MONASH University

Sphingolipids in cardiac remodelling: Molecular mechanisms and potential therapeutic targets

Ruth Rebecca Magaye

MSc., BSc.

A thesis submitted for the degree of *Doctor of Philosophy* at
Monash University in 2020
Faculty of Medicine, Nursing and Health Sciences
School of Public Health and Preventive Medicine
Department of Epidemiology and Preventive Medicine

October 2020

Copyright notice

Abstract

Cardiac remodelling plays a major role in the progression of cardiomyopathies to heart failure (HF) and is recognised as a clinical determinant for HF. The process of cardiac remodelling is driven by a plethora of molecular and cellular events. Among these events, the lipid synthesis pathways, such as the sphingolipids synthesis pathway, is dysregulated. The *de novo* sphingolipid synthesis pathway harbours several lipids and enzymes that have not been explored in terms of their effects on cardiac remodelling. These sphingolipids include dihydrosphingosine 1 phosphate (dhS1P) and dihydrosphingosine (dhSph), and the enzyme dihydroceramide desaturase 1 (DES1). This dissertation explored the effects of dhS1P and dhSph on known remodelling signalling pathways such as the transforming growth factor beta (TGFβ), phosphatidyl inositol 3-kinase (PI3K)/ protein kinase B (Akt), and Janus Kinase (JAK)- signal transducer and activator of transcription (STAT) pathways *in vitro* in primary neonatal rat cardiac fibroblast (NCFs) and myocytes (NCMs). This thesis also hypothesizes that, shifting the balance of sphingolipids towards the dihydrosphingolipids by inhibiting DES1 can reduce cardiac remodelling in a mice ischemic reperfusion (I/R) injury model. Exogenous dhS1P increased collagen synthesis in NCFs through the PI3K/Akt and JAK/STAT signalling pathways. DhS1P also increased hypertrophy in NCMs through the JAK/STAT pathway. While exogenous dhSph reduced TGFβ mediated collagen synthesis in primary cardiac fibroblasts by increasing the metabolism of specific dihydrosphingolipids, such as dhS1P, in the *de novo* synthesis pathway. Investigation of the benefits of the DES1 inhibitor CIN038 in a mouse I/R injury model suggests beneficial effects on cellular and molecular markers of cardiac remodelling. Taken together, the data presented in this

dissertation suggests that dihydrosphingolipids such as dhS1P and dhSph can play a role in cardiac remodelling and sheds light on the potential of DES1 enzyme targeted therapy for cardiac remodelling.

Declaration

This thesis is an original work of my research and contains no material which has been accepted for the award of any other degree or diploma at any university or equivalent institution and that, to the best of my knowledge and belief, this thesis contains no material previously published or written by another person, except where due reference is made in the text of the thesis.

Signature:

Print Name: Ruth Rebecca Magaye

Date: 16/10/2020

Publications, Awards and Presentations during enrolment

Publications (Published as first author and submitted for editorial review)

1. **Magaye R**, Savira F, Hua Y, Xiong X, Huang L, Reid C, Flynn B, Liew D, Wang BW. Exogenous dihydrosphingosine 1 phosphatemediates collagen synthesis in cardiac fibroblasts through JAK/STAT signalling and TIMP1. Cellular Signalling. 2020;72:109620.

2. **Magaye R**, Savira F, Hua Y, Kelly DJ, Reid C, Flynn B, Liew D, Wang BW. The role of dihydrosphingolipids in disease. Cellular Molecular Life Science. 2019;76(6):1107-34.

3. **Magaye R**, Savira F, Hua Y, Xiong X, Huang L, Reid C, Flynn BL, Kaye D, Liew D, Wang BH. Attenuating PI3K/Akt-mTOR pathway reduces dihydrosphingosine 1 phosphate mediated fibrosis and hypertrophy in cardiac cells. *Submitted for publication.*

4. **Magaye R**, Savira F, Xiong X, Huynh K, Meikle PJ, Reid C, Flynn BL, Kaye D, Liew D, Wang BH. Dihydrosphingosine driven enrichment of sphingolipids attenuates TGFβ induced collagen synthesis in cardiac fibroblasts. *Submitted for publication.*

5. **Magaye R**, Savira F, Xiong X, Natalie Melett, Huynh K, Meikle PJ, Daniel Donner, Helen Kiriazis, Aascha Brown, Reid C, Flynn BL, Kaye D, Liew D, Wang BH. DES1 inhibition attenuates cardiac remodelling markers and inflammatory pathways in a mouse ischemia reperfusion model. *Submitted for publication.*

Publications (Published as co- author and submitted for editorial review)

1. Savira F, **Magaye R**, Liew D, Reid C, Kelly DJ, Kompa AR, Sangaralingham SJ, Burnett JC, Kaye D, Wang BH. Cardiorenal syndrome: Multi-organ dysfunction involving the heart, kidney and vasculature. British Journal of Pharmacology. 2020;177(13):2906-2922.

2. Savira F, **Magaye R**, Liew D, Reid, Kaye D, Marwick T, Wang BH. Molecular mechanisms of protein-bound uremic toxin-mediated cardiac, renal and vascular effects: underpinning intracellular targets for cardiorenal syndrome therapy. Toxicology Letters. 2019;308:34-49.

3. Lu L, Guo J, Hua Y, Huang K, **Magaye R**, Cornell J, Kelly DJ, Reid C, Liew D, Zhou Y, Chen A, Xiao W, Fu Q, Wang BH. Cardiac fibrosis in the ageing heart: Contributors and mechanisms. Clinical and Experimental Pharmacology & Physiology. 2017; 44(S1):55-63.

4. Savira F, Kompa AR, Kell DJ, **Magaye R**, Xiong X, Huang L, Liew D, Reid C, Scullino CV, Pitson SM, Flynn BL , Wang BH. The effect of dihydroceramide desaturase 1 inhibition on endothelial impairment induced by indoxyl sulfate. *Submitted for publication.*

5. Savira F, **Magaye R**, Scullino CV, Flynn BL, Xiong X, Kompa AR, Wang BH. Sphingolipid imbalance and inflammatory effects induced by uremic toxins in heat and kidney cells are reversed by dihydroceramide desaturase 1 inhibition. *Submitted for publication.*

Awards

List of awards received in relation to PhD studies

1. Monash Postgraduate Publication Award (2020)

Conference Presentations

1. E- POSTER

   15th Annual Basic Cardiovascular Science Scientific Sessions, American Heart Association/Online, July 2020

2. MINI ORAL

   66th Annual Scientific Meeting of Cardiac Society of Australia and New Zealand/ Brisbane, August 2018

Conference Proceedings

1. **Magaye R**, Savira F, Xiong X, Flynn BL, Wang BH. Exogenous dihydrosphingosine 1 phosphate mediates collagen synthesis in cardiac fibroblasts through PI3K/mTOR signalling pathway. Circ Research. 2020;127(1):A487.

2. **Magaye R**, Savira F, Hua Y, Huang L, Flynn B, Wang B. Sphingosine 1 phosphate mediates cardiac fibrosis through JAK/STAT signalling pathways. Heart Lung Circ. 2018;27(2):S132.

3. Hua Y, **Magaye R**, Savira F, Huang L, Flynn B, Wang B. Dihydroceramide desaturase 1 inhibitor CIN038 ameliorates cardiac cellular remodelling. Heart Lung Circ. 2018;27(2):S93.

Thesis including published works declaration

I hereby declare that this thesis contains no material which has been accepted for the award of any other degree or diploma at any university or equivalent institution and that, to the best of my knowledge and belief, this thesis contains no material previously published or written by another person, except where due reference is made in the text of the thesis.

This thesis includes two original papers published in peer reviewed journals and three submitted publications. The core theme of the thesis is "Sphingolipids in Cardiac Remodelling". The ideas, development and writing up of all the papers in the thesis were the principal responsibility of myself, the student, working within the School of Public Health and Preventive Medicine under the supervision of Associate Professor Bing H. Wang.

The inclusion of co-authors reflects the fact that the work came from active collaboration between researchers and acknowledges input into team-based research.

In the case of chapters 1, 2, 3, 4 and 5 my contribution to the work involved the following:

Thesis Chapter	Publication Title	Status *(published, in press, accepted or returned for revision, submitted)*	Nature and % of student contribution	Co-author name(s) Nature and % of Co-author's contribution	Monash student Y/N
1	The role of dihydrosphingolipids in disease	Published (*Cellular and Molecular Life Sciences, Q1 Journal, IF 7.0, Cite Score 6.12*)	75%. Concept literature search and compilation and wrote first draft	Feby Savira-input into manuscript	Yes
				Hua Yue, Darren Kelly, Christopher Reid, Bernard Flynn, Danny Liew, Bing Wang-input into manuscript	No *(All Co-authors contributed equally)*
2	Exogenous dihydrosphingosine 1 phosphate mediates collagen synthesis in cardiac fibroblasts through JAK/STAT signalling and TIMP1	Published (*Cellular Signalling, Q1 Journal, IF 3.38, Cite Score 6.8*)	70%. Designed and performed experiments. Collated and analysed the data. Wrote first draft	Feby Savira-Assisted in performing experiments and editing manuscript	Yes
				Yue Hua, Xin Xiong, Li Huang, assisted in performing experiments	No *(All co-authors contributed equally)*
				Christopher Reid, Bernard Flynn, Danny Liew, Bing Wang, Data validation and manuscript editing	

3	Attenuating PI3K/Akt-mTOR pathway reduces dihydrosphingosine 1 phosphate mediated fibrosis and hypertrophy in cardiac cells	Submitted	70% Designed and performed experiments. Collated and analysed the data. Wrote first draft	Feby Savira Assisted in-performing experiments and editing manuscript	Yes
				Yue Hua, Xin Xiong, Li Huang-assisted in performing experiments	No *(All co-authors contributed equally)*
				Christopher Reid, Bernard Flynn, David Kaye, Danny Liew, Bing Wang-Data validation and manuscript editing	
4	Dihydrosphingosine driven enrichment of sphingolipids attenuates TGFβ induced collagen synthesis in cardiac fibroblasts	Submitted	70% Designed and performed experiments. Collated and analysed the data. Wrote first draft	Feby Savira-Assisted in performing experiments and editing manuscript	Yes
				Yue Hua, Xin Xiong, Li Huang - Assisted in performing experiments	No *(All co-authors contributed equally)*
				Kevin Huynh, Peter Meikle Performed lipidomics analysis, data validation and manuscript editing	
				Christopher Reid, Bernard Flynn, David Kaye, Danny Liew, Bing Wang-Data validation and manuscript editing	

5	DES1 inhibition attenuates cardiac remodelling markers and inflammatory pathways in a mouse ischemia reperfusion model	Submitted	65% Assisted in I/R surgery, animal husbandry, echocardiography, hemodynamic analysis, and lipidomics. Performed biomolecular analysis experiments. Collated and analysed the data. Wrote first draft	Feby Sevira-Assisted in performing experiments and editing manuscript	Yes
				Xin Xiong,-Assisted in performing experiments	No (*all co-authors contributed equally*)
				Kevin Huynh, Natalie Melett, Peter Meikle-Performed lipidomics analysis, data validation and manuscript editing	
				Daniel Donner, Helen Kiriazis, Aascha Brown-Performed I/R surgery, echocardiography, hemodynamic analysis, data validation and manuscript editing	
				Christopher Reid, Bernard Flynn, David Kaye, Danny Liew, Bing Wang-Data validation and manuscript editing	

I have renumbered sections of submitted or published papers in order to generate a consistent presentation within the thesis.

Student name: Ruth Rebecca Magaye

Student signature: **Date:** 16/10/2020

I hereby certify that the above declaration correctly reflects the nature and extent of the student's and co-authors' contributions to this work. In instances where I am not the responsible author I have consulted with the responsible author to agree on the respective contributions of the authors.

Main Supervisor name: Bing Hui Wang

Main Supervisor signature: **Date:** 16/10/2020

Acknowledgement

This thesis would not have been possible without the support of many along the way. Firstly, I thank God for faith and grace to persevere. I would have given up if it were not for Philippians 4:13. To my primary supervisor, Associate Professor Bing H. Wang, thank you for your guidance, encouragement, and support. The confidence and insight you showed when I lacked it, gave me courage. To Associate Professor Bernard L. Flynn, thank you for your continuous support and attention to detail in all that you have assisted me with.

Along the way I have gained many colleagues and friends. Thank you to my everyday family at the Biomarker Discovery Laboratory, Feby Savira, Yue Hua, Xin Xiong, and Li Huang, for your help, support and most of all your friendship. I am so grateful to the staff and colleagues at the school of Public Health and Preventive Medicine for your constant support and encouragement throughout the candidature. Thank you to colleagues and fellow PhD students at the Baker Institute for your welcome and scientific support.

I want to thank the Baker Heart and Diabetes Institute's microsurgery platform, metabolomics and proteomics group and the animal house staff for all your expert contributions. Thank you to Associate Professor Bernard Flynn's laboratory at the Monash Institute of Pharmaceutical Sciences for their contribution of the sphingolipids and the CIN038 compound.

I am grateful for the funding provided by the Australian government and Monash University to undertake this thesis. This research was supported by an Australian Government Research Training Program (RTP) Scholarship, through the

"Monash International postgraduate research scholarship" and the "Monash Graduate Scholarship".

Finally, to my family and friends who have been my source of sanity and refreshment. To Jonathan D'Sylva, Cheryl Teo, Renee Conroy and Cynthia Fo, only God knows how much your friendship has meant to me in the last four years and I will forever be indebted. To Dr. Samsel and Frances Kenston, thank you for your enduring friendship and encouragement. To my parents, and siblings, thank you for always believing in me. Without you all, this would not be possible.

Table of contents

List of tables

List of figures

List of abbreviations

Akt	Protein kinase B
αMHC	Alpha myosin heavy chain
αSKA	Alpha skeletal muscle actin
α-SMA	Alpha smooth muscle actin
ANP	Atrial natriuretic peptide
β1AR	β1- adrenergic receptor
βMHC	β myosin heavy chain
BNP	Brain natriuretic peptide
CAD	Coronary artery disease
Cer	Ceramide
Cer1P	Ceramide 1 phosphate
CO	Cardiac output
Coll1a1	Collagen 1a1
Coll3a1	Collagen 3a1
CTGF	Connective tissue growth factor
CVD	Cardiovascular disease
DAMPs	Danger associated- molecular patterns
DEGS1	Delta 4-Desaturase, Sphingolipid 1 gene
DES1	Dihydroceramide desaturase 1 enzyme
DhCer	Dihydroceramide
DhS1P	Dihydrosphingosine 1 phosphate
Ea	Arterial elastance
EF	Ejection fraction
ECM	Extracellular Matrix

ER	Endoplasmic Reticulum
ERK	Extracellular-signal-regulated kinase
EDPVR	End diastolic pressure volume relationship
ESPVR	End systolic pressure volume relationship
FA	Fatty acid
FS	Fractional shortening
GAPDH	Glyceraldehyde 3 –phosphate dehydrogenase
GF	Growth factor
HDL	High density lipoprotein
H&E	Hematoxylin and eosin
HF	Heart failure
HR	Heart rate
IL-1β	Interleukin 1 beta
IL-6	Interleukin 6
JAK	Janus Kinase
KXA	Ketamine/ xylazine/atropine
LAD	Left anterior descending artery
LAP	Latency associated protein
LDL	Low density lipoprotein
LV	Left ventricle
MI	Myocardial Infarct
MMP2 and 9	Matrix metalloproteinase 2 and 9
mTOR	Mammalian target for rapamycin
NCF	Neonatal cardiac fibroblasts
NCM	Neonatal cardiac myocytes
NFκB	Nuclear factor kappa B

P38- MAPK	P38 mitogen activated protein kinase
PC	Phosphatidylcholine
PI3K	Phosphatidylinositol-3-kinase
PKC	Protein kinase C
PSR	Picrosirius red
PV	Pressure-volume loop
RPS6	Ribosomal protein S6
S1P	Sphingosine 1 phosphate
S1PRs	Sphingosine 1 phosphate receptors
S1PR1 to 5	Sphingosine 1 phosphate receptor 1 to 5
SK1	Sphingosine kinase 1
SM	Sphingomyelin
Sph	Sphingosine
STAT1 and 3	Signal transducer and activator of transcription 1 and 3
SV	Stroke volume
TG	Triglycerides
TGFβ	Transforming growth factor β
TIMP1 and 2	Tissue inhibitor of metalloproteinase 1 and 2
TNFα	Tumour necrosis factor alpha
TNFR	Tumour necrosis factor alpha receptor
Ved	Volume at end of diastole
Ves	Volume at end of systole

Preface

The introductory chapter (chapter 1) incorporates both unpublished (section 1.1 to 1.4) and published work (section 1.5) that has been modified from a comprehensive review on dihydrosphingolipids in a variety of diseases in the following published article;

Magaye R, Savira F, Hua Y, Kelly DJ, Reid C, Flynn B, Liew D, Wang BW. The role of dihydrosphingolipids in disease. Cellular Molecular Life Science. 2019;76(6):1107-34.

Published work is attached in **Appendix 1.1**.

Chapter 1: Introduction and literature review

1.1 General introduction

Lipids are the basic building blocks of cells [1]. Their functions and roles within the biological system range from supporting the structural integrity of cells to acting as mediators of cell signalling events [1, 2]. These roles and functions are also divergent in terms of species, target site, and disease states. Perturbation of the metabolic pathways that govern each category or group of lipids can also impose effects on other lipid categories or pathways, especially in disease states where dyslipidemia poses a risk for further complications such as cardiovascular diseases (CVD). Dyslipidemia as a risk factor in heart failure (HF) is well documented for classical lipids such as cholesterol, high density lipids (HDLs), low density lipids (LDLs), and triglycerides (TG) [3, 4]. In the last century, technological advances in small molecule analysis have led to increased characterization and delineation of other lipid categories and their synthetic pathways [5]. This has allowed advancement in scientific research regarding their roles in physiological and pathological states. The sphingolipids are among the low abundance lipids that are now being investigated for their role in the aetiology of cardiovascular diseases.

The heart responds to biochemical stresses and mechanical stimuli through what is known as cardiac remodelling [6]. Cardiac remodelling plays a major role in progression of cardiomyopathies to HF, that ultimately results in death [7]. It can occur in both physiological and pathological states [7, 8]. Clinically it is evident as morphometric and functional changes in the heart [9]. These clinical changes are the result of a combination of a series of events occurring at the cellular, and

molecular level in the myocardium [6, 9]. The degree of remodelling in the heart depends on the extent of injury or change in pathophysiology of the myocardium [6]. The focus of this thesis is on the molecular events in the pathophysiology of cardiac remodelling in the context of myocardial infarction (MI).

1.2 Physiology of the myocardium

The heart comprises four chambers; the left and right aorta, and the left and right ventricles [10]. These work in rhythmic cohesion to maintain locale and global perfusion. It is a muscular pump made up of a meshwork of muscle fibres, cells, and vasculature [10].

The heart wall consists of three different layers; the pericardium- comprising two different layers made up of simple mesothelial cells (visceral) and fibrous elastic tissue (parietal), the myocardium- or the muscle layer, makes up the bulk of the heart, and the endocardium- or the endothelial layer inside the myocardium [10]. The thickness of the myocardium is determined by the pressure present in the chamber; thus, the ventricles have greater wall thickness than the atria. In adults the left ventricle wall is three folds thicker than the right, due to the higher pressure in the systemic circulation than the pulmonary circuit [10].

The cellular structure of the myocardium consists of the muscle cells or myocytes (cardiomyocytes) and non- cardiomyocytes [11, 12]. Both the cardiomyocytes and the non- cardiomyocytes are essential for normal heart homeostasis, efficient contraction and long term survival of the heart [12]. Numerically, the cardiomyocytes are less in number compared to other cell populations. Recent assessment of cell populations in the murine heart have shown that 36% of the cells were cardiac myocytes, and 64% endothelial cells, including 15% fibroblasts, and 9% leukocytes [11]. These make up three integrated components in the

myocardium; the myocytes, extracellular matrix (ECM), and the microvascular circulation [13].

1.2.1 The myocytes

The cardiac myocyte is a terminally differentiated cell, that is composed of myofibrils that are bundled together [10]. The myofibrils contain myofilaments made up of the myosin and actin proteins which form the thick and thin filaments, respectively [10]. The basic contractile unit of the myocyte is the sarcomere which is defined as the structure between two Z-lines or discs within the myofilament [10]. The myosin is the molecular motor that drives the contraction. Contraction occurs when the central bipolar myosin thick filaments use adenosine triphosphate (ATP) generated at the head by the myosin ATPase, to pull the thin filaments [14] [15]. This allows the two types of filaments to slide across each other reducing the sarcomere length, therefore generating the contractile force during the process of excitation- contraction coupling [15]. The thin filaments are composed of three proteins; actin, tropomyosin, and troponin (troponin- T and troponin-C).

Apart from the sarcomeres, cardiac myocytes have other structures that are vital for proper functioning of the heart. Adherence to other myocytes are maintained by intercalated discs at the periphery of the cell [10]. Gap junctions at the intercalated discs allow electrical communication between cells [10, 16]. They also have transverse tubules or T tubules that are extensions from the myocyte plasma membrane which helps maintain the sarcoplasmic reticulum (SR) calcium (Ca^{2+}) storage and regulation [10, 17]. The terminal cisternae in the SR mechanically couples to T tubules and voltage sensitive ryanodine receptors that release Ca^{2+}[15, 17]. The binding affinity of Ca^{2+} to troponin C drives the force generating

response [10]. Ca^{2+} is also an important regulator of cell metabolism, apoptosis and transcription [17].

1.2.2 The ECM

The myocytes are coupled with the ECM which acts as a viscoelastic scaffold that is stress tolerant [13]. The dynamic and complex architectural structure of the ECM consists of both structural proteins and non- structural proteins that allow for its plasticity[13, 18, 19]. The Structural proteins of the ECM mainly consist of collagen type I and III [18]. The ECMs non- structural properties include accommodating multiple proteins with cell receptor and growth factor receptor binding properties and cells types such as the cardiac fibroblasts, myofibroblasts, leukocytes and vasculature [13, 19]. These properties enable the ECM to serve as a reservoir, processing site and a communication hub for signalling molecules, proteins and genetic information [18, 19].

1.2.3 The microvascular circulation

The microvascular circulation of the myocardium serves as the transport system and exchange interface for substrates [20, 21]. These microvasculature are fed with arterial blood through the coronary arteries; right anterior coronary artery to the right side of the heart, and the left anterior coronary artery, which branches out into the left anterior descending (LAD) and left circumflex (LCX) artery in about 58% of human beings, which supply the left side of the heart [10, 20]. The coronary circulation in the heart is unique in that pressure, capacitance and resistance differs in the larger arteries (500 μM- 5 mm), arterioles (100- 500 μM)

and transmural arterioles (< 100 μM) [21]. Blood flow in the microvasculature is determined by the ventricular contraction/relaxation and lumen space of pre-capillary arterioles [21].

1.3 Cardiac remodelling

Injury or insult to the myocardium results in alterations in the physiology of the myocardium, in-order to maintain cardiac function [6, 7]. These alterations eventually lead to the pathology of cardiac remodelling.

1.3.1 Definition of cardiac remodelling

The term "cardiac remodelling" was first used by Hochman and Bulkley in 1982 in a MI model describing the formation of scar tissue at the site of infarction [22]. Their definition has now been expanded upon and encompasses a plethora of events at the genomic, molecular, cellular and interstitial level which is clinically evident as changes in the size, shape and function of the heart in both physiological and pathological remodelling [6]. It is aimed at supporting and maintaining ventricular wall integrity and preventing myocardial rapture post injury [7].

1.3.2 Clinical aspect of cardiac remodelling

Clinically, remodelling after a MI has a unique pattern of presentation [13, 23]. The acute loss of myocytes due to necrosis, has a sudden effect on the loading conditions, evident as a 20% increase in left ventricular end diastolic volume (LVEDV) [13, 23]. The left ventricular end systolic volume (LVESV) and ejection

fraction (EF) have also been considered as clinical endpoints [23]. The hearts morphology also changes, in terms of cavity diameter, mass, wall thickness, shape and area [9, 24]. The extent of remodelling differs across the different phases of MI (acute, subacute and late), and progresses toward HF [9].

1.3.3 Molecular mechanisms of cardiac remodelling

The resultant increase in load due to an injury or insult also triggers a cascade of cellular, molecular and biochemical signalling processes that initiate and subsequently modulate reparative changes, which include dilatation, hypertrophy inflammatory infiltrates, and fibrosis [6, 13].

1.3.3.1 Cardiac myocyte death

The process of cell death can occur through autophagy, apoptosis and necrosis [25]. Autophagy and apoptosis play important roles in ischemia/reperfusion (I/R) and cardiomyocyte death [25, 26]. Autophagic cell death is activated initially as a response to depleted APT levels due to low oxygen supply [26]. The cardiac myocytes derive 95% of the energy they need to function from oxidative phosphorylation [27]. In re-perfused conditions, autophagy is driven by oxidative stress (OS), mitochondrial damage, endoplasmic stress, and calcium overload [26]. Autophagy can be adaptive or maladaptive depending on the context.

The regulated and energy dependent process of apoptosis is activated upon cellular stress or injury [28]. The process occurs through the extrinsic or death receptor pathway and the intrinsic or mitochondrial pathway and converge on the same terminal pathway [28, 29]. The terminal pathway involves the activation of effector caspases 3, 6 and 7 which then cleave essential cellular substrates leading

to apoptosis [29]. Apoptosis appears in 50-60% of patients 24 h after an MI and correlates with the presence of HF or arrhythmias and left ventricular remodelling [30, 31]. The amount and presence of apoptosis differs across the regions of injury (infarct zone, border zone, remote zone), and the MI phases [28].

Unlike autophagy and apoptosis, the process of necrosis initiates remodelling[31, 32]. The injured or stressed cardiomyocytes and damaged ECM release substrates that act as danger signals [32]. These substrates include interleukin 1α, heat shock protein 60 and 70 (HSP60 & 70), mitochondrial DNA, single and double stranded RNA, uric acid, ATP, the DNA binding nuclear protein (high mobility group box 1 -HMGB1), calcium binding cytoplasmic proteins (S100A8 and S100A9), low molecular weight hyaluronic acid, and fibronectin-EDA [32, 33]. Collectively termed danger associated- molecular patterns (DAMPs). DAMPs bind to cognate pattern recognition receptors (PRRs) expressed intracellularly or on the surface of innate immune cells resident in tissue (macrophages, fibroblasts, mast cells, dendritic cells), and in circulation (monocytes and neutrophils)[33]. These PRRs include the toll like receptors (TLRs), interleukin 1 receptor (IL-R), nucleotide-binding oligomerization domain- like receptor (NLRs) and receptor for advanced glycation end-products (RAGE) [34]. All of which converge downstream on mitogen activated protein kinases (MAPKs) and the nuclear factor kappa B (NFκB) [33, 34]. These then drive the increased expression and secretion of inflammatory factors that trigger the inflammatory cascade. Necrosis also results in release of intracellular proteins such as creatine kinase (CK), myoglobin, troponins T and I and lactate dehydrogenase (LDH) [35, 36]. These substrates leak into the interstitial spaces and enter the microcirculation and are considered as biomarkers for an active MI.

1.3.3.2 Myocyte hypertrophy

Broadly, hypertrophy can be defined as the enlargement of individual myocyte size, enhanced protein synthesis, and heightened organization of the sarcomeres [37, 38]. Classically, pathological hypertrophy is categorized as concentric hypertrophy; which is characterized by parallel addition of sarcomeres and lateral growth of individual cardiomyocytes due to pressure overload, or eccentric hypertrophy; which is characterized by addition of sarcomeres in series (end to end) and longitudinal cell growth due to volume overload [37]. In MI induced cardiac remodelling, the mechanical and physiological stress impairs cardiac function which causes the cardiac myocyte to undergo eccentric hypertrophy as a compensatory response to reduce wall stress and oxygen consumption [38, 39]. The adaptive responses become maladaptive leading to dysregulation of Ca^{2+} handling proteins (plus others), reactivation of fetal gene expression, altered protein synthesis and function, mitochondrial dysfunction, oxidative stress and metabolic reprogramming [38]. These biochemical changes activate G protein coupled intracellular signalling pathways that are involved in their regulation. Which include the calcineurin/ nuclear factor of activated T cells (NFAT) pathway, phospholipase C (PLC)/ protein kinase C (PKC) pathway, tyrosine kinase pathway, extracellular signal-regulated kinase (ERK) pathway, c-JUN N-terminal kinase (JNK) pathway, p38 MAP kinase (p38) pathway, Rho family of small G-proteins, PI3K/Akt pathway, and JAK/STAT pathway [40-43]. The activation of the β and α Adrenergic receptors (β-AR and α-AR), adenosine receptors, angiotensin receptors, endothelin receptors and muscarinic receptors by their respective ligands also impact the downstream molecular targets of these

signalling pathways [44]. The activation of these pathways and receptors further contribute to fibrosis and angiogenesis.

At the genetic level, these signalling pathways and receptors lead to the reactivation of latent fetal genes such as β-myosin heavy chain (β-MHC), skeletal α-Actin (αSKA), and the atrial and brain natriuretic peptides (ANP and BNP), and reductions in α-myosin heavy chain (αMHC) [39, 40]. Metabolically, the myocyte in the state of hypertrophy switches from fatty acid oxidation to glucose utilization as its main source of ATP, resulting in increased glycolysis and the activity of its associated enzymes [45]. This switch to glucose catabolism is promoted by the 5' AMP- activated protein kinase (AMPK), which acts as a central censor for cellular energy status. AMPK responds to increase in AMP/ ATP ratios and induces numerous pathways that contribute to lipid metabolism, protein synthesis and glucose catabolism [46].

1.3.3.3 Neurohormonal factors

Myocyte death and hypertrophy impairs pump function. This is sensed by peripheral arterial baroreceptors as "underfilling", which activate a series of compensatory mechanisms involving neurohormonal factors. However, prolonged activation of these factors contributes to disease progression towards HF. The two main neurohormonal systems involved in cardiac remodelling are the renin angiotensin aldosterone system (RAAS) and the sympathetic nervous system (SNS). The activation of the RAAS and SNS during remodelling leads to activation of intracellular signalling pathways that stimulate the synthesis of proteins in myocytes and fibroblasts, contributing to cellular hypertrophy, fibrosis and LV dilation [9]. The main products of SNS activation are the catecholamines, adrenaline and noradrenaline, which act as compensatory mechanisms to maintain

CO through ionotropic and chronotropic effects. Even though this produces protective effects, excessive production elevates the heart rate by aggravating the ischaemic damage [47]. The increased SNS outflow may cause desensitization of the β-AR (β1, β2) and α-AR, depletion of noradrenalin stores, destruction of sympathetic innervation, arrhythmias, and impairment of diastolic and systolic function.

The RAAS is the most important hormonal system that controls and regulates the systemic blood pressure, renal blood flow and glomerular filtration rate. The hypo-perfusion of organs including the kidney, together with an activated SNS leads to activation of the RAAS and the production of angiotensin II (Ang II). The components of the RAAS can act in autocrine or paracrine manner, independently. Ang II can affect the heart directly or indirectly by eliciting systemic effects. Ang II acts on the heart by increasing inotropy, decreasing lecithotrophy and coronary vasoconstriction. It drives fibroblast division and collagen production causing myocardial fibrosis, and myocyte hypertrophy [48]. The systemic effects of Ang II include sodium (Na) reabsorption by increasing aldosterone secretion and by stimulating water intake by direct effect on the tubules. It also causes vasoconstriction directly and may facilitate the release of noradrenaline by acting on the sympathetic nerve endings. The stimulatory effects of Ang II occur after the peptide binds to its G protein-coupled cell surface receptors (GPCR), most notably angiotensin receptor type 1 (AT1). Renin is the rate limiting factor in the production of Ang II, alterations in the production of renin have been linked to cardiac and vascular disorders [49]. The release of renin is inhibited by ANP and BNP [50]. In the circulation ANP and BNP bind to different natriuretic peptide receptors (NPRs) and exert their effects: NPR-A, NPR-B and NPR-C. ANP and BNP primarily bind with NPR-A which activates

the 3'-5'-guanosine monophosphate (cGMP) signalling thus increasing vasodilation, diuresis and natriuresis, leading to decrease in renin and aldosterone, cell proliferation and cardiac fibrosis [51]. Ang II can also trigger the release of other vasoactive substances such as arginine Vasopressin (AVP), and endothelin, and reduces nitric oxide (NO) which contribute to endothelial dysfunction [48, 52-54]. Due to the diverse systemic and myocardial effects of Ang II, coupled with clinical trials that have shown survival benefit, angiotensin converting enzyme (ACE) inhibitors are recommended in patients with MI [13, 55, 56].

1.3.3.4 Inflammation

Necrosis of the cardiac myocytes also triggers a complex inflammatory process involving multiple players in the heart [35, 57]. These include resident myocardial cells; cardiomyocytes, endothelial cells, and fibroblasts, and circulating immune cells; neutrophils, monocytes, macrophages, dendritic cells and lymphocytes. The initial inflammatory phase triggered by the DAMPs after an MI assists in digesting and clearing damaged cells and the ECM, in the infarct zone [32, 33]. The PRR driven increased expression and secretion of inflammatory cytokines such as tumour necrosis factor- α (TNF-α), interleukin-1β (IL-1β), interleukin-6 (IL-6), and interleukin-18 (IL-18); CXC chemokines; CC chemokines; cell adhesion molecules and complement factor B enable recruitment and migration of macrophages, monocytes and neutrophils into the infarct zone [32]. The endothelial layer also undergoes activation and changes in its permeability to allow cellular component migration between compartments. These further enhance and amplify the immune response and promotes efferocytosis of dying cells and damaged tissue digestion through the release of proteolytic enzymes and oxidases [58]. Thus, preparing the microenvironment in the infarct zone for repair.

The reparative phase is anti-inflammatory and allows wound healing and scar formation to prevent cardiac rupture. The cytokine, IL-1β, induces the production of Matrix Metalloproteinases (MMPs) by fibroblasts, which breaks down the ECM [59]. This encourages infiltration of the infarcted zone by neutrophils and monocytes which clear the wound of dead cells and matrix debris. As the infarct zone is cleared up, the inflammatory response progressively decreases. The large infiltrates of neutrophils into the infarcted myocardium undergo apoptosis due to their short lifespan and are phagocytosed by macrophages. The dying neutrophils release mediators that inhibit further neutrophil recruitment, such as annexin 1 and lactoferrin [60, 61]. Macrophages further suppress the inflammation process by secreting transforming growth factor β (TGF-β), interleukin-10 (IL-10) and other lipid mediators such as resolvins and protectins which prevent additional neutrophil transmigration [62, 63]. The balance and transition between these two phases determine the extent of cardiac or left ventricular remodelling.

1.3.3.5 Fibrosis

The fibrogenic effect is initiated by MI and involves the acute innate immune response. Which leads to activation of effector cells, such as fibroblasts, myocytes, myofibroblasts, fibrocytes, epithelial cells undergoing mesenchymal transformation (EMT), endothelial cells undergoing mesenchymal transformation (EnMT) and pericytes, which then increase excretion and deposition of ECM.

The process of fibrosis follows from the reparative phase during inflammation (1.3.3.2), which can be termed as the proliferative phase, to the maturation phase. Suppression of inflammation during the reparative phase, allows for infiltration of the infarct with fibroblasts and endothelial cells which increase profibrotic signalling, which involves the activation of the TGF-β dependent and independent

cascades, ultimately leading to trans-differentiation of fibroblast into myofibroblast phenotype. Myofibroblasts express α-Smooth Muscle Actin (α-SMA), and contractile proteins such as actin, troponin, and titin [64]. They synthesize and deposit matrix proteins such as collagen type III and I. Collagen deposition is crucial to increase the tensile strength and prevent myocardial rapture [65]. The myofibroblasts also produce matricellular proteins such as thrombospondin-1 (TSP-1) and tenascin C, and fibronectin with extra domain A (EDA-FN) which further promote myofibroblasts migration [66]. A massive angiogenesis process accompanies this phase to allow for oxygen and nutrients provision to the metabolically active wound [67]. The RAAS has also been shown to play a role in promoting myofibroblasts proliferation and stimulation of matrix synthesis; through circulating Ang II and aldosterone as well as locally produced Ang II which interacts with nuclear angiotensin receptors in cardiac fibroblasts [68, 69].

Proliferation subsides and transition to the maturation phase follows replacement of collagen type I with collagen type III by the remaining myofibroblasts. During this phase, the reparative cells are either deactivated or undergo apoptosis. The STOP signals that are responsible for terminating the proliferative stage is not well defined. The activation of these signals, inhibits and terminates TGF-β and Ang II signalling. The synthetic activity of the fibroblasts maybe inhibited by clearance of the matricellular proteins that promote survival and activity of the myofibroblasts. As the scar matures, the ECM becomes cross-linked allowing for increased tensile strength and contraction of the scar. This alters the geometry of the chamber and contributes to remodelling in the remote areas of the ventricular wall [70]. Even though in other tissues the myofibroblasts are all cleared from the scar area, they have been found to persist in the infarct scar decades after the insult

[71]. When there is an imbalance between resorption and deposition of ECM, HF can occur. This balance is governed by senescence, apoptosis and autophagy of effector cells.

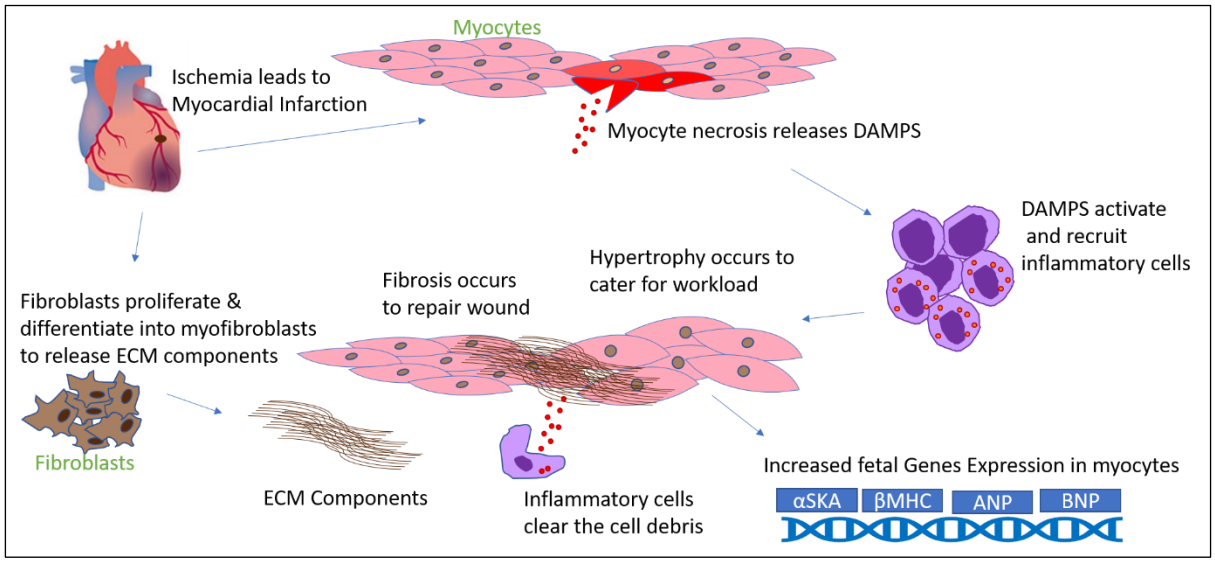

Figure 1.1 Initiation of myocardium repair after an infarction. Summative figure derived from section 1.3.3 and illustrated with Microsoft power point software, 2019.

1.4 Dysregulation of lipids in cardiac remodelling

Shifts in energy demand and supply in the injured myocardium also contribute to contractile dysfunction. The heart is sometimes described as a "metabolic omnivore". Several factors in cardiac metabolism have been linked to lipid metabolism. These factors include an imbalance in the supply and demand for oxygen and the switching of fatty acid (FA) β-oxidation to glycolysis leading to accumulation of TGs [72]. FAs are the main source of fuel in the heart, except in the post prandial state. The oxidation of FAs in the heart generates about 70 to 90% of ATP [73]. FAs can be supplied to the heart as free FAs (non-esterified)

bound to albumin or released from TG following hydrolysis from chylomicrons or very low density lipoproteins (VLDL) by lipoprotein lipase [74]. Approximately 20 % of free FAs are taken up by the heart and converted to TGs. The TG pool in the myocardium plays a key role in regulating lipid homeostasis of the heart. In the setting of HF or ischemia FAs levels are significantly raised [75, 76]. The imbalance in FA uptake and oxidation results in accumulation of long chain FAs which are esterified to TGs and phospholipids from esterified fatty acyl-CoA. Fatty acyl-CoA, particularly palmitoyl-CoA, lead to *de novo* synthesis of sphingolipids such as Cer, which are involved in several cellular regulatory processes [77].

1.5 Sphingolipids

The sphingolipids are a class of lipids discovered in the 1800s by a scientist named Thudichum from brain extracts [78]. These class of lipids are characterized by a common carbon backbone called, "sphingosine", to which other head groups are added [78]. The length of the carbon chain in sphingolipids is determined by the type of fatty acid metabolized in the beginning of the *de novo* synthesis pathway and the enzymes that catalyse the reactions in the pathway. Sphingolipids are found through-out the body and are structural components of the plasma membrane [79]. They are found in circulation bound to HDL and are produced by platelets [79-81].

1.5.1 Sphingolipid synthesis and metabolism

The sphingolipids are amphipathic lipids that are synthesized through the *de novo* synthesis pathway, the hydrolytic or sphingomyelin pathway, and the salvage

pathway [78]. The main synthetic pathway is the *de novo* synthesis pathway which occurs in the endoplasmic reticulum (ER)[82]. This pathway begins at the condensation of palmitoyl-CoA and Serine by the enzyme serine palmotyl-transferase (SPT) to form 3-ketosphinganine. 3-ketosphinganine is reduced by 3 keto-sphinganine reductase (3-KSR) to dihydrosphingosine (dhSph). The acylation of dhSph by ceramide synthase 1-6 (CerS1-6) derives dihydroceramide (dhCer), while it's phosphorylation by sphingosine kinase 1 and 2 (SK1 and 2) leads to the formation of dihydrosphingosine 1 phosphate (dhS1P). The six different ceramide synthases, CerS1-6, utilize differing chain lengths of fatty acyl CoAs for *N*-acylation of dhCer, indicate that they may have distinct functions both in pathological and physiological stimuli [83]. DhCer is then desaturated by the enzyme dihydroceramide desaturase 1 and 2 (DES1 & 2) in a non- reversible reaction to ceramides (Cer). Cer is metabolized by ceramidase (CDase) to produce sphingosine (Sph), acylated by sphingomyelin synthase to form Sphingomyelin (SM), and is also converted to other complex lipids such as glucosylceramide. The production of sphingosine 1 phosphate (S1P) from Sph is exclusively phosphorylated by K1 & 2. S1P is then degraded to ethanolamine phosphate (EAP) and trans- 2- hexadecenal by S1P lyase (SPL) [84]. The latter forms the base for globosides. DhS1P & S1P can be converted back to dhSph and Sph by S1P phosphatase (S1PP).

Cer is also produced through the hydrolysis or sphingomyelin (SM) pathway, from complex sphingolipids and SM. SM is catabolized by sphingomyelinases (SMase). The SM pathway is activated at the plasma membrane, golgi apparatus and in the mitochondria. The Cer formed through the sphingomyelin pathway accounts for most of the Ceramide 1 phosphate (Cer1P) in circulation. This conversion is catalysed by ceramide kinase (CERK) [85, 86]. The salvage pathway takes place in

the lysosomes and endosomes, where complex sphingolipids such as glycosphingolipids and glucosphingolipids are catabolized. Sph is the resultant catabolic end- product of complex sphingolipids, which is then recycled through acylation to produce Cers [87].

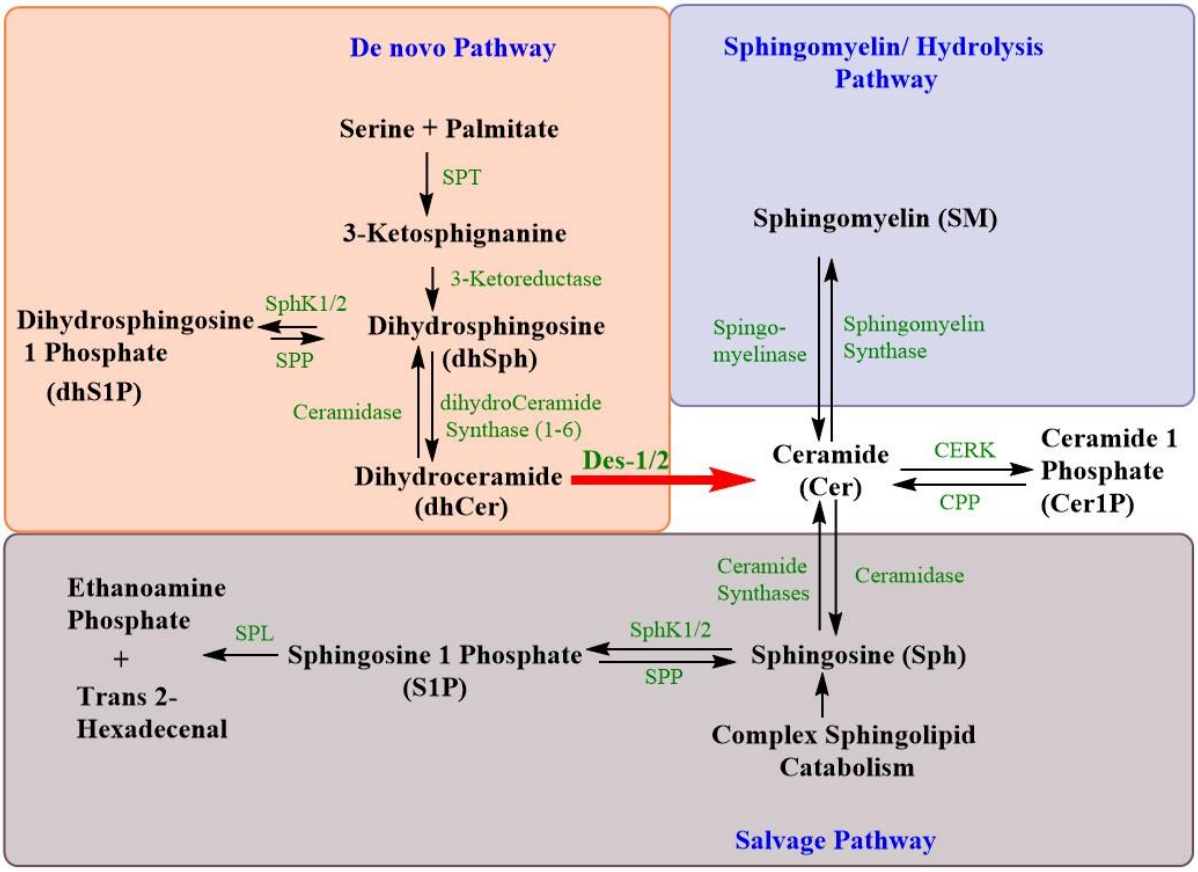

Figure 1.2. Sphingolipid synthesis pathway. Schematic diagram illustrated using Microsoft power point, 2016.

1.5.2 Sphingolipid transport

The intra-and extracellular transport of sphingolipids is governed by their biophysical properties. These movement maybe within a membrane or between membranes [88-91]. Sphingolipids found on the membranes of all eukaryotic cell types. Cer and Cer1P, are transported to the golgi apparatus for further processing

by lipid transfer proteins (LPTs) such as Cer transfer protein (CERT) and Cer1P transfer protein (CPTP) [89, 90]. Cer is known to undergo spontaneous flip-flop; passively moves from one lipid bilayer to another as dictated by concentration gradients [91]. While the amphipathic nature of Sph and dhSph allows them to diffuse and flip between membranes leaflets [78]. The ionization of their free amino groups also allows them to accumulate in acidic pH organelles. S1P and dhS1P are soluable in hydrophilic environment but are unable to traverse membranes without the aid of lipid transporters such as Spinster-Homolog-2 (encoded by the gene SPNS2) and the major facilitator superfamily transporter 2b (Msfd2b) [92, 93]. These transporters aid dhS1P and S1P in their roles as "inside-out signalling" molecules. SNPS2 is mainly localized in epithelial cells and tissues and plays a role in the effect of S1P on lymphocyte traffic, while Msfd2b is abundant in plasma membranes of erythrocytes, platelets and bone marrow [94, 95]. Apart from these, the ATP binding cassette (ABC) transporters also transport S1P and the other sphingolipids. In the plasma about 65% of S1P is bound to HDL specifically through apolipoprotein M, and another 30% is bound by albumin, while dhS1P is un-specifically bound to HDL [79, 96].

1.5.3 Sphingolipid function

Sphingolipid function is reliant upon a complex interplay between the sphingolipids and the metabolic pathway enzymes, the transport system and membrane receptors. The segment of the pathway that begins at DES1 & 2 to S1P which includes Cer, Sph, S1P including SM, has been studied the most and their functions are well documented [83, 97-99]. Briefly, Cer has been known for a long time to be an important biological molecule that is involved in apoptosis,

lipid metabolism, fibrosis and stress response. Cer, due to the differing acyl CoAs that can be used to produce it, is technically a class of molecules rather than a single molecule and therefore may have different biological functions depending on the acyl chain it is composed of. Although Cers are physiological modulators, they become pathological or toxic when they are in excess or their quality is compromised [100]. Apart from Cers, Sph, S1P and SM may exert different effects on their downstream targets, their levels in cellular or biological compartments also differ both in physiological and pathological states. Sph is known to promote apoptosis and cell cycle arrest by targeting sphingosine dependent kinase (SDK) and protein kinase Cδ (PKCδ) [101]. S1P is a bioactive molecule that binds specifically to G-protein coupled receptors termed Sphingosine 1 Phosphate receptors (S1PR). There are five characterized S1P receptors (S1PR1-5). In mammals the S1PR1-3 are most abundant, and their functions have been delineated. S1P functions through these receptors and mediates various intracellular signalling pathways. It is thought of as a lipid mediator involved in cell proliferation, cell growth, cell survival, cell migration, inflammation, angiogenesis, and resistance to apoptotic cell death [102]. SM is dominant in most cellular plasma membranes and its functions range from regulation of endocytosis and receptor mediated ligand uptake, G protein and ion channel signalling, and is known to be the preferred choice of substrate for cholesterol to interact with [85]. The functional attributes of sphingolipids such as dhSph, dhS1P and dhCer have not been fully delineated yet. This is due to them being intermediates in the pathway, therefore rapidly metabolized through the *de novo* pathway resulting in low levels in both tissue and circulation.

1.5.4 Sphingolipids in cardiac remodelling

The evidence for sphingolipids in cardiac remodelling so far targets the Cer-S1P-SM arm of the pathway. Indeed, S1P is the most studied sphingolipid in terms of its effects on the myocardium. Its inside out signalling capabilities, together with the affinity of binding to HDL in plasma have made it a potential target for cardiovascular disease therapy [80]. Here I discuss the mechanisms regarding sphingolipid in cardiac fibrosis and hypertrophy. Figure 1.3 summarises what is known and unknown about the effect of sphingolipids in terms of cardiac remodelling.

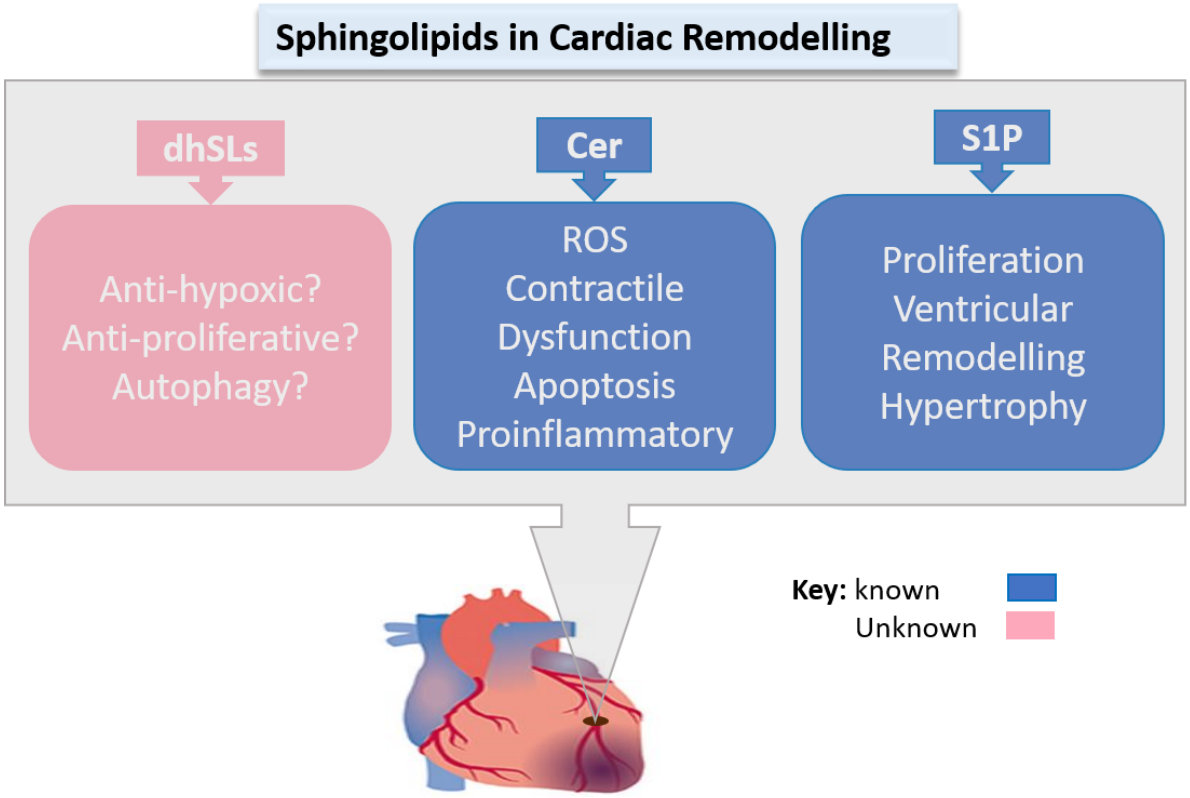

dhSLs, dihydrosphingolipids; Cer, Ceramide; S1P, Sphingosine 1 phosphate

Figure 1.3. Summary of sphingolipid effects in cardiac remodelling. Schematics summarized from section 1.5.4 and illustrated in Microsoft power-point, 2016.

1.5.4.1 S1P in cardiac remodelling

The effects of S1P on cardiac cells seem to differ from fibroblasts, myocytes and endothelial cells. These differences may also be dependent on the type of S1P receptors being activated, the pathophysiological conditions under which they are investigated, and model. For example, a recent population study proposed that S1P is causally involved in the pathophysiology of HF [103]. However, some cell and animal studies have revealed that S1P signalling through S1PRs in post ischemic conditions maybe cardio-protective [104, 105]. S1P may be able to promote hypertrophy[106] and hyperplastic cardiac remodelling [107] effects due to its growth promoting ability as observed in tumors [108]. Multiple studies have found that S1P signalling through its receptors have differing effects on downstream targets. The most abundant S1P receptor in cardiac myocytes is S1PR1 followed by S1PR3 and S1PR2, while in cardiac fibroblasts S1PR3 is most abundant [109, 110]. Inside- out signalling by S1P due to increased TGFβ activates S1PR2 in cardiac fibroblasts leading to increased collagen synthesis [107]. S1P/S1PR2 signalling has been found to regulate myogenic responses in progressive HF with increased activation of p38 MAPK and ERK 1/2 and inhibition of myosin light chain Protein (MLCP) [111]. The activation of S1PR3 in endothelial progenitor cells activated the PI3K/Akt pathway promoting proliferation, while PI3K/Akt activation through S1PR1 reduced apoptosis [112]. S1PR2/3 knockout in cardiac myocytes leads to reduced ERK activation and abrogation of Akt activity, even in the presence of S1PR1, while Akt activation through S1PR2 and 3 protects against ischemia reperfusion[104, 110]. Additionally, S1PR1 knockout in myocytes has been associated with perinatal lethality in mice as a result of defects in myocardial development [113]. Inversely,

S1PR1 overexpression in mice fibroblasts leads to cardiac remodelling involving increased ang II, IL-6 and STAT3 activation [114]. Together with S1PRs, the enzyme SK1 is also an important factor in S1Ps activity [115, 116]. The SK1/ S1P/S1PR1 axis has been targeted the most and is known to have proliferative effects on vascular cells and cardiac fibroblasts [115, 117, 118]. In cardiac myocytes this axis contributes to proinflammatory signalling by stimulating β1AR [119]. In fact, S1PR1 behaved similarly to β1AR and could be regulated by G protein coupled receptor kinase 2 (GRK2)[105]. Their reduction by GRK2 activation led to progression toward remodelling and hypertrophy, implicating S1PR1s protective role in post ischemic conditions. When SK1 is overexpressed, Rho GTPase, and SMAD are activated, with increased ROS production resulting in cardiac fibrosis through S1PR3 (84). Additionally, the enzyme SK1 is also a target for TGFβ, which enhances Sph metabolism with the resultant increase of S1P in the cells [120-122]. Increased SK1 by TGFβ also leads to upregulation of TIMP1 in cardiac fibroblasts [120]. Increased S1P as observed in overexpressed SK1 results in detrimental effects on cardiac myocytes [123].. The inhibition of SK1 by PF-543 prevented cardiac dysfunction and reduced the expression of remodelling markers such as ANP, BNP, and β-MHC [119], and also downregulated S1PR1, STAT3, ERK 1/ 2, protein kinase C (PKC), and Rho associated protein kinase (ROCK) and increased Sph in ang II induced cardiac hypertrophy [124]. Figure 1.4 is a summative illustration of S1Ps activation of pathways in cardiac remodelling.

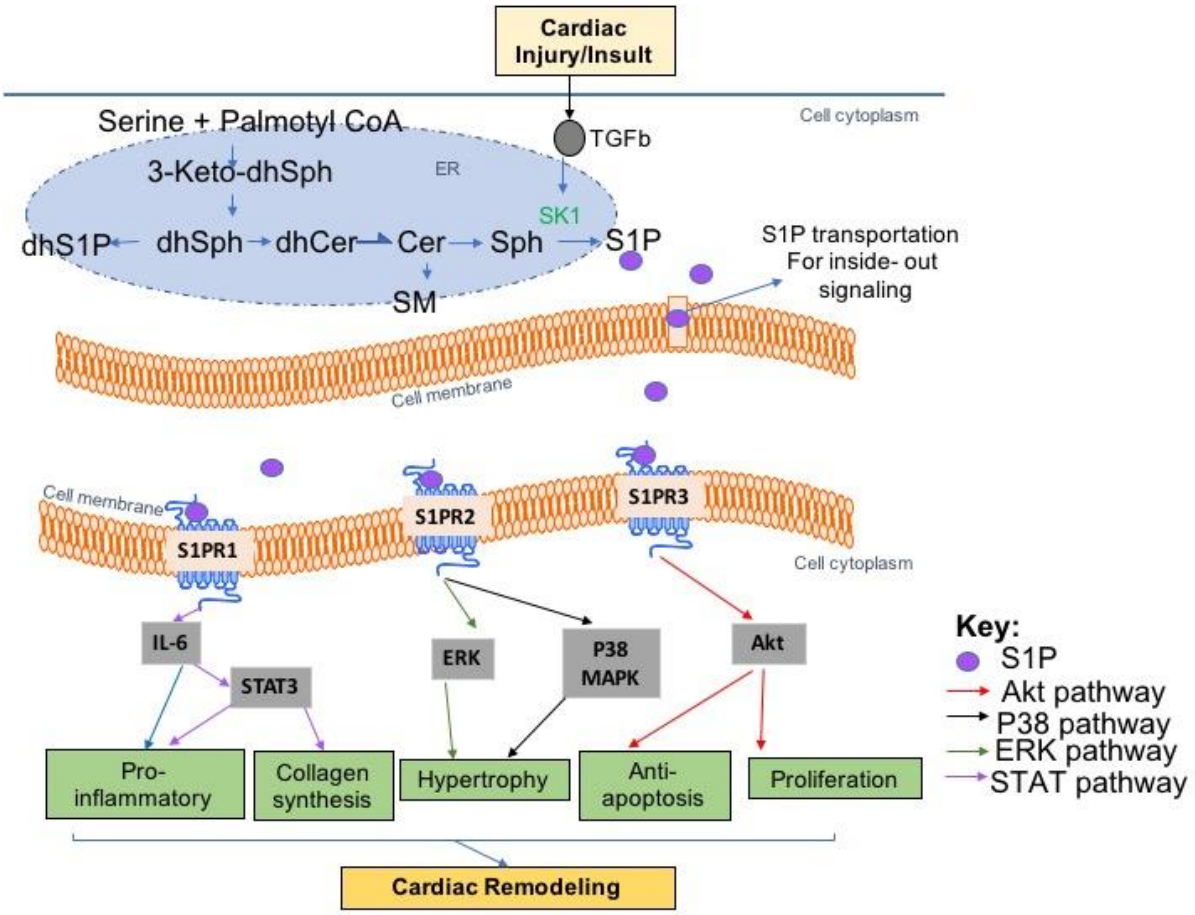

Figure 1.4 Simplified schematic of S1P in cardiac remodelling. Cardiac injury or insult increases expression and synthesis of cytokines and growth factors such as TGFβ. TGFβ mediates SK1 expression and activity leading to increase in increased S1P in in cardiac cells. S1P through its inside out signalling mechanism activates intracellular signalling pathways involving ERK, P38 MAPK, STAT3 and Akt through its receptors. These then increase factors that contribute to cardiac remodelling. This diagram has been summarized from the text in section 1.5.4.1 and illustrated with Microsoft Power point, 2016.

1.5.4.2 Cer in cardiac remodelling

Recent animal and human studies have shown that different Cer chain lengths have potential as biomarkers for heart diseases [125, 126]. Due to Cer being

synthesised through multiple pathways, and the different chain lengths having different effects, the evidence for Cer in cardiac remodelling is still being assembled. However, its main mechanism of effect is linked to its apoptotic effects as observed in cancer therapy. In this regard, Cer generated through the SM pathway has been linked to exacerbated IR injury (i.e., apoptosis) due to increased TNFα activation and ROS generation [127]. Cer is able to have this effect by increasing the formation of 'lipid rafts' that recruit and amplify signal transduction cascades and apoptosis signalling pathways [128]. Targeting certain enzymes in the *de novo* pathway has been shown to reduce Cer accumulation, accompanied by improved cardiac function. For example, inhibition of the upstream enzyme in the *de novo* pathway, SPT, has been shown to reduce the accumulation of certain Cer (C16, C24:1 and C24) species and reduced ventricular remodelling, and macrophage content [129, 130]. A recent gain of function study targeting acid ceramidase saw improved cardiac function after MI with low cell death rate, and low abundance of detrimental proinflammatory neutrophils [131]. Cer accumulation has also been shown to affect sarcomeric maintenance, contractile dysfunction, reduce Ca^{2+} influx, and caspase activation [132-134]. However, these latter findings are related to lipotoxic cardiomyopathy, thus, they are yet to be translated in terms of cardiac remodelling. Figure 1.5 gives a summative illustration of Cer's role in cardiac remodelling.

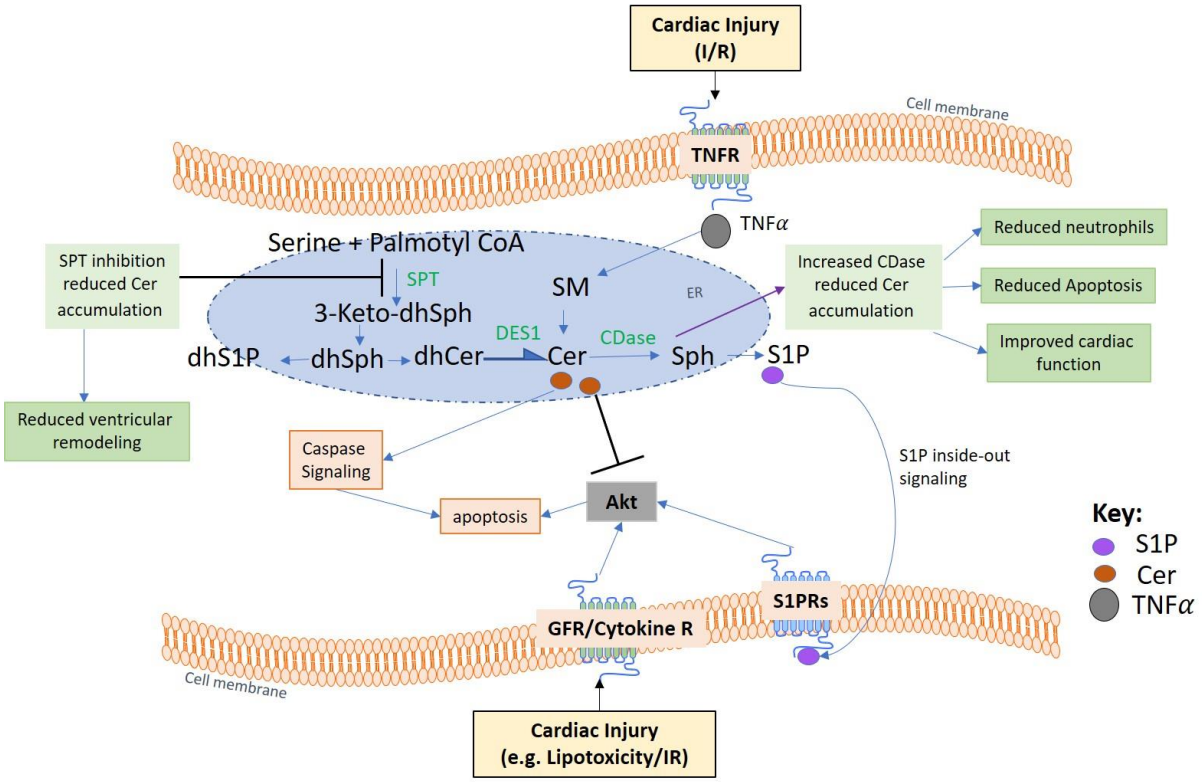

Figure 1.5 Cer in cardiac remodelling. Cardiac injury or insult increases activation of cytokines and growth factor (GF) receptors such as TNFα receptor (TNFR) which increases TNFα. TNFα increases formation of Cer through the SM pathway which inhibits Akt activation. Cer also increases caspase signalling which increases apoptosis. Reduced Akt activation reduces cardiac cell apoptosis through Akt activation. Cer inhibition by inhibiting SPT and increasing CDase lowers cell death, improves cardiac function and reduces ventricular remodelling. Blue arrows represent pathway activation, perpendicular bars represent inhibition and purple arrow represents increase. This diagram has been derived from the text in section 1.5.4.2 and illustrated with Microsoft Power point, 2016.

1.5.4.3 Dihydrosphingolipids in cardiac remodelling

Collectively, the evidence for dihydrosphingolipids (dhSph, dhCer and dhS1P) in disease is spatial (summarized in the published work in appendix 1.1), especially the mechanistic pathways through which they could contribute to disease.

The role of dhS1P in both physiology and pathophysiology is assumed to be similar to S1P. However, studies in neuronal cells, nerve cells, scleroderma fibroblasts and dermal fibroblasts, have shown that they can have differing effects on cell proliferation and differentiation [135-137]. DhS1P has been shown to be anti-fibrotic in dermal fibroblasts by acting as an antagonist of TGF-β/SMAD-ERK signalling through S1PR1 [135, 137]. DhS1P promoted the expression of MMP1 in these cells, by upregulating phosphatase and tensin homolog (PTEN). PTEN is a negative regulator of Akt and suppresses cardiac hypertrophy, while MMPs such as MMP1 are key regulators of the cardiac remodelling process [138-140]. Furthermore, there is evidence for its involvement in promoting plaque stability and increasing endothelial barrier function [141-143], which could reduce risk of coronary heart disease. DhS1P levels have also been shown to be altered in tissue and plasma of animal models and patients with MI [144-146]. However, its exact role and molecular mechanisms in the pathophysiology of cardiomyopathies remains obscure. The level of dhS1P in cell systems can be reduced by inhibiting the first rate limiting enzyme SPT and increased by inhibition of CerS, and DES1.

Inhibition of CerS leads to reduced *N*-acylation to dhCer and increases the level of dhSph which consequently increases dhS1P [147]. The accumulation of dhSph has been associated with fumonisin tocixity in animals and humans [148-150]. Fumonisin competitively inhibits CerS, because fumonisin and dhSph are structurally similar and differ only in the free amino group at C_1 [151]. Several

studies have reported elevated dhSph levels in the plasma of MI patients [146, 152] and urine of HF patients sun [153], whether this has any effect on cardiac remodelling has not been evaluated.

Targeting DES1, the enzyme at the centre of the conversion of dhCer to Cer, also leads to increased dhS1P and dhSph levels in neuronal cells, which was attributed to the inhibitor also targeting S1PL [154]. Studies specifically targeting DES1 in cardiomyopathies have been lacking. Most studies that have targeted DES1 gene ablation or inhibition in other cell types were focussed on reporting increases in dhCer. DhCer has been shown to have cellular effects that are opposite to Cer [155]. Including autophagy, inhibition of cell proliferation, oxidative stress, anti-apoptotic and anti-hypoxic effects [156-160]. In terms of overall disease processes there are a number of evidence available showing; 1) dhCers can be used as a tool in predicting type 2 diabetes, 2) dhCer could also play a role in reducing adipogenesis and increasing autophagy in adipocytes, 3) dhCer may be associated with hypoxia, 4) dhS1P and dhSph could be involved in plague stability, 5) dhS1P could have anti-tumour effects through suppression of T cell proliferation, 6) dhS1P binds to albumin, and 8) dhS1P regulation by SK1 could be stimulus, cell type and complex dependent, as I have summarized in my literature review [161]. The sparsity of studies related to dihydrosphingolipids in CVDs and cardiac remodelling shows that there is lack of basic data in terms of the molecular mechanisms and effects of these dihydrosphingolipids on cardiac pathophysiology. In this thesis I examine the effects of dhS1P, and dhSph on certain aspects of cardiac remodelling and explore the potential for targeting DES1 as a therapy for remodelling in ischemia induced MI.

1.7 Thesis aims and objectives

1.7.1 Aims

The two main questions my thesis is trying to answer are;

1. Do these dihydrosphingolipids such as dihydrosphingosine 1 phosphate and dihydrosphingosine, in the *de novo* synthesis pathway play a role in the cardiac fibrosis and hypertrophy?
2. Is there a therapeutic potential for targeting the gate keeper enzyme, DES1, in the *de novo* sphingolipid pathway for cardiac remodelling therapy?

1.7.2 Objectives

In chapter 1 I give an overview of the normal myocardium and how each of the components in the myocardium are involved in cardiac remodelling. I also provide an overview of sphingolipid synthesis, transport and function, and summarise what is known about their effects in terms of cardiac remodelling.

In chapter 2 I investigate the effect of exogenous dhS1P on cardiac cells in comparison to S1P and elucidate its effects on the JAK/STAT signalling pathway.

In chapter 3 I investigate the effect of exogenous dhS1P on cardiac cells in comparison to S1P and elucidate its effects on the PI3K/Akt signalling pathway.

In chapter 4 I investigate the effect of exogenous dhSph and Sph on various pathways in cardiac fibroblasts

In chapter 5 I examine the potential for DES1 inhibition in an animal model ischemia induced MI using the novel DES1 inhibitor compound, CIN038 also known as MIPS247.

Preface

The work incorporated in chapter two describes the effects of dhS1P on primary cardiac cells and its ability to activate the JAK/STAT signalling pathway to induce collagen synthesis and myocyte hypertrophy. This work has been published as follows;

Magaye R, Savira F, Hua Y, Xiong X, Huang L, Reid C, Flynn B, Liew D, Wang BW. Exogenous dihydrosphingosine 1 phosphatemediates collagen synthesis in cardiac fibroblasts through JAK/STAT signalling and TIMP1. Cellular Signalling. 2020;72:109620.

Published work is attached in Appendix 1.2.

Chapter 2: Exogenous dihydrosphingosine 1 phosphate mediates collagen synthesis in cardiac fibroblasts through JAK/STAT signalling and regulation of TIMP1

Authors

Ruth R. Magaye[1, 2], Feby Sevira[1, 2], Hua Yue[2, 3], Xin Xiong[2, 4], Li Huang[1, 2], Christopher Reid[2,5], Bernard Flynn[6], David Kaye[7], Danny Liew[2], Bing H. Wang[1, 2*]

1. Biomarker Discovery Laboratory, Baker Heart and Diabetes Institute, Melbourne, Australia
2. Monash Centre of Cardiovascular Research and Education in therapeutics, Melbourne, Australia
3. School of Traditional Chinese Medicine, Southern Medical University, Guangzhou, China
4. Shanghai Institute of Heart Failure, Research Centre for Translational Medicine, Shanghai East Hospital, Tongji University, School of Medicine, Shanghai 200120, P. R. China
5. School of Public Health School, Curtin University, Perth, Australia
6. Australian Translational Medicinal Chemistry Facility, Medicinal Chemistry, Monash Institute of Pharmaceutical Sciences, Monash University, Melbourne, Australia
7. Heart Failure Research Group, Baker Heart and Diabetes Institute, Melbourne, Australia. *Corresponding author: bing.wang@baker.edu.au and bing.wang@monash.edu.

2.1 Abstract

Cardiac fibrosis and myocyte hypertrophy are hallmarks of the cardiac remodelling process in cardiomyopathies such as HF. Dyslipidemia or dysregulation of lipids contributes to HF. The dysregulation of HDL could lead to altered levels of other lipid metabolites that are bound to it such as S1P. Recently, it has been shown that S1P and its analogue dhS1P are bound to HDL in plasma. The effects of dhS1P on cardiac cells have been obscure. The findings in this study show that extracellular dhS1P increases collagen synthesis in NCFs and causes hypertrophy of NCMs. The JAK/STAT signalling pathway was involved in the increased collagen synthesis by dhS1P, through sustained increase of TIMP1. Extracellular dhS1P increased phosphorylation levels of STAT1 and STAT3 proteins. It also caused an early increase in TGFβ1 gene expression, and sustained increase in TIMP1 gene. Inhibition of JAKs led to inhibition of TIMP1 and TGFβ gene and protein expression. Additionally, this study shows that dhS1P causes NCM hypertrophy through S1PR1 signalling which is opposite to that of its analogue, S1P. Taken together, the results show that dhS1P increases collagen synthesis in cardiac fibroblasts causing fibrosis through dhS1P-JAK/ STAT-TIMP1 signalling.

2.2 Introduction

DhS1P and S1P are both metabolic products of the *de novo* sphingolipid synthesis pathway present in all cells. dhS1P differs from S1P by its backbone structure which is composed of dhSph, in contrast to sphingosine for S1P. S1P's role as a lipid mediator is widely known. It modulates multiple signalling pathways involved in cellular events such as white cell migration, inflammation, proliferation, apoptosis and fibrosis by binding to S1P specific membrane bound G protein coupled receptors (GPCRs). Recently, several reviews have highlighted the effects of S1P and its receptors, S1PR1-3, in cardiac pathophysiology such as cardiac remodelling [115, 116, 162]. Unlike S1P, due to its low levels within the biological system, the role of dhS1P in disease processes such as cardiac remodelling is ill-defined. But it has been speculated to be similar to that of S1P, since it also activates the S1PRs. This is despite evidence in skin fibroblasts showing dhS1P to have opposite effects to that of S1P by downregulating fibrotic markers such as matrix metalloproteinase 1 (MMP1) and phosphorylated SMAD 3 [163]. Recently, others have shown that dhS1P is able to bind to HDL in plasma in a non-specific manner compared to S1P which requires apo lipoprotein M [79]. S1P activates several downstream signalling pathways in cardiac fibroblasts and myocytes including the TGFβ/ SMAD, and JAK/STAT pathways leading to cardiac remodelling [120] or cardio-myocyte protection [104, 119]. S1P activation of the JAK/STAT pathway is known to be receptor dependent as indicated by S1P/S1PR2/3 signalling in cardiac myocytes in I/R injury [104, 164]. The JAK/STAT signalling pathway confers short-term cardiac protection, however its prolonged activation is thought to worsen the disease state thus requiring a balance in the activation of this pathway. Cardiac remodelling is marked by increased deposition of the ECM such as collagen causing fibrosis and loss of myocyte

function due to myocyte hypertrophy. The phosphorylation of STAT1 and STAT3 have also been shown to mediate proliferation of cardiac fibroblasts and collagen synthesis induced by high glucose in the heart [165]. Therefore, the aim of this study is to determine whether exogenous dhS1P leads to cardiac cellular remodelling through activation of the JAK/STAT signalling pathway and explore differences in downstream signalling mechanisms between dhS1P and S1P.

2.3 Materials and methods

2.3.1 Primary neonatal rat cardiac cell isolation and culture

Primary NCMs and NCFs were extracted from 1-2 days old Sprague-Dawley rat pups using enzymatic collagenase digestion routinely used in the laboratory for in vitro assays [19]. Pups were purchased from the Monash Animal Research Platform (Clayton, Vic), and complied with the guidance from the National Health and Medical Research Council of Australia. The animals used for this study were approved by the Alfred Medical Research and Education Precinct Animal Ethics Committee (E/1653/2016/M). Briefly, the hearts were excised and washed in cold PBS to remove blood cells. 3-5 mm thick pieces of the ventricles were digested in a magnetic cell stir glass with 1:25 ratio of collagenase I (Sigma Aldrich, St. Louis, Missouri, USA) in 1 X Ads buffer solution for enzyme digestion. The tissue was digested at 10-minute intervals with a constant slow agitation. 2 ml of the cell digestion mixture was gently pipetted onto 15 mL falcon tubes containing the percoll gradient and centrifuged at 3300 rpm for 30 minutes, after washing with 1X Ads Buffer. The different cell layers (top layer; fibroblasts, bottom layer; myocytes) were then collected in separate tubes and washed with 1X Ads Buffer before resuspending in DMEM + 10% new born calf serum (NBCS) medium at

a pH of 7.2 for plating. While, NCMs suspended in 10% NBCS + DMEM were seeded straight into experimental plates coated with 0.2% gelatin. The NCFs were maintained in 10 % fetal bovine serum (FBS) + DMEM in T75 flasks until passage 2.

On the day of seeding, the NCFs were washed twice with 1 X PBS at a pH of 7.2. 2 mL of Trypsin EDTA, at a ratio of 1:4 diluted in 1X PBS, was added to T75 flasks containing NCFs after 2 minutes incubation or until all cells were floating (as observed under a microscope). 5mL DMEM + 10% FBS was added to the flask to stop trypsin activity. The mixture was then transferred into 50 mL Falcon tubes for washing, after the flasks were gently pipetted to dislodge the cells and aggregate them. The cells were then seeded as desired and maintained in DMEM + 10% FBS for the first 24 h. This method is routinely used in the laboratory for in vitro assays [166].

2.3.2 Measurement of collagen synthesis in NCFs

Induction of collagen synthesis by S1P, dhS1P and the S1PR1 agonist, SEW2871, in NCFs was determined using the ^{3}H-proline incorporation assay [167]. Briefly, after determining optimum dose of dhS1P and S1P for collagen synthesis, NCFs at 50 000 cells/ well were pre-treated with the JAKs inhibitor, also known as Pyridone 6 (P6, 0.01-1.0 μM- Calbiochem, Darmstadt, Germany), and a specific S1PR1 antagonist (W146, 0.1- 5.0 μM- Tocris Bioscience, Bristol, UK) for 2 h. This was performed 48 h after serum starvation in DMEM with 0.5 % BSA. The cells were then stimulated with 3 μM dhS1P, 1 μM S1P, and 10 μM SEW2871 (Monash Institute of Pharmaceutical Sciences, Melbourne, Australia) for 48 h in DMEM F12 medium supplemented with 1% vitamin C and 0.5% bovine serum

albumin (BSA). 1 μCi ^{3}H proline was added to the cell culture media and included ad hoc with S1P, dhS1P and SEW2871 (the doses used were pre-determined as shown in Figure 2.1A). After precipitation with 10% trichloroacetic acid (TCA) for 30 minutes, the cell pellets were detached in 1 M sodium hydroxide (NaOH), and solubilized in 1:10 ratio of 1 M hydrochloric acid (HCl) with scintillation fluid. The levels of ^{3}H-proline incorporation were determined on a 300SL beta counter at counts per minute (cpm). The tool compounds, sphingolipids and inhibitors, were reconstituted in dimethyl sulfoxide (DMSO), while Ang II was reconstituted with treatment media.

2.3.3 Measurement of NCM hypertrophy

To determine whether exogenous dhS1P and S1P induced NCM hypertrophy, ^{3}H-leucine incorporation which measures the increase in protein synthesis in myocytes (approximate measure of hypertrophy) was used as described previously [166]. Briefly, NCM media was changed 24 h after isolation to special media containing DMEM supplemented with essential and non-essential amino acids, insulin, apolipoprotein with potassium chloride to prevent contact-induced spontaneous contraction of the plated NCMs. After 48 h the media was changed and the NCMs were pre-treated for 2 h, at similar doses of P6 and W146 as used in NCF and treated with S1P (1 μM) and dhS1P (3 μM) at predetermined time points of 60 h and 48 h, respectively. The optimum dose and times point for stimulation were validated prior to the experiments as shown in Figure 2.10A.

2.3.4 Measurement of cell viability in NCFs and NCMs

Cell viability was measured using the Alamar blue assay (Invitrogen- Thermo Fischer Scientific, Carlsbad, CA, United States). Cells were seeded in 96-well plates at a density of 1.5 x 10^4 and 1 x 10^5 cells per well for NCFs and NCM, respectively. After 48 h or 60 h treatment as described for collagen synthesis and myocyte hypertrophy assays, respectively. The reduction of resazurin by viable cells to resorufin was measured after further incubation with 1:10 ratio of Alamar reagent to media for 4-6 h, and the absorbance was read at 570 and 600 nm wavelength on a NanoStar spectrometer (BMG Labtech, Ortenberg, BW, Germany).

2.3.5 Western blot analysis of protein expression

The expression of specific proteins related to the JAK/STAT signalling pathway and cardiac remodelling were analysed using Western Blot assay. Both NCFs (3 x 10^5 cells/ Flask) in T25 flasks and NCMs (1 x 10^6 cells/ Well) in 6 well plates were pre-treated for 2 h with P6 (0.3 & 1 μM), and W146 (3 & 5 μM) and treated with 3 μM dhS1P, 1 μM S1P, and 10 μM SEW2871 (*NCF only*), for 15 to 30 minutes for phosphorylated proteins and 24 h for total proteins. These were performed 48 h after serum starvation as described in section 3.3.2 for NCFs and section 3.3.3 for NCMs. 10 μg/μL cell lysates were separated on 7.5, 10, or 12% gels by SDS-polyacrylamide gel electrophoresis (SDS-PAGE), and transferred onto nitrocellulose blotting membranes (GE HealthCare, Chicago, IL, United States). The blots were probed for phosphorylated STAT1, STAT3, c-JUN, and SMAD2 from Cell Signalling Technologies (CST: 8826S, 9145L, 2361S, and 3108L) after blocking with 5% bovine serum albumin (BSA). They were also probed for TGFβ (CST: 3709S, 3711S), collagen I (coll1) (Abcam, Cambridge, UK: Ab209539),

TIMP1 (Novus Biologica, Centennial, CO, United States: NBP1- 96554), α-smooth muscle actin, α-SMA (Abcam: Ab124964) after blocking with 5% Milk in Tris-buffered saline with 0.1% Tween 20 (TBS-T). Bands were detected using Super Signal West Pico Chemiluminescence substrate (Thermo Fisher Scientific, Rockford, IL, United States) on BioRad Chemidoc instrument and analysed using Image lab software (BioRad Laboratories, Hercules, CA, United States). Proteins were normalized to Glyceraldehyde –phosphate dehydrogenase (GAPDH) (CST: 2118L) or β-Actin (CST: 4970).

2.3.6 PCR analysis of hypertrophic and fibrotic gene markers

NCFs (5 x 10^5/ well) and NCMs (1 x 10^6 / well) seeded in 6 well plates were pre-treated with the inhibitors as mentioned above for 2 h, after 48 h serum starvation. The NCFs were further incubated with SEW2871 (10 μM) for 18 h, and dhS1P (3μM) and S1P (1 μM) for 6 h (stimulation time points based on TGFβ gene expression as shown in Figure 2.4A). NCMs were incubated for 18 h with each of the lipids. Total RNA was extracted and isolated using MagMAX-96 Total RNA Isolation for Microarray Kit according to the manufacturer's instructions (Thermo Fisher Scientific, Rockford, IL, United States). 5 or 10 ng/μL of RNA was reverse transcribed into cDNA using Multi-Scribe (Applied Bio systems, Foster City, CA, USA). The expression levels of the fibrotic markers; TGFβ, CTGF, TIMP1, collagen 1a1 (Coll1a1), collagen 3a1 (Coll3aI), the S1P receptors (1-3), and the enzyme SK1 were quantified by real time polymerase chain reaction (PCR) on the Quan-Studio 12K Flex Real Time PCR System (Applied Bio systems) with SYBR Green as detector (Applied Bio systems). The gene expression levels of pro-hypertrophic markers such as ANP, BNP, βMHC, and α-SKA were also

quantified. Refer to Appendix 2.1 for full sequence of primers. 18s mRNA was used as the endogenous controls.

2.3.7 Immunohistochemistry

Immunohistochemical analysis was carried out on passage 1 NCFs plated in glass bottom 6 well plates (1 x 10^5 cells/well) and treated with SEW2871 (10 μM), S1P (1 μM), & dhS1P (3 μM) and TGFβ (10 μM) for 48 h. Abcam's online immunostaining protocol was followed with minor modifications. Briefly, the cells were washed three times with PBS, before fixing for 5 minutes with ice cold methanol. The fixed cells were then washed with cold PBS before blocking with 1% BSA in TBST. After blocking the cells were incubated with α-SMA (Sigma) at 1:500; and Vimentin (Abcam, Cambridge, MA, USA) at 1:1000. Actin filaments were labelled with Alexa Fluor tagged secondary anti-bodies at 1: 1000. The nuclei were labelled with Hoerscht at 1:1000 (Sigma). Images were captured with the Nikon TI Eclipse Widefield microscope (Nikon, Minato, TKY, Japan), and analysed using NIS elements viewer software (Nikon).

2.3.8 Statistical analysis

All cell culture experiments were performed in triplicates, with at least three repeated experiments for the hypertrophy and collagen synthesis assays and two repeated experiments for western blots and PCR. The results are presented as the percentage of unstimulated controls (mean ± SEM). For western blot analyses, ratio of phosphorylated over GAPDH levels were analysed. For real-time PCR, gene expression levels in NCF and NCM were normalized with 18s (housekeeping

gene). One-way ANOVA with Bonferroni's multiple comparison post hoc tests was used for statistical analyses for comparison between multiple groups and unpaired *t*-test was used for comparison between two groups. A statistically significant result was determined with a two-tailed *p*-value of less than 0.05. GraphPad Prism Version 8 (GraphPad Software Inc., San Diego, CA, United States) were used to perform all the statistical analyses.

2.4 Results

2.4.1 DhS1P induced collagen synthesis in NCFs

The sphingolipid, S1P, is now known to cause cardiac fibrosis and myocyte hypertrophy [104, 115, 116]. This study, investigated whether extracellular dhS1P, the analogue of S1P, was able to induce collagen synthesis at similar doses to that of S1P and the S1PR1 agonist- SEW2871 at 48 h of stimulation using tritiated (^{3}H) proline incorporation assay. The results in Figure 2.1A show that dhS1P at 3 μM significantly ($p < 0.01$) induced collagen synthesis in NCFs. However, at the highest dose of 10 μM, dhS1P caused significant cell death as corroborated by the results from the Alamar cell viability assay ($p < 0.01$, Figure 2.1D). Reductions in cell viability could have non-specific inhibitory effects on collagen synthesis therefore, this dose was excluded in the study. It should be noted that the doses chosen for testing did not affect the cell viability. Figure 2.1A shows that SEW2871 caused a dose dependent increase in collagen synthesis, while S1P induced collagen synthesis was significant at 1 μM ($p < 0.01$) and 3 μM ($p < 0.005$), showing similar non-linear effects as dhS1P. These increases in collagen synthesis were comparable to that induced by 100 nM Ang II which was used as a positive control, $p < 0.01$-0.005 vs. control.

2.4.2 DhS1P, S1P & SEW2871 induce collagen synthesis by activating JAKs

Since dhS1P, S1P and SEW2871 were able to induce collagen synthesis in NCFs, the relationship between their activation of the JAK/STAT signalling pathway and collagen synthesis was examined. The JAKs (JAK1, JAK2, JAK3, TYK1, and TYK2) are a group of cytoplasmic tyrosine kinases that transduce signals from membrane receptors to the STAT proteins which can translocate to the nucleus and act as transcription factors. The introduction of the JAKs inhibitor, P6 [168], had similar potency at doses over 0.1 μM on collagen synthesis by 3 μM dhS1P ($p < 0.05$, Figure 2.1B). Comparatively, P6 was also able to significantly inhibit 1 μM S1P induced collagen synthesis in NCFs with no observable trend of dose-dependency (Figure 2.1B). These differences may be due to S1P and dhS1P activating different types of S1P receptors leading to activation of different pathways such as the mitogen activated protein kinase (MAPK/ ERK) pathway, which has been shown to have increased phosphorylation in mice overexpressing S1PR1 [114]. In cells treated with 10 μM of the S1PR1 agonist, SEW2871, there was a dose response effect when P6 was introduced, although not with a big gradient difference (Figure 2.1B).

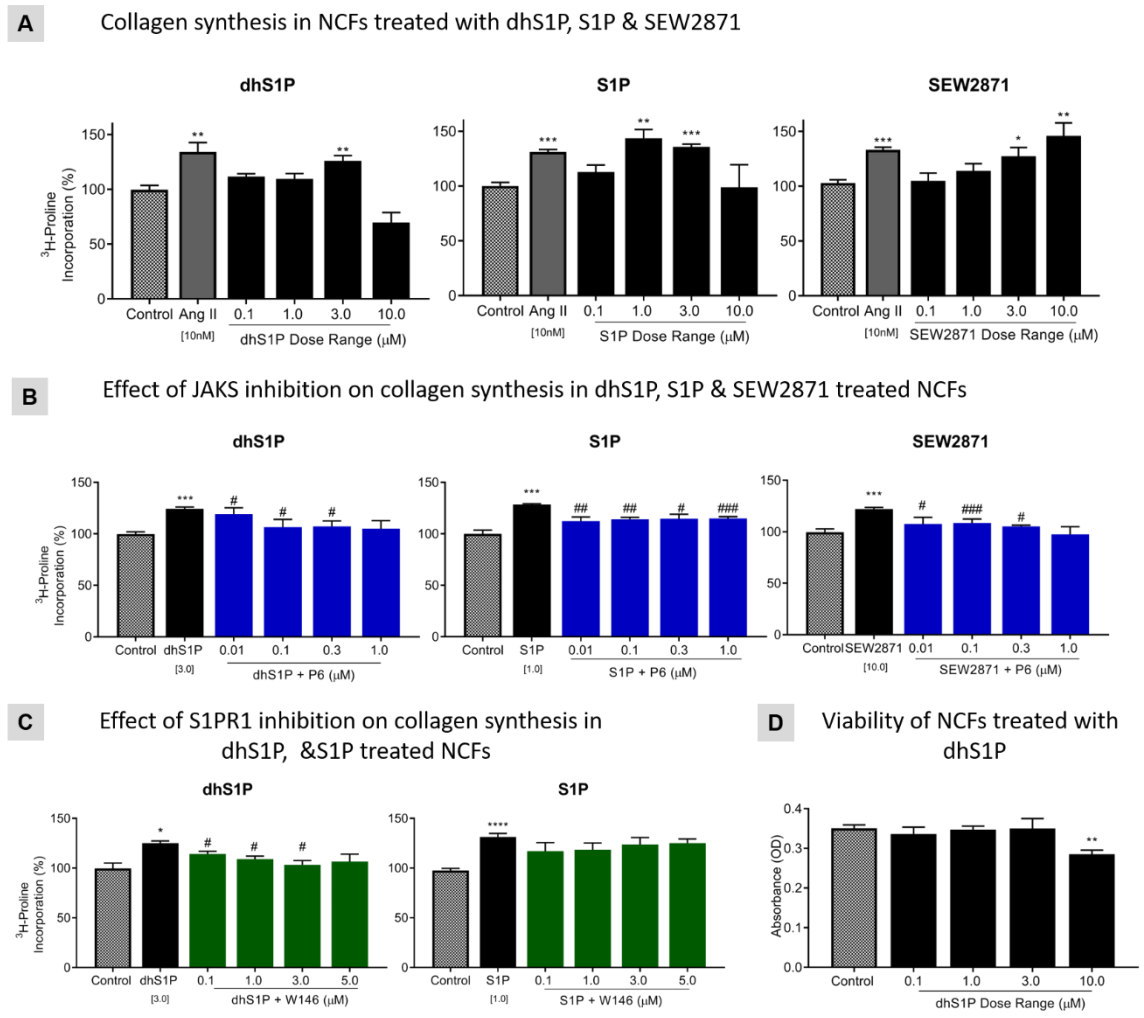

Figure 2.1. DhS1P/ S1P/ SEW2871 induced collagen synthesis in NCFs.

(A) Significant increase in collagen synthesis were observed for dhS1P at 3 μM, S1P at 1 μM & 3 μM, and SEW2871 at 3 μM & 10 μM vs. control. (B) Inhibition of JAKs significantly reduced collagen synthesis in NCF induced by dhS1P, S1P, & SEW2871 vs. Ang II. (C) Inhibition of S1PR1 significantly reduced collagen synthesis stimulated by dhS1P, but the effects on S1P stimulated collagen synthesis were not statistically significant. (D) DhS1P (10 μM) reduced the viability of NCFs at 48 h of treatment. $^{###}p < 0.005$, $^{##}p < 0.01$, $^{#}p < 0.05$ vs. dhS1P/S1P/SEW2871, and $^{**}p < 0.01$, $^{*}p < 0.05$ vs. Control. $^{***}p < 0.00$, $^{**}p < 0.01$ vs. Control. Values

presented as mean ± standard error of mean (SEM) of at least three independent experiments with 3 replicates in each.

2.4.3 DhS1P/S1PR1 signalling increased collagen synthesis

Targeting S1P/S1PR1 signalling has shown potential in cancer therapy [169], but evidence for its role in cardiac fibrosis is limited. Therefore, the specific S1PR1 antagonist, W146, was used to determine if S1PR1 was essential for collagen synthesis by dhS1P and S1P. The results in Figure 2.1C show that W146 had a dose dependent effect on the inhibition of collagen synthesis increased by dhS1P ($p < 0.05$). However, for S1P, W146 was not able to significantly inhibit collagen synthesis, despite showing reduction in collagen synthesis as determined by 3H-proline incorporation at all concentrations tested. This indicates that S1P may activate other targets, compensating for inhibition of S1PR1, possibly through S1PR2/3 activation, as shown by Quint *et.al* [170].

2.4.4 DhS1P, S1P & SEW2871 activated fibroblast to myofibroblast differentiation

The phenotypic differentiation of fibroblasts to myofibroblasts is associated with cardiac remodelling. Myofibroblasts have an increased expression of the α-SMA with reduced expression of vimentin [171], one of the intermediate filaments found in many non-muscle cells. Fibrotic factors such as TGFβ are known to activate the differentiation process leading to increased production of the ECM [57]. Immunofluorescence staining methods were used to determine if SEW2871, dhS1P and S1P and TGFβ (used as positive control) led to increased cytosolic

expression of α-SMA in NCFs. Figure 2.2A shows that dhS1P, S1P and SEW2871 increased cytosolic α-SMA, but was less intense when compared to TGFβ. This effect is comparative to those shown by Western Blot protein quantification of α-SMA (Figure 2.2B), showed that TGFβ ($p < 0.05$) and SEW2871 ($p < 0.01$) caused significant increase in α-SMA protein levels vs. control. TGFβ also seemed to increase the intensity of vimentin in NCFs.

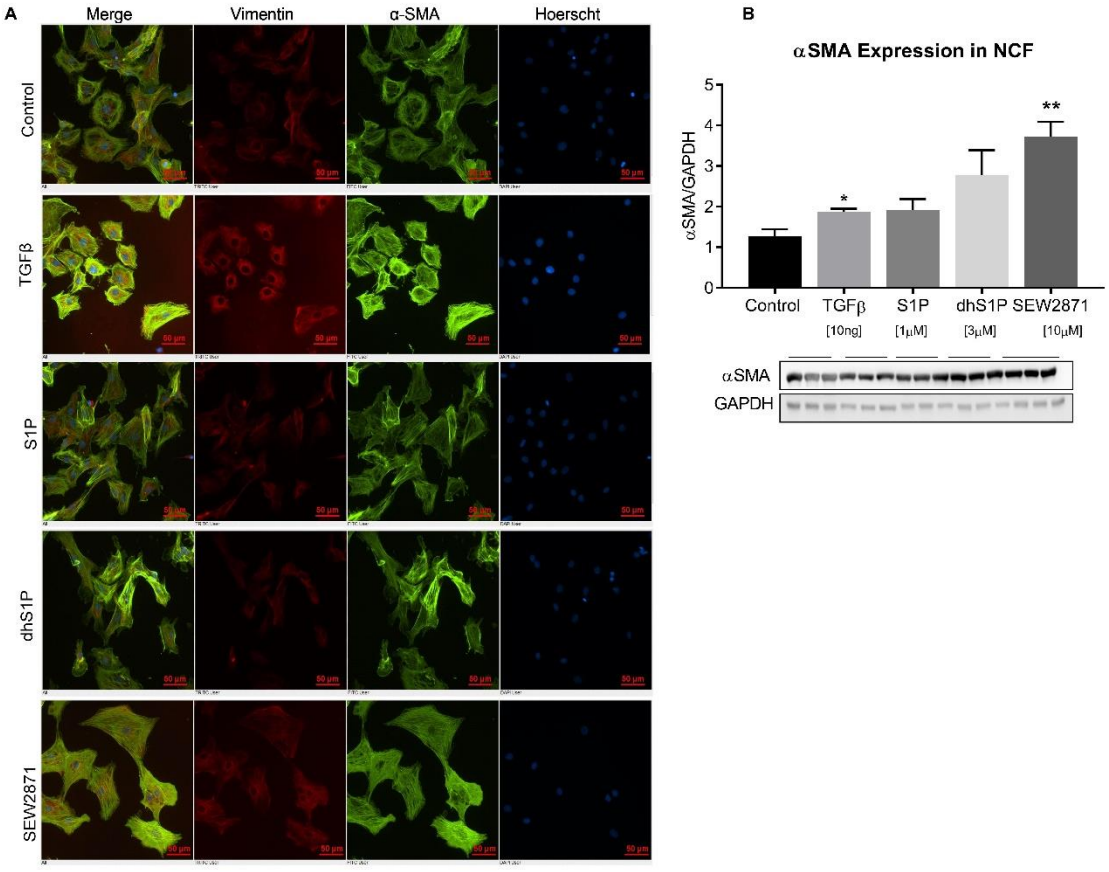

Figure 2.2. SEW2871, S1P and dhS1P activated trans-differentiation of fibroblast to myofibroblast. (A) Immunofluorescent staining of α-SMA (green), vimentin (red) and Nuclei (Blue) by Hoerscht. 10 μM TGFβ, 1 μM S1P, 3 μM dhS1P & 10 μM SEW2871 have increased α-SMA expression. Original magnification X200. (B) Western blot α-SMA protein expression in NCFs compared to the different treatments at 48 h incubation, *p <0.05 & **p < 0.01

vs. control. Values presented as mean ± standard error of mean (SEM) of at least three independent experiments with 3 replicates in each.

2.4.5 Increased dhS1P phosphorylation of STAT1 in NCF was reduced when JAKs were inhibited

The ability of dhS1P and S1P to activate STAT1 and STAT3 proteins were also evaluated using Western Blot in NCFs. Of the seven known mammalian STAT proteins, the activation and translocation of STAT1 and 3 to the nucleus leads to the transcription of genes including those that regulate inflammation, cell proliferation and fibrosis [172, 173]. Both dhS1P and S1P were able to significantly increase pSTAT1 levels ($p < 0.01$ & $p < 0.05$ vs. control) at 15 minutes of stimulation, and there was a strong trend toward a reduction when inhibited by P6 (1 μM) (Figure 2.3A-B). Pre-treatment of NCFs with P6 completely abolished the expression of phosphorylated STAT3 in both dhS1P and S1P treated cells. DhS1P did not increase phosphorylation of STAT3 at the time point tested (Figure 2.3A). This may imply that STAT3 phosphorylation is delayed as seen in Figure 2.3C, which was stimulated for 20 mins. STAT3 phosphorylation at tyrosine 705 leads to its dimerization forming homodimers or heterodimers with other STATs such as STAT1. Both phosphorylated STAT3α (86 kDa-upper band) and STAT3β (79 kDa-lower band) were expressed in primary rat NCFs (see representative blots in Figure 2.3). STAT3 has been shown to affect collagen synthesis in the heart more than STAT1 [174].

A Effect of P6 on STATs protein expression in dhS1P treated NCFs

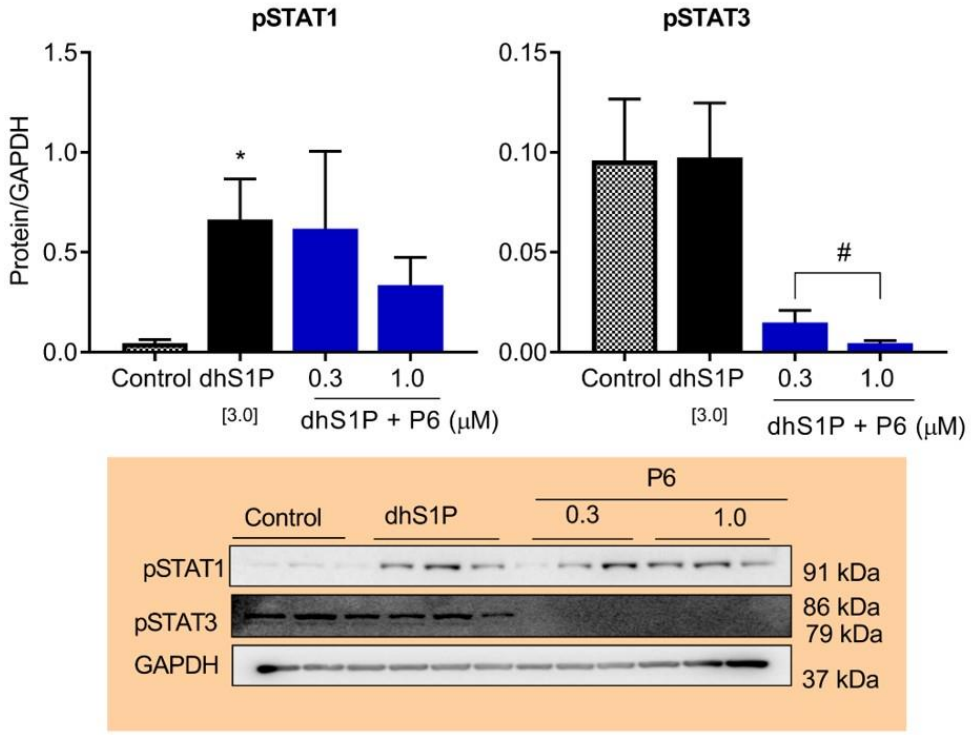

B Effect of P6 on STATs protein expression in S1P treated NCFs

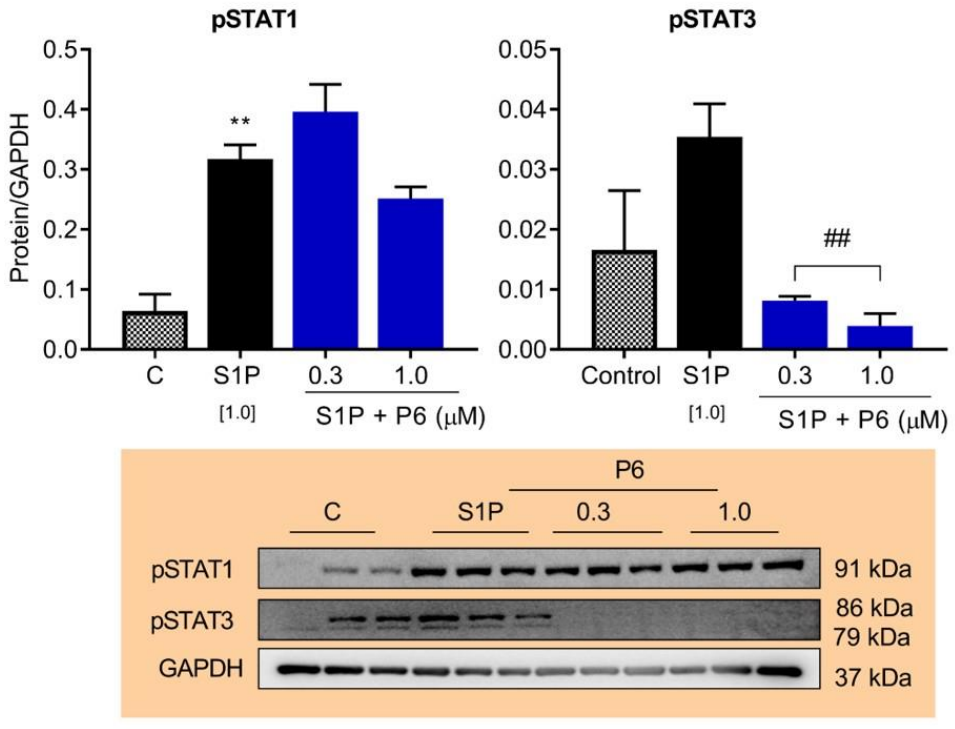

Figure 2.3. Effect of DhS1P and S1P on phosphorylation of STAT1/3. (A) P6 reduced dhS1P (3 μM) induced phosphorylation of STAT1, and completely abrogated STAT3. (B) S1P (1 μM) induced phosphorylation of STAT1 and not STAT3. Treatment with P6 abrogated STAT3 phosphorylation. $^{\#\#}p < 0.01$, $^{\#}p < 0.05$ vs. dhS1P/S1P, and $^{**}p < 0.01$, $^{*}p < 0.05$ vs. Control. Values are presented as ± SEM of at least 3 replicates with two independent repeats.

2.4.6 Differential regulation of STAT1/3 by dhS1P/S1PR1 and S1P/S1PR1 axis in NCF

Since the JAKs are associated with GPCRs such as the S1PRs, the activation of STAT1 and 3 through S1PR1 signalling by both dhS1P and S1P was investigated. Treatment of NCF with W146 led to reduced phosphorylation of STAT1 stimulated by S1P at the highest dose of 5 μM ($p < 0.01$, Figure 2.4B). On the other hand, S1PR1 inhibition by W146 in dhS1P stimulated NCFs seemed to have synergistic increase in STAT1 phosphorylation level at 5μM (Figure 2.4A) but was statistically insignificant.

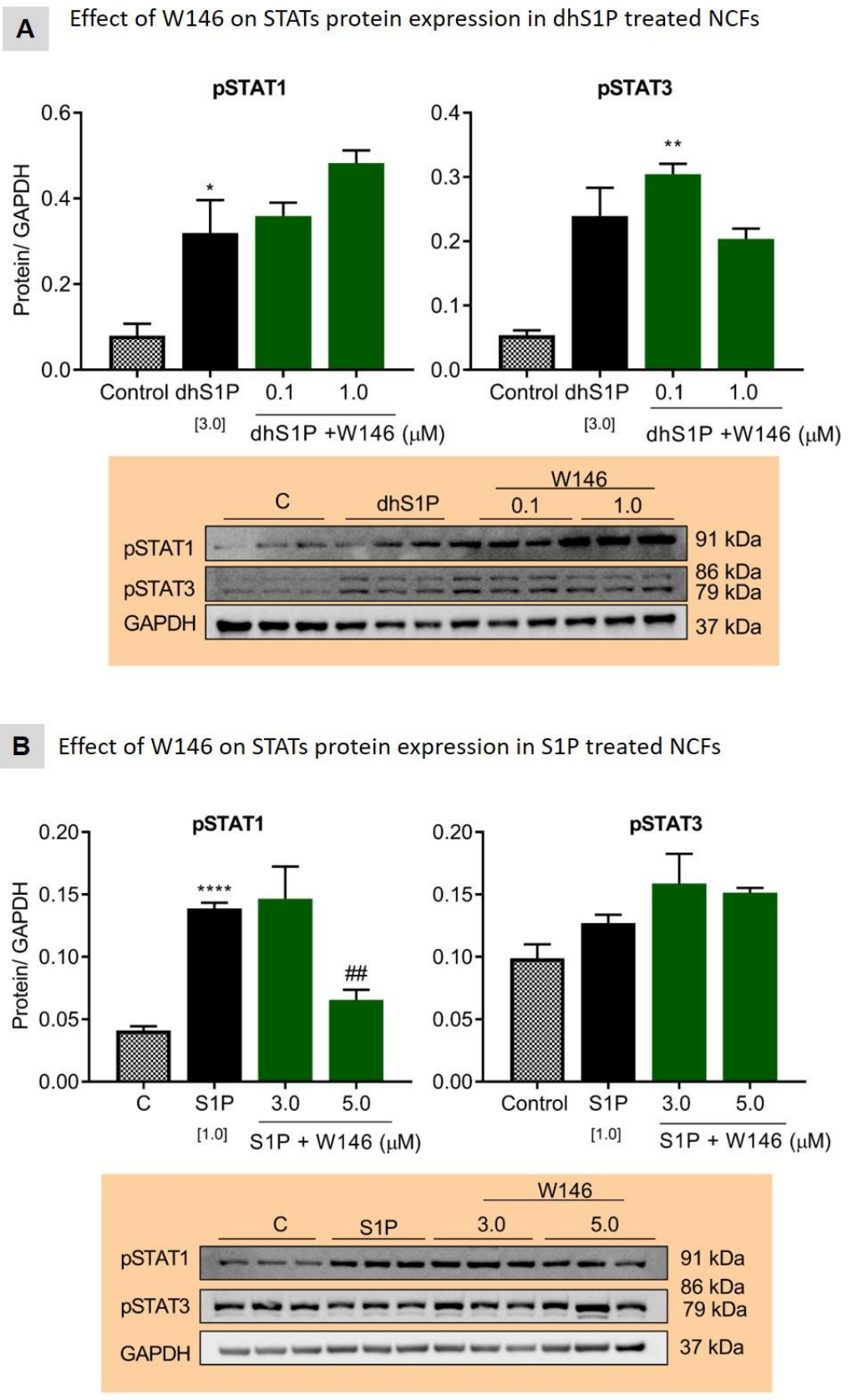

Figure 2.4. Effect of DhS1P/S1PR1 and S1P/S1PR1 axis on phosphorylation of STAT1/3. (A) Inhibition of S1PR1 had a synergistic effect on dhS1P induced

STAT1 phosphorylation. (B) Inhibition of S1PR1 reduced S1P induced STAT1 phosphorylation. $^{\#\#}p < 0.01$ vs. dhS1P/S1P, and $^{****}p < 0.0001$, $^{*}p < 0.05$ vs. Control. Values are presented as ± SEM of at least 3 replicates with two independent repeats.

2.4.7 S1P and dhS1P increased TGFβ, TIMP1 and SK1 gene expression

We then investigated whether S1P and dhS1P caused an increase in mRNA expression of known fibrotic markers such as TGFβ. First, a time course analysis was performed. The treatment of NCFs with extracellular S1P (Figure 2.5G) or dhS1P (Figure 2.5A) led to a significant early increase (at 6 h of stimulation) in TGFβ1 gene expression ($p = 0.0001$ and $p < 0.0001$, respectively).

Additionally, the mRNA expression of TIMP1 and SK1 at this time point were greatly enhanced by both S1P ($p < 0.0001$, Figure 2.5G-H) and dhS1P ($p < 0.0001$, Figure 2.5B-C). SK1 has been shown to mediate TIMP1 increase [120]. There was sustained significant increase in TIMP1 mRNA at all the time points investigated in both dhS1P (Figure 2.5B) and S1P (Figure 2.5GH) stimulated cells, however there was no changes in SK1 or TGFβ1 mRNA expression at other time points tested. Both S1P and dhS1P had no effect on dihydroceramide desaturase 1 gene (DEGS1) in the sphingolipid pathway (Figure 2.5F and L). Others have shown that 48 h of exposure of C57BL/6 mice cardiac fibroblasts to TGFβ led to increased SK1 and Coll1a1 mRNA by 0.1 μM S1P [107]. It should be noted that, at the time points of 6, 18 & 24 h, Coll1a1 (Figure 2.5D & J) and Coll3a1 (Figure 2.5E & I) were not increased by extracellular S1P or dhS1P. Instead, at 24 h there

was significant reduction in Coll1a1 ($p < 0.01$) mRNA in S1P stimulated cells (Figure 2.5I) and Coll3a1 ($p < 0.05$) in dhS1P stimulated cells (Figure 2.5D), which may have been a result of feedback inhibition prompted by the enhanced effect on TIMP1 gene expression. In addition, collagen mRNA expression has a lag phase of 6 h with maximal increases seen at 3 days of exposure [175], which could explain the lack of response at the early time points. These results may indicate that the pro-fibrotic effects of S1P and dhS1P are not directly due to activation of ECM synthesis pathways but rather due to activation of ECM degradation inhibition pathways such as TIMP1.

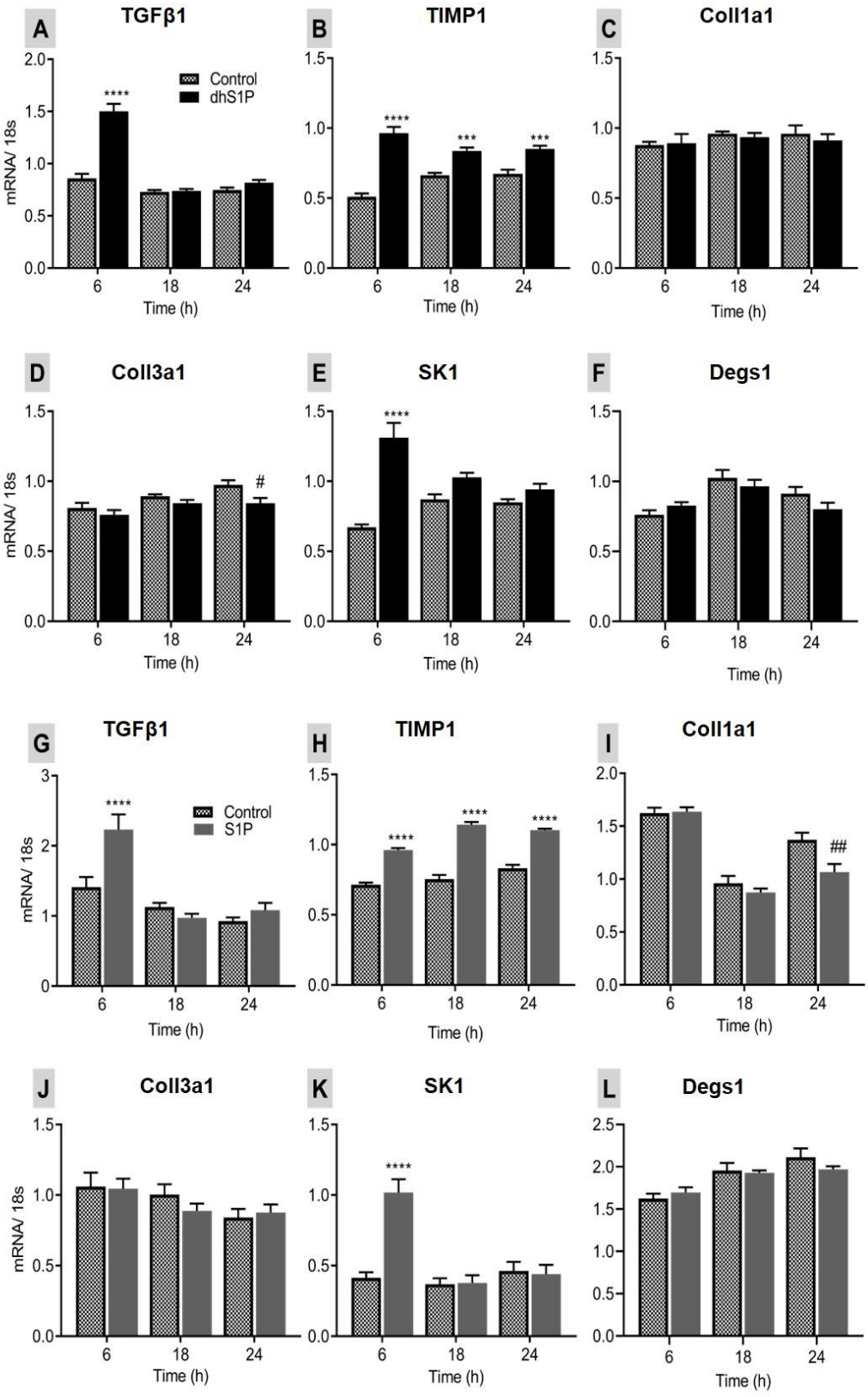

Figure 2.5. Time course analysis of extracellular S1P and dhS1P induced RNA expression in NCFs. (A) DhS1P (3μM) significantly increased the

expression of TGFβ at 6 h, (B) TIMP1 was increased throughout all time points, (C) had no effect on Coll1a1, (D) significantly reduced Coll3a1 at 24 h, (E) greatly increased SK1 at 6 h and (F) had no effect on DEGS1 mRNA levels. (G) S1P greatly increased TGFβ at 6 h, (H) increased TIMP1 at all-time points, (I) significantly reduced Coll1a1 at 24 h, (J) had no effect on Coll3a1, (K) significantly increased SK1 at 6 h, and (I) had no effect on DEGS1. $^{****}p < 0.0001$ and $^{\#\#}p < 0.01$, $^{\#}p < 0.05$ vs. control. Values are presented as ± SEM of at least 3 replicates with two independent repeats.

2.4.8 Inhibition of JAKs attenuated pro-fibrosis gene expression

Next, the role of the JAK/STAT pathway in the early increase in regulation of pro-fibrotic gene expression by dhS1P and S1P was explored. As shown in Figure 2.56A & C, P6 significantly inhibited the increase in TGFβ1, TIMP1, and SK1 genes expression at 6 h stimulation by both dhS1P ($p < 0.01$, $p < 0.005$, and $p < 0.005$) and S1P ($p < 0.05$, $p < 0.01$, and $p < 0.05$). These results show that the JAKs are involved in downstream transmission of cellular signals activated by extracellular dhS1P and S1P that leads to increase in TGFβ1, TIMP1, & SK1 genes. S1P signalling is known to increase TGFβ1 genes expression which subsequently increases SK1 gene expression [107, 120]. The results show that dhS1P may also have similar effects. Additionally, in NCFs pre-treated with P6, DEGS1 gene expression was significantly increased at the lower dose (0.3 μM), and shifted toward a reduction at the higher dose in dhS1P treated NCFs.

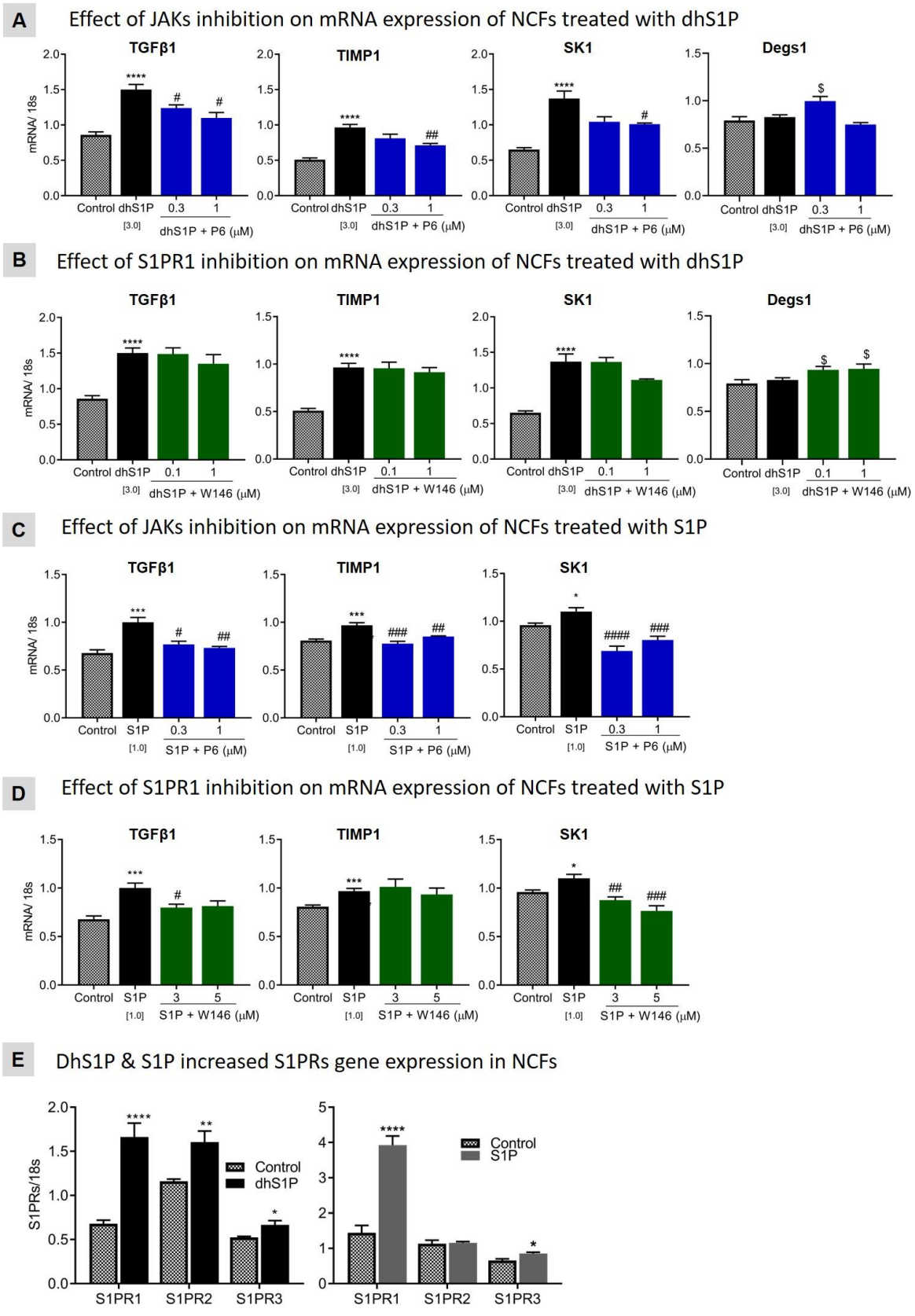

Figure 2.6. Inhibition of JAKs leads to reduction in genes increased by S1P or dhS1P/S1PRs signalling. (A) TGFβ1, TIMP1 & SK1 genes were dose

dependently reduced when JAKs was inhibited in dhS1P treated NCFs. Inhibition of JAKs at the lower dose (0.3 μM) raised DEGS1 gene expression in the presence of dhS1P. (B) Inhibiting S1PR1 in dhS1P treated NCFs had less effect on the raised TGFβ1, TIMP1, & SK1; DEGS1 was significantly increased at both doses. (C) In S1P treated NCFs TGFβ1, TIMP1 & SK1 genes were dose dependently reduced when JAKs was inhibited. (D) TGFβ1 & SK1 were significantly inhibited when S1PR1 was inhibited in S1P treated NCFs. (E) DhS1P significantly increased S1PR1-3 at 6 h, while S1P increased S1PR1. $^{\#}p < 0.05$, $^{\#\#}p < 0.01$, $^{\#\#\#}p < 0.005$ & $^{\#\#\#\#}p < 0.001$ and $^{\$}p < 0.05$ vs. dhS1P/ S1P & 3, $^{*}p < 0.05$, $^{***}p < 0.005$ & $^{****}p < 0.001$ vs. control. Values are presented as ± SEM of at least 3 replicates with two independent repeats.

2.4.9 DhS1P and S1P increased TGFβ1, and SK1 mRNA through S1PR1 activation

Since, the S1PR1 agonist led to increase in collagen synthesis phenotypically, the inhibition of S1PR1 by W146 could inhibit the increase in TGFβ, SK1 and TIMP1 mRNA expression was investigated. The results show that both dhS1P and S1P caused a significant increase in S1PR1 mRNA at 6 h (Figure 2.6E). Surprisingly, inhibition of S1PR1, did not inhibit TIMP1 mRNA expression in NCFs, for both dhS1P and S1P (Figure 2.6B & D), implying that the increase in TIMP1 by S1P and dhS1P is not dependent on S1PR1 activation alone at the time point tested. This may be due to S1P and dhS1P increasing TIMP1 expression through a signalling cascade that involves the other S1P receptors at this time point, even though S1P increased S1PR1 mRNA was greater than dhS1P, Figure 2.5E.

Inhibition of S1PR1 significantly increased DEGS1 expression at both doses (0.1 and 1.0 μM). Additionally, Figure 2.6E also shows that S1P significantly increased S1PR3 ($p < 0.05$) expression while, dhS1P caused significant increase in mRNA expression of both S1PR2 ($p < 0.01$) and S1PR3 ($p < 0.05$) at 6 h. Others have implicated S1PR2 as the target through which S1P increased collagen synthesis at 48 h [107]. The inhibition of S1PR1 by W146 did reduce SK1 mRNA expression induced by dhS1P (Figure 2.6B) at the higher dose, and produced a significant dose dependent reduction for S1P induced SK1 ($p < 0.005$, Figure 2.6D) and TGFβ ($p < 0.05$) mRNA.

2.4.10 JAKs are involved in specific S1PR1 agonist mediated increase in fibrotic gene markers

Next, the ability of SEW2871, the S1PR1 specific agonist, to increase expression of the fibrotic markers in NCFs was investigated, due to the partial nature of S1PR1 involvement in NCFs when activated by dhS1P and S1P. The treatment of NCFs with SEW2871 for 18 h significantly increased the genetic expression of TGFβ, TIMP1 and Coll1a1 as shown in Figure 2.7 A-C. These findings are like those reported by Shea et.al [176], in terms of lung fibrosis, where prolonged exposure to SEW2871 led to increased fibrosis and vascular leakage. The results also show that inhibiting JAKs did reduce the expression of levels of these fibrotic markers; TGFβ ($p < 0.001$, Figure 2.7A), TIMP1 ($p < 0.01$, Figure 2.7B) and Coll1a1 ($p < 0.01$, Figure 2.7C), significantly. This finding supports the proposition that a dhS1P and S1P induced TIMP1 is not dependent on S1PR1, since these ligands do bind to multiple receptors.

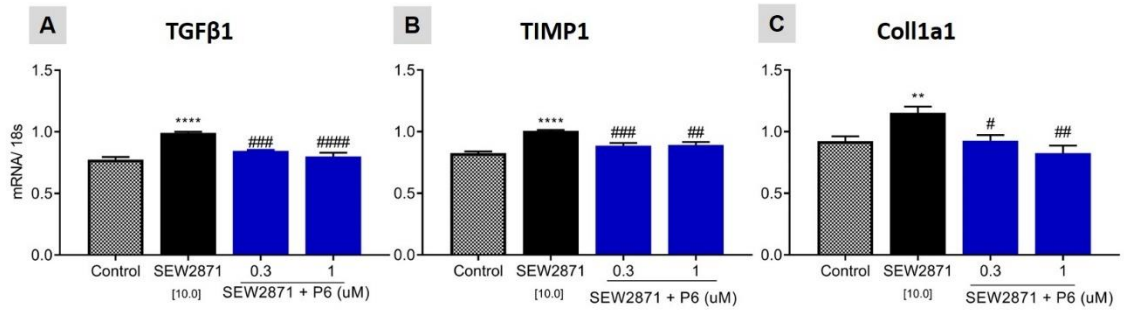

Figure 2.7. Inhibition of JAKs reduced mRNA levels of fibrotic markers increased by activation of S1PR1. (A) S1PR1 specific agonist, SEW2871, increased TGFβ, (B) TIMP1 and, (C) Coll1a1. These were significantly reduced when JAKs were inhibited by P6. $^{\#}p < 0.05$, $^{\#\#}p < 0.01$, $^{\#\#\#}p < 0.005$ & $^{\#\#\#\#}p < 0.001$ vs. SEW2871, and $^{**}p < 0.001$, $^{****}p < 0.0001$ vs. control. Data are presented as ± SEM of at least 3 replicates with two independent repeats.

2.4.11 Inhibition of JAKs reduced intracellular TGFβ protein secretion and activation by dhS1P and S1P

Since there were no changes in gene expression of TGFβ1 at the later time points of 18 h and 24 h, cellular protein expression levels of TGFβ at 24 h of treatment with dhS1P and S1P were conducted. Extracellular activity of TGFβ is regulated by conversion of latent TGFβ to active TGFβ through proteolytic degradation of the latency associated protein (LAP) which renders TGFβ inactive. TGFβ proteins are synthesized as latent precursor molecules (LTGF-β) in a complex with latent TGFβ binding protein (LTBP) [177] that forms the large latent complex (LLC), which is secreted and stored in the ECM [178]. DhS1P increased the levels of both the 65 ($p < 0.01$) and 45 kDa latent TGFβ protein, but P6 inhibited only the 65 kDa ($p < 0.005$) TGFβ as shown in Figure 2.8A. P6 also significantly reduced

dhS1P increased protein expression of the 12 kDa TGFβ monomer ($p < 0.05$) and 25 kDa mature ($p < 0.05$) TGFβ levels. Similar effects were also observed in S1P treated cells. S1P significantly increased the expression of latent TGFβ proteins (65 kDa; $p < 0.0001$, and 45 kDa; $p < 0.001$) and the 12 kDa TGFβ monomer ($p < 0.05$), which were significantly inhibited by P6 ($p < 0.001$, $p < 0.05$, & $p < 0.05$, respectively), Figure 2.8B. These increases in latent TGFβ and mature TGFβ indicate that S1P and dhS1P did increase secretion of TGFβ in NCFs that could result in the fibrotic effect observed in the phenotypic collagen sensitive ^{3}H proline incorporation assay. However, due to MMPs being completely reduced by dhS1P and S1P at 24 h (Figure 2.9A), the increase did not activate the canonical TGFβ/ SMAD signalling pathway that is known to increase the expression of fibrotic gene markers. Even at 6 h when TIMP1 and TGFβ1 were significantly inhibited by P6, MMP2 levels remained unchanged (Figure 2.9B). The proteolytic action of the MMPs and integrins ($\alpha_V\beta_6$ and $\alpha_V\beta_8$) cleave TGFβ from LAP releasing it from the ECM and allowing it to bind to the TGFβ receptor. P6 also reduced dhS1P stimulated increase in TIMP1 protein levels at 24 h (Figure 2.8C).

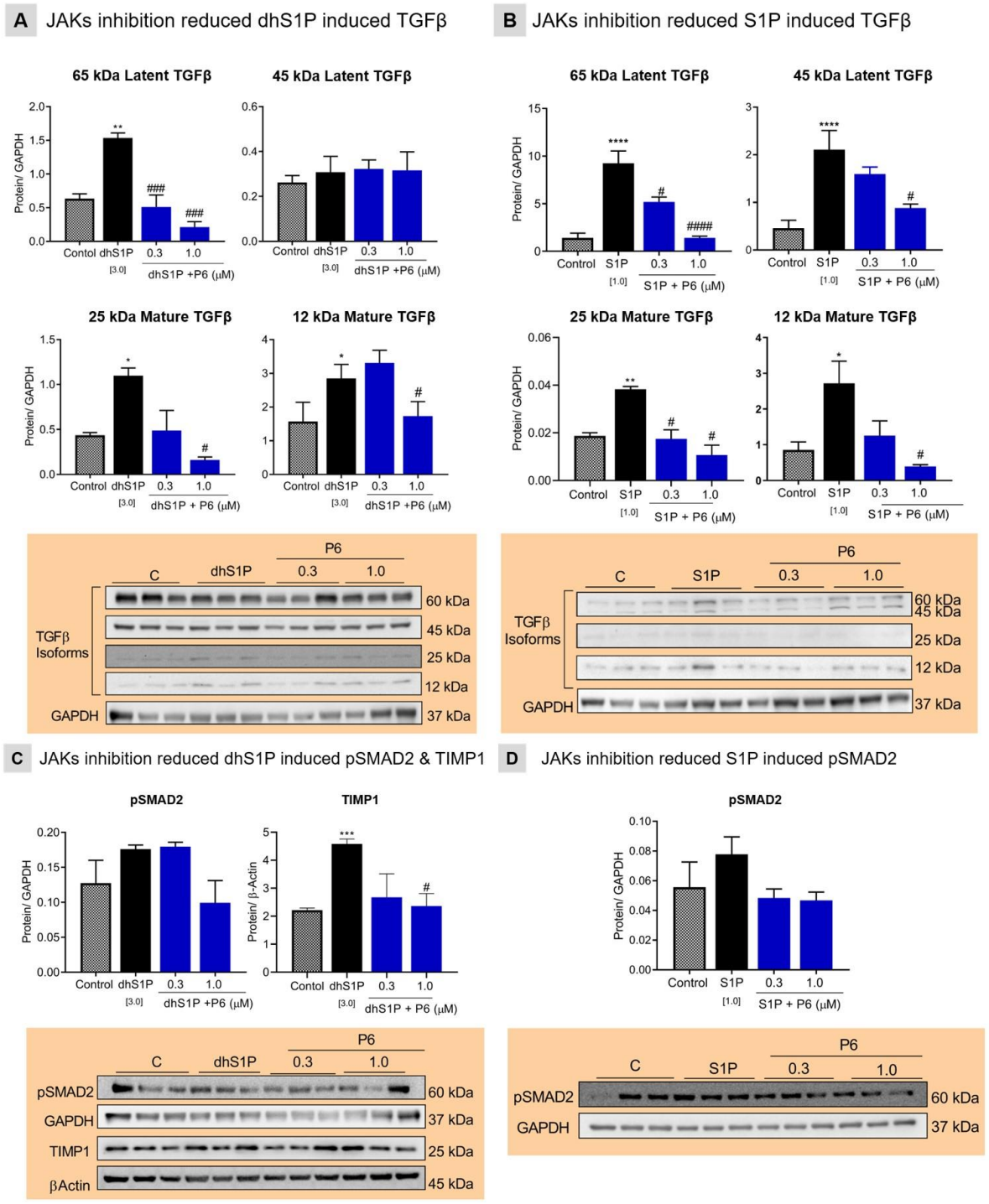

Figure 2.8. P6 reduced TGFβ protein expression and pSMAD2 activation by dhS1P and S1P. (A) dhS1P increased the protein expression of TGFβ isoforms of 65, 45, 25 & 12 kDa in NCFs at 24 h, while P6 inhibited all except the 45 kDa. (B) S1P also increased the 65, 45, 25 & 12 kDa TGFβ isoforms and all

were inhibited by P6 at 24 h. (C) dhS1P activated pSMAD2 at 30 minutes of treatment was inhibited by P6 at the highest dose, and P6 also reduced TIMP1 protein expression at 24 h. (D) S1P activated pSMAD2 was also inhibited by P6, but both were statistically insignificant. $^{*}p < 0.05$, $^{**}p < 0.01$, $^{****}p < 0.001$, vs. control & $^{\#}p < 0.05$, $^{\#\#}p < 0.01$, $^{\#\#\#}p < 0.005$ vs. treatment. Values are presented as ± SEM of at least 3 replicates with two independent repeats.

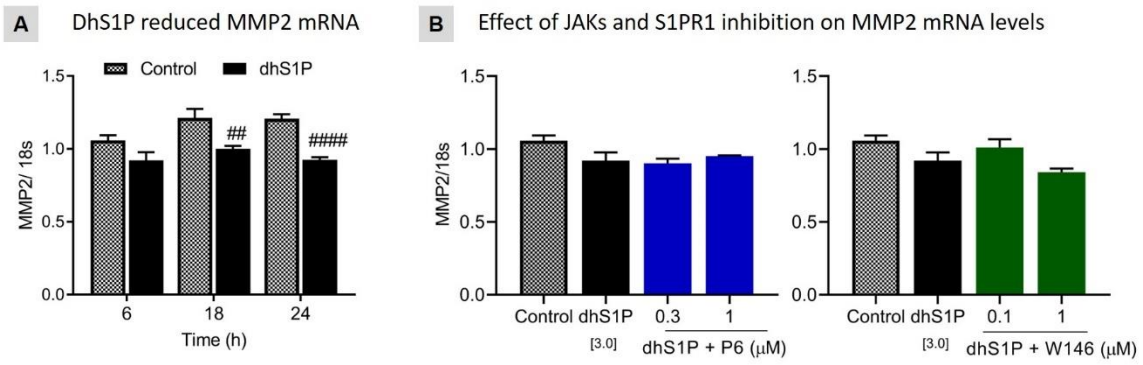

Figure 2.9. Effect of dhS1P on MMP2 mRNA & protein. (A) DhS1P significantly reduced MMP2 mRNA expression at 18 and 24 h. (B) MMP2 mRNA expressions did not increase when cells were treated with P6 and W146 for 6 h. $^{\#\#}p < 0.01$, $^{\#\#\#\#}p < 0.001$, vs. control. Values are presented as ± SEM of at least 3 replicates with two independent repeats.

2.4.12 DhS1P and S1P had a delayed effect on pSMAD2 activation

We then investigated SMAD2 phosphorylation, to determine if it is involved in dhS1P and S1P mediated intracellular signalling. The activation of TGFβ causes phosphorylation of the TGFβ receptors 1 & 2 leading to activation of downstream

targets. The primary target of this activation is the SMAD family of proteins, including SMAD2, resulting in the activation of the canonical TGFβ/SMAD signalling pathway. NCFs treated with S1P and dhS1P showed that they did increase the phosphorylation level of SMAD2 at 30 minutes of treatment, Figure 2.8C & D. Even though treatment with P6 did lead to reduced activation of phosphorylated SMAD2 levels in both dhS1P and S1P stimulations, these were not statistically significant. The slow activation of SMAD2 by S1P was also observed in mesangial cells [179], and may be the result of non-canonical pathways such as the ERK/MAPK being activated [180]. This supports the premise that the canonical TGFβ/SMAD signalling pathway may not be the primary cause of extracellular dhS1P and S1P induced increase in collagen synthesis.

2.4.13 JAKs are involved in the phosphorylation of c-JUN by dhS1P and S1P

Since TIMP1 has the AP-1 response element to which SK1 binds to [120], the ability of P6 to inhibit the phosphorylation of c-JUN, a component of the AP-1 transcription factor was investigated. The results in Figure 2.10A show that both dhS1P and S1P slightly increased phosphorylation of c-JUN, and were significantly reduced when JAKs was inhibited by P6 ($p < 0.05$, and $p < 0.01$, respectively). Figure 2.10B also shows that W146, the S1PR1 antagonist caused a further non-significant increase in c-JUN at the higher doses. This result supports the previous results (Figure 2.6B & C) for gene expression where W146 was unable to inhibit TIMP1 mRNA increase.

A C-JUN activation by dhS1P & S1P reduced by JAKs inhibition

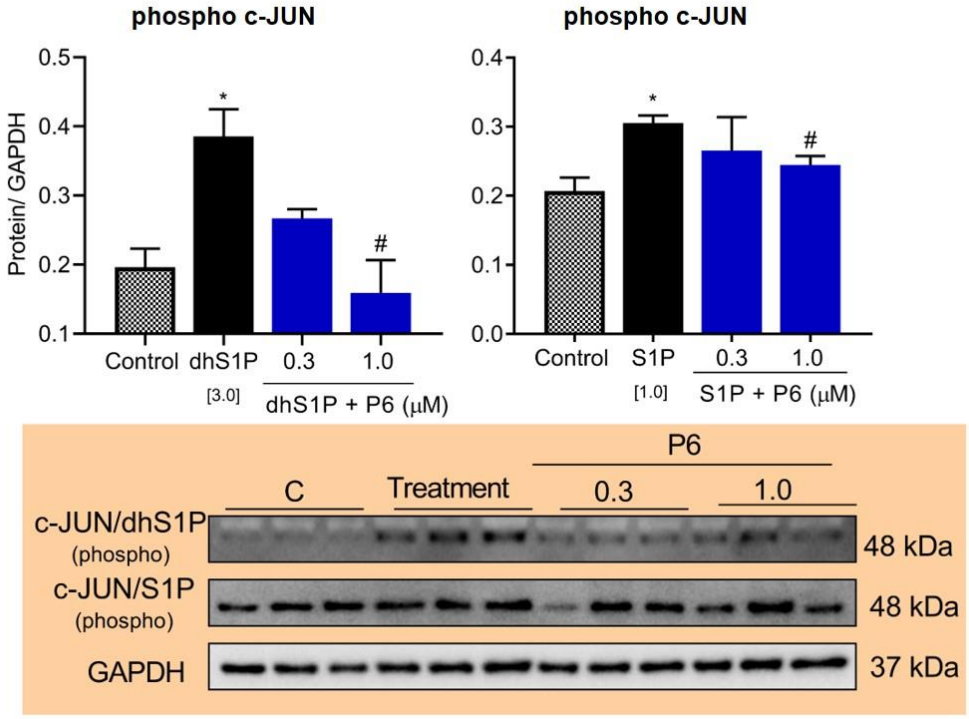

B C-JUN activation by dhS1P & S1P not affected by S1PR1 inhibition

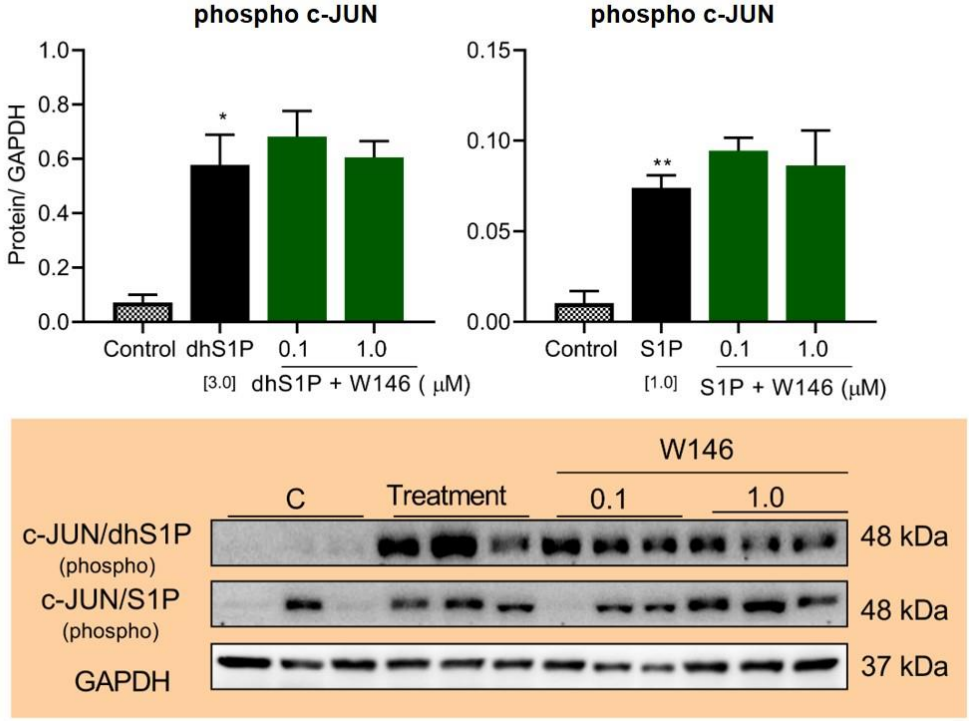

Figure 2.10. C-JUN phosphorylation by dhS1P and S1P was inhibited by P6 and not W146. (A) P6 reduced dhS1P & S1P phosphorylated c-JUN at 15 minutes of treatment. (B) W146 did not reduce dhS1P and S1P phosphorylation of c-JUN. $^{*}p < 0.05$, vs. control & $^{\#}p < 0.05$, $^{\#\#}p < 0.01$ vs. dhS1P/S1P. Values are presented as mean ± SEM of at least 3 replicates with two independent repeats.

2.4.14 DhS1P and S1P caused myocyte hypertrophy

Next, the effects of extracellular dhS1P to S1P in causing hypertrophy, in cardiac myocytes isolated from 1-2 days old rat pups were compared. Previous experiments have shown both hypertrophic [106] and anti-hypertrophic [181, 182] effects of S1P, depending on the conditions under which it has been investigated. The results in Figure 2.11A show that 1 μM and 3 μM dhS1P was also able to induce statistically significant hypertrophic effects when treated within 48 h ($p < 0.05$), 60 h ($p < 0.05$) and 72 h ($p < 0.05$), and within 48 h ($p < 0.05$) and 72 h ($p < 0.01$), respectively.

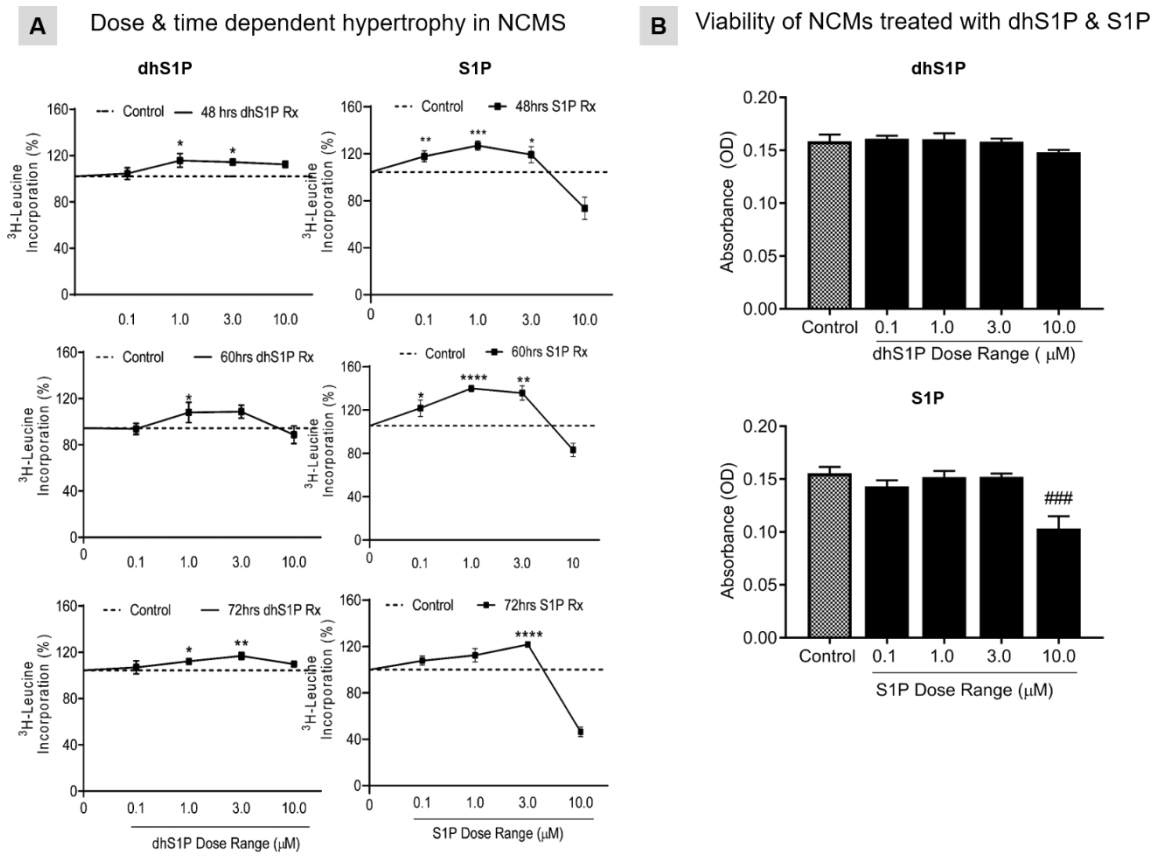

Figure 2.11. DhS1P & S1P induced myocyte hypertrophy. (A) ^{3}H-Leucine incorporation assay showing cardiac myocyte hypertrophy induced by dhS1P and S1P in NCM at 48, 60 & 72 h, at dose ranges of 0.1, 1, 3 & 10 μM. Ang II was used as positive control (data not shown). (B) 0.1, 1, 3, & 10 μM dhS1P treatment alone at 48 h did not reduce the viability of NCMs, while S1P reduced NCM viability at 10 μM as measured by Alamar blue assay. Data is representative of at least 4 replicates at each time point and dose with 3 repeated experiments. $^{*}p < 0.05$, $^{**}p < 0.01$, $^{***}p < 0.005$, $^{****}p < 0.001$ vs. Control, $^{\#\#\#}p < 0.005$ vs. stimulant. Values are presented as ± SEM.

This was comparatively lower than S1P at similar dose and time points, and 10 nM Ang II at 60 h (Figure 2.12C). Compared to the control SEW2871 had

significant hypertrophic effects (Figure 2.12A) at 60 (p <0.01) and 72 h (p< 0.05), but was much lower than the effects of dhS1P and S1P. It should be noted that 1 μM S1P induced hypertrophic effects were like that of Ang II at 60 h (Figure 2.12C). In addition, 48 h stimulation of NCMs with different doses of dhS1P (0.1, 1, 3 & 10 μM) did not reduce their viability as measured by the Alamar blue assay, while S1P significantly reduced NCM viability at 10 μM, Figure 2.11B.

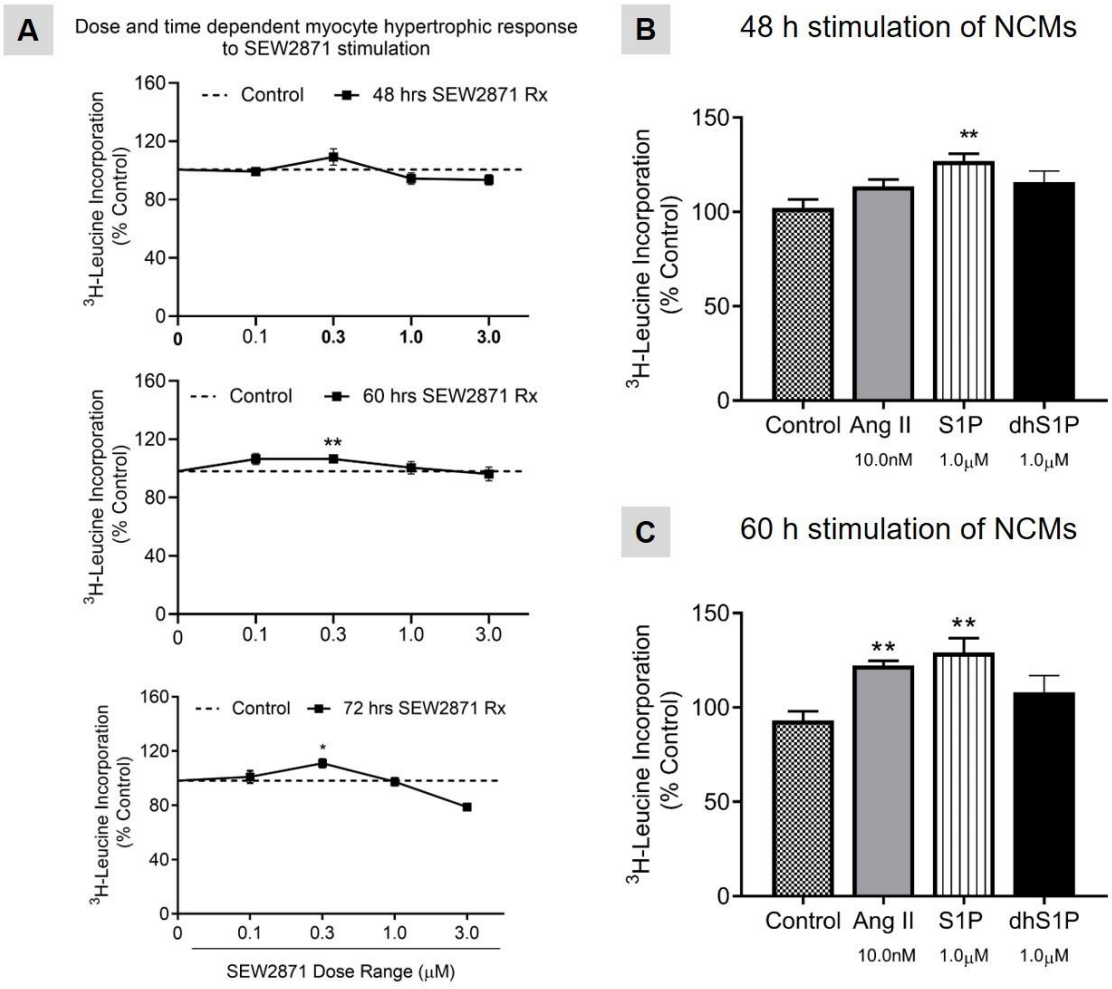

Figure 2.12. Comparative hypertrophic effect of Ang II/S1P/ dhS1P and SEW2871. (A) The hypertrophic effects induced by SEW2871 at 0.1, 0.3, 1.0 & 3.0 μM was significant at 60 h and 72 h for 0.3 μM. (B) At 48 h of treatment 10 nM Ang II & 1 μM dhs1P did not increase hypertrophy, while 1 μM S1P did. (C) At 60 h of treatment, 10 nM Ang II and 1 μM S1P increased hypertrophy while 1

μM dhS1P did not. ** $p < 0.01$, * $p < 0.05$ vs. Control. Values are presented as ± SEM of four independent experiments at each time point with three replicates in each.

2.4.15 Inhibition of JAKs slightly reduced dhS1P and S1P induced NCM hypertrophy

Next, whether inhibition of JAKs led to a reduction in the hypertrophic effects induced by dhS1P at 48 h, and S1P at 60 h in NCMs were explored. Phenotypically, the addition of P6 significantly reduced the dhS1P induced hypertrophic effects at the three higher doses; 0.1 μM ($p < 0.01$), 0.3 μM ($p < 0.05$) and 1 μM ($p < 0.05$), Figure 2.13A. Comparatively, P6 did not reduce myocyte hypertrophy induced by extracellular S1P, indicating JAK/STAT pathway maybe involved in extracellular dhS1P but not S1P induced myocyte hypertrophy. JAK/STAT signalling in cardiac myocytes can either be cardio-protective or cardio-offensive, depending on the disease state and type of injury or insult. In terms of S1P induced activation of the JAK/STAT pathway, increased JAK/STAT signalling in ischaemic reperfusion injury has been shown to be cardio-protective [164].

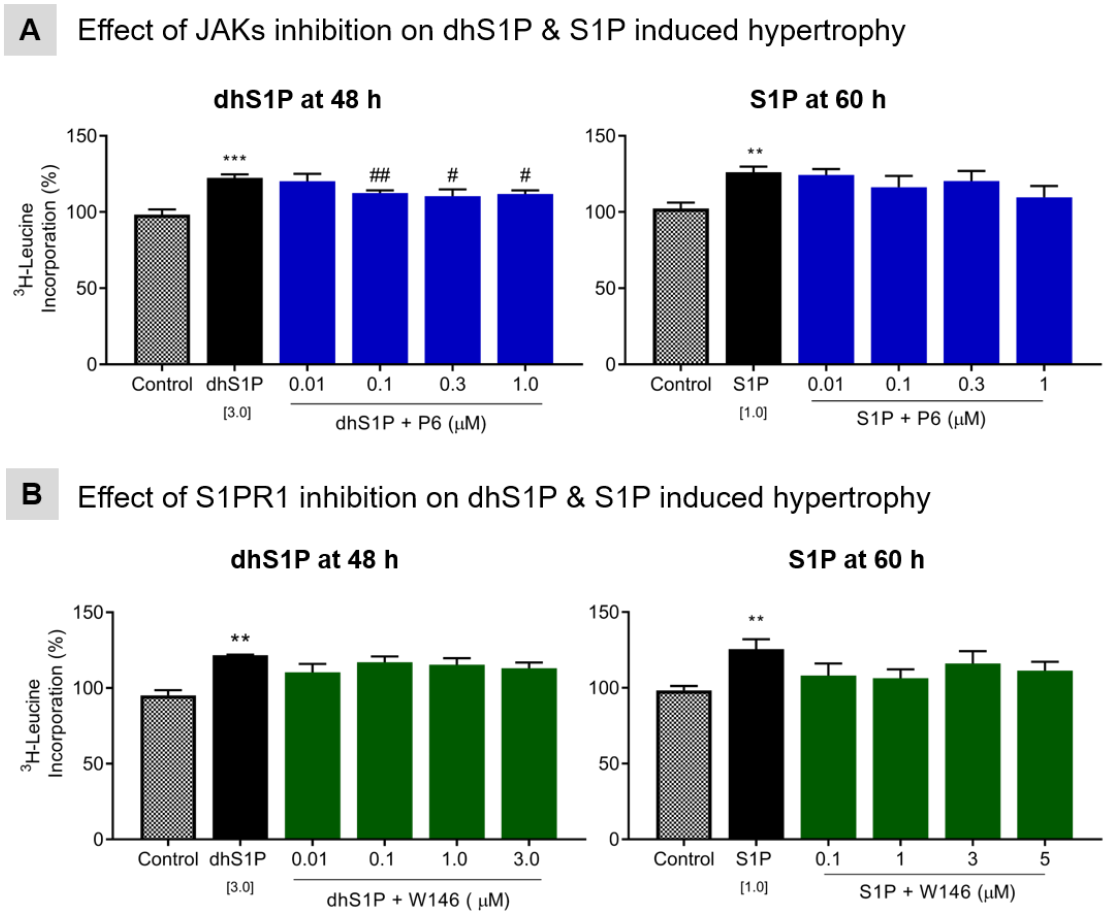

Figure 2.13. P6 inhibited dhS1P & S1P induced myocyte hypertrophy. (A) Inhibition of JAKs led to reductions in hypertrophy induced by dhS1P and S1P, however these reductions were insignificant for S1P. (B) Inhibition of S1PR1 had varying degrees of inhibition across the different doses in both dhS1P and S1P treated NCMs, which were not significant. Data is representative of at least 4 replicates at each time point and dose with 3 repeated experiments. $^{*}p < 0.05$, $^{**}p < 0.01$, $^{***}p < 0.005$, $^{****}p < 0.001$ vs. Control, $^{\#}p < 0.05$, $^{\#\#}p < 0.01$, $^{\#\#\#}p < 0.005$ vs. stimulant.

2.4.16 Inhibition of S1PR1 had little effect on dhS1P and S1P induced NCM hypertrophy

The S1P/S1PR1 axis in NCMs is also known to be cardio-protective against the effects of β_1-adrenergic receptor (β1AR) overstimulation in HF [105]. Therefore, the effects of S1PR1 inhibition on dhS1P and S1P treated NCMs were compared. Phenotypically, the treatment with W146 had no statistically significant effect on hypertrophy induced by extracellular dhS1P and S1P (Figure 2.13B). This is despite both showing trends toward a reduction in myocyte hypertrophy.

2.4.17 Inhibiting JAKs reduced dhS1P stimulated pSTAT1 and S1P stimulated pSTAT1/3 in NCM

We then determined if there was any difference in the levels of phosphorylated STAT1 and STAT3 proteins in NCMs stimulated with dhS1P and S1P. Both dhS1P and S1P significantly increased phosphorylated STAT1 ($p < 0.05$, Figure 2.14A & B) at 15 minutes of stimulation in NCMs. The addition of P6 significantly inhibited S1P stimulated STAT1 phosphorylation at the highest dose of 1 µM ($p < 0.05$, Figure 2.14B). P6 did not have inhibitory effects on dhS1P stimulated phosphorylation of STAT1. At 15 minutes, the increase in phosphorylated STAT3 by S1P was not significant, but P6 abrogated its expression, Figure 2.14B. In contrast, dhS1P stimulation significantly reduced phosphorylated STAT3 ($p < 0.05$, Figure 2.14A), and the addition of P6 rescinded it further. For S1P, these findings are expected since it has been shown to increase activation of pSTAT3 following MI [119]. However, for dhS1P, the results show for the first time that it seems to affect phosphorylated STAT1 and STAT3 in NCMs differently.

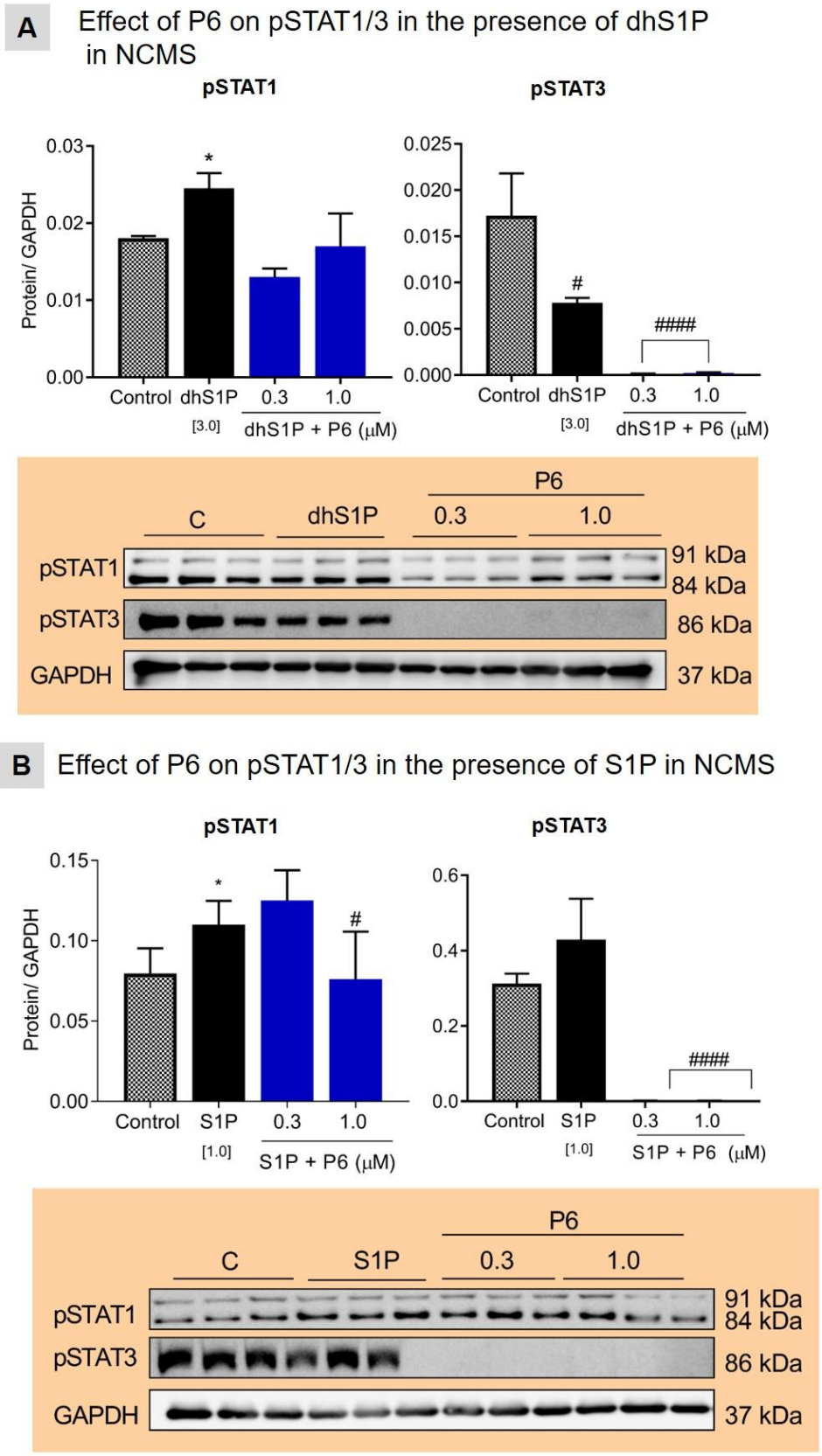

Figure 2.14. Effect of dhS1P and S1P on pSTAT1/ 3. (A) P6 inhibited 3μM dhS1P stimulated STAT1 phosphorylation, and completely abrogated dhS1P

dephosphorylated STAT3, (B) P6 inhibited 1μM S1P stimulated STAT1, and STAT3 phosphorylation. $^{**}p$ <0.01 vs. control and, $^{\#}p$ < 0.05 vs. stimulant. Values are presented as mean ± SEM of at least 3 replicates with two independent repeats.

2.4.18 The dhS1P/ S1PR1 axis is not required for JAKs/STAT1/3 activation in NCMs

S1PR1 was inhibited to determine whether the dhS1P/ S1PR1 axis was involved in activating JAKs/STAT1 and 3 signalling. W146 was not able to reduce the phosphorylation levels of STAT1 stimulated by both dhS1P (Figure 2.15A) and S1P (Figure 2.15B), despite showing a reductive effect. This may indicate that the S1P & dhS1P/ S1PR1 axis is not involved in activation of JAKs/STAT1 signalling in myocyte hypertrophy. STAT3 plays differing roles in cardiac myocytes depending on the type of stimulant or insult in both physiological and pathophysiological states. Inhibition of S1PR1 had no effect on pSTAT3 increased by S1P (p < 0.05. Figure 2.15B), indicating that the phosphorylation of STAT3 is not dependent on the S1P/S1PR1 axis. In comparison, dhS1P tended to reduce pSTAT3 but was not significant (Figure 2.15A). Inhibition of S1PR1 by W146 had no effect on pSTAT3 in the presence of dhS1P.

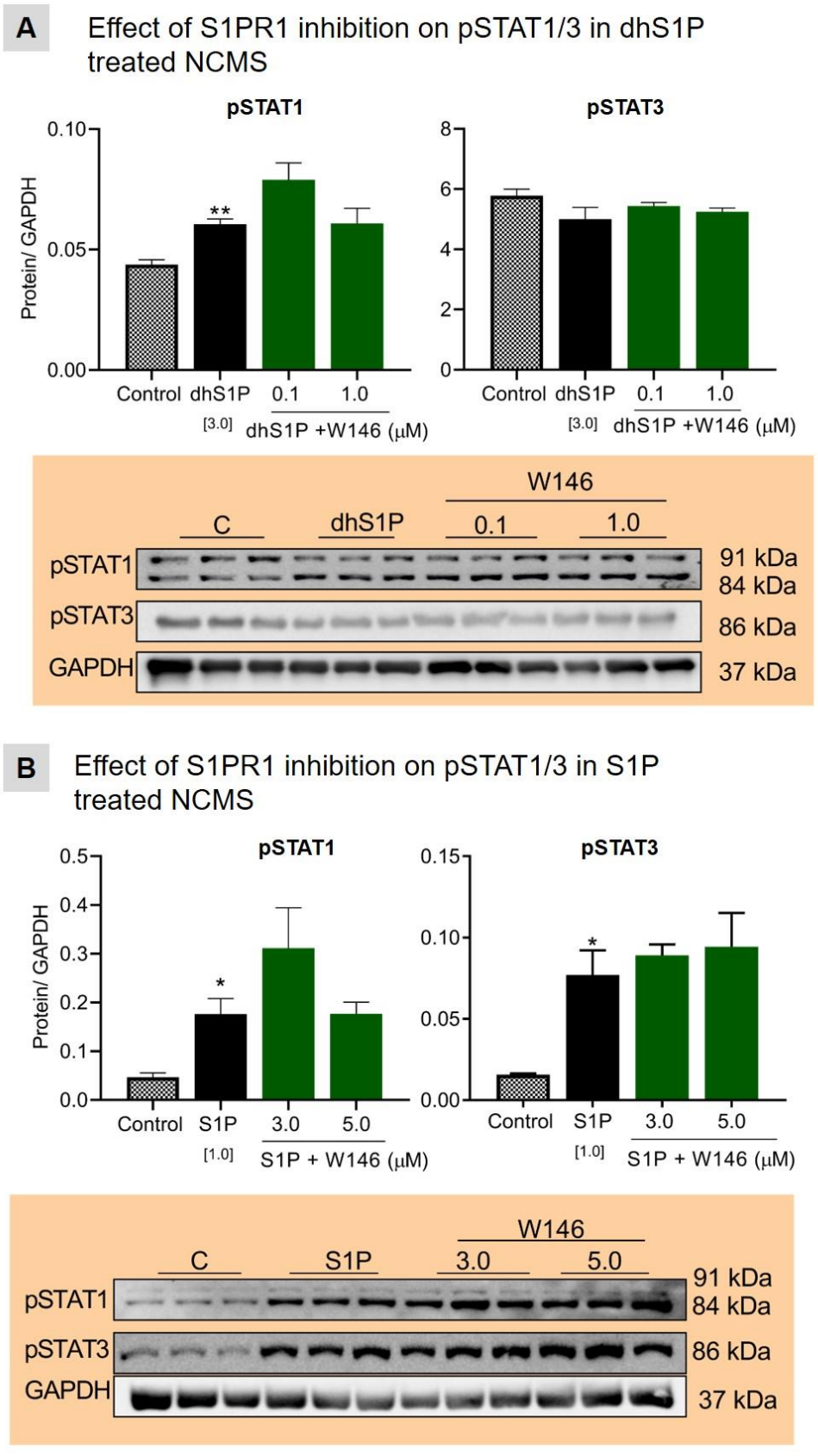

Figure 2.15. Effect of dhS1P/S1PR1 and S1P/S1PR1 axis activation on pSTAT1/3. Inhibition of S1PR1 did not affect STAT1 and STAT3

phosphorylation in NCMs treated with (A) dhS1P and (B) S1P. $^{*}p$ <0.05 vs. control. Values are presented as mean ± SEM of at least 3 replicates with two independent repeats.

2.4.19 Inhibition of JAKs in NCMs led to synergistic increase in expression of myocyte hypertrophy gene markers

Next, dhS1P and S1P's capacity to induce expression of certain hypertrophic markers in the NCMs were examined. Both S1P (p < 0.001- 0.0001, Figure 2.16B and D) and dhS1P (p < 0.0001, Figure 2.16A and C) significantly increased the expression of the hypertrophic markers investigated. The addition of P6 caused significant synergistic increases in βMHC (p < 0.01), ANP (p < 0.005) and BNP (p < 0.005) by dhS1P, and αSKA (p < 0.01) by S1P (Figure 2.16A & B, respectively). ANP and BNP secretion is increased as a counter measure by myocytes in response to the increased hypertrophic stimuli [183], indicated by the increase in βMHC. Apart from the JAK/STAT pathway other pathways are also known to be involved in signalling ANP and BNP increase which may account for the synergistic increase. These results indicate that inhibition of JAKs in dhS1P induced NCM hypertrophy may not be sufficient to reduce the hypertrophic genes. However, P6 had no effect on S1P induced ANP, BNP and βMHC, and dhS1P induced αSKA mRNA. The differing effects on αSKA expression by JAKs inhibition in S1P and dhS1P treated NCMs Show that inhibition of JAKs in S1P treated cells may have a greater hypertrophic effect than dhS1P. αSKA expression is known to be increased in proportion to the progression of hypertrophy[184]. Considering that other hypertrophic signalling pathways could possibly be

simultaneously activated, it may account for the disparities between the phenotypic, protein and gene expression results in terms of JAKs inhibition.

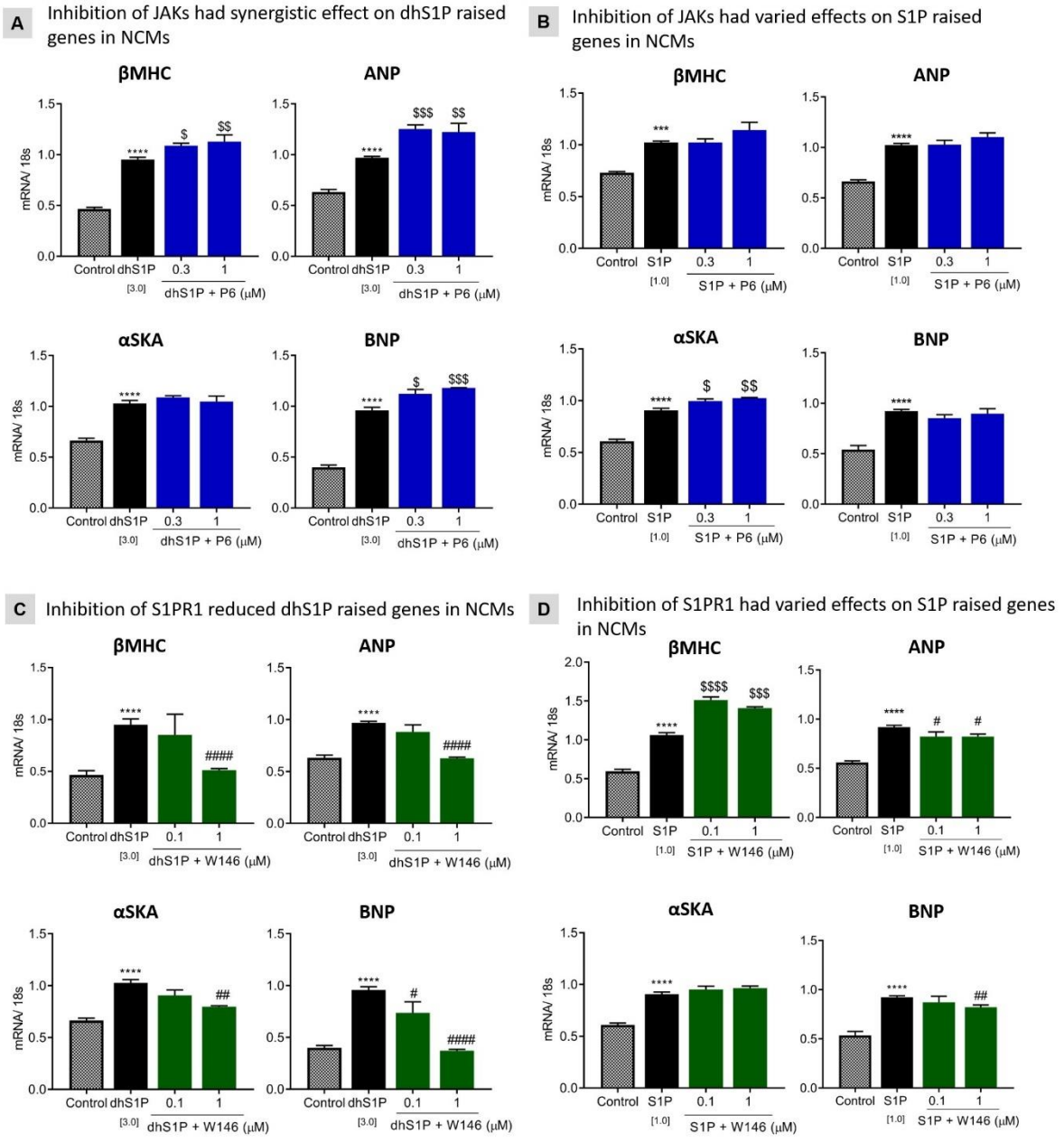

Figure 2.16. Inhibition of JAKs and S1PR1 have opposite effects on dhS1P and S1P induced expression of myocyte hypertrophy genes. Both 3 μM dhS1P and 1 μM S1P significantly increased mRNA expression of βMHC, ANP, αSKA and BNP at 18 h of treatment. (A) JAKs inhibition caused significant

synergistic effects on βMHC, & BNP mRNA increase by dhS1P, and had no effect on αSKA mRNA. (B) JAKs inhibition had significant synergistic effect on αSKA mRNA increased by S1P, with slight increases in βMHC, & ANP mRNA, and no effect on BNP mRNA. (C) All hypertrophy gene markers were significantly reduced when S1PR1 was inhibited in dhS1P stimulated cells. (D) Inhibition of S1PR1 led to significant reductions in ANP and BNP, synergistic increase in βMHC and no effect on αSKA mRNA in S1P treated cells. $^{\#\#}p < 0.01$, $^{\#\#\#\#}p < 0.001$, $^{\$}p < 0.05$, $^{\$\$\$}p < 0.005$ & $^{\$\$\$\$}p < 0.001$ vs. dhS1P/S1P, and $^{***}p < 0.005$ & $^{****}p < 0.001$ vs. control. Values are presented as mean ± SEM of at least 3 replicates with two independent repeats.

2.4.20 DhS1P/S1PR1 axis signalling is involved in increased mRNA expression of myocyte hypertrophy markers

The association between the increased mRNA expression of the hypertrophic markers and activation of S1PR1 by dhS1P and S1P was also examined. W146 significantly inhibited all the hypertrophic markers increased by dhS1P (βMHC; p <0.0001, ANP; p <0.0001, αSKA; p <0.001 & BNP; p <0.0001), as shown in Figure 2.16C. Suggesting that dhS1P induced myocyte hypertrophy maybe S1PR1 dependent, through other signalling pathways. The inhibition of S1PR1 caused a significant synergistic increase in βMHC expression ($p < 0.0001$), while significantly reducing ANP ($p < 0.05$) and BNP ($p < 0.01$) expression, and had no effect on αSKA gene expression increased by S1P (Figure 2.16D). These findings support those reported by others showing that the S1P/S1PR1 axis in NCMs is cardio-protective [105, 185].

2.5 Discussion

S1Ps role in cardiac remodelling through its receptors whether in cell or animal studies has been highlighted by many over the years, although not fully explored. Its role in inflammation and cancer biology is becoming an area for target therapy. On the other hand, S1P signalling through the JAK/STAT pathway is less understood especially in terms of cardiac fibroblasts. DhS1P's overall effect on the cardiovascular system and especially cardiac remodelling to our knowledge has not been investigated. It's level in plasma is known to be altered and has recently been linked to increased cardiac dysfunction in aging, where cardiac remodelling is known to occur [186]. One of the major goals of this study has been to determine the role of the JAK/STAT pathway in terms of dhS1P and S1P signalling and for the first time describe any differences in signalling by these sphingolipid analogues. Increased inflammatory cells in circulation [187] and activation of other fibrotic factors such as TGFb in the infarcted wall [188] can increase dhS1P in circulation and tissue resulting in increased activation of intracellular pathways.

The results show that extracellular dhS1P increases primary NCF collagen synthesis like that of S1P (Figure 2.1). Similarly, both sphingolipids activated STAT1 protein (Figure 2.3 and 2.4), but this activation was not entirely dependent on JAKs activation as indicated by the non-significant reductions by P6 (Figure 2.3). Signalling through the S1PRs activates other GPRC dependent pathways such as ERK pathway which may have contributed to STAT1 phosphorylation [189]. The activation of STAT1 protein by S1P occurs through the S1P/S1PR1 axis in NCFs while dhS1P may activate it through either S1PR2 or 3 (Figure 2.4). The non-significant and inconsistent increase in STAT3 phosphorylation by both dhS1P and S1P may indicate a delayed effect (Figure 2.3 and 2.4), and under our

experimental conditions, it's activation may depend on JAKs activation as indicated by its complete abrogation by P6 (Figure 2.3). This is of importance in relation to the reduced collagen synthesis since STAT3 is known as a key transcription factor involved fibrosis [190].

It is also interesting to note that both dhS1P and S1P caused an early increase in the expression of TGFβ1 gene and even at 24 h of treatment, TIMP1 mRNA rather than TGFβ1 mRNA was still increased (Figure 2.5). The results show that the early increase in TGFβ1 mRNA expression was accompanied by an early increase in SK1 mRNA, which was reduced together with TGFβ1 at 24 h (Figure 2.5). In dermal fibroblasts TGFβ was shown to induce SK1 [120], and that SK1 co-operated with TGFβ to mediate the increase in TIMP1. In addition, others have shown that SK1 upregulation alone increased TIMP1 but had no effect on TGFβ [121]. However, since TIMP1 mRNA remained significantly high even after 24 h stimulation, with receding SK1 and TGFβ1 mRNA expression, it can be assumed that the extracellular dhS1P and S1P induced fibrosis in rat NCFs was primarily due to the sustained TIMP1 activation. See summative diagram in Figure 2.17A & C.

This led us to investigate c-JUN protein activation, since TIMP1 harbours an AP-1 response element on its promoter site [120]. The reduced activation of c-JUN proteins by dhS1P and S1P when JAKs was inhibited and not when S1PR1 was inhibited showed that S1P and dhS1P potentially signal through JAK/STATs-AP-1- TIMP1 pathway and is not S1PR1 dependent (Figure 2.10). Furthermore, STAT3 and not STAT1, interacts with c-JUN [191]. Apart from these interactions, TIMP1 also harbours a functional binding site for STAT3 [192]. TIMP1 is an effective inhibitor of the proteolytic degradation of ECM by factors such as the MMPs, which results in the accumulation of ECM products [193]. A recent study

indicated that TIMP1 increases *de novo* collagen synthesis by activating SMAD2/3 and β-catenin in in-vivo models of cardiac fibrosis which were independent of MMPs [194]. Studies on neuronal progenitor cells using pharmacological inhibition of sphingolipid pathway have shown that dhS1P increases SMAD2 to a greater degree than S1P, which has an effect on proliferation and differentiation [135].

Since TGFβ signalling is regulated by the balance between TIMPs and MMPs, the sustained activation of TIMP1 may have a feedback inhibition effect on the transcription of TGFβ, but not on its post transcriptional secretion and activation, as shown by the increased TGFβ protein levels at 24 h of treatment for S1P and dhS1P (Figure 2.8A and B). The increased TIMP1 led to a significant reduction in MMP2 mRNA, up to 20% at 24 h compared to control in dhS1P stimulated NCFs, and did not recover with the addition of P6 and W146 (Figure 2.9A). The lack of recovery through the S1PR1/JAKs/STAT signalling indicate that these effects on MMP2 maybe through other signalling cascades. While, the downstream signalling of JAK/STAT pathways in increasing TIMP1 mRNA may have contributed to the accumulation of TGFβ protein.

The effects of dhS1P and S1P may not be receptor subtype specific, even though the effects of both were greatest on the early increase in S1PR1 mRNA expression. Clinically the plasma concentration of dhS1P and S1P have been found to be reduced within the first 6 h after an MI [145, 146]. Whether this is a cumulative effect or a result of the MI remains yet to be determined. While, in animal models of MI, the expression of S1PR1 has been found to be reduced [105], thus the authors suggested S1PR1 targeted gene therapy. In contrast, the results show that perhaps long-term activation of S1PR1 alone could aggravate fibrosis. It is also

possible that the initial increase in TGFβ may contribute to reparative fibrosis rather than reactive fibrosis at the initial onset of injury such as an MI.

The JAK/STAT signalling pathway in cardio-myocytes is known to be protective, especially STAT3 activation [195]. The increased expression of hypertrophic gene markers when JAKS were inhibited in dhS1P and S1P treated NCMs support this and show that it could further aggravate hypertrophy, Figure 2.16B & D. Clinically, hypertrophic markers such as BNP and ANP are considered as compensatory mechanisms in terms of HF [183]. Their increase in experimental conditions highlight the hypertrophic effects of the agents used. In this study, the synergistic increase in ANP and BNP mRNA levels despite inhibition of JAKs/STATs signalling also indicated the existence of other hypertrophic signals. This may be the reason for the minimal yet significant anti-hypertrophic effects exhibited phenotypically when JAKs were inhibited. Our findings also show that dhS1P and S1P have similar activating effects on the mRNA expression of βMHC and αSKA in NCMs (Figure 2.16A and B). However, the inhibition of JAKs and S1PR1 led to deferring effects. There is potential for further investigations in regards to these differences in relation to dhS1Ps effect on pacemaker cells or cardiac electrophysiology. This is in light of the growing number of evidence showing that S1P can have an effect on contractile activity of the heart through S1PR1 and S1PR3 signalling as summarized by Ningjun Li and Fan Zhang [196]. The differences in STAT1/3 protein phosphorylation (Figure 2.14) may perhaps be due to the dichotomous role of the JAK/STAT pathway in myocytes as explained by van Empel et.al [197]. The complete abrogation of STAT3 and its lack of activation at similar time points to STAT1 indicate that it's activation maybe delayed and dhS1P has opposite effects on STAT3 compared to S1P (Figure 2.14). Eventhough there are mechanisms known to negatively regulate

STAT3 [198], whether the reduced phosphorylation of STAT3 by dhS1P reflects this is beyond the scope of this thesis. The inhibition of S1PR1 in dhS1P treated cells did not show that myocyte hypertrophy could occur through the dhS1P/S1PR1 signalling axis (Figure 2.15A). Additionally, the activation of this axis could be ligand dependent, since the S1PR1 agonist, SEW2871, stimulated myocyte hypertrophy was lower than that of dhS1P or S1P (Figure 2.12A). This is also supported by the lack of inhibition shown in our phenotypic studies (Figure 2.13B). Additionally, this shows that the effect of dhS1P/S1PR1 signalling is opposite to the effects of S1P/S1PR1 signalling which is reported to be anti-hypertrophic [105, 185], and corroborated by the findings on the inhibitory effects of W146 on ANP and BNP gene expression (Figure 2.16D).

In addition, targeting the intracellular signalling molecules such as JAKs or STATs is likely to have more selective effects than indirect effects through dhS1P signalling at receptor level. Therefore, it is of particular importance to further investigate the role of individual JAKs or STATs in the functioning of cardiac myocytes and fibroblasts that is likely to produce more effective therapies.

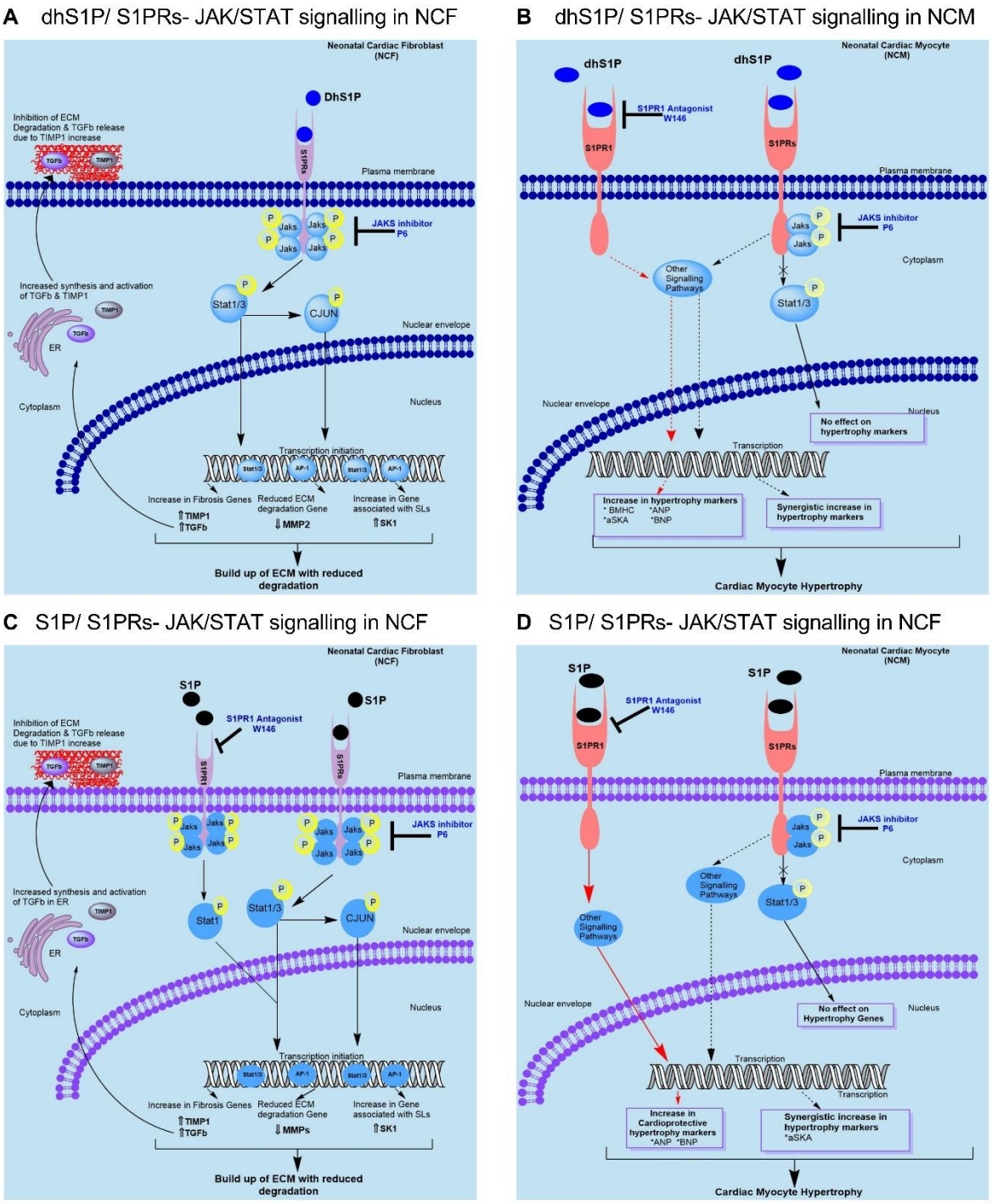

Figure 2.17. Summary of dhS1P/S1P/S1PR1-JAKs/STAT signalling in NCFs and NCMs. (A) Exogenous dhS1P activates the JAKs/STAT signalling pathway in NCFs through the S1PRs. The phosphorylation of STAT1/3 together with c-JUN leads to their nuclear translocation and increase in the transcription of fibrotic genes; TGFβ & TIMP1, SL synthesis related gene; SK1, and reduces

ECM degradation gene; MMP2. The increase in TGFβ mRNA encourages increase in TGFβ secretion, activation and transport to the ECM from the endoplasmic reticulum (ER). However, due to the abundance of TIMP1, ECM degradation and TGFβ release is inhibited, resulting in ECM accumulation. The inhibition of JAKs by P6, was able to inhibit the dhS1P/S1PRs-JAKs/STAT-TIMP1 signalling. (B) In NCMs exogenous addition of dhS1P activates JAKs/STAT signalling pathway through S1PR1. The effect of STAT1/3 phosphorylation and translocation to the nucleus has no effect on the transcription of hypertrophy genes such as βMHC, αSKA, ANP & BNP (bold black arrow). However, the inhibition of JAKs synergistically increases these markers through other pathways (dashed black arrow). dhS1P/ S1PR1 axis signalling through other pathways can cause myocyte hypertrophy by increasing the hypertrophy markers (bold red arrow). (C) Exogenous S1P activates JAKs/STAT pathway similarly to dhS1P in NCFs. S1P is also able to increase collagen synthesis in NCFs through the S1P/S1PR1/JAKs/STAT1 signalling cascade. (D) In NCMs, S1P activation of JAKs/STAT signalling also has no effect on hypertrophy gene markers (bold black arrow). However, it may have synergistic effects on the expression of αSKA genes (dashed black arrow). The S1P/S1PR1 may activate other pathways to that encourage increased expression of cardio-protective hypertrophy markers such as ANP and BNP (bold red arrows). The inhibition of S1PR1 by W146, reduces the levels of these hypertrophy genes. However, the inhibition of JAKs by P6, may lead to increased activation of other signalling pathways resulting in synergistic increase in the myocyte hypertrophy genes. Illustration derived through ChemDraw Professional 17.0 (Perkin Elmer, Waltham, MA, USA).

2.6 Conclusion

This chapter establishes the fibrotic and hypertrophic effects of extracellular dhS1P on primary rat cardiac cells. It shows that dhS1P-JAK/STAT-TIMP1 signalling can increase collagen synthesis in NCFs. While, dhS1P/S1PRs signalling in myocytes leads to hypertrophy. Since dhS1P can have inside-out signalling effects, targeting de novo sphingolipid pathway enzymes such as SK1 could improve outcomes in cardiac remodelling. These findings also increase the possibility of exploring effects of dhS1P on current trends in cardiac research such as stem cells and further exploration of dhS1Ps effect on cardiac electrophysiology. Considering current progress in therapies targeting the S1PRs and the *de novo* sphingolipid synthesis pathway, the impact of these therapies on their targets in other body systems should be considered.

Published article copy attached in **appendix 1.2**

Preface

Chapter three describes the effect of dhS1P on the PI3K/Akt signalling pathway in cardiac cells in terms of collagen synthesis and myocyte hypertrophy. This work has been submitted for publication.

Chapter 3: Attenuating PI3K/Akt-mTOR pathway reduces dihydrosphingosine 1 phosphate mediated fibrosis and hypertrophy in cardiac cells

Authors
Ruth R. Magaye[1, 2], Feby Savira[1, 2], Yue Hua[2, 3], Xin Xiong[2, 4], Li Huang[1, 2], Christopher Reid[2,5], Bernard L. Flynn[6], David Kaye[7], Danny Liew[2], Bing H. Wang[1, 2*]

8. Biomarker Discovery Laboratory, Baker Heart and Diabetes Institute, Melbourne, Australia
9. Monash Centre of Cardiovascular Research and Education in therapeutics, Melbourne, Australia
10. School of Traditional Chinese Medicine, Southern Medical University, Guangzhou, China
11. Shanghai Institute of Heart Failure, Research Centre for Translational Medicine, Shanghai East Hospital, Tongji University, School of Medicine, Shanghai 200120, P. R. China
12. School of Public Health School, Curtin University, Perth, Australia
13. Monash Institute of Pharmaceutical Sciences, Monash University, Melbourne, Australia
14. Heart Failure Research Group, Baker Heart and Diabetes Institute, Melbourne, Australia

*Corresponding author:

bing.wang@baker.edu.au and bing.wang@monash.edu

3.1 Abstract

Cardiac fibrosis and myocyte hypertrophy play contributory roles in the progression of diseases such as HF through what is collectively termed cardiac remodelling. The phosphoinositide 3- kinase (PI3K), protein kinase B (Akt) and mammalian target for rapamycin (mTOR) signalling pathway (PI3K/Akt- mTOR) pathway is an important pathway in protein synthesis, cell growth, cell proliferation, and lipid metabolism. The sphingolipid, dhS1P has been shown to bind to high density lipids in plasma. Unlike its analogue, S1P, the role of dhS1P in cardiac fibrosis is still being deciphered. This study was conducted to investigate the effect of dhS1P on PI3K/Akt signalling in cardiac fibrosis and hypertrophy. The findings demonstrate that inhibiting PI3K reduced collagen synthesis in NCFs, and hypertrophy in NCMs induced by dhS1P, in vitro. Reduced activation of the PI3K/Akt- mTOR signalling pathway led to impaired translation of fibrotic proteins such as Coll1 and TGFβ, and inhibited the transcription and translation of TIMP1. PI3K inhibition also affected the S1P receptors and enzymes such as DEGS1 and SK1 in the *de novo* sphingolipid pathway. While in myocytes, PI3K inhibition reduced myocyte hypertrophy induced by dhS1P by reducing αSKA, and reduced protein translation due to increased glycogen synthase kinase 3β (GSK3β) mRNA expression. The findings show a relationship between the PI3K/Akt- mTOR signalling cascade and exogenous dhS1P induced collagen synthesis and hypertrophy in cardiac cells.

3.2 Introduction

Remodelling in the injured myocardium, characterised by increased activation of hypertrophic and fibrotic factors, has detrimental effects in progressive HF [7]. Years of research have linked many peptide hormones, growth factors, cytokines, lipid mediators, and their downstream effectors to the process of cardiac remodelling [38, 199]. Research from chapter 2 and others have implicated sphingolipids, S1P and its analogue dhS1P, in cardiac fibrosis and hypertrophy [106, 114, 200, 201]. These lipids are ubiquitously present in biological systems and function as lipid mediators. In circulation they are bound to HDL and albumin, [79, 80]. In human platelet depleted plasma, their concentration ranges from 0.1 to 0.6 μM, with dhS1P at the lower end [202]. Their levels are altered in plasma, erythrocytes and platelets of patients with cardiomyopathies [81, 187, 203]. They interact with the sphingosine 1 phosphate receptors (S1PRs) on cell membranes, which are G protein coupled receptors [106, 204], leading to activation of downstream signalling pathways such as the phosphatidylinositol 3-kinase/ Protein Kinase B (PI3K/ Akt) pathway..

Lipid Kinases such as the PI3Ks are increasingly being targeted for cancer and immune disorder therapies [205]. PI3Ks are composed of three different classes of enzymes involved in cellular function. Class 1 PI3K activates Akt, which serves as the main downstream effector of PI3K. Among other substrates, Akt then phosphorylates mTOR, which acts on other proteins such as RPS6 to increase ribosomal RNA, nuclear protein synthesis, growth regulatory gene product, and cyclin D [206]. Together with the other broad range of cascading signals, activation of the PI3K/Akt pathway contributes to tissue and organ fibrosis, cell proliferation and survival [207-211]. PI3K/ Akt also plays an important role in cellular lipid metabolism [212, 213].

The JAK/STAT pathway investigated in chapter 2, and the PI3K/Akt pathway described here are important factors in remote ischemic preconditioning for cardio-protection, known as the SAFE and RISK pathways [214]. Considering the role of the S1P/S1PR1 axis activation in cardio-protection, the activation of PI3K/ Akt- mTOR signalling by S1P and its analogue, dhS1P in terms of cardiac remodelling is needed. This is because it could unveil potential differences in the molecular mechanisms of dhS1P and S1P's effect on these pathways and contribute to understanding the systemic effects of targeting sphingolipids for therapy. Therefore, in this chapter the effects of PI3K/ Akt- mTOR signalling pathway activation by dhS1P and S1P in isolated primary cardiac fibroblasts and myocytes was explored.

3.3 Methods

The methods used in chapter 2 were applied in this chapter. Please refer to section 2.3 for more details.

3.3.1 Measurement of cardiac fibroblast collagen synthesis

The ^{3}H-proline incorporation assay, as described in section 2.3.1 and 2.3.2, was used to determine collagen synthesis in NCFs induced by 1μM S1P, 3μM dhS1P and 10 μM of the S1PR1 agonist, SEW2871 [167]. The NCFs were seeded at 50 000 cells/ well and pre-treated for 2 h with the PI3K inhibitor, Wortmannin (W, 0.01-10.0 μM- SelleckChem, Houston, TX, USA), and the specific S1PR1 antagonist (W146, 0.1- 5.0μM- Torcris Bioscience, Bristol, UK). The levels of ^{3}H-proline incorporation were determined on a 300SL beta counter (cpm).

3.3.2 Measurement of neonatal cardiac myocyte hypertrophy

^{3}H-leucine incorporation was used as described previously [166], as described in section 2.3.3 was used to determine whether exogenous dhS1P and S1P induced NCM hypertrophy. Briefly, NCMs were pre-treated for 2 h at similar doses of W and W146 as used in NCF and treated with S1P (1μM) and dhS1P (3.0μM) at predetermined time points of 60 h and 48 h, respectively.

3.3.3 Measurement of cell viability in rat NCFs and NCMs

Cell viability was measured as described in section 2.3.4

3.3.4 Quantitative measurement of protein levels in NCFs and NCMs

Western blotting was performed as described in section 2.3.5, to investigate the expression of specific proteins related to the PI3K/Akt signalling pathway and cardiac remodelling. The blots were probed for phosphorylated Akt, mTOR, rpS6, and SMAD2 from Cell Signalling Technologies (CST, Danvers, MA, USA:4060L, 5536T, 5364T, and 3108L). They were also probed for TGFβ, and connective tissue growth factor (CTGF), Coll I, TIMP1, and α-SMA. Proteins were normalized to or β-Actin.

3.3.5 Quantitative measurement of genes expressed in cardiac remodelling

RT PCR was performed as described in section 2.3.7, to ascertain the changes in gene expression induced by dhS1P, S1P and SEW2871. The gene expression levels of the fibrotic markers; TGFβ, CTGF, TIMP1, Coll1a1, the S1PR1-3, and the sphingolipid enzymes SK1 and DEGS1 were quantified. The gene expression levels of pro-hypertrophic markers such as ANP & BNP, βMHC, α-SKA, GATA binding protein 4 (GATA4) and glycogen synthase kinase 3 β (GSK3β) were also quantified. Refer to appendix 1.1 for full sequence of primers. 18s mRNA was used as the endogenous controls.

3.3.6 Statistical Analysis

Similar statistical methods as used in section 2.3.8 were applied.

3.4 Results

3.4.1 Inhibition of PI3K led to reduction of dhS1P & S1P induced collagen synthesis

One of the hallmarks of fibrosis in tissues including the heart is exacerbated collagen synthesis by cells such as fibroblasts. In chapter 2, it was shown that dhS1P and S1P at doses of 3 μM and 1 μM induced collagen synthesis in primary NCFs [200]. Whether this increased collagen synthesis could be reduced by inhibiting the PI3K/Akt pathway, using a potent PI3K inhibitor (W), was investigated here. The results in Figure 3.1 show that wortmannin was able to inhibit both dhS1P (p < 0.01- 0.001, Figure 3.1A) & S1P (p <0.01- 0.001, Figure

3.1B) induced collagen synthesis in a dose dependent manner. Whether Inhibition of PI3K in NCFs treated with the S1PR1 agonist, SEW2871, could reduce collagen synthesis, was also investigated. As shown in Figure 3.1C, wortmannin significantly reduced SEW2871 (p <0.0001) induced collagen synthesis at all doses tested. The viability of NCFs exposed to wortmannin alone, was reduced at the highest dose (10 μM, p <0.01, Figure 3.1D). Since reductions in cell viability could have non-specific inhibitory effects on collagen synthesis, the viability of cells in the presence of both wortmannin and dhS1P was tested. The results showed that cell viability was not reduced in cells treated with wortmannin in the presence of either dhS1P or S1P as shown in Figure 3.1E and F, respectively. Thus, the reduced collagen synthesis can be attributed to PI3K inhibition.

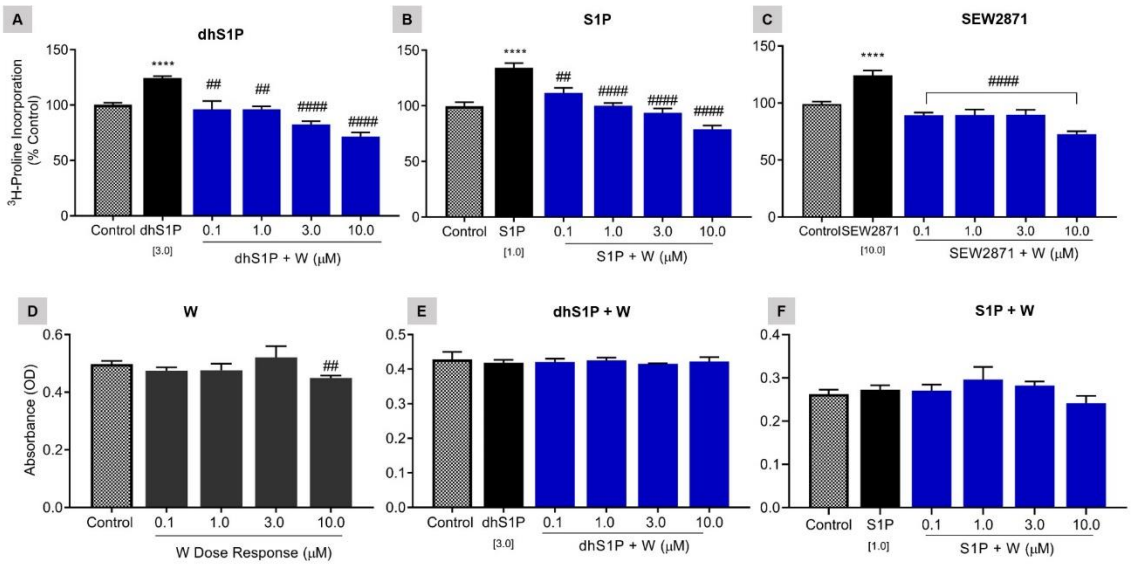

Figure 3.1. Inhibition of PI3K by wortmannin reduces dhS1P, S1P & SEW2871 induced collagen synthesis. Collagen synthesis by (A) 3 μM dhS1P and (B) 1 μM S1P was dose dependently reduced in NCFs treated with wortmannin for 48 h. (C) W also inhibited 10 μM SEW2871 induced collagen synthesis. (D) The viability NCFs was reduced by wortmannin at the highest dose (10 μM), but there was no effect on the viability of NCFs in the presence of (E)

dhS1P and (F) S1P for 48 h. $^{\#}p$ <0.05, $^{\#\#}p$ <0.01, $^{\#\#\#}p$ <0.005, $^{\#\#\#\#}p$ <0.001 vs. dhS1P/S1P/SEW2871, $^{**}p$ <0.01, $^{***}p$ <0.005, $^{***}p$ <0.001 vs. Control. Data are presented as ± SEM of 3 replicates.

3.4.2 DhS1P and S1P activate PI3K/Akt signalling

The PI3K/Akt- mTOR pathway is a critical pathway involved in cell proliferation, differentiation, metabolism and survival [215]. Western blot assays were conducted to determine if known PI3K/Akt- mTOR related signalling pathway proteins were perturbed by the inhibition of PI3K in the presence dhS1P and S1P. Both dhS1P (Figure 3.2B, p <0.01) and S1P (Figure 3.2F, p <0.05) increased the phosphorylation of Akt at 12 minutes in NCFs. S1P also increased phosphorylation of mTOR (Figure 3.2E, p <0.05) and RPS6 (Figure 3.2G, p < 0.05) at this time point, but dhS1P did not. In NCFs pre- treated for 2 h with the highest doses of wortmannin (3 & 10 μM), there was complete obliteration of phosphorylated Akt (Figure 3.2B and F, p <0.0001). wortmannin also reduced mTOR phosphorylation in NCFs in the presence of dhS1P (Figure 3.2A, p <0.01) and S1P (Figure 3.2E, 3 μM; p <0.01, 10 μM; p <0.05). Furthermore, wortmannin reduced phosphorylation of RPS6, which is downstream of mTOR in both dhS1P (Figure 3.2C, 3 μM; p <0.01, 10 μM; p <0.001) and S1P (Figure 3.2G, p <0.01) treated NCFs.

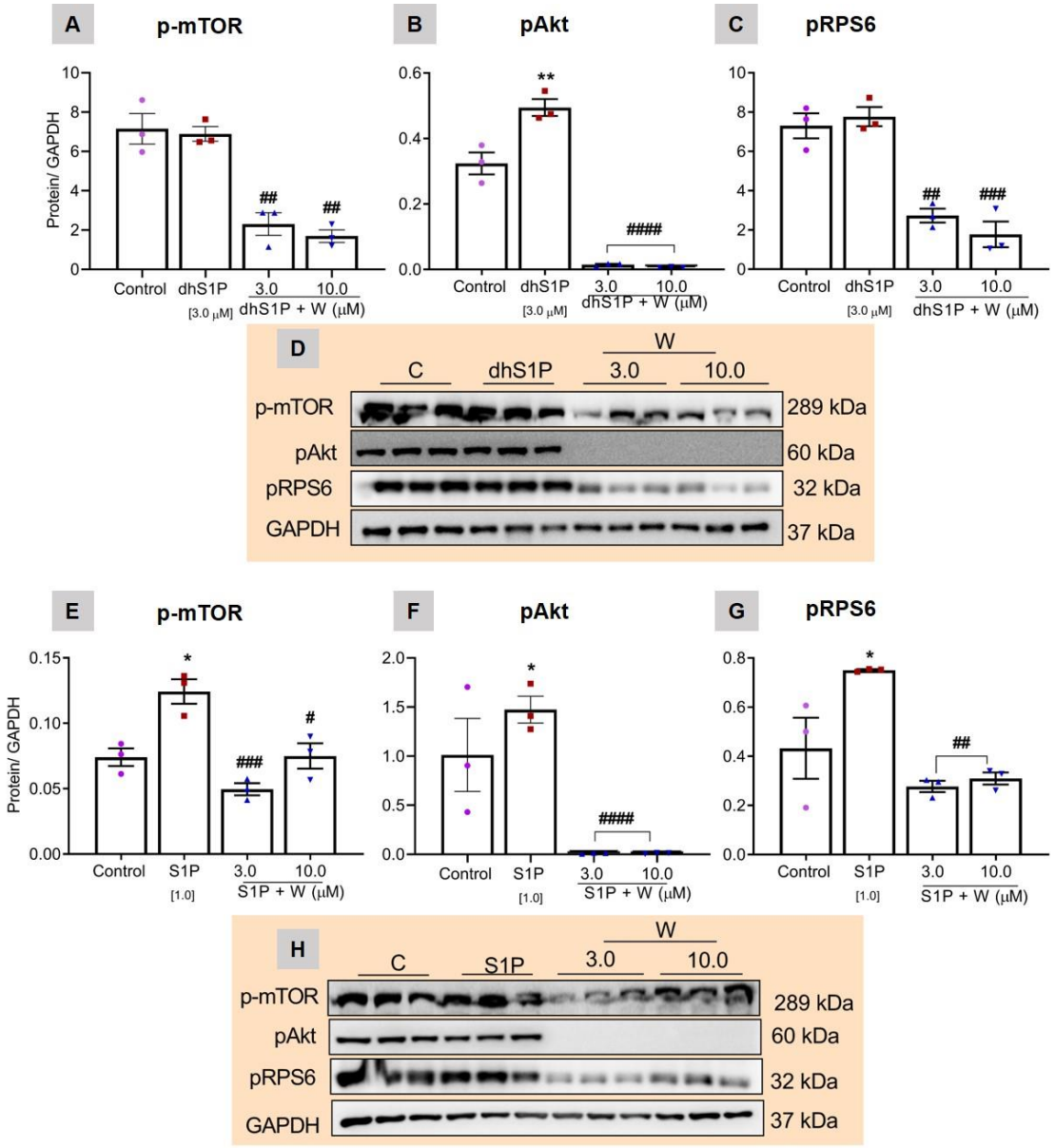

Figure 3.2. Activation of PI3K/Akt signalling by dS1P and S1P. In NCFs, 12 minutes of treatment with 3 μM dhS1P (A) did not increase the level of p-mTOR, (B) significantly phosphorylated Akt, (C) and had no effect on pRPS6. These were reduced in NCFs pre- treated with wortmannin for 2 h (3 μM and 10 μM). S1P (1 μM) increased phosphorylation of (E) mTOR, (F) Akt, and (G) RPS6 in NCFs at 12 minutes. Pre- treatment with wortmannin significantly reduced them. (D and H) Representative blots. $^{*}p$ <0.05, $^{**}p$ <0.01 vs. Control, $^{\#}p$ <0.05, $^{\#\#}p$ <0.01, $^{\#\#\#}p$ <0.005, $^{\#\#\#\#}p$ <0.001 vs. dhS1P. Data are presented as ± SEM of 3 replicates.

3.4.3 DhS1P modulates protein expression of TGFβ and Collagen I through PI3K/Akt Signalling

Since PI3K inhibition was able to reduce collagen synthesis stimulated by dhS1P, its effect on the expression of the fibrotic protein, TGFβ, in NCFs at 24 h was investigated. The results in Figure 3.3 shows that dhS1P increase all TGFβ isoforms. The expression level of latent 65 kDa (Figure 3.3A, p <0.005) and 45 kDa (Figure 3.3B, p <0.05) isoforms, and the mature 25 kDa isoform were increased by dhS1P (Figure 3.3C, p < 0.05), but had no significant effect on the active 12 kDa isoform (Figure 3.3D). PI3K inhibition significantly reduced 65 kDa TGFβ dose dependently (p <0.01 & p <0.005) and 25 kDa TGFβ at the highest dose (10 μM, p <0.05). However, it had no effect on the 45 kDa isoform.

The effect of S1P (1 μM) on TGFβ isoforms with kDa of 65, 45 and 25 (Figure 3.3H- J) were not significant. PI3K inhibition did significantly reduce the 65 kDa and 25 kDa proteins significantly. Even though S1P significantly increased the 12 kDa TGFβ isoform, it's inhibition by wortmannin did not reach statistical significance. The increased Coll1 protein expression by dhS1P at 24 h was not significant (Figure 3.3E). This was significantly reduced by PI3K inhibition (3 μM; p <0.05, 10 μM; p <0.01). PI3K inhibition also led significant reductions in Coll 1 (3 and 10 μM; p <0.01) protein expression raised by S1P in NCFs (Figure 3.3L, p <0.05).

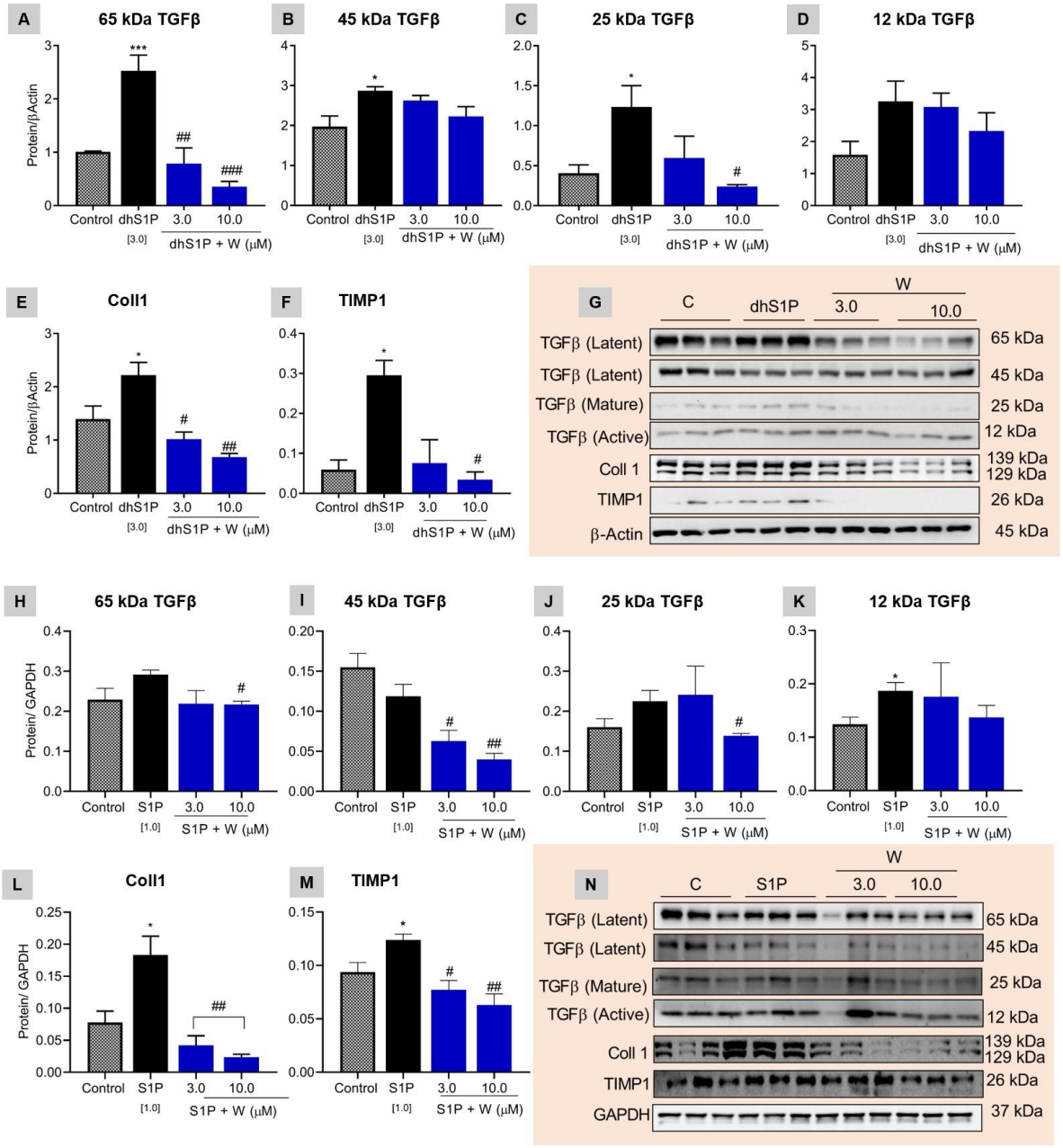

Figure 3.3. Modulation of TGFβ & Collagen I by dhS1P and S1P through PI3K/Akt signalling. 24 h treatment of NCFs with dhS1P (3 μM) increased protein level of (A) 65 kDa, (B) 45 kDa, (C) 25 kDa, and (D) 12 kDa TGFβ protein isoforms. It also increased (E) Coll 1 and, (F) TIMP1 protein expression. These were reduced dose dependently when PI3K was inhibited by wortmannin. S1P (1 μM) (H) slightly increased 65 kDa, (I) had no effect on 45 kDa, (J) increased 25 kDa, and (K) 12 kDa TGFβ isoforms. S1P also increased (L) coll 1, and (M) TIMP1 protein levels. These were reduced by wortmannin. (G and N)

Representative blots. $^{****}p$ <0.001, $^{*}p$ <0.05 vs. Control, $^{###}p$ <0.001, $^{##}p$ <0.01, $^{#}p$ <0.05 vs. dhS1P. Data are presented as ± SEM of 3 replicates.

3.4.4 Inhibition of PI3K/Akt signalling affects TIMP1 protein expression in NCFs

In chapter 2 it was shown that dhS1P and S1P signalling has an effect on TIMP1 protein expression in NCFs [200]. Here the effects of PI3K inhibition on TIMP1 protein expression was investigated. The results in Figure 3.3F shows that PI3K inhibition (p <0.05) significantly reduced dhS1P induced (p <0.05) increase in TIMP1 protein expression in NCFs. Similarly, PI3K inhibition (Figure 3.3M, 3 μM; p <0.05, 10 μM; p <0.01) significantly reduced S1P induced (p <0.05) TIMP1 protein expression.

3.4.5 S1PR1 inhibition does not reduce dhS1P/S1P - Akt Signalling

Furthermore, the effects of S1PR1 inhibition on Akt signalling were investigated, since **wortmannin** reduced the S1PR1 agonist, SEW2871, induced collagen synthesis. Inhibition of S1PR1 synergistically increased mTOR phosphorylation by dhS1P (Figure 3.4A, p < 0.01) and S1P (Figure 3.4E, p <0.05) in NCFs. S1PR1 inhibition in NCFs did not cause significant changes in RPS6 phosphorylation in the presences of both dhS1P and S1P (Figure 3.4C and 3.4G). However, S1PR1 inhibition synergistically increased Akt phosphorylation Figure 3.4F, p <0.05) in the presence of S1P. There was no difference in Akt phosphorylation (Figure 3.4B) when S1PR1 was inhibited in the presence of dhS1P.

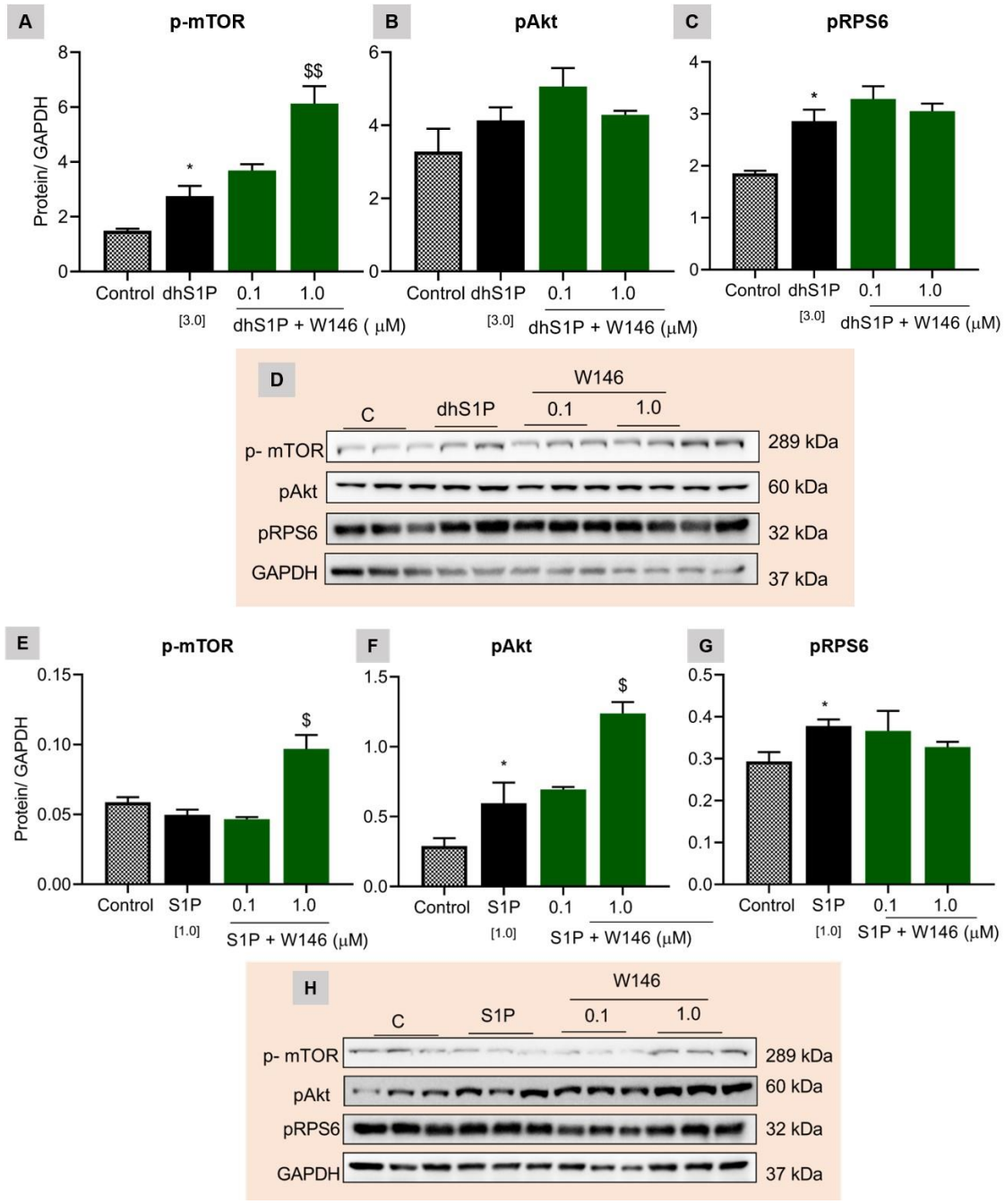

Figure 3.4. Effect of S1PR1 inhibition on Akt signalling. Inhibition of S1PR1 by pre- treating with W146 (A) synergistically increased phosphorylation of mTOR, (B) and had no effect on Akt, and (C) RPS6 in NCFs treated with dhS1P (3 μM) for 12 minutes. In S1P (1 μM) treated NCFs, inhibition of S1PR1 synergistically increased (E) p-mTOR, and (F) pAkt, (G) but had no effect on pRPS6. (D and H) representative blots. $^{\$\$}p$ <0.01, $^{\$}$p<0.05 vs. treatment. $^{*}p$ <0.05, $^{\#}p$ <0.05 vs. Control. Data are presented as ± SEM of 3 replicates.

3.4.6 DhS1P increases mRNA expression of TIMP1 through PI3K/Akt Pathway

The effect on PI3K inhibition on the expression of genes involved in fibrosis such as TGFβ1, Coll 1, CTGF, MMP2, TIMP1 and TIMP2 were investigated. The results in Figure 3.5A show that inhibition of the PI3K/Akt pathway had significant reductive effect on TIMP1 mRNA transcription but not on TGFβ1, CTGF, Coll1, and TIMP2 mRNA levels at 6 h treatment in NCFs. At this time point dhS1P increased TGFβ1 (p <0.0001, Figure 3.5A) and CTGF (p <0.05) mRNA levels significantly but had no effect on Coll1a1 and TIMP2. MMP2 mRNA levels also trended downward in the presence of dhS1P, which was significant when the ratio of MMP2 to TIMP1 was measured (p <0.005, Figure 3.5A). In NCFs treated with wortmannin, the MMP2 to TIMP1 ratio improved significantly (3 μM, p <0.05).

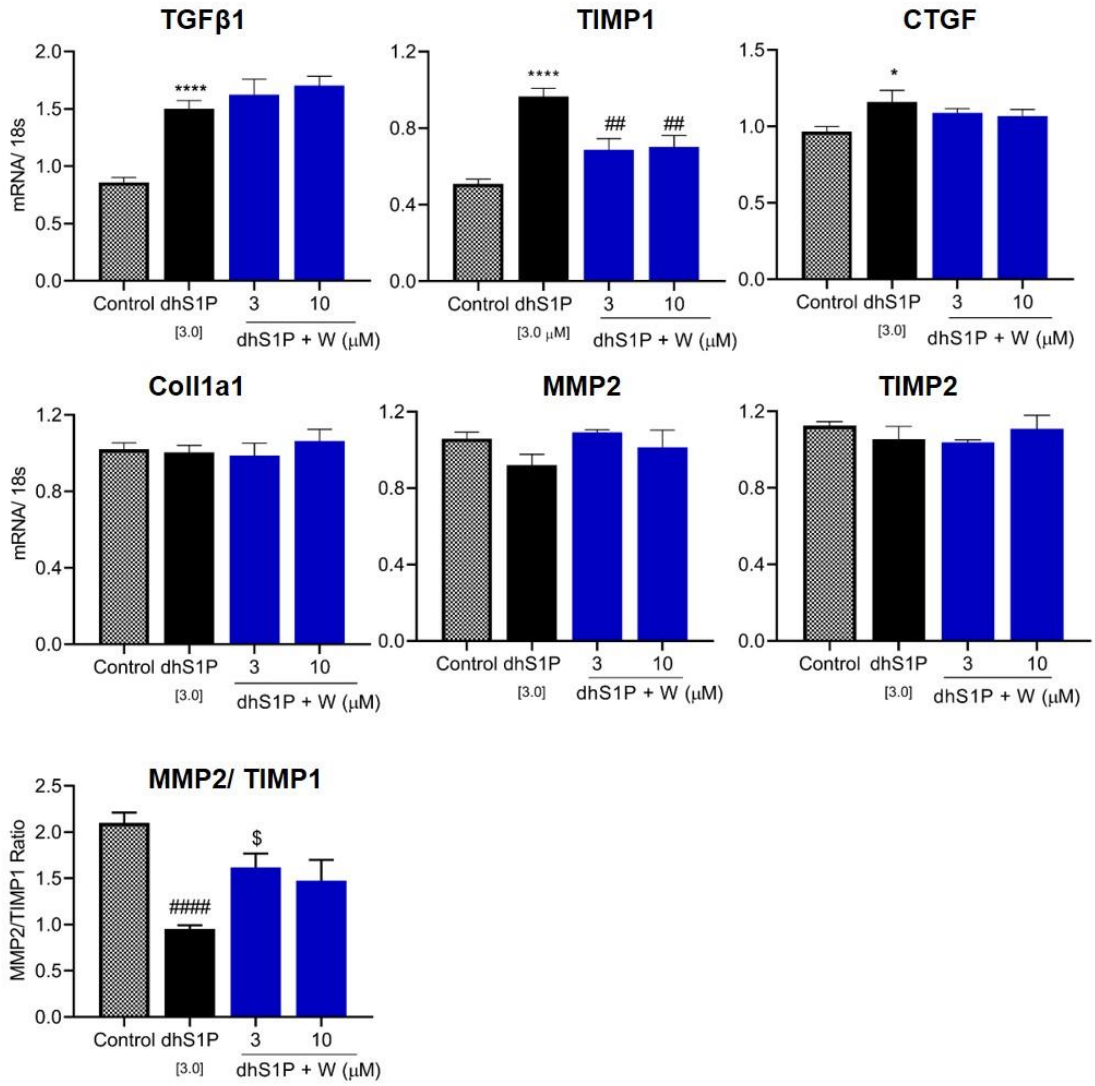

Figure 3.5. Effect of PI3K inhibition on mRNA levels in NCF. Inhibition of PI3K by wortmannin reduced TIMP1 mRNA levels raised by dhS1P at 6 h treatment, but had no effect on TGFβ1, CTGF, Coll1, MMP2, and TIMP2 mRNA levels. While PI3K inhibition increased the MMP2/TIMP1 ratio reduced by dhS1P. $^{****}p$ <0.001, $^{*}p < 0.05$ vs. Control, $^{\#\#\#}p < 0.001$, $^{\#\#}p < 0.01$ vs. treatment, $^{\$}p < 0.05$ vs. treatment. Data presented as ± SEM of 3 replicates.

3.4.7 PI3K inhibition reduced TIMP1 mRNA expression in NCFs treated with S1P and SEW2871

The effect of PI3K inhibition on S1P and SEW2871 induced mRNA levels were also investigated. TIMP1 and TGFβ1 mRNA transcription levels were significantly raised in cells treated with S1P (Figure 3.6A) and SEW2871 (Figure 3.6B). PI3K inhibition had significant dose dependent inhibitory effects on S1P ($p < 0.001$, Figure 3.5B) and SEW2871 ($p < 0.0005$, Figure 3.6B) induced TIMP1 mRNA transcription levels. The results in Figure 3.6 also shows that PI3K inhibition did not reduce the expression of Coll1a1, TGFβ1 and TIMP2 raised by SEW2871, or TGFβ1 raised by S1P. These imply that dhS1P and S1P mediated PI3K/Akt signalling through S1PR1 affects TIMP1 mRNA levels but not TGFβ1.

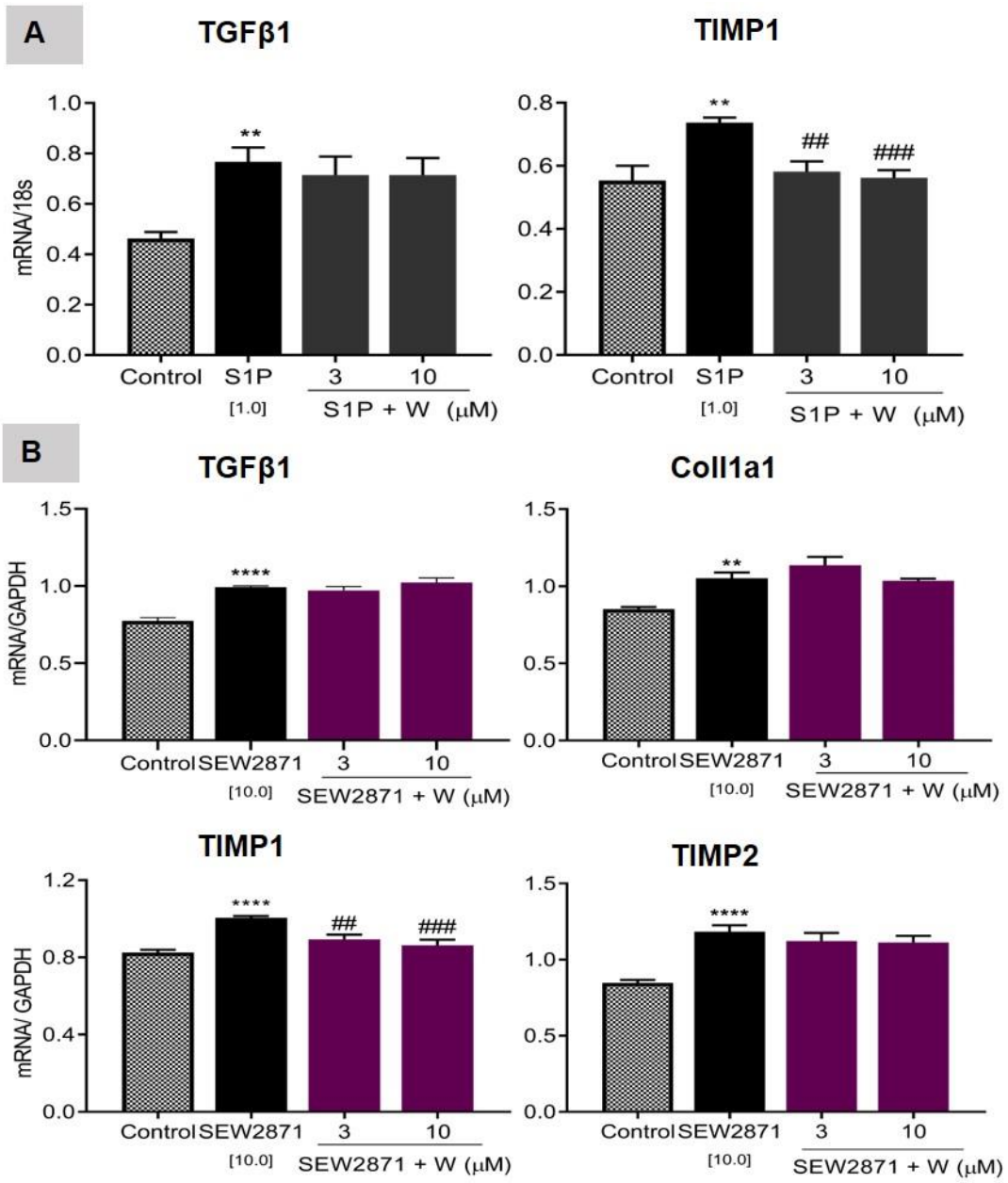

Figure 3.6. Effect of PI3K inhibition on mRNA levels in S1P and SEW2871 treated NCF. (A) PI3K inhibition also reduced S1P induced TIMP1 mRNA expression but had no effect on TGFβ1 at 6 h. (B) In NCFs treated for 18 h with SEW2871, PI3K inhibition had no effect on Coll1a1, TGFβ1 and TIMP2 mRNA expression, but reduced TIMP1 significantly. $^{****}p$ <0.001, $^{**}p < 0.01$, $^{*}p < 0.05$ vs. Control, $^{###}p < 0.001$, $^{##}p < 0.01$, $^{#}p < 0.05$ vs. treatment. Data presented as ± SEM of 3 replicates.

3.4.8 Inhibiting PI3K increases GSK3β and GATA4 mRNA in NCFs treated with dhS1P

Increased activation of the PI3K/Akt pathway is known to inactivate GSK3β by phosphorylating it, allowing increased cell metabolism, protein synthesis and proliferation [216, 217]. The effects of PI3K inhibition on GSK3β gene expression in the presence of dhS1P was also explored. Inhibiting PI3K significantly increased the expression of GSK3β mRNA levels at the higher dose (10 μM; $p < 0.05$, Figure 3.7A). However, the S1PR1 antagonist, W146, had no effect on GSK3β mRNA and GATA4 mRNA levels (Figure 3.7B). GATA4 in cardiac cells is linked to the cross talk between cardiac fibroblasts and myocytes in relation to the level of natriuretic peptides and negatively regulates PI3K [218, 219]. Treatment of NCFs with dhS1P significantly raised GATA4 mRNA levels (10 μM; $p < 0.0001$) when PI3K was inhibited, Figure 3.7A.

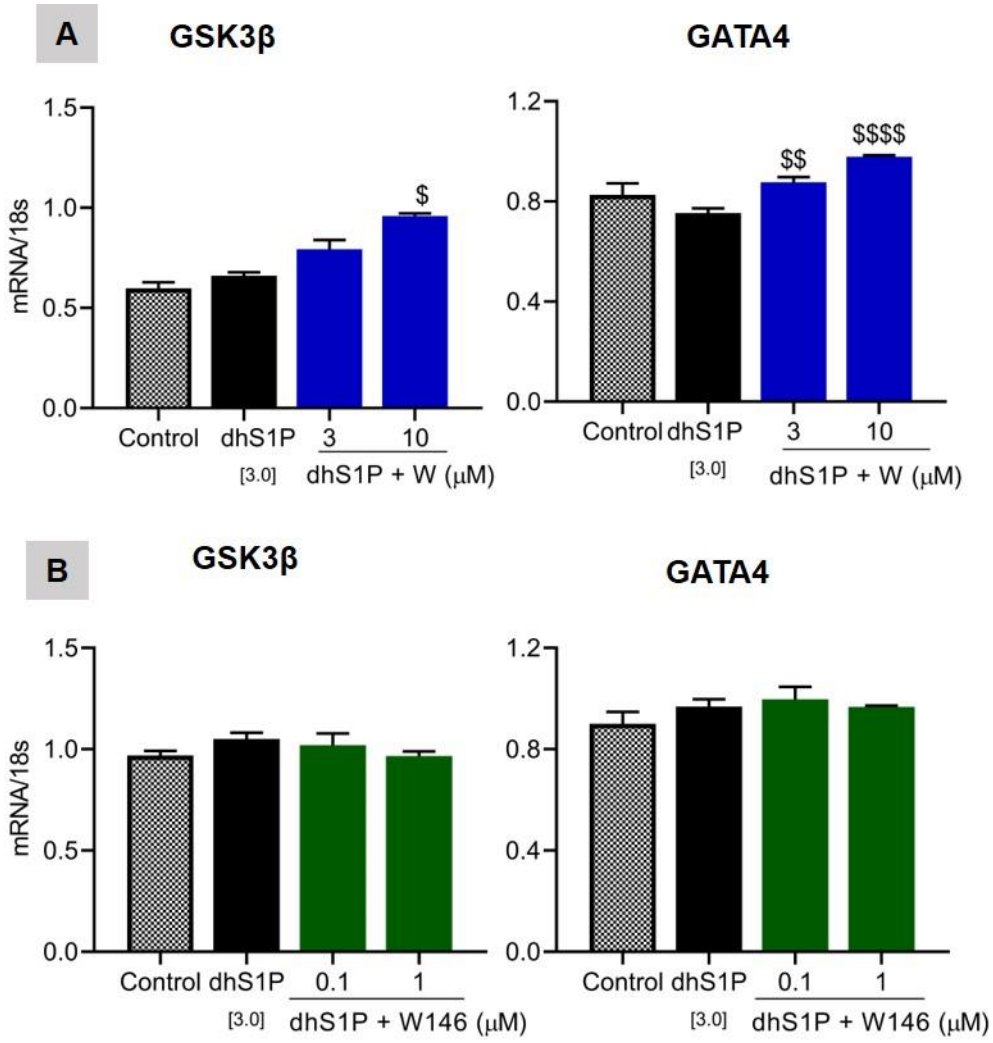

Figure 3.7. Effect of PI3K and S1PR1 inhibition on GSK3β and GATA4 mRNA levels in NCF. (A) PI3K inhibition significantly increased the level of GSK3β and GATA4 mRNA at 10 μM in the presence of dhS1P. (B) W146 had no effect on GSK3β and GATA4 mRNA levels. $^{\$\$\$}p < 0.001$, $^{\$\$}p < 0.01$, $^{\$}p < 0.05$ vs. treatment. Data presented as ± SEM of 3 replicates.

3.4.9 DhS1P activated sphingolipid related genes were altered by PI3K inhibition

Others have shown that Akt interacts with the sphingolipid pathway [220, 221], therefore, here the effects of PI3K inhibition on other sphingolipid related genes was explored. Figure 3.8A shows that inhibition of PI3K in dhS1P treated NCFs led to significant reductions in the S1P receptors; S1PR1 ($p < 0.05$), S1PR2 ($p < 0.01$) and S1PR3 ($p < 0.0001$), Figure 3.8A. PI3K inhibition also reduced SK1 mRNA expression significantly ($p < 0.01$). DEGS1 encodes the gene for DES1 enzyme. This enzyme is responsible for converting dihydroceramide to ceramide in the *de novo* sphingolipid synthesis pathway [100]. There were significant elevations in DEGS1 mRNA ($p < 0.05$) expression When PI3K was inhibited. However, dhS1P did not influence DEGS1 mRNA expression.

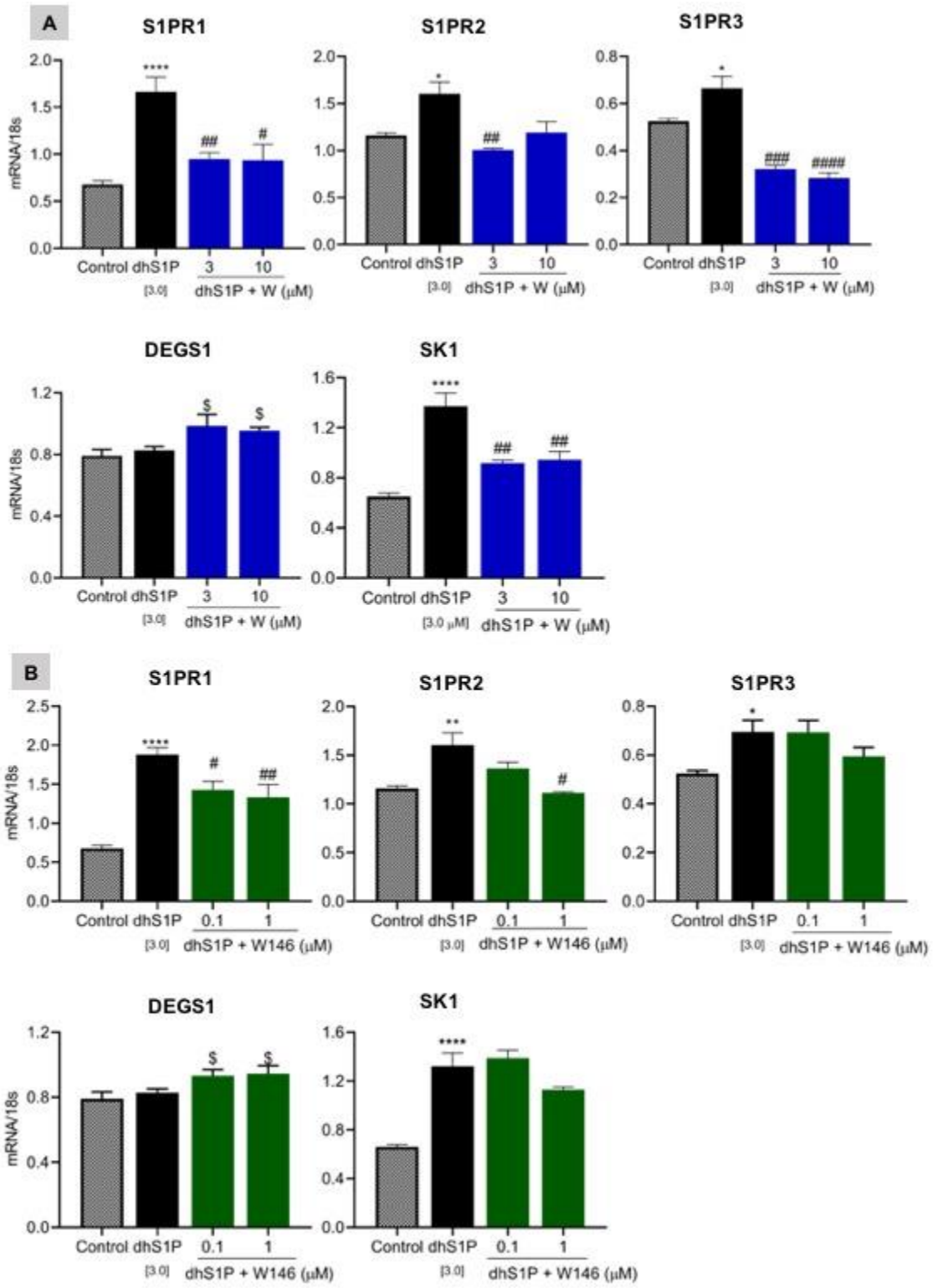

Figure 3.8. Effect of PI3K and S1PR1 inhibition on sphingolipid related genes in NCF. (A) Inhibition of PI3Ks by wortmannin reduced S1PR1, S1PR2, S1PR3, and SK1 mRNA levels raised by dhS1P at 6 h treatment, and increased

DEGS1 mRNA levels. (B) S1PR1 inhibition did not affect SK1 and S1PR3 mRNA levels. It did reduce S1PR1, and S1PR2 mRNA levels, and increased DEGS1 mRNA levels. $^{****}p < 0.001$, $^{**}p < 0.01$, $^{*}p < 0.05$ vs. Control, $^{\#\#\#}p < 0.001$, $^{\#\#}p < 0.01$, $^{\#}p < 0.05$, $^{\$}p < 0.05$ vs. treatment. Data are presented as ± SEM of 3 replicates.

3.4.10 S1PR1 inhibition affects the expression of sphingolipid related genes in NCFs

Although S1PR1 is less abundant in NCFs, the results showed that PI3K inhibition did affect genes increased by the S1PR1 agonist, SEW2871, in NCFs. Therefore, the effect of S1PR1 on other enzymes and receptors related to sphingolipids were investigated. Figure 3.8B shows that inhibition of S1PR1 by its receptor antagonist, W146, reduced S1PR1 mRNA expression significantly in a dose dependent manner ($p < 0.001$). Additionally, it was noted that W146 reduced the expression of S1PR2 mRNA levels significantly at the highest dose (1 μM, $p < 0.05$), but not S1PR3. The mRNA expression of SK1 was also significantly reduced when S1PR1 was inhibited ($p < 0.05$). Additionally, there was a significant synergistic effect on DEGS1 mRNA levels ($p < 0.05$). These results are comparable to that seen in PI3K inhibition implying the S1PR1/2-PI3K signalling pathway indirectly influences the transcription levels of SK1 and DEGS1.

3.4.11 Inhibition of PI3K/Akt signalling reduces dhS1P & S1P induced myocyte hypertrophy

Furthermore, the effect of PI3K inhibition in primary cardiac myocytes treated with dhS1P and S1P were investigated. There was increased hypertrophy of myocytes in both dhS1P and S1P at 48 h ($p < 0.01$, Figure 3.7A) and 60 h ($p < 0.001$, Figure 3.7B) of treatment, respectively. These were significantly reduced when PI3K was inhibited by wortmannin at the higher doses (1.0 μM, $p < 0.01$; 3.0 μM, $p < 0.05$; & 10.0 μM, $p < 0.01$), in dhS1P treated cells. In S1P treated cells, PI3K inhibition also reduced myocyte hypertrophy significantly (3.0 μM, $p < 0.05$, & 10.0 μM $p < 0.01$). There were no effects on the viability of NCMs treated exclusively with wortmannin at 0.1, 1.0, 3.0, & 10.0 μM (Figure 3.7E). Additionally, combined treatment of NCMs with wortmannin, and either dhS1P (Figure 3.7C) or S1P (Figure 3.7D) had no significant effect on cell viability.

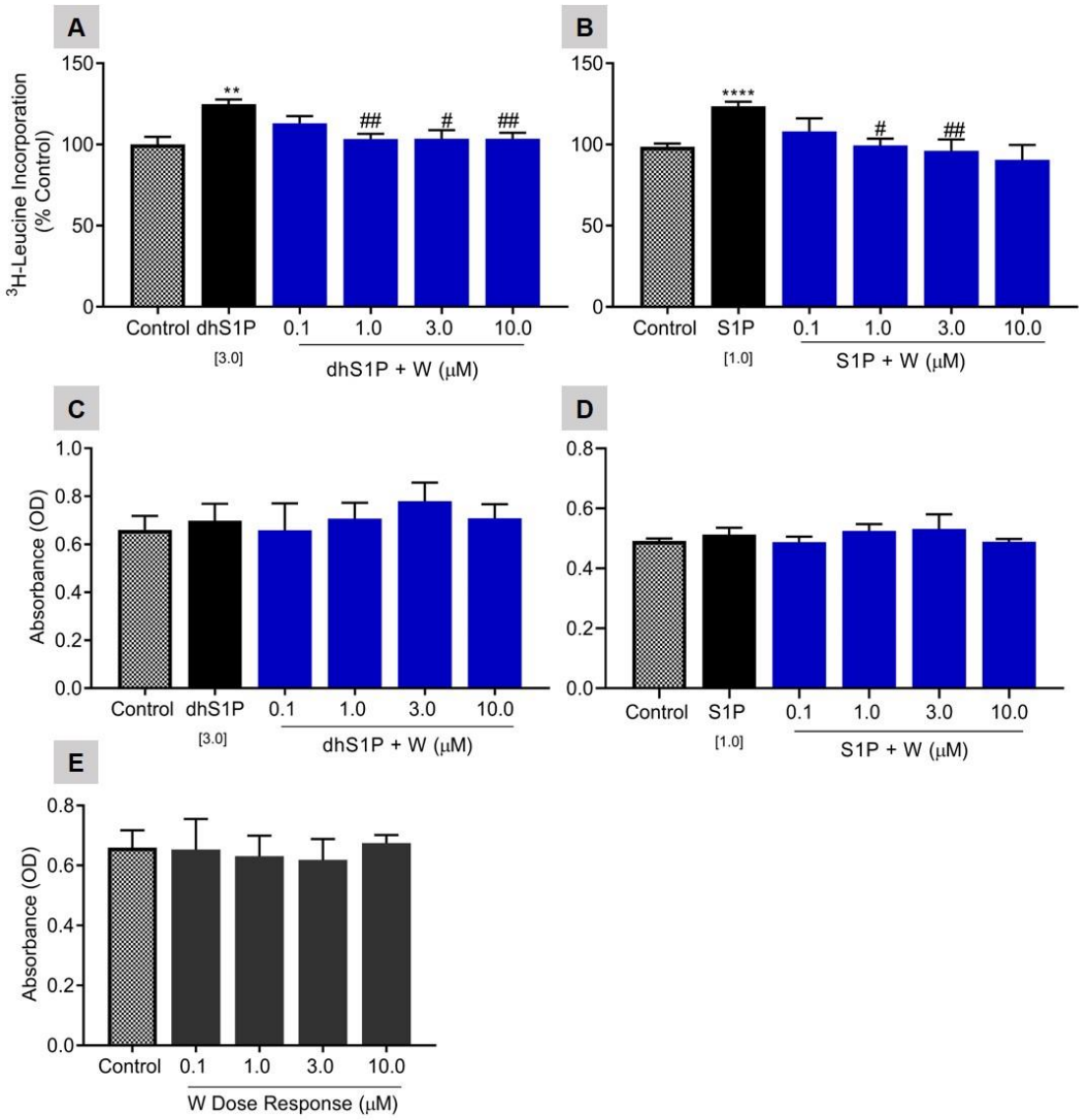

Figure 3.9. Involvement of PI3K in dhS1P & S1P induced myocyte hypertrophy. PI3K inhibition reduced (A) dhS1P (3 μM) induced myocyte hypertrophy at 48 h and (B) S1P (1 μM) at 60 h. The viability of NCMs treated with wortmannin in the presence of (C) dhS1P and (D) S1P did not change at 48 h and 60 h of treatment. (E) NCM viability in the presence of wortmannin at 60 h was not affected. $^{****}p < 0.001$, $^{***}p < 0.005$, $^{**}p < 0.01$ vs. Control, $^{###}p < 0.001$, $^{##}p < 0.01$, $^{#}p < 0.05$ vs. dhS1P & S1P. Data are presented as ±SEM of 4 replicates.

3.4.12 Wortmannin reduces PI3K/Akt- mTOR phosphorylation in the presence of dhS1P and S1P in NCMs

Next, the effect of PI3K inhibition on PI3K/Akt- mTOR pathway proteins in the presence of dhS1P in NCMs was investigated. PI3K inhibition led to significant reductions in the downstream phosphorylation of mTOR ($p < 0.0001$), RPS6 ($p < 0.001$), and completely abrogated Akt ($p < 0.0001$), Figure 3.9A. These results were comparable to those observed in S1P treated NCMs as shown in Figure 3.8B. However, 15 minutes treatment of NCMs with dhS1P did not show exacerbated effects on the phosphorylation of these protein in the PI3K/Akt- mTOR pathway, but S1P significantly phosphorylated Akt ($p < 0.05$) and RPS6 ($p < 0.05$). Indicating S1P as the more active analogue.

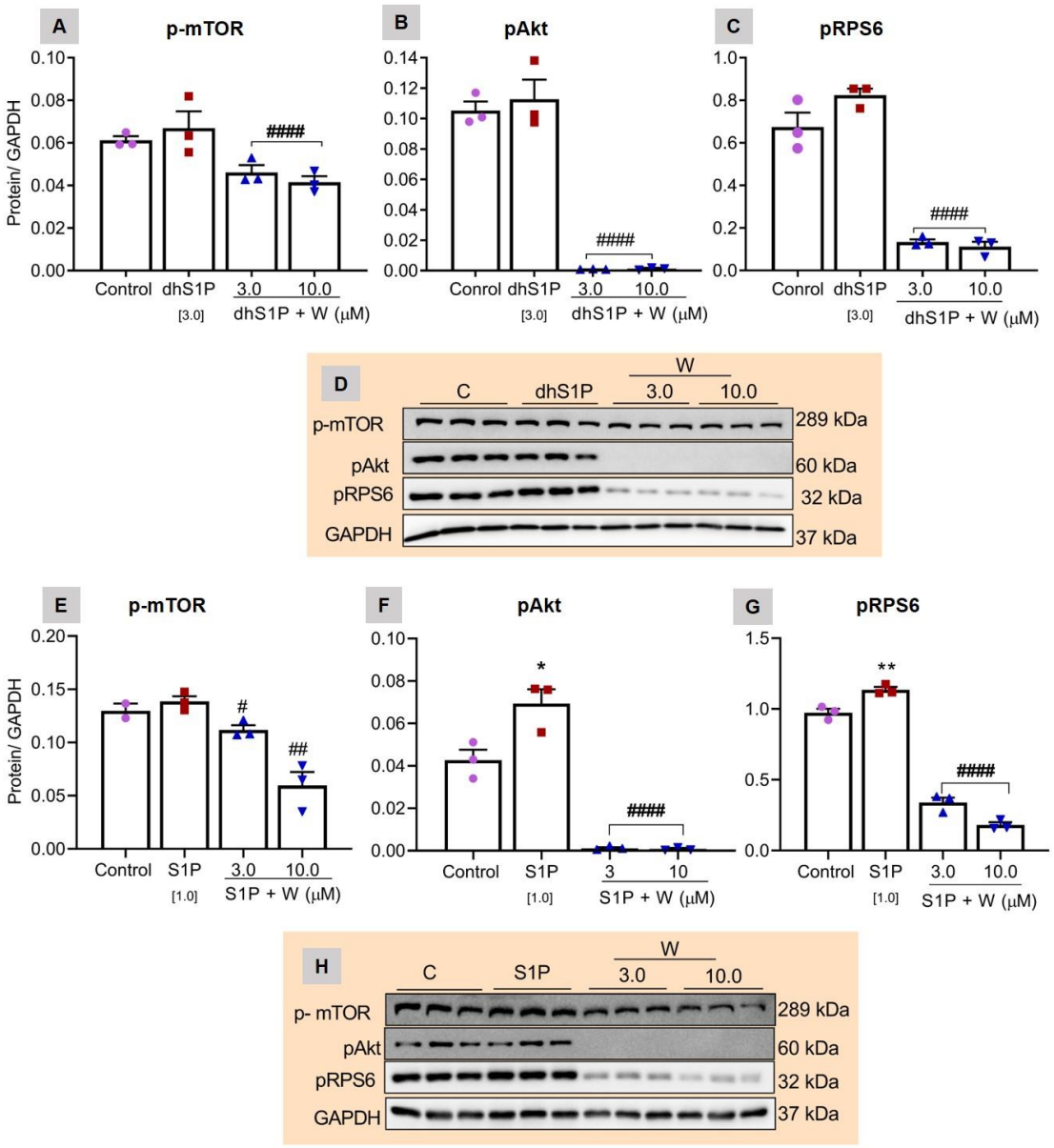

Figure 3.10. Effects of PI3K inhibition on PI3K/Akt- mTOR pathway proteins in NCMs. (A) Inhibition of PI3K in NCMs significantly reduced p-mTOR, pAkt, and pRPS6 in NCMs, but 15 minutes stimulation with dhS1P (3 μM) had no effect on them. (B) The significant increase in phosphorylation of Akt and RPS6 by S1P (1 μM) was notably reduced by wortmannin. $^{**}p < 0.01$, $^{*}p < 0.05$ vs. Control, $^{\#\#\#}p < 0.001$, $^{\#}p < 0.05$ vs. dhS1P & S1P. Data are presented as ±SEM of 3 replicates.

3.4.13 S1PR1 inhibition reduced RPS6 phosphorylation in both dhS1P and S1P treated NCMs

Furthermore, the effects of S1PR1 inhibition on the PI3K/Akt- mTOR signalling pathway in NCMs was explored. Figure 3.11 shows that S1PR1 inhibition by W146 significantly reduced phosphorylation of RPS6 in the presence of dhS1P (0.1 μM; p <0.05, 1.0 μM; p <0.01, Figure 3.11A,) and S1P (1.0 μM; p < 0.05, Figure 3.11B). Inhibiting S1PR1 had no effect on mTOR and Akt phosphorylation in both treatments at 15 minutes.

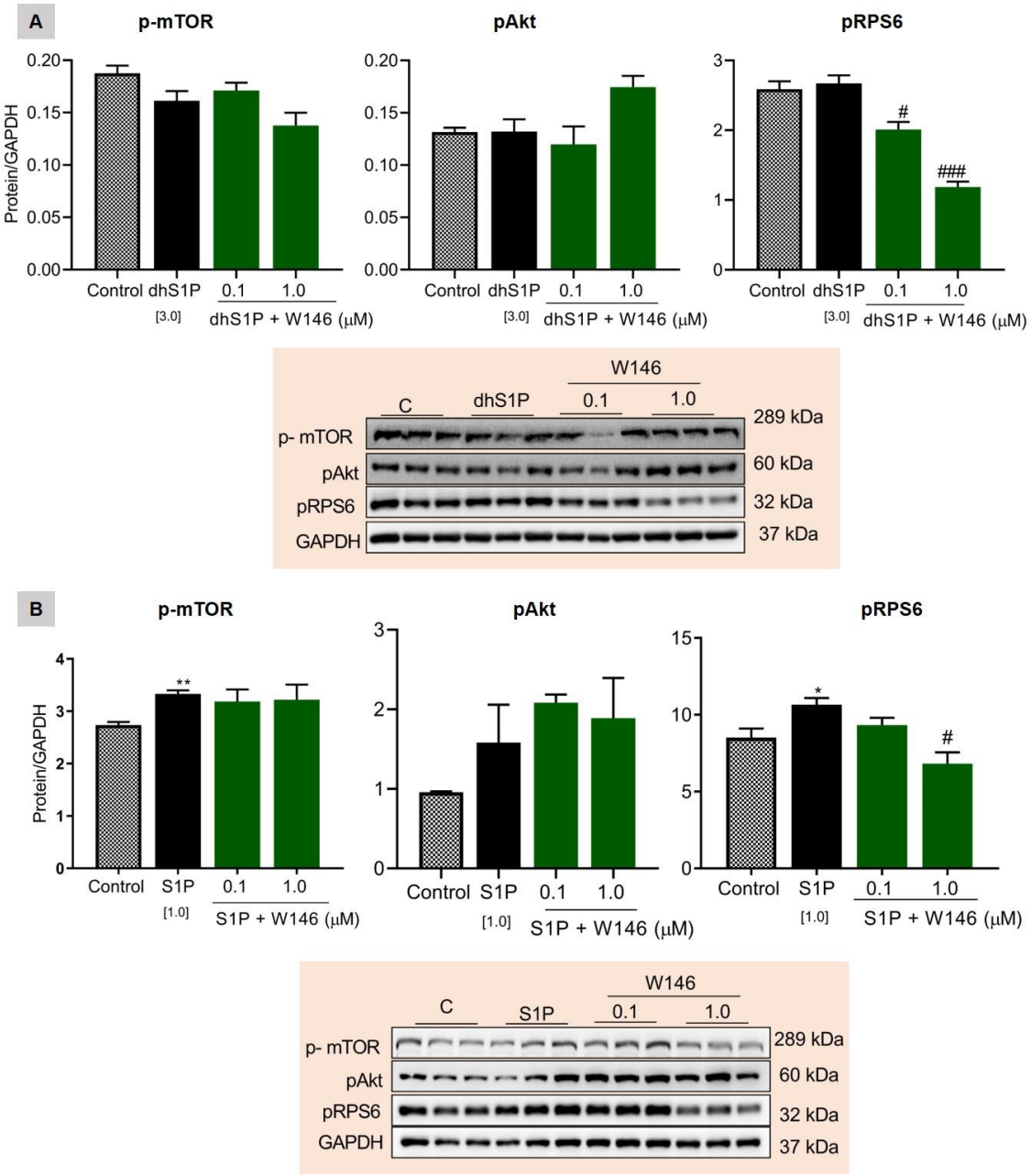

Figure 3.11. Effects of S1PR1 inhibition on PI3K/Akt- mTOR pathway proteins in NCMs. (A) Inhibition of S1PR1 by W146 reduced pRPS6 (0.1 μM and 1.0 μM), but not p-mTOR and pAkt in dhS1P stimulated cells. (B) S1P increased phosphorylation of RPS6, and mTOR. Inhibition of S1PR1 reduced RPS6 but not mTOR and Akt. $^{**}p < 0.01$, $^{*}p < 0.05$ vs. Control, $^{###}p < 0.001$, $^{\#}p < 0.05$ vs. dhS1P & S1P. Data are presented as ±SEM of 3 replicates.

3.4.14 Both S1P & dhS1P had synergistic effects on hypertrophic genes

The genetic effects of PI3K inhibition in dhS1P and S1P treated NCMs were explored. DhS1P (Figure 3.12A, $p < 0.0001$) and S1P (Figure 3.12B, $p < 0.0001$) significantly increased all the genes associated with myocyte hypertrophy (βMHC, ANP, BNP, and αSKA) at 18 h of treatment. Myocytes undergoing hypertrophy revert to expressing fetal genes such as βMHC, with proportional increase in antagonist genes such ANP and BNP [222, 223]. In cells treated with dhS1P, inhibiting PI3K had significant synergistic effect on βMHC (3 μM; $p < 0.05$), BNP (3 μM; $p < 0.05$), and ANP (3 & 10 μM; $p < 0.001$), while significantly reducing αSKA mRNA expression levels (3 μM; $p < 0.0005$, 10 μM; $p < 0.0001$). Similarly, in S1P treated cells, PI3K inhibition had synergistic effects on all the hypertrophic genes tested, including, βMHC (3 & 10 μM; $p < 0.0001$), BNP (3 μM; $p < 0.05$, 10 μM; $p < 0.0001$), ANP (3 μM; $p < 0.0005$, 10 μM; $p < 0.0001$), and αSKA (3 μM; 10 μM; $p < 0.0001$).

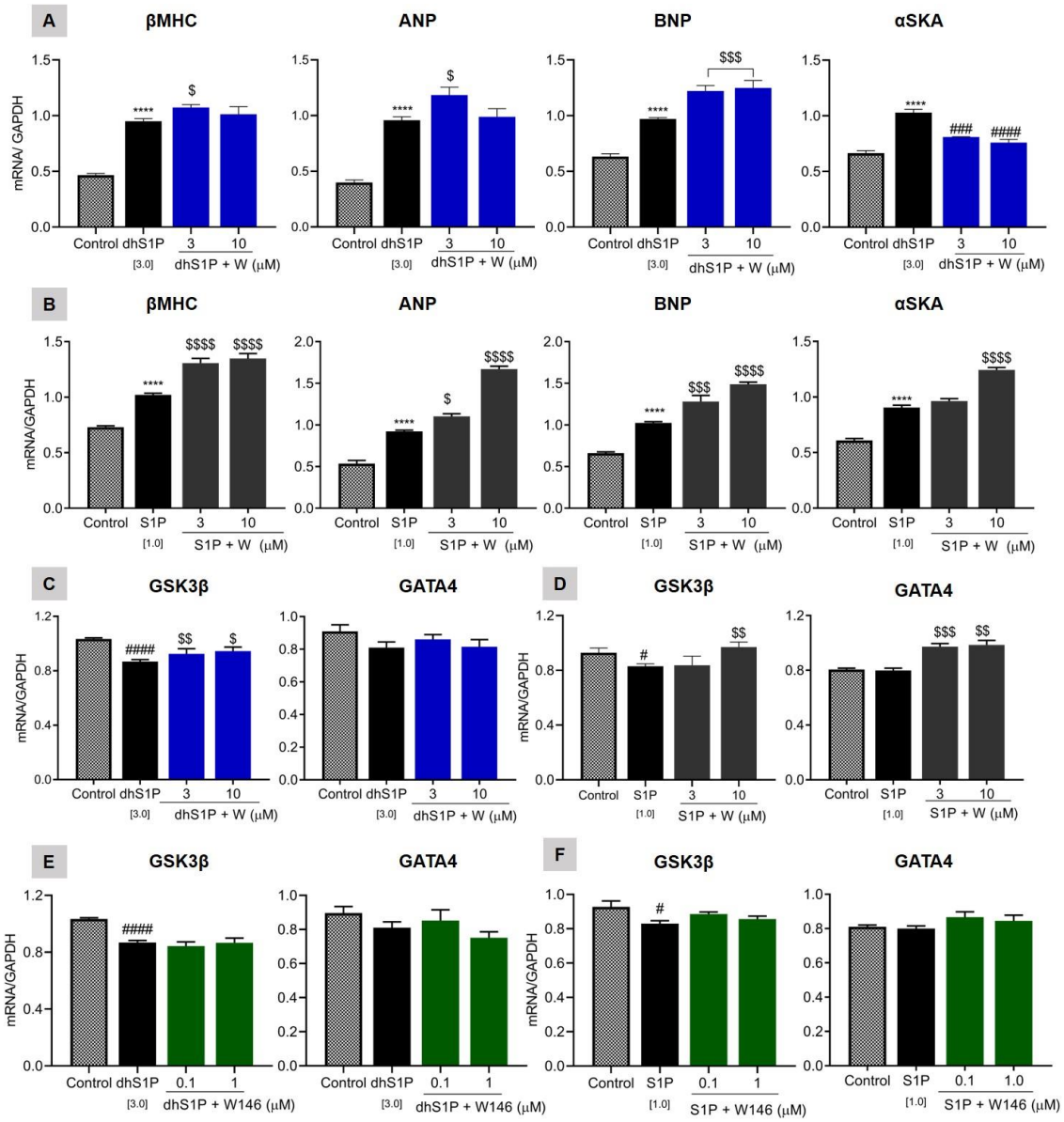

Figure 3.12. Effect of PI3K and S1PR1 inhibition on mRNA levels in NCM. (A) Inhibition of PI3K synergistically increased βMHC, BNP, ANP and reduced αSKA mRNA levels raised by dhS1P (3 μM) at 18 h of treatment. (B) PI3K inhibition synergistically increased all the hypertrophic genes in NCMs treated with S1P (1 μM) for 18 h. (C) DhS1P reduced GSK3β gene expression, this was recovered when PI3K was inhibited, but dhS1P had no effect on GATA4 mRNA levels. (D) PI3K inhibition augmented GATA4 mRNA and raised 1 μM S1P

reduced GSK3β. (E) S1PR1 inhibition by W146 had no effect on GSK3β and GATA4 mRNA levels in NCMs treated with dhS1P, and (F) S1P. $^{****}p < 0.001$, $^{**}p < 0.01$, $^{*}p < 0.05$ vs. Control, $^{\#\#\#}p < 0.001$, $^{\#\#}p < 0.01$, $^{\#}p < 0.05$, $^{\$\$\$\$}p < 0.0001$, $^{\$\$\$}p < 0.005$, $^{\$\$}p < 0.01$, $^{\$}p < 0.05$ vs. treatment. Data are presented as ± SEM of 3 replicates.

3.4.15 DhS1P altered GSK3β and GATA4 mRNA expression in NCMs

The transcription levels of GSK3β and GATA4 in NCMs were also analysed. GSK3β is a critical regulator of the cardiac myocyte cell cycle in embryogenesis, and its deletion results in hypertrophic cardiomyopathy [224]. DhS1P (3 μM) and S1P (1 μM) significantly reduced GSK3β mRNA transcription ($p < 0.0001$, and $p < 0.05$), these was rescued by PI3K inhibition (Figure 3.12B, 3 μM; $p < 0.001$, 10 μM; $p < 0.05$, and Figure 3.12C, 10 μM; $p < 0.0001$). The transcription factor, GATA4, is required for full activation of mechanical stress genes such as ANP and BNP [225]. Surprisingly, PI3K inhibition increased GATA4 expression in S1P treated (3 μM; $p < 0.001$, and 10μM; $p < 0.001$), but not dhS1P treated NCMs (Figure 3.12D). This is despite both dhS1P and S1P having no effect on GATA4 mRNA expression. S1PR1 inhibition had no effect on either GSK3β or GATAT4 mRNA levels in both dhS1P (Figure 3.12E) and S1P (Figure 3.12F) treated NCMs.

3.4.16 Sphingolipid related genes were reduced in PI3K and S1PR1 inhibited NCMs

The effects of PI3K and S1PR1 inhibition on the expression of DEGS1, SK1, and S1PR1 gene expression in NCMs at 18 h of treatment with dhS1P (3 μM) were compared. DEGS1 ($p < 0.05$), SK1 ($p < 0.01$), and S1PR1 ($p < 0.005$) mRNA levels were increased significantly by dhS1P in NCMs, Figure 3.13A-B. Inhibition of PI3K and S1PR1 had significant effect on these genes. DEGS1 (10 μM; $p < 0.05$), SK1 ($p < 0.05$) and S1PR1 ($p < 0.05$) were markedly reduced when PI3K was inhibited by wortmannin (Figure 3.13A). Similarly, marked reductions in DEGS1 (1 μM; $p < 0.05$), SK1 (0.1 μM; $p < 0.05$, 1 μM; $p < 0.01$) and S1PR1 (0.1 μM; $p < 0.05$, 1 μM; $p < 0.01$) transcription levels were observed when S1PR1 was inhibited in NCMs (Figure 3.13B).

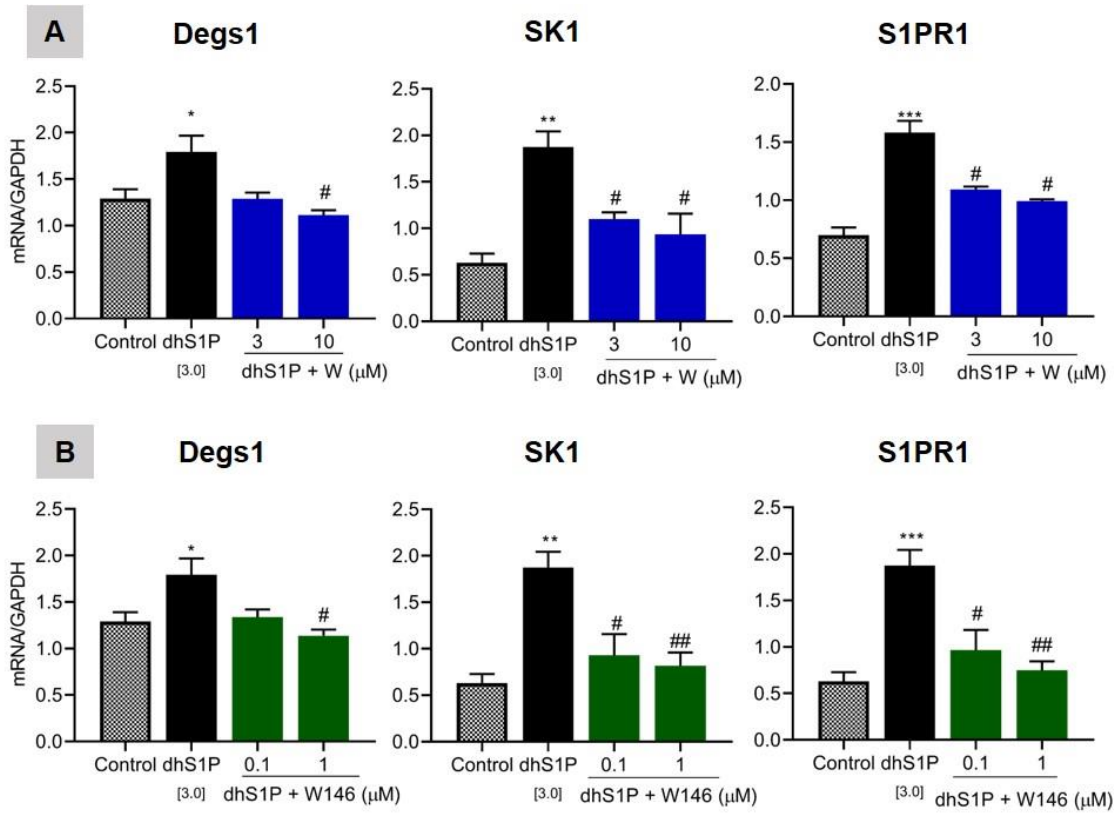

Figure 3.13. Effect of PI3K and S1PR1 inhibition on Sphingolipid related genes in NCM. (A) Inhibition of PI3K by wortmannin reduced DEGS1, SK1 and S1PR1 mRNA levels raised by dhS1P at 18 h treatment. (B) Inhibition of S1PR1 by W146 also reduced DEGS1, SK1 and S1PR1 mRNA levels raised by dhS1P. $^{***}p < 0.005$, $^{**}p < 0.01$, $^{*}p < 0.05$ vs. Control, $^{\#\#}p < 0.01$, $^{\#}p < 0.05$ vs. treatment. Data are presented as ± SEM of 3 replicates.

3.5 Discussion

In this study, the role of the PI3K/Akt- mTOR pathway in terms of collagen synthesis and myocyte hypertrophy mediated by the sphingolipids, dhS1P and S1P, in primary cardiac fibroblasts and myocytes was investigated. The results in chapter 2 and others have shown that exogenous application of the sphingolipids,

S1P and dhS1P, can contribute to collagen synthesis in fibroblasts and cause myocyte hypertrophy which contribute to cardiac remodelling [84, 200, 226].

3.5.1 Multiple effects of PI3K/Akt- mTOR cascade inhibition on dhS1P induced fibrosis

The PI3K/Akt signalling pathway is well described as a critical pathway in cell metabolism, proliferation, differentiation, and survival, and in lipid metabolism [211]. Activation of PI3K through GPCRs such as the S1PRs, subsequently leads to phosphorylation of Akt, thereby activating it. Akt indirectly activates mTOR (mTORC1 and mTORC2) further downstream. mTORC1 is one of the major effectors of PI3K/Akt signalling, and a regulator of fibrosis [215]. One of the key indicators of fibrosis is excessive synthesis and accumulation of the ECM such as collagen. In this study, inhibiting PI3K reduced the excessive collagen synthesis induced by extracellular dhS1P and S1P in primary rat NCFs, Figure 3.1. Pathway analysis through protein immunoblotting showed reduced activation of Akt, mTOR and RPS6, Figure 3.2. The downstream targets of mTORC1 include; p70 S6 kinase (S6K1), phosphorylates RPS6, and the eukaryotic initiation factor 4E (EI4E) binding protein 1 (4EBP1), and they promote mRNA translation [227, 228]. Therefore, the reduced translation and synthesis of Coll1 and TGFβ proteins in both dhS1P and S1P treated NCFs correspond to the reduced mTOR and RPS6 activity due to PI3K inhibition (Figure 3.3). Interestingly, these reductions were not reflected in the gene expression levels for TGFβ1 and Coll1a1, Figure 3.5. The mRNA levels of TIMP2 and CTGF, also remained unchanged. This is not surprising, since dhS1P and S1P can activate other GPCR related signalling pathways, which can influence the expression of these fibrotic genes. However,

PI3K inhibition did reduce both TIMP1 mRNA and protein expression levels, and increased MMP2/TIMP1 ratio (Figure 3.5A). Indicating a delayed mechanism of transcription control for TIMP1, which may be related to TGFβ and Coll1 protein translation. Combined with the increased MMP2/TIMP1 mRNA ratio, the increased GSK3β and GATA4 mRNA levels may have also contributed to ECM degradation (Figure 3.5D). This is because increased GSK3β results in reduced glycolysis, leading to degradation of ECMs such as collagen [229]. Inversely, accelerated collagen synthesis and fibrogenesis were reported in cells and mouse models with deletion of global and cardiac specific GSK3β [230] [231]. GSK3β is abundant in normal cells, but in conditions where growth pathways such as the PI3K/Akt/mTOR are activated its levels are reduced[217]. Therefore, it is thought to act as a negative regulator of growth pathways. GSK3β partners with the transcription factor GATA4 in regulating cardiac development [217]. The increase in GATA4 mRNA levels also allude to the activation of other pathways. Inhibiting the PI3K/Akt- mTOR signalling pathway also reduced sphingolipid pathway related genes such as SK1. The reduced mTOR activation and TGFβ protein translation and could have led to reduced SK1 transcription. SK1 activity is increased by TGFβ and is linked to increased fibrosis and disease progression [115, 226, 232, 233]. Additionally, mTORC1 signalling promotes transcription of SREBPs; a family of transcription factors that encode genes for lipogenic enzymes such as SK1 [234, 235]. This effect on SK1 mRNA level was not observed in S1PR1 inhibited NCFs where there was a synergistic increase in mTOR activity. Interestingly, PI3K and S1PR1 inhibition had an inverse effect on DEGS1 mRNA levels. DEGS1 encodes the gene for the DES1 enzyme, known as the gatekeeper, in the *de novo* sphingolipid biosynthesis pathway [100]. The increase in DEGS1 mRNA level may be related to a positive feedback mechanism involving S1PR1

on the *de novo* sphingolipid pathway since S1PR1 mRNA levels were reduced. This feedback mechanism has been described elsewhere [236]. Furthermore, S1PR2 could also be involved in this feedback mechanism since its mRNA levels were also reduced in both PI3K and S1PR1 inhibition. Even though S1PR3 mRNA was reduced by PI3K inhibition, it was not reduced by S1PR1 inhibition, Figure 3.8. This activation may have contributed to the increased Akt and mTOR activity observed in S1PR1 inhibited cells, Figure 3.4. Activation of S1PR3 has been shown to increase proliferation through PI3K/Akt pathway [112]. These results reveal a link between the PI3K/Akt pathway and dhS1Ps activation of the S1PRs. Taken together, these findings indicate that inhibition of PI3K/Akt – mTOR signalling cascade in NCFs treated with dhS1P has anti-fibrotic effects by reducing translation of growth factors and increased degradation of ECM. It also affects basal transcription levels of sphingolipid enzymes and receptors.

3.5.2 PI3K/Akt- mTOR cascade is associated with dhS1P induced cardiac myocyte contractility and stretch

Cardiac hypertrophy involves increased myocyte size and protein content, with complex alterations in translation and transcription processes. The PI3K/Akt-mTOR pathway is known to play a key role in myocyte hypertrophy [237]. The findings in this chapter show that inhibiting PI3K in dhS1P and S1P treated NCMs reduced phenotypic hypertrophic effects, with reductions in Akt, mTOR and RPS6 activity, Figure 3.9- 3.10. Interestingly, the inhibition led to a synergistic increase in the hypertrophic marker, βMHC, with relative increase in ANP and BNP (Figure 3.9A- B). Clinically, ANP and BNP are considered to be compensatory markers for HF [183]. Their increase also highlights the

hypertrophic effect of the agents used. In contrast, inhibiting PI3K reduced αSKA transcripts in dhS1P treated NCMs, but not in those treated with S1P. Highlighting a significant difference between S1P and dhS1P induced myocyte hypertrophy. αSKA mRNA increase has been linked to increased myocyte stretch and contractility [238, 239]. The reduced levels of βMHC, ANP, BNP and αSKA mRNA when S1PR1 was inhibited in dhS1P treated NCMs is shown in chapter 2 [200]. Increased GSK3β activity impedes protein initiation and translation by EIF2Bε, thus negatively regulating myocyte hypertrophy [240-242]. Interestingly, inhibition of PI3K and not S1PR1 rescued GSK3β mRNA levels in both treatments (Figure 3.9). Additionally, inhibiting S1PR1 led to reduction in RPS6 phosphorylation triggered by both dhS1P and S1P in NCMs (Figure 3.8C- D). Apart from activation by ribosomal p70 S6 kinase in the Akt- mTOR pathway, RPS6 phosphorylation is also triggered by other kinases [243-245]. Even though GSK3β is known to negatively regulate GATA4 in myocytes resulting in reduced hypertrophic makers [246], the inhibition of PI3K increased GATA4 in S1P treated NCMs. These results suggest that inhibiting the PI3K/Akt pathway alone is insufficient to reduce hypertrophic gene transcription but may influence myocyte protein expression.

In terms of the expression levels of sphingolipid related genes in NCMs, inhibition of both PI3K and S1PR1 led to reductions in DEGS1, SK1 and S1PR1 mRNA (Figure 3.10). The effect of PI3K inhibition on DEGS1 mRNA is notably different from those observed in NCFs for dhS1P. Differences in cell type, cellular metabolism, and nutrient supplements in the NCM media, maybe have influenced these results. Further research may help unveil the mechanisms behind these differences. The similar inhibitory effects on the sphingolipid related genes by PI3K and S1PR1 inhibition suggests that the dhS1P- S1PR1 axis can interaction

with the PI3K/Akt- mTOR cascade in NCMs. However, it is noted that targeted inhibition of individual downstream proteins such as Akt and mTOR maybe necessary to fully decipher the effects of dhS1P on fibrogenesis and hypertrophy through the Pi3K/Akt -mTOR pathway. This is in view of PI3K's ability to regulate other signalling pathways.

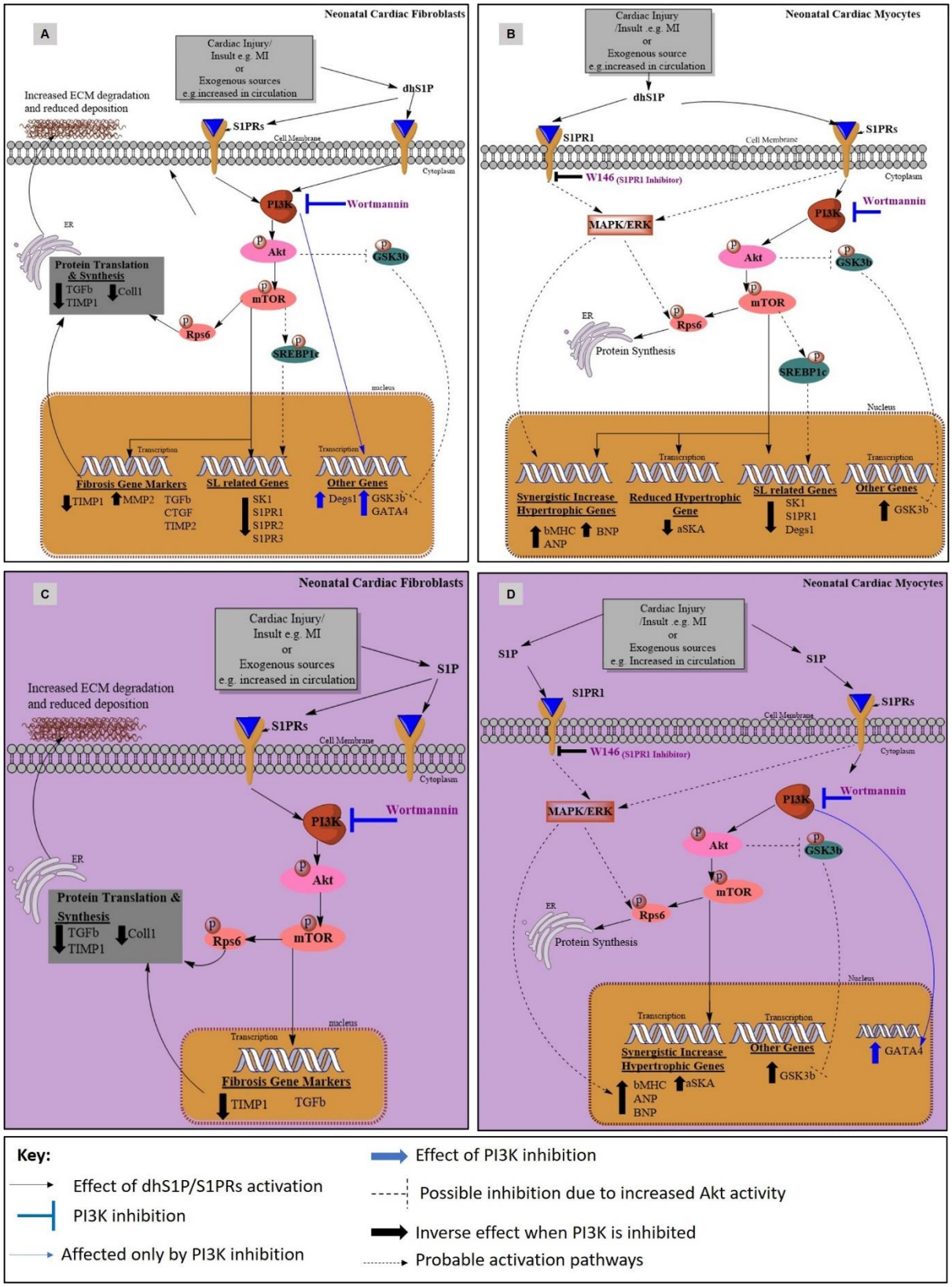

Figure 3.11. DhS1P and S1P signalling through S1PR- PI3K/Akt- mTOR in NCFs and NCMs. Inhibiting the activation of the dhS1P/S1PRs- PI3K/Akt-mTOR signalling cascade with wortmannin in the event of cardiac insults such an

MI or increased dhS1P in circulation could lead to, (A) to reduced deposition and increased degradation of the ECM, as a result of reduced translation and synthesis of fibrotic proteins such as TGFβ, Coll1, and TIMP1. These reductions are due to reduction in RPS6 phosphorylation downstream of PI3K/Akt-mTOR signalling. Reduced mTOR phosphorylation reduced TIMP1 mRNA and increased MMP2 mRNA in NCFs, but had no effect on dhS1P increased TGFβ1, CTGF and TIMP2 mRNA levels. The reduced mTOR activity could lead to reduced SREBP1c activity resulting in the observed reduction in sphingolipid related mRNAs such as the S1PRs and SK1. GSK3β, DEGS1 and GATA4 mRNA levels were increased only when PI3K activity was inhibited in the presence of dhS1P. (B) PI3K inhibition in NCM reduced dhS1P/S1PR signalling induced hypertrophy by reducing αSKA, increasing GSK3β mRNA level, and reduce protein expression by reducing RPS6 activity. It also decreases the sphingolipid related genes, probably through reduced mTOR-SREBP1c activity. Despite the PI3K inhibition, there was a synergistic increase βMHC, ANP and BNP mRNA levels, possibly due to signalling through other dominant pathways such as MAPK/ERK via the dhS1P/S1PR1 axis. Inhibition of S1PR1 by W146, results in reduced expression of these makers. C) Reduced deposition and increased degradation of the ECM, as a result of reduced translation and synthesis of fibrotic proteins such as TGFβ, Coll1, and TIMP1 were also observed when PI3K was inhibited in S1P/S1PRs-PI3K/Akt signalling. These were due to reductions in RPS6 phosphorylation downstream of PI3K/Akt-mTOR signalling. Reduced mTOR phosphorylation reduced TIMP1 mRNA levels but had no effect on dhS1P increased TGFβ1 mRNA levels. D) PI3K inhibition in NCM reduced S1P/S1PR signalling induced hypertrophy by increasing GSK3β mRNA levels and reducing protein expression as a result of reduced RPS6 activity. Despite the

PI3K inhibition, there was a synergistic increase in βMHC, αSKA, ANP and BNP mRNA, possibly due to signalling through other dominant pathways such as MAPK/ERK via the S1P/S1PR1 axis. Inhibition of S1PR1 by W146, results in reduced expression of these makers. Illustration derived through ChemDraw Professional 17.0 (Perkin Elmer, Waltham, MA, USA).

It is well understood that PI3K/Akt signalling is a critical pathway in many cellular events in both diseased and physiological states. It is also riddled with feedback activation loops depending on exposure levels, cell types, ligands and experimental models. Its role in cellular metabolism and cell survival is also another aspect that could have an impact on these findings. Besides these, other limitations such as the phosphorylation levels of GSK3β and expression of proteins related to sphingolipid pathway are some of the limitations of this study. Therefore, the findings here are considered as preliminary.

3.6 Conclusion

The PI3K/Akt- mTOR signalling pathway plays a complex role in dhS1P and S1P induced cardiac fibrosis and myocyte hypertrophy. Although, these findings are preliminary, they show links between the PI3K/ Akt- mTOR cascade and the receptors targeted by dhS1P and S1P, and the enzymes involved in sphingolipid synthesis. PI3K inhibition affects collagen synthesis in NCFs post transcriptionally, leading to delayed effects on others like TIMP1 at the transcription level. Additionally, there is implications of it playing balancing roles in lipogenesis of sphingolipids and GSK3β in promoting its anti-fibrotic effects. Although PI3K inhibition in NCMs had little effect on the major hypertrophic

gene markers, what was evident is its augmentative effect on GSK3β, which may have influenced the reduction in both dhS1P and S1P induced myocyte hypertrophy by increasing protein degradation. Additionally, in dhS1P treated NCMs, PI3K inhibition did result in reduction of the gene related to contractility and stretch, αSKA. The results demonstrated in this chapter indicate the PI3K pathway can be further explored in terms of dhS1P and S1P mediated cardiac remodelling and expanded upon with targeted inhibition of downstream proteins in the pathway.

Manuscript submitted

Preface

Chapter four describes the effects of dhSph and Sph on collagen synthesis in cardiac fibroblasts and highlights a sphingolipid pathway driven inhibition of collagen synthesis. This work has been submitted for publication.

Chapter 4: Dihydrosphingosine driven enrichment of sphingolipids attenuates TGFβ induced collagen synthesis in cardiac fibroblasts

Authors

Ruth R. Magaye[1, 2], Feby Savira[1, 2], Xin Xiong[1,2, 3], Kevin Huynh[4], Peter J. Meikle[4,5], Christopher Reid[2,5], Bernard L. Flynn[6], David Kaye[7], Danny Liew[2], Bing H. Wang[1, 2*]

1. Biomarker Discovery Laboratory, Baker Heart and Diabetes Institute, Melbourne, Australia
2. Monash Centre of Cardiovascular Research and Education in therapeutics, Melbourne, Australia
3. Shanghai Institute of Heart Failure, Research Centre for Translational Medicine, Shanghai East Hospital, Tongji University, School of Medicine, Shanghai 200120, P. R. China
4. Metabolomics Research Group, Baker Heart and Diabetes Institute, Melbourne, Australia
5. School of Public Health School, Curtin University, Perth, Australia
6. Monash Institute of Pharmaceutical Sciences, Monash University, Melbourne, Australia
7. Heart Failure Research Group, Baker Heart and Diabetes Institute, Melbourne, Australia

*Corresponding author:

bing.wang@baker.edu.au and bing.wang@monash.edu

4.1 Abstract

The sphingolipid *de novo* synthesis pathway, encompassing the sphingolipids, the enzymes and the cell membrane receptors, are being investigated for their role in diseases and as potential therapeutic targets. The intermediate sphingolipids such as dhSph and Sph have not been investigated due to them being thought of as precursors to other more active lipids such as Cer and S1P. Their effects in terms of collagen synthesis in NCFs are investigated in this chapter. Our results in rat NCFs showed that both dhSph and Sph did not induce collagen synthesis, whilst dhSph reduced collagen synthesis induced by TGFβ. The mechanisms of these inhibitory effects were related to the increased activation of the *de novo* synthesis pathway that led to increased dhS1P. Subsequently, through a negative feedback mechanism that may involve substrate-enzyme receptor interactions, S1P receptor 1 expression was reduced.

4.2 Introduction

The sphingolipids such as Cer and S1P have been targeted in recent years for therapeutic interventions in cancer therapy due to their apoptotic and proliferative effects on cancer cells. Apart from these, several of the so called "intermediate" lipids in the *de novo* sphingolipid synthesis pathway may have a role in several pathologies including cardiovascular diseases [161]. In the setting of a number of cardiomyopathies, other researchers have shown these intermediate sphingolipids (dhSph and Sph) are also altered in both plasma and tissue of animal models [144, 247] and in the blood of patients [145, 203, 248]. However, due to the lack of basic mechanistic pathway research regarding their effects or interactions with well-known cardiac remodelling markers such as the TGFβ, no conclusions could be drawn in regards to what these alterations may imply.

Within the cellular system, Sph is produced either because of the metabolic effects of ceramidase on Cer or salvaged in the lysosome from the breakdown products of sphingolipids. While dhSph is derived from the *de novo* synthesis pathway and is a product of the reducing effects of 3-ketoreductase on 3-ketosphingosine. The phosphorylation of both Sph and dhSph by SK1 & 2 results in the production S1P and dhS1P, respectively. Furthermore, the acylation of dhSph results in the production of dhCer which is then converted to Cer in a non-reversible reaction catalysed by DES1 and 2. Several feedback mechanisms are at play in the *de novo* pathway [249], involving both the sphingolipids and the enzymes to regulate these sphingolipids in the disease states, therefore, the possibility of them interacting with factors such as TGFβ, are irrefutable. However, they have hardly been investigated in cardiac cells. Inhibition of DES1; which results in cellular accumulation of sphingolipid species such as dhCer and dhSph, in liver cells, and cancer cells have shown reduced cell/cycle progression and proliferation [250-

252]. The growth and proliferative effects of TGFβ on cells, including cardiac cells leading to increased proliferation and collagen synthesis, is well understood. There is evidence of TGFβ increasing SK1 activity in muscle cells giving rise to fibrosis [253]. This study was conducted to determine whether extracellular dhSph and Sph influence TGFβ induced collagen synthesis in cardiac fibroblasts in a primary cell culture system.

4.3 Methods

The methods used in chapter 2 were applied in this chapter. Please refer to section 2.3 for more details.

4.3.1 Measurement of cardiac fibroblast collagen synthesis

The ^{3}H-proline incorporation assay[167] as described in section 2.3.1 and 2.3.2, was used to determine collagen synthesis in NCFs induced by TGFβ (100-21C, PeproTech, Rocky Hill, NJ, USA) 3 μM dhS1P and 10 μM of the S1PR1 agonist, SEW2871. The NCFs were seeded at 50 000 cells/ well and pre-treated for 2 h with pre-treated for 2 h with the Sph and dhSph (0.01-10.0 μM- Toronto Chemical Research Incorporated, North York, ON, Canada). The levels of ^{3}H-proline incorporation were determined on a 300SL beta counter (cpm).

4.3.2 Measurement of cell viability in rat NCFs

Alamar Assay (Invitrogen- Thermo Fischer Scientific, Carlsbad, CA, USA) was used to determine the cell viability of NCFs in the presence of the sphingolipids and TGFβ according to manufacturer's guidelines as reported previously [254].

4.3.3 Quantitative measurement of protein levels in NCFs

Western blotting was performed as described in section 2.3.5, to investigate the expression of specific proteins related to the PI3K/Akt signalling pathway and cardiac remodelling. The blots were probed for phosphorylated, protein kinase B (Akt), inhibitor of nuclear kappa B (NFKβ) kinase alpha and beta (IKKα/β), NFKβ, P38- MAPK, extracellular-signal-regulated kinase (ERK), RPS6, STAT1, and SMAD2 from Cell Signalling Technologies (CST, Danvers, MA, USA: 4060L, 2694, 4631, 3033, 9101, and 3108L). They were also probed for TGFβ. Proteins were normalised to GAPDH or β-actin.

4.3.4 Quantitative measurement of genes expressed in cardiac remodelling

RT PCR was performed as described in section 2.3.7, to ascertain the changes in gene expression induced by dhS1P, S1P and SEW2871. The gene expression levels of the fibrotic markers; TGFβ, CTGF, TIMP1, TIMP2, MMP2, Coll1a1, the S1PR1-3, and the sphingolipid enzymes SK1 and DEGS1 were quantified. Refer to Appendix 2.1 for full sequence of primers. 18s mRNA was used as the endogenous controls.

4.3.5 Tracing relative d7-dhSph in NCFs

Cardiac fibroblasts extracted from neonatal rats were cultured in 6 well plates at 200 000 cells/ well at passage 2. After 48 h serum starvation, the cells were treated with 1 μM d7-dhSph (Cayman Chemicals, Ann Arbor, MI, USA) in DMEM F12

with 0.5% BSA at different time points. The cells were then washed 3 times with PBS, scrapped in 1 mL PBS, transferred into Eppendorf tubes and placed on ice. NCFs were then sonicated (Misonix S4000- Ultrasonic Liquid Processor, Qsonica, Newton, CT, United States) at 25 amplitudes for 10 seconds each. Samples were then snap frozen on dry ice until processed for liquid chromatography- mass spectrophotometry (LC- MS) according to previously published methods with modification for cultured cells [255, 256]. The Agilent 6490 QQQ mass spectrometer with an Agilent 1290 series HPLC system and a ZORBAX eclipse plus C18 column (2.1x100mm 1.8µm, Agilent) with the thermostat set at 45°C was used to analyse the cell extracts. Mass spectrometry analysis was performed with dynamic scheduled multiple reaction monitoring (MRM) in positive ion mode. Scanning was conducted for both the endogenous sphingolipids and sphingolipids with tracer incorporation were scanned for, where tracer incorporation utilised a 7 Da offset for the precursor and/or product ion depending on the sphingolipid species. Relative enrichment was calculated as area of the labelled species / (area of labelled species + area of non-labelled species).

4.3.6 Statistical analysis

Similar statistical methods as used in section 2.3.8 were applied.

4.4 Results

4.4.1 Extracellular Sph and dhSph alone did not induce collagen synthesis in NCFs

To ascertain whether exogenous dhSph and Sph have effects on collagen synthesis, their effect on cultured NCFs were determined using the ^{3}H-proline

incorporation Assay. As shown in Figure 4.1A at the doses of 0.1, 0.3, 1 and 3 μM both dhSph and Sph did not induce collagen synthesis. However, dhSph at the highest dose of 3 μM ($p < 0.01$) significantly reduced ^{3}H-proline incorporation levels compared to the control. This was corroborated by the cell viability results which showed that 3 μM dhSph treatment significantly reduced NCF viability ($p < 0.001$), while Sph had no effect (Figure 4.1B).

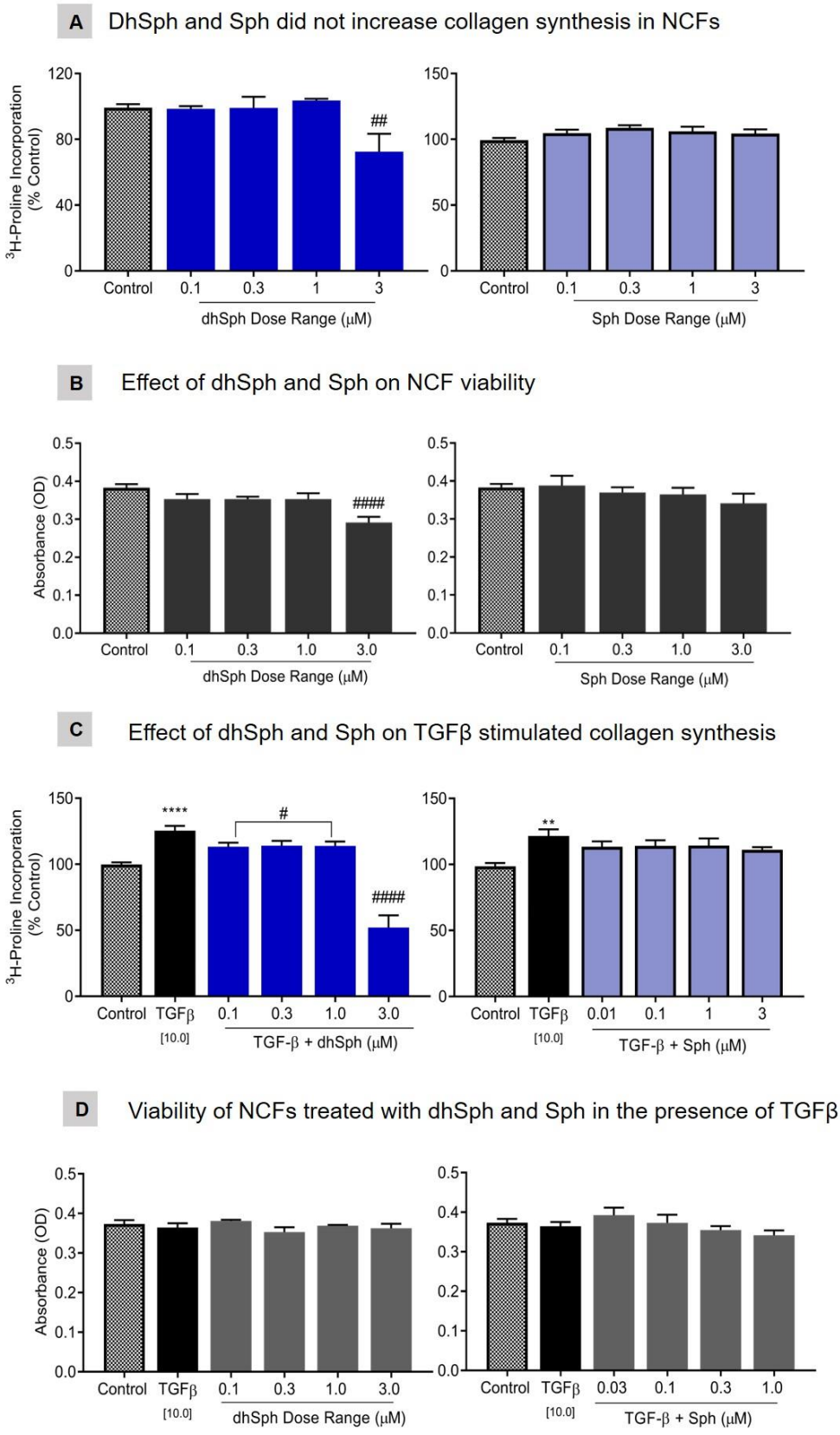

Figure 4.1. Effect of dhSph and Sph on collagen synthesis and viability in NCFs. (A) Treatment of NCFs with dhSph and Sph at 0.1, 0.3, 1 and 3 μM for

48 h did not induce collagen synthesis. (B) dhSph significantly reduced the viability of NCFs at 3 μM ($p < 0.005$), but Sph had no significant effect on NCFs at all doses tested. (C) DhSph (0.1, 0.3, 1.0, and 3.0 μM) significantly reduced collagen synthesis in NCFs induced by TGFβ at 48 h, while the effects of Sph were not statistically significant. (D) The viability of NCFs were not affected by dhSph and Sph treatment in the presence of TGFβ. $^{\#\#\#\#}p < 0.001$, $^{\#\#}p < 0.01$, $p < 0.05$ vs. treatment, $^{\#\#\#}p < 0.005$, $^{\#\#}p < 0.01$ $^{****}p < 0.0001$ vs. control. Data are presented as ± SEM of 3 replicates.

4.4.2 DhSph reduced collagen synthesis induced by TGFβ

The potential for dhSph and Sph to reduce collagen synthesis induced by a known collagen inducing agent, TGFβ was investigated. dhSph (0.1, 0.3, and 1 μM; $p < 0.05$, 3 μM; $p < 0.0001$) significantly reduced collagen synthesis induced by TGFβ ($p < 0.0001$) as shown in Figure 4.1C, Sph did not have significant effect on TGFβ induced collagen synthesis at the doses investigated. The viability of NCFs treated with dhSph and Sph were not affected in the presence of TGFβ (Figure 4.1D. TGFβ's ability to modulate cell growth may have counteracted the effects of dhSph alone as observed in Figure 4.1A & B.

4.4.3 DhSph reduces SMAD2 phosphorylation stimulated by TGFβ

TGFβ utilises the canonical TGFβ/SMAD signalling pathway to induce collagen synthesis, therefore since dhSph reduced collagen synthesis in NCFs, its ability to attenuate SMAD2 phosphorylation was explored. DhSph significantly diminished

SMAD2 phosphorylation stimulated by TGFβ in NCFs at 1 μM ($p < 0.05$), Figure 4.2A. Sph had no effect on TGFβ induced SMAD2 phosphorylation.

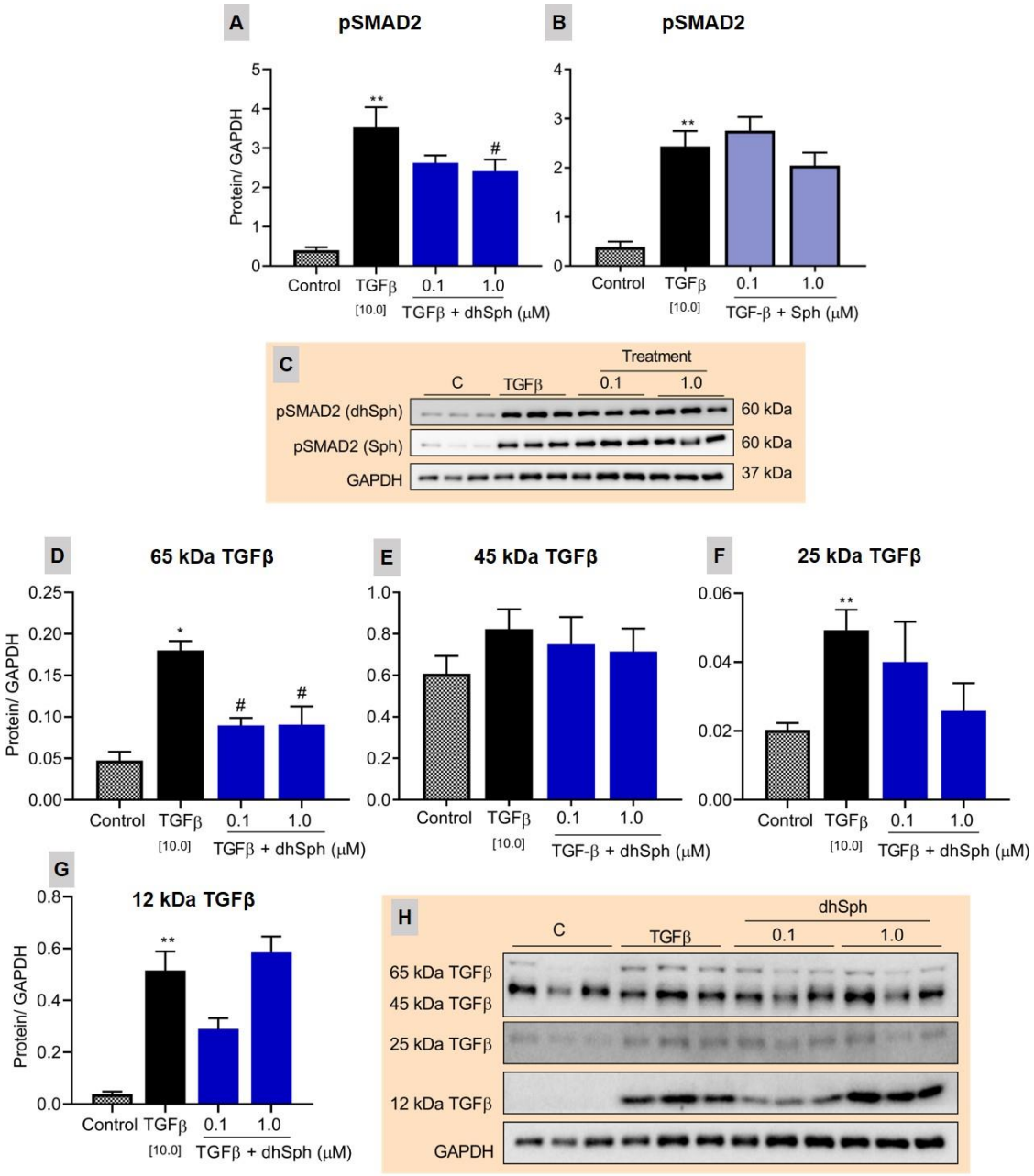

Figure 4.2. Effect of dhSph on the canonical TGFβ pathway. (A) Pre-treatment of NCFs with 1 μM dhSph significantly reduced SMAD2 phosphorylation stimulated by 10 ng/ml TGFβ at 18 minutes ($p < 0.05$). (B) Sph (0.1 and 1 μM) had no effect on TGFβ induced phosphorylation of SMAD2. dhSph significantly reduced (C) the 65 kDa latent TGFβ, but (D) had no effect on

45 kDa latent TGFβ, and the (F) 25 kDa mature TGFβ in NCFs treated with the human recombinant TGFβ. (E) and (G) show representative blots. Refer to supplementary Figure 2 for original blots. $^{\#}p < 0.05$ vs. TGFβ, $^{**}p < 0.01$, $^{*}p < 0.05$ vs. control. Data are presented as ± SEM of 3 replicates.

4.4.4 DhSph reduces TGFβ protein expression

The human recombinant TGFβ activates TGFβ receptor 1 and 2 resulting in increased TGFβ protein expression in the cell. DhSph (0.1 and 1 μM) treatment significantly inhibited the increased expression of 65 kDa latent TGFβ protein in NCFs (Figure 4.2C) but had no significant effect on the 45 kDa isoform (Figure 4.2D). There was a trend toward a reduction on the mature 25 kDa TGFβ protein isoform by dhSph (Figure 4.2F), however it did not reach significance.

4.4.5 DhSph affects Akt- RPS6 signalling in TGFβ treated cells

The effects of dhSph and Sph on Akt-RPS6 signalling was compared. Both dhSph ($p < 0.05$) and Sph ($p < 0.05$) reduced Akt phosphorylation by TGFβ in NCFs (Figure 4.3C). Additionally, dhSph and Sph had significant effect on the phosphorylation of the downstream protein RPS6 in the Akt pathway ($p < 0.05$ and $p < 0.005$, Figure 4.3D).

4.4.6 DhSph and Sph have no effect on other pathways and transcription factors

Furthermore, the effects of Sph and dhSph on the ERK, P38- MAPK and IKK pathway and transcription factors such as STAT1 and NFκB were compared. Both dhSph and Sph did not have any effect on the phosphorylation levels of P38-MAPK (Figure 4.3A) and ERK (Figure 4.3B), which were elevated by TGFβ ($p < 0.05$ and $p < 0.01$, respectively). TGFβ increased phosphorylation of IKKα/β ($p<0.01$, Figure 4.3F), while dhSph and Sph had no effect on IKKα/β and its downstream target, the transcription factor, NFκB (Figure 4.3G). Even though dhSph raised the phosphorylation level of the transcription factor STAT1 (Figure 4.3E) in the presence of TGFβ, the difference was not statistically significant.

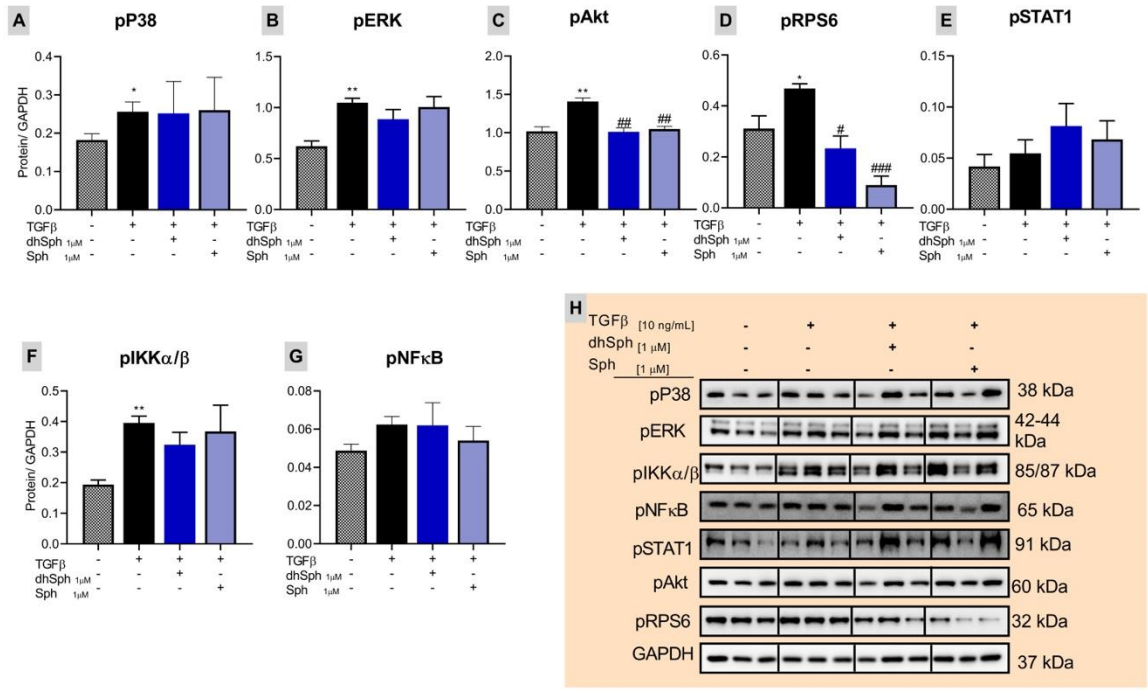

Figure 4.3. Effect of dhSph and Sph on non-canonical TGFβ pathways. Pre-treatment of NCFs with 1 μM dhSph and Sph had no significant effect on (A) P38-MAPK, and (B) ERK phosphorylation induced by 10 ng/ml TGFβ at 18

minutes. (C) DhSph and Sph (1 μM) reduced TGFβ induced phosphorylation of Akt and (D) RPS6. DhSph and Sph had no effect on the phosphorylation levels of (E) STAT1, (F) IKKα/β and (G) NFκB in NCFs. (H) Representative blots in the presence and absence of TGFβ, Sph, and dhSph. $^{###}p < 0.005$, $^{##}p < 0.01$ vs. treatment, $^{**}p < 0.01$, $^{*}p < 0.05$ vs. control. Data are presented as ± SEM of 3 replicates.

4.4.7 DhSph-d7 enriches sphingolipids in a predictive manner in NCFs

DhSph is an intermediate lipid in the sphingolipid pathway, therefore its incorporation enriches other lipids in the *de novo* sphingolipid pathway. Isotopically (deuterium) labelled dhSph (dhSph-d7) were used to determine the time at which dhSph is incorporated into NCFs and assessed the type of lipids that were enriched. Looking at Figure 4.4A1, it appears that dhSph-d7 is converted into dhCer quite rapidly, but it's not until 60 minutes where more complex sphingolipids like sphingomyelins (SM) begin to form (Figure 4.4B3). Albeit at very minor quantities relative to endogenous, likely due to the stability of SM in membranes. Others such as Cer was enriched at approximately 30 minutes (Figure 4.4A2).

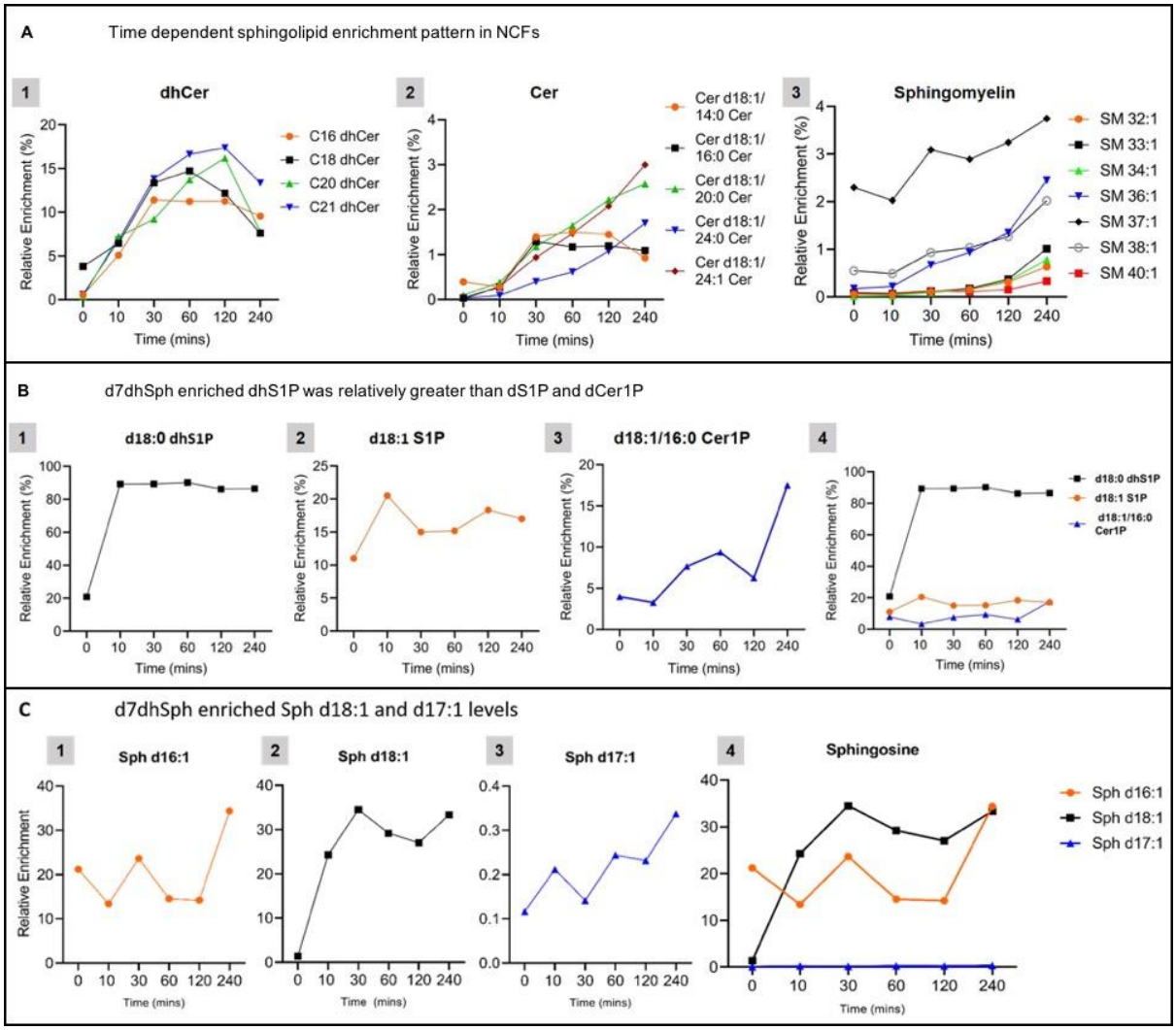

Figure 4.4. Enrichment of sphingolipids by d7dhSph. In NCFs treated with deuterium isotopically labelled dhSph (d7dhSph), (A1) dhCer was enriched at around 10 minutes, (A2) Cer at 30 minutes (A3) and sphingomyelin at 120 to 240 minutes. D7dhSph also enriched the phosphorylated lipids (B1) d18:0 dhS1P, and (B2) d18:1 S1P within 10 minutes, and (B3) d18:1/ 16:0 Cer1P at 30 minutes. (B4) A comparative graph showing the enrichment of the three lipids across different time points. Data are presented as relative enrichment of 3 independent replicates. (C1) Sph d16:1 was not enriched by D7dhSph, but (C2) d18:1 and (C3) d17:1 were enriched. (C4) d18:1 Sph was increased at all times compared to d16:1 and d17:1.

4.4.8 DhSph-d7 enriched dhS1P more than S1P and Ceramide 1 phosphate (Cer1P)

The phosphorylated sphingolipids target the G protein coupled S1PRs to activate intracellular signalling pathways. DhSph-d7 is almost immediately converted into dhS1P and hits saturation point, likely for removal in response to such high concentrations of exogenous sphingosines. The incorporation of dhSph-d7 enriched d18:0 dhS1P at 10 minutes to about 80 %, which remained at this level throughout the time points tested (Figure 4.4B1). S1P and Cer1P were enriched at 10 to 30 minutes after dhSph-d7 treatment in NCFs (Figure 4.4B2-3). The increase in S1P enrichment at 10 minutes maybe due to the dhSph-d7 being contaminated with d8-Sph. DhS1P was enriched more than S1P and Cer1P by dhSph-d7 (Figure 4.4B4). Even though Sph d18:1 and d17:1 levels were enriched (Figure 4.4C2 and 3) their level of increase were also lower than dhS1P levels at similar time points. This increase was predictably higher than S1P, since S1P is phosphorylated from Sph.

4.4.9 Exogenous dhS1P had synergistic effect on TGFβ induced collagen

Since dhS1P enrichment was increased early and remained for the duration of the experiment, the effects of dhS1P on TGFβ induced collagen synthesis in NCFs was explored. Exogenous dhS1P had a synergistic effect on TGFβ induced collagen synthesis at 3 μM (p <0.05). Additionally, the highest dose of dhS1P (10 μM) reduced collagen synthesis by TGFβ (Figure 4.5A, $p < 0.05$). However, this effect was likely due to reduced viability of NCFs as shown in Figure 4.5B.

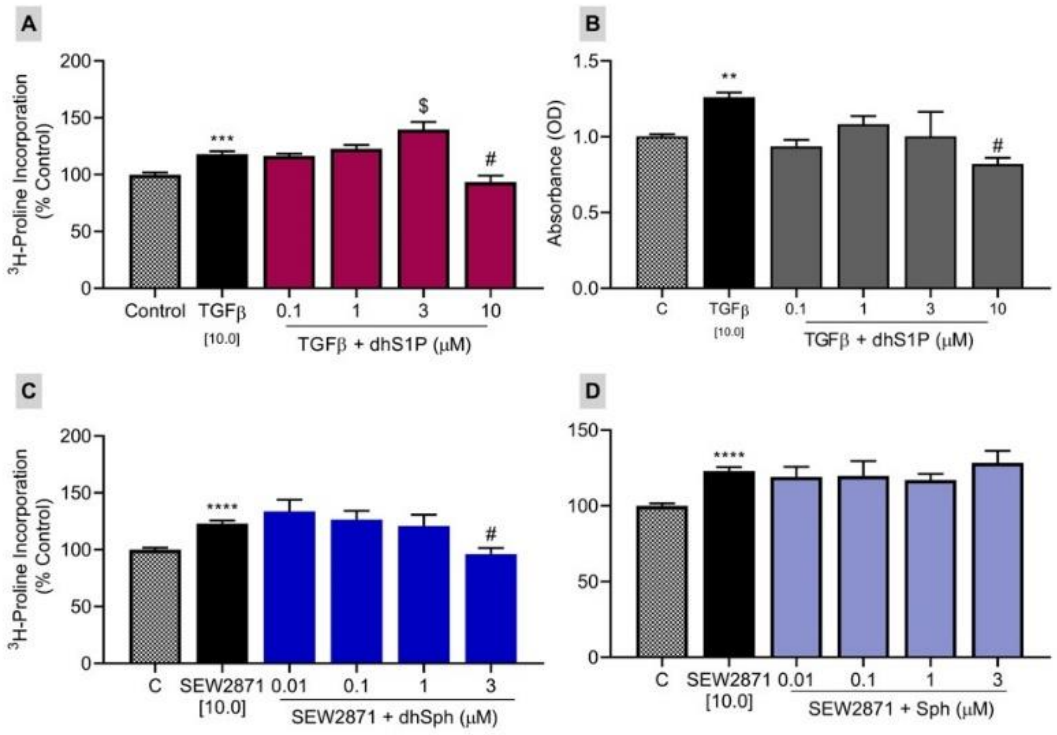

Figure 4.5. Effect of dhS1P on TGFβ induced collagen synthesis. (A) In NCFs treated with dhS1P in the presence of TGFβ for 48 h, dhS1P (10 μM) reduced collagen synthesis. (B) The viability of NCFs was reduced by dhS1P (10 μM) in the presence of TGFβ for 48 h. (C) Treatment of NCFs with the S1PR1 agonist, SEW2871, increased collagen synthesis after 48 h, which was reduced by dhSph (3 μM). (D) Sph had no effect on SEW2871 induced collagen synthesis. $^{\#}p < 0.05$ vs. treatment, $^{****}p < 0.0001$, $^{***}p < 0.001$, $^{**}p < 0.01$, vs. control. Data are presented as ± SEM of 3 replicates.

4.4.10 DhSph reduces S1PR1 agonist, SEW2871, induced collagen synthesis

Next, the effects of dhSph on collagen synthesis induced by the S1PR1 agonist, SEW2871, was examined. DhSph significantly reduced SEW2871 induced

collagen synthesis at the highest dose of 3 μM (Figure 4.5C, $p < 0.05$). Sph had no effect on collagen synthesis induced by SEW2871 (Figure 4.5D).

4.4.11 DhSph and Sph had differing effects on TGFβ induced fibrotic genes

The, the effects of dhSph and Sph on TGFβ induced fibrotic genes were investigated. In primary rat NCFs, stimulation with TGFβ for 18 h significantly increased TGFβ1 ($p < 0.01$), TIMP1 ($p < 0.005$) and CTGF mRNA levels ($p < 0.001$, Figure 4.6A). DhSph significantly reduced TGFβ1 and TIMP1 at the higher dose of 1 μM ($p < 0.05$), but had no effect on CTGF mRNA. Sph had no effect on TGFβ1 and TIMP1 mRNA, but increased CTGF mRNA at the lower dose of 0.1 μM ($p < 0.05$, Figure 4.7B). After 18 h of treatment with TGFβ, there was no change in Coll1a1 mRNA level in NCFs. Additionally, at this time point MMP2 ($p < 0.005$) mRNA level was significantly reduced. Both dhSph and Sph had no effect on Coll1a1 and MMP2 mRNA levels in the presence of TGFβ.

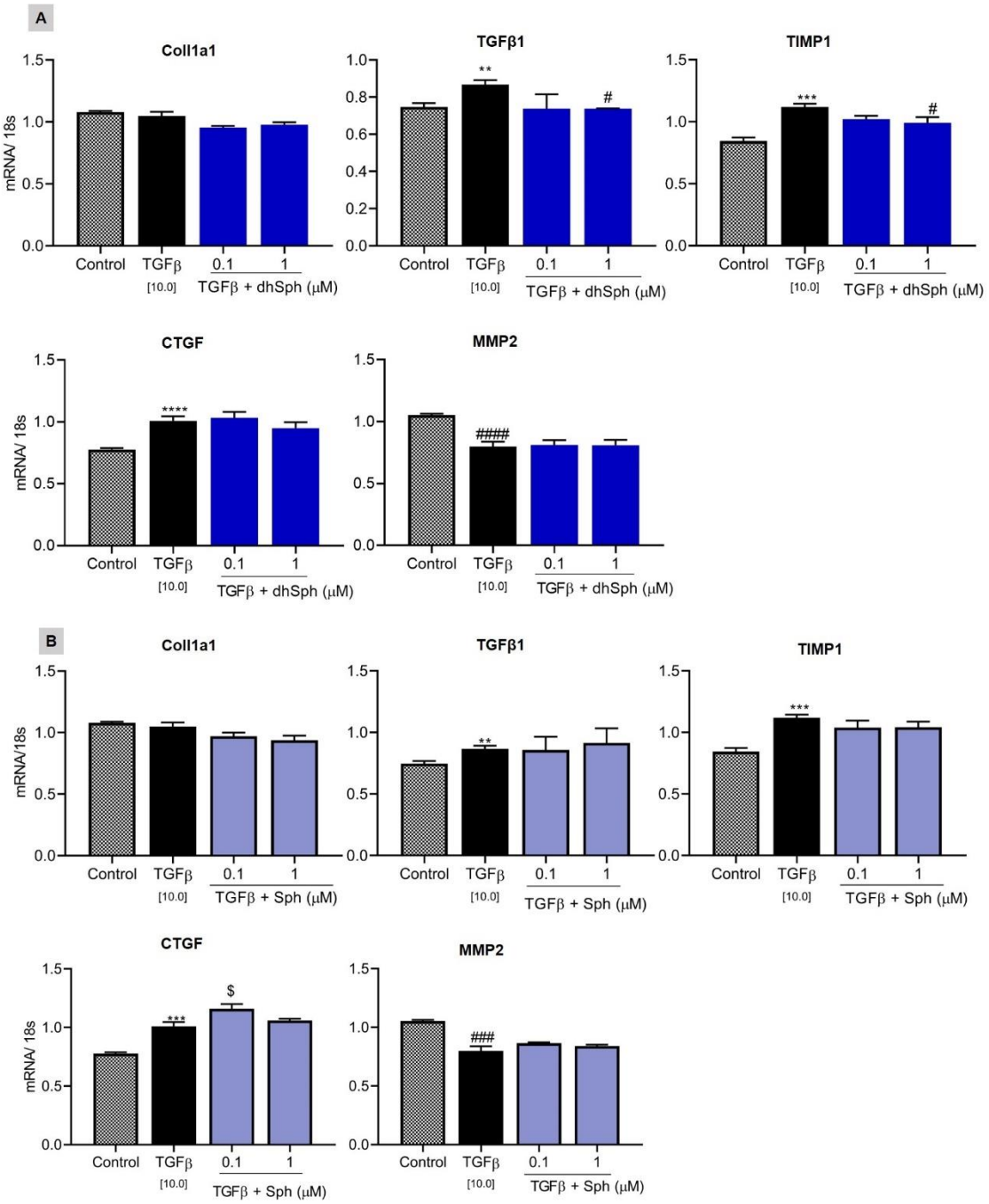

Figure 4.6. Effect of dhSph and Sph on TGFβ induced fibrotic genes. In NCFs treated with 10 μM TGFβ for 18 h (A) dhSph reduced TGFβ and TIMP1 mRNA levels but had no effect on Coll1a1, CTGF and MMP2. While (B) Sph a synergistic effect on CTGF mRNA levels, but had no effect on TGFβ1, Coll1a1, TIMP1 and MMP2. $^{\#}p < 0.05$, $^{*}p < 0.05$, and $^{\$}p < 0.05$ vs. treatment, $^{\#\#\#\#}p < 0.0001$, and $^{****}p < 0.0001$ vs. control. Data are presented as ± SEM of 3 replicates.

4.4.12 DhSph reduced S1PR1 mRNA levels in NCFs

TGFβ is known to increase SK1 activity, therefore the effect of dhSph and Sph on sphingolipid related genes were examined. TGFβ significantly increased the mRNA levels of the *de novo* sphingolipid pathway enzymes, SK1 ($p < 0.01$) and DEGS1 ($p < 0.01$) at 18 h, Figure 4.7. Both dhSph and Sph had no effect on the expression levels of these genes. While, TGFβ had no effect on S1PR1-3 mRNA levels, dhSph significantly reduced S1PR1 mRNA levels ($p < 0.05$, Figure 4.7A). DhSph also had no effect on S1PR2 and S1PR3 mRNA levels. Curiously, Sph increased S1PR2 and 3 mRNA levels significantly ($p < 0.05$, Figure 4.7B).

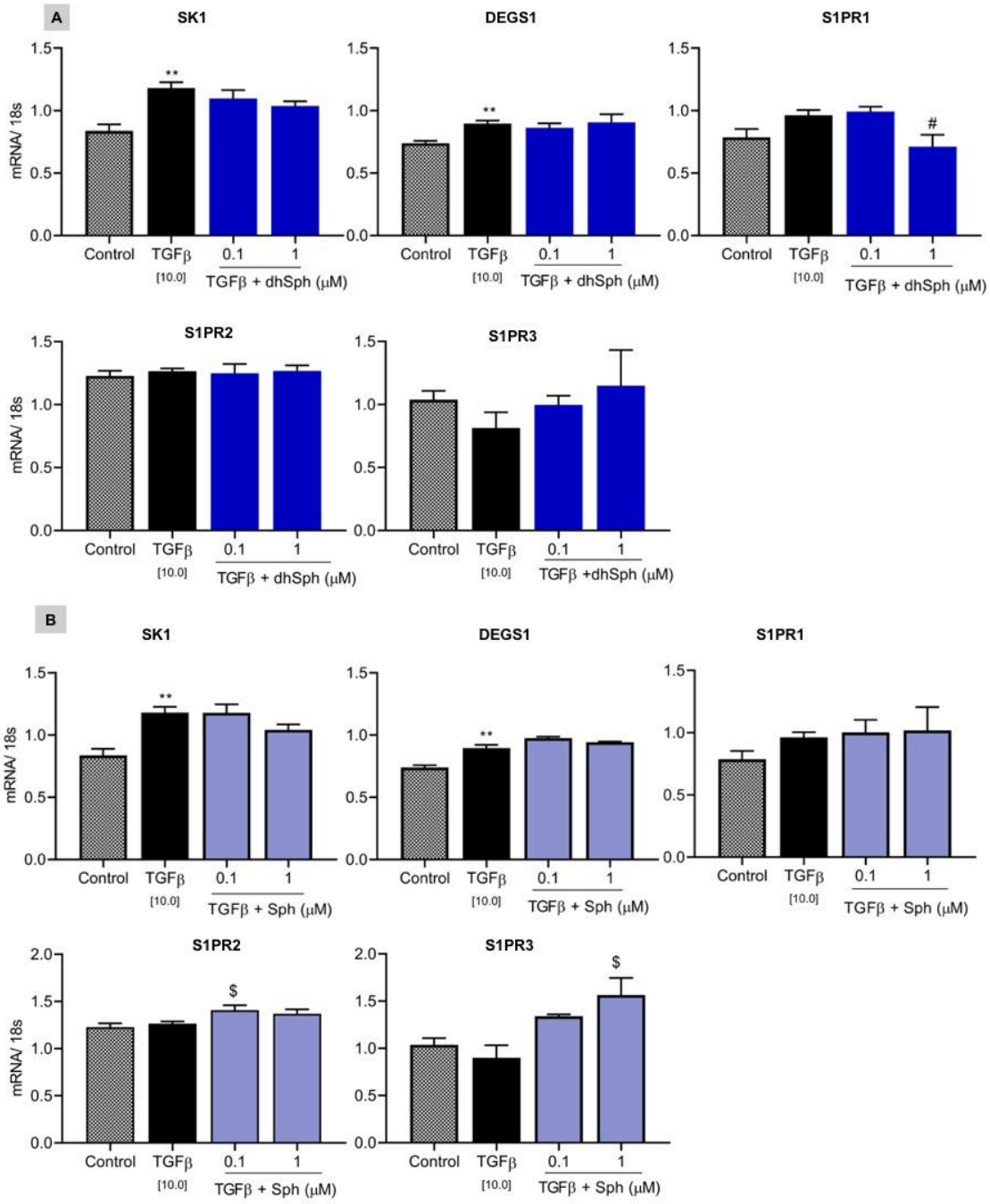

Figure 4.7. Effect of dhSph and Sph on TGFβ induced sphingolipid related genes. (A) In NCFs treated with TGFβ 10 (ng/ml) for 18 h dhSph reduced S1PR1 mRNA levels but had no effect on SK1, DEGS1, S1PR2 and S1PR3. While (B) Sph increased S1PR2 & 3 in the presence of TGFβ (10 ng/ml) and had no effect on S1PR1, SK1 and DEGS1 mRNA levels. $^{\#}p < 0.01$, $^{\$}p < 0.05$ vs.

treatment, and $^{**}p < 0.0001$ vs. control. Data are presented as ± SEM of 3 replicates.

4.4.13 DhSph reduced fibrotic genes induced by the S1PR1 agonist

The effect of dhSph on collagen synthesis stimulated by SEW2871 and S1PR1 mRNA level in the presence of TGFβ led us to investigate its effect on SEW2871 induced changes in NCF genes expression. SEW2871 significantly raised Coll1a1 ($p < 0.01$, TGFβ1 ($p < 0.0001$), CTGF ($p < 0.05$), TIMP1 ($p < 0.0001$) and TIMP2 ($p < 0.0001$) mRNA levels, Figure 4.8A-D. DhSph significantly reduced Coll a1, TGFβ1 ($p < 0.05$), CTGF, TIMP1 and TIMP2 ($p < 0.0001$) at the doses tested.

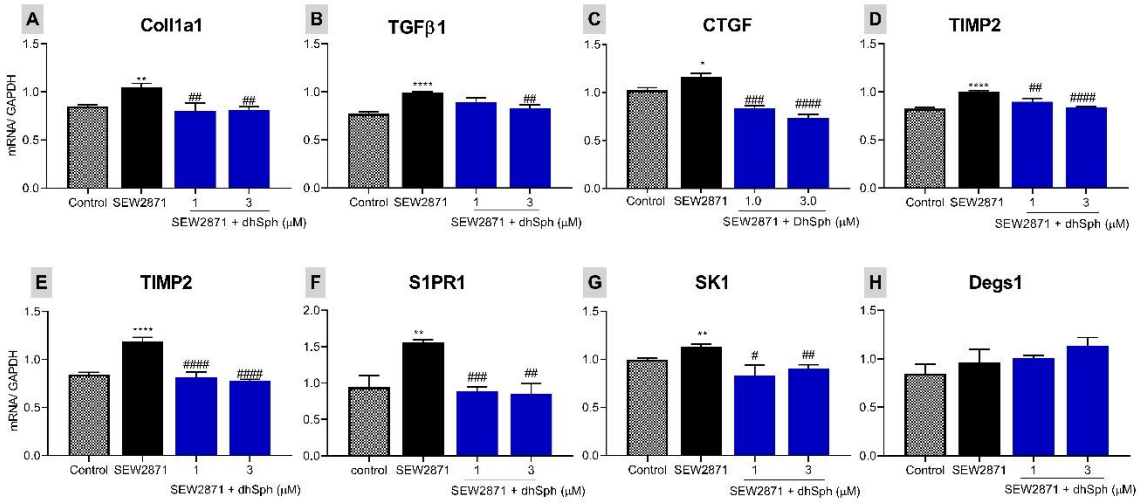

Figure 4.8. Effects of dhSph on SEW2871 induced fibrotic and sphingolipid related genes. (A-E) DhSph reduced the fibrotic genes; Coll1a1, TGFβ1, CTGF, TIMP1, and TIMP2 mRNA levels elevated by SEW2871, in NCFs treated with SEW2871 (10 μM) for 18 h (A-E). (F-G) DhSph also reduced S1PR1 and SK1 mRNA levels. Both SEW2871 and dhSph had no effect on DEGS1gene expression. $^{\#\#\#\#}p < 0.0001$, $^{\#\#\#}p < 0.005$, $^{\#\#}p < 0.01$, $^{\#}p < 0.05$ vs. treatment, and

$^{****}p < 0.0001$, $^{**}p < 0.01$, $^{*}p < 0.05$ vs. control. Data are presented as ± SEM of 3 replicates.

4.4.14 DhSph reduced S1PR1 and SK1 genes elevated by SEW2871

Furthermore, the effects of SEW2871 on sphingolipid related genes such as S1PR1, SK1 and DEGS1 were explored. SEW2871 (10 μM) increased S1PR1 and SK1 gene expression levels in NCFs (Figure 4.8F-G). The expression levels of these genes were significantly reduced by dhSph (1 and 3 μM). SEW2871 did not have significant effect on the DEGS1 gene (Figure 4.8H). However, dhSph showed a non-significant trend toward an increase in DEGS1 gene expression in the presence of SEW2871.

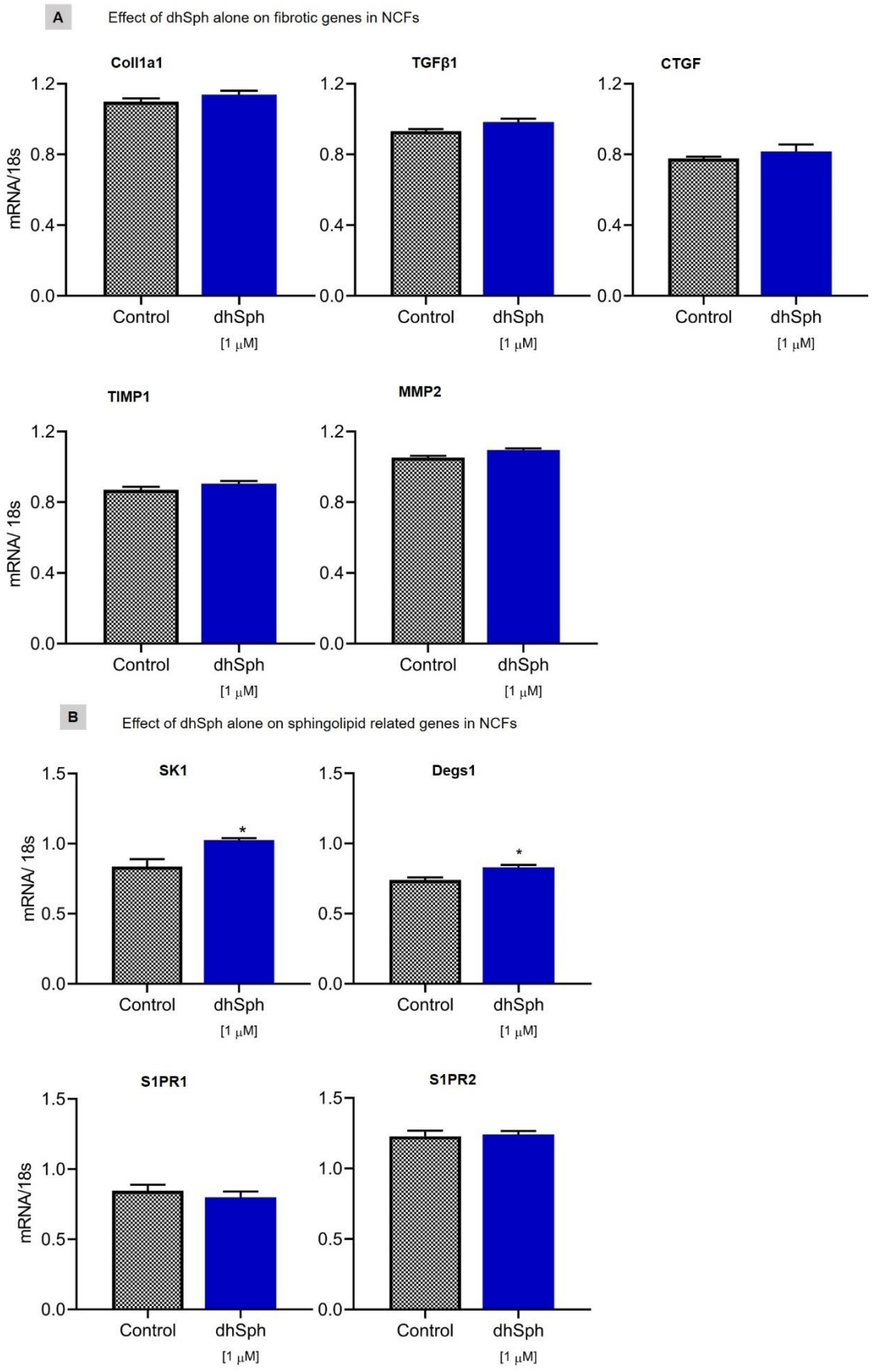

Figure 4.9. Effect on NCF genes when treated exclusively with dhSph. (A) Changes in gene expression in NCFs treated with exogenous dhSph alone. At 18

h of treatment with dhSph there were no significant changes in the expression of fibrotic genes. (B) SK1 and Degsl gene expression were increased significantly by dhSph, while there were no changes in S1PR1 and 2 gene expression. *$p < 0.05$ vs. control. Data are presented as ± SEM of 3 replicates.

4.5 Discussion

The sphingolipids, dhSph and Sph, are intermediate lipids in the *de novo* sphingolipid pathway. They are rapidly metabolised in the pathway to give rise to other patho-physiologically relevant lipids such as Cer and S1P. Their rapid metabolism also results in low detection levels in plasma and tissue. Due to these reasons, their molecular effects on the pathway, and in disease models such as cardiac remodelling are rarely explored. Recent studies on cell proliferation, apoptosis, autophagy and migration have alluded to the possibilities of targeting the sphingolipid pathway for therapeutics [257, 258]. The growth factor, TGFβ, is known to increase activation of SK1 in the sphingolipid synthesis pathway [253]. Considering the pivotal role TGFβ plays in collagen synthesis and its role in cardiac remodelling, here the effects of exogenous dhSph and Sph on primary NCFs in the presence TGFβ was investigated.

In cardiac fibroblasts, TGFβ is known to increase collagen synthesis and drive the trans- differentiation of fibroblasts into myofibroblasts. TGFβ binds to either TGFβ receptor 1 and 2, which then activates the canonical pathway, involving the receptor activated SMADS (R-SMADs); SMAD2 and 3. Exogenous dhSph significantly reduced collagen synthesis stimulated by TGFβ in NCFs (fig. 1C). The effect of dhSph on phosphorylation of SMAD2 (Figure 4.2A), and Akt (Figure 4.3A & B) implied that it was able to reduce collagen synthesis by targeting

both canonical and non- canonical TGFβ signalling pathways [259]. However, the inhibitory effect on the non-canonical signalling pathway did not include NFκB phosphorylation (Figure 4.3D). TGFβ signalling can be both rapid and delayed depending on experimental conditions. Direct activation of P38-MAPK by TGFβ occurs through MKK3 and MKK6, as a result of TGFβ activating kinase 1 (TAK1) activation which is a part of the MAP kinase kinase kinase (MAPK3K) [260]. TGFβ activation of Akt can occur through TRAF6 ubiquitination which also activates TAK1 [261]. Considering our experimental conditions, these pathways maybe directly activated by TGFβ at 18 minutes in NCFs, while NFκB activation was likely delayed.

Due to dhSph being rapidly metabolized, to further understand how dhSph was affecting TGFβ induced collagen synthesis, the relative enrichment of other lipids in NCFs using deuterium labelled dhSph was investigated. As expected, addition of d7-dhSph to cultured NCFs led to enrichment of dhCer, Cer, SM and dhS1P (Figure 4.4). The enrichment of dhS1P and dhCer occurred at around 10 minutes and stayed elevated for the duration of the study. The effects of dhSph on Akt could be a result of the increase in Cer [262]. This is highly likely in view of the similarity between Sph and dhSph effect on Akt and RPS6 phosphorylation as shown in Figure 4.3C and D. When Sph is incorporated into cells, enrichment of Cer predominates [263]. The downstream Akt target, RPS6, mediates transcription of genes including proliferation, and cell survival [227, 228]. TGFβ can activate the PI3K/ Akt signalling and can be dependent or independent of SMADs [264, 265]. The addition of Sph and dhSph was able to inhibit this signalling interactions. Our findings indicate that the inhibition of collagen synthesis and the TGFβ/SMAD2 signalling by dhSph seems to be independent of the effects on Akt due to an increase in Cer. This is because addition of Sph also inhibited Akt

but had no effect on fibrotic markers, and the addition of Sph to some cell types preferentially increases S1P rather than Cer [266]. It is noteworthy that small amounts of both dhSph and Sph can be converted to Cer leading to the observed inhibitory effects on Akt. Additionally, these inhibitory effects did not involve other downstream non-canonical signalling pathways and molecules such as ERK, P38-MAPK, NFκB and STAT1 (Figure 4.3A-B, E-G).

Despite dhS1P being consistently enriched at different time points in this study (Figure 4.4B1), and a previous report suggesting anti-fibrotic effects in dermal fibroblasts [163], exogenous dhS1P had a synergistic influence on TGFβ induced collagen synthesis in NCFs (Figure 4.5A). Our previous findings have shown that exogenous dhS1P alone can induce collagen synthesis [254]. Additionally, SK1 preferentially increases dhS1P and not S1P when dhSph is added exogenously [249]. Studies from our group and others have shown that dhS1P and S1P activate signalling pathways through their G protein coupled receptors, S1PRs, and are capable of "inside-out" signalling [84, 254]. Therefore, there is a possibility that the increased intracellular dhS1P, via inside out signalling, may have inhibited the TGFβ/SMAD signalling through its effects on phosphatase and tensin homolog (PTEN) as described by Bu and colleagues [137]. Additionally, the immunomodulator, fingolimod (FTY-720), has been shown to increase intracellular dhS1P [267], and was recently demonstrated to reduce existing cardiac hypertrophy and fibrosis in a pressure overload model [268].

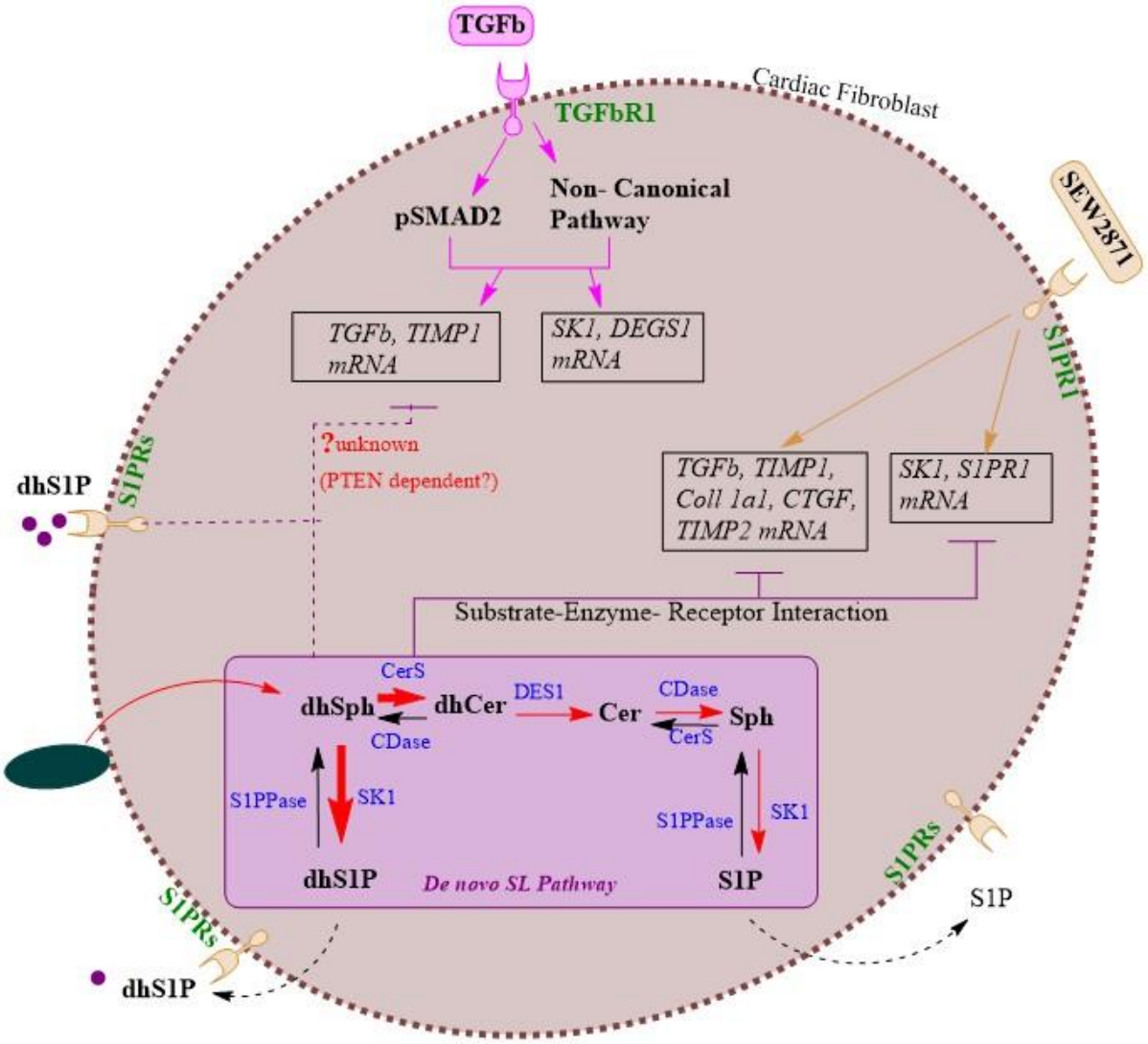

Figure 4.10. DhSph driven increase in *de novo* sphingolipid synthesis inhibits collagen synthesis in NCFs by TGFβ. Exogenous dhSph drives the *de novo* sphingolipid synthesis pathway as indicated with the red arrows. DhCer and dhS1P (bold red arrows) were increased the most. Increased intracellular S1P and dhS1P, due to increased pathway activation, are capable of activating S1PRs through "inside out" signalling (dashed black arrows). The increased activation of the *de novo* pathway was able to 1) inhibit pSMAD2 and non-canonical pathways activated by TGFβ (pink arrows and lines), which also led to reduced expression of fibrotic markers such as TGFβ1 and TIMP1. These effects were likely via "inside-out" signalling by dhS1P through an unknown mechanism that may

involve PTEN (dashed purple lines). 2) DhSph inhibited the S1PR1 agonist, SEW2871, induced collagen synthesis by reducing TGFβ1, TIMP1, CTGF, and TIMP2 mRNA expression (yellowish-brown arrows), perhaps through a substrate- enzyme-receptor interaction. Illustrated using ChemDraw Professional 7.0 (Perkin Elmer, MA, USA).

Apart from the increased enrichment of dhS1P, exogenous dhSph inhibited collagen synthesis induced by the S1PR1 agonist, SEW2871 (Figure 4.5C). This inhibition also led to profound reductions in the transcription levels of known fibrotic markers, such as TGFβ1, Coll1a1, CTGF, TIMP1 and TIMP2 (Figure 4.8A-E). Similar effects were observed in TGFβ induced increase in mRNA levels of TGFβ1 and TIMP1 (Figure 4.6A), which were reduced by dhSph. There were no changes in these genes in Sph treated cells (Figure 4.6B and 4.7B). Moreover, dhSph inhibition of S1PR1 transcription levels were observed in both TGFβ (Figure 4.7A) and SEW2871 (Figure 4.8F) treated cells, implying a connection between the receptor and dhSph activated sphingolipid pathway. Unlike S1PR2 and 3, S1PR1 exclusively couples to the G_i protein to transduce its signals [269]. One of the main downstream pathways that Gi proteins activate is the PI3K/Akt pathway, however similar inhibitory effects were not observed in cells that had Sph added exogenously. Further examination of dhSph effects on the transcription level of sphingolipid pathway enzymes showed some differences between TGFβ and SEW2871 treated NCFs. TGFβ increased both SK1 and DEGS1 mRNA expression (Figure 4.7A). The effects of TGFβ on SK1 are known [253], while its effect on DEGS1 transcription is a new finding. Exogenous dhSph did not have any effect on SK1 and DEGS1 mRNA levels in the presence

of TGFβ and SEW2871, perhaps due to the independent effect of dhSph in the absence of other stimulants (Figure 4.9). Contrarily, exogenous dhSph reduced SK1 mRNA levels in the presence of SEW2871 (Figure 4.8G), indicating that the transcription of SK1 in SEW2871 treated NCFs may depend on S1PR1 activation. TGFβ's direct effect on SK1 may have counteracted the effects of S1PR1 inhibition by dhSph [253]. There was no effect on DEGS1 transcription after dhSph co-treatment in the presence SEW2871 in NCFs (Figure 4.8H). The inhibition of collagen synthesis through S1PR1 inhibition by dhSph implies the existence of a negative feedback mechanism employed by the increased dhSph substrate availability on S1PR1. Berdysev and colleagues have alluded to the existence of such a mechanism which they termed the substrate-enzyme-receptor complex [249]. The DES1 enzyme could be the mediator between dhSph and S1PR1 in this case, as there was no effect on its transcription levels in the presence of either TGFβ or SEW2871, furthermore it is classically known as the "gate keeper" enzyme in the sphingolipid pathway. It should be noted that inhibiting SK1 and SK2 may not necessarily yield similar results in NCFs to those observed in this study. Therefore the findings of this study be regarded as preliminary.

In conclusion, the collagen reducing effects of dhSph in the presence of TGFβ, can be attributed to increased sphingolipids, such dhS1P, in the *de novo* synthetic pathway. Further studies are needed to determine which sphingolipid had the inhibitory effect. This study further highlighted the involvement of sphingolipid metabolic pathway's substrate-enzyme-receptor interactions in pathological events such as fibrosis, and thus, the need for investigating the effects of intracellularly generated dhS1P.

Preface

Chapter five describes the therapeutic potential of inhibiting the DES1 enzyme in the sphingolipid pathway for cardiac remodelling in a mouse I/R model using a tool compound, CIN038. Due to the length of the ipidomics results, they have been attached as appendix 3, to allow for a coherent flow to the chapter. This work has been submitted for publication.

Chapter 5: DES1 inhibition attenuated cardiac remodelling markers and inflammatory pathways in a mouse ischemia reperfusion model

Authors

Ruth R. Magaye[1, 2], Feby Savira[1, 2], Xin Xiong[1,2, 3], Daniel D. Donner[4], Helen Kiriazis[4], Aascha Brown[4], Li Huang[1, 2], Natalie Mellet[5], Kevin Huynh[5], Peter J. Meikle[5,6,] Christopher Reid [2,6], Bernard L. Flynn[7], David Kay[e8], Danny Liew[2], Bing H. Wang[1, 2*]

1. Biomarker Discovery Laboratory, Baker Heart and Diabetes Institute, Melbourne, Australia
2. Centre of Cardiovascular Research and Education in Therapeutics, School of Public Health and Preventive Medicine, Melbourne, Australia
3. Shanghai Institute of Heart Failure, Research Centre for Translational Medicine, Shanghai East Hospital, Tongji University, School of Medicine, Shanghai, P. R. China
4. Preclinical Cardiology and Microsurgery Imaging Platform, Baker Heart and Diabetes Institute, Melbourne, Australia
5. Metabolomics Research Group, Baker Heart and Diabetes Institute, Melbourne, Australia
6. School of Public Health, Curtin University, Perth, Australia
7. Monash Institute of Pharmaceutical Sciences, Monash University, Melbourne, Australia
8. Heart Failure Research Group, Baker Heart and Diabetes Institute, Melbourne, Australia

*Corresponding author:

bing.wang@baker.edu.au and bing.wang@monash.edu

Affiliations:

Daniel D. Donner and Helen Kiriazis: Department of Cardiometabolic Health, School of Medicine, University of Melbourne, Melbourne, Australia

5.1 Abstract

Rationale: In patients with MI, the level of sphingolipids such as Cer are increased and are associated with increased risk of progression towards HF. The DES1 enzyme is responsible for the conversion of dhCer into Cer in the *de novo* sphingolipids pathway.

Objective: Investigate the effects of DES1 inhibition on cardiac remodelling in a mouse model of ischemia-reperfusion (I/R) using a novel selective DES1 inhibitor, CIN038.

Methods and Results: Adult male C57Bl/6 mice underwent I/R surgery or sham and were randomly allocated to sham (n= 8), I/R+Vehicle (n=11) and I/R+CIN038 (n=11) groups. The I/R+Vehicle and I/R+CIN038 groups were given the vehicle (Trappsol) or 50 mg/kg CIN038 daily (*i.p*), beginning at day four post-surgery. Echocardiography was performed on day 27. On day 28, cardiac pressure-volume (PV) catherisation was conducted prior to being euthanised, and tissue and plasma were collected for downstream histochemistry and molecular analysis. DES1 inhibition by CIN038 reduced infarct size and cardiac stiffness. Furthermore, the DES1 inhibitor CIN038 attenuated myocyte hypertrophy and fibrotic marker gene expression, including coll1a1 and TGFβ1, as well as protein and tissue levels of α-SMA. The expression of IL-1β and IL-6 were also reduced by CIN038 treatment, leading to downregulation of STAT1/3 and ERK signalling pathways.

Conclusion: DES1 inhibitor CIN038 reduced cardiac remodelling markers in a I/R mice model by attenuating certain fibrotic, hypertrophic responses and inflammatory pathways.

5.2 Introduction

Recently, interest in sphingolipids, in the pathophysiology of CVD has gained momentum, due to their altered levels in clinical and animal studies [270-272], and could have therapeutic implications for cardiac remodelling. The enzyme DES1 acts as a gatekeeper in the *de novo* sphingolipid biosynthesis pathway, catalysing the insertion of a 4,5-trans-double bond into dhCer to form Cer [78, 86, 100]. Cer can be regarded as a metabolic hub, acting as a substrate for complex sphingolipids, Cer 1 phosphate (Cer1P), and eventually S1P from Sph. Cer levels have been found to be elevated in the plasma of patients with coronary artery disease (CAD), and cardiac tissues of small animal models [125, 273]. It also increases the risk for HF in patients, which may be attributed to Cers ability to induce apoptosis [129, 274, 275]. In contrast, S1P is a bioactive molecule capable of activating cellular signalling pathways through its cell surface receptors (S1PR1-5) conferring both cardioprotective and injurious effects depending on the aetiology and the subtype of receptor being activated [196, 276]. It also induces cell proliferation and is known to increase fibrosis in vitro, mimicking TGFβ mediated signalling through the SK1/S1P axis [122, 254, 277, 278].

The benefits of DES1 inhibition have been targeted for cancer therapy utilizing phenolic compounds, and both sphingolipid and non-sphingolipid analogues. For example, inhibition of DES1 by the synthetic retinoic acid, fenretinide, reduces Cer and raises dhCer levels resulting in increased apoptosis, reduced proliferation and angiogenesis in various cancers[100, 279, 280]. In terms of metabolic disorders such as diabetes mellitus, DES1 inhibition increases insulin sensitivity, reduces adipocyte differentiation and senescence [100, 158]. Despite these demonstrations of the therapeutic potential of DES1 inhibition, the use of non-specific inhibitors has led to some contradictory findings. Furthermore, the effects of DES1

inhibition in the context of CVDs including cardiac remodelling in MI has not been explored. We investigated the therapeutic potential of a novel DES1 inhibitor, CIN038, in a mouse model of I/R. CIN038 is a synthetic sphingolipid derived specific inhibitor of the DES1 enzyme with an IC_{50} of 0.55 μM as published by Aurelio et.al [281]. It is compound number 38 in the article, with the chemical name 4-((5-(4-trifluoromethyl) phenyl)-1,3,4-oxadiazol-2-yl) amino)-phenol.

5.3 Methods

This study was approved by the Alfred Research Alliance Animal Ethics Committee (AEC no. E/1949/2019/B). All animal experiments were conducted in accordance with the Australian Code of Practice for "the Care and Use of Animals for Scientific Purposes" of the National Health and Medical Research Council of Australia. Male C57Bl/6 mice (n=30, age= 3 months) were obtained and housed at the Alfred Research Alliance Precinct Animal Care Facility. Mice were randomized to receive either myocardial I/R surgery (n= 22) or sham (n= 8).

5.3.1 I/R surgery

Adult C57Bl/6 mice were randomly assigned to undergo either the I/R or sham procedures. Briefly, mice were anaesthetised using a mixture of Ketamine (100 mg/ kg), xylazine (20 mg/kg) and atropine (1.2 mg/kg) (KXA). Prior to incision, mice received subcutaneous injection of meloxicam and localised injection of bupivacaine around the surgical site (0.5 mg/kg). A left thoracotomy was performed via the fourth intercostal space to expose the left anterior descending

(LAD) coronary artery with the aid of a surgical microscope as described previously [282, 283]. The LAD coronary artery was ligated using a 7- 0 silk suture with slip-knot enclosing a releasing ring. Regional ischemia was induced for 40 minutes, and blood flow through the LAD was re- established by releasing the slip- knots. Sham animals underwent the same procedures but were not ligated. Mice were randomly assigned to receive vehicle (Trappsol, 50 mg/kg/day, n= 11) or CIN038 (50 mg/ kg/ day CIN038, n= 11) commencing at four days after I/R surgery and were followed for a period of one-month post-surgery. The investigator was blinded. The 50 mg/kg daily i.p. dose was based on the enzyme activity of the drug in vitro cellular activity assays and initial PK studies. The i.p. route was chosen to determine if there were any toxicological or global effects, apart from the anti- fibrotic effects, as part of this compounds preliminary study.

5.3.2 Echocardiography

Left ventricular size and function were assessed on day 27 post-surgery through echocardiography. Mice were anaesthetized with isoflurane at approximately 4.5 % induction and maintained at approximately 1.7% during image capture, with body temperature ~37◦. Transthoracic echocardiography was performed using a Vevo2100 ultrasound system equipped with a 40 MHz linear-array transducer. B-mode loops of the long-axis parasternal view were captured and analysed offline in a blinded fashion, using Vevo LAB software (version 3.2.5).

5.3.3 Cardiac hemodynamic assessment

Mice were anesthetized with isofluorine and placed in a supine position. A 1.4 Fr Millar Pressure-Volume catheter was inserted into the artery and LV with 10kHz and connected to a Powerlab System (AD instruments) were used. Hemodynamic assessment was conducted for established parameters through a catheter placed into the LV through the right carotid artery, as described previously [284]. Cardiac performance was measured as stroke work (SW) and end diastolic and systolic volume (Ved and Ves). LV systolic preload dependent function was measured as maximal rate of LV pressure change (dP/dt_{max}) and end systolic pressure (Pes). End systolic and end-diastolic pressure volume relationships (ESPVR and EDPVR) were analysed as measures of preload and load independent LV systolic and diastolic function. Diastolic load dependent LV function was quantified by end diastolic pressure (Ped), the isovolumetric relaxation constant (tau, τ), and the minimal rate of LV pressure change (dP/dt_{min}). The LV developing pressure (Pdev), maximum and minimum LV pressure (Pmax and Pmin) and arterial elastance (Ea) were also assessed. Two mice (one in each group) were excluded due to incomplete measurement of parameters.

5.3.4 Plasma and tissue collection

After cardiac catherization, while anaesthetised, mice were euthanized after cardiac catheterisation through cardiac puncture using a 26-gauge needle and syringe. Cardiac blood was used to calibrate the hemodynamic data collected. This was then transferred into 1.5 mL Eppendorf tubes and centrifuged at 1800 rpm for 5 minutes to separate the plasma. 100 μL aliquots of plasma were snap frozen on dry ice and stored for subsequent analysis. Tissue weights were determined

after necropsy. The LV was dissected into three portions; the base, mid-section, and apex. The first portion of the re-sectioned mid-section was separated into the infarct zone, boarder zone and remote zone and snap frozen in separate Eppendorf tubes. The second portion of the LV mid-section, and other tissues were processed for histochemistry. 2 -3 mm pieces of other tissues were also snap frozen in liquid nitrogen for western blot, lipidomics and PCR, accordingly.

5.3.5 Plasma and liver lipidomic

Plasma and liver samples from mice were processed for lipidomics analysis. The liver was chosen to determine whether CIN038 affected global lipid synthesis and due to less cardiac tissue available to process for lipidomics after utilising it for other assays. Liver tissue weight of about 16.19 ± 1.82 mg were homogenized using the Bullet Blender Gold (BB24-AU-CE, Next Advance, Troy, NJ, USA) at 4◦C for 15 seconds. Samples were then sonicated on a Misonix ultrasonic liquid processor (S-4000, Misonix, Inc., Farmingdale, NY, USA) at 25 amplitudes for 10 seconds on ice. 5 µL aliquots of samples were separated for protein quantification before snap-frozen on dry ice.

Lipids were extracted from 10 µL of approximately 9.3 ± 2.7 µg/mL protein from homogenized liver tissues and 10 µL of plasma samples and processed for liquid chromatography-mass spectrophotometry (LC-MS) according to previously published methods [255]. The Agilent 6490 QQQ mass spectrometer with an Agilent 1290 series HPLC system and a ZORBAX eclipse plus C18 column (2.1 x 100 mm, 1.8 µm, Agilent) with the thermostat set at 60°C was used to analyse the cell extracts. Mass spectrometry analysis was performed with dynamic scheduled multiple reaction monitoring (MRM) in positive ion mode. After

characterizing the lipids, the Mass Hunter (B.07.00, Agilent Technologies) software was used to integrate chromatographic peaks. Lipids were assigned to a specific lipid species based on MRM (precursor/product) ion pairs and retention time. The ratio of each analyte peak with the corresponding internal standard, was used to quantify the lipids.

5.3.6 Histochemical analysis of cardiac tissue sections

Mid LV tissue sections were fixed in 10% neutral buffered formalin for 24 h and embedded in paraffin blocks. 4 μm thin sections were prepared on salinized glass and stained with Picosirius red (PSR) to determine the extent of fibrosis [16]. Infarct size was measured as an averaged percentage of the endocardial and epicardial scarred circumferences of the whole LV within each group (Figure 5.1). Slides were scanned using Aperio Scanscope CS digital scanner (Aperio ScanScope Console v.8.0.0.1058, Aperio Technologies, Inc.) at x20 magnification and analysed using ImageScope (v11.1.2.760, Aperio Technologies).

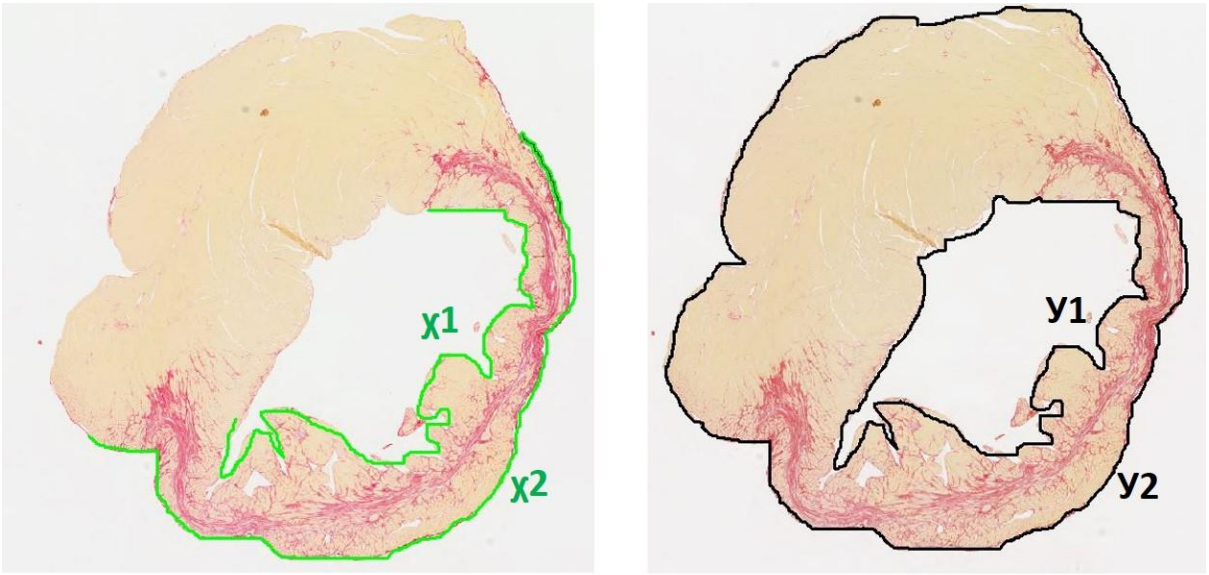

Figure 5.1. Infarct size measurement illustration. Infarct size was measured

using the following formula: Infarct size (%) = [(x1/y1) + (x2/y2)] / 2 *100, where x1: infarct length on the endocardium (μM), y1: total length of endocardium (μM), x2: infarct length on the epicardium (μM), y2: total length of epicardium (μM).

The hematoxylin and eosin (H&E) stain was used to assess cell morphology and myocyte hypertrophy, from approximately 50 myocyte per LV in the subendocardial region of the LV with similar-sized nuclei and intact cellular membranes. Individual cell membranes were traced to determine the cross-sectional area, and these were averaged as a measure of hypertrophy. Sections were also processed for immunohistochemistry to assess cardiac expression of tissue specific Coll 1 and 3, SMADs, TGFβ, and α-SMA. CD45 and CD68 positive staining were used as inflammatory cell markers for lymphocytes and macrophages. All sections were counterstained with hematoxylin. Antibody staining was detected by diaminobenzidine as previously reported [285], and quantitated for percentage area using ImageScope. The total number of CD45 and CD68 immunoreactive cell infiltration and SMAD2 phosphorylation (pSMAD2)-stained nuclei in non-infarct zone of the LV were individually counted from an average of 25 fields of view using ImageScope at x40 magnification. All data were acquired and analysed by a single blinded observer. Further information on antibodies for immunohistochemical staining are provided in Appendix 2.3.

5.3.7 Cardiac tissue protein expression analysis through Western Blot

Tissues from the infarct and remote zone of the LV were homogenised in 300 µL lysis buffer with inhibitor cocktails, for 10-15 seconds on ice. Aliquots of the lysate were snap frozen on dry ice after centrifuging at 12 000 g for 10 minutes. Proteins were quantified using the Bradford assay. Protein were denatured at 98 ◦C in sample buffer and equal amount of protein (10 µg) from each sample were separated on 7.5% and 10% gels by SDS-PAGE, and transferred onto nitrocellulose membranes (GE HealthCare, Chicago, IL, USA). Western blotting was performed as described in section 2.3.5. The membranes were probed for phosphorylated, Akt, STAT1 and 3, ERK, mTOR, RPS6, nuclear factor kappa B (NFκB: CST, Danvers, MA, USA: 3192), and p38 mitogen activated protein kinase (p38-MAPK: CST, Danvers, MA, USA: 5536). They were also probed for TGFβ, TIMP1, and α-SMA. Bands were detected using Super Signal West Pico Chemiluminescence Substrate (Thermo Fisher Scientific, Rockford, IL, United States) on the BioRad Chemidoc instrument and analysed using Image lab software (BioRad Laboratories, Hercules, CA, USA). Proteins were normalized to GAPDH or β-Actin.

5.3.8 PCR analysis of gene expression

RT PCR was used to ascertain changes in gene expression. Infarct and remote zone heart tissue sections were homogenized in 300 µL trizol for 10-15 seconds on ice. RT PCR was performed as described in section 2.3.7. The expression levels of the fibrotic markers; TGFβ1, CTGF, TIMP1 and 2, Coll1a1, Coll3aI, and MMP2 and 9, the S1P receptors; S1PR1-3, the enzymes; SK1, and DES1

(DEGS1), hypertrophy markers; alpha myosin heavy chain (αMHC), ANP and BNP, and inflammatory markers; tumour necrosis factor alpha (TNFα), interleukin 1 beta and 6 (IL-1β and IL-6) were quantified. Refer to Appendix 2.2 for full sequence of primers. 18s rRNA was used as the endogenous control.

5.3.9 Cardiac fibroblasts lipidomics analysis

Primary NCFs were isolated and cultured as described in section 2.3. Briefly, NCFs cultured were cultured at a density of 2.5 $X10^5$ cells/ well. These were treated with 3.0 and 10 μM CIN038 for 5 and 24 h. The cells were harvested and processed for lipidomics as described in section 4.3.5. The fibrotic agent Ang II was used at both time points as a comparison.

5.3.10 Data Analysis

One-way ANOVA followed by Bonferroni's post hoc test was used to determine statistical significance in more than two groups. Student t-test was used to assess difference between two groups. Lipidomics data analysis was performed using either student t-test or One-way ANOVA, both were tested for false discovery rate (FDR) by multiple comparisons (Benjamini Hochberg method). The results are presented as mean ± SEM. A statistically significant result was determined with a two-tailed *p*-value of less than 0.05. GraphPad Prism Version 9 (GraphPad Software Inc., San Diego, CA, United States) was used to perform all the statistical analyses.

5.4 Results

A total of 28 mice were included in the study. A mouse in the I/R+Vehicle group was excluded due to a non- drug related adverse event at day 14 of the study (Figure 5.2). Another mouse in the CIN038 treatment group was excluded in the analysis process due to small infarct size (8%) as indicated by histochemistry, and by echocardiography.

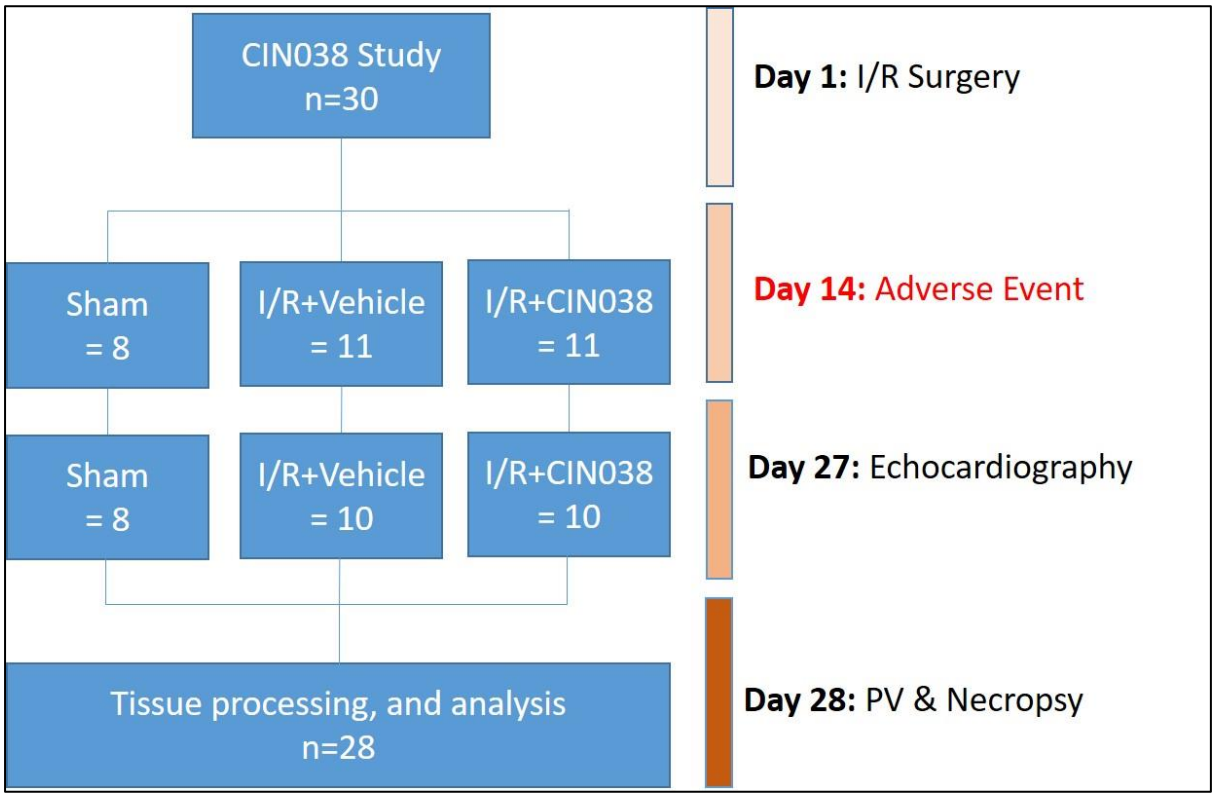

Figure 5.2. Schematic representation of the CIN038 study.

In the I/R+Vehicle group there was a strong trend toward an increase in heart weight to body weight ratio (hw/bw) (p= 0.058) compared to the sham group. There were no significant changes in lung weight to body weight ratio (lw/bw). The effects of CIN038 on hw/bw and lw/bw compared to the I/R+Vehicle group were not significant (Table 5.1). There were no differences in the body weight between the groups.

Table 5.1. Differences in body weight and heart weight of mice. * sham vs. I/R+Vehicle. BW; body weight; HW; heart weight; LW, lung weight. Data are presented as mean ± SEM.

Group	BW (g)		HW/BW Ratio (mg/g)		LW/ BW Ratio (mg/g)	
	Mean	*p* Value	Mean	*p* Value	Mean	*p* Value
Sham (8)	30.68 ± 2.34		4.65 ± 0.13		5.28 ± 0.26	
I/R+Vehicle (10)	28.31± 2.32	0.071	5.59 ± 0.49	0.058	5.56 ± 0.56	0.71
I/R+CIN038 (10)	28.31± 1.61	0.77	4.90 ± 0.28	0.13	5.28 ± 0.22	0.64

5.4.1 Echocardiography

Echocardiography showed that CIN038 treatment had no significant effect on cardiac function (Table 5.2). The LV volume at diastole and systole (p= 0.01, and p= 0.003, respectively) and LV area at systole (p= 0.005) were significantly increased in the I/R+Vehicle group. The ejection fraction (EF), and stoke volume (SV) were reduced by 44%, and 19% in the I/R+Vehicle group compared to sham (p=<0.0001, and p=0.0629, respectively). The 16% reduction in cardiac output (CO) in the I/R+Vehicle group compared to sham was not significant (p= 0.11). The changes in these parameters in the I/R+CIN038 compared to the I/R+Vehicle group were not significant. There were no significant differences in the heart rate (HR) between the groups. Representative echocardiography image provided in Figure 5.3A.

Table 5.2 Echocardiography assessment at day 27. DES1 inhibition had no significant on cardiac function parameters altered by IR induced MI. Values are presented as mean ± SEM. *significant *p* value vs. Sham. Sham=8, I/R+Vehicle= 10, I/R+CIN038=10.

Parameters	Sham	I/R+Vehicle		I/R+CIN038	
(Units)	Mean ± SEM	Mean ± SEM	*p* value vs. Sham	Mean ± SEM	*p* value vs. I/R+ Vehicle
HR (bpm)	466.8±16.1	482.2±11.4	0.434	503±11.9	0.21
Area_s (mm)	14.4±0.4	21.2±1.9	0.005*	19.9±1.5	0.57
Area_d (mm)	22.3±0.7	26.7±1.8	0.052	25.8±1.2	0.65
Vol_s (uL)	26.4±1.4	64.2±9.4	0.003*	56.7±7.0	0.51
Vol_d (uL)	56.2±3	88.4±9.8	0.0136*	82.4±6.1	0.59
SV (uL)	29.8±1.7	24.2±1.9	0.048*	25.8±1.3	0.50
EF (%)	52.9±0.8	29.5±3.3	<0.0001*	32.8±3.3	0.46
CO (ml/min)	13.9±0.9	11.7±0.9	0.103	12.9±0.6	0.26

5.4.2 Cardiac hemodynamic parameters

CIN038 treatment did not improve cardiac hemodynamic parameters in mice with I/R (Table 5.3). The Ves and Ved showed a strong trend toward an increase in the I/R+Vehicle group (p= 0.07, and p= 0.08, respectively), implying increased workload. The LV dP/dt_{max}, Pdev, and Pes were significantly reduced in the I/R+Vehicle group compared to sham (p= 0.001, p= 0.0007 and p= 0.002, respectively). Tau (τ) was significantly prolonged by 30% and dP/dt_{min} was increased in the I/R+Vehicle group compared to sham (p= <0.0001 and p= 0.0002, respectively). Contractile function as measured by the ESPVR had a strong trend toward a reduction in the I/R+Vehicle group compared to sham group (p= 0.08). The changes in these parameters in the I/R+CIN038 group compared to the I/R+Vehicle group were not significant. There were no significant differences

between groups in the other parameters such as EDPVR, Ea, SW, Ped and Pmin. Representative echocardiography image provided in Figure 5.3B.

Table 5.3 Hemodynamic parameters measured by PV analysis at day 28. Values are presented as ± SEM. * significant *p* value vs. Sham. Sham= 8, I/R+Vehicle= 9, I/R+CIN038= 9. Two mice were excluded, due to incomplete measurements.

PV Loop Parameters	Sham	I/R+Vehicle		I/R+CIN038	
	Mean ±SEM	Mean ±SEM	*p* value vs. Sham	Mean ±SEM	*p* value vs. I/R+Veh
SW (mmHg*μL)	1893.7±190.9	1604.3± 146.9	0.2	1604.9± 101.6	0.99
ESPVR (mmHg/ml)	2.8±0.6	1.7±0.3	0.08	1.4±0.2	0.43
EDPVR ((mmHg/ml)	0.4±0.06	0.5±0.08	0.4	0.4±0.09	0.41
Ves (μL)	23.1±4.3	53.1±13.8	0.07	43.1±7.2	0.53
Ved (μL)	42.6±6.6	73.5±14.1	0.08	63.1±6.3	0.51
Pmax (mmHg)	98.2±2.4	85.3±1.9	0.0007*	84.2±1.7	0.68
Pmin (mmHg)	-0.0001± 0.00008	0.03±0.03	0.3	0.00001± 0.00009	0.28
Pdev (mmHg)	98.2±2.4	85.3±1.9	0.0007*	84.2±1.7	0.69
Pes (mmHg)	93.5±2.1	81.9±2.3	0.002*	81.5±1.7	0.89
Ped (mmHg)	5.2±0.4	6.01±0.8	0.4	6.6±0.8	0.60
Ea (mmHg/μL)	4.4±0.7	3.6±0.4	0.3	3.4±0.3	0.70
dP/dt max (mmHg/s)	10771.8± 766.6	7515.7± 352.34	0.001*	7824.2± 473.6	0.61
dP/dt min (mmHg/s)	-9523.00± 690.5	-5881.9± 328.1	0.0002*	-6172.1± 353.3	0.55
τ (ms)	5.5±0.1	7.2±0.3	0.0001*	6.7±0.2	0.25

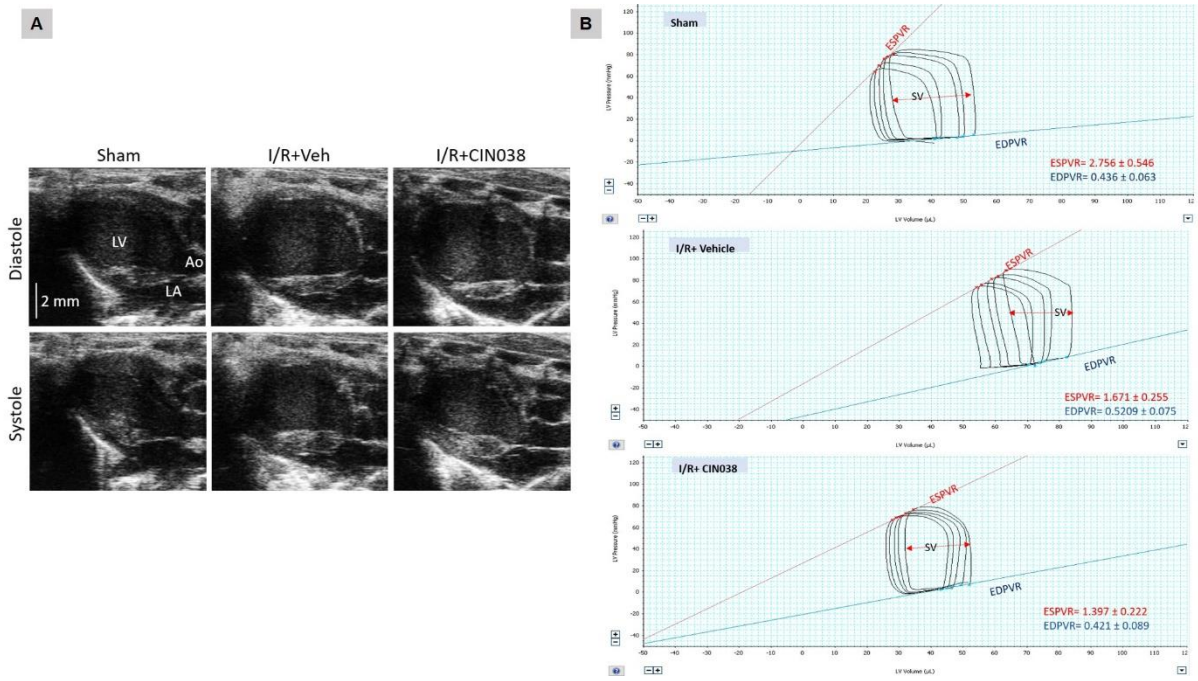

Figure 5.3. Representative images of echocardiography and PV loops. (A) Representative long axis echocardiography images at diastole and systole. LV, left ventricle; LA, left atrium; Ao, Aorta. (B) Representative PV loops from sham, I/R+Vehicle, and I/R+CIN038 group.

5.4.3 Infarct size and tissue fibrosis

The I/R surgery caused MI as indicated by the substantially large infarct size in the I/R+Vehicle animals (p= <0.0001, Figure 5.4B). Mice treated with CIN038, had a strong trend toward a reduction in infarct size by 22% compared to the I/R+Vehicle group (p= 0.0518). In the I/R+Vehicle group tissue interstitial fibrosis was significantly increased (p= <0.0001), together with significant increase in tissue expression of Coll 1, Coll 3 and α-SMA (p= <0.0001, p= 0.0002 and p= 0.0314, respectively). CIN038 treatment in the I/R+CIN038 group had a strong trend toward reduction in Coll 3 tissue expression, with no significant (NS) effect on interstitial fibrosis, Coll 1 and α-SMA expression compared to I/R+Vehicle

group. Immunohistochemical staining of cardiac tissue demonstrated a significant increase in TGFβ1 (p= 0.0008) protein expression in the I/R+Vehicle group. Tissue nuclear protein expression of phosphorylated SMAD2 (pSMAD2) also tended to increase (p= 0.0971). CIN038 treatment significantly reduced TGFβ1 in the I/R+CIN038 animals compared to I/R+Vehicle (p= 0.0155), and despite a reduction in pSMAD2 which was not significant (p= 0.0809).

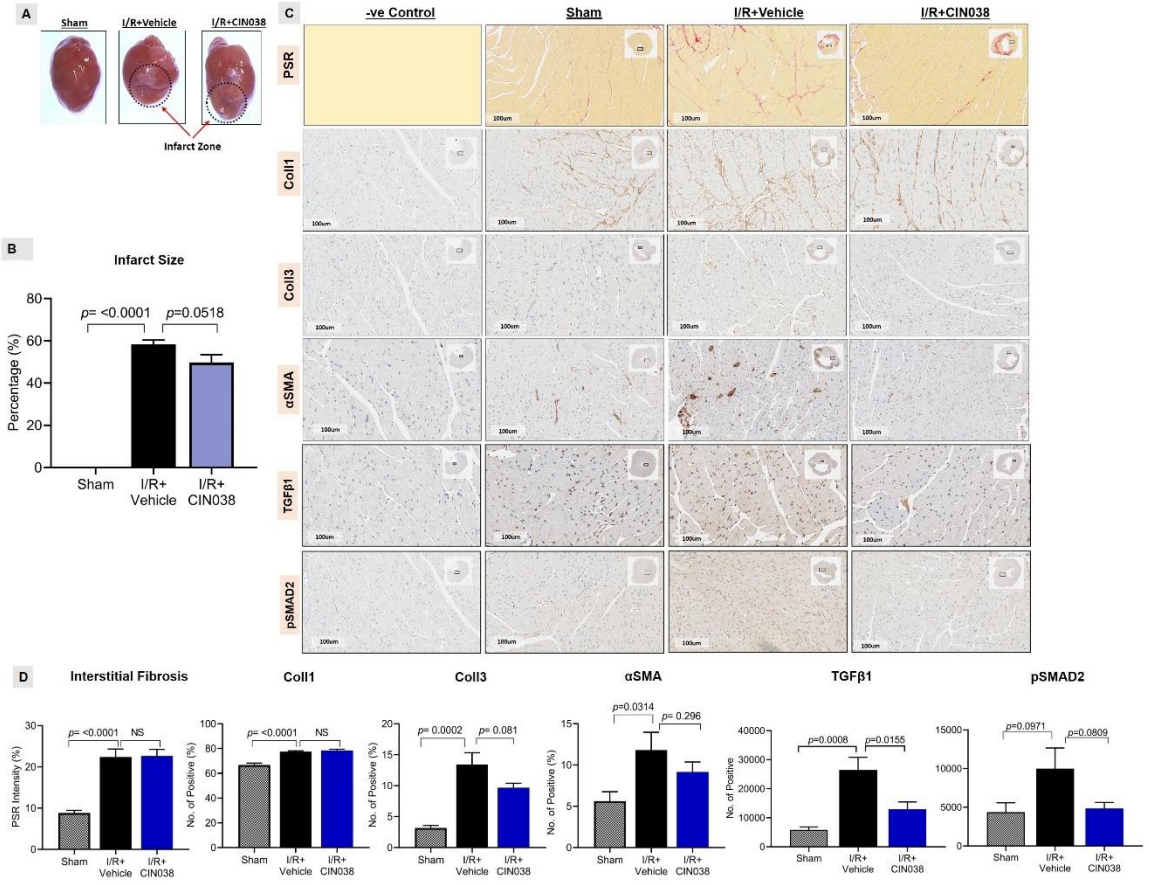

Figure 5.4. Effect of DES1 inhibition on infarct size and tissue expression of fibrotic markers. (A) Representative picture of the heart from each group. (B) Infarct size was increased in the I/R+Vehicle group, which was reduced in the I/R+CIN038 group. (C) Representative immunohistochemistry photomicrographs of PSR, Coll1, Coll3, α-SMA, TGFβ1 and pSMAD2 staining. Scale bar: 100μm. (D) Quantification of PSR staining for interstitial fibrosis, and

Coll1, Coll3 and α-SMA immunohistochemical staining. Values are presented as mean ± SEM.

5.4.4 Cardiac myocyte hypertrophy

DES1 inhibition significantly reduced myocyte hypertrophy in mice with I/R. The myocyte cross-sectional area in the I/R+Vehicle group was significantly increased compared to sham (p= 0.0003, Figure 5.5B). This was significantly reduced in the I/R+CIN038 group compared to the I/R+Vehicle group.

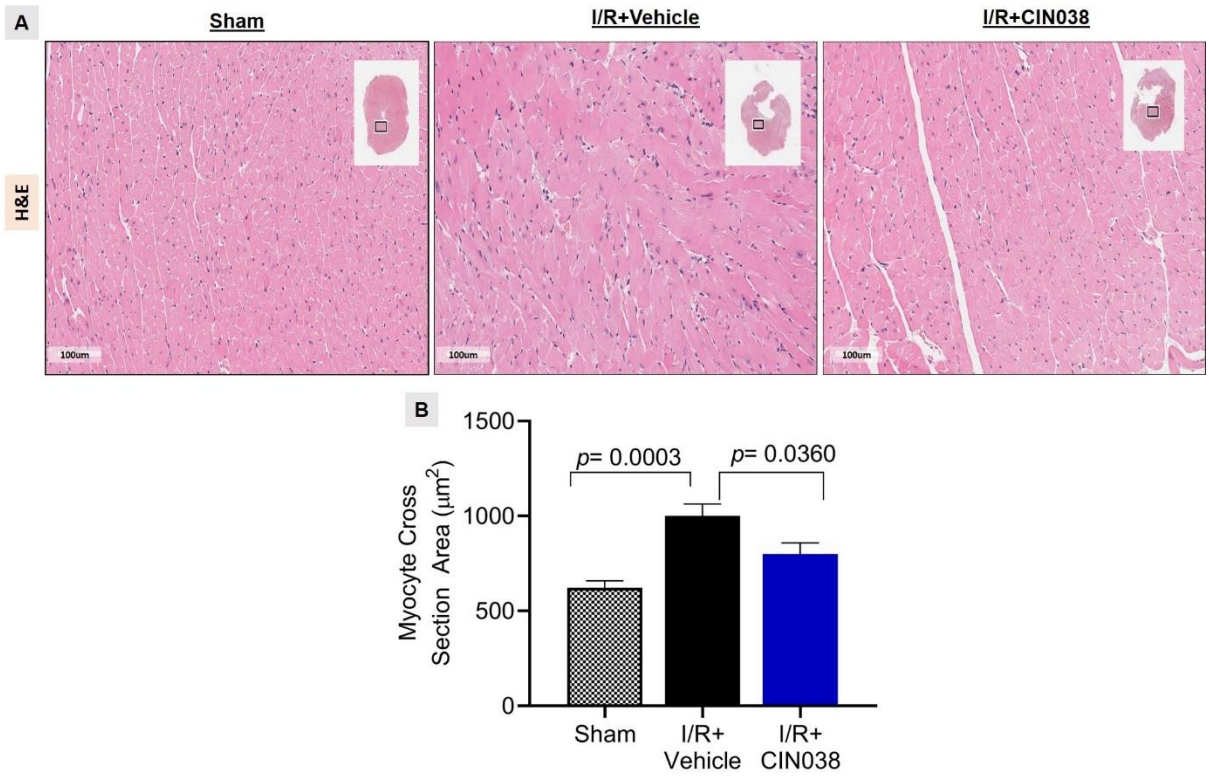

Figure 5.5. Effect of DES1 inhibition on cardiac myocyte hypertrophy. (A) Representative histochemistry photomicrographs of H&E staining. Scale bar: 100 μm. (B) I/R significantly increased myocyte area in the I/R+Vehicle group, this was reduced in the I/R+CIN038 group. Data are presented as ± SEM.

5.4.5 Cardiac CD68 and CD45 positive cell infiltration

Compared to sham animals, analysis of inflammatory cell infiltration in the myocardium as demonstrated by immunohistochemistry showed significant increase in CD45 (p= 0.0068) and CD68 (p= 0.0006) positive immune cell staining in the I/R+Vehicle group compared to the Sham group (Figure 5.6A and B). Changes in both CD45 and CD68 positive immune cell staining in the I/R+CIN038 group compared to the I/R+Vehicle group were not significant (p= 0.2015 and p= 0.5646, respectively).

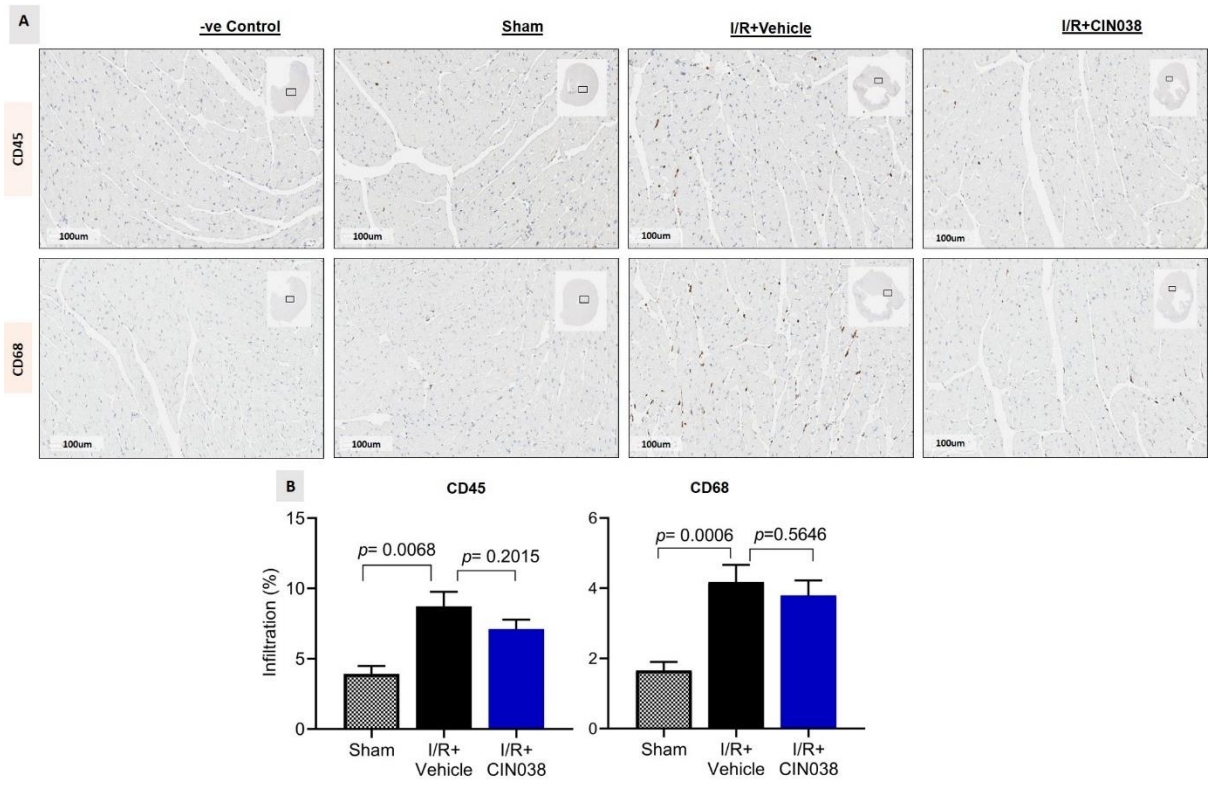

Figure 5.6. Effect of DES1 inhibition on lymphocyte and macrophage infiltration. (A) Representative immunohistochemistry photomicrographs of CD45+ and CD68+ staining. Scale bar: 100 μm. (B) Percentage of CD45+ and CD68+ cell infiltrates in the cardiac tissue were increased in the I/R+Vehicle group. Data are presented as mean ± SEM.

5.4.6 Cardiac fibrotic markers gene expression

Examination of fibrotic gene markers revealed that CIN038 treatment significantly reduced Coll1a1 (p= 0.0383) and TGFβ1 (p= 0.0459) mRNA levels in the I/R+CIN038 group compared to the I/R+Vehicle group in the infarct zone (Figure 5.7A & C). CIN038 had no significant effects on Coll 3a1, CTGF, TIMP1, TIMP2, MMP2 and MMP9. These markers were all significantly increased in the I/R+Vehicle mice compared to sham mice, except for MMP9. In the remote zone Coll1a1 mRNA expression was significantly reduced (p= 0.0381), while Coll3a1 (p=0.0552), TIMP1 (p= 0.0925), and MMP9 (p= 0.0591) mRNA expression showed trends of reduction in the I/R+CIN038 group, compared to the I/R+Vehicle group (Figure 5.7I-L).

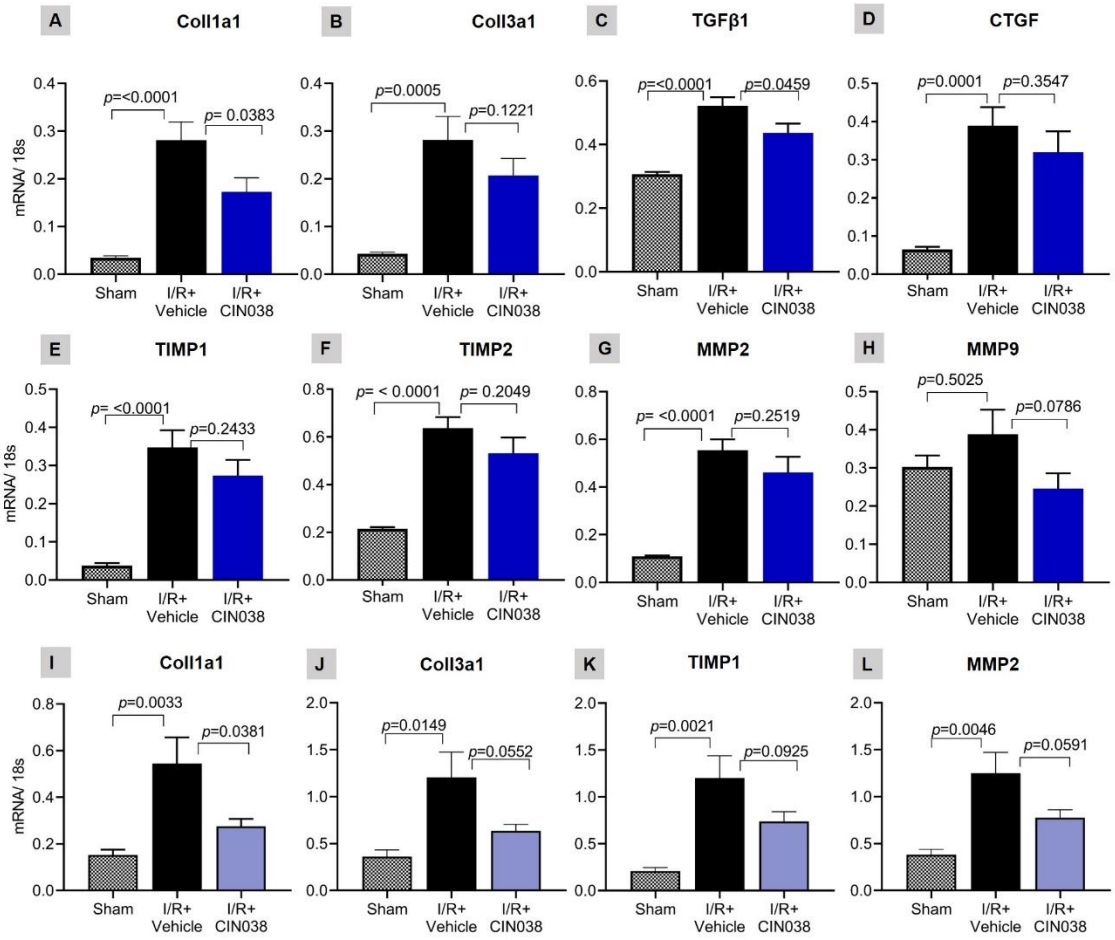

Figure 5.7. Effect of DES1 inhibition on the gene expression of fibrotic markers. (A-H) DES1 inhibition significantly ameliorated the mRNA expression levels of Coll1a1, and TGFβ1 in the infarct zone. No significant effects on Coll3a1, CTGF, TIMP1, TIMP2, MMP2 and MMP9 mRNA expression were observed. (I-L) In the remote zone, Coll1a1, Coll3a1, TIMP1 and MMP2 were reduced in the I/R+CIN038 group compared to sham.

5.4.7 Cardiac hypertrophic and inflammatory gene expression

In the I/R+Vehicle mice, hypertrophic gene markers such as αMHC was significantly reduced, while ANP and BNP were significantly increased in the infarct and remote zones (Figure 5.8A and B). CIN038 treatment increased αMHC

mRNA expression in I/R+CIN038 group (p= 0.0353) but had no effect on ANP and BNP mRNA expression compared to the I/R+Vehicle group in the infarct zone. In the remote zone, the changes in αMHC, ANP and BNP mRNA expression were not altered significantly by CIN038.

IL-1β (p= 0.0013) and IL-6 (p= <0.0001) gene expression levels in the infarct zone were significantly increased in the I/R+Vehicle mice compared to sham mice (Figure 5.8C). In the I/R+CIN038 mice IL-6 expression showed a trend of reduction compared to the I/R+Vehicle mice (p= 0.0635), but had no effect on IL-1β. There was no difference in TNFα mRNA expression between the groups in the infarct zone.

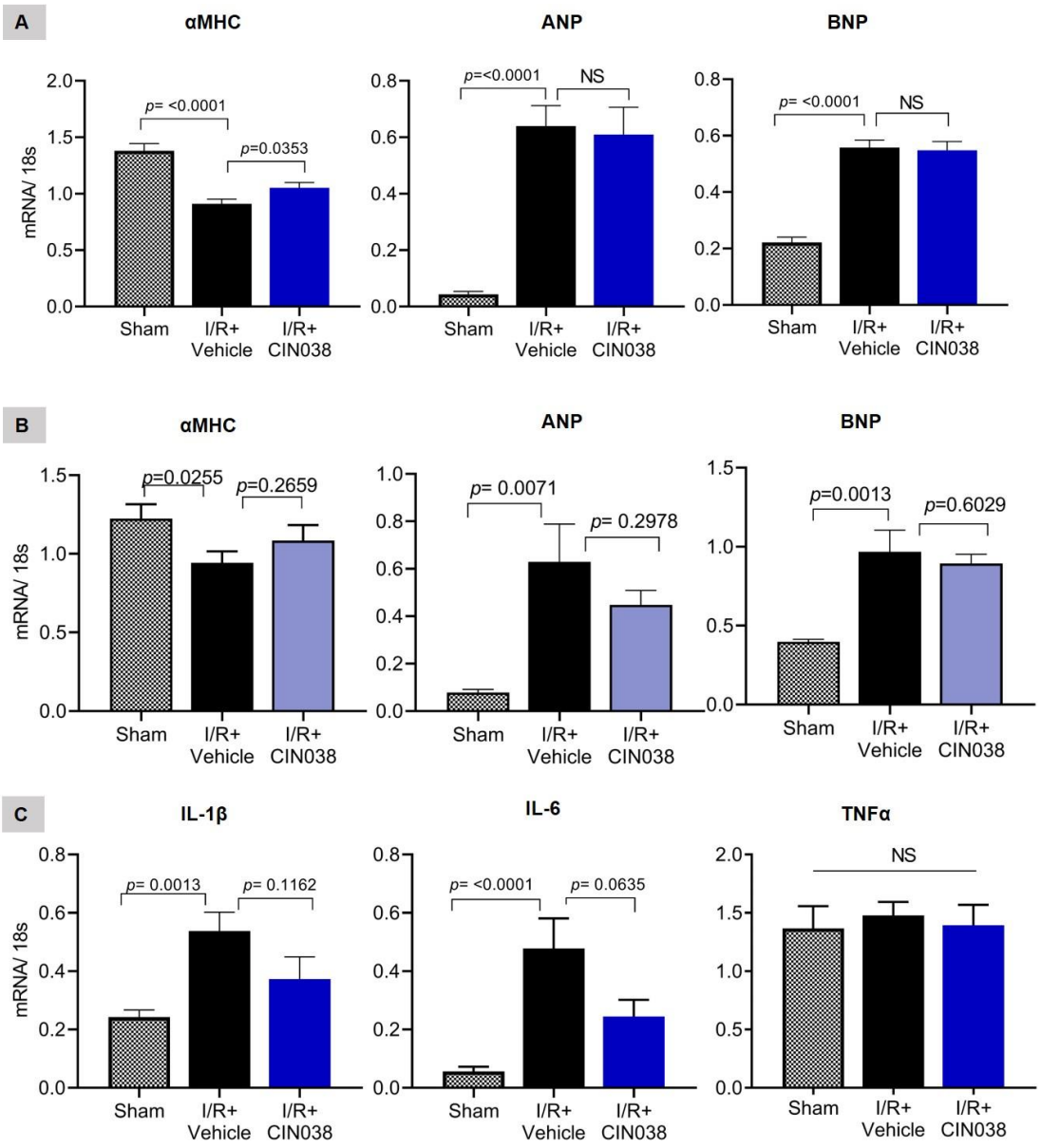

Figure 5.8. Effect of DES1 inhibition on hypertrophic and inflammatory gene expression. (A) Expression of hypertrophic markers αMHC, ANP and BNP were altered in the infarct zone, (B) and in the remote zone of I/R hearts. (C) Changes in IL-1β, and IL-6 gene expression in the infarct zone of I/R hearts. Data are presented as mean ± SEM.

5.4.6 Expression of sphingolipid related genes in the heart

Analysis of sphingolipid related gene expression in the infarct zone demonstrated that SK1 (p= <0.0001), and S1PR2 (p= <0.0001) mRNA were significantly elevated in the I/R+Vehicle group compared to sham (Figure 5.9A and D). The mRNA level of S1PR1 was reduced significantly (p=0.011), but the reduction in S1PR3 mRNA was not significant (p=0.077), Figure 5.9C and E, respectively. CIN038 treatment in the I/R+CIN038 group had no significant effect on these genes compared to the I/R+Vehicle group. The mRNA level of the DEGS1 gene was not altered in all treatment arms in the infarct and remote zones (Figure 5.9B and F).

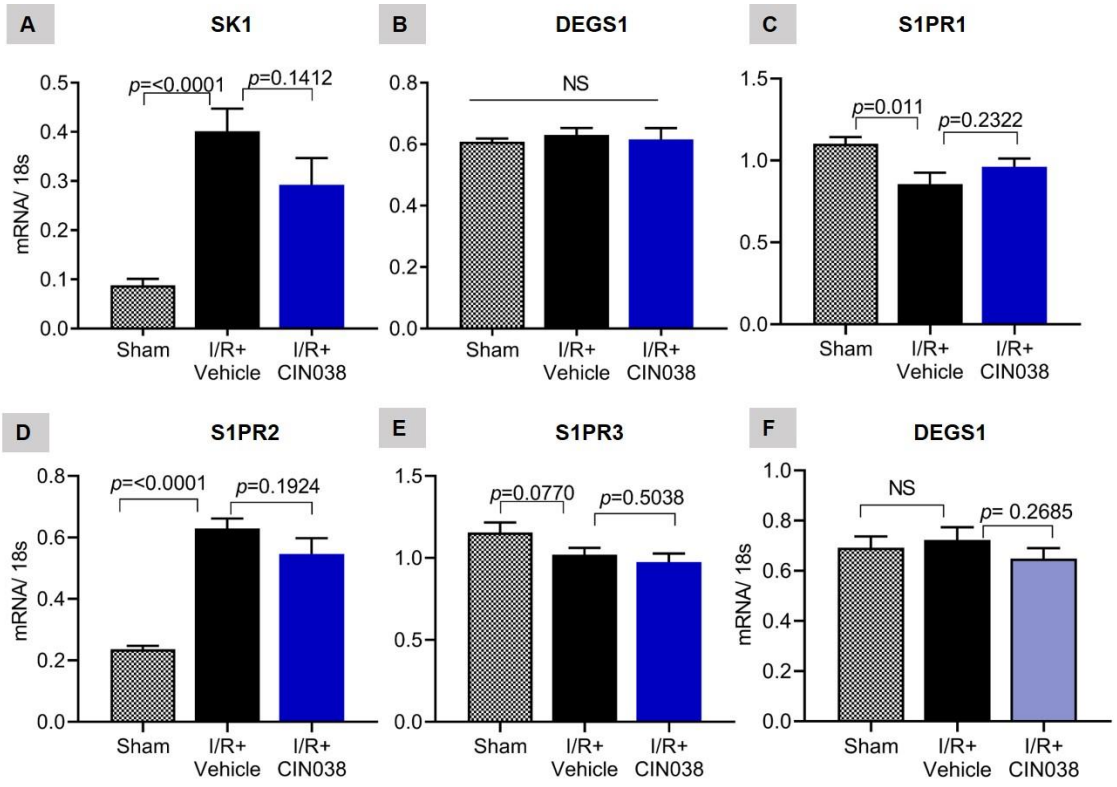

Figure 5.9. Effect of DES1 inhibition on the expression of sphingolipid related genes. (A-E) DES1 inhibition had no significant effect on SK1, DEGS1, S1PR1-3 gene expression in the infarct zone of I/R+CIN038 mice compared to I/R+Vehicle mice. (F) DES1 inhibition had no significant effect on DEGS1 gene

expression in the remote zone of I/R+CIN038 mice compared to I/R+Vehicle mice.

5.4.9 Fibrotic protein expression in cardiac tissue

α-SMA and TGFβ were remarkably increased in the I/R+Vehicle mice compare to sham (p= 0.0009 and p=0.0162, respectively), while the shift toward an increase in TIMP1 protein expression was not significant (p= 0.1573). CIN038 treatment significantly reduced α-SMA (p= 0.034) and TGFβ (p= 0.042) protein expression, while there was a strong trend toward reduction in TIMP1 (p= 0.066) expression in the infarct zone of I/R+CIN038 mice compared to the I/R+Vehicle mice.

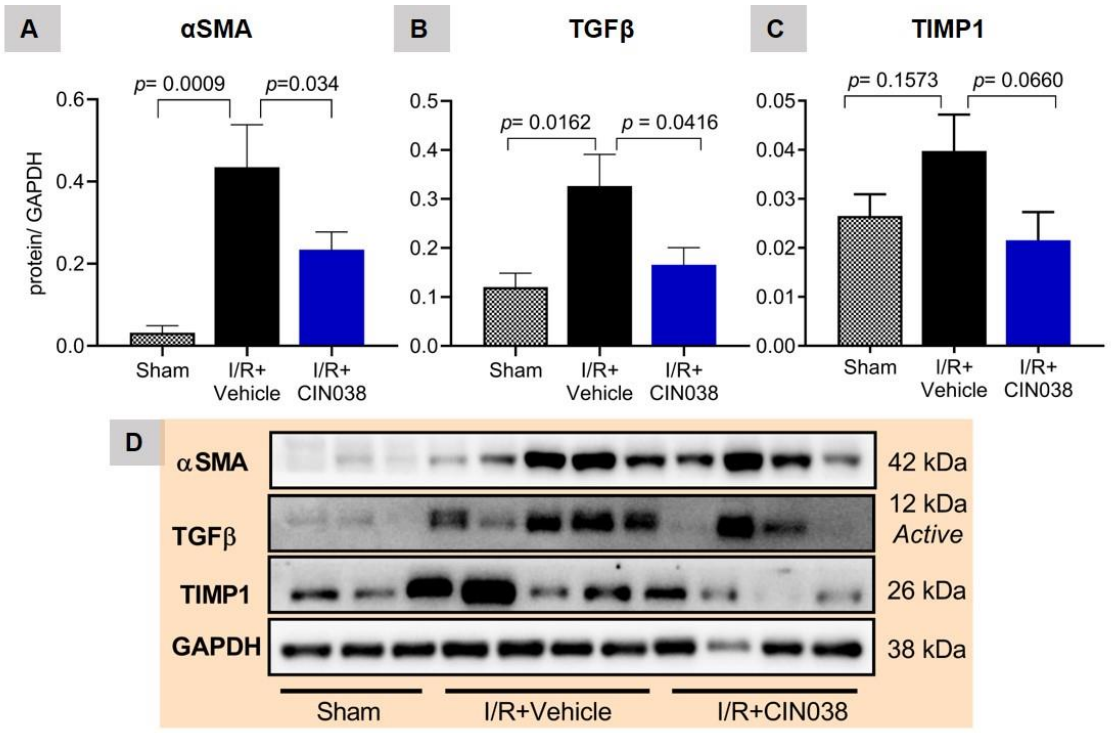

Figure 5.10. Effect of DES1 inhibition on fibrotic proteins in the heart. Protein expression of (A) α-SMA, (B) TGFβ and (C) TIMP1 were reduced by DES1 inhibition in I/R+CIN038 mice compared to I/R+Vehicle mice. Data are presented as mean ± SEM. (D) Representative images of western blots.

5.4.10 Des1 inhibition modulates phosphorylation of ERK

The effects of DES1 inhibition on P38-MAPK and ERK signalling pathways in the heart were examined. P38-MAPK phosphorylation (pP38) was significantly reduced (p= 0.0207) in the infarct zone but not in the remote zone of the I/R+Vehicle group compared to sham (Figure 5.11A and B). Reduced P38-MAPK phosphorylation in the infarct zone has been reported previously [286]. The increase in pP38 by DES1 inhibition in the I/R+CIN038 group compared to the I/R+Vehicle group was not significant. ERK phosphorylation (pERK) was significantly increased in the infarct (p= <0.0001) and remote zone (p= 0.029) of I/R+Vehicle group compared to sham. DES1 inhibition in the I/R+CIN038 group reduced pERK in the infarct zone (p=0.017) and not the remote zone, compared to the I/R+Vehicle group.

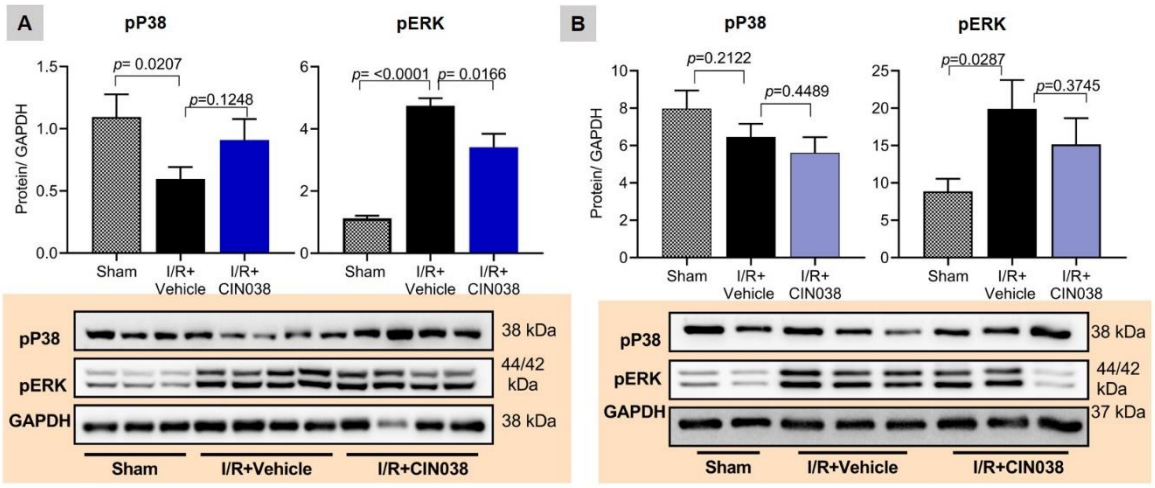

Figure 5.11. Effect of DES1 inhibition on MAPK and ERK signalling. (A) DES1 inhibition reduced pERK and had little effect on pP38 in the infarct zone of the I/R+CIN038 group. (B) The effect of DES1 inhibition on pP38 and pERK in the remote zone were not significant in the I/R+CIN038 group. Graphed data are presented as mean ± SEM.

5.4.11 Effect of CIN038 treatment on STAT and Akt Signalling

STAT1 and 3 phosphorylation were significantly increased in the I/R+Vehicle mice compared to sham mice in the infarct zone (p= 0.0026, and p= 0.0046, respectively), Figure 5.12A-B. CIN038 treatment in the I/R+CIN038 group demonstrated significant reduction in pSTAT1 (p= 0.0494) but not pSTAT3 compared to the I/R+Vehicle mice. There was a trend toward an increase in NFκB phosphorylation (pNFκB) in the Vehicle-treated MI animals, however it was not significant (p= 0.2399). In the remote zone, pSTAT3 was significantly increased (p= 0.0127) and pNFκB (p= 0.0558) phosphorylation trended strongly toward an increase in the I/R+Vehicle mice, compared to sham (Figure 5.12E-F). CIN038 treatment in the I/R+CIN038 mice reduced pNFκB significantly compared to I/R+Vehicle mice (p= 0.0464). However, the reduction in pSTAT3 in the I/R+CIN038 mice was not significant (p= 0.0775).

In view of the evidence for reduced Akt phosphorylation due to DES1 ablation [287, 288], we also investigated the expression of Akt signalling pathway proteins. Western blot analysis demonstrated that in the infarct zone, the differences in pAkt, p-mTOR, and pRPS6 were not significant between the groups (Figure 5.12C-D).

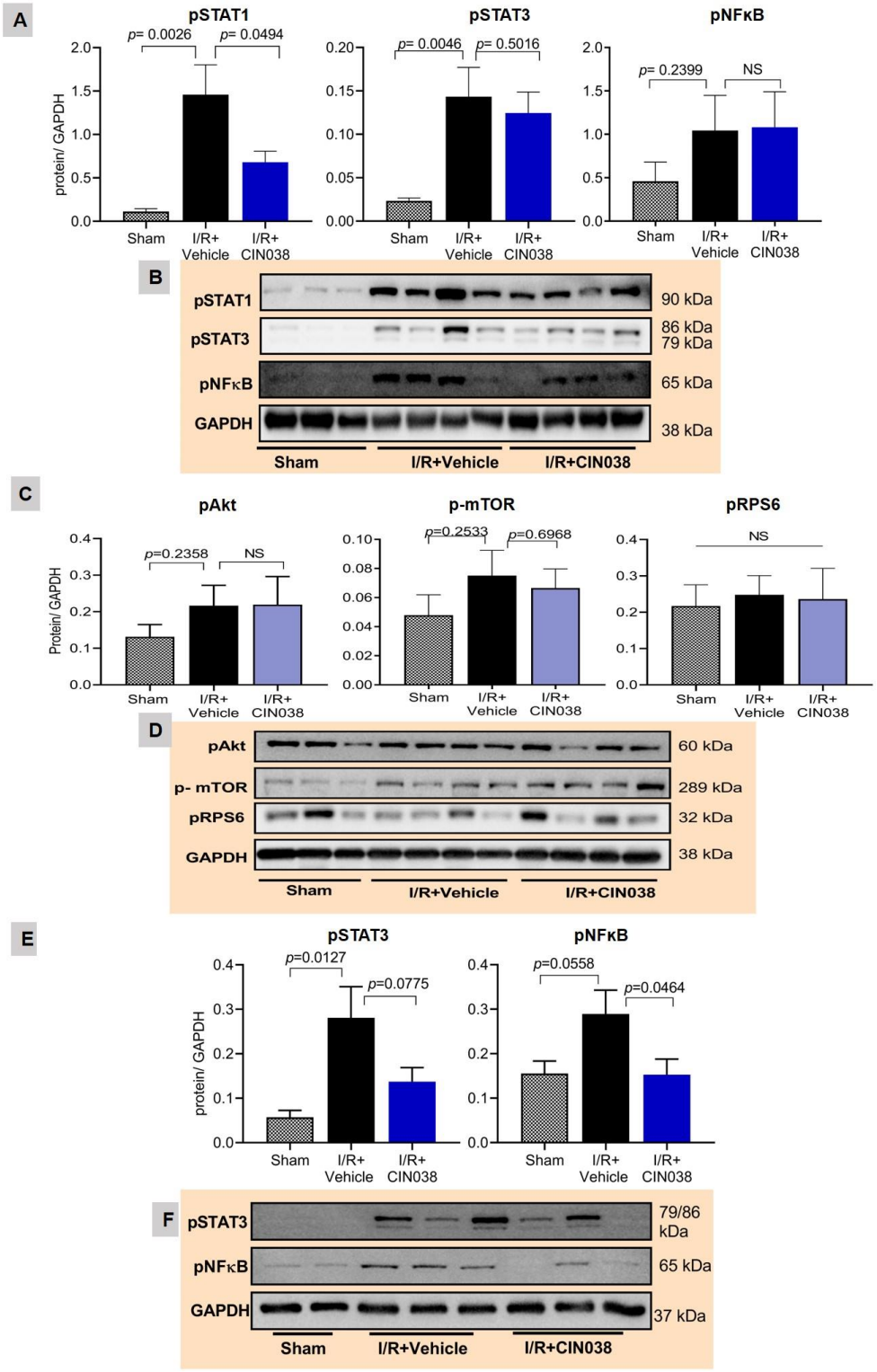

Figure 5.12. Effect of DES1 inhibition on STAT and Akt signalling proteins in the heart. (A) DES1 inhibition in the I/R+CIN038 group showed a strong trend toward a reduction in pSTAT1 but had no effect on pSTAT3 and pNFκB compared to the I/R+Vehicle group in the infarct zone. (C) No significant effects

were observed for pAkt pathway related protein such pAkt, p-mTOR and pRPS6 in the infarct zone. (E) DES1 inhibition reduced pSTAT3 and pNFκB in the remote zone of I/R+CIN038 group. (B, D & F) Representative images of western blots. Graphed data are presented as mean ± SEM.

5.4.12 Changes in total plasma lipid profile after DES1 inhibition

Analysis of the lipid profile in plasma through lipidomics demonstrated that total dehydrocholesterol ester-DE (30.54%, p= 0.0068), lisophosphatidylcholine-LPC (12.31%, p= 0.0279), lysophosphatidylethanolamine-LPE (11.37%, p= 0.0271), lysophosphatidylinositol-LPI (23.18%, p= 0.0210), phosphatidylinositol-PI (14.61%, p= 0.0402), and S1P (24.31 %, p= 0.0189) were significantly reduced in the I/R+Vehicle group compared to sham (Table 5.4). However, these were all not significant after multiple comparisons using the Benjamini and Hochberg method. CIN038 treatment in I/R+CIN038 group also had no effect on these total lipids compared to the I/R+Vehicle group. There was no significant difference between groups for total sphingolipids such as dhCer, Cer and SM. Other sphingolipid metabolites are found at extremely low levels in both physiological and pathological states, therefore the mass spectrophotometry method employed was unable to detect quantifiable amounts of these metabolites.

Table 5.4. Total lipids in the plasma of I/R+Vehicle vs. sham and I/R+CIN038 vs. I/R+Vehicle. Significant values in red font. Data are presented as mean ±SEM. NS= Not significant.

No.	Lipid Species	Mean Values		Percentage Difference I/R+Vehicle vs. Sham (%)	Direction of Change	p- Value (t-Test)	Mean Values	Percentage Difference I/R+CIN038 vs. I/R+Vehicle (%)	Direction of Change	p- Value (t-Test)
		Sham (± SEM)	I/R+vehicle (± SEM)				I/R+CIN038 (± SEM)			
1	DE	7890.15 ± 677.75	5480.27 ± 437.05	30.54%	Decrease	0.007	6346.42 ± 594.25	15.80%	NS	0.256
2	LPC	501797.94 ± 19825.55	440012.36 ± 16463.76	12.31%	Decrease	0.028	488550.45 ± 24584.01	11.03%	NS	0.118
3	LPE	20722.07 ± 917.79	18365.99 ± 466.37	11.37%	Decrease	0.027	17315.06 ± 1202.97	5.72%	NS	0.426
4	LPI	2343.69 ± 155.81	1800.40 ± 143.21	23.18%	Decrease	0.021	2087.73 ± 294.30	15.96%	NS	0.392
5	PI	290441.55 ± 16502.01	248020.99 ± 10763.37	14.61%	Decrease	0.040	241134.36 ± 12222.78	2.78%	NS	0.677
6	S1P	686.08 ± 55.43	519.33 ± 36.18	24.31%	Decrease	0.019	670.56 ± 73.59	29.12%	NS	0.082

5.4.13 Effect of CIN038 treatment on individual lipid species in plasma

A total of 27 individual lipid species levels in plasma were significantly altered in the I/R+Vehicle group compared to sham, Appendix 3.1. These included two species each of CE, plasmalogen (PC(P)) and TG, and one specie of lysoalkylphosphatidylcholine (LPC(O)) were significantly increased. While, seven SM species, five LPC species, three species of DE, two species each of alkenyl phosphatidylethanolamine (PE(P)) and PI, and one specie each of S1P and phosphatidylcholine (PC) were significantly reduced. None of these were significantly changed in the I/R+CIN038 group compared to the I/R+Vehicle group. However, CIN038 treatment did affect other species that were not changed in the I/R+Vehicle group. Lipid species such as fatty acids-FA (18:2; p= 0.0367), PC (P-16:0/16:0; p= 0.007), and SM (44:3; p=0.031, and d18:1/17:0; p= 0.011) were significantly increased in the I/R+CIN038 group compared to the I/R+Vehicle group. While the PC species 33:2 (p= 0.034) 16:1_18:2 (p= 0.043) and 17:1_18:2 (p= 0.0003) were reduced significantly. After multiple comparisons for false discoveries, only the lysoalkylphosphatidylcholine (LPC(O-24:0), p= 0.022) species was significantly increased in the I/R+Vehicle group compared to sham. This was not change in the I/R+CIN038 group compared to the I/R+Vehicle group. Analysis of dhCer/Cer ratio for matching individual species in plasma showed no significant changes.

5.4.14 Changes in total liver lipid profile after CIN038 treatment

Analysis of liver lipid profile demonstrated that total free cholesterol (COH, 9.73%), alkyl phosphatidylcholine (PC(O), 26.77%) and plasmalogen (PC(P), 47.63%) were increased significantly, while diacylglycerol (DG, -37.43%), LPE (-14.22%), PI (-11.28%), TG(SIM) (-54.11%) and ubiquinone (-26.83%) were significantly reduced in the I/R+Vehicle group compared to sham (Table 5.5). Only the total (PC(O), p= 0.0276) and PC(P) (p= 0.0276) remained significant after multiple comparisons for false discoveries. These were not changed significantly with CIN038 in the I/R+CIN038 group compared to the I/R+Vehicle group. Additionally, there were no changes in total sphingolipids such as dhCer, Cer and SM in the liver between the groups.

Table 5.5. Total lipids altered in the liver of I/R+Vehicle vs. sham and I/R+ CIN038 vs. I/R+Vehicle. Significant values in red font. Data are presented as mean ±SEM. NS =Not significant.

No.	Lipid Species	Mean Values		Percentage Difference I/R+Vehicle vs. Sham (%)	Direction of Change	p- Value (t-Test)	Mean Values	Percentage Difference I/R+CIN038 vs. I/R+Vehicle (%)	Direction of Change	p- Value (t-Test)
		Sham (± SEM)	I/R+vehicle (± SEM)				I/R+CIN038 (± SEM)			
1	COH	93006 ± 3313	102051 ± 2455	9.73%	Increase	0.0395	103798.68 ± 1884.28	1.71%	NS	0.579315
2	DG	365111 ± 52602	228448 ± 23083	37.43%	Decrease	0.0210	242351.07 ± 25273.68	6.09%	NS	0.689405
3	Hex2Cer	16 ± 11	114 ± 19	632.80%	Increase	0.0008	78.07 ± 24.63	31.50%	NS	0.265332
4	LPE	13404 ± 854	11498 ± 398	14.22%	Decrease	0.0459	10507.84 ± 691.35	8.62%	NS	0.230375
5	PC(O)	5136 ± 324	6511 ± 165	26.77%	Increase	0.0010	6035.56 ± 313.03	7.30%	NS	0.196343
6	PC(P)	1138 ± 107	1680 ± 99	47.63%	Increase	0.0019	1766.71 ± 142.97	5.16%	NS	0.623686
7	PI	560608 ± 13611	497396 ± 14400	11.28%	Decrease	0.0065	499841.23 ± 11019.27	0.49%	NS	0.894204
8	TG(SIM)	771002 ± 155221	353848 ± 63724	54.11%	Decrease	0.0162	395011.13 ± 59094.07	11.63%	NS	0.641448
9	Ubiquinone	329 ± 31	241 ± 16	26.83%	Decrease	0.0169	249.35 ± 14.76	3.65%	NS	0.694699

5.4.15 Effect of DES1 inhibition on individual lipid species in liver

A total of 171 individual lipid species were significantly altered in the liver in the I/R+Vehicle group compared to sham (Appendix 3.2). 90 TG species, 11 DG species, two FA, LPE, and PI species, and one each of CE, and Cer species were significantly reduced in the I/R+Vehicle group compared to sham. CIN038 treatment in the I/R+CIN038 group had significantly reduced PC (O- 34:1; p= 0.031, and O-36:0, p= 0.027), and SM (d18:0/16:0, p=0.048) species in the liver, but had no effect on the others. Additionally, 21 PC(O) species, 20 PC(P) species, eight SM species, four PE species, three CE species, and one each of COH and phosphatidylserine (PS) species were significantly increased in the I/R+Vehicle group compared to sham, while ubiquinone was reduced significantly. CIN038 treatment reduced PC (O-34:1; p= 0.031, and O-36:0; p= 0.027) and SM(d18:0/16:0) in the I/R+CIN038 group compared to the I/R+Vehicle group, however CIN038 had no effect on the other lipids. After multiple comparisons for false discovery, only the PC(O) (O-32:1, O-34:1, O-36:0, O-18:0/18:1, and O-45:0; p= 0.041), PC(P-18:0/18:2, p= 0.041), PE (P-18:1/22:4, p= 0.041) and DG(18:0/24:0, p= 0.041) species remained significant in the I/R+ vehicle group compared to the sham.

Interestingly, other lipid species in the I/R+CIN038 group were significantly altered, that were not changed in the I/R+Vehicle group. These included significant reductions in PC (16:0_16:0; p= 0.02), PE (P-16:0/18:1; p= 0.028, and P-16:0/20:3; p= 0.006) and SM ((38:3) (b); p= 0.037) species in the I/R+CIN038 group compared to the I/R+Vehicle group. In addition, the following TG species were significantly increased in the I/R+CIN038 group compared to the

I/R+Vehicle group; O-50:1[NL-15:0] (p= 0.042), O-52:1 [NL-16:0] (p= 0.031), O-50:2 SIM (p= 0.024), O-52:2 [NL-16:0] (p= 0.011), O-52:2 [NL-17:1] (p= 0.022), O-52:2 [NL-18:1] (p= 0.026), O-54:2 [NL-17:1] (p= 0.039), O-54:3 [NL-17:1] (p= 0.011), O-54:3 [NL-18:1] (p= 0.008), and O-54:4 SIM (p= 0.027), and LPC (26:0 [sn1] (p= 0.031). However, these were not significant after FDR testing. Analysis of dhCer/Cer ratio for matching individual species also showed no apparent changes.

5.4.16 Effect of DES1 inhibition on dhCer and Cer in cardiac fibroblasts

Lipidomics analysis on neonatal cardiac fibroblasts showed that at 5 h of treatment with Ang II+CIN038 there was a 55-fold (10 μM) and 20-fold (3.0 μM) increase in dhCer (d38:0) (Figure 5.13). There was no change in dhCer levels in cells treated with the fibrotic agent, Ang II. There was a 14-fold increase in dhCer levels at 24 h of treatment with Ang II+CIN038 (10 μM, and a 0.5-fold reduction was observed in Ang II treated cells. Cer (d38:1) levels remained unchanged at 5 h and 24 h.

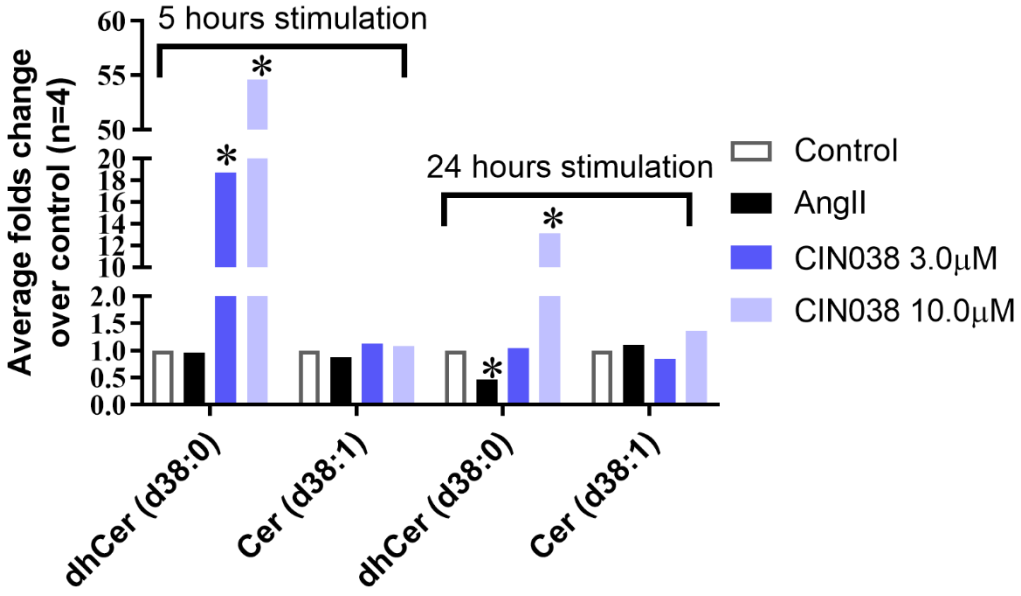

Figure 5.13 Effect of DES1 inhibition on dhCer and Cer in cardiac fibroblasts. In CIN038 (10 μM) treated NCFs, there was > 15-fold increase in dhCer levels at 5 and 24 h. Data presented as average fold change over control. *p <0.05 vs. control.

5.5 Discussion

Recently, sphingolipids such as S1P and Cer have been implicated in CVDs [271, 273, 274, 276]. Targeting the nodal enzyme, DES1, in the *de novo* sphingolipid biosynthesis pathway alters their levels [100]. Despite, evidence for the beneficial effects of DES1 inhibition in cancer and insulin resistance, research in CVDs targeting DES1 have been slow and lacking [155, 258, 288-290]. This chapter demonstrates the cardioprotective effects of Des1 inhibition for the first time in a mouse model of I/R utilizing a novel selective DES1 inhibitor (CIN038) [281]. No compound related adverse events were recorded during the study period.

Remodelling alters ventricular architecture and induces phenotypic changes in myocytes and the ECM [6, 9]. The infarct size is strongly correlated to remodelling and impacts cardiac function after an MI [291]. DES1 inhibition showed some effect on infarct size (Figure 5.4B). These were accompanied by significant changes in some gene, protein, and tissue expression of markers related to fibrosis and hypertrophy. Fibrosis in the myocardium is characterised by increased expression and deposition of ECM components such as Coll1 and 3, α-SMA, and TGFβ [32, 57, 292]. DES1 inhibitor CIN038 reduced Coll1a1 and TGFβ1 gene expression significantly in the infarct zone (Figure 5.7). Similar effects were observed for genes examined in the remote zone. These changes corresponded with reductions in α-SMA, and TGFβ (mature form) protein expression (Figure 5.10). The increased secretion of the ECM components play an integral part in the scar formation and contributes to LV stiffness [292, 293]. Des1 inhibition reduced tissue deposition of Coll3 (Figure 5.4D), together with reductions in tissue expression of TGFβ1 (Figure 5.7A), implying that DES1 inhibition can reduce activation of the TGFβ signalling which contributes immensely to fibrosis [37].

DES1 inhibitor CIN038 recovered the expression of the hypertrophic gene marker, αMHC (Figure 5.8A), with significant apparent reductions in the diameter of myocytes in tissue (Figure 5.5) and reduced activation of hypertrophic signalling pathways such as the ERK pathway (Figure 5.11) [286, 294]. The natriuretic peptides, ANP and BNP, are antagonists of hypertrophy, and are secreted as compensatory mechanisms in HF in response to myocyte injury and necrosis [183]. The lack of effect by CIN038 on these peptides implies that cardiac dysfunction persists. This is concurred by the lack of improvement in cardiac function as measured through echocardiographic (section 5.4.1) and hemodynamic analysis (section 5.4.2).

Inflammation exacerbates post MI LV remodelling, as evidenced by the increase in monocyte/macrophage infiltrates, which secrete proinflammatory cytokines, in the infarction site and plasma [295, 296]. CIN038 treatment showed reductive effects on the gene expression of the proinflammatory cytokine, IL-6, in the infarct zone (Figure 5.8C). CIN038 treatment also reduced phosphorylation of STAT1 in the infarct zone, and STAT3 and NFκβ in the remote zone, (Figure 5.12A, and E), which can lead to reductions in activation of inflammatory pathways such as the IL-6/JAK/STAT pathway which is strongly linked to hypertrophy [195, 297]. Taken together, DES1 inhibition demonstrates anti-inflammatory effects by ameliorating major transcription factors such as NFκB, and STAT1/3. These factors are downstream targets of IL-6 and can amplify inflammatory processes [298, 299].

In terms of changes in lipid profiles, the changes in the plasma and liver lipids were not significant in both the I/R+vehicle and I/R+CIN038 groups after multiple comparisons. Changes in sphingolipid profile have been reported in both patients and animals with HF, obesity, and MI [119, 129, 152, 300]. Most of these studies have associated elevated Cer, SM and S1P levels in plasma with disease progression. In this study, the mouse I/R model showed that there was a lack of change in liver and plasma sphingolipids such as dhCer and Cer. It also indicated that a more effective dose of CIN038 may be required to observe changes in dhCer and Cer level in animals. This is supported by the increased dhCer levels in NCFs (Figure 15.3). Other factors including, 1) pharmacokinetic parameters such as ineffective drug PK metabolic profiles, 2) compensatory feedback and salvage mechanisms, 3) short half-life in circulation evidenced by the lack of change in lipidomics, may have also reduced its effects on the sphingolipid pathway. Therefore, the effects observed on remodelling factors may show reduced effect

rather than off-target effects. Additionally, the mice in this study received their final treatment 24 h prior to hemodynamic analysis and sacrifice. Studies have shown sphingolipid levels returning to control levels from 24 h to 30 days after a major cardiac event in plasma, myocardium and erythrocytes [145, 146, 187, 188]. Since CIN038 is an inhibitor targeting DES1 enzyme activity and not the DEGS1 gene, it is not likely to have effects on the DEGS1 gene in cardiac tissue as we observed (Figure 5.9B and F). Additionally, I/R significantly affected other sphingolipid related genes that were tested, but they were not changed by CIN038 treatment.

5.6 Conclusion

In conclusion, DES1 inhibitor CIN038 can reduce some fibrosis, hypertrophy, and inflammatory pathway genes and proteins. However, with improvements in the compound pharmacokinetics these findings could be improved upon. This study also highlights DES1 inhibition may be an effective target for cardiac remodelling therapy, with a compound that has better PK properties than CIN038.

5.7 Limitations

The study was conducted as a preliminary proof of concept study towards understanding the effects of DES1 inhibition with a pharmacological tool compound, CIN038. The findings could be considerably different with improvements in compound pharmacokinetics. Analysing lipid profiles at different time points, for example a few hours after surgery, and before commencing treatment at day four, in addition to the endpoint could have

supplied more details in delineating any effects DES1 inhibition may have had on lipid dysregulation. Comparing CIN038 with other DES1 inhibitors on the market could have also contributed to better understanding its mode and mechanism of action.

5.8 Key Findings

DES1 inhibitor CIN038 altered certain markers of cardiac remodelling such as;

1. reducing TGFβ, Coll1, and α-SMA in fibrosis,
2. recovering αMHC gene expression in hypertrophy and
3. attenuating STAT and NFκB related pathway activation in inflammation.

Manuscript submitted for publication.

Chapter 6: General discussion, conclusion and future direction

6.1 General discussion and conclusion

Cardiac remodelling is a detrimental factor propelling the progression towards HF in patients with cardiomyopathies. Lipids, such as sphingolipids can contribute to the pathophysiology of CVDs. Therefore, this thesis, set out to decipher the role of sphingolipids such as dhS1P and dhSph in cardiac remodelling and demonstrate the therapeutic potential of inhibiting the "gatekeeper" enzyme, DES1, in the *de novo* sphingolipid pathway in the setting of I/R.

The three main findings demonstrated for the first time in this thesis include;
1) dhS1P's ability to induce collagen synthesis and hypertrophy in primary cardiac cells, through the JAK/STAT pathway and collagen synthesis through the PI3K pathway. 2) Exogenous application of dhSph, reduced TGFβ induced collagen synthesis in cardiac fibroblasts. 3) Provides evidence that DES1 inhibition may be able to reduce cardiac remodelling after an I/R. The mechanisms of maybe involve reducing the expression of fibrosis, hypertrophy markers and inflammatory signalling pathways through inhibition of transcription factors such as STAT1 and STAT3.
The results for dhS1P contradict the claims of Bu et.al [98], that it has anti-fibrotic effects. Differences in cell types maybe have played a role in the different effects observed. However, considering the inhibitory effect of dhSph on collagen synthesis, and the results from DES1 inhibition in the I/R animal model, the dihydrosphingolipids may have anti- fibrotic effects. The activation of JAK/STAT signalling pathway by exogenous dhS1P and its attenuation by DES1

inhibition also implies an import link between the dihydrosphingolipids and inflammatory pathways that play a major role in disease processes such as cardiac remodelling. This is interesting since, the sphingolipid S1P in association with its receptors, is known to influence immune cell trafficking from the bone marrow [274]. Whether or not dhS1P has opposing effects to S1P in inflammation is beyond the scope of this thesis. Additionally, due to the lack of data on intracellular generated dihydrosphingolipids, lack of enzyme essays related to the sphingolipid pathway and inferior tool compound for DES1 inhibition, the interpretations of these findings are limited.

These findings imply that dhS1P and dhSph do play a role in cardiac fibrosis and hypertrophy and that the DES1 enzyme could be targeted for cardiac remodelling therapy. It also provides a basis to explore their roles in other CVD related disciplines such as CAD, and metabolic disorders that contribute to CVD such as diabetes.

6.2 Future directions

Further investigations into the effects of other dihydrosphingolipids is critical in understanding their role in cardiac remodelling, enabling and enhancing the development of more effective therapies targeting the sphingolipid synthesis pathway including DES1. This can be achieved by;

1) Encouraging mechanistic research that build on the findings outlined in this thesis, using specific molecular and genetic methods and animal models that target the *de novo* pathway in cardiac related fields. Especially in terms of exploring the effects of intracellular and extracellular dihydropshingolipids in diseases. This is

because the inhibition of DES1 increases the saturated sphingolipids [221], resulting in increased autophagy and reduced cell proliferation.

2) Improving and incorporating the use of advanced analytical tools such as LC-MS for the measurement of small molecules, such as sphingolipids, in the clinical setting should be encouraged. This would allow for collection of more accurate clinical and epidemiological data, broadening our understanding of the role these lipids have in disease processes.

Bibliography

1. Muro, E., G.E. Atilla-Gokcumen, and U.S. Eggert, *Lipids in cell biology: how can we understand them better?* Molecular biology of the cell, 2014. **25**(12): p. 1819-1823.
2. Storck, E.M., C. Özbalci, and U.S. Eggert, *Lipid Cell Biology: A Focus on Lipids in Cell Division.* Annual Review of Biochemistry, 2018. **87**(1): p. 839-869.
3. Mach, F., et al., *2019 ESC/EAS Guidelines for the management of dyslipidaemias: lipid modification to reduce cardiovascular risk: The Task Force for the management of dyslipidaemias of the European Society of Cardiology (ESC) and European Atherosclerosis Society (EAS).* European Heart Journal, 2020. **41**(1): p. 111-188.
4. Jellinger, P.S., *American Association of Clinical Endocrinologists/American College of Endocrinology Management of Dyslipidemia and Prevention of Cardiovascular Disease Clinical Practice Guidelines.* Diabetes Spectrum, 2018. **31**(3): p. 234.
5. McLuckey, S.A. and J.M. Wells, *Mass Analysis at the Advent of the 21st Century.* Chemical Reviews, 2001. **101**(2): p. 571-606.
6. Cohn, J.N., R. Ferrari, and N. Sharpe, *Cardiac remodeling--concepts and clinical implications: a consensus paper from an international forum on cardiac remodeling. Behalf of an International Forum on Cardiac Remodeling.* J Am Coll Cardiol, 2000. **35**(3): p. 569-82.
7. Galli, A. and F. Lombardi, *Postinfarct Left Ventricular Remodelling: A Prevailing Cause of Heart Failure.* Cardiology research and practice, 2016. **2016**: p. 2579832-2579832.
8. Cheng, S., et al., *Correlates of echocardiographic indices of cardiac remodeling over the adult life course: longitudinal observations from the Framingham Heart Study.* Circulation, 2010. **122**(6): p. 570-578.
9. Azevedo, P.S., et al., *Cardiac Remodeling: Concepts, Clinical Impact, Pathophysiological Mechanisms and Pharmacologic Treatment.* Arq Bras Cardiol, 2016. **106**(1): p. 62-9.
10. Klabunde, R.E., *Cardiovascular Physiology Concepts*. 2nd ed. 2011, Baltimore, USA: Lippincott, Williams & Wilkins.
11. Pinto, A.R., et al., *Revisiting Cardiac Cellular Composition.* Circulation research, 2016. **118**(3): p. 400-409.
12. Zhou, P. and W.T. Pu, *Recounting Cardiac Cellular Composition.* Circulation research, 2016. **118**(3): p. 368-370.
13. Sutton, M.G.S.J. and N. Sharpe, *Left Ventricular Remodeling After Myocardial Infarction.* Circulation, 2000. **101**(25): p. 2981-2988.
14. Katz Arnold, M. and H. Lorell Beverly, *Regulation of Cardiac Contraction and Relaxation.* Circulation, 2000. **102**(suppl_4): p. Iv-69-Iv-74.
15. Hwang, P.M. and B.D. Sykes, *Targeting the sarcomere to correct muscle function.* Nature Reviews Drug Discovery, 2015. **14**(5): p. 313-328.
16. Tirziu, D., J. Giordano Frank, and M. Simons, *Cell Communications in the Heart.* Circulation, 2010. **122**(9): p. 928-937.
17. Gautel, M. and K. Djinović-Carugo, *The sarcomeric cytoskeleton: from molecules to motion.* The Journal of Experimental Biology, 2016. **219**(2): p. 135.
18. Spinale, F.G., et al., *Crossing Into the Next Frontier of Cardiac Extracellular Matrix Research.* Circulation research, 2016. **119**(10): p. 1040-1045.

19. Rienks, M., et al., *Myocardial Extracellular Matrix.* Circulation Research, 2014. **114**(5): p. 872-888.
20. Villa, A.D., et al., *Coronary artery anomalies overview: The normal and the abnormal.* World journal of radiology, 2016. **8**(6): p. 537-555.
21. Vijayan, S., et al., *Assessing Coronary Blood Flow Physiology in the Cardiac Catheterisation Laboratory.* Current cardiology reviews, 2017. **13**(3): p. 232-243.
22. Hochman, J.S. and B.H. Bulkley, *Expansion of acute myocardial infarction: an experimental study.* Circulation, 1982. **65**(7): p. 1446-50.
23. Cokkinos, D.V. and C. Belogianneas, *Left Ventricular Remodelling: A Problem in Search of Solutions.* European cardiology, 2016. **11**(1): p. 29-35.
24. Xie, M., S. Burchfield Jana, and A. Hill Joseph, *Pathological Ventricular Remodeling.* Circulation, 2013. **128**(9): p. 1021-1030.
25. Chen, Y., et al., *Distinct Types of Cell Death and the Implication in Diabetic Cardiomyopathy.* Frontiers in Pharmacology, 2020. **11**(42).
26. Gustafsson Åsa, B. and A. Gottlieb Roberta, *Autophagy in Ischemic Heart Disease.* Circulation Research, 2009. **104**(2): p. 150-158.
27. Wu, D., K. Zhang, and P. Hu, *The Role of Autophagy in Acute Myocardial Infarction.* Frontiers in pharmacology, 2019. **10**: p. 551-551.
28. Teringova, E. and P. Tousek, *Apoptosis in ischemic heart disease.* Journal of translational medicine, 2017. **15**(1): p. 87-87.
29. Green, D.R. and F. Llambi, *Cell Death Signaling.* Cold Spring Harbor perspectives in biology, 2015. **7**(12): p. a006080.
30. Rabkin, S.W., *Apoptosis in Human Acute Myocardial Infarction: The Rationale for Clinical Trials of Apoptosis Inhibition in Acute Myocardial Infarction.* Scholarly Research Exchange, 2009. **2009**: p. 979318.
31. Baldi, A., et al., *Apoptosis and post-infarction left ventricular remodeling.* J Mol Cell Cardiol, 2002. **34**(2): p. 165-74.
32. Prabhu, S.D. and N.G. Frangogiannis, *The Biological Basis for Cardiac Repair After Myocardial Infarction.* Circulation Research, 2016. **119**(1): p. 91-112.
33. Newton, K. and V.M. Dixit, *Signaling in innate immunity and inflammation.* Cold Spring Harbor perspectives in biology, 2012. **4**(3): p. a006049.
34. Mann, D.L. and L. Kirschenbaum, *The Emerging Role of Innate Immunity in the Heart and Vascular System.* Circulation Research, 2011. **108**(9): p. 1133-1145.
35. Frangogiannis, N.G., *Inflammation in cardiac injury, repair and regeneration.* Current opinion in cardiology, 2015. **30**(3): p. 240-245.
36. Hammarsten, O., et al., *Possible mechanisms behind cardiac troponin elevations.* Biomarkers, 2018. **23**(8): p. 725-734.
37. Travers, J.G., et al., *Cardiac Fibrosis: The Fibroblast Awakens.* Circ Res, 2016. **118**(6): p. 1021-40.
38. Schirone, L., et al., *A Review of the Molecular Mechanisms Underlying the Development and Progression of Cardiac Remodeling.* Oxidative medicine and cellular longevity, 2017. **2017**: p. 3920195-3920195.
39. Wu, Q.Q., et al., *Mechanisms contributing to cardiac remodelling.* Clin Sci (Lond), 2017. **131**(18): p. 2319-2345.
40. Clerk, A., et al., *Signaling pathways mediating cardiac myocyte gene expression in physiological and stress responses.* Journal of Cellular Physiology, 2007. **212**(2): p. 311-322.
41. Proud, C.G., *Ras, PI3-kinase and mTOR signaling in cardiac hypertrophy.* Cardiovascular Research, 2004. **63**(3): p. 403-413.

42. Yokota, T. and Y. Wang, *p38 MAP kinases in the heart.* Gene, 2016. **575**(2 Pt 2): p. 369-376.
43. Vega, R.B., R. Bassel-Duby, and E.N. Olson, *Control of Cardiac Growth and Function by Calcineurin Signaling.* Journal of Biological Chemistry, 2003. **278**(39): p. 36981-36984.
44. Wang, J., C. Gareri, and H.A. Rockman, *G-Protein–Coupled Receptors in Heart Disease.* Circulation Research, 2018. **123**(6): p. 716-735.
45. Tran Diem, H. and V. Wang Zhao, *Glucose Metabolism in Cardiac Hypertrophy and Heart Failure.* Journal of the American Heart Association, 2019. **8**(12): p. e012673.
46. Herzig, S. and R.J. Shaw, *AMPK: guardian of metabolism and mitochondrial homeostasis.* Nature reviews. Molecular cell biology, 2018. **19**(2): p. 121-135.
47. Chaggar, P.S., et al., *Neuroendocrine effects on the heart and targets for therapeutic manipulation in heart failure.* Cardiovasc Ther, 2009. **27**(3): p. 187-93.
48. Parajuli, N., et al., *The Role of Neurohumoral Activation in Cardiac Fibrosis and Heart Failure*, in *Cardiac Fibrosis and Heart Failure: Cause or Effect?*, I.M.C. Dixon and J.T. Wigle, Editors. 2015, Springer International Publishing: Cham. p. 347-381.
49. Wang, W., et al., *Role of ACE2 in diastolic and systolic heart failure.* Heart Fail Rev, 2012. **17**(4-5): p. 683-91.
50. Calvieri, C., S. Rubattu, and M. Volpe, *Molecular mechanisms underlying cardiac antihypertrophic and antifibrotic effects of natriuretic peptides.* J Mol Med (Berl), 2012. **90**(1): p. 5-13.
51. Skulnick, H.I., et al., *Structure-based design of nonpeptidic HIV protease inhibitors: the sulfonamide-substituted cyclooctylpyramones.* J Med Chem, 1997. **40**(7): p. 1149-64.
52. Sugden, P.H. and A. Clerk, *Endothelin signalling in the cardiac myocyte and its pathophysiological relevance.* Curr Vasc Pharmacol, 2005. **3**(4): p. 343-51.
53. Sugden, P.H., *An overview of endothelin signaling in the cardiac myocyte.* J Mol Cell Cardiol, 2003. **35**(8): p. 871-86.
54. Tschöpe, C. and S. Van Linthout, *New Insights in (Inter)Cellular Mechanisms by Heart Failure with Preserved Ejection Fraction.* Current Heart Failure Reports, 2014. **11**(4): p. 436-444.
55. Dimou, C., et al., *A systematic review and network meta-analysis of the comparative efficacy of angiotensin-converting enzyme inhibitors and angiotensin receptor blockers in hypertension.* Journal of Human Hypertension, 2019. **33**(3): p. 188-201.
56. *Effect of ramipril on mortality and morbidity of survivors of acute myocardial infarction with clinical evidence of heart failure. The Acute Infarction Ramipril Efficacy (AIRE) Study Investigators.* Lancet, 1993. **342**(8875): p. 821-8.
57. Frangogiannis, N.G., *Cardiac fibrosis: Cell biological mechanisms, molecular pathways and therapeutic opportunities.* Mol Aspects Med, 2019. **65**: p. 70-99.
58. Li, Y., Q. Li, and G.-C. Fan, *Macrophage Efferocytosis in Cardiac Pathophysiology and Repair.* Shock, 9000. **Publish Ahead of Print**.
59. Prabhu, S.D. and N.G. Frangogiannis, *The Biological Basis for Cardiac Repair After Myocardial Infarction.* Circulation Research, 2016. **119**(1): p. 91.
60. Sugimoto, M.A., et al., *Annexin A1 and the Resolution of Inflammation: Modulation of Neutrophil Recruitment, Apoptosis, and Clearance.* Journal of immunology research, 2016. **2016**: p. 8239258-8239258.
61. Okubo, K., et al., *Lactoferrin Suppresses Neutrophil Extracellular Traps Release in Inflammation.* EBioMedicine, 2016. **10**: p. 204-215.

62. Wynn, T.A. and L. Barron, *Macrophages: master regulators of inflammation and fibrosis.* Seminars in liver disease, 2010. **30**(3): p. 245-257.
63. de Oliveira, S., E.E. Rosowski, and A. Huttenlocher, *Neutrophil migration in infection and wound repair: going forward in reverse.* Nature reviews. Immunology, 2016. **16**(6): p. 378-391.
64. Chang, H.Y., et al., *Diversity, topographic differentiation, and positional memory in human fibroblasts.* Proc Natl Acad Sci U S A, 2002. **99**(20): p. 12877-82.
65. Talman, V. and H. Ruskoaho, *Cardiac fibrosis in myocardial infarction—from repair and remodeling to regeneration.* Cell and Tissue Research, 2016. **365**(3): p. 563-581.
66. Toba, H. and M.L. Lindsey, *Extracellular matrix roles in cardiorenal fibrosis: Potential therapeutic targets for CVD and CKD in the elderly.* Pharmacology & therapeutics, 2019. **193**: p. 99-120.
67. Chen, W. and N.G. Frangogiannis, *Fibroblasts in post-infarction inflammation and cardiac repair.* Biochimica et biophysica acta, 2013. **1833**(4): p. 945-953.
68. Sun, Y. and K.T. Weber, *Angiotensin Converting Enzyme and Myofibroblasts during Tissue Repair in the Rat Heart.* Journal of Molecular and Cellular Cardiology. **28**(5): p. 851-858.
69. Tadevosyan, A., et al., *Intracellular Angiotensin-II Interacts With Nuclear Angiotensin Receptors in Cardiac Fibroblasts and Regulates RNA Synthesis, Cell Proliferation, and Collagen Secretion.* Journal of the American Heart Association, 2017. **6**(4).
70. van den Borne, S.W., et al., *Myocardial remodeling after infarction: the role of myofibroblasts.* Nat Rev Cardiol, 2010. **7**(1): p. 30-7.
71. Willems, I.E., et al., *The alpha-smooth muscle actin-positive cells in healing human myocardial scars.* The American Journal of Pathology, 1994. **145**(4): p. 868-875.
72. Doenst, T., D. Nguyen Tien, and E.D. Abel, *Cardiac Metabolism in Heart Failure.* Circulation Research, 2013. **113**(6): p. 709-724.
73. Lopaschuk, G.D., et al., *Myocardial Fatty Acid Metabolism in Health and Disease.* Physiological Reviews, 2010. **90**(1): p. 207-258.
74. Goldberg, Ira J., Chad M. Trent, and P.C. Schulze, *Lipid Metabolism and Toxicity in the Heart.* Cell Metabolism, 2012. **15**(6): p. 805-812.
75. Schulze, P.C., *Myocardial lipid accumulation and lipotoxicity in heart failure.* Journal of lipid research, 2009. **50**(11): p. 2137-2138.
76. Folmes, C.D., et al., *High rates of residual fatty acid oxidation during mild ischemia decrease cardiac work and efficiency.* J Mol Cell Cardiol, 2009. **47**(1): p. 142-8.
77. Bikman, B.T. and S.A. Summers, *Ceramides as modulators of cellular and whole-body metabolism.* J Clin Invest, 2011. **121**(11): p. 4222-30.
78. Gault, C.R., L.A. Obeid, and Y.A. Hanun, *An Overview of Sphingolipid Metabolism: From Synthesis to Breakdown*, in *Sphingolipids as Signaling and Regulatory Molecules*, C. Chalfant and M. De Poeta, Editors. 2010, Springer New York. p. 1-23.
79. Mishima, Y., et al., *Dihydro-sphingosine 1-phosphate interacts with carrier proteins in a manner distinct from that of sphingosine 1-phosphate.* Bioscience reports, 2018. **38**(5): p. BSR20181288.
80. Diarte-Añazco, E.M.G., et al., *Novel Insights into the Role of HDL-Associated Sphingosine-1-Phosphate in Cardiometabolic Diseases.* Int J Mol Sci, 2019. **20**(24).

81. Jadczyk, T., et al., *Bioactive Sphingolipids, Complement Cascade, and Free Hemoglobin Levels in Stable Coronary Artery Disease and Acute Myocardial Infarction*. Mediators of inflammation, 2018. **2018**: p. 2691934-2691934.
82. Merrill, A.H., Jr., *Sphingolipid and glycosphingolipid metabolic pathways in the era of sphingolipidomics*. Chemical reviews, 2011. **111**(10): p. 6387-6422.
83. Stiban, J., R. Tidhar, and A.H. Futerman, *Ceramide synthases: roles in cell physiology and signaling*. Adv Exp Med Biol, 2010. **688**: p. 60-71.
84. Shea, B.S. and A.M. Tager, *Sphingolipid regulation of tissue fibrosis*. Open Rheumatol J, 2012. **6**: p. 123-9.
85. Slotte, J.P., *Biological functions of sphingomyelins*. Prog Lipid Res, 2013. **52**(4): p. 424-37.
86. Pralhada Rao, R., et al., *Sphingolipid Metabolic Pathway: An Overview of Major Roles Played in Human Diseases*. Journal of Lipids, 2013. **2013**: p. 12.
87. Kitatani, K., J. Idkowiak-Baldys, and Y.A. Hannun, *The sphingolipid salvage pathway in ceramide metabolism and signaling*. Cellular signalling, 2008. **20**(6): p. 1010-1018.
88. Riboni, L., P. Giussani, and P. Viani, *Sphingolipid Transport*, in *Sphingolipids as Signaling and Regulatory Molecules*, C. Chalfant and M.D. Poeta, Editors. 2010, Springer New York: New York, NY. p. 24-45.
89. Yamaji, T. and K. Hanada, *Sphingolipid Metabolism and Interorganellar Transport: Localization of Sphingolipid Enzymes and Lipid Transfer Proteins*. Traffic, 2015. **16**(2): p. 101-122.
90. Hanada, K., et al., *CERT-mediated trafficking of ceramide*. Biochim Biophys Acta, 2009. **1791**(7): p. 684-91.
91. Ogushi, F., et al., *Rapid flip-flop motions of diacylglycerol and ceramide in phospholipid bilayers*. Chemical Physics Letters, 2012. **522**: p. 96-102.
92. Kawahara, A., et al., *The sphingolipid transporter spns2 functions in migration of zebrafish myocardial precursors*. Science, 2009. **323**(5913): p. 524-7.
93. Vu, T.M., et al., *Mfsd2b is essential for the sphingosine-1-phosphate export in erythrocytes and platelets*. Nature, 2017. **550**(7677): p. 524-528.
94. Nagahashi, M., et al., *Spns2, a transporter of phosphorylated sphingoid bases, regulates their blood and lymph levels, and the lymphatic network*. Faseb j, 2013. **27**(3): p. 1001-11.
95. Samaha, D., et al., *Sphingolipid-Transporting Proteins as Cancer Therapeutic Targets*. International journal of molecular sciences, 2019. **20**(14): p. 3554.
96. King, M.W. *Synthesis of Sphingosine and the Ceramides*. 2017 [cited 2017 10 May]; Available from: https://themedicalbiochemistrypage.org/sphingolipids.php.
97. Levkau, B., *Cardiovascular effects of sphingosine-1-phosphate (S1P)*. Handb Exp Pharmacol, 2013(216): p. 147-70.
98. Colacios, C., et al., *Basics of Sphingolipid Metabolism and Signalling*, in *Bioactive Sphingolipids in Cancer Biology and Therapy*, Y.A. Hannun, et al., Editors. 2015, Springer International Publishing: Cham. p. 1-20.
99. Petrache, I. and E.V. Berdyshev, *Ceramide Signaling and Metabolism in Pathophysiological States of the Lung*. Annu Rev Physiol, 2016. **78**: p. 463-80.
100. Rodriguez-Cuenca, S., N. Barbarroja, and A. Vidal-Puig, *Dihydroceramide desaturase 1, the gatekeeper of ceramide induced lipotoxicity*. Biochimica et Biophysica Acta (BBA) - Molecular and Cell Biology of Lipids, 2015. **1851**(1): p. 40-50.

101. Kanno, T., A. Gotoh, and T. Nishizaki, *Sphingosine arrests the cell cycle and induces apoptosis by targeting sphingosine-dependent protein kinase and protein kinase Cδ in vitro.* Personalized Medicine Universe, 2014. **3**: p. 22-27.
102. Bartke, N. and Y.A. Hannun, *Bioactive sphingolipids: metabolism and function.* J Lipid Res, 2009. **50 Suppl**: p. S91-6.
103. Polzin, A., et al., *Plasma sphingosine-1-phosphate concentrations are associated with systolic heart failure in patients with ischemic heart disease.* J Mol Cell Cardiol, 2017. **110**: p. 35-37.
104. Means, C.K., et al., *Sphingosine 1-phosphate S1P2 and S1P3 receptor-mediated Akt activation protects against in vivo myocardial ischemia-reperfusion injury.* Am J Physiol Heart Circ Physiol, 2007. **292**(6): p. H2944-51.
105. Cannavo, A., et al., *beta1-adrenergic receptor and sphingosine-1-phosphate receptor 1 (S1PR1) reciprocal downregulation influences cardiac hypertrophic response and progression to heart failure: protective role of S1PR1 cardiac gene therapy.* Circulation, 2013. **128**(15): p. 1612-22.
106. Robert, P., et al., *EDG1 receptor stimulation leads to cardiac hypertrophy in rat neonatal myocytes.* J Mol Cell Cardiol, 2001. **33**(9): p. 1589-606.
107. Gellings Lowe, N., et al., *Sphingosine-1-phosphate and sphingosine kinase are critical for transforming growth factor-β-stimulated collagen production by cardiac fibroblasts.* Cardiovasc Res, 2009. **82**(2): p. 303-312.
108. Rodriguez, Y.I., et al., *Sphingosine-1 Phosphate: A New Modulator of Immune Plasticity in the Tumor Microenvironment.* Frontiers in oncology, 2016. **6**: p. 218-218.
109. Landeen, L.K., et al., *Sphingosine-1-phosphate receptor expression in cardiac fibroblasts is modulated by in vitro culture conditions.* Am J Physiol Heart Circ Physiol, 2007. **292**(6): p. H2698-711.
110. Means, C.K., et al., *S1P1 receptor localization confers selectivity for Gi-mediated cAMP and contractile responses.* The Journal of biological chemistry, 2008. **283**(18): p. 11954-11963.
111. Hoefer, J., et al., *Sphingosine-1-phosphate-dependent activation of p38 MAPK maintains elevated peripheral resistance in heart failure through increased myogenic vasoconstriction.* Circ Res, 2010. **107**(7): p. 923-33.
112. Wang, H., H. Huang, and S.F. Ding, *Sphingosine-1-phosphate promotes the proliferation and attenuates apoptosis of Endothelial progenitor cells via S1PR1/S1PR3/PI3K/Akt pathway.* Cell Biol Int, 2018. **42**(11): p. 1492-1502.
113. Clay, H., et al., *Sphingosine 1-phosphate receptor-1 in cardiomyocytes is required for normal cardiac development.* Dev Biol, 2016. **418**(1): p. 157-165.
114. Ohkura, S.I., et al., *Augmented sphingosine 1 phosphate receptor-1 signaling in cardiac fibroblasts induces cardiac hypertrophy and fibrosis through angiotensin II and interleukin-6.* PLoS One, 2017. **12**(8): p. e0182329.
115. Cannavo, A., et al., *Sphingosine Kinases and Sphingosine 1-Phosphate Receptors: Signaling and Actions in the Cardiovascular System.* Front Pharmacol, 2017(556).
116. Vestri, A., et al., *Sphingosine 1-Phosphate Receptors: Do They Have a Therapeutic Potential in Cardiac Fibrosis?* Front Pharmacol, 2017. **8**: p. 296.
117. Brakch, N., et al., *Evidence for a role of sphingosine-1 phosphate in cardiovascular remodelling in Fabry disease.* Eur Heart J, 2010. **31**(1): p. 67-76.
118. Chao, H.H., et al., *L-Carnitine attenuates angiotensin II-induced proliferation of cardiac fibroblasts: role of NADPH oxidase inhibition and decreased sphingosine-1-phosphate generation.* J Nutr Biochem, 2010. **21**(7): p. 580-8.

119. Zhang, F., et al., *Sphingosine 1-phosphate signaling contributes to cardiac inflammation, dysfunction, and remodeling following myocardial infarction.* Am J Physiol Heart Circ Physiol, 2016. **310**(2): p. H250-61.
120. Yamanaka, M., et al., *Sphingosine kinase 1 (SPHK1) is induced by transforming growth factor-beta and mediates TIMP-1 up-regulation.* J Biol Chem, 2004. **279**(52): p. 53994-4001.
121. Wang, S., et al., *Transforming Growth Factor beta1 (TGF-beta1) Appears to Promote Coronary Artery Disease by Upregulating Sphingosine Kinase 1 (SPHK1) and Further Upregulating Its Downstream TIMP-1.* Med Sci Monit, 2018. **24**: p. 7322-7328.
122. Beach, J.A., et al., *Sphingosine kinase 1 is required for TGF-β mediated fibroblastto- myofibroblast differentiation in ovarian cancer.* Oncotarget, 2016. **7**(4): p. 4167-4182.
123. Tao, R., et al., *Deletion of the Sphingosine Kinase-1 gene influences cell fate during hypoxia and glucose deprivation in adult mouse cardiomyocytes.* Cardiovascular Research, 2007. **74**(1): p. 56-63.
124. Józefczuk, E., et al., *Cardiovascular Effects of Pharmacological Targeting of Sphingosine Kinase 1.* Hypertension, 2020. **75**(2): p. 383-392.
125. Tham, Y.K., et al., *Lipidomic Profiles of the Heart and Circulation in Response to Exercise versus Cardiac Pathology: A Resource of Potential Biomarkers and Drug Targets.* Cell Rep, 2018. **24**(10): p. 2757-2772.
126. Peterson, L.R., et al., *Ceramide Remodeling and Risk of Cardiovascular Events and Mortality.* Journal of the American Heart Association, 2018. **7**(10): p. e007931.
127. He, X. and E.H. Schuchman, *Ceramide and Ischemia/Reperfusion Injury.* Journal of Lipids, 2018. **2018**: p. 3646725.
128. Gulbins, E., *Regulation of death receptor signaling and apoptosis by ceramide.* Pharmacological Research, 2003. **47**(5): p. 393-399.
129. Ji, R., et al., *Increased de novo ceramide synthesis and accumulation in failing myocardium.* JCI Insight, 2017. **2**(9).
130. Reforgiato, M.R., et al., *Inhibition of ceramide de novo synthesis as a postischemic strategy to reduce myocardial reperfusion injury.* Basic Research in Cardiology, 2016. **111**(2): p. 12.
131. Hadas, Y., et al., *Altering Sphingolipid Metabolism Attenuates Cell Death and Inflammatory Response After Myocardial Infarction.* Circulation, 2020. **141**(11): p. 916-930.
132. Walls, S.M., et al., *Ceramide-Protein Interactions Modulate Ceramide-Associated Lipotoxic Cardiomyopathy.* Cell Rep, 2018. **22**(10): p. 2702-2715.
133. Liu, S.J. and R.H. Kennedy, *Positive inotropic effect of ceramide in adult ventricular myocytes: mechanisms dissociated from its reduction in Ca2+ influx.* American Journal of Physiology-Heart and Circulatory Physiology, 2003. **285**(2): p. H735-H744.
134. Park, T.-S., et al., *Ceramide is a cardiotoxin in lipotoxic cardiomyopathy.* Journal of Lipid Research, 2008. **49**(10): p. 2101-2112.
135. Callihan, P., et al., *Distinct generation, pharmacology, and distribution of sphingosine 1-phosphate and dihydrosphingosine 1-phosphate in human neural progenitor cells.* Neuropharmacology, 2012. **62**(2): p. 988-96.
136. Edsall, L.C., G.G. Pirianov, and S. Spiegel, *Involvement of sphingosine 1-phosphate in nerve growth factor-mediated neuronal survival and differentiation.* J Neurosci, 1997. **17**(18): p. 6952-60.

137. Bu, S., et al., *Opposite effects of dihydrosphingosine 1-phosphate and sphingosine 1-phosphate on transforming growth factor-beta/Smad signaling are mediated through the PTEN/PPM1A-dependent pathway.* J Biol Chem, 2008. **283**(28): p. 19593-602.
138. Schwartzbauer, G. and J. Robbins, *The Tumor Suppressor Gene PTEN Can Regulate Cardiac Hypertrophy and Survival.* Journal of Biological Chemistry, 2001. **276**(38): p. 35786-35793.
139. Roe, N.D., et al., *Targeted deletion of PTEN in cardiomyocytes renders cardiac contractile dysfunction through interruption of Pink1-AMPK signaling and autophagy.* Biochimica et biophysica acta, 2015. **1852**(2): p. 290-298.
140. DeLeon-Pennell, K.Y., et al., *Matrix Metalloproteinases in Myocardial Infarction and Heart Failure.* Progress in molecular biology and translational science, 2017. **147**: p. 75-100.
141. Dobierzewska, A., et al., *Plasma cross-gestational sphingolipidomic analyses reveal potential first trimester biomarkers of preeclampsia.* PLoS ONE, 2017. **12**(4): p. e0175118.
142. Sugiura, T., et al., *Circulating microRNA-126 as a potential biomarker for recovery from smoking-related vascular endothelial damage.* European Heart Journal, 2013. **34**(suppl_1): p. P2417-P2417.
143. Argraves, K.M., et al., *S1P, dihydro-S1P and C24:1-ceramide levels in the HDL-containing fraction of serum inversely correlate with occurrence of ischemic heart disease.* Lipids in Health and Disease, 2011. **10**: p. 70-70.
144. Górski, J., et al., *Effect of atrial pacing on the level of bioactive sphingolipids in the heart ventricles of the rat.* Atherosclerosis. **241**(1): p. e122-e123.
145. Knapp, M., et al., *Plasma sphingosine-1-phosphate concentration is reduced in patients with myocardial infarction.* Med Sci Monit, 2009. **15**(9): p. CR490-3.
146. Knapp, M., et al., *Sustained decrease in plasma sphingosine-1-phosphate concentration and its accumulation in blood cells in acute myocardial infarction.* Prostaglandins Other Lipid Mediat, 2013. **106**: p. 53-61.
147. Gelineau-van Waes, J., et al., *Increased sphingoid base-1-phosphates and failure of neural tube closure after exposure to fumonisin or FTY720.* Birth Defects Res A Clin Mol Teratol, 2012. **94**(10): p. 790-803.
148. Riley, R.T. and K.A. Voss, *Differential sensitivity of rat kidney and liver to fumonisin toxicity: organ-specific differences in toxin accumulation and sphingoid base metabolism.* Toxicol Sci, 2006. **92**(1): p. 335-45.
149. Riley, R.T., et al., *Evidence for Fumonisin Inhibition of Ceramide Synthase in Humans Consuming Maize-Based Foods and Living in High Exposure Communities in Guatemala.* Molecular nutrition & food research, 2015. **59**(11): p. 2209-2224.
150. Voss, K.A. and R.T. Riley, *Fumonisin Toxicity and Mechanism of Action: Overview and Current Perspectives.* Food Safety, 2013. **1**(1): p. 2013006-2013006.
151. Merrill, A.H., et al., *Sphingolipid metabolism: roles in signal transduction and disruption by fumonisins.* Environmental Health Perspectives, 2001. **109**(suppl 2): p. 283-289.
152. Huang, L., et al., *Plasma Metabolic Profile Determination in Young ST-segment Elevation Myocardial Infarction Patients with Ischemia and Reperfusion: Ultra-performance Liquid Chromatography and Mass Spectrometry for Pathway Analysis.* Chin Med J (Engl), 2016. **129**(9): p. 1078-86.

153. Sun, M., et al., *Urinary Metabonomics Study of Heart Failure Patients with HILIC and RPLC Separation Coupled to TOF–MS*. Chromatographia, 2014. **77**(3): p. 249-255.
154. Triola, G., et al., *Specificity of the dihydroceramide desaturase inhibitor N-[(1R,2S)-2-hydroxy-1-hydroxymethyl-2-(2-tridecyl-1-cyclopropenyl)ethyl]octanami de (GT11) in primary cultured cerebellar neurons*. Mol Pharmacol, 2004. **66**(6): p. 1671-8.
155. Siddique, M.M., et al., *Dihydroceramides: From Bit Players to Lead Actors*. J Biol Chem, 2015. **290**(25): p. 15371-9.
156. Signorelli, P., et al., *Dihydroceramide intracellular increase in response to resveratrol treatment mediates autophagy in gastric cancer cells*. Cancer Letters. **282**(2): p. 238-243.
157. Zhou, W., et al., *Overexpression of degenerative spermatocyte homolog 1 up-regulates the expression of cyclin D1 and enhances metastatic efficiency in esophageal carcinoma Eca109 cells*. Molecular Carcinogenesis, 2009. **48**(10): p. 886-894.
158. Barbarroja, N., et al., *Increased dihydroceramide/ceramide ratio mediated by defective expression of degs1 impairs adipocyte differentiation and function*. Diabetes, 2015. **64**(4): p. 1180-92.
159. Obeid, L.M., et al., *Programmed cell death induced by ceramide*. Science, 1993. **259**(5102): p. 1769.
160. Devlin, C.M., et al., *Dihydroceramide-based Response to Hypoxia*. The Journal of Biological Chemistry, 2011. **286**(44): p. 38069-38078.
161. Magaye, R.R., et al., *The role of dihydrosphingolipids in disease*. Cell Mol Life Sci, 2019. **76**(6): p. 1107-1134.
162. Meikle, P.J. and S.A. Summers, *Sphingolipids and phospholipids in insulin resistance and related metabolic disorders*. Nat Rev Endocrinol, 2017. **13**(2): p. 79-91.
163. Bu, S., et al., *Dihydrosphingosine-1 phosphate has a potent anti-fibrotic effect in Scleroderma fibroblasts via normalization of PTEN levels*. Arthritis Rheum, 2010. **62**(7): p. 2117-2126.
164. Wang, Y., et al., *Role of JAK-STAT pathway in reducing cardiomyocytes hypoxia/reoxygenation injury induced by S1P postconditioning*. Eur J Pharmacol, 2016. **784**: p. 129-136.
165. Dai, B., et al., *STAT1/3 and ERK1/2 synergistically regulate cardiac fibrosis induced by high glucose*. Cell Physiol Biochem, 2013. **32**(4): p. 960-71.
166. Lekawanvijit, S., et al., *Does indoxyl sulfate, a uraemic toxin, have direct effects on cardiac fibroblasts and myocytes?* Eur Heart J, 2010. **31**(14): p. 1771-1779.
167. Simpson, P., *Stimulation of hypertrophy of cultured neonatal rat heart cells through an alpha 1-adrenergic receptor and induction of beating through an alpha 1- and beta 1-adrenergic receptor interaction. Evidence for independent regulation of growth and beating*. Circ Res, 1985. **56**(6): p. 884-94.
168. Pedranzini, L., et al., *Pyridone 6, A Pan-Janus–Activated Kinase Inhibitor, Induces Growth Inhibition of Multiple Myeloma Cells*. Cancer Res, 2006. **66**(19): p. 9714.
169. Rostami, N., et al., *S1PR1 as a Novel Promising Therapeutic Target in Cancer Therapy*. Mol Diagn Ther, 2019.
170. Quint, P., et al., *Sphingosine 1-phosphate (S1P) receptors 1 and 2 coordinately induce mesenchymal cell migration through S1P activation of complementary kinase pathways*. J Biol Chem, 2013. **288**(8): p. 5398-5406.
171. Negmadjanov, U., et al., *TGF-beta1-mediated differentiation of fibroblasts is associated with increased mitochondrial content and cellular respiration*. PLoS One, 2015. **10**(4): p. e0123046.

172. Chuang, P.Y. and J.C. He, *JAK/STAT signaling in renal diseases.* Kidney Int, 2010. **78**(3): p. 231-234.
173. Hirahara, K., et al., *Asymmetric Action of STAT Transcription Factors Drives Transcriptional Outputs and Cytokine Specificity.* Immunity, 2015. **42**(5): p. 877-889.
174. Mir, S.A., et al., *Inhibition of signal transducer and activator of transcription 3 (STAT3) attenuates interleukin-6 (IL-6)-induced collagen synthesis and resultant hypertrophy in rat heart.* J Biol Chem, 2012. **287**(4): p. 2666-2677.
175. Schwarz, R.I., *Collagen I and the fibroblast: High protein expression requires a new paradigm of post-transcriptional, feedback regulation.* Biochem Biophys Rep, 2015. **3**: p. 38-44.
176. Shea, B.S., et al., *Prolonged exposure to sphingosine 1-phosphate receptor-1 agonists exacerbates vascular leak, fibrosis, and mortality after lung injury.* American journal of respiratory cell and molecular biology, 2010. **43**(6): p. 662-673.
177. Verrecchia, F. and A. Mauviel, *Transforming growth factor-beta and fibrosis.* World journal of gastroenterology, 2007. **13**(22): p. 3056-3062.
178. Annes, J.P., J.S. Munger, and D.B. Rifkin, *Making sense of latent TGFbeta activation.* J Cell Sci, 2003. **116**(Pt 2): p. 217-24.
179. Xin, C., et al., *Sphingosine 1-Phosphate Cross-activates the Smad Signaling Cascade and Mimics Transforming Growth Factor-β-induced Cell Responses.* J Biol Chem, 2004. **279**(34): p. 35255-35262.
180. Funaba, M., C.M. Zimmerman, and L.S. Mathews, *Modulation of Smad2-mediated signaling by extracellular signal-regulated kinase.* J Biol Chem, 2002. **277**(44): p. 41361-8.
181. Yan, H., et al., *Sphingosine-1-phosphate ameliorates the cardiac hypertrophic response through inhibiting the activity of histone deacetylase-2.* Int J Mol Med, 2018. **41**(3): p. 1704-1714.
182. Karliner, J.S., et al., *The lysophospholipids sphingosine-1-phosphate and lysophosphatidic acid enhance survival during hypoxia in neonatal rat cardiac myocytes.* J Mol Cell Cardiol, 2001. **33**(9): p. 1713-7.
183. Nishikimi, T., N. Maeda, and H. Matsuoka, *The role of natriuretic peptides in cardioprotection.* Cardiovasc Res, 2006. **69**(2): p. 318-28.
184. Stilli, D., et al., *Correlation of a-skeletal actin expression, ventricular fibrosis and heart function with the degree of pressure overload cardiac hypertrophy in rats.* Experimental Physiology, 2006. **91**(3): p. 571-580.
185. Chen, Y.-Z., et al., *Sphingosine 1 phosphate receptor-1 (S1PR1) signaling protects cardiac function by inhibiting cardiomyocyte autophagy.* Journal of geriatric cardiology : JGC, 2018. **15**(5): p. 334-345.
186. Ahuja, G., et al., *Loss of genomic integrity induced by lysosphingolipid imbalance drives ageing in the heart.* EMBO reports, 2019. **20**(4): p. e47407.
187. Knapp, M., et al., *Myocardial infarction differentially alters sphingolipid levels in plasma, erythrocytes and platelets of the rat.* Basic Research in Cardiology, 2012. **107**(6): p. 294.
188. Knapp, M., et al., *Myocardial Infarction Changes Sphingolipid Metabolism in the Uninfarcted Ventricular Wall of the Rat.* Lipids, 2012. **47**(9): p. 847-853.
189. Xuan, Y.-T., et al., *Role of the Protein Kinase C-ε–Raf-1–MEK-1/2–p44/42 MAPK Signaling Cascade in the Activation of Signal Transducers and Activators of Transcription 1 and 3 and Induction of Cyclooxygenase-2 After Ischemic Preconditioning.* Circulation, 2005. **112**(13): p. 1971-1978.
190. Zhao, J., Y.-F. Qi, and Y.-R. Yu, *STAT3: A key regulator in liver fibrosis.* Annals of Hepatology, 2020.

191. Zhang, X., et al., *Interacting regions in Stat3 and c-Jun that participate in cooperative transcriptional activation.* Mol Cell Biol, 1999. **19**(10): p. 7138-7146.
192. Bugno, M., et al., *Identification of the interleukin-6/oncostatin M response element in the rat tissue inhibitor of metalloproteinases-1 (TIMP-1) promoter.* Nucleic Acids Res, 1995. **23**(24): p. 5041-7.
193. Arpino, V., M. Brock, and S.E. Gill, *The role of TIMPs in regulation of extracellular matrix proteolysis.* Matrix Biol, 2015. **44-46**: p. 247-254.
194. Takawale, A., et al., *Tissue Inhibitor of Matrix Metalloproteinase-1 Promotes Myocardial Fibrosis by Mediating CD63-Integrin beta1 Interaction.* Hypertension, 2017. **69**(6): p. 1092-1103.
195. Kurdi, M., C. Zgheib, and G.W. Booz, *Recent Developments on the Crosstalk Between STAT3 and Inflammation in Heart Function and Disease.* Front Immunol, 2018. **9**: p. 3029.
196. Li, N. and F. Zhang, *Implication of sphingosin-1-phosphate in cardiovascular regulation.* Frontiers in bioscience (Landmark edition), 2016. **21**: p. 1296-1313.
197. van Empel, V.P.M. and L.J. De Windt, *Myocyte hypertrophy and apoptosis: a balancing act.* Cardiovasc Res, 2004. **63**(3): p. 487-499.
198. Kim, M., et al., *Protein Tyrosine Phosphatases as Potential Regulators of STAT3 Signaling.* International journal of molecular sciences, 2018. **19**(9): p. 2708.
199. Nabben, M., J.J.F.P. Luiken, and J.F.C. Glatz, *Metabolic remodelling in heart failure revisited.* Nature Reviews Cardiology, 2018. **15**(12): p. 780-780.
200. Magaye, R.R., et al., *Exogenous dihydrosphingosine 1 phosphate mediates collagen synthesis in cardiac fibroblasts through JAK/STAT signalling and regulation of TIMP1.* Cellular Signalling, 2020: p. 109629.
201. Schwalm, S., J. Pfeilschifter, and A. Huwiler, *Sphingosine-1-phosphate: a Janus-faced mediator of fibrotic diseases.* Biochim Biophys Acta, 2013. **1831**(1): p. 239-50.
202. Berdyshev, E.V., et al., *Quantitative analysis of sphingoid base-1-phosphates as bisacetylated derivatives by liquid chromatography-tandem mass spectrometry.* Anal Biochem, 2005. **339**(1): p. 129-36.
203. Egom, E.E., et al., *Serum sphingolipids level as a novel potential marker for early detection of human myocardial ischaemic injury.* Frontiers in Physiology, 2013. **4**: p. 130.
204. Means, C.K. and J.H. Brown, *Sphingosine-1-phosphate receptor signalling in the heart.* Cardiovascular research, 2009. **82**(2): p. 193-200.
205. Yang, J., et al., *Targeting PI3K in cancer: mechanisms and advances in clinical trials.* Molecular Cancer, 2019. **18**(1): p. 26.
206. Avendaño, C. and J.C. Menéndez, *Chapter 9 - Drugs That Inhibit Signalling Pathways for Tumor Cell Growth and Proliferation*, in *Medicinal Chemistry of Anticancer Drugs*, C. Avendaño and J.C. Menéndez, Editors. 2008, Elsevier: Amsterdam. p. 251-305.
207. Wei, L., et al., *Asiatic acid attenuates CCl4-induced liver fibrosis in rats by regulating the PI3K/AKT/mTOR and Bcl-2/Bax signaling pathways.* International Immunopharmacology, 2018. **60**: p. 1-8.
208. Hsu, H.-S., et al., *Involvement of ER stress, PI3K/AKT activation, and lung fibroblast proliferation in bleomycin-induced pulmonary fibrosis.* Scientific Reports, 2017. **7**(1): p. 14272.
209. Liu, F. and S. Zhuang, *Role of Receptor Tyrosine Kinase Signaling in Renal Fibrosis.* International Journal of Molecular Sciences, 2016. **17**(6): p. 972.

210. Liang, M., et al., *Vertical inhibition of PI3K/Akt/mTOR signaling demonstrates in vitro and in vivo anti-fibrotic activity.* Journal of Dermatological Science, 2014. **76**(2): p. 104-111.
211. Ghigo, A., et al., *PI3K and Calcium Signaling in Cardiovascular Disease.* Circulation Research, 2017. **121**(3): p. 282-292.
212. Ortega-Molina, A., et al., *Pharmacological Inhibition of PI3K Reduces Adiposity and Metabolic Syndrome in Obese Mice and Rhesus Monkeys.* Cell Metabolism, 2015. **21**(4): p. 558-570.
213. Krycer, J.R., et al., *The Akt-SREBP nexus: cell signaling meets lipid metabolism.* Trends Endocrinol Metab, 2010. **21**(5): p. 268-76.
214. Somers, S.J., et al., *Interplay between SAFE and RISK pathways in sphingosine-1-phosphate-induced cardioprotection.* Cardiovasc Drugs Ther, 2012. **26**(3): p. 227-37.
215. Lawrence, J. and R. Nho, *The Role of the Mammalian Target of Rapamycin (mTOR) in Pulmonary Fibrosis.* International journal of molecular sciences, 2018. **19**(3): p. 778.
216. Maurer, U., et al., *GSK-3 – at the crossroads of cell death and survival.* Journal of Cell Science, 2014. **127**(7): p. 1369.
217. Lal, H., et al., *The GSK-3 Family as Therapeutic Target for Myocardial Diseases.* Circulation Research, 2015. **116**(1): p. 138-149.
218. Jankowski, M., *GATA4, a new regulator of cardiac fibroblasts, is sensitive to natriuretic peptides.* Cardiovascular Research, 2009. **84**(2): p. 176-177.
219. Ang, Y.-S., et al., *Disease Model of GATA4 Mutation Reveals Transcription Factor Cooperativity in Human Cardiogenesis.* Cell, 2016. **167**(7): p. 1734-1749.e22.
220. Park, S.W., et al., *Sphinganine-1-phosphate protects kidney and liver after hepatic ischemia and reperfusion in mice through S1P1 receptor activation.* Lab Invest, 2010. **90**(8): p. 1209-24.
221. Jiang, Q., et al., *Gamma-tocotrienol induces apoptosis and autophagy in prostate cancer cells by increasing intracellular dihydrosphingosine and dihydroceramide.* International Journal of Cancer. Journal International du Cancer, 2012. **130**(3): p. 685-693.
222. Pandya, K. and O. Smithies, *β-MyHC and Cardiac Hypertrophy.* Circulation Research, 2011. **109**(6): p. 609-610.
223. Booz George, W., *Putting the Brakes on Cardiac Hypertrophy.* Hypertension, 2005. **45**(3): p. 341-346.
224. Kerkela, R., et al., *Deletion of GSK-3beta in mice leads to hypertrophic cardiomyopathy secondary to cardiomyoblast hyperproliferation.* J Clin Invest, 2008. **118**(11): p. 3609-18.
225. Välimäki, M.J. and H.J. Ruskoaho, *Targeting GATA4 for cardiac repair.* IUBMB life, 2020. **72**(1): p. 68-79.
226. Liu, X., et al., *Transforming growth factor-beta-sphingosine kinase 1/S1P signaling upregulates microRNA-21 to promote fibrosis in renal tubular epithelial cells.* Exp Biol Med (Maywood), 2016. **241**(3): p. 265-72.
227. Hannan, K.M., et al., *mTOR-Dependent Regulation of Ribosomal Gene Transcription Requires S6K1 and Is Mediated by Phosphorylation of the Carboxy-Terminal Activation Domain of the Nucleolar Transcription Factor UBF†.* Molecular and Cellular Biology, 2003. **23**(23): p. 8862.
228. Holz, M.K., et al., *mTOR and S6K1 Mediate Assembly of the Translation Preinitiation Complex through Dynamic Protein Interchange and Ordered Phosphorylation Events.* Cell, 2005. **123**(4): p. 569-580.

229. Rabinowitz, J.D. and G.M. Mutlu, *A metabolic strategy to reverse fibrosis?* Nature Metabolism, 2019. **1**(1): p. 12-13.
230. Kapoor, M., et al., *GSK-3β in mouse fibroblasts controls wound healing and fibrosis through an endothelin-1–dependent mechanism.* The Journal of Clinical Investigation, 2008. **118**(10): p. 3279-3290.
231. Lal, H., et al., *Cardiac Fibroblast Glycogen Synthase Kinase-3β Regulates Ventricular Remodeling and Dysfunction in Ischemic Heart.* Circulation, 2014. **130**(5): p. 419-430.
232. Liu, S.Q., et al., *[Sphingosine kinase 1 enhances the proliferation and invasion of human colon cancer LoVo cells through up-regulating FAK pathway and the expression of ICAM-1 and VCAM-1].* Zhonghua Zhong Liu Za Zhi, 2013. **35**(5): p. 331-6.
233. Sferra, R., et al., *Interaction between sphingosine kinase/sphingosine 1 phosphate and transforming growth factor-β/Smads pathways in experimental intestinal fibrosis. An in vivo immunohistochemical study.* European journal of histochemistry : EJH, 2018. **62**(3): p. 2956.
234. Kim, K.H., et al., *Regulatory Role of Glycogen Synthase Kinase 3 for Transcriptional Activity of ADD1/SREBP1c.* Journal of Biological Chemistry, 2004. **279**(50): p. 51999-52006.
235. Horton, J.D., J.L. Goldstein, and M.S. Brown, *SREBPs: transcriptional mediators of lipid homeostasis.* Cold Spring Harb Symp Quant Biol, 2002. **67**: p. 491-8.
236. Wang, P., et al., *Roles of sphingosine-1-phosphate signaling in cancer.* Cancer Cell International, 2019. **19**(1): p. 295.
237. Aoyagi, T. and T. Matsui, *Phosphoinositide-3 kinase signaling in cardiac hypertrophy and heart failure.* Current pharmaceutical design, 2011. **17**(18): p. 1818-1824.
238. Suurmeijer, A.J., et al., *Alpha-actin isoform distribution in normal and failing human heart: a morphological, morphometric, and biochemical study.* J Pathol, 2003. **199**(3): p. 387-97.
239. Hewett, T.E., et al., *Alpha-skeletal actin is associated with increased contractility in the mouse heart.* Circ Res, 1994. **74**(4): p. 740-6.
240. Morisco, C., et al., *The Akt-Glycogen Synthase Kinase 3β Pathway Regulates Transcription of Atrial Natriuretic Factor Induced by β-Adrenergic Receptor Stimulation in Cardiac Myocytes.* Journal of Biological Chemistry, 2000. **275**(19): p. 14466-14475.
241. Haq, S., et al., *Glycogen Synthase Kinase-3β Is a Negative Regulator of Cardiomyocyte Hypertrophy.* Journal of Cell Biology, 2000. **151**(1): p. 117-130.
242. Hardt, S.E., et al., *Phosphorylation of Eukaryotic Translation Initiation Factor 2Bε by Glycogen Synthase Kinase-3β Regulates β-Adrenergic Cardiac Myocyte Hypertrophy.* Circulation Research, 2004. **94**(7): p. 926-935.
243. Roux, P.P., et al., *RAS/ERK Signaling Promotes Site-specific Ribosomal Protein S6 Phosphorylation via RSK and Stimulates Cap-dependent Translation.* Journal of Biological Chemistry, 2007. **282**(19): p. 14056-14064.
244. Biever, A., et al., *PKA-Dependent Phosphorylation of Ribosomal Protein S6 Does Not Correlate with Translation Efficiency in Striatonigral and Striatopallidal Medium-Sized Spiny Neurons.* The Journal of Neuroscience, 2015. **35**(10): p. 4113.

245. Tao, R., et al., *Cardiomyocyte S1P1 receptor-mediated extracellular signal-related kinase signaling and desensitization.* Journal of cardiovascular pharmacology, 2009. **53**(6): p. 486-494.
246. Morisco, C., et al., *Glycogen Synthase Kinase 3β Regulates GATA4 in Cardiac Myocytes.* Journal of Biological Chemistry, 2001. **276**(30): p. 28586-28597.
247. Sun, L., et al., *Comprehensive metabonomic analysis of heart tissue from isoproterenol-induced myocardial infarction rat based on reversed-phase and hydrophilic interaction chromatography coupled to mass spectrometry.* Journal of Separation Science, 2017. **40**(10): p. 2198-2206.
248. Knapp, M., et al., *Decreased free sphingoid base concentration in the plasma of patients with chronic systolic heart failure.* Advances in Medical Sciences, 2012. **57**(1): p. 100-105.
249. Berdyshev, E.V., et al., *De novo biosynthesis of dihydrosphingosine-1-phosphate by sphingosine kinase 1 in mammalian cells.* Cell Signal, 2006. **18**(10): p. 1779-92.
250. Kraveka, J.M., et al., *Involvement of dihydroceramide desaturase in cell cycle progression in human neuroblastoma cells.* J Biol Chem, 2007. **282**(23): p. 16718-28.
251. Breen, P., et al., *Dihydroceramide Desaturase Knockdown Impacts Sphingolipids and Apoptosis after Photodamage in Human Head and Neck Squamous Carcinoma Cells.* Anticancer research, 2013. **33**(1): p. 77-84.
252. Ruangsiriluk, W., et al., *Silencing of enzymes involved in ceramide biosynthesis causes distinct global alterations of lipid homeostasis and gene expression.* Journal of Lipid Research, 2012. **53**(8): p. 1459-1471.
253. Cencetti, F., et al., *Transforming Growth Factor- 1 Induces Transdifferentiation of Myoblasts into Myofibroblasts via Up-Regulation of Sphingosine Kinase-1/S1P3 Axis.* Molecular biology of the cell, 2010. **21**: p. 1111-24.
254. Magaye, R.R., et al., *Exogenous dihydrosphingosine 1 phosphate mediates collagen synthesis in cardiac fibroblasts through JAK/STAT signalling and regulation of TIMP1.* Cell Signal, 2020. **72**: p. 109629.
255. Huynh, K., et al., *High-Throughput Plasma Lipidomics: Detailed Mapping of the Associations with Cardiometabolic Risk Factors.* Cell Chemical Biology, 2019. **26**(1): p. 71-84.e4.
256. Weir, J.M., et al., *Plasma lipid profiling in a large population-based cohort.* Journal of Lipid Research, 2013. **54**(10): p. 2898-2908.
257. Ogretmen, B., *Sphingolipid metabolism in cancer signalling and therapy.* Nature Reviews Cancer, 2018. **18**(1): p. 33-50.
258. Lewis, A.C., et al., *Targeting sphingolipid metabolism as an approach for combination therapies in haematological malignancies.* Cell Death Discovery, 2018. **4**(1): p. 72.
259. Zhang, Y.E., *Non-Smad Signaling Pathways of the TGF-β Family.* Cold Spring Harbor perspectives in biology, 2017. **9**(2): p. a022129.
260. Yamaguchi, K., et al., *Identification of a member of the MAPKKK family as a potential mediator of TGF-beta signal transduction.* Science, 1995. **270**(5244): p. 2008-11.
261. Yang, W.-L., et al., *The E3 ligase TRAF6 regulates Akt ubiquitination and activation.* Science (New York, N.Y.), 2009. **325**(5944): p. 1134-1138.
262. Schubert, K.M., M.P. Scheid, and V. Duronio, *Ceramide Inhibits Protein Kinase B/Akt by Promoting Dephosphorylation of Serine 473.* Journal of Biological Chemistry, 2000. **275**(18): p. 13330-13335.

263. Riboni, L., et al., *The Effects of Exogenous Sphingosine on Neuro2a Cells Are Strictly Related to the Overall Capacity of Cells to Metabolize Sphingosine1*. The Journal of Biochemistry, 1998. **124**(5): p. 900-904.
264. Yi, J.Y., I. Shin, and C.L. Arteaga, *Type I transforming growth factor beta receptor binds to and activates phosphatidylinositol 3-kinase*. J Biol Chem, 2005. **280**(11): p. 10870-6.
265. Wilkes, M.C., et al., *Transforming growth factor-beta activation of phosphatidylinositol 3-kinase is independent of Smad2 and Smad3 and regulates fibroblast responses via p21-activated kinase-2*. Cancer Res, 2005. **65**(22): p. 10431-40.
266. Yatomi, Y., et al., *N,N-Dimethylsphingosine Inhibition of Sphingosine Kinase and Sphingosine 1-Phosphate Activity in Human Platelets*. Biochemistry, 1996. **35**(2): p. 626-633.
267. Berdyshev, E.V., et al., *FTY720 Inhibits Ceramide Synthases and Up-regulates Dihydrosphingosine 1-Phosphate Formation in Human Lung Endothelial Cells*. The Journal of Biological Chemistry, 2009. **284**(9): p. 5467-5477.
268. Liu, W., et al., *A Novel Immunomodulator, FTY-720 Reverses Existing Cardiac Hypertrophy and Fibrosis From Pressure Overload by Targeting NFAT (Nuclear Factor of Activated T-cells) Signaling and Periostin*. Circulation: Heart Failure, 2013. **6**(4): p. 833-844.
269. Lee, M.J., M. Evans, and T. Hla, *The inducible G protein-coupled receptor edg-1 signals via the G(i)/mitogen-activated protein kinase pathway*. J Biol Chem, 1996. **271**(19): p. 11272-9.
270. Alessenko, A.V., A. Lebedev, and I.N. Kurochkin, *[The role of sphingolipids in cardiovascular pathologies]*. Biomed Khim, 2018. **64**(6): p. 487-495.
271. Lim, G.B., *Sphingolipids are biomarkers of coronary disease*. Nature Reviews Cardiology, 2020. **17**(4): p. 200-200.
272. Borodzicz, S., et al., *Sphingolipids in cardiovascular diseases and metabolic disorders*. Lipids Health Dis, 2015. **14**: p. 55.
273. Poss, A.M., et al., *Machine learning reveals serum sphingolipids as cholesterol-independent biomarkers of coronary artery disease*. The Journal of Clinical Investigation, 2020. **130**(3): p. 1363-1376.
274. Lemaitre Rozenn, N., et al., *Plasma Ceramides and Sphingomyelins in Relation to Heart Failure Risk*. Circulation: Heart Failure, 2019. **12**(7): p. e005708.
275. Thomas, D.M. and M.O. Lina, *Ceramide and Apoptosis: Exploring the Enigmatic Connections between Sphingolipid Metabolism and Programmed Cell Death*. Anti-Cancer Agents in Medicinal Chemistry, 2012. **12**(4): p. 340-363.
276. Jozefczuk, E., T.J. Guzik, and M. Siedlinski, *Significance of sphingosine-1-phosphate in cardiovascular physiology and pathology*. Pharmacological Research, 2020. **156**: p. 104793.
277. Wang, E., X. He, and M. Zeng, *The Role of S1P and the Related Signaling Pathway in the Development of Tissue Fibrosis*. Frontiers in pharmacology, 2019. **9**: p. 1504-1504.
278. Wang, J., et al., *SphK1/S1P mediates TGF-β1-induced proliferation of pulmonary artery smooth muscle cells and its potential mechanisms*. Pulm Circ, 2019. **9**(1): p. 2045894018816977.
279. Casasampere, M., et al., *Inhibitors of dihydroceramide desaturase 1: Therapeutic agents and pharmacological tools to decipher the role of dihydroceramides in cell biology*. Chem Phys Lipids, 2016. **197**: p. 33-44.

280. Orienti, I., et al., *A new bioavailable fenretinide formulation with antiproliferative, antimetabolic, and cytotoxic effects on solid tumors.* Cell Death & Disease, 2019. **10**(7): p. 529.
281. Aurelio, L., et al., *From Sphingosine Kinase to Dihydroceramide Desaturase: A Structure–Activity Relationship (SAR) Study of the Enzyme Inhibitory and Anticancer Activity of 4-((4-(4-Chlorophenyl)thiazol-2-yl)amino)phenol (SKI-II).* Journal of Medicinal Chemistry, 2016. **59**(3): p. 965-984.
282. Gao, X.-M., et al., *Infarct size and post-infarct inflammation determine the risk of cardiac rupture in mice.* International Journal of Cardiology, 2010. **143**(1): p. 20-28.
283. Gao, X.-M., et al., *Mouse model of post-infarct ventricular rupture: time course, strain- and gender-dependency, tensile strength, and histopathology.* Cardiovascular Research, 2005. **65**(2): p. 469-477.
284. Du, X.-J., et al., *β2-Adrenergic Receptor Overexpression Exacerbates Development of Heart Failure After Aortic Stenosis.* Circulation, 2000. **101**(1): p. 71-77.
285. Liu, S., et al., *Subtotal nephrectomy accelerates pathological cardiac remodeling post-myocardial infarction: implications for cardiorenal syndrome.* Int J Cardiol, 2013. **168**(3): p. 1866-80.
286. Yeh, C.-C., et al., *Distinctive ERK and p38 signaling in remote and infarcted myocardium during post-MI remodeling in the mouse.* Journal of cellular biochemistry, 2010. **109**(6): p. 1185-1191.
287. Siddique, M.M., et al., *Ablation of dihydroceramide desaturase 1, a therapeutic target for the treatment of metabolic diseases, simultaneously stimulates anabolic and catabolic signaling.* Mol Cell Biol, 2013. **33**(11): p. 2353-69.
288. Siddique, M.M., et al., *Ablation of Dihydroceramide Desaturase Confers Resistance to Etoposide-Induced Apoptosis In Vitro.* PLOS ONE, 2012. **7**(9): p. e44042.
289. Casasampere, M., et al., *Dihydroceramide desaturase inhibitors induce autophagy via dihydroceramide-dependent and independent mechanisms.* Biochimica et Biophysica Acta (BBA) - General Subjects, 2017. **1861**(2): p. 264-275.
290. Chaurasia, B., et al., *Targeting a ceramide double bond improves insulin resistance and hepatic steatosis.* Science, 2019. **365**(6451): p. 386.
291. Palazzuoli, A., et al., *The impact of infarct size on regional and global left ventricular systolic function: a cardiac magnetic resonance imaging study.* The International Journal of Cardiovascular Imaging, 2015. **31**(5): p. 1037-1044.
292. Mehta, N., et al., *Transdifferentiation of cardiac fibroblasts to myofibroblast phenotype and its regulation by extracellular matrix compostion and mechanics.* Journal of the American College of Cardiology, 2014. **63**(12 Supplement): p. A851.
293. Baum, J. and H.S. Duffy, *Fibroblasts and myofibroblasts: what are we talking about?* Journal of cardiovascular pharmacology, 2011. **57**(4): p. 376-379.
294. Gallo, S., et al., *ERK: A Key Player in the Pathophysiology of Cardiac Hypertrophy.* International journal of molecular sciences, 2019. **20**(9): p. 2164.
295. Maekawa, Y., et al., *Effect of granulocyte-macrophage colony-stimulating factor inducer on left ventricular remodeling after acute myocardial infarction.* Journal of the American College of Cardiology, 2004. **44**(7): p. 1510-1520.
296. Anzai, T., *Inflammatory Mechanisms of Cardiovascular Remodeling.* Circ J, 2018. **82**(3): p. 629-635.
297. Coles, B., et al., *Classic interleukin-6 receptor signaling and interleukin-6 trans-signaling differentially control angiotensin II-dependent hypertension, cardiac signal*

transducer and activator of transcription-3 activation, and vascular hypertrophy in vivo. Am J Pathol, 2007. **171**(1): p. 315-25.
298. Liu, T., et al., *NF-κB signaling in inflammation.* Signal Transduction and Targeted Therapy, 2017. **2**(1): p. 17023.
299. Harhous, Z., et al., *An Update on the Multifaceted Roles of STAT3 in the Heart.* Frontiers in Cardiovascular Medicine, 2019. **6**(150).
300. Haus, J.M., et al., *Plasma ceramides are elevated in obese subjects with type 2 diabetes and correlate with the severity of insulin resistance.* Diabetes, 2009. **58**(2): p. 337-343.

Appendice

Appendix 1

The following pages contain publications directly arising from the studies described in this thesis. They include:

1. **Magaye RR**, Savira F, Hua Y, Kelly DJ, Reid C, Flynn B, Liew D, Wang BW. The role of dihydrosphingolipids in disease. Journal of Cellular Molecular Life Science. 2019;76(6):1107-34.

2. **Magaye RR**, Savira F, Hua Y, Xiong X, Huang L, Reid C, Flynn B, Liew D, Wang BW. Exogenous dihydrosphingosine 1 phosphatemediates collagen synthesis in cardiac fibroblasts through JAK/STAT signalling and TIMP1. Journal of Cellular Signalling. 2020;72:109620.

Appendix 1.1

Magaye RR, Savira F, Hua Y, Kelly DJ, Reid C, Flynn B, Liew D, Wang BW. The role of dihydrosphingolipids in disease. Journal of Cellular Molecular Life Science. 2019;76(6):1107-34.

The role of dihydrosphingolipids in disease

Ruth. R. Magaye, Feby Savira, Yue Hua, Darren J. Kelly, Christopher Reid, Bernard Flynn, Danny Liew & Bing H. Wang

Cellular and Molecular Life Sciences

ISSN 1420-682X

Cell. Mol. Life Sci.
DOI 10.1007/s00018-018-2984-8

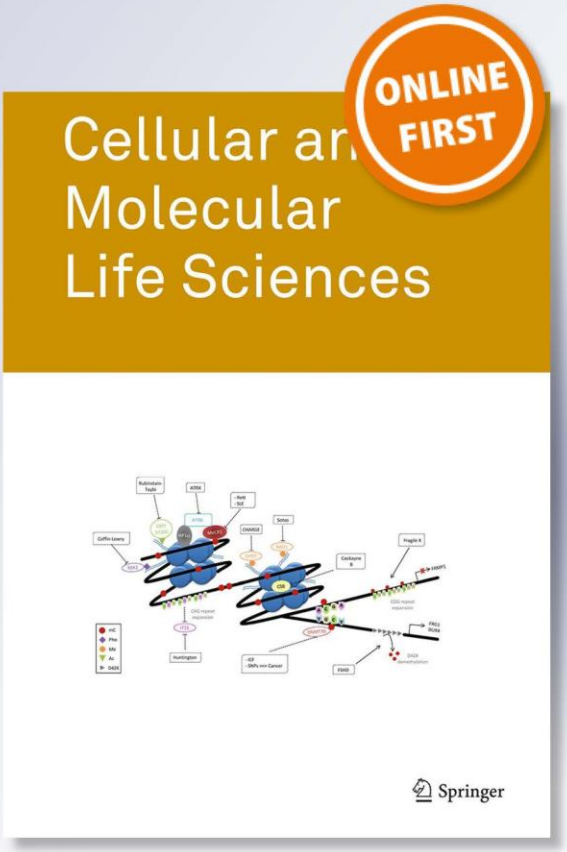

Springer

Cellular and Molecular Life Sciences
https://doi.org/10.1007/s00018-018-2984-8

Cellular and Molecular Life Sciences

REVIEW

The role of dihydrosphingolipids in disease

Ruth. R. Magaye[1] · Feby Savira[1] · Yue Hua[1] · Darren J. Kelly[2] · Christopher Reid[1] · Bernard Flynn[3] · Danny Liew[1] · Bing H. Wang[1]

Received: 19 July 2018 / Revised: 6 November 2018 / Accepted: 26 November 2018

Abstract

Dihydrosphingolipids refer to sphingolipids early in the biosynthetic pathway that do not contain a C4-*trans*-double bond in the sphingoid backbone: 3-ketosphinganine (3-ketoSph), dihydrosphingosine (dhSph), dihydrosphingosine-1-phosphate (dhS1P) and dihydroceramide (dhCer). Recent advances in research related to sphingolipid biochemistry have shed light on the importance of sphingolipids in terms of cellular signalling in health and disease. However, dihydrosphingolipids have received less attention and research is lacking especially in terms of their molecular mechanisms of action. This is despite studies implicating them in the pathophysiology of disease, for example dhCer in predicting type 2 diabetes in obese individuals, dhS1P in cardiovascular diseases and dhSph in hepato-renal toxicity. This review gives a comprehensive summary of research in the last 10–15 years on the dihydrosphingolipids, 3-ketoSph, dhSph, dhS1P and dhCer, and their relevant roles in different diseases. It also highlights gaps in research that could be of future interest.

Keywords Adipocyte · Aging · Airway hypersensitivity · Apoptosis · Autophagy · Cancer · Cardiomyopathy · Ceramide · Ceramide synthase · Dihydroceramide desaturase 1-Des-1 · Diabetes · Dihydrosphinganine · FB1 toxicity · Hypoxia · Neurodegenerative · Sphingosine kinase · Serine palmitoyl transferase · Sphingosine-1-phosphate—S1P · Sphingosine-1-phosphate receptors · 4-HRP fenretinide

Abbreviations

3-KR	3-Ketosphinganine Reductase
4-HPR	*N*-(4-Hydroxyphenyl) retinamideFenretinide
γ-TE	γ-Tocotrienol
ACER3	Alkaline ceramidase 3
ACSL5	Acyl-coenzyme A synthase
ACSL5	Δ20 acyl-coenzyme A synthase lacking exon 20
ADH	Adiponectin hormone
AHA	American Heart Association
Akt	Protein kinase B
AMPK	AMP activated protein kinase
BMI	Body mass index
CAD	Coronary artery disease
cAMP	Cyclic adenosine 3′,5′-monophosphate
cDase	Ceramidase
cdk2	Cyclin dependent kinase 2
Cer	Ceramide
CERKL	Ceramide like kinase
CERK	Ceramide kinase
CerS	Ceramide synthase
CFTR	Cystic fibrosis transmembrane conductance regulator
COX-2	Cyclooxygenase 2
CRF	Cardiorespiratory fitness
CTGF	Connective tissue growth factor
CVD	Cardiovascular disease
Des1	Dihydroceramide desaturase 1
Des2	Dihydroceramide desaturase 2

✉ Bing H. Wang
bing.wang@monash.edu

Ruth. R. Magaye
ruth.magaye@monash.edu

Feby Savira
feby.savira@monash.edu

Yue Hua
luna.hua@monash.edu

[1] Monash Centre of Cardiovascular Research and Education in Therapeutics, School of Public Health and Preventive Medicine, Monash University, Melbourne, Australia

[2] Department of Medicine, St Vincent's Hospital, University of Melbourne, Fitzroy, VIC, Australia

[3] Australian Translational Medicinal Chemistry Facility, Medicinal Chemistry, Monash Institute of Pharmaceutical Sciences, Monash University, Melbourne, Australia

Published online: 06 December 2018

DhCer	Dihydroceramide
DhSph	Dihydrosphingosine/Dihydrosphinganine
DhS1P	Dihydrosphingosine 1 phosphate/dihydrosphinganine 1 phosphate
EAP	Ethanolamine phosphate
ER	Endoplasmic reticulum
ERK	Extracellular signal regulated kinases
FAK	Focal adhesion kinase
FB1	Fumonisin B 1
FFA	Free fatty acid
HDAC2	Histone deacetylase 2
HDL	High density lipid
HepG2	Human hepato-carcinoma cell
HIF1-α	Hypoxia inducible factor 1-α
HOMA-IR	Homestasis model of insulin resistance
HSP27	Heat shock protein 27
HUVEC	Human umblical endothelial cell
FTY720	Fingolimod
IL-1	Interleukin 1
IL-6	Interleukin 6
JNK	c-Jun N terminal kinase
LDL	Low density lipid
LPS	Lipopolysaccharide
LRS	Lipidomic risk score
MAPK	Mitogen activated protein kinases
MI	Myocardial infarct
MnTBAP	Manganese(III) tetrakis (4-benzoic acid) porphyrin
MTORC1	Mammalian target of rapamycin complex 1
NADH	Nicotinamide adenine nucleotide
NADPH	Nicotinamide adenine nucleotide phosphate
NAFLD	Non-alcoholic fatty liver disease
NFATC	Nuclear factor of activated T cells
NK-kβ	Nuclear factor kappa light chain enhancer of B cell
Nrf2	Nuclear factor erythroid related factor 2
PDGF	Platelet derived growth factor
PDT	Photodynamic therapy
PeIF2α	Phosphorylated eukaryotic translation initiation factors 2α
PERK	PKR like endoplasmic reticulum kinase
PKCα	Protein kinase Cα
PLD	Phospholipase D
PPARγ	Peroxisome proliferator-activated receptor γ
RAR	Retinoic acid receptor
RMC	Renal mesengial cell
ROS	Reactive oxygen species
S6K	Ribosomal protein S6 kinase
SAFHS	San Antonio Family Heart Study
SEK-1	Dual specificity mitogen activated protein kinase kinase 1
SD	Sprague Dawley
SK 1 and 2	Sphingosine kinase 1 and 2
S1P	Sphingosine 1 phosphate
S1PP	Sphingosine 1 phosphate phophatase
S1PR1–5	Sphingosine 1 phosphate receptor 1–5
SPL	Sphingosine 1 phosphate lyase
SPT	Serine palmitoyltransferase
SPLTC1	Serine palmitoyltransferase long chain base 1
SPTLC3	Serine palmitoyltransferase long chain base 3
STEMI	ST-segment elevation myocardial: infarct
SCC19	Squamous cell carcinoma cell
T2DM	Type 2 diabetes mellitus
TNF-α	Tumour necrosis factor α
VEGF	Vascular endothelial growth factor
WC	Waist circumference

Background

Since their discovery in the 1800s, sphingolipids have been shown to play key roles in physiological and pathological states by functioning as mediators or effectors of cellular signals. They are integral components of all eukaryotic cell membranes. It is now known that sphingolipids play a role in cell apoptosis, autophagy, oxidative stress and inflammation [1, 2, 3] and in disease states such as cancer, multiple sclerosis and diabetes [4, 5, 6]. These cellular events are effected through activation and interaction of the sphingosine 1 phosphate receptors (S1PR1–5), enzymes such as sphingosine kinases (SK 1 and 2), ceramide synthases (CerS1–6) or sphingolipids such as sphingosine 1 phosphate (S1P), and ceramides (Cers) [7]. Accordingly, there is significant interest in targeting the enzyme of sphingolipid metabolism and S1PRs in the discovery of new therapies. The term sphingolipids extends to a lot of other lipids and enzymes within the sphingolipid de novo biosynthesis pathway (Fig. 1). These include 3-ketoSph, dhSph, dhS1P and dhCer, as well as enzymes such as serine palmitoyltransferase (SPT), dihydroceramide desaturases (Des 1 and 2), and ceramidases (CDases). Here we, attempt to give a comprehensive review of literature focusing on the evidence for the role of the aforementioned dihydropshingolipids in relevant disease states and the associative effects they may have or the possible roles they may play. The information presented in this review was derived through data searches in Ovid, Medline and Embase using the MeSH terms (dihydrosphingosine 1-phsophate, sphinganine 1 phosphate, 3-ketosphinganine, dihydroceramide, dihydrosphinganine and dihydrosphingosine) and keyword searches of the same. The articles derived from the search were limited to human and animal studies and the English language. It is hoped that this review will also shed light on much needed areas of research on the relevance of dihydrosphingolipids and their roles in diseases.

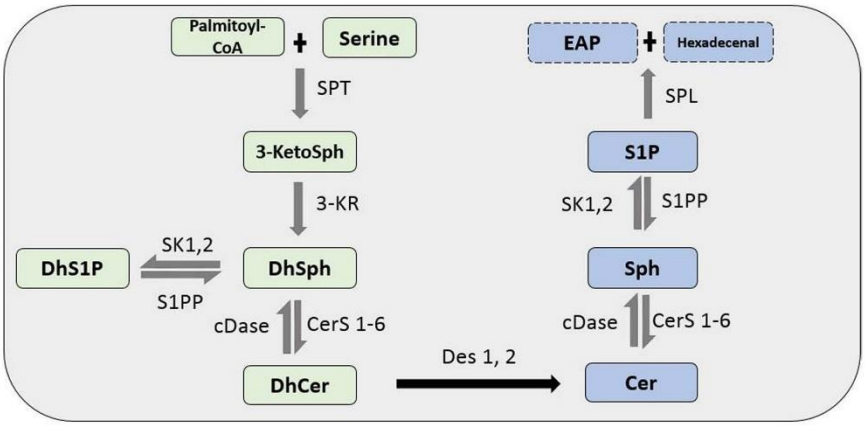

Fig. 1 De novo sphingolipid biosynthesis pathway. In the de novo pathway, the condensation of palmitoyl-CoA and serine by the enzyme SPT forms 3-ketoSph. This is then reduced by 3-KR to dhSph. The acylation and phosphorylation of dhSph by CerS1-6 and SK 1 and 2 leads to the formation of dhCer and dhS1P, respectively. Des-1 and -2 then catalyze the desaturation of dhCer to Cer, which is a non-reversible reaction. The metabolization of Cer by CDase produces Sph. The production of S1P from Sph is exclusively phosphorylated by SK 1 and 2. S1P is then degraded to ethanolamine phosphate (EAP) and trans-2-hexadecenal by S1P lyase (SPL). DhS1P and S1P can be converted back to dhSph and Sph by S1P phosphatase (S1PP) and dhSph and Sph to dhCer and Cer, respectively, by cDase

De novo synthesis of sphingolipids

Briefly, apart from the de novo synthesis pathway (Fig. 1), sphingolipids are also synthesized through the salvage pathway and the sphingomyelin pathway. Regulation of plasma levels of sphingolipids generally occurs through the de novo synthesis pathway [8]. The backbone of the sphingolipids are Sph and dhSph, which are composed of an amino alcohol, from which all the other sphingolipids are derived by the enzymatic activity of a number of enzymes along the pathway. Most of the enzymatic activities along the de novo synthesis pathway are reversible except a few, including the conversion of dhCer to Cer. Thus, the enzymes responsible for this, Des-1 and -2, have now been described as gatekeepers [9].

The segment of the pathway that begins at Des-1 and -2 to S1P which includes Cer, Sph and S1P has been studied the most and their relevance in disease is well documented by other reviewers [10–13]. Therefore, in this review, the focus is on highlighting dhCer, dhS1P, dhSph and 3-ketoSph; dihydrosphingolipids; and the possible regulatory and contributory effects of these dihydrosphingolipids in diseases.

DhCer in disease

Overview and structure

DhCers lack the C4-double bond observed in Cers (Fig. 2); however, they also serve as precursors of complex sphingolipids such as dihydrosphingomyelins and dihydrogangliosides. For years, dhCers were thought to be biologically inactive due to them being less abundant, compared to Cers. This perception changed with the development of fenretinide [(*N*-(4-hydroxyphenyl)retinamide]-(4-HPR), which was found to inhibit Des-1 by the Merill Group [14]. Des-1 is found in all tissues, whereas Des-2 has been found in skin, intestine and kidney [15]. A later study further showed that the ablation of Des-1 and 2 shifts sphingolipid synthesis pathway toward the sphingolipid lacking the double bond introduced by Des-1 and -2, such as dhS1P,

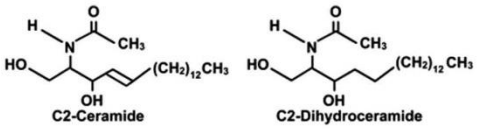

Fig. 2 Comparison of C2-ceramide with C2-dihydroceramide, without the double bond

dhSph, dhsphingomyelin (dhSM) and especially dhCer [16]. Together, these discoveries led to new functional discoveries for dhCers in apoptosis, autophagy, hypoxia and cell proliferation, as reviewed by Siddique et al. [17].

In the conventional sphingolipid synthesis pathway, dhCers are produced as a result of the addition of fatty acyl-CoAs of differing chain lengths to dhSph by the enzyme CerS. The six isoforms of CerS expressed in mammalians are encoded by different chromosomes and exhibit preference for a defined chain length of fatty acyl-CoA [18], therefore portraying different functional, structural and biochemical attributes [19]. The dhCer chain lengths that are mentioned in this review are summarized in Table 1, except for the studies in cancer cells. It should be noted that most of the studies referenced in the table also had alterations in the Cer levels; however, they have not been mentioned due to the focus of the review in highlighting dhCers and the other dihydrosphingolipids. The majority of the studies in which dhCer has been mentioned, from 1990s to 2009, used cell penetrant dhCer bearing short acyl chains as negative controls in experiments tailored toward elucidating the effects of Cers in biological systems or disease conditions [20–22]. Due to the way in which these were used, most reported no effects and thus will not be included here. However, evidence contained in more recent studies paint a different picture of longer chain dhCers in terms of diseases.

DhCer in brain diseases

Research on sphingolipids in the brain has focussed on the glycolipids which include the cerebrosides, gangliosides and ceramide oligosaccharides as well as on Cers. Though Sun et al. [60] give a comprehensive review of the role of sphingolipids in stroke, the review does not highlight dihydrosphingolipids, which may be due to most of the studies focussing on other sphingolipids. Here, we highlight studies that have mentioned dhCer levels in brain-related diseases.

A study investigating the effects of hypoxia on sphingolipid metabolism in human cerebral endothelial cells found that dhCers (long chains) were increased together with other sphingolipids [23]. In addition, increased dhCer levels were also seen after subarachnoid haemorrhage [24]. Both of these studies allude to the involvement of dhCer in the mechanisms of disease in oxygen deprivation states such as stroke. Not only this, but dhCer levels have also been noted to be altered in studies related to certain neuronal diseases such as luekodystrophia [26], Alzheimer's [61], Huntington's disease (HD) [62] and in episodic migraineurs [25]. Though the cause of migraines is not so clear, genetic anomalies in the enzymes could have played a part in the reduced levels of dhCer seen in the migraine study, as shown by Matesanz et al. [63]. This study hypothesized that the splice variant of the acyl-coenzyme A synthase 5 (ACSL5) gene which lacked exon 20 (ACSL5-Δ20), could have led to the decrease in CerS, and thus dhCer levels. On the other hand, genetic mutations in other enzymes such as ACER3, which is an alkaline ceramidase (CDase), have been linked to elevated dhCer (C18:1 and C20:1) levels observed in the plasma of childhood leukodystrophic twin patients with a genetic mutation at p.E33G, responsible for the catalytic activity of ACER3. In Alzheimer's disease, the inhibition of the gatekeeper enzyme, Des-1 byXM461 and XM462, increased dhCer levels in Alzheimer's transgenic mice, which led to the induction of autophagy and reduced amyloid secretion by neuronal cells through loss of ribosomal protein S6 kinase (S6K) activity due to reduced mammalian target of rapamycin complex 1 (MTORC1) activity [64]. The autophagy effect exerted by increased dhCer observed in this study is corroborated by studies in cancer cells that have shown similar effects [65, 66]. However, clinically, others have shown that increased plasma dihydroshingomyelin/dhCer and sphingomyelin/Cer ratios are predictive of slower progression among Alzheimer's disease patients [61]. In addition, reduced dhCer (C18:0) including dhSph and dhS1P levels and mRNA expression of the enzymes CerS1 and serine palmotyltransferase long chain base 1 (SPLTC1) have been observed in transgenic mice brains manifesting HD. These reductions may be a result of the reduced level of SPLTC1, which impacts the entire de novo sphingolipid synthesis pathway. These studies show an association of dhCer with the progression of degenerative brain diseases as well as in other brain-related diseases, which makes it a potential target as a biomarker. There are also conceivable genetic associations of the enzymes in the sphingolipid pathway with neurodegenerative diseases. However, whether or not dhCer has a causal effect is an area that warrants further research.

DhCer in diabetes

It is now known that dyslipidaemia commonly occurs in diabetes [67], which is a major risk factor for developing cardiovascular diseases (CVDs) [68]. The main characteristic of dyslipidemia in diabetes is high triglyceride levels, reduced high-density lipids (HDL) and slightly elevated low-density lipids (LDL)-cholesterol, with a dominance of the atherogenic small dense LDL [69]. Studies have shown that the sphingolipid, S1P, is bound to HDL in plasma and its distribution is shifted to other non-HDL carriers in the plasma, when HDL levels are low [70]. A number of studies also support the role of Cer and Cer16:0 in particular, in insulin resistance and glucose intolerance [71–74]. These evidences show that sphingolipid metabolism and transport, including dhCer, can be altered in diabetes affecting insulin resistance and mitochondrial and adipose tissue homeostasis.

Table 1 Summary of the dhCer acyl chain length-specific effects in the different pathologies mentioned in the review

Effects	Study type	Type of cell, animal or sample	Pathways involved	dhCer acyl chain length	Levels	References
Brain disease and dhCer						
Hypoxia	In vitro	Cerebral endothelial cells		Long chain (unspecified)	↑	[23]
Subarachnoid haemorrhage	Human	CSF		Unspecified	↑	[24]
Episodic migraine	Human	Plasma		Very long chain (unspecified)	↑	[25]
Leukodystrophia	Human	Plasma		Unspecified	↑	[26]
Diabetes, aging and dhCer						
Insulin inhibition by palmitate	In vitro	C2C12 muscle cell	Inhibition of Akt/PKB pathway	Unspecified	↑	[27]
Gluoco-lipotoxicity	In vitro	β-Islet cells		C16:0, C18:0, C22:0, C24:1	↑	[28]
	In vitro	Isolated β-islet cells		C16:0	↑	[29]
Reduced mitochondrial respiration	In vitro	C2C12 myotubes		Long chain (unspecified)	↑	[30, 31]
Cer channel formation in mitochondria	In vitro	Isolated mitochondria		C16:0, C2:0	↑	[32]
Increased dhCer	In vitro	Mature adipocytes	Nutrient stress pathway involving AMPK	Unspecified	↑	[33]
Increased insulin sensitivity by overexpressing adiponectin	In vitro	Rat single muscle cells		C20:0	↓	[34]
Inhibition of plasma insulin signalling and amino acid transport	In vitro	Primary human trophoblast cells		Unspecified	↑	[35]
Insulin resistance in high fat and high fructose diet	In vivo	Rhesus monkeys		Unspecified	↑	[36]
	In vivo	Rat single muscle cells		C20:0	↓	[37]
Insulin resistance due to adiposity	In vivo	Lactating cows		Unspecified	↑	[38]
Associated with BMI and increased waist to hip ratio	Human	Plasma		Unspecified	↑	[39, 40]
Associated with higher plasma cholesterol and statin use	Human	Plasma		C20:0	↑	[40]
Correlated with waist circumference	Human	Plasma		C18:0, C20:0, C22:0, C24:1	↑	[41]
Obesity and type 2 diabetes	Human	Plasma		C24:1, C18:0	↑	[42–44]
Increased insulin sensitivity due to diet and exercise and antidiabetes therapy	Human	Plasma		Unspecified, C18:0, C24:1	↓	[45, 46]
Associated with lower cardio-respiratory fitness in older adults (< 55 years)	Human	Plasma		C20:0	↑	[47]
Hypoxia	In vivo	Right ventricles of rats		C16:0	↑	[48]
Cardiovascular disease and dhCer						
Induced apoptosis in the presence of high concentrations of saturated fat	In vivo	Cardiac myocytes		C16:0	↑	[49]

Table 1 (continued)

Effects	Study type	Type of cell, animal or sample	Pathways involved	dhCer acyl chain length	Levels	References
Coronary artery disease	In vivo	Atherosclerotic plaques	Induced IL-6	Unspecified	↑	[50, 51]
Lung disease and dhCer						
Cystic fibrosis	In vitro	Lung epithelial cells		C16:0	↑	[52]
Effect of inhibition of CerS by FTY720	In vitro	Human lung epithelial cells	Defective expression of CFTR gene	Unspecified	↓	[53]
Emphysema, autophagy in hypoxic state, decreased lung cell proliferation	In vivo	SD rat lung, lung epithelial cells	Reduced HIF-1α and VEGF protein expression	Unspecified	↑	[54] [55]
Liver disease and dhCer						
Inflammation	In vitro	HeG2 Cells		Unspecified	↑	[56]
Knock down of Des-1	In vitro	Huh7 hepatocyte cells		Unspecified	↑	[57]
Raised in hepato cell carcinoma than hepatic cirrhosis	Human	plasma		Unspecified	↑	[58]
Raised in non-alcoholic fatty liver disease	Human	plasma		C16:0, C18:0, C24:0, C24:1	↑	[59]

Insulin resistance

Insulin resistance is an important factor in type 2 diabetes and pre-diabetes [75], while chronic exposure to free fatty acids (FFA), such as palmitate, causes insulin resistance. In cellular models (C2C12 myotubes and isolated β-islet cells) of insulin resistance induced by palmitate, increased dhCer (C16:0), Cer (C16:0) and dhSph have been noted [27, 29]. The study in C2C12 myotubes also indicated the inhibition of the Akt/PKB pathway in promoting the insulin resistance [27], which is similar to how Cer has been shown to antagonize insulin signalling [72]. Others have shown that palmitate causes an increase in specific dhCer (C16:0, C18:0, C22:0, C24:1) and Cer chain lengths, resulting in glucolipotoxicity in beta cells [28]. These studies denote the changes in dhCer as associative effects, rather than a causal effect. There are recent studies which imply that dhCer and the de novo sphingolipids could have an additive effect to that of Cers. For example, Reali et al. [71] showed in their model of *ob/ob* mice macrophage that increases in the enzymatic activity of CerS6 led to increased Cer C16:0 and that the impairment of insulin signalling in these model occurred at 16 weeks when the levels of all the sphingolipids were upregulated. This increase in all sphingolipids provides a link to the clinical [76] and animal [36] studies that have shown increases in both dhCer and Cer levels. This is further supported by findings that the enzymes SPT, CerS and Des-1 are not specific to one type of sphingolipid in their sensitivity but quite diffuse [71], implying that they contribute towards balancing the regulation of sphingolipids. Perhaps, this is one of the reasons for the insignificant changes in Cer levels seen in the same cohort of patients with significant increase in dhCer levels [76]. Moreover, the type of abundant saturated fats available in the system could also determine the type of dhCer species produced. For example, when SPT is induced by high saturated fats, it has been shown to switch substrate specificity (palmitate to myristate), producing different dhCer C16:0 species [49]. In terms of therapy, increasing the expression of adiponectin receptors in single muscles of rats fed a high fat diet did increase the insulin sensitivity and also reduced the level of dhCer and Cer [77], which may be occurring through the adiponectin/AMP-activated protein kinase (AMPK) pathway. Activation of the adiponectin–AMPK pathway leads to inhibition of manoyl-CoA resulting in the increase of cartinine palmitoyltransferase 1 (CPT1), the rate-limiting step in fatty acid oxidation [78]. Furthermore, two other studies have also noted increase in the levels of dhCer and Cer in primary human trophoblasts (PHT) [35], and in cows transitioning from gestation to lactation [38], implicating these sphingolipids in gestational diabetes.

These studies show that the changes in dhCer levels in lipid-driven insulin signalling are directly related to it being a precursor to Cers and that Cer is involved in insulin resistance. However, it should be noted that these studies were aimed at Cer; therefore, the question of the effect that dhCers has on insulin signalling still remains unanswered.

Mitochondrial homeostasis

The clinical complications associated with type 2 diabetes such as dyslipidaemia, hyperglycaemia and insulin resistance are linked to mitochondrial defragmentation [79]. Mitochondrial homeostasis is maintained through a balance

of fusion and fission, mitochondrial biogenesis and degradation. Increased longer chain dhCer due to ablation of *Des-1*$^{-/-}$ in mouse embryonic fibroblasts and Des-1 inhibition in C2C12 myotubes reduced mitochondrial respiration and complex IV (cytochrome c oxidase) expression in the presence of lipopolysaccharides (LPS) [31, 80]. Complex IV catalyses the final step in the mitochondrial electron transfer chain and is thought to be a major regulation site for oxidative phosphorylation [30]. A reduction in complex IV would impair ATP synthesis. Introduction of LPS to the C2C12 myotubes caused an increase in Cers and had opposite effect to dhCers. LPS also increased oxidative stress and mitochondrial fission through dynamin-related protein 1 (DRP1) which was inhibited when SPT was inhibited by myriocin. Increase in DRP1 and oxidative stress leads to increased mitochondrial defragmentation and insulin resistance [81]. Another study has shown that dhCer (C2, 95% and C16, 51%) can inhibit Cer channel formation in mitochondria [32], inhibiting apoptosis. The study in mouse embryonic fibroblasts also found the *Des-1*$^{-/-}$ cells to be resistant to apoptosis through the Akt/PkB pathway, but had increased autophagy through AMPK activation as a result of the impaired ATP synthesis. These studies show that dhCer can disrupt the processes of mitochondrial biogenesis and degradation, and contribute towards improving mitochondrial function by increasing autophagy and decreasing apoptosis, inhibiting mitochondrial respiration and possibly inhibiting DRP1 and oxidative stress.

Apidose tissue homeostasis

A number of researchers have shown how the selective manipulation of Des-1 and its substrates may be a pathophysiologically advantageous strategy to improve adipose tissue homeostasis and ameliorate the burden of obesity-associated metabolic complications. For example, Barbarroja et al. [33] showed that an ablation in expression of Des-1 or the pharmacological inhibition of Des-1 in 3T3-L cells led to an increase in dhCer/Cer ratio with concurrent increases in oxidative stress, cell death and inhibition of cell differentiation. Their results also showed an increase in the protein expression of GLUT4, which facilitates the uptake of glucose from the plasma. Moreover, 5- to 16-fold increases in dhCer with activation of p38-MAPK, protein phosphorylated eukaryotic translation initiation factor 2α (PeIF2α) and autophagy markers (Beclin1 and LC3B II) have been observed in mature adipocytes treated with 4-HPR-fenretinide [34]. PeIF2α is involved in the nutrient stress response pathway, which has been shown to contribute to the pathogenesis of diabetes. In this study, 4-HPR-fenretinide was shown to utilize both retinoic acid receptor (RAR)-dependent and -independent pathways to regulate adipogenesis and prevent obesity in mice fed a high fat diet. The RA-dependent pathway results in increased Cer despite the presence of 4-HPR-fenretinide, an example of which is given by Bikman et al. [37]. 4-HPR-fenretinide is a structural derivative of retinoic acid, and research in cancer cells has also shown that this compound and dhCer are associated with the activation of cellular stress responses and induction of autophagy [65, 82]. In fact, a recent study in kidney cells has shown that 4-HRP-fenretinide induced polyubiquitination of Des-1, which exhibited "gain of function" and activated pro-survival pathways, p38 MAPK, JNK and X-Box Protein-1s [83]. In addition, dhCers directly suppressed the transcriptional activity of peroxisome proliferator-activated receptor gamma (PPARγ) similar to that seen in Degs1 (Des-1 regulatory gene) ablation, which also suppressed cyclins (D1, D3 and E) and cyclin-dependent kinase 2 (cdk2), thus impairing adipocyte programming in pre-adipocytes [33]. PPARγ plays a central role in adipogenesis and lipid metabolism [84]. We would like to note that the inhibition or ablation of Des-1 led to feedback inhibition and downregulation of SPLTC1 and CerS6, a systemic counter balancing mechanism which could be triggered by the increased dhCer levels.

These studies showed that dhCer could be involved in the disruption of adipogenesis and cause cell death either as a direct result of Des-1 inhibition or by itself. Since the inhibition of Des-1 certainly leads to dhCer accumulation, it is possible that it disrupted adipogenesis early on through inhibition of PPARγ transcription, which is necessary for the terminal differentiation of the adipocytes, and the increased oxidative stress and cell death through autophagy can be attributed to dhCer. However, whether it functions as a ligand or has lipid–protein interactions or lipid–enzyme interactions is elusive since these studies focussed on Des-1.

Epidemiological findings

Epidemiological studies aimed at decoding the associations between sphingolipids and known risk factors [42, 43, 85] or markers for diabetes [39, 40] show increases in dhCer to be precedent of increases in Cer, with concomitant reductions seen when diet, exercise and anti-diabetics are introduced [45, 46]. While others found it to have no longitudinal or cross-sectional association with pre-diabetes or diabetes, Cer (C18:0, C22:1) did [39]. This can be attributed to the progression of the de novo synthesis pathway towards Cer. However, there are at least two studies which show dhCer levels to be opposite to that of Cers. One study found dhCer to be genetically correlated with waist circumference [41], while Cer was not, even after adjusting for confounders such as age and sex, and accounting for genetic differences by using polygenic models. The other study found dhCer to be elevated in the abdominal adipose tissue of obese and non-obese diabetics when compared to lean non-diabetics

[39, 41, 86], with negative correlation between homeostasis model of insulin resistance score (HOMA-IR) and Cer. It is possible that sampling differences (plasma vs. adipose tissue from abdominal area) could account for the differences; however, the latter study did not adjust for patients taking the anti-diabetic metformin, which could have had an effect on the HOMA-IR scores. Despite these, there is evidence for dhCer to be used as a predictor for developing type 2 diabetes. A study showed dhCer C18:0 to be the single best predictor for progression to diabetes, with those progressing from non-diabetic to diabetic within 10 years having higher dhCer C18:0 at baseline [87]. Furthermore, researchers in the USA have recommended that the lipidomic risk score (LRS) assessment criteria—dhCer (C18:0) included in the criteria—be used in conjunction with metformin supplementation for individuals with high risk of developing type 2 diabetes [88]. The LRS score predicted future type 2 diabetes independently of prediabetes with an accuracy of 76%. Therefore, dhCer lipid profiling in obese patients could be a tool for predicting the onset of pre-diabetes and diabetes in this population.

In summary, apart from the epidemiological evidence showing its value as a predictor for developing type 2 diabetes, the in vitro and in vivo studies show a possible therapeutic potential in targeting the Des-1 enzyme and elevating dhCer, which could increase autophagy, reduce adipogenesis and lipid accumulation, leading to increased insulin sensitivity and glucose uptake as summarized in Fig. 3.

DhCer in aging and disease

As age increases, lipid dysregulation increases also and gives rise to the risk of developing CVDs. A current epidemiological report released by the American Heart Association (AHA) highlighted that 48.6% of adults aged ≥ 40 years in the USA are eligible for statin "lipid-lowering" therapy [89]. Chronological aging has a tremendous effect on cardiorespiratory fitness (CRF) and low levels are representative of risk factors for CVDs, dyslipidaemia and hypertension [90–92]. CRF refers to the ability of the cardiac and respiratory systems to supply oxygen to skeletal muscles during sustained physical activity. Increased C20:0 dhCer was found to be strongly associated with lower CRF in both men and women aged 54–96 years [47], while C24:0 dhCer was not. This connection of dhCer to hypoxia is supported by evidence in mice hypoxia models, which showed elevated levels of dhCer C16:0 in the right ventricles [48] and in the heart [93] from week 4 to week 8, with a concomitant decrease in Cer and expression of Des-1. The latter study identified that the Des-1 promoter harbours overlapping sites for *HAND2* and nuclear factor of activated T cell (NFATC) transcription factors, which have been shown to be important in the development of cardiac systems. Both of these factors were required for upregulation of Des-1, while the re-activation of HAND2 in failing hearts due to co-operation between NFATC and miRNA-125 has been shown to aid cardiac dysfunction [94]. Whether the hypoxia-induced dhCer is a protective mechanism even in reduced CRF through autophagic flux remains to be answered. Furthermore, increased local dhCer levels were shown to be associated with reductions in thymocyte apoptosis and age-associated thymic involution in aged mice, when growth hormones were introduced [95]. This most likely fostered autophagy in thymic epithelial cells, which shapes the T cell repertoire and tolerance. These contrasting effects of hypoxia and autophagy point to tissue-specific associations of dhCer. However, this remains inconclusive due to the lack of evidence with regard to dhCer in aging. Therefore, including dhCer and dihydrosphingolipids in future lipidomic profiling studies in the elderly should be encouraged.

DhCer in cardiovascular disease

Though cholesterol is vital for healthy bodily functions, excess amounts in the blood due to increased dietary intake of saturated fats can lead to buildup of atherosclerotic plaque and coronary artery disease (CAD), increasing the risk for heart attacks. Cers are known to be associated with cholesterol in terms of lipid rafts formation [96], which serve as the basis for signal transduction during inflammatory responses. In human atherosclerotic plaques [50] and rat models of hypercholesterolaemia [97], dhCers were found to be increased. Both dhCer and Cer correlated with the release of the inflammatory cytokine interleukin 6 (IL-6), but only dhCer correlated with macrophage inflammatory protein 1β (MIP-1β) release [50]. Elevated IL-6 levels in atherosclerosis results in effects on endothelial cells (activation), platelets (prothrombotic effect), muscle cells (proliferation) and macrophages (lipid accumulation) that are involved in lipid processing and plaque formation [98], while increased MIP-1β (also known as chemokine CC motif ligand 4—CCL4) in patients was linked to atherosclerosis and plaque instability [99]. What role this increase in dhCer plays in plaque stability is still debatable, since the extracellular addition of dhCer to human aortic smooth muscle cells did not cause apoptosis, whereas Cer did [50]. Apoptosis of cells in the vessel walls increases plaque instability. Apart from these CAD-related studies, dhCer levels have also been found to be elevated in patients with rheumatoid arthritis [100], patients with "HeartWare" left ventricular assist devices [101], hypertensive rats [102] and in doxorubicin-induced cardiac toxicity [103]. These studies point to the possible role of dhCer as a marker for cardiac pathology. The correlation between MIP-1β and dhCer should also be investigated further, since MIP-1β is also implicated in type 2 diabetes. However, there is a lack of mechanistic studies

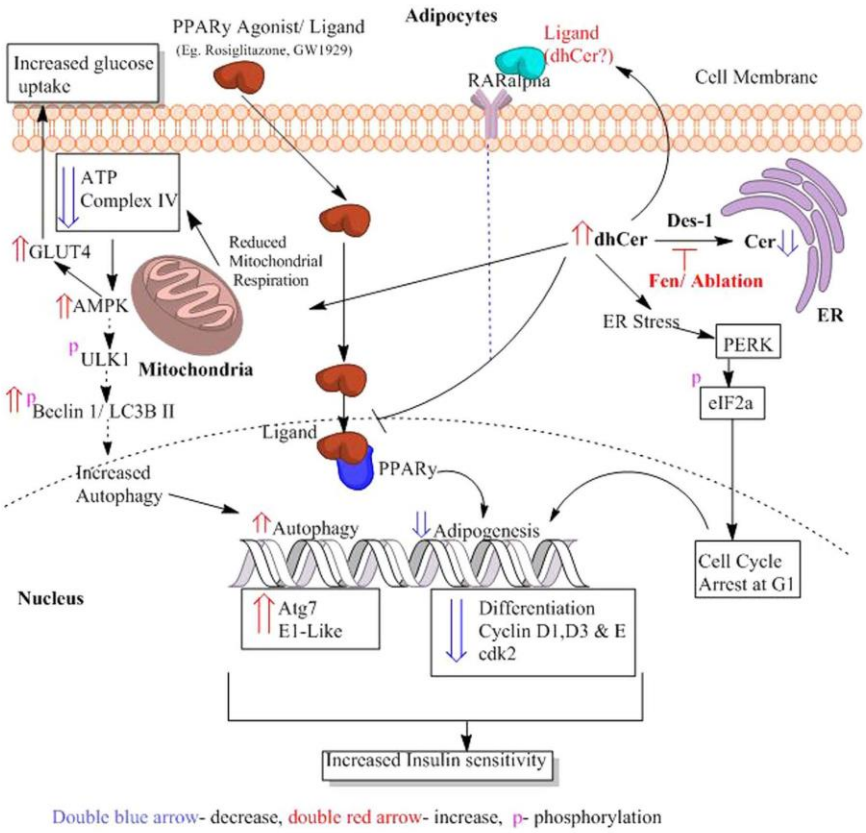

Fig. 3 Possible effects of dhCer on adipocytes. The ablation or inhibition of Des-1 by drugs such as Fen (4-HRP-fenretinide) in adipocytes leads to increased dhCer, (1) reducing adipogenesis and (2) increasing autophagy and resulting in increased insulin sensitivity and glucose uptake. (1) Increased dhCer reduces adipogenesis by (a) causing endoplasmic reticulum (ER) stress or nutrient stress which then phosphorylates eIF2alpha downstream of PERK (Protein Kinase R-like Endoplasmic Reticulum Kinase), resulting in cell cycle arrest at G1, and (b) the increased dhCer also inhibits ligand activation of PPARγ. Both of these lead to reduced differentiation of adipocytes due to reduced expression of cyclins D1, D3 and E and cdk2. (2) DhCer also increases autophagy by reducing mitochondrial respiration and complex IV, which results in reduced ATP synthesis. The impaired ATP synthesis leads to increased AMPK, activating the phosphorylation of ULK1 (unc-51 like Autophagy Activating Kinase 1), Beclin 1 and LC3B II, which are involved in the initiation and formation of autophagomsomes. This leads to increased expression of autophagy genes such as atg7 and E1-like, thus increasing autophagy. An increase in AMPK also increases GLUT4 translocation to the cell membrane, leading to increased glucose uptake. The hypothesis of dhCer acting as a ligand to activate RARα thus inhibiting PPARγ remains to be deciphered (light blue dotted line)

that are directed at determining whether dhCer has an associative or causal effect in CVDs.

DhCer in lung disease

Studies in lung diseases investigating dhCer were outnumbered by studies investigating Cer, S1P and Sph. As can be seen below, the few studies that did mention dhCer compared its role in hypoxia as opposed to Cer. 4-HPR-fenretinide treatment of Sprague–Dawley (SD) rat lungs with emphysema showed that there was increase in the dhCer levels with a decrease in hypoxia-inducible factor1-α (HIF1-α) and vascular endothelial growth factor (VEGF) protein expression [54], which was rescued with concurrent S1P treatment. Additionally, it is now known that dhCer does accumulate in states of hypoxia through the induction of autophagy and

inhibits proliferation of primary rat lung-transformed cells [55]. These researchers proposed that the dhCer desaturation step acts as an oxygen sensor, based on the amplitude and kinetics of increased dhCer at physiological alterations of oxygen concentration. This can be explained by the requirement for oxygen by Des-1 and -2 to convert dhCer to Cer in the reaction involving nicotinamide adenine dinucleotide phosphate (NADPH) and nicotinamide adenine dinucleotide (NADH) [15]. In immortalized lung epithelial cells (IB3, A549 and C38) with defective expression of the cystic fibrosis transmembrane conductance regulator (CFTR) gene, the levels of C16:0 dhCer, Sph, SM and Cer (C22, C24 and C26) were increased [52]. The use of 4-HPR-fenretinide and fumonisin (FB_1) reduced the level of these sphingolipids (individual species measurement not given) without affecting the level of CFTR, showing that CFTR could function in a feedback loop manner, sequestering sphingolipids and or altering the membrane structure. The increase in dhCer in mice with defective CFTR gene expression is comparable to the increase seen in those with emphysema, since both pathologies have an underlying hypoxic condition. However, in states of infection, the response differs, as shown by the increased airway sensitivity caused by reduced levels of de novo sphingolipids including dhCer (due to deletion of SPLTC2) in mice lung infected with rhinovirus [104], showing that sphingolipids may be protective in lung hypersensitivity reactions. These studies show regulating dhCer levels by targeting the enzymes involved in its modulation could be potential therapeutic targets for hypoxia-related disorders in the lung. However, whether the increased dhCer contributes to the disease or occurs as a coping mechanism is yet to be deciphered.

DhCer in liver disease

The excessive accumulation of lipids within hepatocytes is one of the factors listed in the pathogenesis of fatty liver or non-alcoholic fatty liver disease (NAFLD), which can progress to hepatic fibrosis and cancer if not managed well. Raised dhCer levels together with Cer have been observed in both NAFLD and hepatocellular carcinoma patients when compared to hepatitis C infection and cirrhosis patients, respectively [58, 59, 105]. However in diabetic patients with NAFLD, up to 12% of increase in dhCer has been noted, with negative correlations with insulin resistance [106]. However, cell and animal studies show some conflicting results. For example, reductions in the de novo sphingolipid pathway (knockout of SPTLC1) led to the occurrence of fatty liver, insulin resistance and elevated fasting glucose in mice [107], while knockdown of Des-1 in Huh7 hepatocyte cells led to increased dhCer, FFAs and diacylglrcerol [57]. This study also showed that silencing SPLTC1–3 showed positive effects such as increased nutrient uptake and reduction in lipid synthesis, whereas Des-1 silencing led to prominent changes in amino acid, sugar, and nucleotide metabolism and vesicle trafficking between organelles in Huh7 hepatocyte cells. These contrasting effects may be reconciled if SPLTC2 and 3 are considered to be still functional in the former study. This also implies that the ablation of Des-1 in hepatocytes may be detrimental, since increasing levels of FFA and diacylglycerol can cause lipotoxicity which activates a chain of events that eventually leads to hepatocyte death.

In human hepatocarcinoma (HepG2) cells, interleukin 1 (IL-1)-mediated sterile inflammation downregulated orosomucoid like protein 3 (ORMDL3), a key regulator of SPT, leading to increased dhCers, dhSph and Cers [56]. Also, an integrated lipidomics and transcriptomics study in balb/c mice showed that the anti-inflammatory and immunosuppressive drug triptolide caused reductions in dhCer C18:0, C18:1, C20:0, C22:0 and C24:0 in the liver, and C22:0, C24:0, and C24:1 in plasma [108]. These studies suggest that inflammatory processes can also affect alterations in the level of individual species of dhCer in the liver and contribute to liver pathologies.

In the liver, dhCer together with sphingolipids seems to be part of the lipid pool that accumulates in disease states. However, due to the limited amount of studies specifically targeting dhCer in the liver, whether it has any effect remains to be answered.

DhCer in cancer and cancer therapy

As the investigation on Cer increased in cancer cells for combination therapy with various cancer treatments, due to its apoptotic property [109] it became apparent that dhCer could be bioactive. Most studies have regarded dhCer as a precursor to Cer [110–112]. However, there are studies that have demonstrated dhCer's potential role in cancer cell autophagy [14, 66, 113], in cancer induced bone pain [114] and cell cytotoxicity [115]. The changes in the levels of dhCer and Cer in cancer cells also seem to differ according to the site of origin of the cancer. For example, in melanoma cells, dhCers (d18:0/16:0) and Cers were significantly lowered compared to non-malignant melanocytes [116], while in cancerous tissue of human endometrial cells the level of dhCer was increased 3- to 4.6-fold, and Cer and S1P were increased 1.6- to 1.9-fold [117]. The most effective way to understand the effects of dhCer on a biological system is through the inhibition of the gatekeeper enzyme, Des-1, which is now a target for cancer therapy.

DhCer induced autophagy as a result of Des-1 inhibition

The Des-1 inhibitor, 4-HPR-fenretinide, is currently under clinical trial for use in breast cancer therapy [118]. The

anti-cancer effects of 4-HPR-fenretinide are thought to occur through the modulation of endogenous sphingolipids. A study by Rahmaniyan et al. [119] showed that 4-HPR-fenretinide does directly inhibit Des-1 with an IC_{50} of 2.32 μM in SMS-KCNR neuroblastoma cells. Others have shown that inhibiting SK sensitizes cells to 4-HPR-fenretinide's cytotoxic effects due to increased dhCers [120]. These show that there is possible interaction between 4-HPR-fenretinide inhibition of Des-1 and SK activity, which has also been noted by others [113, 121–123]. Apart from these pharmacological agents, oxidative stress can also inhibit Des-1 in cancer cell lines such as HEK293, MCF 7, 549 and SMS-KCNR cells, leading to increased dhCers [124]. The raised exogenous dhCer levels seems to be capable of inducing autophagy; as shown inT98G, U87MG glioblastoma cells [66] and DU145 cells [14] and also reduce the proliferation of castration-resistant prostate cancer cells [125]. In the prostate cancer cells, reduction in proliferation occurred without inducing apoptosis and autophagy, perhaps through effects on the cell cycle. Additional support for dhCers autophagic effects in cancer cells is found in a study on human gastric cancer cell line, HGC-27, where the inhibition of Des-1 by XM462 and resveratrol led to the accumulation of dhCer at 16 h with induction of autophagy, whereas Cer was increased only slightly [113]. In addition, another study on U937 cells showed that dhCer did not induce apoptosis through DNA fragmentation, compared to Cers and tumour necrosis factor-α (TNF-α) [126]. The autophagy effect of dhCer seems to occur only when the de novo sphingolipid biosynthesis pathway is altered. This is because in studies where dhCer levels increased together with Cers, apoptosis occurred rather than autophagy. For instance, the anti-tumour effect of TNF-α in MCF-7 cells occurred through increased activity of CerS, which then drove the de novo sphingolipid synthesis forward, leading to accumulation of dhCers (C16:0, C18:0, C20:0, C22:0, C24:0, C24:1) and Cers [127] and thus regulating focal adhesion kinase (FAK) and apoptosis. Since the role of autophagy in tumours is highly context driven and can lead to either regression or advancement of tumours [128], this could also apply to targeting Des-1 inhibition as an anti-cancer therapy. This is evident in a recent study in leukaemia cells which found that dhCer accumulation and ROS generation were distinct and non-essential events in 4-HPR-fenretinide-induced cell death [129]. This is further confounded considering that 4-HPR-fenretinide can have both retinoic acid (RA)-dependent and -independent effects [34], and that it induces polyubiquitination of the enzyme [83]. Apart from these, Des-1 inhibition is also promising in terms of restraining metastasis. Studies have linked Des-1 to promotion of metastasis in prostate cancer cells [130], and oesophageal carcinoma [131]. It is worth mentioning that this promotional effect was regulated by RA without affecting the proliferative potential of the cell [130], maybe because Des-1 also increases cyclin D1 expression as a result of NF-κB activation [131].

In an effort to beat resistance to Foscan photodynamic therapy (PDT), some have studied its combination with 4-HPR-fenretinide. Their findings showed that the apoptotic effect was greater when combined, compared to either alone in SCC19 cell by increasing dhCer C16:0 and not Cer [132]. This combination also enhanced mitochondrial depolarization. PDT alone has been shown to induce accumulation of dhCer in SCC cells [133, 134] and was thought to effect the resistance by inhibiting the formation of ceramide channels in the mitochondria [133]. The reason for the enhanced effect when combined may be due to enhanced CerS activity and mitochondrial dysfunction [132]. This is supported by two different studies by Separovic et al. [135], which showed that SCC cells with silenced CerS1 or knockout of CerS6 genes treated with PDT had reduced levels of global Cers, dhCers (C18:0, C18:1 and C20:0) and decreased apoptosis. These findings also imply ROS as a mediator between Des-1 and CerS, since PDT induces cell cytotoxicity through ROS generation.

These studies contribute to the evidence that raised dhCer levels could potentially mean increased autophagic flux. Collectively, increasing dhCer levels to increase autophagy and inhibiting metastasis through Des-1 inhibition are promising targets for cancer therapy.

DhCer induced ER stress

Vitamin E, γ-tocotrienol (γ-TE), has been demonstrated to confer its anti-cancer effects through modulation of dhCer. A study by Jiang et al. [136] showed that γ-TE induced autophagy, necrosis and apoptosis in prostate cancer cells by increasing intracellular dhCer and dhSph, suppressing Akt phosphorylation. Suppression of the PI3K/Akt signalling pathway which leads to inhibition of NF-κB is a known target for γ-TEs anti- breast cancer effects [137]. In fact, in RAW264.7 macrophages, the shorter chain dhCer, C8:0, was linked to the anti-NF-κB effects of γ-TE, by enhancing ER stress and attenuating TNF-α-triggered increase in NF-κB [138]. What is interesting to note in this study is that dhCer C8:0 mimicked the effects of γ-TE by increasing the expression of the zinc finger protein A20, which is a negative feedback regulator of NF-κB. This also led to increased phosphorylation of eIF2α, cJun N-terminal kinase (JNK) and NF-κB inhibitor α (IκBα). Phosphorylation of the ER stress marker, eIF2α, has also been noted in adipocytes treated with 4-HPR-fenretinide [34]. In contrast, increased A20 in adipocytes has been shown to enhance adipogenesis by supressing NF-κB even in the presence of TNF-α [139]. These differences may be due to different NF-κB pathways being activated: canonical (involves TNF-α) vs. non canonical, apart from cellular differences. It is also possible that

γ-TE may be inhibiting Des-1 or even the expression of certain CerS. Interference of the expression of CerS2, 5 and 6 has been shown to increase dhCer C16:0 and hexosylceramide which also promoted ER stress [140]. This study also noted that the observation of the expression levels of individual CerS in MCF-7 cells leads to counter regulation of non-targeted CerS species with no significant differences in total sphingolipids.

DhCer in other diseases

In the kidney, Cer triggers the mitogen-activated protein kinase (MAPK/ ERK) cascade in glomerular mesangial cells [141] and the stress-activated protein kinase (SAPK/ JNK) cascade in the endothelial cell; however, dhCer was not able to trigger the SAPK/JNK cascade [142] and whether it triggers the MAPK/ERK is yet to be deciphered. Dermatological studies have indicated dhCer's possible role in heterogeneity of the stratum corneum layer [143]. In addition, others have found altered expressions of the enzymes CerS, cDase and SPT in the skin disease, "hidradenitis suppurativa" [144]. However, lack of measurement of the different sphingolipids was a limitation in this study. In the eye, increased dhCer (C18:1, C16:0) has been indicated as a possible contributor to cataracts in 64–70 year old [145].

Collectively, dhCers' association with hypoxia possibly triggering autophagy is a recurrent finding in the brain, diabetes, aging, lung and cancer. The relevance of this effect depends on the pathophysiology of the disease, therefore indicating its potential applications as a biomarker or therapeutic target. The mechanistic aspects of this link between dhCer and hypoxia remain to be elucidated. Figure 4 gives a summary of the possible effects of increased dhCer as highlighted in this review.

DhS1P in disease

Overview and structure

DhS1P is derived from the phosphorylation of dhSph by SK1 and 2, and it is known to accumulate when CerS is inhibited [146]. It differs from S1P in that its backbone structure is composed of dhSph instead of Sph. The role of its chemical analog, S1P, as a signalling molecule in the regulation of cellular processes such as cell proliferation [147, 148] and neuroprotection [149] are now known and are being targeted for therapy. As in the case of the other dihydropshingolipids, research into the relevance of dhS1P in the cellular mechanisms of disease is fairly new and quite limited.

DhS1P in cerebrovascular disease

DhS1P has been shown to activate S1PRs [150] in neuronal progenitor cells, and the orphaned receptor GPR63 in the thalamus and nuclear-caudatus of the brain [151]. Recent studies have demonstrated reduced dhS1P levels in the

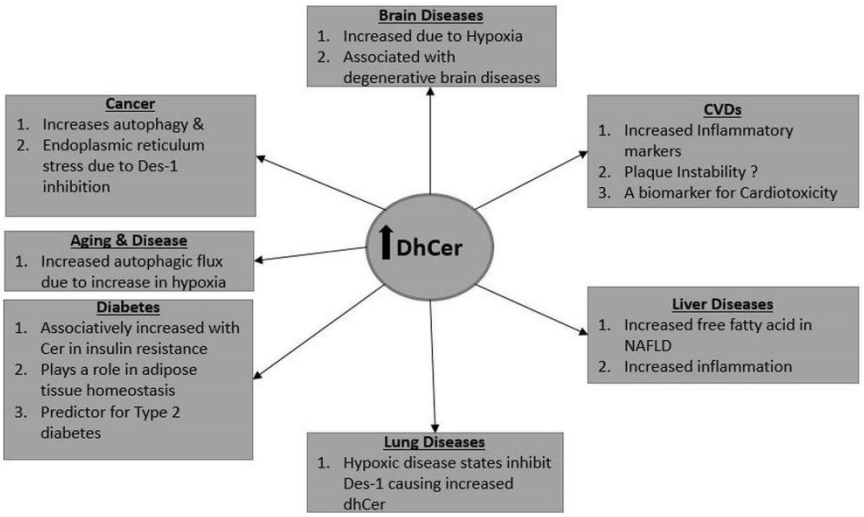

Fig. 4 DhCer in diseases. A summary of the potential effects of increased dhCer as highlighted in this review

brains of rat models of Alzheimer's disease [152] and HD [62]. The reduced availability of dhSph due to a perturbation in the de novo synthesis pathway may led to reduced dhS1P levels, since it occurred in conjunction with reduced levels of dhSph and dhCer and the enzymes SPTLC1 and CerS1. Raised DhS1P may have a protective role in HD, since the accumulation of nuclear dhS1P has been shown to inhibit histone deacetylases (HDAC) [146], which is being targeted for HD therapy [153, 154]. The inhibition of HDAC results in increased gene expression that leads to increased cell proliferation, migration and decreased cell apoptosis. In addition, studies in neuronal cells also found that dhS1P increases Smad phosphorylation compared to S1P [150]. Smads are involved in neuronal precursor proliferation and differentiation. However, in nerve cells (PC12), dhS1P did not protect the cells from apoptosis, whereas S1P did [155]. The different cellular microenvironments could be the reason for this difference. This is exemplified by the inhibition of TGFβ-induced Smad 2/3 phosphorylation by dhS1P in dermal fibroblasts [156], which is opposite to the effects seen in neuronal cells. Other studies have also shown that the pharmacological inhibition of Des-1 in cerebellar neuron cells [157], hypoxia in cerebellar endothelial cells [23], and CerS inhibition by FB1 in neuronal progenitor cells [158] can raise the dhS1P levels. In addition, dhS1P has been identified as a potential marker in FB1–neural tube defect risk assessment [158]. These studies show that the inhibition of Des-1 or CerS reverses the sphingolipid metabolism reaction towards the dihydrosphingolipids and that of dhS1P, possibly by interfering with the activity levels of SPT and S1P lyase. It is obvious that DhS1P does have some form of influence on neuronal cells proliferation and differentiation, and could be a potential therapeutic target for neurodegenerative diseases such as HD.

DhS1P in cardiovascular disease

Similar to S1P, plasma erythrocyte and platelet levels of dhS1P differ in physiological states. In states of physical strain such as exercise, the dhS1P levels differ according to the type of activity, duration and training [159–161]. For example, in untrained man, the erythrocyte levels of dhS1P at 60 min of pedalling were elevated and remained markedly elevated post-exercise [159]. Thus, these differences are also most likely to be present in pathophysiological states.

Both in animal models of cardiomyopathies and patients with cardiomyopathies, altered sphingolipid levels have been noted. Having a major cardiac event such as a myocardial infarct (MI) has been shown to alter the levels of dhS1P in plasma (reduced at 1–6 h), erythrocytes (increased at 6 and 24 h), and platelets (reduced) in rats [162]. Reduced dhS1P and S1P have also been observed in left ventricular tissue of Wistar rats subjected to tachycardia [163]. Similar trends in plasma (reduced early on) and erythrocytes (increased early on) have been observed in patients with acute ST-segment elevation myocardial infarct (STEMI) [164], and MI [165]. It has been suggested that reduced plasma S1P enables erythrocytes to increase S1P production by increasing SK1 protein expression and activity [166]. Hypothetically, this may also be the case for dhS1P, since both were incidentally increased or decreased. Samples from patients in the Copenhagen City Heart Study (CCHS) showed that there was an inverse relationship between reduced dhS1P, S1P and Cer C24:1, and the occurrence of ischaemic heart disease (IHD) in the plasma fraction containing HDL [167]. This may be due to the decreased availability of HDL, implying that dhS1P may be bound to HDL just as S1P [168]. S1P is known to be positively and negatively correlated to CAD depending on the plasma HDL or non-HDL fraction it is bound to [70], while S1P released from activated platelets preferentially binds to the non-HDL fraction—Albumin [169]. Studies that have investigated dhS1P together with S1P have shown that dhS1P is found in non-activated platelets [170, 171], and it was increased in and released by activated platelets [170, 172]. Whether albumin-bound dhS1P and S1P influenced the outcomes observed in the CCHS study was not investigated.

Moreover, a shift in the balance between dhS1P, S1P and Cer within the platelets rather than erythrocytes may be aiding the cross talk in CAD, as observed in patients with multivessel CAD [171]. Together with the findings of reduced dhS1P contributing to reduced endothelial barrier [173], its positive correlation with increased miRNA-122 and 126 in improved endothelial barrier function [174], and dhS1P as a potent inducer of S1PR1-dependent endothelial barrier function and endothelial cell migration [167], it can be inferred that dhS1P may promote plaque stability. Even in human umbilical vein endothelial cells (HUVEC), dhS1P has been shown to inhibit chemotaxis and Rac activation stimulated by platelet-derived growth factor (PDGF) [175], which is known to promote atherosclerosis. Furthermore, dhS1P has been shown to induce matrix metalloproteinase 1 (MMP1) in dermal and scleroderma fibroblasts [176, 177], which is involved in plaque stability [178] and linked to reduced risk of coronary heart disease [179]. The downregulation of MMP1 is also a known marker for cardiac fibrosis. The study on scleroderma fibroblasts showed that dhS1P not only normalized MMP1 expression through the upregulation of phosphatase and tensin homolog (PTEN), but also inhibited factors known to promote fibrosis such as phosphorylated Smad3 (pSmad3), and collagen [177]. In the dermal fibroblasts, dhS1P induced the ERK 1/2-Etsl pathway, leading to increased MMP1 through one of its pertussis toxin-dependent receptors. In the setting of atherosclerosis, this pathway facilitates and promotes vascular smooth muscle cell proliferation, thus promoting fibrous cap stability, while S1P led

to the induction of the inflammatory factor, cyclooxygenase 2 (COX-2) in the same study. However, MMP1 activation or reduction by dhS1P in endothelial cells is not known, It is possible to hypothesize from these studies that dhS1P may also play a role in vascular fibrosis. Considering the common factors involved in fibrosis in the cardiac and circulatory system such as the renin–angiotensin–aldosterone system (RAAS), the effects of dhS1P in the cardiac system needs to be investigated. Furthermore, raised dhS1P levels were demonstrated to have a strong relationship with survival from cardiac arrest in SK1-knockout mice, while S1P did not [180]. The increase in dhS1P can be attributed to the increased activity of the enzyme SK2, which is localized in the nucleus [181]. Taking into account the inhibitory effects of dhS1P on HDAC in the nucleus [146], the potential for it to impact on survival through increased proliferation is highly likely. Another area that warrants further research is studies detailing what impact commonly prescribed cardiac medications may have on dhS1P's role in CVDs, since dhS1P levels were shown to be reduced in plasma of healthy subjects taking a 300 mg loading dose of aspirin [182].

These animal and clinical studies clearly show that dhS1P may be involved in the pathophysiology of CVDs and that platelets and erythrocyte levels of dhS1P influence the plasma levels of dhS1P and S1P for that matter. Applying this to CAD, hypothetically, there could be increased albumin-bound dhS1P. However, how this may influence the outcome of the disease is unknown, especially since the studies also show that dhS1P may promote plaque stability through improved endothelial barrier function. Another area that warrants further research is dhS1P's role in cardiac fibrosis.

DhS1P in lung disease

In terms of lung diseases, sphingolipids and sphingolipid metabolism have been suggested as potential contributors to the pathogenesis of asthma [183], especially in relation to the interactions between ORMDL3 and SPT. A recent study has shown that the inhibition of ORMDL3 increased SPTLC1 and S1P, which then increased smooth muscle contraction rather than inflammation, causing airway hypersensitivity (AHR) [184]. Increases in both S1P and dhS1P have been noted in relation to dust mite allergy, increasing AHR and the asthmatic phenotype [185]. However, it is likely that the prominent increase in S1P led to the effects. The immunomodulatory molecule FTY720, which is known to reduce ORMLD3 leading to reduced AHR and inflammation [186], was able to inhibit CerS4 and increase SK1, leading to decreased S1P and increased dhS1P levels in human lung endothelial cells [53]. This suggests that therapeutic agents such as FTY720 could be more useful than those that inhibit ORMDL3 alone, assuming dhS1P potentially has a different effect than S1P. Furthermore, Berdyshev et al. [187] have shown in their study that the increase in SK1 derails the metabolic pathway of sphingolipids towards that of dhS1P generation, rather than S1P in respiratory syncytial virus (RSV) infection of human bronchial epithelial cells (HBEpC) and HPAEC. They also suggested that SK1 forms a substrate membrane enzymatic complex that impacts on this derailment. Additionally, dhS1P has been shown to compete for cystic fibrosis transmembrane receptor uptake with S1P in C127 cells [188], while in the setting of radiation-induced pulmonary fibrosis both S1P and dhS1P, and the expression of SK1 were increased [189]. Considering the contrasting findings in dermal cells and neuronal cells in terms of dhS1P in activating or inhibiting certain fibrotic factors, and those of S1P in cardiac fibrosis, the role of dhS1P in pulmonary fibrosis needs to be investigated. What is apparent in these latter studies is the regulation of dhS1P and S1P by SK1 increase may be stimulus, cell type, and complex dependent as hinted by Berdyshev et al. [187].

DhS1P in liver and kidney disease

Studies have demonstrated the protective effects of dhS1P against ischaemic–reperfusion injury (IRI) in mice hepatic and renal tissues [190, 191]. DhS1P was able to confer protection against IRI by activating S1PR1, which led to phosphorylation of MAPK/ERK, Akt, and heat shock protein 27 (HSP27) [190]. Exogenous treatment of the mice subjected to hepatic IRI with low doses of dhS1P led to reduced hepatic and renal necrosis and apoptosis, neutrophil infiltration, preserved endothelial cell integrity and reduced pro-inflammatory mRNA [191]. It should be noted that there were no changes observed in S1P levels and S1P conferred protection through S1PR3. DhS1P has also been recommended as a marker for FB1 toxicity [192]. This is supported by studies in cells [193], ducks [194] and human [195] serum or tissue, which showed an increase in dhS1P after exposure to FB1. Apart from it being a marker for toxicity, it may also contribute to cell proliferation. The accumulation of dhS1P due to FB1 toxicity in renal cells led to transient activation of PKCα within 5 min of exposure, compared to dhSph, Sph, S1P and Cer [193]. PKCα mediates the mitogenic effect of PDGF in renal mesangial cells (RMC) [196]. PDGF has been shown to induce increased expression of SK1 mRNA [197], which diverts dhSph towards phosphorylation to give dhS1P instead of Cer, promoting cell survival [198]. In addition, both S1P and dhS1P were able to stimulate similar gene expression waves as PDGF in RMC [199]. In dhS1P-stimulated cells, the angiotensin II receptor type 2 (AT2R) expression was lower than in S1P-stimulated cells, implying that dhS1P has a higher mitogenic effect. In fact, this study also showed that dhS1P had a greater degree of intracellular calcium mobilization than S1P, which explains the transient

activation of PKCα seen in FB1 toxicity [193]. The calcium/PKC pathway is one of the signal transduction pathway for growth factors such as PDGF. Both dhS1P and S1P also induced growth factors such as heparin-binding EGF-like growth factor (HB-EGF) and connective tissue growth factor (CTGF), a fibrotic protein, which was not induced upon stimulation with PDGF [199].

It can be summarized from these studies that dhS1P is able to activate proliferation either on its own through the calcium/ PKC pathway or by interacting with other signalling molecules, including ERK, MAPK and Akt, and HSP27 in the kidney and liver at lower doses while conferring toxic effects at higher doses. How this may impact upon the long-term systemic effects such as fibrosis and in the setting of different pathologies needs to be evaluated.

DhS1P in cancer and cancer therapy

In terms of cancer therapy, dhS1P may help promote survival of neuronal cells [200], inhibit migration, invasion of melanomas through S1PR2 activation [201] and could even be harnessed as a therapeutic tool for tumours [202]. In C6 glioma cells, dhS1P was able to activate the ERK/early growth factor response 1 (EGR-1)/fibroblast growth factor 2 (FGF-2) pathway through S1PR1 [200]. FGF-2 is a neurotrophic factor involved in neuronal differentiation and survival. DhS1P also activated phospholipase D (PLD), a mitogenic factor, through S1PR2 but at lower levels than S1P. The activation of S1PR2 by dhS1P and S1P in B16 melanoma cells led to inhibition of cell migration through regulation of RhoA and Rac which are involved in cell motility [201]. One of the limitations to cancer treatment has been the systemic immune suppression caused by tumour-associated inflammation effected through myeloid lineage cells. Barth and colleagues showed that a recent therapeutic tool targeted at this phenomenon, termed "Photo-ImmunoNano-Therapy", improved the outcome in mice models as a result of dhS1P (S1P to a lesser degree) abrogating myeloid lineage cells and allowing the expansion of anti-tumour lymphocytes [202]. The increase in dhS1P was attributed to increase in SK2, which is known to have epigenetic effects [203], rather than SK1. They also injected tumour-bearing mice with dhS1P and found it to have anti-tumour effect, while S1P promoted tumour growth. Incubation of T cells stimulated with the immune-suppressive drugs anti-CD3 and anti-CD28 with dhS1P induced the release of interleukin 2 (IL-2) and interferon-γ (INF-γ), respectively [204]. Thus, dhS1P inhibits T cell proliferation which could suppress tumour growth and survival. However, this may not be true for all types of cancers, since patients with hepatocellular carcinoma were found to have raised serum dhS1P levels. Despite this, it can be surmised that dhS1P is a potential anti-cancer biomolecule that needs to be further investigated (Fig. 5).

DhSph in disease

Overview and structure

Sphinganine or dihydrosphingosine (dhSph) forms the backbone of dihydrosphingolipids. It has a molecular weight of 301.5 g/mol and is produced mostly in the endoplasmic reticulum. DhSph serves as a precursor to dhS1P synthesis by SK1 and 2 and dhCer by ceramide synthases. In biological systems, early studies in the 1990s seem to have used dhSph as a protein kinase C (PKC) inhibitor with regard to cell proliferation and vasoconstriction studies [205–207]. Here, we look at its role in different diseases.

DhSph in hepatic and renal diseases

Much relevance has been given to the enzymes involved in dhSph metabolism, thus overlooking its role in pathophysiology. Only a few studies have considered dhSph, especially in terms of FB1 toxicity which increases the dhSph and dhSph/Sph ratio. The extent of FB1 toxicity in humans has been reviewed by Voss et al. [208]. A number of studies have found raised dhSph levels due to FB1 exposure in the liver and kidney [209], the brain of calves [210], gastrointestinal tract (GIT) of chickens [211], pregnant mice and fish (with no fetal toxicity) [212, 213], and in urine samples from humans [214]. Apart from FB1 toxicity, dhSph was also increased in the plasma in other instances, such as in hepatotoxicity due to *Guynuria Segetum*, Fabry's disease, endemic nephropathy, hepatitis C infection, type 2 diabetes-induced NAFLD, disease models of glucocorticoid-induced osteoporotic rats and dyslipidaemia, remote ischaemic preconditioning (RIPC) strategy for IRI, and genetic ablation of CerS2 in the liver [106, 215–222]. The key factor in all of these increases is the inhibition of the CerS enzyme which catalyses the acylation of dhSph to dhCer. FB1 competitively inhibits CerS due to it being structurally similar to dhSph and differing only in the free amino group at C_1 [223]. This inhibition not only raises dhSph levels, but also the levels of dhS1P which is known to have autocrine–paracrine functions on the S1PRs, further complicating the mechanistic pathways of FB1 toxicity. Whether or not the increased dhS1P is also able to inhibit CerS2 by directly interacting with the S1P receptor-like motif on CerS2 is unknown [224]. FB1 toxicity is accompanied by an increase in TNF-α expression causing increased cell apoptosis and induction of cytokines such as IL-12 p40 and IFNγ [225, 226]. However, He et al. [227] stated that this is not directly related to the increase in dhSph or Sph as shown by the continuous

expression of TNF-α despite the inhibition of SPT in the presence of FB1 in kidney cells. However, earlier studies by Sharma et al. [228] in TNF-α receptor knockout mice showed that there was some increase in dhSph in the liver and kidney, but these were lower than in the wild types. These studies imply that there may be partial interactions between TNF-α and dhSph or the de novo pathway.

Reduced dhSph levels have been noted in the seminal plasma of infertile male patients with Kidney–Yang syndrome [229], adenine-induced chronic renal failure in rats [230], and in type 2 diabetes-induced diabetic nephropathy [231]. These studies were metabolomics and metabonomics studies aimed at discovering biomarkers for these disease conditions. Their findings showed the sphingolipid metabolism may be perturbed, the mechanisms of which remain unknown. Regardless, it is likely that the beginning of the de novo pathway is perturbed in these disease conditions, causing the reduced levels seen. DhSph has also been mentioned as a possible biomarker for kidney cancer [232]. It is worth considering the causal increase in dhS1P levels in these studies which could influence the outcomes observed. Therefore, to explore the effect of dhSph, research that takes into account this aspect would be valuable.

DhSph in cardiovascular disease

Elevated levels of dhSph have been noted in the hearts of rats exercising to exhaustion in 30 min [233], or pacing for 60 min [234], both of which show that increased cardiac workload not only affects SLs levels, but dhSLs as well.

Cardiomyopathies

In terms of cardiomyopathies, various other researchers have shown altered dhSph levels. For example, raised levels of dhSph were shown in plasma and tissues from rat MI models [162, 235–237], in the right ventricle after 60 min of tachycardia [163] and in cardiac muscle of male Wistar rats with drug-induced hyperthyroidism [238]. DhSph and phytosphingosine were identified as biomarkers in relation to the efficacy of traditional Chinese medicine (TCM) therapies in two of the MI studies [236, 237]. Phytosphingosine is derived from dhSph (as characterized in yeast) and causes apoptosis of cancer cells by caspase 8 activation and Bcl-2- associated X protein (Bax) translocation [239]. However, another study employing similar analytical methods and experimental conditions for MI indicated phytosphingosine as a biomarker and not dhSph [240]. The reason for this may lie in the rate of metabolism of dhSph in the tissue and plasma. The latter study was carried out on heart tissue. Reducing solid tissue de novo synthesis of sphingolipids were also shown to affect the level of dhSph in plasma (decreased) and platelets (increased) [241]. The disruption of the sphingolipid metabolic pathway showing increases in dhSph in cardiomyopathies has also been shown in the plasma of young (STEMI) patients [164, 242]. This study showed that dhSph had high specificity and sensitivity to the prognosis related to major adverse cardiovascular events after patients were discharged [242]. Prior to this study, 25–27% reductions in plasma dhSph were reported in chronic systolic heart failure patients, independent of the underlying cause of heart failure [243], with no changes observed in the plasma level of S1P and dhS1P, perhaps due to metabolic clearance as noted in another study where urine levels of dhSph and phytosphingosine were increased in HF patients [244]. Disease onset and duration could have also influenced these findings. For example, the STEMI study reported elevated levels upon admission, which were reduced at 1, 5, and 30 days after admission, while others have shown no changes in plasma dhSph levels in MI patients at the time of admission and 5 days after [165].

Coronary artery disease

Raised dhSph levels have been indicated in the progression of atherosclerotic dyslipidaemia [245], in spontaneously hypertensive rats [246], and has also been investigated as a biomarker for atherosclerosis in a rabbit model [247]. In patients with multi-vessel CAD, the level of dhSph and Sph in platelets has been shown to be higher than in the controls, whereas their levels in plasma and erythrocytes were stable or similar [171]. In addition, a study in patients with temporary coronary occlusion found that 1 min after PCI in the coronary sinus, dhSph levels were raised to 614%, and 272% in peripheral blood, but dropped below baseline at 12 h [248]. The inhibition of SPT by myriocin in apolipoprotein E (ApoE)-deficient mice led to significant reductions in dhSph and other sphingolipids levels, with a stable plaque formation and reductions in cholesterol and LDL [249], but in ApoE null mice fed with a high fat diet, dhSph levels were raised which positively correlated with total cholesterol and LDL-C [245]. Thus, inhibition of the sphingolipid de novo synthesis pathway may be beneficial to lowering atherogenic plasma lipids and encourage stable plaque formation. However, studies that could inform the mechanisms of this interaction between cholesterol and dhSph or sphingolipids are lacking. Therefore, these findings are speculative at this time.

DhSph in other diseases

The intracellular increase in dhSph is either as a result of overall increase in the de novo sphingolipid synthesis leading to effects similar to that of Cer, or due to inhibitions at the CerS enzymes, the effects of which are still elusive. The extracellular addition of dhSph also leads to Cer-type effects

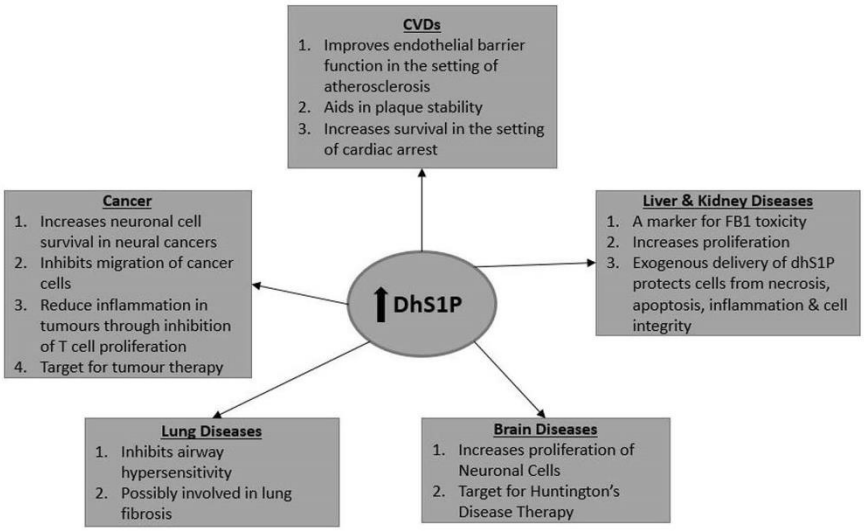

Fig. 5 DhS1P in disease. A summary of the potential effects of increased dhS1P as highlighted in this review

Table 2 List of sporadic studies on different disease models of SPT or CerS interventions with effects on dhSph levels

Disease or disease event studied	Target organ/tissue	Experimental model	Method of de novo pathway perturbation	Changes in dhSph	References
Hypoxic state	Brain	Human cerebral endothelial cells	CerS inhibition	Increase	[23]
Colitis	GIT	Mice	CerS2 knockout mice	Increase	[259]
Gastric smooth muscle dysfunction	GIT	Mice	CerS2 null mice	Increase	[260]
Pancreatitis	Pancreas	Human plasma	De novo synthesis pathway[a]	Increase	[261]
Myopia	Eye	Human aqueous humour	De novo synthesis pathway[a]	Increase	[262]
Rheumatoid arthritis	Joints	Human Plasma	De novo synthesis pathway[a]	Increase	[263]
Pre-eclampsia	Uterus	Human plasma/placenta	De novo synthesis pathway[a]	Increase	[264]
Rhino virus infection	Lungs	Rat	Deletion of SPLTC2	Decrease	[104]
Wolfram syndrome	Brain	Human plasma	De novo synthesis pathway[a]	Decrease (C17:0)	[265]

[a]Metabolomics or metabonomics studies that show the de novo synthesis pathway may be perturbed, indicating dhSph as a biomarker. However, the mechanisms of this perturbation are less understood

such as apoptosis in cancer cells [250]. De novo sphingolipid synthesis can be perturbed by inhibiting or overexpressing the enzyme SPT. The yeast orthologues of ORMDLs have been shown to inhibit SPT by forming a conserved complex with SPT reducing sphingolipids such as dhSph [251, 252]. Lowering the level of the enzymes at both ends of the de novo pathway such as that seen HD rat models [62]: SPLTC1 and CerS1, results in reductions in dhSph, dhCer and dhS1P. However, dhSph could be a promising target for therapy in dermatological diseases such as atopic dermatitis, where Sph and dhSph ratios were found to influence barrier abnormalities observed in human stratum corneum (SC) [253]. For example, dhSph was found to play a role in contributing to the formation of more rigid lattice of lipids in the SC [254]. It has also been suggested as a biomarker in neurodegenerative disease and diabetes. The altering of dhSph levels in diabetic disease states and models by the inhibition of the sphingolipid pathway or anti-diabetics that regulate lipid and cholesterol also supports dhSph being a possible biomarker for diabetes and diabetes therapy [255–258]. Such

applications could allow for early detection of insulin resistance and patient response to therapy, because it is a necessary step in the de novo pathway that leads to Cers. Overall, studies in which dhSph is implicated are sporadic, which makes them difficult to discuss; therefore we have collated them in Table 2.

3-Ketosphinganine in disease

3-KetoSph is the product of the condensation of palmitoyl-CoA and serine catalysed by the enzyme SPT in the ER, which is the rate-limiting enzyme in the de novo sphingolipid metabolism pathway. The inhibition of the enzyme SPT in relation to disease seems to be studied more than the effects of the product 3-ketoSph, due to it being metabolized rapidly. In fact, an increasing number of studies are reporting links of mutations in the gene that encodes SPT, SPLTC1 and 2, to hereditary peripheral neuropathies [266–268]. There are also reports of new novel SPT inhibitors for cancer that have shown to reduce 3-ketoSph in human lung adenocarcinoma cells [269]. Mutations or missense in the enzyme that reduces 3-ketoSph, 3-ketodihydrosphingosine reductase (KDSR), have been linked to recessive progressive symmetric erythrokeratoderma [270], keratinization disorders associated with thrombocytopaenia [271] and bovine spinal muscular atrophy [272]. Long-term exposure of cancer cells (HGC27, T98G and U87MG) to 3 ketoSph has been shown to induce autophagy and overexpression of Des-1 [273].

The evidence for 3 ketoSph in disease is quite scarce owing to its rapid metabolism in the de novo sphingolipid synthesis pathway; however, the enzymes involved in its synthesis and metabolism are targets for further studies.

Conclusion and perspectives

Collectively, the evidence for dihydrosphingolipids in disease is spatial across the board and thus requires a lot more research in terms of their roles in disease, especially the mechanistic pathways through which they could contribute to disease. There are a number of areas that have been examined in this review that should be the focus of further research. These include: (1) the value of dhCers in predicting type 2 diabetes in relation to obesity, (2) the possible role of dhCer in reducing adipogenesis and increasing autophagy in adipocytes, (3) the reoccurring theme of dhCer in association with hypoxia, (4) the role of dhS1P and dhSph in plaque stability, (5) the anti-tumour effects of dhS1P conferred through suppression of T cell proliferation, (6) the binding of dhS1P to albumin and the effects of this in terms of IHD, (7) the possible therapeutic effect of dhS1P in terms of HD, and (8) the stimulus, cell type and complex-dependent regulation of dhS1P by SK1. There are also a number of studies in terms of CVDs showing alterations in sphingolipid levels; however, what is lacking are mechanistic studies to show if these alterations can contribute to the pathophysiology of the disease. The role of dhSph as a biomarker in cardiomyopathies, drug-induced toxicities, as well as liver and kidney toxicity due to FB1 is imperative, especially in determining if the de novo sphingolipid synthesis pathway is perturbed. Future studies applying current lipidomics tools should be encouraged, together with studies that take into consideration both the metabolites and the enzymatic interactions of the de novo pathway. The use of more potent and selective Des-1 inhibitors should be encouraged for investigating the effects of dhCer or Des-1 inhibition in light of the recent polyubiquitination findings for 4-HRP-fenretinide. Finally, the altering role of dihydrosphingolipids in the different organs seems to depend not only upon the initial insults and the disease processes, but also the key players along the de novo sphingolipid pathway.

Author contributions RM and BW conceived and designed review question, conducted preliminary data search, and sorting the papers. FS and YH conducted literature search and screening. DK, CR, BF and DL assisted drafting and edited of the paper and had responsibility for its final content. All authors read and approved the final manuscript.

Funding This research was supported by National Health and Medical Research Council of Australia Program Grants (1092642) (BHW, DL, CR and DJK) and Project Grant (1087355) (BHW). RM and FS are sponsored by a Monash Graduate Scholarship and Monash International Postgraduate Research Scholarship for their doctoral studies.

Compliance with ethical standards

Conflict of interest The authors declare that there is no conflict of interest.

References

1. Young MM, Kester M, Wang H-G (2013) Sphingolipids: regulators of crosstalk between apoptosis and autophagy. J Lipid Res 54(1):5–19. https://doi.org/10.1194/jlr.R031278
2. Cutler RG, Kelly J, Storie K, Pedersen WA, Tammara A, Hatanpaa K, Troncoso JC, Mattson MP (2004) Involvement of oxidative stress-induced abnormalities in ceramide and cholesterol metabolism in brain aging and Alzheimer's disease. Proc Natl Acad Sci USA 101(7):2070–2075. https://doi.org/10.1073/pnas.0305799101
3. Kitatani K, Iwabuchi K, Snider A, Riboni L (2016) Sphingolipids in inflammation: from bench to bedside. Mediators Inflamm 2016:7602526. https://doi.org/10.1155/2016/7602526
4. Ogretmen B (2017) Sphingolipid metabolism in cancer signalling and therapy. Nat Rev Cancer 18:33. https://doi.org/10.1038/nrc.2017.96
5. Halmer R, Walter S, Fassbender K (2014) Sphingolipids: important players in multiple sclerosis. Cell Physiol Biochem 34(1):111–118. https://doi.org/10.1159/000362988

6. Russo SB, Ross JS, Cowart LA (2013) Sphingolipids in obesity, Type 2 diabetes, and metabolic disease. Handb Exp Pharmacol 216:373–401. https://doi.org/10.1007/978-3-7091-1511-4_19
7. Gulbins E, Petrache I (2013) Sphingolipids in disease. In: Gulbins E, Petrache I (eds) Hand book of experimental pharmacology, vol 216. Springer, Vienna. https://doi.org/10.1007/978-3-7091-1511-4
8. Giles C, Takechi R, Mellett NA, Meikle PJ, Dhaliwal S, Mamo JC (2017) Differential regulation of sphingolipid metabolism in plasma, hippocampus, and cerebral cortex of mice administered sphingolipid modulating agents. J Neurochem 141(3):413–422. https://doi.org/10.1111/jnc.13964
9. Rodriguez-Cuenca S, Barbarroja N, Vidal-Puig A (2015) Dihydroceramide desaturase 1, the gatekeeper of ceramide induced lipotoxicity. Biochim Biophys Acta Mol Cell Biol Lipids 1851(1):40–50. https://doi.org/10.1016/j.bbalip.2014.09.021
10. Levkau B (2013) Cardiovascular effects of sphingosine-1-phosphate (S1P). Handb Exp Pharmacol 216:147–170. https://doi.org/10.1007/978-3-7091-1511-4_8
11. Colacios C, Sabourdy F, Andrieu-Abadie N, Ségui B, Levade T (2015) Basics of Sphingolipid Metabolism and Signalling. In: Hannun YA, Luberto C, Mao C, Obeid LM (eds) Bioactive sphingolipids in cancer biology and therapy. Springer, Cham, pp 1–20. https://doi.org/10.1007/978-3-319-20750-6_1
12. Stiban J, Tidhar R, Futerman AH (2010) Ceramide synthases: roles in cell physiology and signaling. Adv Exp Med Biol 688:60–71
13. Petrache I, Berdyshev EV (2016) Ceramide signaling and metabolism in pathophysiological states of the lung. Annu Rev Physiol 78:463–480. https://doi.org/10.1146/annurev-physiol-021115-105221
14. Zheng W, Kollmeyer J, Symolon H, Momin A, Munter E, Wang E, Kelly S, Allegood JC, Liu Y, Peng Q, Ramaraju H, Sullards MC, Cabot M, Merrill AH (2006) Ceramides and other bioactive sphingolipid backbones in health and disease: lipidomic analysis, metabolism and roles in membrane structure, dynamics, signaling and autophagy. Biochim Biophys Acta Biomembr 1758(12):1864–1884. https://doi.org/10.1016/j.bbamem.2006.08.009
15. Casasampere M, Ordonez YF, Pou A, Casas J (2016) Inhibitors of dihydroceramide desaturase 1: therapeutic agents and pharmacological tools to decipher the role of dihydroceramides in cell biology. Chem Phys Lipids 197:33–44. https://doi.org/10.1016/j.chemphyslip.2015.07.025
16. Siddique MM, Bikman BT, Wang L, Ying L, Reinhardt E, Shui G, Wenk MR, Summers SA (2012) Ablation of dihydroceramide desaturase confers resistance to etoposide-induced apoptosis in vitro. PLoS One 7(9):e44042. https://doi.org/10.1371/journal.pone.0044042
17. Siddique MM, Li Y, Chaurasia B, Kaddai VA, Summers SA (2015) Dihydroceramides: from bit players to lead actors. J Biol Chem 290(25):15371–15379. https://doi.org/10.1074/jbc.R115.653204
18. Wegner MS, Schiffmann S, Parnham MJ, Geisslinger G, Grosch S (2016) The enigma of ceramide synthase regulation in mammalian cells. Prog Lipid Res 63:93–119. https://doi.org/10.1016/j.plipres.2016.03.006
19. Cingolani F, Futerman AH, Casas J (2016) Ceramide synthases in biomedical research. Chem Phys Lipids 197:25–32. https://doi.org/10.1016/j.chemphyslip.2015.07.026
20. Samadi A (2007) Ceramide-induced cell death in lens epithelial cells. Mol Vis 13:1618–1626
21. Chien CC, Shen SC, Yang LY, Wu CY, Liau JS, Chen YC (2009) Activation of telomerase and cyclooxygenase-2 in PDGF and FGF inhibition of C2-ceramide-induced apoptosis. J Cell Physiol 218(2):405–415. https://doi.org/10.1002/jcp.21613
22. Wong K, Li X-B, Hunchuk N (1995) *N*-Acetylsphingosine (C-ceramide) inhibited neutrophil superoxide formation and calcium influx. J Biol Chem 270(7):3056–3062. https://doi.org/10.1074/jbc.270.7.3056
23. Testai FD, Kilkus JP, Berdyshev E, Gorshkova I, Natarajan V, Dawson G (2014) Multiple sphingolipid abnormalities following cerebral microendothelial hypoxia. J Neurochem 131(4):530–540. https://doi.org/10.1111/jnc.12836
24. Testai FD, Xu HL, Kilkus J, Suryadevara V, Gorshkova I, Berdyshev E, Pelligrino DA, Dawson G (2015) Changes in the metabolism of sphingolipids after subarachnoid hemorrhage. J Neurosci Res 93(5):796–805. https://doi.org/10.1002/jnr.23542
25. Peterlin BL, Mielke MM, Dickens AM, Chatterjee S, Dash P, Alexander G, Vieira RV, Bandaru VV, Dorskind JM, Tietjen GE, Haughey NH (2015) Interictal, circulating sphingolipids in women with episodic migraine: a case–control study. Neurology 85(14):1214–1223. https://doi.org/10.1212/WNL.0000000000002004
26. Edvardson S, Yi JK, Jalas C, Xu R, Webb BD, Snider J, Fedick A, Kleinman E, Treff NR, Mao C, Elpeleg O (2016) Deficiency of the alkaline ceramidase ACER3 manifests in early childhood by progressive leukodystrophy. J Med Genet 53(6):389
27. Park M, Kaddai V, Ching J, Fridianto KT, Sieli RJ, Sugii S, Summers SA (2016) A role for ceramides, but not sphingomyelins, as antagonists of insulin signaling and mitochondrial metabolism in C2C12 myotubes. J Biol Chem 291(46):23978–23988
28. Veret J, Coant N, Berdyshev EV, Skobeleva A, Therville N, Bailbe D, Gorshkova I, Natarajan V, Portha B, Le Stunff H (2011) Ceramide synthase 4 and de novo production of ceramides with specific *N*-acyl chain lengths are involved in glucolipotoxicity-induced apoptosis of INS-1 beta-cells. Biochem J 438(1):177–189. https://doi.org/10.1042/BJ20101386
29. Roomp K, Kristinsson H, Schvartz D, Ubhayasekera K, Sargsyan E, Manukyan L, Chowdhury A, Manell H, Satagopam V, Groebe K, Schneider R, Bergquist J, Sanchez J-C, Bergsten P (2017) Combined lipidomic and proteomic analysis of isolated human islets exposed to palmitate reveals time-dependent changes in insulin secretion and lipid metabolism. PLoS One 12(4):e0176391. https://doi.org/10.1371/journal.pone.0176391
30. Li Y, Park J-S, Deng J-H, Bai Y (2006) Cytochrome c oxidase Subunit IV is essential for assembly and respiratory function of the enzyme complex. J Bioenerg Biomembr 38(5–6):283–291. https://doi.org/10.1007/s10863-006-9052-z
31. Hansen ME, Simmons KJ, Tippetts TS, Thatcher MO, Saito RR, Hubbard ST, Trumbull AM, Parker BA, Taylor OJ, Bikman BT (2015) Lipopolysaccharide disrupts mitochondrial physiology in skeletal muscle via disparate effects on sphingolipid metabolism. Shock 44(6):585–592. https://doi.org/10.1097/SHK.0000000000000468
32. Stiban J, Fistere D, Colombini M (2006) Dihydroceramide hinders ceramide channel formation: implications on apoptosis. Apoptosis 11(5):773–780. https://doi.org/10.1007/s10495-006-5882-8
33. Barbarroja N, Rodriguez-Cuenca S, Nygren H, Camargo A, Pirraco A, Relat J, Cuadrado I, Pellegrinelli V, Medina-Gomez G, Lopez-Pedrera C, Tinahones FJ, Symons JD, Summers SA, Oresic M, Vidal-Puig A (2015) Increased dihydroceramide/ceramide ratio mediated by defective expression of degs1 impairs adipocyte differentiation and function. Diabetes 64(4):1180–1192. https://doi.org/10.2337/db14-0359
34. McIlroy GD, Tammireddy SR, Maskrey BH, Grant L, Doherty MK, Watson DG, Delibegovic M, Whitfield PD, Mody N (2016) Fenretinide mediated retinoic acid receptor signalling and inhibition of ceramide biosynthesis regulates adipogenesis, lipid accumulation, mitochondrial function and nutrient stress signalling in

adipocytes and adipose tissue. Biochem Pharmacol 100:86–97. https://doi.org/10.1016/j.bcp.2015.11.017
35. Aye ILMH, Gao X, Weintraub ST, Jansson T, Powell TL (2014) Adiponectin inhibits insulin function in primary trophoblasts by PPARα-mediated ceramide synthesis. Mol Endocrinol 28(4):512–524. https://doi.org/10.1210/me.2013-1401
36. Brozinick JT, Hawkins E, Hoang Bui H, Kuo MS, Tan B, Kievit P, Grove K (2013) Plasma sphingolipids are biomarkers of metabolic syndrome in non-human primates maintained on a Western-style diet. Int J Obes 37(8):1064–1070. https://doi.org/10.1038/ijo.2012.191
37. Bikman BT, Guan Y, Shui G, Siddique MM, Holland WL, Kim JY, Fabriàs G, Wenk MR, Summers SA (2012) Fenretinide prevents lipid-induced insulin resistance by blocking ceramide biosynthesis. J Biol Chem 287(21):17426–17437. https://doi.org/10.1074/jbc.M112.359950
38. Rico JE, Saed Samii S, Mathews AT, Lovett J, Haughey NJ, McFadden JW (2017) Temporal changes in sphingolipids and systemic insulin sensitivity during the transition from gestation to lactation. PLoS One 12(5):e0176787. https://doi.org/10.1371/journal.pone.0176787
39. Mielke MM, Bandaru VV, Han D, An Y, Resnick SM, Ferrucci L, Haughey NJ (2015) Demographic and clinical variables affecting mid- to late-life trajectories of plasma ceramide and dihydroceramide species. Aging Cell 14(6):1014–1023. https://doi.org/10.1111/acel.12369
40. Weir JM, Wong G, Barlow CK, Greeve MA, Kowalczyk A, Almasy L, Comuzzie AG, Mahaney MC, Jowett JBM, Shaw J, Curran JE, Blangero J, Meikle PJ (2013) Plasma lipid profiling in a large population-based cohort. J Lipid Res 54(10):2898–2908. https://doi.org/10.1194/jlr.P035808
41. Mamtani M, Meikle PJ, Kulkarni H, Weir JM, Barlow CK, Jowett JB, Bellis C, Dyer TD, Almasy L, Mahaney MC, Duggirala R, Comuzzie AG, Blangero J, Curran JE (2014) Plasma dihydroceramide species associate with waist circumference in mexican american families. Obesity (Silver Spring, MD) 22(3):950–956. https://doi.org/10.1002/oby.20598
42. Meikle PJ, Wong G, Barlow CK, Weir JM, Greeve MA, MacIntosh GL, Almasy L, Comuzzie AG, Mahaney MC, Kowalczyk A, Haviv I, Grantham N, Magliano DJ, Jowett JBM, Zimmet P, Curran JE, Blangero J, Shaw J (2013) Plasma lipid profiling shows similar associations with prediabetes and Type 2 diabetes. PLoS One 8(9):e74341. https://doi.org/10.1371/journal.pone.0074341
43. Lopez X, Goldfine AB, Holland WL, Gordillo R, Scherer PE (2013) Plasma ceramides are elevated in female children and adolescents with type 2 diabetes. J Pediatr Endocrinol Metab 26(9–10):995–998. https://doi.org/10.1515/jpem-2012-0407
44. Racette SB, Evans EM, Weiss EP, Hagberg JM, Holloszy JO (2006) Abdominal adiposity is a stronger predictor of insulin resistance than fitness among 50–95 year olds. Diabetes Care 29(3):673–678
45. Dubé JJ, Amati F, Toledo FGS, Stefanovic-Racic M, Rossi A, Coen P, Goodpaster BH (2011) Effects of weight loss and exercise on insulin resistance, and intramyocellular triacylglycerol, diacylglycerol and ceramide. Diabetologia 54(5):1147–1156. https://doi.org/10.1007/s00125-011-2065-0
46. Warshauer JT, Lopez X, Gordillo R, Hicks J, Holland WL, Anuwe E, Blankfard MB, Scherer PE, Lingvay I (2015) Effect of pioglitazone on plasma ceramides in adults with metabolic syndrome. Diabetes Metab Res Rev 31(7):734–744. https://doi.org/10.1002/dmrr.2662
47. Fabbri E, Yang A, Simonsick EM, Chia CW, Zoli M, Haughey NJ, Mielke MM, Ferrucci L, Coen PM (2016) Circulating ceramides are inversely associated with cardiorespiratory fitness in participants aged 54–96 years from the Baltimore Longitudinal Study of Aging. Aging Cell 15(5):825–831. https://doi.org/10.1111/acel.12491
48. Noureddine L, Azzam R, Nemer G, Bielawski J, Nasser M, Bitar F, Dbaibo GS (2008) Modulation of total ceramide and constituent ceramide species in the acutely and chronically hypoxic mouse heart at different ages. Prostaglandins Other Lipid Mediat 86(1–4):49–55. https://doi.org/10.1016/j.prostaglandins.2008.02.003
49. Russo SB, Tidhar R, Futerman AH, Cowart LA (2013) Myristate-derived d16:0 sphingolipids constitute a cardiac sphingolipid pool with distinct synthetic routes and functional properties. J Biol Chem 288(19):13397–13409. https://doi.org/10.1074/jbc.M112.428185
50. Edsfeldt A, Dunér P, Ståhlman M, Mollet IG, Asciutto G, Grufman H, Nitulescu M, Persson AF, Fisher RM, Melander O, Orho-Melander M, Borén J, Nilsson J, Gonçalves I (2016) Sphingolipids contribute to human atherosclerotic plaque inflammation. Arterioscler Thromb Vasc Biol 36(6):1132
51. Ellims AH, Wong G, Weir JM, Lew P, Meikle PJ, Taylor AJ (2014) Plasma lipidomic analysis predicts non-calcified coronary artery plaque in asymptomatic patients at intermediate risk of coronary artery disease. Eur Heart J Cardiovasc Imaging 15(8):908–916. https://doi.org/10.1093/ehjci/jeu033
52. Hamai H, Keyserman F, Quittell LM, Worgall TS (2009) Defective CFTR increases synthesis and mass of sphingolipids that modulate membrane composition and lipid signaling. J Lipid Res 50(6):1101–1108. https://doi.org/10.1194/jlr.M800427-JLR200
53. Berdyshev EV, Gorshkova I, Skobeleva A, Bittman R, Lu X, Dudek SM, Mirzapoiazova T, Garcia JGN, Natarajan V (2009) FTY720 inhibits ceramide synthases and up-regulates dihydrosphingosine 1-phosphate formation in human lung endothelial cells. J Biol Chem 284(9):5467–5477. https://doi.org/10.1074/jbc.M805186200
54. Yasuo M, Mizuno S, Allegood J, Kraskauskas D, Bogaard HJ, Spiegel S, Voelkel NF (2013) Fenretinide causes emphysema, which is prevented by sphingosine 1-phoshate. PLoS One 8(1):e53927. https://doi.org/10.1371/journal.pone.0053927
55. Devlin CM, Lahm T, Hubbard WC, Van Demark M, Wang KC, Wu X, Bielawska A, Obeid LM, Ivan M, Petrache I (2011) Dihydroceramide-based response to hypoxia. J Biol Chem 286(44):38069–38078. https://doi.org/10.1074/jbc.M111.297994
56. Cai L, Oyeniran C, Biswas DD, Allegood J, Milstien S, Kordula T, Maceyka M, Spiegel S (2016) ORMDL proteins regulate ceramide levels during sterile inflammation. J Lipid Res 57(8):1412–1422. https://doi.org/10.1194/jlr.M065920
57. Ruangsiriluk W, Grosskurth SE, Ziemek D, Kuhn M, des Etages SG, Francone OL (2012) Silencing of enzymes involved in ceramide biosynthesis causes distinct global alterations of lipid homeostasis and gene expression. J Lipid Res 53(8):1459–1471. https://doi.org/10.1194/jlr.M020941
58. Grammatikos G, Schoell N, Ferreirós N, Bon D, Herrmann E, Farnik H, Köberle V, Piiper A, Zeuzem S, Kronenberger B, Waidmann O, Pfeilschifter J (2016) Serum sphingolipidomic analyses reveal an upregulation of C16-ceramide and sphingosine-1-phosphate in hepatocellular carcinoma. Oncotarget 7(14):18095–18105. https://doi.org/10.18632/oncotarget.7741
59. Grammatikos G, Mühle C, Ferreiros N, Schroeter S, Bogdanou D, Schwalm S, Hintereder G, Kornhuber J, Zeuzem S, Sarrazin C, Pfeilschifter J (2014) Serum acid sphingomyelinase is upregulated in chronic hepatitis C infection and non alcoholic fatty liver disease. Biochim Biophys Acta Mol Cell Biol Lipids 1841(7):1012–1020. https://doi.org/10.1016/j.bbalip.2014.04.007
60. Sun N, Keep RF, Hua Y, Xi G (2016) Critical role of the sphingolipid pathway in stroke: a review of current utility and potential

therapeutic targets. Transl Stroke Res 7(5):420–438. https://doi.org/10.1007/s12975-016-0477-3
61. Mielke MM, Haughey NJ, Bandaru VV, Weinberg DD, Darby E, Zaidi N, Pavlik V, Doody RS, Lyketsos CG (2011) Plasma sphingomyelins are associated with cognitive progression in Alzheimer's disease. J Alzheimers Dis 27(2):259–269. https://doi.org/10.3233/JAD-2011-110405
62. Di Pardo A, Basit A, Armirotti A, Amico E, Castaldo S, Pepe G, Marracino F, Buttari F, Digilio AF, Maglione V (2017) De novo synthesis of sphingolipids is defective in experimental models of Huntington's disease. Front Neurosci 11:698. https://doi.org/10.3389/fnins.2017.00698
63. Matesanz F, Fedetz M, Barrionuevo C, Karaky M, Catalá-Rabasa A, Potenciano V, Bello-Morales R, López-Guerrero J-A, Alcina A (2016) A splice variant in the ACSL5 gene relates migraine with fatty acid activation in mitochondria. Eur J Hum Genet 24(11):1572–1577. https://doi.org/10.1038/ejhg.2016.54
64. Ordóñez-Gutiérrez L, Benito-Cuesta I, Abad JL, Casas J, Fábrias G, Wandosell F (2018) Dihydroceramide desaturase 1 inhibitors reduce amyloid-β levels in primary neurons from an Alzheimer's disease transgenic model. Pharm Res 35(3):49. https://doi.org/10.1007/s11095-017-2312-2
65. Gagliostro V, Casas J, Caretti A, Abad JL, Tagliavacca L, Ghidoni R, Fabrias G, Signorelli P (2012) Dihydroceramide delays cell cycle G1/S transition via activation of ER stress and induction of autophagy. Int J Biochem Cell Biol 44(12):2135–2143. https://doi.org/10.1016/j.biocel.2012.08.025
66. Casasampere M, Ordóñez YF, Casas J, Fabrias G (2017) Dihydroceramide desaturase inhibitors induce autophagy via dihydroceramide-dependent and independent mechanisms. Biochim Biophys Acta Gen Subj 1861(2):264–275. https://doi.org/10.1016/j.bbagen.2016.11.033
67. Schofield JD, Liu Y, Rao-Balakrishna P, Malik RA, Soran H (2016) Diabetes dyslipidemia. Diabetes Ther 7(2):203–219. https://doi.org/10.1007/s13300-016-0167-x
68. Mooradian AD (2009) Dyslipidemia in type 2 diabetes mellitus. Nat Clin Pract Endocrinol Metab 5:150. https://doi.org/10.1038/ncpendmet1066
69. Mark L, Dani G (2016) Diabetic dyslipidaemia and the atherosclerosis. Orv Hetil 157(19):746–752. https://doi.org/10.1556/650.2016.30441
70. Sattler KJ, Elbasan S, Keul P, Elter-Schulz M, Bode C, Graler MH, Brocker-Preuss M, Budde T, Erbel R, Heusch G, Levkau B (2010) Sphingosine 1-phosphate levels in plasma and HDL are altered in coronary artery disease. Basic Res Cardiol 105(6):821–832. https://doi.org/10.1007/s00395-010-0112-5
71. Reali F, Morine MJ, Kahramanoğulları O, Raichur S, Schneider H-C, Crowther D, Priami C (2017) Mechanistic interplay between ceramide and insulin resistance. Sci Rep 7:41231. https://doi.org/10.1038/srep41231. https://www.nature.com/articles/srep41231#supplementary-information
72. Stratford S, Hoehn KL, Liu F, Summers SA (2004) Regulation of insulin action by ceramide: dual mechanisms linking ceramide accumulation to the inhibition of AKT/protein kinase B. J Biol Chem 279(35):36608–36615. https://doi.org/10.1074/jbc.M406499200
73. Turpin SM, Nicholls HT, Willmes DM, Mourier A, Brodesser S, Wunderlich CM, Mauer J, Xu E, Hammerschmidt P, Bronneke HS, Trifunovic A, LoSasso G, Wunderlich FT, Kornfeld JW, Bluher M, Kronke M, Bruning JC (2014) Obesity-induced CerS6-dependent C16:0 ceramide production promotes weight gain and glucose intolerance. Cell Metab 20(4):678–686. https://doi.org/10.1016/j.cmet.2014.08.002
74. Raichur S, Wang ST, Chan PW, Li Y, Ching J, Chaurasia B, Dogra S, Ohman MK, Takeda K, Sugii S, Pewzner-Jung Y, Futerman AH, Summers SA (2014) CerS2 haploinsufficiency inhibits beta-oxidation and confers susceptibility to diet-induced steatohepatitis and insulin resistance. Cell Metab 20(4):687–695. https://doi.org/10.1016/j.cmet.2014.09.015
75. Taylor R (2012) Insulin resistance and type 2 diabetes. Diabetes 61(4):778
76. Szpigel A, Hainault I, Carlier A, Venteclef N, Batto A-F, Hajduch E, Bernard C, Ktorza A, Gautier J-F, Ferré P, Bourron O, Foufelle F (2018) Lipid environment induces ER stress, TXNIP expression and inflammation in immune cells of individuals with type 2 diabetes. Diabetologia 61(2):399–412. https://doi.org/10.1007/s00125-017-4462-5
77. Patel SA, Hoehn KL, Lawrence RT, Sawbridge L, Talbot NA, Tomsig JL, Turner N, Cooney GJ, Whitehead JP, Kraegen EW, Cleasby ME (2012) Overexpression of the adiponectin receptor AdipoR1 in rat skeletal muscle amplifies local insulin sensitivity. Endocrinology 153(11):5231–5246. https://doi.org/10.1210/en.2012-1368
78. Qu Q, Zeng F, Liu X, Wang QJ, Deng F (2016) Fatty acid oxidation and carnitine palmitoyltransferase I: emerging therapeutic targets in cancer. Cell Death Dis 7:e2226. https://doi.org/10.1038/cddis.2016.132
79. Williams M, Caino MC (2018) Mitochondrial dynamics in Type 2 diabetes and cancer. Front Endocrinol 9:211. https://doi.org/10.3389/fendo.2018.00211
80. Siddique MM, Li Y, Wang L, Ching J, Mal M, Ilkayeva O, Wu YJ, Bay BH, Summers SA (2013) Ablation of dihydroceramide desaturase 1, a therapeutic target for the treatment of metabolic diseases, simultaneously stimulates anabolic and catabolic signaling. Mol Cell Biol 33(11):2353–2369. https://doi.org/10.1128/MCB.00226-13
81. Jheng H-F, Tsai P-J, Guo S-M, Kuo L-H, Chang C-S, Su I-J, Chang C-R, Tsai Y-S (2012) Mitochondrial fission contributes to mitochondrial dysfunction and insulin resistance in skeletal muscle. Mol Cell Biol 32(2):309
82. Lai WL, Wong NS (2008) The PERK/eIF2 alpha signaling pathway of unfolded protein response is essential for *N*-(4-hydroxyphenyl)retinamide (4HPR)-induced cytotoxicity in cancer cells. Exp Cell Res 314(8):1667–1682. https://doi.org/10.1016/j.yexcr.2008.02.002
83. Alsanafi M, Kelly SL, Jubair K, McNaughton M, Tate RJ, Merrill AH, Pyne S, Pyne NJ (2018) Native and polyubiquitinated forms of dihydroceramide desaturase are differentially linked to human embryonic kidney cell survival. Mol Cell Biol 38:e00222
84. Grygiel-Górniak B (2014) Peroxisome proliferator-activated receptors and their ligands: nutritional and clinical implications—a review. Nutr J 13(1):17. https://doi.org/10.1186/1475-2891-13-17
85. Bergman BC, Brozinick JT, Strauss A, Bacon S, Kerege A, Bui HH, Sanders P, Siddall P, Wei T, Thomas MK, Kuo MS, Perreault L (2016) Muscle sphingolipids during rest and exercise: a C18:0 signature for insulin resistance in humans. Diabetologia 59(4):785–798. https://doi.org/10.1007/s00125-015-3850-y
86. Blachnio-Zabielska AU, Pulka M, Baranowski M, Nikolajuk A, Zabielski P, Gorska M, Gorski J (2012) Ceramide metabolism is affected by obesity and diabetes in human adipose tissue. J Cell Physiol 227(2):550–557. https://doi.org/10.1002/jcp.22745
87. Curran JE, Weir, Jacquelyn M., Bellis, Claire., Carless, Melanie A., Jowett, Jeremy B., Mahaney, Michael C., Dyer, Thomas D., Goring, Harald H., Comuzzie, Anthony G., Almasy, Laura., Meikle, Peter J., Blangero, John. (2011) Genetic analysis of lipidomic profiles influencing diabetes risk in Mexican Americans. Paper presented at the American Diabetes Association, 71st Scientific Sessions
88. Mamtani M, Kulkarni H, Wong G, Weir JM, Barlow CK, Dyer TD, Almasy L, Mahaney MC, Comuzzie AG, Glahn DC, Maglianо DJ, Zimmet P, Shaw J, Williams-Blangero S, Duggirala R,

Blangero J, Meikle PJ, Curran JE (2016) Lipidomic risk score independently and cost-effectively predicts risk of future type 2 diabetes: results from diverse cohorts. Lipids Health Dis 15(1):67. https://doi.org/10.1186/s12944-016-0234-3

89. Benjamin EJ, Virani SS, Callaway CW, Chang AR, Cheng S, Chiuve SE, Cushman M, Delling FN, Deo R, de Ferranti SD, Ferguson JF, Fornage M, Gillespie C, Isasi CR, Jiménez MC, Jordan LC, Judd SE, Lackland D, Lichtman JH, Lisabeth L, Liu S, Longenecker CT, Lutsey PL, Matchar DB, Matsushita K, Mussolino ME, Nasir K, O'Flaherty M, Palaniappan LP, Pandey DK, Reeves MJ, Ritchey MD, Rodriguez CJ, Roth GA, Rosamond WD, Sampson UKA, Satou GM, Shah SH, Spartano NL, Tirschwell DL, Tsao CW, Voeks JH, Willey JZ, Wilkins JT, Wu JHY, Alger HM, Wong SS, Muntner P (2018) Heart disease and stroke statistics—2018 update: a report from the American Heart Association. Circulation 137(12):e67–e492
90. Fagard RH (1999) Physical activity in the prevention and treatment of hypertension in the obese. Med Sci Sports Exerc 31(11 Suppl):S624–S630
91. Paterson DH, Govindasamy D, Vidmar M, Cunningham DA, Koval JJ (2004) Longitudinal study of determinants of dependence in an elderly population. J Am Geriatr Soc 52(10):1632–1638. https://doi.org/10.1111/j.1532-5415.2004.52454.x
92. Laaksonen DE, Lakka HM, Salonen JT, Niskanen LK, Rauramaa R, Lakka TA (2002) Low levels of leisure-time physical activity and cardiorespiratory fitness predict development of the metabolic syndrome. Diabetes Care 25(9):1612–1618
93. Azzam R, Hariri F, El-Hachem N, Kamar A, Dbaibo G, Nemer G, Bitar F (2013) Regulation of de novo ceramide synthesis: the role of dihydroceramide desaturase and transcriptional factors NFATC and Hand2 in the hypoxic mouse heart. DNA Cell Biol 32(6):310–319. https://doi.org/10.1089/dna.2013.1993
94. Dirkx E, Gladka MM, Philippen LE, Armand A-S, Kinet V, Leptidis S, el Azzouzi H, Salic K, Bourajjaj M, da Silva GJJ, Olieslagers S, van der Nagel R, de Weger R, Bitsch N, Kisters N, Seyen S, Morikawa Y, Chanoine C, Heymans S, Volders PGA, Thum T, Dimmeler S, Cserjesi P, Eschenhagen T, da Costa Martins PA, De Windt LJ (2013) Nfat and miR-25 cooperate to reactivate the transcription factor Hand2 in heart failure. Nat Cell Biol 15:1282. https://doi.org/10.1038/ncb2866. https://www.nature.com/articles/ncb2866#supplementary-information
95. de Mello-Coelho V, Cutler RG, Bunbury A, Tammara A, Mattson MP, Taub DD (2017) Age-associated alterations in the levels of cytotoxic lipid molecular species and oxidative stress in the murine thymus are reduced by growth hormone treatment. Mech Ageing Dev 167:46–55. https://doi.org/10.1016/j.mad.2017.08.015
96. Brown DA, London E (2000) Structure and function of sphingolipid- and cholesterol-rich membrane rafts. J Biol Chem 275(23):17221–17224. https://doi.org/10.1074/jbc.R000005200
97. González-Peña D, Checa A, de Ancos B, Wheelock CE, Sánchez-Moreno C (2017) New insights into the effects of onion consumption on lipid mediators using a diet-induced model of hypercholesterolemia. Redox Biol 11:205–212. https://doi.org/10.1016/j.redox.2016.12.002
98. Reiss AB, Siegart NM, De Leon J (2017) Interleukin-6 in atherosclerosis: atherogenic or atheroprotective? Clin Lipidol 12(1):14–23. https://doi.org/10.1080/17584299.2017.1319787
99. Chang T-T, Chen J-W (2016) Emerging role of chemokine CC motif ligand 4 related mechanisms in diabetes mellitus and cardiovascular disease: friends or foes? Cardiovasc Diabetol 15(1):117. https://doi.org/10.1186/s12933-016-0439-9
100. Fang L, Mundra PA, Fan F, Galvin A, Weir JM, Wong G, Chin-Dusting J, Cicuttini F, Meikle P, Dart AM (2016) Plasma lipidomic profiling in patients with rheumatoid arthritis. Metabolomics 12(8):136. https://doi.org/10.1007/s11306-016-1086-6
101. Fine B, Marx A, Topkara V, Gomez EA, Vunjak-Novakovic G, Colombo P (2017) (223)—An integrated analysis of metabolomics after left ventricular assist device implantation. J Heart Lung Transplant 36(4, Supplement)):S93. https://doi.org/10.1016/j.healun.2017.01.235
102. Liu A, Chu Y-J, Wang X, Yu R, Jiang H, Li Y, Zhou H, Gong L-L, Yang W-Q, Ju J (2018) Serum metabolomics study based on LC-MS and antihypertensive effect of uncaria on spontaneously hypertensive rats. Evid Based Complement Altern Med 2018:11. https://doi.org/10.1155/2018/9281946
103. Ji R, Chang JY, Liao X, Zhang X, Kennel P, Castillero E, Brunjes D, Akashi H, Homma S, Goldberg I, Schulze PC (2015) Abstract 17320: inhibition of ceramide synthesis preserves cardiac function and increases survival in doxorubicin-induced cardiomyopathy. Circulation 132(Suppl 3):A17320
104. Sharma A, Sung B, Veerappan A, Silver RB, Kim B, Worgall TS, Worgall S (2017) Decreased Sphingolipid Synthesis Enhances Rhinovirus-Triggered Airway Hyperreactivity. In: A36. Host defense against viral infection. American Thoracic Society International Conference Abstracts, American Thoracic Society, pp A1381–A1381. https://doi.org/10.1164/ajrccm-conference.2017.195.1_meetingabstracts.a1381
105. Mucke VT, Gerharz J, Jakobi K, Thomas D, Ferreiros Bouzas N, Mucke MM, Trotschler S, Weiler N, Welker MW, Zeuzem S, Pfeilschifter J, Grammatikos G (2018) Low serum levels of (dihydro-)ceramides reflect liver graft dysfunction in a real-world cohort of patients post liver transplantation. Int J Mol Sci. https://doi.org/10.3390/ijms19040991
106. Apostolopoulou M, Gordillo R, Koliaki C, Gancheva S, Jelenik T, De Filippo E, Herder C, Markgraf D, Jankowiak F, Esposito I, Schlensak M, Scherer PE, Roden M (2018) Specific hepatic sphingolipids relate to insulin resistance, oxidative stress, and inflammation in nonalcoholic steatohepatitis. Diabetes Care. https://doi.org/10.2337/dc17-1318
107. Alexaki A, Clarke BA, Gavrilova O, Ma Y, Zhu H, Ma X, Xu L, Tuymetova G, Larman BC, Allende ML, Dunn TM, Proia RL (2017) De novo sphingolipid biosynthesis is required for adipocyte survival and metabolic homeostasis. J Biol Chem 292(9):3929–3939. https://doi.org/10.1074/jbc.M116.756460
108. Qu L, Qu F, Jia Z, Wang C, Wu C, Zhang J (2015) Integrated targeted sphingolipidomics and transcriptomics reveal abnormal sphingolipid metabolism as a novel mechanism of the hepatotoxicity and nephrotoxicity of triptolide. J Ethnopharmacol 170:28–38. https://doi.org/10.1016/j.jep.2015.05.010
109. Li F, Zhang N (2015) Ceramide: therapeutic potential in combination therapy for cancer treatment. Curr Drug Metab 17(1):37–51
110. Park MA, Mitchell C, Zhang G, Yacoub A, Allegood J, Häussinger D, Reinehr R, Larner A, Spiegel S, Fisher PB, Voelkel-Johnson C, Ogretmen B, Grant S, Dent P (2010) Vorinostat and sorafenib increase CD95 activation in gastrointestinal tumor cells through a Ca^{2+}-de novo ceramide-PP2A-ROS dependent signaling pathway. Can Res 70(15):6313–6324. https://doi.org/10.1158/0008-5472.CAN-10-0999
111. Gencer EB, Ural AU, Avcu F, Baran Y (2011) A novel mechanism of dasatinib-induced apoptosis in chronic myeloid leukemia; ceramide synthase and ceramide clearance genes. Ann Hematol 90(11):1265–1275. https://doi.org/10.1007/s00277-011-1212-5
112. Maeng HJ, Song J-H, Kim G-T, Song Y-J, Lee K, Kim J-Y, Park T-S (2017) Celecoxib-mediated activation of endoplasmic reticulum stress induces de novo ceramide biosynthesis and apoptosis in hepatoma HepG2 cells. BMB Rep 50(3):144–149. https://doi.org/10.5483/bmbrep.2017.50.3.197
113. Signorelli P, Munoz-Olaya JM, Gagliostro V, Casas J, Ghidoni R, Fabriàs G (2009) Dihydroceramide intracellular increase

in response to resveratrol treatment mediates autophagy in gastric cancer cells. Cancer Lett 282(2):238–243. https://doi.org/10.1016/j.canlet.2009.03.020
114. Grenald SA, Doyle TM, Zhang H, Slosky LM, Chen Z, Largent-Milnes TM, Spiegel S, Vanderah TW, Salvemini D (2017) Targeting the S1P/S1PR1 axis mitigates cancer-induced bone pain and neuroinflammation. Pain 158(9):1733–1742. https://doi.org/10.1097/j.pain.0000000000000965
115. Holliday MW Jr, Cox SB, Kang MH, Maurer BJ (2013) C22:0- and C24:0-dihydroceramides confer mixed cytotoxicity in T-Cell acute lymphoblastic leukemia cell lines. PLoS One 8(9):e74768. https://doi.org/10.1371/journal.pone.0074768
116. Realini N, Palese F, Pizzirani D, Pontis S, Basit A, Bach A, Ganesan A, Piomelli D (2016) Acid ceramidase in melanoma: expression, localization, and effects of pharmacological inhibition. J Biol Chem 291(5):2422–2434. https://doi.org/10.1074/jbc.M115.666909
117. Knapp P, Baranowski M, Knapp M, Zabielski P, Błachnio-Zabielska AU, Górski J (2010) Altered sphingolipid metabolism in human endometrial cancer. Prostaglandins Other Lipid Mediat 92(1):62–66. https://doi.org/10.1016/j.prostaglandins.2010.03.002
118. Cazzaniga M, Varricchio C, Montefrancesco C, Feroce I, Guerrieri-Gonzaga A (2012) Fenretinide (4-HPR): a preventive chance for women at genetic and familial risk? J Biomed Biotechnol 2012:172897. https://doi.org/10.1155/2012/172897
119. Rahmaniyan M, Curley RW, Obeid LM, Hannun YA, Kraveka JM (2011) Identification of dihydroceramide desaturase as a direct in vitro target for fenretinide. J Biol Chem 286(28):24754–24764. https://doi.org/10.1074/jbc.M111.250779
120. Illuzzi G, Bernacchioni C, Aureli M, Prioni S, Frera G, Donati C, Valsecchi M, Chigorno V, Bruni P, Sonnino S, Prinetti A (2010) Sphingosine kinase mediates resistance to the synthetic retinoid *N*-(4-hydroxyphenyl)retinamide in human ovarian cancer cells. J Biol Chem 285(24):18594–18602. https://doi.org/10.1074/jbc.M109.072801
121. Noack J, Choi J, Richter K, Kopp-Schneider A, Regnier-Vigouroux A (2014) A sphingosine kinase inhibitor combined with temozolomide induces glioblastoma cell death through accumulation of dihydrosphingosine and dihydroceramide, endoplasmic reticulum stress and autophagy. Cell Death Dis 5:e1425. https://doi.org/10.1038/cddis.2014.384
122. Valsecchi M, Aureli M, Mauri L, Illuzzi G, Chigorno V, Prinetti A, Sonnino S (2010) Sphingolipidomics of A2780 human ovarian carcinoma cells treated with synthetic retinoids. J Lipid Res 51(7):1832–1840. https://doi.org/10.1194/jlr.M004010
123. Wang H, Maurer BJ, Liu YY, Wang E, Allegood JC, Kelly S, Symolon H, Liu Y, Merrill AH Jr, Gouaze-Andersson V, Yu JY, Giuliano AE, Cabot MC (2008) *N*-(4-Hydroxyphenyl)retinamide increases dihydroceramide and synergizes with dimethylsphingosine to enhance cancer cell killing. Mol Cancer Ther 7(9):2967–2976. https://doi.org/10.1158/1535-7163.MCT-08-0549
124. Idkowiak-Baldys J, Apraiz A, Li L, Rahmaniyan M, Clarke CJ, Kraveka JM, Asumendi A, Hannun YA (2010) Dihydroceramide desaturase activity is modulated by oxidative stress. Biochem J 427(2):265–274. https://doi.org/10.1042/BJ20091589
125. Venant H, Rahmaniyan M, Jones EE, Lu P, Lilly MB, Garrett-Mayer E, Drake RR, Kraveka JM, Smith CD, Voelkel-Johnson C (2015) The sphingosine kinase 2 inhibitor ABC294640 reduces the growth of prostate cancer cells and results in accumulation of dihydroceramides in vitro and in vivo. Mol Cancer Ther 14(12):2744–2752. https://doi.org/10.1158/1535-7163.MCT-15-0279
126. Obeid LM, Linardic CM, Karolak LA, Hannun YA (1993) Programmed cell death induced by ceramide. Science 259(5102):1769
127. Hernandez-Corbacho MJ, Canals D, Adada MM, Liu M, Senkal CE, Yi JK, Mao C, Luberto C, Hannun YA, Obeid LM (2015) Tumor necrosis factor-alpha (TNFalpha)-induced ceramide generation via ceramide synthases regulates loss of focal adhesion kinase (FAK) and programmed cell death. J Biol Chem 290(42):25356–25373. https://doi.org/10.1074/jbc.M115.658658
128. Singh SS, Vats S, Chia AY, Tan TZ, Deng S, Ong MS, Arfuso F, Yap CT, Goh BC, Sethi G, Huang RY, Shen HM, Manjithaya R, Kumar AP (2018) Dual role of autophagy in hallmarks of cancer. Oncogene 37(9):1142–1158. https://doi.org/10.1038/s41388-017-0046-6
129. Apraiz A, Idkowiak-Baldys J, Nieto-Rementería N, Boyano MD, Hannun YA, Asumendi A (2012) Dihydroceramide accumulation and reactive oxygen species are distinct and nonessential events in 4-HPR-mediated leukemia cell death. Biochem Cell Biol 90(2):209–223. https://doi.org/10.1139/o2012-001
130. McNair C, Urbanucci A, Comstock CES, Augello MA, Goodwin JF, Launchbury R, Zhao SG, Schiewer MJ, Ertel A, Karnes J, Davicioni E, Wang L, Wang Q, Mills IG, Feng FY, Li W, Carroll JS, Knudsen KE (2017) Cell cycle-coupled expansion of AR activity promotes cancer progression. Oncogene 36(12):1655–1668. https://doi.org/10.1038/onc.2016.334
131. Zhou W, Ye X-L, Sun Z-J, Ji X-D, Chen H-X, Xie D (2009) Overexpression of degenerative spermatocyte homolog 1 up-regulates the expression of cyclin D1 and enhances metastatic efficiency in esophageal carcinoma Eca109 cells. Mol Carcinog 48(10):886–894. https://doi.org/10.1002/mc.20533
132. Boppana NB, DeLor JS, Van Buren E, Bielawska A, Bielawski J, Pierce JS, Korbelik M, Separovic D (2016) Enhanced apoptotic cancer cell killing after Foscan photodynamic therapy combined with fenretinide via de novo sphingolipid biosynthesis pathway. J Photochem Photobiol B Biol 159(Supplement C):191–195. https://doi.org/10.1016/j.jphotobiol.2016.02.040
133. Breen P, Joseph N, Thompson K, Kraveka JM, Gudz TI, Li LI, Rahmaniyan M, Bielawski J, Pierce JS, Van Buren E, Bhatti G, Separovic D (2013) Dihydroceramide desaturase knockdown impacts sphingolipids and apoptosis after photodamage in human head and neck squamous carcinoma cells. Anticancer Res 33(1):77–84
134. Separovic D, Bielawski J, Pierce JS, Merchant S, Tarca AL, Ogretmen B, Korbelik M (2009) Increased tumour dihydroceramide production after Photofrin-PDT alone and improved tumour response after the combination with the ceramide analogue LCL29. Evidence from mouse squamous cell carcinomas. Br J Cancer 100(4):626–632. https://doi.org/10.1038/sj.bjc.6604896
135. Separovic D, Breen P, Joseph N, Bielawski J, Pierce JS, Van Buren E, Gudz TI (2012) siRNA-mediated down-regulation of ceramide synthase 1 leads to apoptotic resistance in human head and neck squamous carcinoma cells after photodynamic therapy. Anticancer Res 32(7):2479–2485
136. Jiang Q, Rao X, Kim CY, Freiser H, Zhang Q, Jiang Z, Li G (2012) Gamma-tocotrienol induces apoptosis and autophagy in prostate cancer cells by increasing intracellular dihydrosphingosine and dihydroceramide. Int J Cancer 130(3):685–693. https://doi.org/10.1002/ijc.26054
137. Sylvester PW, Ayoub NM (2013) Tocotrienols target PI3K/Akt signaling in anti-breast cancer therapy. Anticancer Agents Med Chem 13(7):1039–1047
138. Wang Y, Park NY, Jang Y, Ma A, Jiang Q (2015) Vitamin E gamma-tocotrienol inhibits cytokine-stimulated NF-kappaB activation by induction of anti-inflammatory A20 via stress adaptive response due to modulation of sphingolipids. J Immunol 195(1):126–133. https://doi.org/10.4049/jimmunol.1403149
139. Dorronsoro A, Lang V, Jakobsson E, Ferrin I, Salcedo JM, Fernández-Rueda J, Fechter K, Rodriguez MS, Trigueros C (2013) Identification of the NF-κB inhibitor A20 as a key

regulator for human adipogenesis. Cell Death Dis 4:e972. https://doi.org/10.1038/cddis.2013.494
140. Mullen TD, Spassieva S, Jenkins RW, Kitatani K, Bielawski J, Hannun YA, Obeid LM (2011) Selective knockdown of ceramide synthases reveals complex interregulation of sphingolipid metabolism. J Lipid Res 52(1):68–77. https://doi.org/10.1194/jlr.M009142
141. Huwiler A, Brunner J, Hummel R, Vervoordeldonk M, Stabel S, van den Bosch H, Pfeilschifter J (1996) Ceramide-binding and activation defines protein kinase c-Raf as a ceramide-activated protein kinase. Proc Natl Acad Sci USA 93(14):6959–6963
142. Huwiler A, Xin C, Brust AK, Briner VA, Pfeilschifter J (2004) Differential binding of ceramide to MEKK1 in glomerular endothelial and mesangial cells. Biochim Biophys Acta 1636(2–3):159–168. https://doi.org/10.1016/j.bbalip.2003.08.010
143. Skolova B, Jandovska K, Pullmannova P, Tesar O, Roh J, Hrabalek A, Vavrova K (2014) The role of the trans double bond in skin barrier sphingolipids: permeability and infrared spectroscopic study of model ceramide and dihydroceramide membranes. Langmuir 30(19):5527–5535. https://doi.org/10.1021/la500622f
144. Dany M, Elston D (2017) Gene expression of sphingolipid metabolism pathways is altered in hidradenitis suppurativa. J Am Acad Dermatol 77(2):268.e266–273.e266. https://doi.org/10.1016/j.jaad.2017.03.016
145. Deeley JM, Hankin JA, Friedrich MG, Murphy RC, Truscott RJW, Mitchell TW, Blanksby SJ (2010) Sphingolipid distribution changes with age in the human lens. J Lipid Res 51(9):2753–2760. https://doi.org/10.1194/jlr.M007716
146. Gardner NM, Riley RT, Showker JL, Voss KA, Sachs AJ, Maddox JR, Gelineau-van Waes JB (2016) Elevated nuclear sphingoid base-1-phosphates and decreased histone deacetylase activity after fumonisin B1 treatment in mouse embryonic fibroblasts. Toxicol Appl Pharmacol 298:56–65. https://doi.org/10.1016/j.taap.2016.02.018
147. Zhang H, Desai NN, Olivera A, Seki T, Brooker G, Spiegel S (1991) Sphingosine-1-phosphate, a novel lipid, involved in cellular proliferation. J Cell Biol 114(1):155–167
148. Olivera A, Spiegel S (1993) Sphingosine-1-phosphate as second messenger in cell proliferation induced by PDGF and FCS mitogens. Nature 365(6446):557–560. https://doi.org/10.1038/365557a0
149. Couttas TA, Kain N, Tran C, Chatterton Z, Kwok JB, Don AS (2018) Age-dependent changes to sphingolipid balance in the human hippocampus are gender-specific and may sensitize to neurodegeneration. J Alzheimers Dis 63(2):503–514. https://doi.org/10.3233/JAD-171054
150. Callihan P, Zitomer NC, Stoeling MV, Kennedy PC, Lynch KR, Riley RT, Hooks SB (2012) Distinct generation, pharmacology, and distribution of sphingosine 1-phosphate and dihydrosphingosine 1-phosphate in human neural progenitor cells. Neuropharmacology 62(2):988–996. https://doi.org/10.1016/j.neuropharm.2011.10.005
151. Niedernberg A, Tunaru S, Blaukat A, Ardati A, Kostenis E (2003) Sphingosine 1-phosphate and dioleoylphosphatidic acid are low affinity agonists for the orphan receptor GPR63. Cell Signal 15(4):435–446
152. Lin W, Zhang J, Liu Y, Wu R, Yang H, Hu X, Ling X (2017) Studies on diagnostic biomarkers and therapeutic mechanism of Alzheimer's disease through metabolomics and hippocampal proteomics. Eur J Pharm Sci 105:119–126. https://doi.org/10.1016/j.ejps.2017.05.003
153. Gray SG (2011) Targeting Huntington's disease through histone deacetylases. Clin Epigenet 2(2):257–277. https://doi.org/10.1007/s13148-011-0025-7
154. Sharma S, Taliyan R (2015) Transcriptional dysregulation in Huntington's disease: the role of histone deacetylases. Pharmacol Res 100:157–169. https://doi.org/10.1016/j.phrs.2015.08.002
155. Edsall LC, Pirianov GG, Spiegel S (1997) Involvement of sphingosine 1-phosphate in nerve growth factor-mediated neuronal survival and differentiation. J Neurosci 17(18):6952–6960
156. Bu S, Kapanadze B, Hsu T, Trojanowska M (2008) Opposite effects of dihydrosphingosine 1-phosphate and sphingosine 1-phosphate on transforming growth factor-beta/Smad signaling are mediated through the PTEN/PPM1A-dependent pathway. J Biol Chem 283(28):19593–19602. https://doi.org/10.1074/jbc.M802417200
157. Triola G, Fabrias G, Dragusin M, Niederhausen L, Broere R, Llebaria A, van Echten-Deckert G (2004) Specificity of the dihydroceramide desaturase inhibitor *N*-[(1R,2S)-2-hydroxy-1-hydroxymethyl-2-(2-tridecyl-1-cyclopropenyl)ethyl]octanamide (GT11) in primary cultured cerebellar neurons. Mol Pharmacol 66(6):1671–1678. https://doi.org/10.1124/mol.104.003681
158. Gelineau-van Waes J, Rainey MA, Maddox JR, Voss KA, Sachs AJ, Gardner NM, Wilberding JD, Riley RT (2012) Increased sphingoid base-1-phosphates and failure of neural tube closure after exposure to fumonisin or FTY720. Birth Defects Res A Clin Mol Teratol 94(10):790–803. https://doi.org/10.1002/bdra.23074
159. Baranowski M, Charmas M, Dlugolecka B, Gorski J (2011) Exercise increases plasma levels of sphingoid base-1 phosphates in humans. Acta Physiol (Oxf) 203(3):373–380. https://doi.org/10.1111/j.1748-1716.2011.02322.x
160. Baranowski M, Gorski J, Klapcinska B, Waskiewicz Z, Sadowska-Krepa E (2014) Ultramarathon run markedly reduces plasma sphingosine-1-phosphate concentration. Int J Sport Nutr Exerc Metab 24(2):148–156. https://doi.org/10.1123/ijsnem.2013-0093
161. Baranowski M, Błachnio-Zabielska AU, Charmas M, Helge JW, Dela F, Książek M, Długołęcka B, Klusiewicz A, Chabowski A, Górski J (2015) Exercise increases sphingoid base-1-phosphate levels in human blood and skeletal muscle in a time- and intensity-dependent manner. Eur J Appl Physiol 115(5):993–1003. https://doi.org/10.1007/s00421-014-3080-x
162. Knapp M, Zendzian-Piotrowska M, Blachnio-Zabielska A, Zabielski P, Kurek K, Gorski J (2012) Myocardial infarction differentially alters sphingolipid levels in plasma, erythrocytes and platelets of the rat. Basic Res Cardiol 107(6):294. https://doi.org/10.1007/s00395-012-0294-0
163. Górski J, Baranowski M, Wójcik B, Chabowski A (2015) Effect of atrial pacing on the level of bioactive sphingolipids in the heart ventricles of the rat. Atherosclerosis 241(1):e122–e123. https://doi.org/10.1016/j.atherosclerosis.2015.04.425
164. Knapp M, Lisowska A, Zabielski P, Musiał W, Baranowski M (2013) Sustained decrease in plasma sphingosine-1-phosphate concentration and its accumulation in blood cells in acute myocardial infarction. Prostaglandins Other Lipid Mediat 106:53–61. https://doi.org/10.1016/j.prostaglandins.2013.10.001
165. Knapp M, Baranowski M, Czarnowski D, Lisowska A, Zabielski P, Gorski J, Musial W (2009) Plasma sphingosine-1-phosphate concentration is reduced in patients with myocardial infarction. Med Sci Monit 15(9):CR490–CR493
166. Książek M, Chacińska M, Chabowski A, Baranowski M (2015) Sources, metabolism, and regulation of circulating sphingosine-1-phosphate. J Lipid Res 56(7):1271–1281. https://doi.org/10.1194/jlr.R059543
167. Argraves KM, Sethi AA, Gazzolo PJ, Wilkerson BA, Remaley AT, Tybjaerg-Hansen A, Nordestgaard BG, Yeatts SD, Nicholas KS, Barth JL, Argraves WS (2011) S1P, dihydro-S1P and C24:1-ceramide levels in the HDL-containing fraction of serum inversely correlate with occurrence of

ischemic heart disease. Lipids Health Dis 10:70. https://doi.org/10.1186/1476-511X-10-70
168. Levkau B (2015) HDL-S1P: cardiovascular functions, disease-associated alterations, and therapeutic applications. Front Pharmacol 6:243. https://doi.org/10.3389/fphar.2015.00243
169. Aoki S, Yatomi Y, Ohta M, Osada M, Kazama F, Satoh K, Nakahara K, Ozaki Y (2005) Sphingosine 1-phosphate-related metabolism in the blood vessel. J Biochem 138(1):47–55. https://doi.org/10.1093/jb/mvi100
170. Dahm F, Nocito A, Bielawska A, Lang KS, Georgiev P, Asmis LM, Bielawski J, Madon J, Hannun YA, Clavien PA (2006) Distribution and dynamic changes of sphingolipids in blood in response to platelet activation. J Thromb Haemost 4(12):2704–2709. https://doi.org/10.1111/j.1538-7836.2006.02241.x
171. Knapp M, Lisowska A (2016) Blood bioactive sphingolipids and activity of acid sphingomyelinase in patients with multivessel coronary artery disease. J Clin Exp Cardiol 7:12. https://doi.org/10.4172/2155-9880.1000482
172. Ono Y, Kurano M, Ohkawa R, Yokota H, Igarashi K, Aoki J, Tozuka M, Yatomi Y (2013) Sphingosine 1-phosphate release from platelets during clot formation: close correlation between platelet count and serum sphingosine 1-phosphate concentration. Lipids Health Dis 12:20. https://doi.org/10.1186/1476-511X-12-20
173. Dobierzewska A, Soman S, Illanes SE, Morris AJ (2017) Plasma cross-gestational sphingolipidomic analyses reveal potential first trimester biomarkers of preeclampsia. PLoS One 12(4):e0175118. https://doi.org/10.1371/journal.pone.0175118
174. Sugiura T, Dohi Y, Yamashita S, Ohte N, Ito S, Sanagawa A, Iwaki S, Ohkawa R, Yatomi Y, Fujii S (2013) Circulating microRNA-126 as a potential biomarker for recovery from smoking-related vascular endothelial damage. Eur Heart J 34(suppl_1):P2417. https://doi.org/10.1093/eurheartj/eht308.p2417
175. Ryu Y, Takuwa N, Sugimoto N, Sakurada S, Usui S, Okamoto H, Matsui O, Takuwa Y (2002) Sphingosine-1-phosphate, a platelet-derived lysophospholipid mediator, negatively regulates cellular rac activity and cell migration in vascular smooth muscle cells. Circ Res 90(3):325
176. Bu S, Yamanaka M, Pei H, Bielawska A, Bielawski J, Hannun YA, Obeid L, Trojanowska M (2006) Dihydrosphingosine 1-phosphate stimulates MMP1 gene expression via activation of ERK1/2-Ets1 pathway in human fibroblasts. FASEB J 20(1):184–186. https://doi.org/10.1096/fj.05-4646fje
177. Bu S, Asano Y, Bujor A, Highland K, Hant F, Trojanowska M (2010) Dihydrosphingosine-1 phosphate has a potent anti-fibrotic effect in Scleroderma fibroblasts via normalization of PTEN levels. Arthritis Rheum 62(7):2117–2126. https://doi.org/10.1002/art.27463
178. Ruddy JM, Ikonomidis JS, Jones JA (2016) Multidimensional contribution of matrix metalloproteinases to atherosclerotic plaque vulnerability: multiple mechanisms of inhibition to promote stability. J Vasc Res 53(1–2):1–16. https://doi.org/10.1159/000446703
179. Ye S, Gale CR, Martyn CN (2003) Variation in the matrix metalloproteinase-1 gene and risk of coronary heart disease. Eur Heart J 24(18):1668–1671
180. Gorshkova IA, Wang H, Orbelyan GA, Goya J, Natarajan V, Beiser DG, Vanden Hoek TL, Berdyshev EV (2013) Inhibition of sphingosine-1-phosphate lyase rescues sphingosine kinase-1-knockout phenotype following murine cardiac arrest. Life Sci 93(9):359–366. https://doi.org/10.1016/j.lfs.2013.07.017
181. Igarashi N, Okada T, Hayashi S, Fujita T, Jahangeer S, S-i Nakamura (2003) Sphingosine kinase 2 is a nuclear protein and inhibits DNA synthesis. J Biol Chem 278(47):46832–46839
182. Knapp M, Lisowska A, Knapp P, Baranowski M (2013) Dose-dependent effect of aspirin on the level of sphingolipids in human blood. Adv Med Sci 58(2):274–281. https://doi.org/10.2478/ams-2013-0021
183. Ono JG, Worgall TS, Worgall S (2015) Airway reactivity and sphingolipids—implications for childhood asthma. Mol Cell Pediatr 2:13. https://doi.org/10.1186/s40348-015-0025-3
184. Miller M, Tam AB, Mueller JL, Rosenthal P, Beppu A, Gordillo R, McGeough MD, Vuong C, Doherty TA, Hoffman HM, Niwa M, Broide DH (2017) Cutting edge: targeting epithelial ORMDL3 increases, rather than reduces, airway responsiveness and is associated with increased sphingosine-1-phosphate. J Immunol
185. Kowal K, Zebrowska E, Chabowski A (2018) Plasma concentration of selected sphingolipids correlates with lung function parameters in house dust mite allergic patients. J Allergy Clin Immunol 141(2, Supplement):AB113. https://doi.org/10.1016/j.jaci.2017.12.360
186. Oyeniran C, Sturgill JL, Hait NC, Huang WC, Avni D, Maceyka M, Newton J, Allegood JC, Montpetit A, Conrad DH, Milstien S, Spiegel S (2015) Aberrant ORM (yeast)-like protein isoform 3 (ORMDL3) expression dysregulates ceramide homeostasis in cells and ceramide exacerbates allergic asthma in mice. J Allergy Clin Immunol 136(4):1035 e1036–1046 e1036. https://doi.org/10.1016/j.jaci.2015.02.031
187. Berdyshev EV, Gorshkova IA, Usatyuk P, Zhao Y, Saatian B, Hubbard W, Natarajan V (2006) De novo biosynthesis of dihydrosphingosine-1-phosphate by sphingosine kinase 1 in mammalian cells. Cell Signal 18(10):1779–1792. https://doi.org/10.1016/j.cellsig.2006.01.018
188. Boujaoude LC, Bradshaw-Wilder C, Mao C, Cohn J, Ogretmen B, Hannun YA, Obeid LM (2001) Cystic fibrosis transmembrane regulator regulates uptake of sphingoid base phosphates and lysophosphatidic acid: modulation of cellular activity of sphingosine 1-phosphate. J Biol Chem 276(38):35258–35264. https://doi.org/10.1074/jbc.M105442200
189. Gorshkova I, Zhou T, Mathew B, Jacobson JR, Takekoshi D, Bhattacharya P, Smith B, Aydogan B, Weichselbaum RR, Natarajan V, Garcia JG, Berdyshev EV (2012) Inhibition of serine palmitoyltransferase delays the onset of radiation-induced pulmonary fibrosis through the negative regulation of sphingosine kinase-1 expression. J Lipid Res 53(8):1553–1568. https://doi.org/10.1194/jlr.M026039
190. Park SW, Kim M, Chen SW, Brown KM, D'Agati VD, Lee HT (2010) Sphinganine-1-phosphate protects kidney and liver after hepatic ischemia and reperfusion in mice through S1P1 receptor activation. Lab Invest 90(8):1209–1224. https://doi.org/10.1038/labinvest.2010.102
191. Park SW, Kim M, Chen SW, D'Agati VD, Lee HT (2010) Sphinganine-1-phosphate attenuates both hepatic and renal injury induced by hepatic ischemia and reperfusion in mice. Shock 33(1):31–42. https://doi.org/10.1097/SHK.0b013e3181c02c1f
192. Kim DH, Yoo HS, Lee YM, Kie JH, Jang S, Oh S (2006) Elevation of sphinganine 1-phosphate as a predictive biomarker for fumonisin exposure and toxicity in mice. J Toxicol Environ Health A 69(23):2071–2082. https://doi.org/10.1080/15287390600746215
193. Gopee NV, Sharma RP (2003) Sphingoid bases and their phosphates: transient activation and delayed repression of protein kinase C isoforms and their possible involvement in fumonisin B1 cytotoxicity. Toxicology 187(2):239–250. https://doi.org/10.1016/S0300-483X(03)00048-9
194. Tardieu D, Tran ST, Auvergne A, Babile R, Benard G, Bailly JD, Guerre P (2006) Effects of fumonisins on liver and kidney sphinganine and the sphinganine to sphingosine ratio during chronic

exposure in ducks. Chem Biol Interact 160(1):51–60. https://doi.org/10.1016/j.cbi.2005.11.004
195. Riley RT, Torres O, Matute J, Gregory SG, Ashley-Koch AE, Showker JL, Mitchell T, Voss KA, Maddox JR, Gelineau-van Waes JB (2015) Evidence for fumonisin inhibition of ceramide synthase in humans consuming maize-based foods and living in high exposure communities in Guatemala. Mol Nutr Food Res 59(11):2209–2224. https://doi.org/10.1002/mnfr.201500499
196. Choudhury GG, Biswas P, Grandaliano G, Abboud HE (1993) Involvement of PKC-alpha in PDGF-mediated mitogenic signaling in human mesangial cells. Am J Physiol 265(5 Pt 2):F634–F642. https://doi.org/10.1152/ajprenal.1993.265.5.F634
197. Katsuma S, Hada Y, Ueda T, Shiojima S, Hirasawa A, Tanoue A, Takagaki K, Ohgi T, Yano J, Tsujimoto G (2002) Signalling mechanisms in sphingosine 1-phosphate-promoted mesangial cell proliferation. Genes Cells 7(12):1217–1230
198. Veret J, Coant N, Gorshkova IA, Giussani P, Fradet M, Riccitelli E, Skobeleva A, Goya J, Kassis N, Natarajan V, Portha B, Berdyshev EV, Le Stunff H (2013) Role of palmitate-induced sphingoid base-1-phosphate biosynthesis in INS-1 beta-cell survival. Biochim Biophys Acta 1831(2):251–262. https://doi.org/10.1016/j.bbalip.2012.10.003
199. Katsuma S, Hada Y, Shiojima S, Hirasawa A, Tanoue A, Takagaki K, Ohgi T, Yano J, Tsujimoto G (2003) Transcriptional profiling of gene expression patterns during sphingosine 1-phosphate-induced mesangial cell proliferation. Biochem Biophys Res Commun 300(2):577–584. https://doi.org/10.1016/S0006-291X(02)02850-4
200. Sato K, Ui M, Okajima F (2000) Differential roles of Edg-1 and Edg-5, sphingosine 1-phosphate receptors, in the signaling pathways in C6 glioma cells. Brain Res Mol Brain Res 85(1–2):151–160
201. Arikawa K, Takuwa N, Yamaguchi H, Sugimoto N, Kitayama J, Nagawa H, Takehara K, Takuwa Y (2003) Ligand-dependent inhibition of B16 melanoma cell migration and invasion via endogenous S1P2 G protein-coupled receptor. Requirement of inhibition of cellular RAC activity. J Biol Chem 278(35):32841–32851. https://doi.org/10.1074/jbc.m305024200
202. Barth BM, Shanmugavelandy SS, Kaiser JM, McGovern C, Altinoglu EI, Haakenson JK, Hengst JA, Gilius EL, Knupp SA, Fox TE, Smith JP, Ritty TM, Adair JH, Kester M (2013) PhotoImmunoNanoTherapy reveals an anticancer role for sphingosine kinase 2 and dihydrosphingosine-1-phosphate. ACS Nano 7(3):2132–2144. https://doi.org/10.1021/nn304862b
203. Hait NC, Allegood J, Maceyka M, Strub GM, Harikumar KB, Singh SK, Luo C, Marmorstein R, Kordula T, Milstien S, Spiegel S (2009) Regulation of histone acetylation in the nucleus by sphingosine-1-phosphate. Science 325(5945):1254–1257. https://doi.org/10.1126/science.1176709
204. Jin Y, Knudsen E, Wang L, Bryceson Y, Damaj B, Gessani S, Maghazachi AA (2003) Sphingosine 1-phosphate is a novel inhibitor of T-cell proliferation. Blood 101(12):4909–4915. https://doi.org/10.1182/blood-2002-09-2962
205. Xu Y, Stenmark KR, Das M, Walchak SJ, Ruff LJ, Dempsey EC (1997) Pulmonary artery smooth muscle cells from chronically hypoxic neonatal calves retain fetal-like and acquire new growth properties. Am J Physiol 273(1 Pt 1):L234–L245. https://doi.org/10.1152/ajplung.1997.273.1.L234
206. Das M, Stenmark KR, Dempsey EC (1995) Enhanced growth of fetal and neonatal pulmonary artery adventitial fibroblasts is dependent on protein kinase C. Am J Physiol 269(5 Pt 1):L660–L667. https://doi.org/10.1152/ajplung.1995.269.5.L660
207. Mann J, Farrukh IS, Michael JR (1991) Mechanisms by which endothelin 1 induces pulmonary vasoconstriction in the rabbit. J Appl Physiol (1985) 71(2):410–416. https://doi.org/10.1152/jappl.1991.71.2.410
208. Voss KA, Riley RT (2013) Fumonisin toxicity and mechanism of action: overview and current perspectives. Food Saf 1(1):2013006. https://doi.org/10.14252/foodsafetyfscj.2013006
209. Riley RT, Voss KA (2006) Differential sensitivity of rat kidney and liver to fumonisin toxicity: organ-specific differences in toxin accumulation and sphingoid base metabolism. Toxicol Sci 92(1):335–345. https://doi.org/10.1093/toxsci/kfj198
210. Mathur S, Constable PD, Eppley RM, Waggoner AL, Tumbleson ME, Haschek WM (2001) Fumonisin B(1) is hepatotoxic and nephrotoxic in milk-fed calves. Toxicol Sci 60(2):385–396
211. Grenier B, Schwartz-Zimmermann HE, Caha S, Moll WD, Schatzmayr G, Applegate TJ (2015) Dose-dependent effects on sphingoid bases and cytokines in chickens fed diets prepared with fusarium verticillioides culture material containing fumonisins. Toxins (Basel) 7(4):1253–1272. https://doi.org/10.3390/toxins7041253
212. Collins TF, Sprando RL, Black TN, Shackelford ME, Laborde JB, Hansen DK, Eppley RM, Trucksess MW, Howard PC, Bryant MA, Ruggles DI, Olejnik N, Rorie JI (1998) Effects of fumonisin B1 in pregnant rats. Part 2. Food Chem Toxicol 36(8):673–685. https://doi.org/10.1016/s0278-6915(98)00036-2
213. LaBorde JB, Terry KK, Howard PC, Chen JJ, Collins TFX, Shackelford ME, Hansen DK (1997) Lack of embryotoxicity of fumonisin B1in New Zealand White Rabbits. Fundam Appl Toxicol 40(1):120–128. https://doi.org/10.1006/faat.1997.2380
214. Domijan AM, Peraica M, Markov K, Fuchs R (2009) Urine ochratoxin a and sphinganine/sphingosine ratio in residents of the endemic nephropathy area in Croatia. Arh Hig Rada Toksikol 60(4):387–393. https://doi.org/10.2478/10004-1254-60-2009-1938
215. Grammatikos G, Dietz J, Ferreiros N, Koch A, Dultz G, Bon D, Karakasiliotis I, Lutz T, Knecht G, Gute P, Herrmann E, Zeuzem S, Mavromara P, Sarrazin C, Pfeilschifter J (2016) Persistence of HCV in acutely-infected patients depletes C24-ceramide and upregulates sphingosine and sphinganine serum levels. Int J Mol Sci 17(6):922. https://doi.org/10.3390/ijms17060922
216. Qiu S, Zhang H, Fei Q, Zhu F, Wang J, Jia X, Chen B (2018) Urine and plasma metabolomics study on potential hepatoxic biomarkers identification in rats induced by Gynura segetum. J Ethnopharmacol 216:37–46. https://doi.org/10.1016/j.jep.2018.01.017
217. Touboul D, Roy S, Germain DP, Baillet A, Brion F, Prognon P, Chaminade P, Laprevote O (2005) Fast fingerprinting by MALDI-TOF mass spectrometry of urinary sediment glycosphingolipids in Fabry disease. Anal Bioanal Chem 382(5):1209–1216. https://doi.org/10.1007/s00216-005-3239-8
218. Ribar S, Mesarić M, Bauman M (2001) High-performance liquid chromatographic determination of sphinganine and sphingosine in serum and urine of subjects from an endemic nephropathy area in Croatia. J Chromatogr B Biomed Sci Appl 754(2):511–519. https://doi.org/10.1016/S0378-4347(01)00041-X
219. Cho K, S-i Min, Ahn S, Min S-K, Ahn C, Yu K-S, Jang I-J, Cho J-Y, Ha J (2017) Integrative analysis of renal ischemia/reperfusion injury and remote ischemic preconditioning in mice. J Proteome Res 16(8):2877–2886. https://doi.org/10.1021/acs.jproteome.7b00167
220. Dekker MJ, Baker C, Naples M, Samsoondar J, Zhang R, Qiu W, Sacco J, Adeli K (2013) Inhibition of sphingolipid synthesis improves dyslipidemia in the diet-induced hamster model of insulin resistance: evidence for the role of sphingosine and sphinganine in hepatic VLDL-apoB100 overproduction. Atherosclerosis 228(1):98–109. https://doi.org/10.1016/j.atherosclerosis.2013.01.041
221. Huang Y, Liu X, Zhao L, Li F, Xiong Z (2014) Kidney tissue targeted metabolic profiling of glucocorticoid-induced osteoporosis and the proposed therapeutic effects of Rhizoma

Drynariae studied using UHPLC/MS/MS. Biomed Chromatogr 28(6):878–884. https://doi.org/10.1002/bmc.3194
222. Pewzner-Jung Y, Park H, Laviad EL, Silva LC, Lahiri S, Stiban J, Erez-Roman R, Brügger B, Sachsenheimer T, Wieland F, Prieto M, Merrill AH, Futerman AH (2010) A critical role for ceramide synthase 2 in liver homeostasis: I. Alterations in lipid metabolic pathways. J Biol Chem 285(14):10902–10910. https://doi.org/10.1074/jbc.m109.077594
223. Merrill AH Jr, Sullards MC, Wang E, Voss KA, Riley RT (2001) Sphingolipid metabolism: roles in signal transduction and disruption by fumonisins. Environ Health Perspect 109(Suppl 2):283–289. https://doi.org/10.1289/ehp.01109s2283
224. Laviad EL, Albee L, Pankova-Kholmyansky I, Epstein S, Park H, Merrill AH Jr, Futerman AH (2008) Characterization of ceramide synthase 2: tissue distribution, substrate specificity, and inhibition by sphingosine 1-phosphate. J Biol Chem 283(9):5677–5684. https://doi.org/10.1074/jbc.M707386200
225. Dugyala RR, Sharma RP, Tsunoda M, Riley RT (1998) Tumor necrosis factor-α as a contributor in Fumonisin B_1 toxicity. J Pharmacol Exp Ther 285(1):317
226. Bhandari N, He Q, Sharma PR (2001) Gender-related differences in subacute fumonisin B1 hepatotoxicity in BALB/c mice, vol 165. https://doi.org/10.1016/s0300-483x(01)00449-8
227. He Q, Riley RT, Sharma RP (2001) Fumonisin-induced tumor necrosis factor-alpha expression in a porcine kidney cell line is independent of sphingoid base accumulation induced by ceramide synthase inhibition. Toxicol Appl Pharmacol 174(1):69–77. https://doi.org/10.1006/taap.2001.9189
228. Sharma RP, Bhandari N, Riley RT, Voss KA, Meredith FI (2000) Tolerance to fumonisin toxicity in a mouse strain lacking the P75 tumor necrosis factor receptor. Toxicology 143(2):183–194. https://doi.org/10.1016/S0300-483X(99)00168-7
229. Chen X, Hu C, Dai J, Chen L (2015) Metabolomics analysis of seminal plasma in infertile males with kidney-yang deficiency: a preliminary study. Evid Based Complement Alternat Med 2015:892930. https://doi.org/10.1155/2015/892930
230. Zhao YY, Cheng XL, Wei F, Xiao XY, Sun WJ, Zhang Y, Lin RC (2012) Serum metabonomics study of adenine-induced chronic renal failure in rats by ultra performance liquid chromatography coupled with quadrupole time-of-flight mass spectrometry. Biomarkers 17(1):48–55. https://doi.org/10.3109/1354750X.2011.637180
231. Zhang J, Yan L, Chen W, Lin L, Song X, Yan X, Hang W, Huang B (2009) Metabonomics research of diabetic nephropathy and type 2 diabetes mellitus based on UPLC—oaTOF-MS system. Anal Chim Acta 650(1):16–22. https://doi.org/10.1016/j.aca.2009.02.027
232. Lin L, Huang Z, Gao Y, Chen Y, Hang W, Xing J, Yan X (2012) LC-MS-based serum metabolic profiling for genitourinary cancer classification and cancer type-specific biomarker discovery. Proteomics 12(14):2238–2246. https://doi.org/10.1002/pmic.201200016
233. Baranowski M, Zabielski P, Blachnio A, Gorski J (2008) Effect of exercise duration on ceramide metabolism in the rat heart. Acta Physiol (Oxf) 192(4):519–529. https://doi.org/10.1111/j.1748-1716.2007.01755.x
234. Wojcik B, Baranowski M, Chabowski A, Gorski J (2015) Effect of atrial pacing on the level of bioactive sphingolipids in the heart ventricles of the rat. J Physiol Pharmacol 66(3):385–389
235. Sun L, Liu J, Sun M, Lin L, Miao L, Ge Z, Yang B (2017) Comprehensive metabonomic analysis of heart tissue from isoproterenol-induced myocardial infarction rat based on reversed-phase and hydrophilic interaction chromatography coupled to mass spectrometry. J Sep Sci 40(10):2198–2206. https://doi.org/10.1002/jssc.201601013
236. Qi Y, Gu H, Song Y, Dong X, Liu A, Lou Z, Fan G, Chai Y (2013) Metabolomics study of resina draconis on myocardial ischemia rats using ultraperformance liquid chromatography/quadrupole time-of-flight mass spectrometry combined with pattern recognition methods and metabolic pathway analysis. Evidence Based Complement Altern Med 2013:10. https://doi.org/10.1155/2013/438680
237. Y-t Liu, H-m Jia, Chang X, W-h Cheng, Zhao X, Ding G, H-w Zhang, D-y Cai, Zou Z-M (2014) Metabolic pathways involved in Xin-Ke-Shu protecting against myocardial infarction in rats using ultra high-performance liquid chromatography coupled with quadrupole time-of-flight mass spectrometry. J Pharm Biomed Anal 90:35–44. https://doi.org/10.1016/j.jpba.2013.11.008
238. Miklosz A, Lukaszuk B, Chabowski A, Rogowski F, Kurek K, Zendzian-Piotrowska M (2015) Hyperthyroidism evokes myocardial ceramide accumulation. Cell Physiol Biochem 35(2):755–766. https://doi.org/10.1159/000369735
239. Park MT, Kang JA, Choi JA, Kang CM, Kim TH, Bae S, Kang S, Kim S, Choi WI, Cho CK, Chung HY, Lee YS, Lee SJ (2003) Phytosphingosine induces apoptotic cell death via caspase 8 activation and Bax translocation in human cancer cells. Clin Cancer Res 9(2):878–885
240. Yang Y, Jia H, Yu M, Zhou C, Sun L, Zhao Y, Zhang H, Zou Z (2018) Chinese patent medicine Xin-Ke-Shu inhibits Ca^{2+} overload and dysfunction of fatty acid β-oxidation in rats with myocardial infarction induced by LAD ligation. J Chromatogr B 1079:85–94. https://doi.org/10.1016/j.jchromb.2018.01.038
241. Błachnio-Zabielska A, Baranowski M, Wójcik B, Górski J (2016) Reduction of ceramide de novo synthesis in solid tissues changes sphingolipid levels in rat plasma, erythrocytes and platelets. Adv Med Sci 61(1):72–77. https://doi.org/10.1016/j.advms.2015.09.006
242. Huang L, Li T, Liu YW, Zhang L, Dong ZH, Liu SY, Gao YT (2016) Plasma metabolic profile determination in young ST-segment elevation myocardial infarction patients with ischemia and reperfusion: ultra-performance liquid chromatography and mass spectrometry for pathway analysis. Chin Med J (Engl) 129(9):1078–1086. https://doi.org/10.4103/0366-6999.180527
243. Knapp M, Baranowski M, Lisowska A, Musiał W (2012) Decreased free sphingoid base concentration in the plasma of patients with chronic systolic heart failure. Adv Med Sci 57(1):100–105. https://doi.org/10.2478/v10039-011-0057-4
244. Sun M, Miao Y, Wang P, Miao L, Liu L, Liu J (2014) Urinary metabonomics study of heart failure patients with HILIC and RPLC separation coupled to TOF–MS. Chromatographia 77(3):249–255. https://doi.org/10.1007/s10337-013-2585-5
245. Chen Y, Wen S, Jiang M, Zhu Y, Ding L, Shi H, Dong P, Yang J, Yang Y (2017) Atherosclerotic dyslipidemia revealed by plasma lipidomics on ApoE(−/−) mice fed a high-fat diet. Atherosclerosis 262:78–86. https://doi.org/10.1016/j.atherosclerosis.2017.05.010
246. Jiang H, Shen Z, Chu Y, Li Y, Li J, Wang X, Yang W, Zhang X, Ju J, Xu J, Yang C (2015) Serum metabolomics research of the anti-hypertensive effects of Tengfu Jiangya tablet on spontaneously hypertensive rats. J Chromatogr B Analyt Technol Biomed Life Sci 1002:210–217. https://doi.org/10.1016/j.jchromb.2015.08.010
247. Liu Y-T, Peng J-B, Jia H-M, Cai D-Y, Zhang H-W, Yu C-Y, Zou Z-M (2014) UPLC-Q/TOF MS standardized Chinese formula Xin-Ke-Shu for the treatment of atherosclerosis in a rabbit model. Phytomedicine 21(11):1364–1372. https://doi.org/10.1016/j.phymed.2014.05.009
248. Egom EE, Mamas MA, Chacko S, Stringer SE, Charlton-Menys V, El-Omar M, Chirico D, Clarke B, Neyses L, Cruickshank JK, Lei M, Fath-Ordoubadi F (2013) Serum sphingolipids level as a novel potential marker for early detection of human myocardial

ischaemic injury. Front Physiol 4:130. https://doi.org/10.3389/fphys.2013.00130
249. Park TS, Rosebury W, Kindt EK, Kowala MC, Panek RL (2008) Serine palmitoyltransferase inhibitor myriocin induces the regression of atherosclerotic plaques in hyperlipidemic ApoE-deficient mice. Pharmacol Res 58(1):45–51. https://doi.org/10.1016/j.phrs.2008.06.005
250. Dolgachev V, Nagy B, Taffe B, Hanada K, Separovic D (2003) Reactive oxygen species generation is independent of de novo sphingolipids in apoptotic photosensitized cells. Exp Cell Res 288(2):425–436. https://doi.org/10.1016/S0014-4827(03)00235-0
251. Miller M, Rosenthal P, Beppu A, Gordillo R, Broide DH (2017) Oroscomucoid like protein 3 (ORMDL3) transgenic mice have reduced levels of sphingolipids including sphingosine-1-phosphate and ceramide. J Allergy Clin Immunol 139(4):1373.e1374–1376.e1374. https://doi.org/10.1016/j.jaci.2016.08.053
252. Breslow DK, Collins SR, Bodenmiller B, Aebersold R, Simons K, Shevchenko A, Ejsing CS, Weissman JS (2010) Orm family proteins mediate sphingolipid homeostasis. Nature 463(7284):1048–1053. https://doi.org/10.1038/nature08787
253. Loiseau N, Obata Y, Moradian S, Sano H, Yoshino S, Aburai K, Takayama K, Sakamoto K, Holleran WM, Elias PM, Uchida Y (2013) Altered sphingoid base profiles predict compromised membrane structure and permeability in atopic dermatitis. J Dermatol Sci 72(3):296–303. https://doi.org/10.1016/j.jdermsci.2013.08.003
254. Obata Y, Sano H, Ohta N, Moriwaki T, Ishida K, Uchida Y, Takayama K (2017) Characterization of simple intercellular lipid model of atopic dermatitis stratum corneum containing sphingosine and sphinganine. J Dermatol Sci 86(2):e43–e44. https://doi.org/10.1016/j.jdermsci.2017.02.128
255. Kurek K, Miklosz A, Lukaszuk B, Chabowski A, Gorski J, Zendzian-Piotrowska M (2015) Inhibition of ceramide de novo synthesis ameliorates diet induced skeletal muscles insulin resistance. J Diabetes Res 2015:154762. https://doi.org/10.1155/2015/154762
256. Dong Y, Chen YT, Yang YX, Zhou XJ, Dai SJ, Tong JF, Shou D, Li C (2016) Metabolomics study of type 2 diabetes mellitus and the antidiabetic effect of berberine in Zucker diabetic fatty rats using Uplc-ESI-Hdms. Phytother Res 30(5):823–828. https://doi.org/10.1002/ptr.5587
257. Jiang W, Gao L, Li P, Kan H, Qu J, Men L, Liu Z, Liu Z (2017) Metabonomics study of the therapeutic mechanism of fenugreek galactomannan on diabetic hyperglycemia in rats, by ultra-performance liquid chromatography coupled with quadrupole time-of-flight mass spectrometry. J Chromatogr B 1044–1045:8–16. https://doi.org/10.1016/j.jchromb.2016.12.039
258. Jung S, Kim M, Ryu HJ, Chae JS, Lee S-H, Lee JH (2015) Age-related increase in LDL-cholesterol is associated with enhanced oxidative stress and disturbed sphingolipid metabolism. Metabolomics 11(1):40–49. https://doi.org/10.1007/s11306-014-0669-3
259. Oertel S, Scholich K, Weigert A, Thomas D, Schmetzer J, Trautmann S, Wegner M-S, Radeke HH, Filmann N, Brüne B, Geisslinger G, Tegeder I, Grösch S (2017) Ceramide synthase 2 deficiency aggravates AOM-DSS-induced colitis in mice: role of colon barrier integrity. Cell Mol Life Sci 74(16):3039–3055. https://doi.org/10.1007/s00018-017-2518-9
260. Choi S, Kim JA, Kim TH, Li HY, Shin KO, Lee YM, Oh S, Pewzner-Jung Y, Futerman AH, Suh SH (2015) Altering sphingolipid composition with aging induces contractile dysfunction of gastric smooth muscle via K(Ca) 1.1 upregulation. Aging Cell 14(6):982–994. https://doi.org/10.1111/acel.12388
261. Xu H, Zhang L, Kang H, Zhang J, Liu J, Liu S (2016) Serum metabonomics of mild acute pancreatitis. J Clin Lab Anal 30(6):990–998. https://doi.org/10.1002/jcla.21969
262. Barbas-Bernardos C, Armitage EG, García A, Mérida S, Navea A, Bosch-Morell F, Barbas C (2016) Looking into aqueous humor through metabolomics spectacles—exploring its metabolic characteristics in relation to myopia. J Pharm Biomed Anal 127:18–25. https://doi.org/10.1016/j.jpba.2016.03.032
263. Sui Z, Li Q, Zhu L, Wang Z, Lv C, Liu R, Xu H, He B, Li Z, Bi K (2017) An integrative investigation of the toxicity of Aconiti kusnezoffii radix and the attenuation effect of its processed drug using a UHPLC-Q-TOF based rat serum and urine metabolomics strategy. J Pharm Biomed Anal 145:240–247. https://doi.org/10.1016/j.jpba.2017.06.049
264. Charkiewicz K, Goscik J, Blachnio-Zabielska A, Raba G, Sakowicz A, Kalinka J, Chabowski A, Laudanski P (2017) Sphingolipids as a new factor in the pathomechanism of preeclampsia—mass spectrometry analysis. PLoS One 12(5):e0177601. https://doi.org/10.1371/journal.pone.0177601
265. Zmyslowska A, Ciborowski M, Borowiec M, Fendler W, Pietrowska K, Parfieniuk E, Antosik K, Pyziak A, Waszczykowska A, Kretowski A, Mlynarski W (2017) Serum metabolic fingerprinting identified putatively annotated sphinganine isomer as a biomarker of Wolfram syndrome. J Proteome Res 16(11):4000–4008. https://doi.org/10.1021/acs.jproteome.7b00401
266. Auer-Grumbach M, Bode H, Pieber TR, Schabhüttl M, Fischer D, Seidl R, Graf E, Wieland T, Schuh R, Vacariu G, Grill F, Timmerman V, Strom TM, Hornemann T (2013) Mutations at Ser331 in the HSN type I gene SPTLC1 are associated with a distinct syndromic phenotype. Eur J Med Genet 56(5):266–269. https://doi.org/10.1016/j.ejmg.2013.02.002
267. Hsiao CT, Chao HC, Liao YC, Lin KP, Soong BW, Lee YC (2017) Investigation for SPTLC1 mutations in a Taiwanese cohort with hereditary neuropathies. J Neurol Sci 381:463–464. https://doi.org/10.1016/j.jns.2017.08.3516
268. Murphy SM, Ernst D, Wei Y, Laura M, Liu YT, Polke J, Blake J, Winer J, Houlden H, Hornemann T, Reilly MM (2013) Hereditary sensory and autonomic neuropathy type 1 (HSANI) caused by a novel mutation in SPTLC2. Neurology 80(23):2106–2111. https://doi.org/10.1212/WNL.0b013e318295d789
269. Kojima T, Asano Y, Kurasawa O, Hirata Y, Iwamura N, Wong T-T, Saito B, Tanaka Y, Arai R, Yonemori K, Miyamoto Y, Sagiya Y, Yaguchi M, Shibata S, Mizutani A, Sano O, Adachi R, Satomi Y, Hirayama M, Aoyama K, Hiura Y, Kiba A, Kitamura S, Imamura S (2018) Discovery of novel serine palmitoyltransferase inhibitors as cancer therapeutic agents. Bioorg Med Chem 26(9):2452–2465. https://doi.org/10.1016/j.bmc.2018.04.008
270. Boyden LM, Vincent NG, Zhou J, Hu R, Craiglow BG, Bayliss SJ, Rosman IS, Lucky AW, Diaz LA, Goldsmith LA, Paller AS, Lifton RP, Baserga SJ, Choate KA (2017) Mutations in KDSR cause recessive progressive symmetric erythrokeratoderma. Am J Hum Genet 100(6):978–984. https://doi.org/10.1016/j.ajhg.2017.05.003
271. Takeichi T, Torrelo A, Lee JYW, Ohno Y, Lozano ML, Kihara A, Liu L, Yasuda Y, Ishikawa J, Murase T, Rodrigo AB, Fernández-Crehuet P, Toi Y, Mellerio J, Rivera J, Vicente V, Kelsell DP, Nishimura Y, Okuno Y, Kojima D, Ogawa Y, Sugiura K, Simpson MA, McLean WHI, Akiyama M, McGrath JA (2017) Biallelic mutations in KDSR disrupt ceramide synthesis and result in a spectrum of keratinization disorders associated with thrombocytopenia. J Invest Dermatol 137(11):2344–2353. https://doi.org/10.1016/j.jid.2017.06.028
272. Krebs S, Medugorac I, Röther S, Strässer K, Förster M (2007) A missense mutation in the 3-ketodihydrosphingosine reductase FVT1 as candidate causal mutation for bovine spinal muscular atrophy. Proc Natl Acad Sci USA 104(16):6746–6751. https://doi.org/10.1073/pnas.0607721104
273. Ordonez YF, Gonzalez J, Bedia C, Casas J, Abad JL, Delgado A, Fabrias G (2016) 3-Ketosphinganine provokes the accumulation of dihydroshingolipids and induces autophagy in cancer cells. Mol BioSyst 12(4):1166–1173. https://doi.org/10.1039/C5MB00852B

Appendix 1.2

Magaye RR, Savira F, Hua Y, Xiong X, Huang L, Reid C, Flynn B, Liew D, Wang BW. Exogenous dihydrosphingosine 1 phosphatemediates collagen synthesis in cardiac fibroblasts through JAK/STAT signalling and TIMP1. Journal of Cellular Signalling. 2020;72:109620.

Cellular Signalling 72 (2020) 109629

Contents lists available at ScienceDirect

Cellular Signalling

journal homepage: www.elsevier.com/locate/cellsig

Exogenous dihydrosphingosine 1 phosphate mediates collagen synthesis in cardiac fibroblasts through JAK/STAT signalling and regulation of TIMP1

Ruth R. Magaye[a,b], Feby Savira[a,b], Yue Hua[b,c], Xin Xiong[b,d], Li Huang[a,b], Christopher Reid[b,e], Bernard Flynn[f], David Kaye[g], Danny Liew[b], Bing H. Wang[a,b,*]

[a] Biomarker Discovery Laboratory, Baker Heart and Diabetes Institute, Melbourne, Australia
[b] Monash Centre of Cardiovascular Research and Education in therapeutics, Melbourne, Australia
[c] School of Traditional Chinese Medicine, Southern Medical University, Guangzhou, China
[d] Shanghai Institute of Heart Failure, Research Centre for Translational Medicine, Shanghai East Hospital, Tongji University, School of Medicine, Shanghai 200120, China
[e] School of Public Health School, Curtin University, Perth, Australia
[f] Australian Translational Medicinal Chemistry Facility, Medicinal Chemistry, Monash Institute of Pharmaceutical Sciences, Monash University, Melbourne, Australia
[g] Heart Failure Research Group, Baker Heart and Diabetes Institute, Melbourne, Australia

ARTICLE INFO

Keywords:
Dihydropshingosine 1 phosphate
Sphingolipid
JAK/STAT signalling
Cardiac remodelling
TIMP1

ABSTRACT

Cardiac fibrosis and myocyte hypertrophy are hallmarks of the cardiac remodelling process in cardiomyopathies such as heart failure (HF). Dyslipidemia or dysregulation of lipids contribute to HF. The dysregulation of high density lipoproteins (HDL) could lead to altered levels of other lipid metabolites that are bound to it such as sphingosine-1- phosphate (S1P). Recently, it has been shown that S1P and its analogue dihydrosphingosine-1-phosphate (dhS1P) are bound to HDL in plasma. The effects of dhS1P on cardiac cells have been obscure. In this study, we show that extracellular dhS1P is able to increase collagen synthesis in neonatal rat cardiac fibroblasts (NCFs) and cause hypertrophy of neonatal cardiac myocytes (NCMs). The janus kinase/signal transducer and activator (JAK/STAT) signalling pathway was involved in the increased collagen synthesis by dhS1P, through sustained increase of tissue inhibitor of matrix metalloproteinase 1 (TIMP1). Extracellular dhS1P increased phosphorylation levels of STAT1 and STAT3 proteins, also caused an early increase in gene expression of transforming growth factor-β (TGFβ), and sustained increase in TIMP1. Inhibition of JAKs led to inhibition of TIMP1 and TGFβ gene and protein expression. We also show that dhS1P is able to cause NCM hypertrophy through S1P-receptor-1 (S1PR1) signalling which is opposite to that of its analogue, S1P. Taken together, our results show that dhS1P increases collagen synthesis in cardiac fibroblasts causing fibrosis through dhS1P-JAK/STAT-TIMP1 signalling.

1. Introduction

Dihydrosphingosine 1 phosphate and sphingosine 1 phospate are both metabolic products of the de novo sphingolipid synthesis pathway present in all cells. dhS1P differs from S1P by its backbone structure which is composed of dihydrosphingosine, in contrast to sphingosine for S1P. S1P's role as a lipid mediator is widely known. It modulates multiple signalling pathways involved in cellular events such as white cell migration, inflammation, proliferation, apoptosis and fibrosis by binding to S1P specific membrane bound G protein coupled receptors (GPCRs). Recently, several reviews have highlighted the effects of S1P and its receptors (S1PR1–3) in cardiac pathophysiology such as cardiac remodelling [1–3]. Unlike S1P, due to its low levels within the biological system, the role of dhS1P in disease processes such as cardiac remodelling are ill-defined but have been speculated to be similar to that of S1P, since it also activates the S1PRs. This is despite evidence in

Abbreviations: ANP, Atrial Natriuretic Peptide; αSKA, α Skeletal Muscle Actin; αSMA, α Smooth Muscle Actin; β1AR, β1- Adrenergic Receptor; βMHC, β Myosin Heavy Chain; BNP, Brain Natriuretic Peptide; Coll1a1, Collagen 1a1; Coll3a1, Collagen 3a1; dhS1P, Dihydrosphingosine 1 phosphate; ECM, Extracellular Matrix; ER, Endoplasmic Reticulum; JAK, Janus Kinase; LAP, Latency Associated Protein; MI, Myocardial Infarct; MMP2, Matrix Metalloproteinase 2; NCF, Neonatal Cardiac Fibroblasts; NCM, Neonatal Cardiac Myocytes; S1P, Sphingosine 1 Phosphate; S1PRs, Sphingosine 1 Phosphate Receptors; S1PR1, Sphingosine 1 Phosphate Receptor 1; SK1, Sphingosine Kinase 1; SL, Spingolipid; STAT1/3, Signal Transducer and Activator of Transcription 1/3; TGFβ, Transforming Growth Factor β; TIMP1, Tissue Inhibitor of Metalloproteinase 1

* Corresponding author at: Biomarker Discovery Laboratory, Baker Heart and Diabetes Institute, Melbourne, Australia.
E-mail addresses: bing.wang@baker.edu.au, bing.wang@monash.edu (B.H. Wang).

https://doi.org/10.1016/j.cellsig.2020.109629
Received 3 January 2020; Received in revised form 30 March 2020; Accepted 1 April 2020
Available online 08 April 2020
0898-6568/

skin fibroblasts showing dhS1P to have opposite effects to that of S1P by downregulating fibrotic markers such as matrix metalloproteinase 1 (MMP1) and phosphorylated SMAD 3 [4]. Recently, others have shown that dhS1P is able to bind to HDL in plasma in a non-specific manner compared to S1P which requires Apo lipoprotein M [5]. S1P activates several downstream signalling pathways in cardiac fibroblasts and myocytes including the transforming growth factor-β (TGFβ)/SMAD, and Janus Kinase/signal transducer and activator (JAK/STAT) pathways leading to cardiac remodelling [6] or cardio-myocyte protection [7,8]. S1P activation of the JAK/STAT pathway is known to be receptor dependent as indicated by S1P/S1PR2/3 signalling in cardiac myocytes in ischaemic reperfusion injury (IRI) [8,9] .The JAK/STAT signalling pathway confers short-term cardiac protection, however its prolonged activation is thought to worsen the disease state thus requiring a balance in the activation of this pathway. Cardiac remodelling is marked by increased deposition of the extracellular matrix (ECM) such as collagen causing fibrosis and loss of myocyte function due to myocyte hypertrophy. The phosphorylation of STAT1 and STAT3 have also been shown to mediate proliferation of cardiac fibroblasts and collagen synthesis induced by high glucose in the heart [10]. Therefore, the aim of this study is to determine whether exogenous dhS1P leads to cardiac cellular remodelling through activation of the JAK/STAT signalling pathway and explore differences in downstream signalling mechanisms between dhS1P and S1P.

2. Materials and methods

2.1. Primary neonatal rat cardiac cells harvest and culture

Primary neonatal cardiac myocytes (NCMs) and fibroblasts (NCFs) were extracted from 1 to 2 days old Sprague-Dawley rat pups using enzymatic collagenase digestion routinely used in our laboratory for in vitro assays [11]. Pups were purchased from the Monash Animal Research Platform (Clayton, Vic), and complied with the guidance from the National Health and Medical Research Council of Australia. The animal used for this study was approved by the Alfred Medical Research and Education Precinct Animal Ethics Committee (E/1653/2016/M).

2.2. Measurement of cardiac fibroblast collagen synthesis

Induction of collagen synthesis by S1P, dhS1P and the S1PR1 agonist, SEW2871, in NCFs was determined using the ^{3}H-proline incorporation assay [12]. Briefly, after determining optimum dose of dhS1P and S1P for collagen synthesis, NCFs at 50000 cells/ well were pre-treated with the JAKs inhibitor (P6, 0.01–1.0 μM- Calbiochem, Darmstadt, Germany), and a specific S1PR1 antagonist (W146, 0.1–5.0 μM- Tocris Bioscience, Bristol, UK) for 2 h. The cells were then stimulated with 3 μM dhS1P, 1 μM S1P, and 10 μM SEW2871 (Monash Institute of Pharmaceutical Sciences, Melbourne, Australia) for 48 h in DMEM F12 medium supplemented with 1% vitamin C and 0.5% BSA. 1 μCi ^{3}H proline was added to the cell culture medium and included ad hoc with S1P, dhS1P and SEW2871 (the doses used were pre-determined as shown in Fig. 1a). The levels of ^{3}H-proline incorporation were determined on a 300SL beta counter at counts per minute (cpm).

2.3. Measurement of neonatal cardiac myocyte hypertrophy

To determine whether exogenous dhS1P and S1P induced NCM hypertrophy, ^{3}H-leucine incorporation was used as described previously [11]. Briefly, NCMs were pre-treated for 2 h at similar doses of P6 and W146 as used in NCF and treated with S1P (1 μM) and dhS1P (3.0 μM) at predetermined time points of 60 h and 48 h, respectively. The optimum dose and times point for stimulation were validated prior to the experiments as shown in Fig. 10a.

2.4. Measurement of cell viability in rat NCFs and NCMs

Cell viability was measured using the Almar Blue Assay (Invitrogen-Thermo Fischer Scientific, Carlsbad, CA, United States). Cells were seeded in 96-well plates at a density of 1.5×10^{4} and 1×10^{5} cells per well for NCFs and NCM, respectively. After 48 h or 60 h treatment as described for collagen synthesis and myocyte hypertrophy assays, respectively. The reduction of resazurin by viable cells to resorufin was measured after further incubation with 1:10 ratio of Almar blue reagent to media for 4–6 h, and the absorbance was read at 570 and 600 nm wavelength on a NanoStar spectrometer (BMG Labtech, Ortenberg, BW, Germany).

2.5. Quantitative measurement of phosphorylated and total protein levels in NCFs and NCMs

The expression of specific proteins related to the JAK/STAT signalling pathway and cardiac remodelling were analysed using Western Blotting. Both NCFs (3×10^{5} cells/ Flask) in T25 flasks and NCMs (1×10^{6} cells/ Well) in 6 well plates were pre-treated for 2 h with P6 (0.3 & 1 μM), and W146 (3 & 5 μM) and treated with 3 μM dhS1P, 1 μM S1P, and 10 μM SEW2871 (*NCF only*), for 15 to 30 min for phosphorylated proteins and 24 h for total proteins. 10 μg/μL cell lysates were separated on 7.5, 10, or 12% gels by SDS-polyacrylamide gel electrophoresis (SDS-PAGE), and transferred onto nitrocellulose blotting membranes (GE HealthCare, Chicago, IL, United States). The blots were probed for phosphorylated STAT1, STAT3, c-JUN, and SMAD2 from Cell Signalling Technologies (CST: 8826S, 9145 L, 2361S, and 3108 L) after blocking with 5% bovine serum albumin (BSA). They were also probed for TGFβ (CST: 3709S, 3711S), Collagen I (Abcam, Cambridge, UK: Ab209539), TIMP1 (Novus Biologica, Centennial, CO, United States: NBP1–96554), α- smooth muscle actin, α-SMA (Abcam: Ab124964) after blocking with 5% Milk in Tris-buffered saline with 0.1% Tween 20 (TBS-T). Bands were detected using Super Signal West Pico Chemiluminescence Substrate (Thermo Fisher Scientific, Rockford, IL, United States) in BioRad Chemidoc instrument and analysed using Image lab software (BioRad Laboratories, Hercules, CA, United States). Proteins were normalized to Glyceraldehyde –phosphate dehydrogenase (GAPDH) (CST: 2118 L) or β-Actin (CST: 4970).

2.6. Quantitative measurement of cardiac remodelling marker RNA expression

NCFs (5×10^{5}/ well) and NCMs (1×10^{6} / well) seeded in 6 well plates were pre-treated with the inhibitors as mentioned above for 2 h after 48 h serum starvation. The NCFs were further incubated with SEW2871 (10 μM) for 18 h, and dhS1P (3 μM) and S1P (1 μM) for 6 h (stimulation time points based on TGFβ gene expression as shown in Fig. 4a) and NCMs were incubated for further 18 h with each of the lipids. Total RNA was extracted and isolated using MagMAX-96 Total RNA Isolation for Microarray Kit according to the manufacturer's instructions (Thermo Fisher Scientific, Rockford, IL, United States). 5 or 10 ng/uL of RNA was reverse transcribed into cDNA using Multi-Scribe (Applied Bio systems, Foster City, CA, USA). The expression levels of the fibrotic markers; TGFβ, CTGF, TIMP1, collagen 1a1 (Coll1a1), collagen 3a1 (Coll3aI), the S1P receptors [1–3], and the enzyme sphingosine kinase-1 (SK1) were quantified by real time polymerase chain reaction (PCR) on the Quan-Studio 12 K Flex Real Time PCR System (Applied Bio systems) with SYBR Green as detector (Applied Bio systems). The gene expression levels of pro-hypertrophic markers such as atrial and brain natriuretic peptide (ANP & BNP), β-myosin heavy chain (βMHC), skeletal α-actin (α-SKA) were also quantified. Refer to Table 1 for full sequence of primers. 18 s mRNA was used as the endogenous controls.

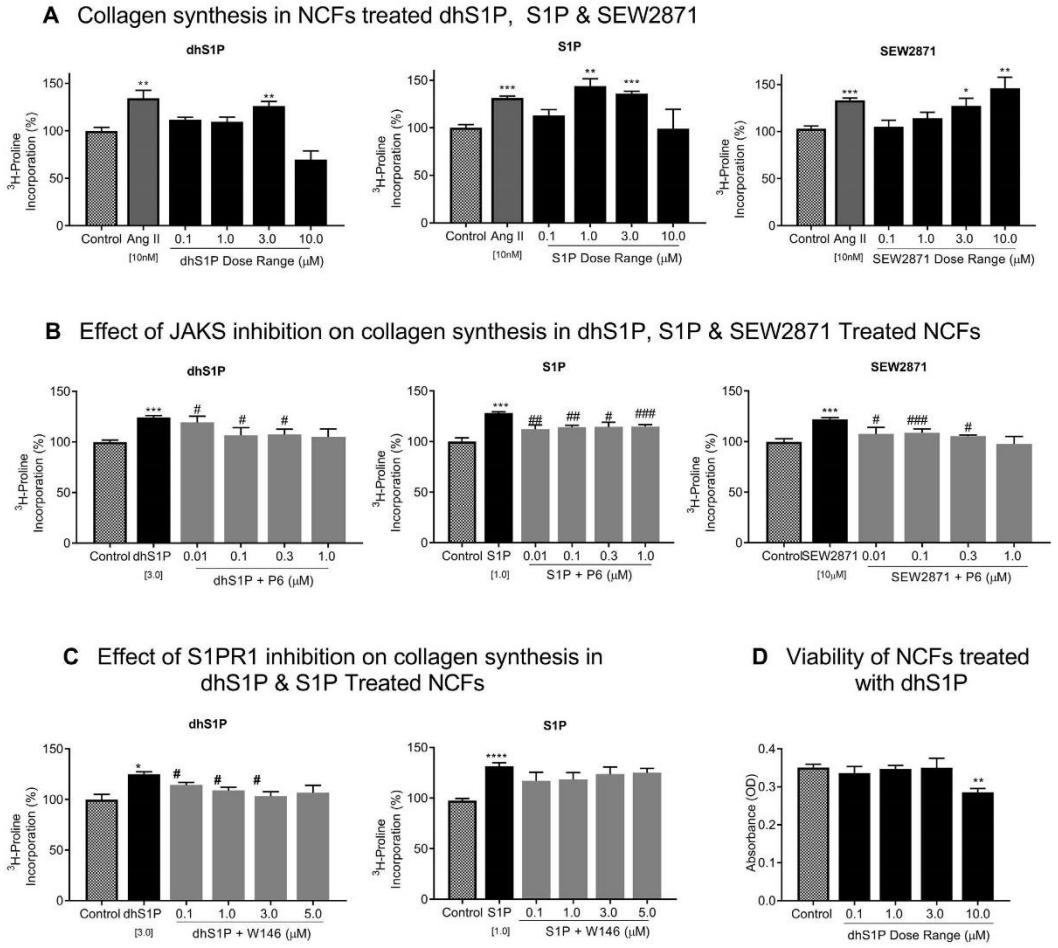

Fig. 1. -dhS1P- or S1P induced collagen synthesis in NCFs. a Significant increase in collagen synthesis were observed for dhS1P at 3 μM ($^{**}p < .01$), S1P at 1 μM ($^{**}p < .01$) & 3 μM ($^{***}p < .005$), and SEW2871 at 3 μM ($^{*}p < .05$) & 10 μM ($^{**}p < .01$) vs. control. b Inhibition of JAKs significantly reduced collagen synthesis in NCF induced by dhS1P ($^{\#}p < .05$), S1P ($^{\#}p < .05$, $^{\#\#}p < .01$, $^{\#\#\#}p < .005$) & SEW2871 ($^{\#}p < .05$, $^{\#\#\#}p < .005$) vs. stimulation. c Inhibition of S1PR1 significantly reduced collagen synthesis stimulated by dhS1P, $^{\#}p < .05$ vs. treatment, but the effects on S1P stimulated collagen synthesis were not statistically significant. d 10 μM dhS1P reduced the viability of NCFs at 48 h of treatment, $^{**}p < .01$ vs. Control. Values presented as mean ± standard error of mean (SEM) of at least three independent experiments with 3 replicates in each.

2.7. Immunohistochemistry

Immunohistochemical analysis was carried out on passage 1 NCFs plated in glass bottom 6 well plates (1×10^5 cells/well) and treated with SEW2871 (10 μM), S1P (1 μM), & dhS1P (3 μM) and TGFβ (10 μM) for 48 h. Abcam's online immunostaining protocol was followed with minor modifications. Briefly, the cells were washed three times with PBS, before fixing for 5 min with ice cold methanol. The fixed cells were then washed with cold PBS before blocking with 1% BSA in TBST (Sigma) at 1:500; and Vimentin (Abcam, Cambridge, MA, USA) at 1:1000. Actin filaments were labelled with Alexa Fluor tagged secondary anti-bodies at 1: 1000. The nuclei were labelled with Hoercsht at 1:1000 (Sigma). Images were captured with the Nikon TI Eclipse Widefield microscope (Nikon, Minato, TKY, Japan), and analysed using NIS elements viewer software (Nikon).

2.8. Statistical analysis

All cell culture experiments were performed in triplicates, with atleast three repeated experiments for the hypertrophy and collagen synthesis assays and two repeated experiments for western blots and PCR. The results are presented as the percentage of unstimulated controls (mean ± SEM). For western blot analyses, ratio of phosphorylated over GAPDH levels were analysed. For real-time PCR, gene expression levels in NCF and NCM were normalized with 18 s (housekeeping gene). One-way ANOVA with Bonferroni's multiple comparison post hoc tests was used for statistical analyses for comparison between multiple groups and unpaired *t*-test was used for

Table 1
List of primers and their sequences.

Primers	Sequence	Manufacturer
TGFb1	*Forward: 5′-CCA GCC GCG GGA CTC* *Reverse: 5′ -TTC CGT TTC ACC AGC TCC AT*	*+Geneworks*
TIMP1	*Forward: 5′-GTA AAG ACC TAT AGT GCT GGC TG* *Reverse: 5′-GAG CAT CTG ATC TGT CCA CAA*	*+Sigma*
SK1	*Forward: 5′- CTT TAA ACT GAT GCT CAC CG* *Reverse: 5′- TAC ATA GGG GTT TCT GGA TG*	*Sigma*
S1PR1	*Forward: 5′- AAA ACC AAG AAG TTC CAC C* *Reverse: 5′- CCA CAA ACA TAC TTC CTT CC*	*Sigma*
S1PR2	*Forward: 5′- CTC TTA TGG CAT CTT AGA AGA CAC C* *Reverse: 5′- CAC AGA CAC ACA TAA ATA CCG*	*Sigma*
S1PR3	*Forward: 5′- AAA ACG CTT AGA AGA CACC* *Reverse: 5′- GTG TGT CTC TGA TGC TAA TC*	*Sigma*
Collagen 3a1	*Forward: 5′- TTT CAA GAT CAA CAC TGA GG* *Reverse: 5′- TAT TTC TCC GCT CTT GAG TTC*	*Sigma*
Collagen 1a1	*Forward: 5′- TGG ATT CCA GTT CGA GAG TAT G* *Reverse: 5′- AGT GAT AGG TGA TGT TCT GG*	*Sigma*
βMHC	*Forward: 5′- TTG GCA CGG ACT GCG TCA TC* *Reverse: 5′- GAG CCT CAA GAG TTT GCT GAA*	*Sigma*
ANP	*Forward: 5′- ATC TGA TGG ATT TCA AGA ACC* *Reverse: 5′- CTC TGA GAC GGG TTG ACT TC*	*Sigma*
BNP	*Forward: 5' ACA ATC CAC GAT GCA GAA GCT* *Reverse: 5′- GGG CCT TGG TCC TTT GAG A*	*Sigma*
αSKA	*Forward: 5′- TCG CGA CCT TAC TGA CTA CCT G* *Reverse: 5′- GCT TCT CTT TGA TGT CGC GC*	*Geneworks*
MMP2	*Forward: 5′- GGG TCC ATT CTG CCA GCA CTC* *Reverse: 5′- CTC CAG AAC TTG TCT CCT GCA A*	*Geneworks*
18 s	*Forward: 5′- TCG AGG CCC TGT AAT TGG AA* *Reverse:5′ - CCC TCC AAT TGG ACC TCG TT*	*Sigma*

* *Sigma,* St. Louis, MO, USA; + *Geneworks*, Thebarton, SA, Australia.

comparison between two groups. A statistically significant result was determined with a two-tailed *p*-value of less than 0.05. GraphPad Prism Version 8 (GraphPad Software Inc., San Diego, CA, United States) were used to perform all of the statistical analyses.

3. Results

3.1. dhS1P induced collagen synthesis in NCFs

The sphingolipid, S1P, is now known to cause cardiac fibrosis and myocyte hypertrophy [1,3,8]. We investigated whether extracellular dhS1P, the analogue of S1P, was able to induce collagen synthesis at similar doses to that of S1P and the S1PR1 agonist- SEW2871 at 48 h of stimulation using the tritiated (^{3}H) proline incorporation assay. Our results in Fig. 1a show that dhS1P at 3 μM significantly ($p < .01$) induced collagen synthesis in NCFs. However, at the highest dose of 10 μM, dhS1P caused significant cell death as corroborated by the results from the Almar Blue cell viability assay ($p < .01$, Fig. 1d).

Fig. 1a also shows that SEW2871 caused a dose dependent increase in collagen synthesis, while S1P induced collagen synthesis was significant at 1 μM ($p < .01$) and 3 μM ($p < .005$), showing similar non-linear effects as dhS1P. These increases in collagen synthesis were comparable to that induced by 100 nM Ang II which was used as a positive control, $p < .01$–0.005 vs. control.

3.2. dhS1P, S1P & SEW2871 induce collagen synthesis by activating JAKs

Since dhS1P, was able to induce collagen synthesis in NCFs, we then investigated whether the JAK/STAT signalling pathway was activated by dhS1P, SEW2871 and S1P. The JAKs (JAK1, JAK2, JAK3, TYK1, and TYK2) are a group of cytoplasmic tyrosine kinases that transduce signals from membrane receptors to the STAT proteins which can translocate to the nucleus and act as transcription factors. The introduction of the JAKs inhibitor, Pyridone 6 (P6) [13], had similar potency at doses over 0.1 μM on collagen synthesis by 3 μM dhS1P ($p < .05$, Fig. 1b). Comparatively, P6 was also able to significantly inhibit 1 μM S1P induced collagen synthesis in NCFs with no observable trend of dose-dependency (Fig. 1b). These differences may be due to S1P and dhS1P activating different types of S1P receptors leading to activation of different pathways such as the mitogen activated protein kinase (MAPK/ Erk) pathway, which has been shown to have increased phosphorylation in mice overexpressing S1PR1 [14]. In cells treated with 10 μM of the S1PR1 agonist, SEW2871, there was a dose response effect when P6 was introduced, although not with a big gradient difference (Fig. 1b).

3.3. dhS1P/S1PR1 signalling increased collagen synthesis

Targeting S1P/S1PR1 signalling has shown potential in cancer therapy [15], but evidence for its role in cardiac fibrosis is limited. Therefore, we then inhibited S1PR1 with its specific antagonist, W146, to determine if S1PR1 was essential for collagen synthesis by dhS1P and S1P. Our results in Fig. 1c show that W146 had a dose dependent effect on the inhibition of collagen synthesis stimulated by dhS1P ($p < .05$). However, for S1P, W146 was not able to significantly inhibit collagen synthesis, despite showing reduction in collagen synthesis as determined by 3H- proline incorporation at all concentrations tested. This indicates that S1P may activate other targets, compensating for inhibition of S1PR1, possibly through S1PR2/3 activation, shown by Quint *et.al* [16].

3.4. dhS1P, S1P & SEW2871 activated fibroblast to myofibroblast differentiation

The phenotypic differentiation of fibroblasts to myofibroblasts is associated with cardiac remodelling. Myofibroblasts have an increased expression of αSMA [17]. Apart from αSMA, myofibroblasts also express vimentin, which is one of the intermediate filaments found in many non-muscle cells. Fibrotic factors such as TGFβ are known to activate the differentiation process leading to increased production of the ECM [18]. We used immunofluorescence staining method to determine if SEW2871, dhS1P and S1P and TGFβ (used as positive control) led to increased cytosolic expression of αSMA in NCFs. Fig. 2a shows that dhS1P, S1P and SEW2871 increased cytosolic αSMA, but was less intense when compared to TGFβ. TGFβ stimulation increased the expression of vimentin in NCFs (Fig. 2a). Such upregulation may reflect TGFβ stimulated fibroblasts differentiation and transformation to myofibroblasts as shown in previous studies. TGFβ has also been shown to increase vimentin expression in cells undergoing trans-differentiation [19]. Western Blot protein quantification of αSMA (Fig. 2b), showed that TGFβ ($p < .05$) and SEW2871 ($p < .01$) caused significant increase in αSMA protein levels vs. control.

3.5. Increased dhS1P phosphorylation of STAT1 in NCF was reduced when JAKs were inhibited

We then evaluated whether dhS1P and S1P could activate STAT1 and STAT3 using Western Blot protein analysis in NCFs. Of the seven known mammalian STAT proteins, the activation and translocation of STAT1 and 3 to the nucleus leads to the transcription of genes including those that regulate inflammation, cell proliferation and fibrosis [20,21]. Both dhS1P and S1P were able to significantly increase pSTAT1 ($p < .01$ & $p < .05$ vs. control) level at 15 min of stimulation, which was inhibited by P6 at 1 μM, even though it was not statistically significant (Fig. 3a-b). Pre-treatment of NCFs with P6 completely abolished the expression of phosphorylated STAT3 in both dhS1P and S1P treated cells. dhS1P did not increase phosphorylation of STAT3 at the time point tested (Fig. 3a). This may imply that STAT3 maybe phosphorylated at a later time point as seen in Fig. 3c, which was stimulated for 30 mins STAT3 phosphorylation at tyrosine 705 leads to its dimerization forming homodimers or heterodimers with other STATs

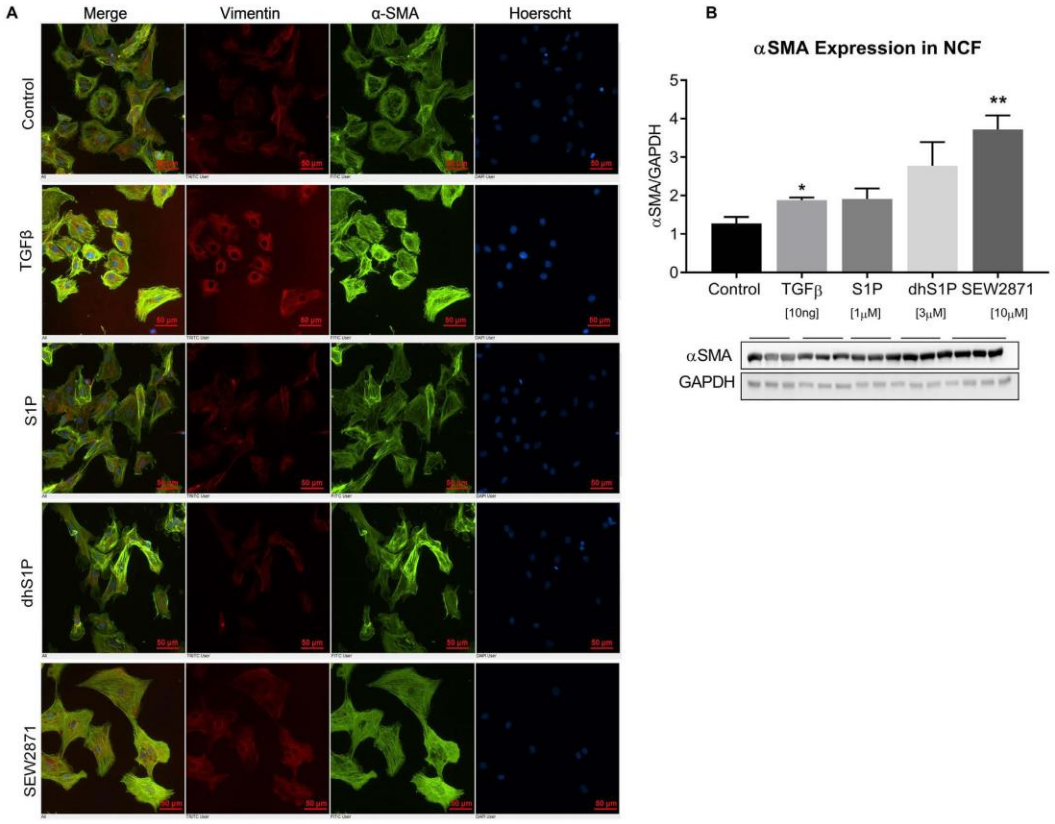

Fig. 2. SEW2871, S1P and dhS1P activated trans-differentiation of fibroblast to myofibroblast. a Immunofluorescent staining of αSMA (green), vimentin (red) and Nuclei (Blue) by Hoerscht. 10 μM TGFβ, 1 μM S1P, 3 μM dhS1P & 10 μM SEW2871 have increased αSMA expression. Original magnification X200. b Western blot αSMA protein expression in NCFs compared to the different treatments at 48 h incubation, $*p < .05$ & $**p < .01$ vs. control. (For interpretation of the references to colour in this figure legend, the reader is referred to the web version of this article.)

such as STAT1. Both phosphorylated STAT3α (86 kDa-upper band) and STAT3β (79 kDa-lower band) were expressed in primary rat NCFs (see representative blots in Fig. 3). STAT3 has been shown to affect collagen synthesis in the heart more than STAT1 [22].

3.6. Differential regulation of STAT1/3 by dhS1P/S1PR1 and S1P/S1PR1 axis in NCF

Since the JAKs are associated with GPCRs such as the S1PRs we investigated whether STAT1 and 3 were activated through S1PR1 signalling by both dhS1P and S1P. Treatment of NCF with W146 led to reduced phosphorylation of STAT1 stimulated by S1P at the highest dose of 5 μM ($p < .01$ (Fig. 3d). On the other hand, S1PR1 inhibition by W146 in dhS1P stimulated NCFs seemed to have synergistic increase in STAT1 phosphorylation level at 1 μM (Fig. 3c) but was statistically not significant.

3.7. S1P and dhS1P increased TGFβ, TIMP1 and SK1 gene expression

We then investigated whether S1P and dhS1P caused an increase in mRNA expression of known fibrotic markers such as TGFβ. First, a time course analysis was performed. The treatment of NCFs with extracellular S1P (Fig. 4f) or dhS1P (Fig. 4a) led to a significant early increase (at 6 h of stimulation) in TGFβ gene expression, $p = .0001$ and $p < .0001$, respectively.

Additionally, the mRNA expression of TIMP1 and SK1 at this time point were greatly enhanced by both S1P, $p < .0001$ (Fig. 4g- h), and dhS1P, $p < .0001$ (Fig. 4b- c). SK1 has been shown to mediate TIMP1 increase [6]. There was sustained significant increase in TIMP1 mRNA at all the time points investigated in both dhS1P (Fig. 4b) and S1P (Fig. 4g) stimulated cells, however there was no changes in SK1 or TGFβ mRNA expression at all other time points tested. Others have shown that 48 h of exposure of C57BL/6 mice cardiac fibroblasts to TGFβ led to increased SK1 mRNA and Coll 1a1 mRNA by 0.1 μM S1P [23]. It should be noted that at these time points (6, 18 & 24 h), other pro fibrotic genes such as Coll1a1 (Fig. 4d & i) and Coll3a1 (Fig. 4e & i) were not increased by extracellular S1P or dhS1P. At 24 h there was significant reduction in Coll1a1 ($p < .01$) mRNA in S1P stimulated cells (Fig. 4j) and Coll3a1 ($p < .05$) in dhS1P stimulated cells (Fig. 4e), which may have been a result of feedback inhibition prompted by the enhanced effect on TIMP1 gene expression. In addition, collagen mRNA expression has a lag phase of 6 h with maximal increases seen at 3 days

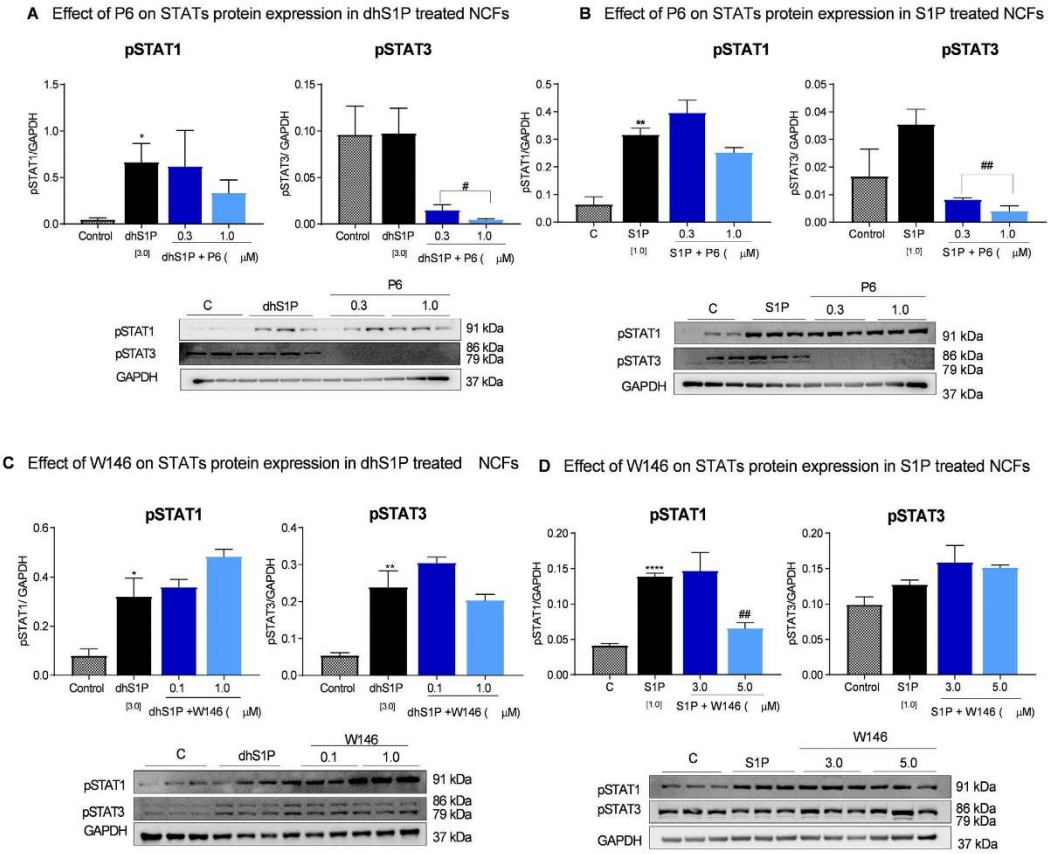

Fig. 3. dhS1P/S1PR1 axis does not induce phosphorylation of STAT1/3. a P6 reduced 3 μM dhS1P induced phosphorylation of STAT1, and completely abrogated STAT3, $^{*}p < .05$ vs. control and, $^{\#\#}p < .01$ vs. dhS1P. b 1 μM S1P induced phosphorylation of STAT1 and not STAT3, but P6 abrogated STAT3 phosphorylation, $^{**}p < .01$ vs. control and, $^{\#\#}p < .01$ vs. S1P. c dhS1P increased phosphorylation of STAT 1 and 3 at 15 and 30 min, respectively. d S1P/S1PR1 signalling increased phosphorylation of STAT1, $^{**}p < .01$ vs. control and, $^{\#\#}p < .01$ vs. S1P. But, had no effect on STAT3. Values are presented as ± SEM of at least 3 replicates with two independent repeats.

of exposure [24], which could explain the lack of response at the early time points. These results may indicate that the pro-fibrotic effects of S1P and dhS1P are not directly due to activation of ECM synthesis pathways but rather due to activation of ECM degradation inhibition pathways such as TIMP1.

3.8. Inhibition of JAKs attenuated pro-fibrosis gene expression

To determine if the increased activation of the JAK/STAT pathway was involved in the early increase in regulation of pro-fibrotic gene expression by dhS1P and S1P, the JAKs inhibitor, P6, was used. As shown in Fig. 5a & c, P6 significantly inhibited the increase in TGFβ; $p < .01$, & $p < .05$, TIMP1; $p < .005$ & $p < .01$, and SK1; $p < .005$ & $p < .05$, genes expression at 6 h stimulation by both dhS1P (Fig. 5a) and S1P (Fig. 5c), respectively. These results show that the JAKs are involved in downstream transmission of cellular signals activated by extracellular dhS1P and S1P that leads to increase in TGFβ, TIMP1, & SK1 genes. S1P signalling is known to increase TGFβ genes expression which subsequently increases SK1 gene expression [6] [23]. Our results show that dhS1P may also have similar effects.

3.9. DhS1P and S1P induced increase in TGFβ, and SK1 mRNA through S1PR1 activation

Since, the S1PR1 agonist led to increase in collagen synthesis phenotypically, we investigated whether the inhibition of S1PR1 by W146 could inhibit the increase in TGFβ, SK1 and TIMP1 mRNA expression. Our results show that both dhS1P and S1P caused a significant increase in S1PR1 mRNA at 6 h (Fig. 5e). Surprisingly, inhibition of S1PR1, did not inhibit TIMP1 mRNA expression in NCFs, for both dhS1P and S1P (Fig. 5b & d), implying that at this time point the increase in TIMP1 by S1P and dhS1P is not dependent on S1PR1 activation alone. This may be due to S1P and dhS1P increasing TIMP1 expression through a signalling cascade that involves the other S1P receptors at this time point, even though S1P increased S1PR1 mRNA was greater than dhS1P, Fig. 5e. Additionally, Fig. 5e also shows that S1P significantly increased S1PR3 ($p < .05$) expression while, dhS1P caused significant increase in mRNA expression of both S1PR2 ($p < .01$) and S1PR3 ($p < .05$) at

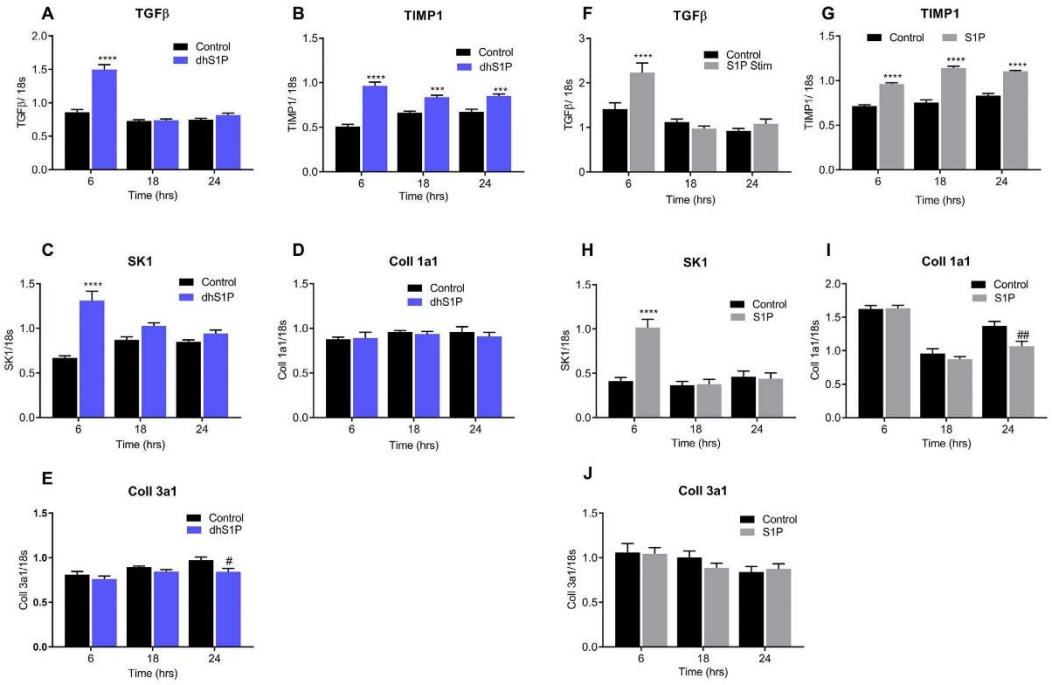

Fig. 4. Time course analysis of extracellular S1P and dhS1P induced RNA expression in NCFs. a 3 μM dhS1P caused significant increase in expression greatly increased TGFβ at 6 h, b TIMP1 was increased throughout all time points, c SK1 was increased at 6 h, d had no effect on Coll1a1 reduced Coll1a1 at 24 h and, e reduced Coll3a1 at 24 h$^{***}p < .005$, $^{****}p < .001$, & $^{\#}p < .05$ vs. control. f 1 μM S1P greatly increased TGFβ at gene expression at 6 h, g increased TIMP1 at all-time points, h SK1 increased only at 6 h, i reduced Coll1a1 at 24 h and, j had no effect on Coll3a1. $^{****}p < .001$ and $^{\#\#}p < .01$ vs. control. Values are presented as ± SEM of at least 3 replicates with two independent repeats.

6 h. Others have implicated S1PR2 as the target through which S1P increased collagen synthesis at 48 h [23]. The inhibition of S1PR1 by W146 did reduce SK1 mRNA expression induced by dhS1P (Fig. 5b) at the higher dose, and produced a significant dose dependent reduction for S1P induced SK1 ($p < .005$, Fig. 5d) and TGFβ ($p < .05$) mRNA.

3.10. JAKs are involved in specific S1PR1 agonist mediated increase in fibrotic gene markers

Due to the partial nature of S1PR1 involvement in NCFs when activated by dhS1P and S1P, we investigated whether SEW2871, the S1PR1 specific agonist, was able to increase expression of the fibrotic markers in NCFs. The treatment of NCFs with SEW2871 for 18 h significantly increased the genetic expression of TGFβ, TIMP1 and Coll 1a1 as shown in Fig. 6a-c. These findings are similar to those reported by Shea et.al [25], in terms of lung fibrosis, where prolonged exposure to SEW2871 led to increased fibrosis and vascular leakage. Our results also show that inhibiting JAKs did reduce the expression of levels of these fibrotic markers; TGFβ ($p < .001$, Fig. 6a), TIMP1 ($p < .01$, Fig. 6b) & Coll1a1 ($p < .01$, Fig. 6c), significantly. This finding supports our proposition that a dhS1P and S1P induced TIMP1 is not dependent on S1PR1, since these ligands do bind to multiple receptors.

3.11. Inhibition of JAKs reduces dhS1P and S1P induced increase in cellular TGFβ protein secretion and activation

Since there were no changes in gene expression of TGFβ at the later time points of 18 h and 24 h, we then investigated whether there were any changes in cellular protein levels of TGFβ at 24 h of treatment with dhS1P and S1P. Extracellular activity of TGFβ is regulated by conversion of latent TGFβ to active TGFβ as a result of proteolytic degradation of the latency associated protein (LAP) which renders TGFβ inactive. TGFβ proteins are synthesized as latent precursor molecules (LTGF-β) in a complex with latent TGFβ binding protein (LTBP) [26] which forms the large latent complex (LLC), which is secreted and stored in the ECM [27]. dhS1P increased the levels of both the 65 ($p < .01$) and 45 kDa latent TGFβ protein, but P6 inhibited only the 65 kDa ($p < .005$) TGFβ as shown in Fig. 7a. P6 also significantly reduced dhS1P increased protein expression of the 12 kDa TGFβ monomer ($p < .05$) and 25 kDa mature ($p < .05$) TGFβ levels. Similar effects were also observed in S1P treated cells. S1P significantly increased the expression of latent TGFβ proteins (65 kDa; $p < .0001$, and 45 kDa; $p < .001$) and the 12 kDa ($p < .05$) TGFβ monomer, which were significantly inhibited by P6 ($p < .001$, $p < .05$, & $p < .05$, respectively), Fig. 7b. These increases in latent TGFβ and mature TGFβ indicate that S1P and dhS1P did increase secretion of TGFβ in NCFs that could result in the fibrotic effect observed in the phenotypic collagen sensitive ^{3}H proline incorporation assay. The proteolytic action of the MMPs and integrins ($\alpha_V\beta_6$ and $\alpha_V\beta_8$) cleave TGFβ from LAP releasing it from the ECM and allowing it to bind to the TGFβ receptor [28]. However, due to MMPs being completely reduced by dhS1P and S1P (Fig. 8) the increase did not activate the canonical TGFβ signalling pathway that is known to increase the expression of fibrotic gene markers such as collagen. It should be noted that P6 was also able to reduce dhS1P stimulated

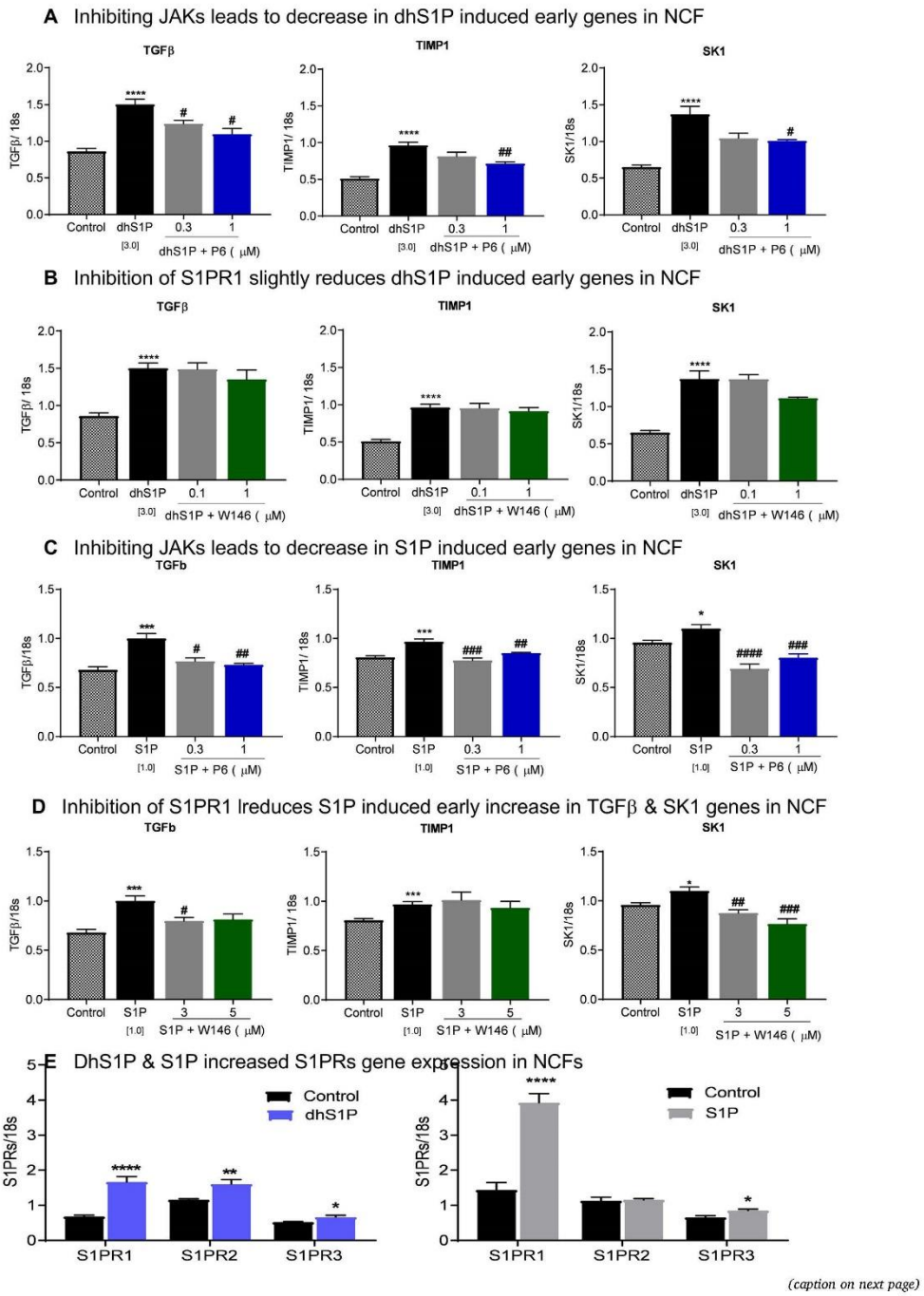

(caption on next page)

Fig. 5. Inhibition of JAKs leads to reduction in genes increased by S1P or dhS1P/S1PRs signalling. a TGFβ, TIMP1 & SK1 genes were dose dependently reduced when JAKs was inhibited in dhS1P treated NCFs, $^{\#}p < .05$, $^{\#\#}p < .01$, $^{\#\#\#}p < .005$ vs. dhS1P. b Inhibiting S1PR1 in dhS1P treated NCFs had less effect on the raised TGFβ, TIMP1, & SK1. c In S1P treated NCFs TGFβ, TIMP1 & SK1 genes were dose dependently reduced when JAKs was inhibited, $^{\#}p < .05$, $^{\#\#}p < .01$, $^{\#\#\#}p < .005$ & $^{\#\#\#\#}p < .001$ vs. S1P. d TGFβ & SK1 were significantly inhibited when S1PR1 was inhibited in S1P treated NCFs, but there was less effect on the increased TIMP1, $^{\#}p < .05$, $^{\#\#}p < .01$, $^{\#\#\#}p < .005$ vs. S1P. e dhS1P increased S1PR1–3 were significantly at 6 h, while S1P increased S1PR1 & 3, $^{*}p < .05$, $^{***}p < .005$ & $^{****}p < .001$ vs. control. Values are presented as ± SEM of at least 3 replicates with two independent repeats,

increase in TIMP1 protein levels at 24 h (Fig. 7c).

3.12. dhS1P and S1P had a delayed effect on pSMAD2 activation

We then investigated SMAD2 phosphorylation, to determine if it is involved in dhS1P and S1P mediated intracellular signalling. The activation of TGFβ causes phosphorylation of the TGFβ receptors 1 & 2 leading to activation of downstream targets. The primary target of this activation is the SMAD family of proteins, including SMAD2, resulting in the activation of the canonical TGFβ/SMAD signalling pathway. NCFs treated with S1P and dhS1P showed that they did increase the phosphorylation level of SMAD2 at 30 min of treatment, Fig. 7c & d. Even though treatment with P6 did lead to reduced activation of phosphorylated SMAD2 levels in both dhS1P and S1P stimulations, these were not statistically significant. The slow activation of SMAD2 by S1P was also observed in mesangial cells [29], and may be the result of non-canonical pathways such as the Erk/MAPK pathway being activated [30]. This supports and implies that the canonical TGFβ/SMAD signalling pathway may not be the primary cause of extracellular dhS1P and S1P induced increase in collagen synthesis.

3.13. JAKs are involved in the phosphorylation of c-JUN by dhS1P and S1P

Since TIMP1 has the AP-1 response element to which SK1 binds to [6], we investigated whether P6 was able to inhibit the phosphorylation of c-JUN, a component of the AP-1 transcription factor. Our results in Fig. 8a show that both dhS1P and S1P slightly increased phosphorylation of c-JUN, and were significantly reduced when JAKs was inhibited by P6, $p < .05$, and $p < .01$, respectively. Fig. 8b also shows that W146, the S1PR1 antagonist caused a further increase in c-JUN at the higher doses, even though this was statistically insignificant. However, this result supports the previous results (Fig. 5b & c) for gene expression where W146 was unable to inhibit TIMP1 mRNA increase.

3.14. dhS1P and S1P caused myocyte hypertrophy

We then compared the effects of extracellular dhS1P to S1P in causing hypertrophy, in cardiac myocytes isolated from 1 to 2 days old rat pups. Previous experiments have shown both hypertrophic [31] and anti-hypertrophic [32,33] effects of S1P, depending on the conditions under which it has been investigated. Our results in Fig. 9a show that 1 μM and 3 μM dhS1P was also able to induce statistically significant

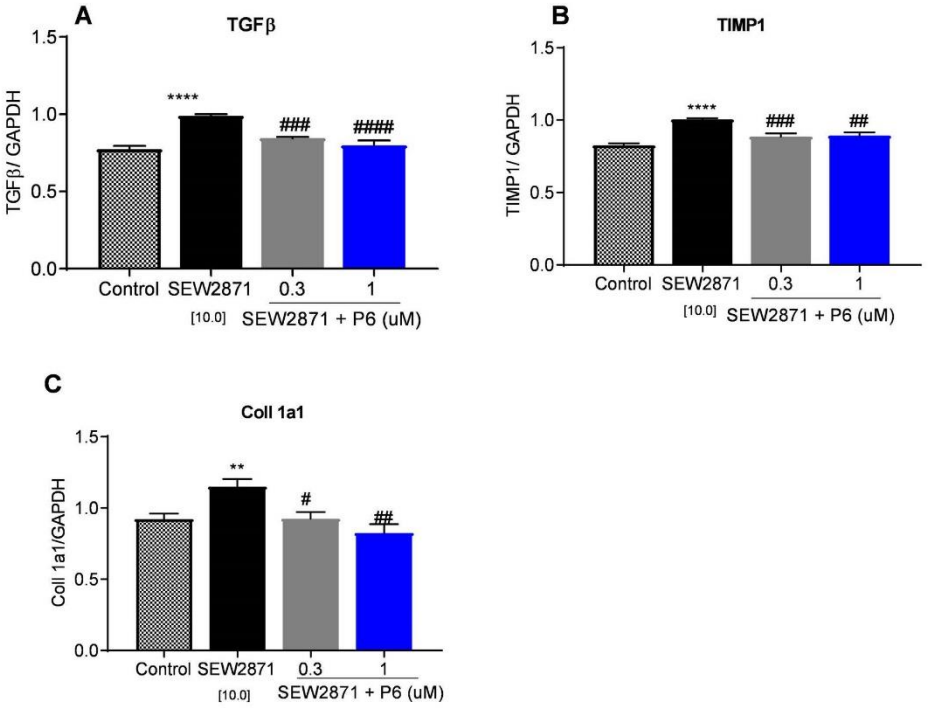

Fig. 6. Inhibition of JAKs reduced mRNA levels of fibrotic markers increased by activation of S1PR1. a The S1PR1 specific agonist, SEW2871, increased TGFβ, $p < .0001$ vs. control, b TIMP1, $p < .0001$ vs. control and, c Coll1a1, $p < .001$ vs. control. These were significantly reduced when JAKs were inhibited by P6. Values are presented as ± SEM of at least 3 replicates with two independent repeats, $^{\#}p < .05$, $^{\#\#}p < .01$, $^{\#\#\#}p < .005$ & $^{\#\#\#\#}p < .001$ vs. SEW2871.

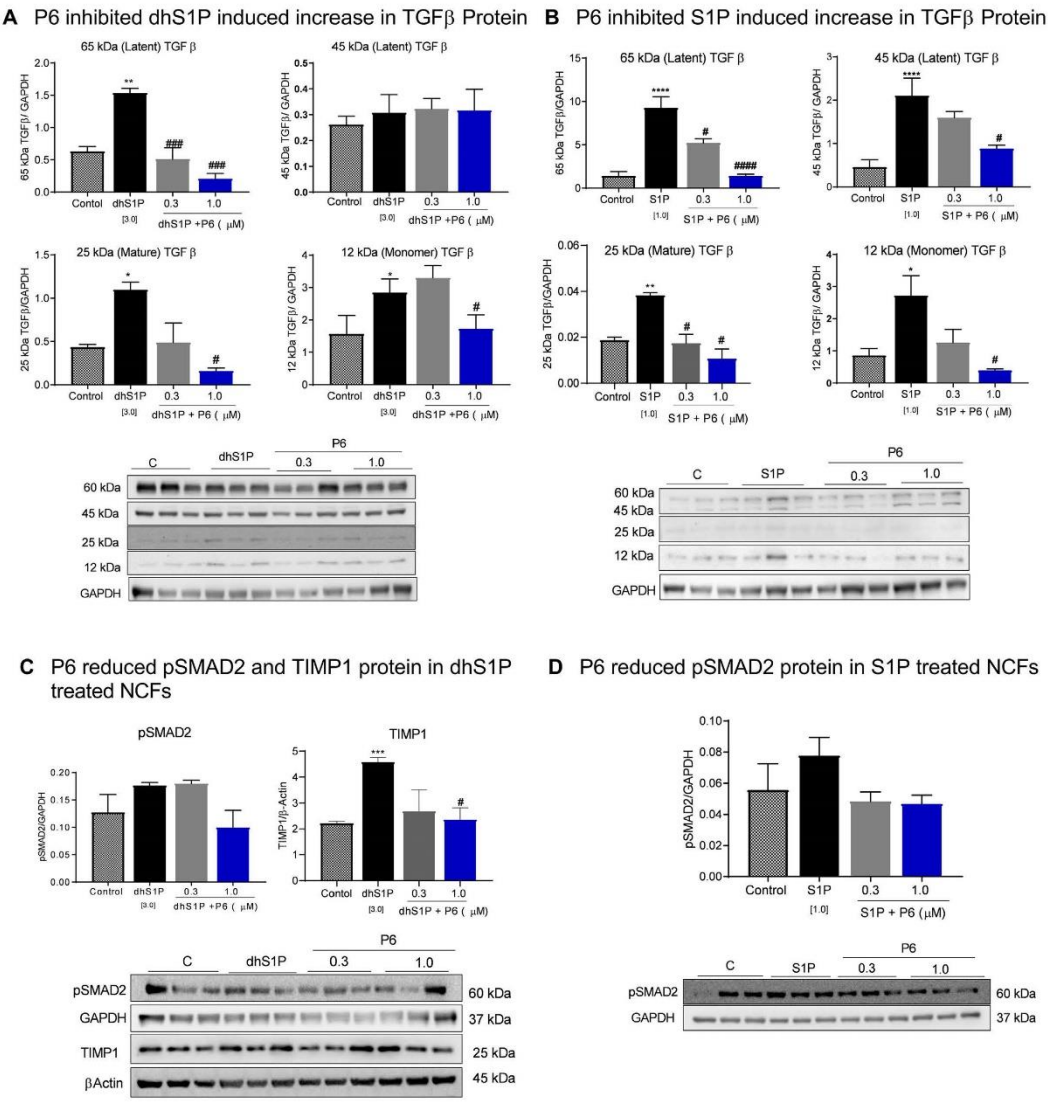

Fig. 7. P6 reduced TGFβ protein expression and pSMAD2 activation by dhS1P and S1P. a dhS1P increased the protein expression of TGFβ isoforms of 65, 45, 25 & 12 kDa in NCFs at 24 h, while P6 inhibited all except the 45 kDa. b S1P also increased the 65, 45, 25 & 12 kDa TGFβ isoforms and all were inhibited by P6 at 24 h. c dhS1P activated pSMAD2 at 30 min of treatment was inhibited by P6 at the highest dose, and P6 also reduced TIMP1 protein expression at 24 h. d S1P activated pSMAD2 was also inhibited by P6, but both were statistically insignificant. $^{*}p < .05$, $^{**}p < .01$, $^{****}p < .001$, vs. control & $^{\#}p < .05$, $^{\#\#}p < .01$, $^{\#\#\#}p < .005$ vs. treatment. Values are presented as ± SEM of at least 3 replicates with two independent repeats.

hypertrophic effects when treated within 48 h ($p < .05$), 60 h ($p < .05$) and 72 h ($p < .05$), and within 48 h ($p < .05$) and 72 h ($p < .01$), respectively. This was comparatively lower than S1P at similar dose and time points and 10 nM Ang II at 60 h (Fig. 11). It should be noted that 1 μM S1P induced hypertrophic effects were similar to that of Ang II at 60 h (Fig. 11b). In addition, 48 h stimulation of NCMs with different doses of dhS1P (0.1, 1, 3 & 10 μM) did not reduce their viability as measured by the Almar blue assay, while S1P significantly reduced NCM viability at 10 μM, Fig. 10d.

3.15. Inhibition of JAKs slightly reduced dhS1P and S1P induced NCM hypertrophy

We then evaluated whether inhibition of JAKs led to a reduction in

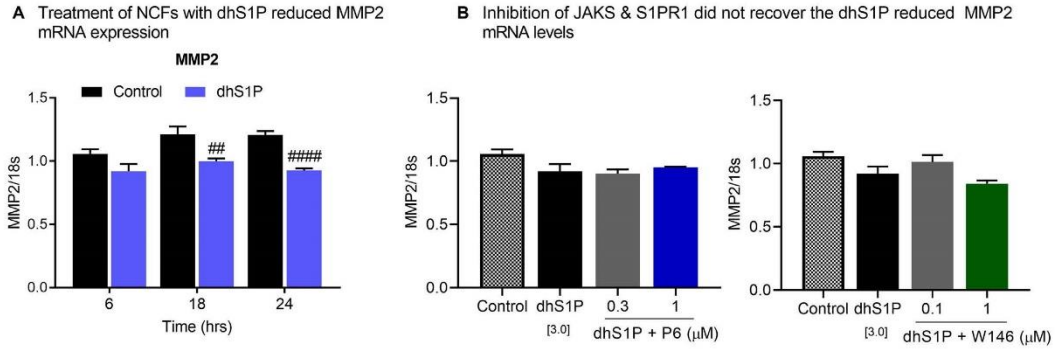

Fig. 8. Effect of dhS1P on MMP2 mRNA & protein. a dhS1P significantly reduced MMP2 mRNA expression at 18 and 24 h. b MMP2 mRNA expressions did not increase when cells were treated with P6 and W146 for 6 h. $^{\#\#}p < .01$, $^{\#\#\#\#}p < .001$, vs. control. Values are presented as ± SEM of at least 3 replicates with two independent repeats.

the hypertrophic effects induced by dhS1P at 48 h, and S1P at 60 h in NCMs. Phenotypically, the addition of P6 significantly reduced the dhS1P induced hypertrophic effects at the three higher doses; 0.1 μM ($p < .01$), 0.3 μM ($p < .05$) and 1 μM ($p < .05$), Fig. 10b. Comparatively, P6 did not reduce myocyte hypertrophy induced by extracellular S1P, indicating JAK/STAT pathway maybe involved in extracellular dhS1P but not S1P induced myocyte hypertrophy. JAK/STAT signalling in cardiac myocytes can either be cardio-protective or cardio-offensive, depending on the disease state and type of injury or insult. In terms of S1P induced activation of the JAK/STAT pathway, increased JAK/STAT signalling in ischaemic reperfusion injury has been shown to be cardio-protective [9].

3.16. Inhibition of S1PR1 had little effect on dhS1P and S1P induced NCM hypertrophy

The S1P/S1PR1 axis in NCMs is also known to be cardio-protective against the effects of β_1-adrenergic receptor (β1AR) overstimulation in heart failure [34]. Therefore, we compared the effects of S1PR1 inhibition on dhS1P and S1P treated NCMs. Phenotypically, the treatment with W146 had no statistically significant effect on hypertrophy induced by extracellular dhS1P and S1P, Fig. 10c. This is despite both showing some reductions in myocyte hypertrophy.

3.17. Inhibiting JAKs reduced dhS1P stimulated STAT1 phosphorylation and S1P stimulated STAT1/3 phosphorylation in NCM

We then determined if there was any difference in the levels of phosphorylated STAT1 and STAT3 proteins in NCMs stimulated with dhS1P and S1P. Both dhS1P and S1P significantly increased phosphorylated STAT1 ($p < .05$, Fig. 12a & b) at 15 min of stimulation in NCMs. The addition of P6 significantly inhibited S1P stimulated STAT1 phosphorylation at the highest dose of 1 μM ($p < .05$, Fig. 12b). P6 did not have inhibitory effects on dhS1P stimulated phosphorylation of STAT1. At the 15 min time point the increase in phosphorylated STAT3 was not significant in S1P treated cells, but P6 abrogated its expression, Fig. 10b. In contrast, dhS1P stimulation significantly reduced phosphorylated STAT3 ($p < .05$, Fig. 12a), and the addition of P6 rescinded it further. For S1P, these findings are expected since it has been shown to increase activation of pSTAT3 following myocardial infarction (MI) [7]. However, for dhS1P we show for the first time that it seems to affect phosphorylated STAT1 and STAT3 in NCMs differently.

3.18. The dhS1P/ S1PR1 axis is required for JAKs/STAT1 activation, and not JAKs/STAT3 activation in NCMs

To determine whether the dhS1P/ S1PR1 axis was involved in

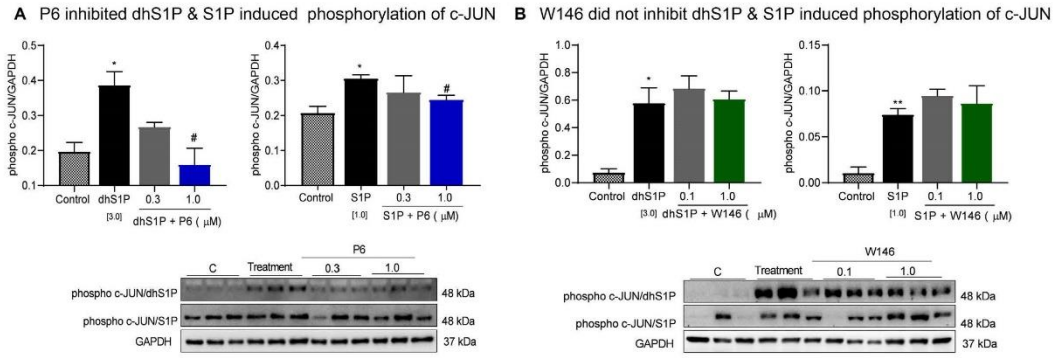

Fig. 9. c-JUN phosphorylation by dhS1P and S1P was inhibited by P6 and not W146. a P6 reduced dhS1P & S1P phosphorylated c-JUN at 15 min of treatment. b While, W146 did not reduce dhS1P and S1P phosphorylation of c-JUN. $^{*}p < .05$, vs. control & $^{\#}p < .05$, $^{\#\#}p < .01$ vs. stimulants. Values are presented as mean ± SEM of at least 3 replicates with two independent repeats.

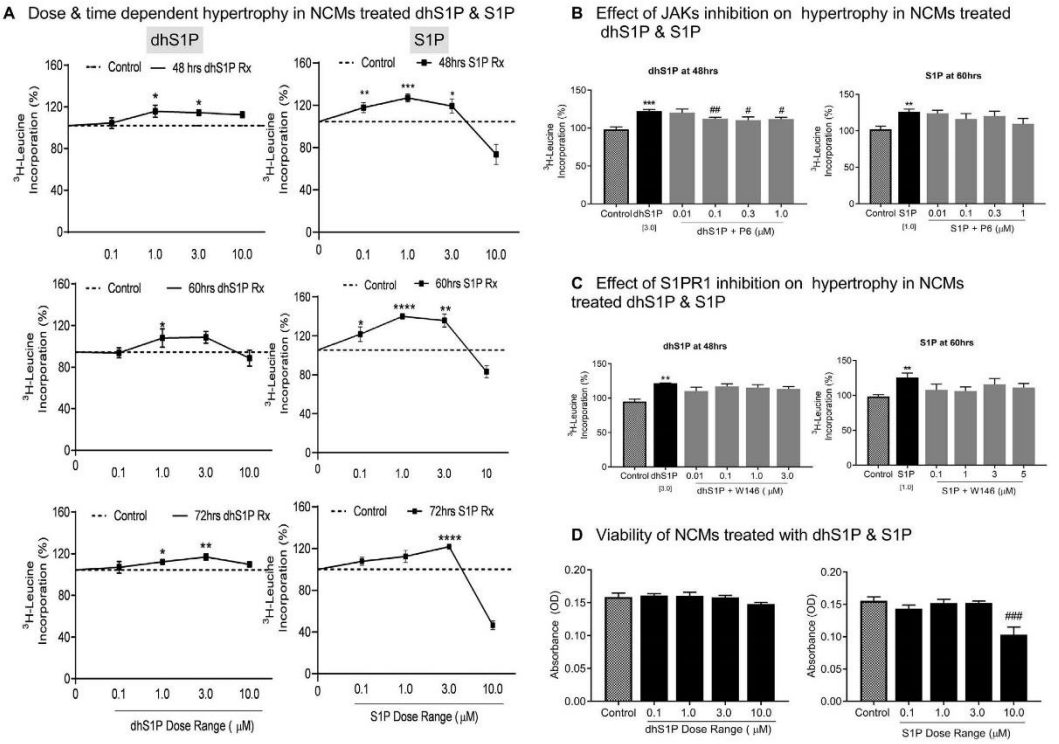

Fig. 10. dhS1P & S1P induced myocyte hypertrophy was inhibited by P6. a ^{3}H-Leucine incorporation assay showing cardiac myocyte hypertrophy induced by dhS1P and S1P in NCM at 48, 60 & 72 h, at dose ranges of 0.1, 1, 3 & 10 μM. Ang II was used as positive control (data not shown). b Inhibition of JAKs led to reductions in hypertrophy induced by dhS1P and S1P, however these reductions were insignificant for S1P. c Inhibition of S1PR1 had varying degrees of inhibition across the different doses in both dhS1P and S1P treated NCMs, which were not significant. d 0.1, 1, 3, & 10 μM dhS1P treatment alone at 48 h did not reduce the viability of NCMs as, while S1P reduced NCM viability at 10 μM asmeasured by Almar Blue assay. Data is representative of at least 4 replicates at each time point and dose with 3 repeated experiments. $^{*}p < .05$, $^{**}, p < .01$, $^{***}p < .005$, $^{****}p < .001$ vs. Control, $^{\#}p < .05$, $^{\#\#}p < .01$, $^{\#\#\#}p < .005$ vs. stimulant. Values are presented as ± SEM of four independent experiments at each time point with three replicates in each.

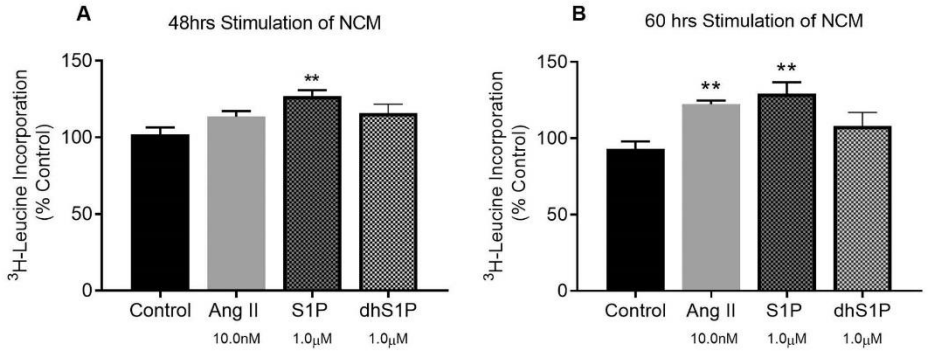

Fig. 11. Comparative hypertrophic effect of Ang II/S1P/ dhS1P. a At 48 h of treatment 10 nM Ang II & 1 μM dhs1P did not increase hypertrophy, while 1 μM S1P did. b At 60 h of treatment, 10 nM Ang II and1 μM S1P increased hypertrophy while 1 μM dhS1P did not. $^{**}p < .01$ vs. Control. Values are presented as ± SEM of four independent experiments at each time point with three replicates in each.

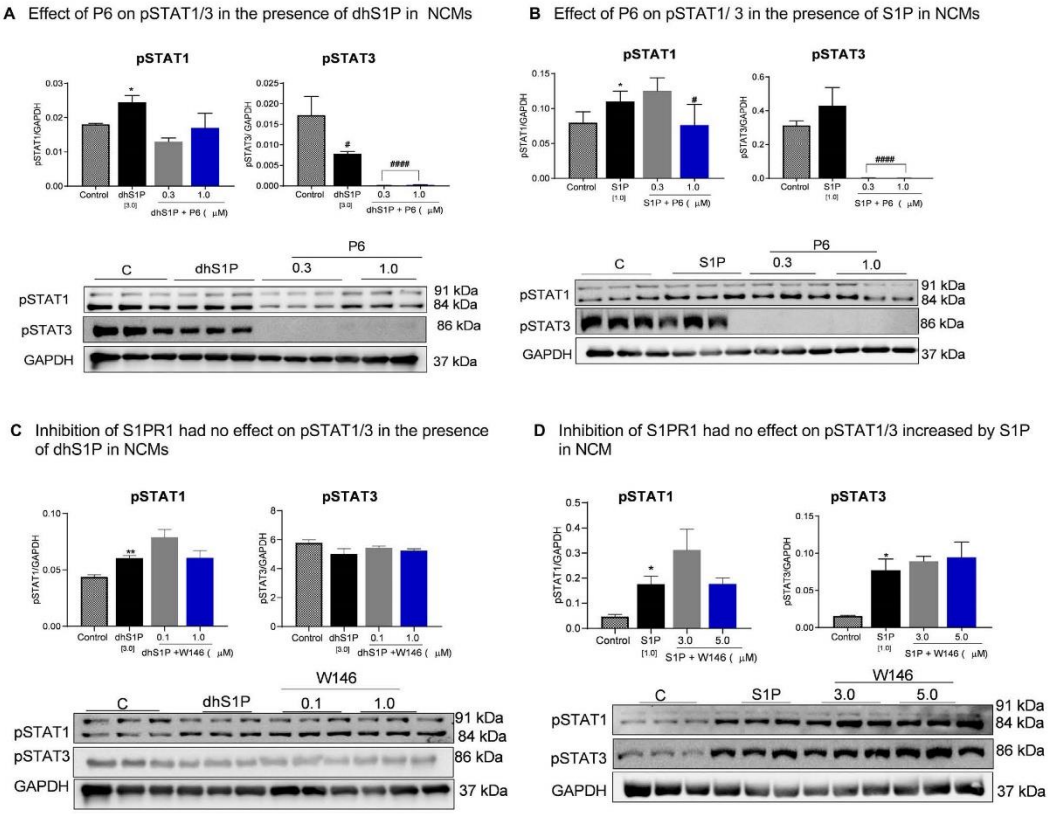

Fig. 12. dhS1P/S1PR1 axis activates pSTAT1 & deactivates pSTAT3, while S1P/S1PR1 axis activates pSTAT1 but not pSTAT3. a P6 inhibited 3 μM dhS1P stimulatedSTAT1 phosphorylation, and completely abrogated dhS1P dephosphorylated STAT3, b P6 inhibited 1 μM S1P stimulated STAT1, and STAT3 phosphorylation. c & d Inhibition of S1PR1 did not affect STAT1 and STAT3 phosphorylation in NCMs treated with dhS1P & S1P, respectively.. $^{**}p < .01$ vs. control and, $^{\#}p < .05$ vs. stimulant. Values are presented as mean ± SEM of at least 3 replicates with two independent repeats.

activating JAKs/STAT1 and 3 pathways, the specific S1PR1 antagonist, W146, was used. W146 was not able to reduce the phosphorylation levels of STAT1 stimulated by both dhS1P (Fig. 12c) and S1P (Fig. 12d), however this was not statistically significant. The lack of effect on phosphorylated STAT1 by W146 indicates that the S1P & dhS1P/S1PR1 axis is not involved in activation of JAKs/STAT1 signalling in myocyte hypertrophy. STAT3 plays differing roles in cardiac myocytes depending on the type of stimulant or insult in both physiological and pathophysiological states. Inhibition of S1PR1 in S1P treated NCMs had no effect on pSTAT3 (Fig. 12d) although this was not significant. This indicates that the phosphorylation of STAT3 is not dependent on the S1P/S1PR1 axis. In comparison, W146 had no effect on the reduced phosphorylation of STAT3 by dhS1P (Fig. 12c), implying that the reduction in STAT3 by dhS1P may not be S1PR1 dependent.

3.19. Inhibition of JAKs in NCMs led to synergistic increase in expression of myocyte hypertrophy gene markers by dS1P and S1P

We then investigated if there were any changes in the expression of certain hypertrophic markers in the NCMs by dhS1P and S1P. Both S1P ($p < .001$–0.0001, Fig. 13a) and dhS1P ($p < .0001$, Fig. 13b) significantly increased the expression of all of the hypertrophic markers investigated. The addition of P6 caused significant synergistic increases in βMHC ($p < .01$, ANP ($p < .005$) and BNP ($p < .005$) by dhS1P, and αSKA ($p < .01$) by S1P as shown in Fig. 13a & b, respectively. ANP and BNP secretion is increased as a counter measure by myocytes in response to the increased hypertrophic stimuli [35], indicated by the increase in βMHC. Apart from the JAK/STAT pathway other pathways are also known to be involved in signalling ANP and BNP increase which may account for the synergistic increase. These result indicate that inhibition of JAKs in dhS1P induced NCM hypertrophy may not be sufficient to reduce the hypertrophic genes. However, P6 had no effect on S1P induced ANP, BNP and βMHC, and dhS1P induced αSKA as shown in Fig. 13a & b, respectively. The differing effects on αSKA expression by JAKs inhibition in S1P and dhS1P treated NCMs Show that inhibition of JAKs in S1P treated cells may have a greater hypertrophic effect than dhS1P. αSKA expression is known to be increased in proportion to the progression of hypertrophy [36]. Considering that other hypertrophic signalling pathways could possibly be simultaneously activated, it may account for the disparities between our phenotypic, protein and gene expression results in terms of JAKs inhibition.

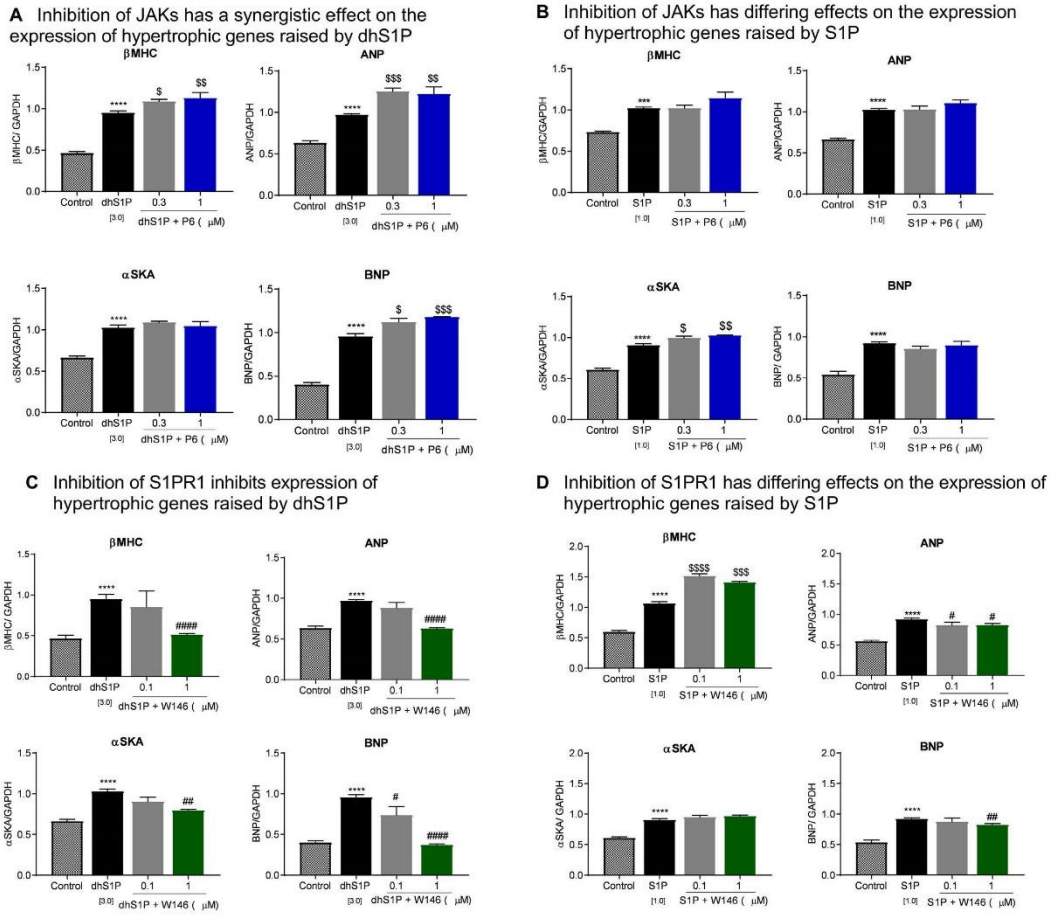

Fig. 13. Inhibition of JAKs and S1PR1 have opposite effects on dhS1P and S1P increased expression of myocyte hypertrophy gene. Both 3 μM dhS1P and 1 μM S1P significantly increased mRNA expression of βMHC, ANP, αSKA and BNP at 18 h of treatment, $^{***}p < .005$ & $^{****}p < .001$ vs. control. a JAKs inhibition caused significant synergistic effects on βMHC, & BNP mRNA increase by dhS1P, and had no effect on αSKA mRNA. b JAKs inhibition had significant synergistic effect on αSKA mRNA increased by S1P, with slight increases in βMHC, & ANP mRNA, and no effect on BNP mRNA. c All hypertrophy gene markers were significantly reduced when S1PR1 was inhibited in dhS1P stimulated cells. d Inhibition of S1PR1 led to significant reductions in ANP and BNP, synergistic increase in βMHC and no effect on αSKA mRNA in S1P treated cells. $^{\#\#}p < .01$, $^{\#\#\#\#}p < .001$, $^{\$}p < .05$, $^{\$\$\$}p < .005$, $^{\$\$\$\$}p < .001$ vs. Stimulant. Values are presented as mean ± SEM of at least 3 replicates with two independent repeats.

3.20. dhS1P/S1PR1 axis signalling is involved in increased mRNA expression of myocyte hypertrophy markers

We then determined whether the increase in the mRNA expression of the hypertrophic markers were due to increased activation of S1PR1 by dhS1P and S1P. W146 significantly inhibited all the hypertrophic markers increased by dhS1P (βMHC; $p < .0001$, ANP; $p < .0001$, αSKA; $p < .001$ & BNP; $p < .0001$), as shown in Fig. 13c. This suggests that dhS1P induced myocyte hypertrophy maybe S1PR1 dependent, through other signalling pathways. The inhibition of S1PR1 by W146 caused a significant synergistic increase in βMHC expression ($p < .0001$), while significantly reducing ANP ($p < .05$) and BNP ($p < .01$) expression, and had no effect on αSKA gene expression stimulated by S1P as shown in Fig. 13d. These findings support those reported by others showing that S1P/S1PR1 signalling in NCMs is cardio-protective [34,37], since ANP and BNP are increased as antagonistic responses to hypertrophic effects.

4. Discussion

S1Ps role in cardiac remodelling through its receptors whether in cell or animal studies has been highlighted by many over the years, although not fully explored. Its role in inflammation and cancer biology is becoming an area for target therapy. On the other hand, S1P signalling through the JAK/STAT pathway is less understood especially in terms of cardiac fibroblasts. dhS1P's overall effect on the cardiovascular system and especially cardiac remodelling to our knowledge has not been investigated. It's level in plasma is known to be altered and has

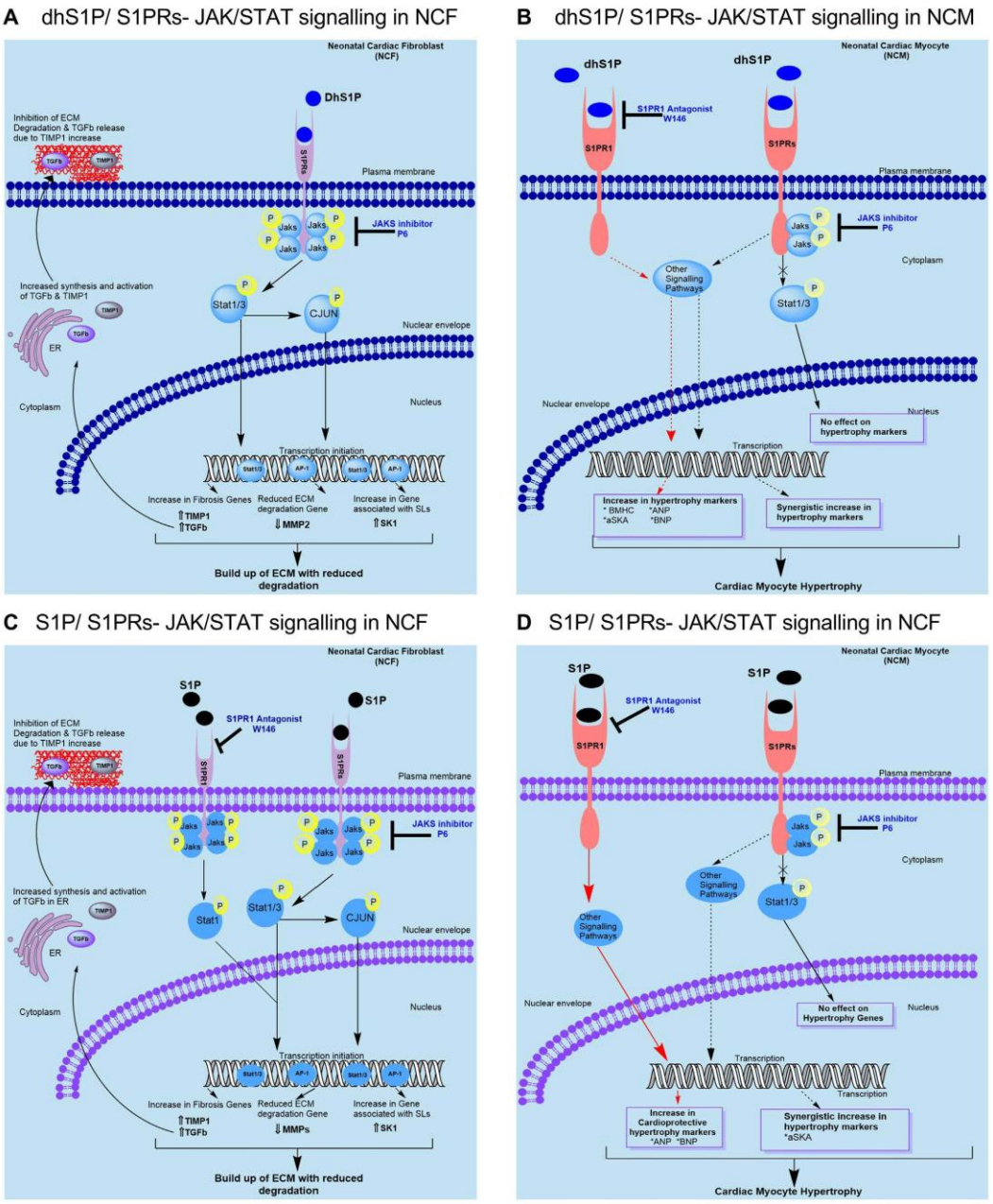

(caption on next page)

Fig. 14. Summary of dhS1P/S1P/S1PR1-JAKs/STAT signalling in NCFs and NCMs. **a** Exogenous dhS1P activates the JAKs/STAT signalling pathway in NCFs through the S1PRs. The phosphorylation of STAT1/3 together with c-JUN leads to their nuclear translocation and increase in the transcription of fibrotic genes; TGFβ & TIMP1, SL synthesis related gene; SK1, and reduces ECM degradation gene; MMP2. The increase in TGFβ mRNA encourages increase in TGFβ secretion, activation and transport to the ECM from the endoplasmic reticulum (ER). However, due to the abundance of TIMP1, ECM degradation and TGFβ release is inhibited, resulting in ECM accumulation. The inhibition of JAKs by P6, was able to inhibit the dhS1P/S1PRs-JAKs/STAT-TIMP1 signalling. **b** In NCMs exogenous addition of dhS1P activates JAKs/STAT signalling pathway through S1PR1. The effect of STAT1/3 phosphorylation and translocation to the nucleus has no effect on the transcription of hypertrophy genes such as βMHC, αSKA, ANP & BNP (bold black arrow). However, the inhibition of JAKs synergistically increases these markers through other pathways (dashed black arrow). dhS1P/S1PR1 axis signalling through other pathways can cause myocyte hypertrophy by increasing the hypertrophy markers (bold red arrow). **c** Exogenous S1P activates JAKs/STAT pathway similarly to dhS1P in NCFs. S1P is also able to increase collagen synthesis in NCFs through the S1P/S1PR1/JAKs/STAT1 signalling cascade. **d** In NCMs, S1P activation of JAKs/STAT signalling also has no effect on hypertrophy gene markers (bold black arrow). However, it may have synergistic effects on the expression of αSKA genes (dashed black arrow). The S1P/S1PR1 may activate other pathways to that encourage increased expression of cardio-protective hypertrophy markers such as ANP and BNP (bold red arrows). The inhibition of S1PR1 by W146, reduces the levels of these hypertrophy genes. However, the inhibition of JAKs by P6, may lead to increased activation of other signalling pathways resulting in synergistic increase in the myocyte hypertrophy genes. Illustration derived through ChemDraw Professional 17.0 (Perkin Elmer, Waltham, MA, USA). (For interpretation of the references to colour in this figure legend, the reader is referred to the web version of this article.)

recently been linked to increased cardiac dysfunction in aging, where cardiac remodelling is known to occur [38]. One of the major goal of this study has been to determine the role of the JAK/STAT pathway in terms of dhS1P and S1P signalling and for the first time describe any differences in signalling by these sphingolipid analogues.

Here we show that extracellular dhS1P is able to increase primary NCF collagen synthesis similar to that of S1P. Similarly, both sphingolipids activated STAT1 and 3 proteins by signalling through S1PRs-JAK/STAT pathway. It is interesting to note that both caused an early increase in the expression of TGFβ gene and even at 24 h of treatment, TIMP1m RNA rather than TGFβ mRNA was still increased. Our results show that the early increase in TGFβ mRNA expression was accompanied by an early increase in SK1 mRNA, which was reduced together with TGFβ at 24 h. In dermal fibroblasts TGFβ was shown to induce SK1 [6], and that SK1 co-operated with TGFβ to mediate the increase in TIMP-1. In addition, others have shown that SK1 upregulation alone increased TIMP1 but had no effect on TGFβ [39]. However, since TIMP1 mRNA remained significantly high even after 24 h stimulation, with receding SK1 and TGFβ mRNA expression, it can be assumed that the extracellular dhS1P and S1P induced fibrosis in rat NCFs was primarily due to the sustained TIMP1 activation. See summative diagram in Fig. 14a & c.

This led us to investigate c-JUN protein activation, since TIMP1 harbours an AP-1 response element on its promoter site [6]. The reduced activation of c-JUN proteins by dhS1P and S1P when JAKs was inhibited and not when S1PR1 was inhibited showed that S1P and dhS1P potentially signalling through JAK/STATs-AP-1- TIMP1 pathway and is not S1PR1 dependent. Furthermore, STAT3 and not STAT1, interacts with c-JUN [40]. Apart from these interactions, TIMP1 also harbours a functional binding site for STAT3 [41]. TIMP1 is an effective inhibitor of the proteolytic degradation of the ECM by factors such as the MMPs, which results in the accumulation of ECM products [42]. A recent study indicated that TIMP1 is capable of causing de novo collagen synthesis by activating SMAD2/3 and β-catenin in in-vivo models of cardiac fibrosis which were independent of MMPs [43]. Studies on neuronal progenitor cells using pharmacological inhibition of sphingolipid pathway have shown that dhS1P increases SMAD2 to a greater degree than S1P, which has an effect on proliferation and differentiation [44].

Since TGFβ signalling is regulated by the balance between TIMPs and MMPs, the sustained activation of TIMP1 may have a feedback inhibition effect on the transcription of TGFβ, but not on its post transcriptional secretion and activation, as shown by the increased TGFβ protein levels at 24 h of treatment by both S1P and dhS1P. The increased TIMP1 led to a significant reduction in MMP2 activity, up to 20% at 24 h compared to control in dhS1P stimulated NCFs, and did not recover when P6 and W146 were added (Fig. 8). The lack of recovery through the S1PR1/JAKs/STAT signalling indicate that these effects on MMP2 maybe through other signalling cascades. While, the downstream signalling of JAK/STAT pathways in increasing TIMP1 mRNA may have contributed to the accumulation of TGFβ protein.

The effects of dhS1P and S1P may not be receptor subtype specific, even though the effects of both were greatest on the early increase in S1PR1 mRNA expression. Clinically the plasma concentration of dhS1P and S1P have been found to be reduced within the first 6 h after an MI [45,46]. Whether this is a cumulative effect or as a result of the MI remains yet to be determined. While, in animal models of MI, the expression of S1PR1 has been found to be reduced [34], thus the authors suggested S1PR1 targeted gene therapy. In contrast, our results show that perhaps long term activation of S1PR1 alone could aggravate fibrosis. It is also possible that the initial increase in TGFβ may contribute to reparative fibrosis rather than reactive fibrosis at the initial onset of injury such as an MI.

The JAK/STAT signalling pathway in cardio-myocytes is known to be protective, especially STAT3 [47]. Our findings for the gene expression of hypertrophic markers support this and show that inhibition of JAKs in dhS1P and S1P treated cells could further aggravate the hypertrophy, Fig. 14b & d. Clinically, hypertrophic markers such as BNP and ANP are considered as compensatory mechanisms in terms of heart failure [35]. Their increase in experimental conditions highlight the hypertrophic effects of the agents used. In our study, the synergistic increase in ANP and BNP mRNA levels despite inhibition of JAKs/STATs signalling indicated the existence of other hypertrophic signals. This may be the reason for the minimal yet significant anti-hypertrophic effects exhibited phenotypically in our study when JAKs were inhibited. Our findings also show that dhS1P and S1P have similar activating effects on the mRNA expression of βMHC and αSKA in NCMs. However, the inhibition of JAKs and S1PR1 led to deferring effects. There is potential for further investigations in regards to these differences in relation to dhS1Ps effect on pacemaker cells or cardiac electrophysiology. This is in light of the growing number of evidence showing that S1P can have an effect on contractile activity of the heart through S1PR1 and S1PR3 signalling as summarized by Ningjun Li and Fan Zhang [48]. The differences in STAT1/3 protein expression may perhaps be due to, the dichotomous role of the JAK/STAT pathway in myocytes as explained by van Empel *et.al* [49]. The complete abrogation of STAT3 and its lack of activation at similar time points to STAT1 indicate that it's activation by dhS1P maybe a delayed effect. The inhibition of S1PR1 in dhS1P treated cells did not show that myocyte hypertrophy could occur through dhS1P/S1PR1 signalling and maybe ligand dependent since the S1PR1 agonist, SEW2871, stimulated myocyte hypertrophy was lower than that of dhS1P or S1P (Supplementary Fig. 1). This is also supported by the lack of inhibition shown in our phenotypic studies. Additionally, this shows that the effect of dhS1P/S1PR1 signalling is opposite to the effects of S1P/S1PR1 signalling which is reported to be anti-hypertrophic [34,37], and corroborated by our findings on the inhibitory effects of W146 on ANP and BNP gene expression.

In addition, targeting intracellular individual signalling molecules such as JAKS or STATs is likely to have more selective effects than

directly targeted at dhS1P signalling at receptor level. Therefore, it is of particular important to further investigate the role of the individual JAKs or STATs in the functioning of cardiac myocytes and fibroblasts that is likely to produce more effective therapies.

5. Conclusion

The present study establishes the fibrotic effects of extracellular dhS1P on primary cardiac fibroblasts and hypertrophic effects in myocytes. It also shows the dhS1P-JAK/STAT-TIMP1 signalling can increase collagen synthesis in NCFs and possibly have an impact on the mitochondria. While, dhS1P/S1PRs signalling leads to myocyte hypertrophy. These findings also open up the possibility of exploring effects of dhS1P on current trends in cardiac research such as stem cells and further exploration of dhS1Ps effect on cardiac electrophysiology including the roles in pacemaker cells of the heart. In light of current progress in therapies targeting the S1PRs and the de novo sphingolipid synthesis pathway, the impact of these therapies on their targets in other body systems should be considered.

Supplementary data to this article can be found online at https://doi.org/10.1016/j.cellsig.2020.109629.

Funding

This research was supported by National Health and Medical Research Council of Australia (Program Grants 1092642 and Project Grant 1087355.

RM and FS were supported by the Monash University International Post Graduate Research Scholarships.

Credit author statement

Ruth R. Magaye: Data curation and analysis, Methodology, Writing- Original draft preparation, Writing - review & editing

Feby Sevira: Data curation and analysis, Writing- Original draft preparation, Writing - review & editing

Hua Yue: Data curation and analysis, Writing - review & editing

Xin Xiong: Data curation and analysis, Writing - review & editing

Li Huang: Data curation and analysis, Writing - review & editing

Christopher Reid: Writing - review & editing

Bernard Flynn: Writing - review & editing

David Kaye: Writing - review & editing

Danny Liew: Writing - review & editing

Bing H. Wang: Conceptualization, Methodology, Supervision, Writing - review & editing

Declaration of Competing Interest

The authors declare no conflict of interest.

Acknowledgement

The authors acknowledge Monash Micro Imaging, Monash University, for the provision of instrumentation, training and technical support. The authors also acknowledge Dr. Andrew Kompa for lending the αSMA antibody for fluorescence microscopy.

References

[1] A. Cannavo, D. Liccardo, K. Komici, G. Corbi, C. de Lucia, G.D. Femminella, et al., Sphingosine kinases and sphingosine 1-phosphate receptors: signaling and actions in the cardiovascular system, Front. Pharmacol. 556 (2017).

[2] P.J. Meikle, S.A. Summers, Sphingolipids and phospholipids in insulin resistance and related metabolic disorders, Nat. Rev. Endocrinol. 13 (2) (2017) 79–91.

[3] A. Vestri, F. Pierucci, A. Frati, L. Monaco, E. Meacci, Sphingosine 1-phosphate receptors: do they have a therapeutic potential in cardiac fibrosis? Front. Pharmacol. 8 (2017) 296.

[4] S. Bu, Y. Asano, A. Bujor, K. Highland, F. Hant, M. Trojanowska, Dihydrosphingosine-1 phosphate has a potent anti-fibrotic effect in scleroderma fibroblasts via normalization of PTEN levels, Arthritis Rheum. 62 (7) (2010) 2117–2126.

[5] Y. Mishima, M. Kurano, T. Kobayashi, M. Nishikawa, R. Ohkawa, M. Tozuka, et al., Dihydro-sphingosine 1-phosphate interacts with carrier proteins in a manner distinct from that of sphingosine 1-phosphate, Biosci. Rep. 38 (5) (2018) BSR20181288.

[6] M. Yamanaka, D. Shegogue, H. Pei, S. Bu, A. Bielawska, J. Bielawski, et al., Sphingosine kinase 1 (SPHK1) is induced by transforming growth factor-beta and mediates TIMP-1 up-regulation, J. Biol. Chem. 279 (52) (2004) 53994–54001.

[7] F. Zhang, Y. Xia, W. Yan, H. Zhang, F. Zhou, S. Zhao, et al., Sphingosine 1-phosphate signaling contributes to cardiac inflammation, dysfunction, and remodeling following myocardial infarction, Am. J. Physiol. Heart Circ. Physiol. 310 (2) (2016) H250–H261.

[8] C.K. Means, C.Y. Xiao, Z. Li, T. Zhang, J.H. Omens, I. Ishii, et al., Sphingosine 1-phosphate S1P2 and S1P3 receptor-mediated Akt activation protects against in vivo myocardial ischemia-reperfusion injury, Am. J. Physiol. Heart Circ. Physiol. 292 (6) (2007) H2944–H2951.

[9] Y. Wang, D. Wang, L. Zhang, F. Ye, M. Li, K. Wen, Role of JAK-STAT pathway in reducing cardiomyocytes hypoxia/reoxygenation injury induced by S1P post-conditioning, Eur. J. Pharmacol. 784 (2016) 129–136.

[10] B. Dai, M. Cui, M. Zhu, W.L. Su, M.C. Qiu, H. Zhang, STAT1/3 and ERK1/2 synergistically regulate cardiac fibrosis induced by high glucose, Cell. Physiol. Biochem. 32 (4) (2013) 960–971.

[11] S. Lekawanvijit, A. Adrahtas, D.J. Kelly, A.R. Kompa, B.H. Wang, H. Krum, Does indoxyl sulfate, a uraemic toxin, have direct effects on cardiac fibroblasts and myocytes? Eur. Heart J. 31 (14) (2010) 1771–1779.

[12] P. Simpson, Stimulation of hypertrophy of cultured neonatal rat heart cells through an alpha 1-adrenergic receptor and induction of beating through an alpha 1- and beta 1-adrenergic receptor interaction. Evidence for independent regulation of growth and beating, Circ. Res. 56 (6) (1985) 884–894.

[13] L. Pedranzini, T. Dechow, M. Berishaj, R. Comenzo, P. Zhou, J. Azare, et al., Pyridone 6, a pan-Janus-activated kinase inhibitor, induces growth inhibition of multiple myeloma cells, Cancer Res. 66 (19) (2006) 9714.

[14] S.I. Ohkura, S. Usui, S.I. Takashima, N. Takuwa, K. Yoshioka, Y. Okamoto, et al., Augmented sphingosine 1 phosphate receptor-1 signaling in cardiac fibroblasts induces cardiac hypertrophy and fibrosis through angiotensin II and interleukin-6, PLoS One 12 (8) (2017) e0182329.

[15] N. Rostami, A. Nikkhoo, A. Ajoolabady, G. Azizi, M. Hojjat-Farsangi, G. Ghalamfarsa, et al., S1PR1 as a novel promising therapeutic target in Cancer therapy, Mol. Diagn. Ther. 23 (4) (2019) 467–487.

[16] P. Quint, M. Ruan, L. Pederson, M. Kassem, J.J. Westendorf, S. Khosla, et al., Sphingosine 1-phosphate (S1P) receptors 1 and 2 coordinately induce mesenchymal cell migration through S1P activation of complementary kinase pathways, J. Biol. Chem. 288 (8) (2013) 5398–5406.

[17] U. Negmadjanov, Z. Godic, F. Rizvi, L. Emelyanova, G. Ross, J. Richards, et al., TGF-beta1-mediated differentiation of fibroblasts is associated with increased mitochondrial content and cellular respiration, PLoS One 10 (4) (2015) e0123046.

[18] N.G. Frangogiannis, Cardiac fibrosis: cell biological mechanisms, molecular pathways and therapeutic opportunities, Mol. Asp. Med. 65 (2019) 70–99.

[19] F. Cheng, Y. Shen, P. Mohanasundaram, M. Lindström, J. Ivaska, T. Ny, et al., Vimentin coordinates fibroblast proliferation and keratinocyte differentiation in wound healing via TGF-β–slug signaling, Proc. Natl. Acad. Sci. 113 (30) (2016) E4320-E7.

[20] P.Y. Chuang, J.C. He, JAK/STAT signaling in renal diseases, Kidney Int. 78 (3) (2010) 231–234.

[21] K. Hirahara, A. Onodera, V. Villarino Alejandro, M. Bonelli, G. Sciumè, A. Laurence, et al., Asymmetric action of STAT transcription factors drives transcriptional outputs and cytokine specificity, Immunity 42 (5) (2015) 877–889.

[22] S.A. Mir, A. Chatterjee, A. Mitra, K. Pathak, S.K. Mahata, S. Sarkar, Inhibition of signal transducer and activator of transcription 3 (STAT3) attenuates interleukin-6 (IL-6)-induced collagen synthesis and resultant hypertrophy in rat heart, J. Biol. Chem. 287 (4) (2012) 2666–2677.

[23] N. Gellings Lowe, J.S. Swaney, K.M. Moreno, R.A. Sabbadini, Sphingosine-1-phosphate and sphingosine kinase are critical for transforming growth factor-β-stimulated collagen production by cardiac fibroblasts, Cardiovasc. Res. 82 (2) (2009) 303–312.

[24] R.I. Schwarz, Collagen I and the fibroblast: high protein expression requires a new paradigm of post-transcriptional, feedback regulation, Biochem. Biophys. Rep. 3 (2015) 38–44.

[25] B.S. Shea, S.F. Brooks, B.A. Fontaine, J. Chun, A.D. Luster, A.M. Tager, Prolonged exposure to sphingosine 1-phosphate receptor-1 agonists exacerbates vascular leak, fibrosis, and mortality after lung injury, Am. J. Respir. Cell Mol. Biol. 43 (6) (2010) 662–673.

[26] F. Verrecchia, A. Mauviel, Transforming growth factor-beta and fibrosis, World J. Gastroenterol. 13 (22) (2007) 3056–3062.

[27] J.P. Annes, J.S. Munger, D.B. Rifkin, Making sense of latent TGFbeta activation, J. Cell Sci. 116 (Pt 2) (2003) 217–224.

[28] D.B. Constam, Regulation of TGFβ and related signals by precursor processing, Semin. Cell Dev. Biol. 32 (2014) 85–97.

[29] C. Xin, S. Ren, B. Kleuser, S. Shabahang, W. Eberhardt, H. Radeke, et al., Sphingosine 1-phosphate cross-activates the Smad signaling Cascade and mimics transforming growth factor-β-induced cell responses, J. Biol. Chem. 279 (34) (2004) 35255–35262.

[30] M. Funaba, C.M. Zimmerman, L.S. Mathews, Modulation of Smad2-mediated

signaling by extracellular signal-regulated kinase, J. Biol. Chem. 277 (44) (2002) 41361–41368.
[31] P. Robert, P. Tsui, M.P. Laville, G.P. Livi, H.M. Sarau, A. Bril, et al., EDG1 receptor stimulation leads to cardiac hypertrophy in rat neonatal myocytes, J. Mol. Cell. Cardiol. 33 (9) (2001) 1589–1606.
[32] H. Yan, S. Yi, H. Zhuang, L. Wu, D.W. Wang, J. Jiang, Sphingosine-1-phosphate ameliorates the cardiac hypertrophic response through inhibiting the activity of histone deacetylase-2, Int. J. Mol. Med. 41 (3) (2018) 1704–1714.
[33] J.S. Karliner, N. Honbo, K. Summers, M.O. Gray, E.J. Goetzl, The lysophospholipids sphingosine-1-phosphate and lysophosphatidic acid enhance survival during hypoxia in neonatal rat cardiac myocytes, J. Mol. Cell. Cardiol. 33 (9) (2001) 1713–1717.
[34] A. Cannavo, G. Rengo, D. Liccardo, G. Pagano, C. Zincarelli, M.C. De Angelis, et al., beta1-adrenergic receptor and sphingosine-1-phosphate receptor 1 (S1PR1) reciprocal downregulation influences cardiac hypertrophic response and progression to heart failure: protective role of S1PR1 cardiac gene therapy, Circulation 128 (15) (2013) 1612–1622.
[35] T. Nishikimi, N. Maeda, H. Matsuoka, The role of natriuretic peptides in cardioprotection, Cardiovasc. Res. 69 (2) (2006) 318–328.
[36] D. Stilli, L. Bocchi, R. Berni, M. Zaniboni, F. Cacciani, C. Chaponnier, et al., Correlation of α-skeletal actin expression, ventricular fibrosis and heart function with the degree of pressure overload cardiac hypertrophy in rats, Exp. Physiol. 91 (3) (2006) 571–580.
[37] Y.-Z. Chen, F. Wang, H.-J. Wang, H.-B. Liu, Sphingosine 1 phosphate receptor-1 (S1PR1) signaling protects cardiac function by inhibiting cardiomyocyte autophagy, J. Geriatr. Cardiol. 15 (5) (2018) 334–345.
[38] G. Ahuja, D. Bartsch, W. Yao, S. Geissen, S. Frank, A. Aguirre, et al., Loss of genomic integrity induced by lysosphingolipid imbalance drives ageing in the heart, EMBO Rep. 20 (4) (2019) e47407.
[39] S. Wang, Q. Zhang, Y. Wang, B. You, Q. Meng, S. Zhang, et al., Transforming growth factor beta1 (TGF-beta1) appears to promote coronary artery disease by upregulating sphingosine kinase 1 (SPHK1) and further upregulating its downstream TIMP-1, Med. Sci. Monit. 24 (2018) 7322–7328.
[40] X. Zhang, M.H. Wrzeszczynska, C.M. Horvath, J.E. Darnell Jr., Interacting regions in Stat3 and c-Jun that participate in cooperative transcriptional activation, Mol. Cell. Biol. 19 (10) (1999) 7138–7146.
[41] M. Bugno, L. Graeve, P. Gatsios, A. Koj, P.C. Heinrich, J. Travis, et al., Identification of the interleukin-6/oncostatin M response element in the rat tissue inhibitor of metalloproteinases-1 (TIMP-1) promoter, Nucleic Acids Res. 23 (24) (1995) 5041–5047.
[42] V. Arpino, M. Brock, S.E. Gill, The role of TIMPs in regulation of extracellular matrix proteolysis, Matrix Biol. 44-46 (2015) 247–254.
[43] A. Takawale, P. Zhang, V.B. Patel, X. Wang, G. Oudit, Z. Kassiri, Tissue inhibitor of matrix metalloproteinase-1 promotes myocardial fibrosis by mediating CD63-integrin beta1 interaction, Hypertension 69 (6) (2017) 1092–1103.
[44] P. Callihan, N.C. Zitomer, M.V. Stoeling, P.C. Kennedy, K.R. Lynch, R.T. Riley, et al., Distinct generation, pharmacology, and distribution of sphingosine 1-phosphate and dihydrosphingosine 1-phosphate in human neural progenitor cells, Neuropharmacology 62 (2) (2012) 988–996.
[45] M. Knapp, M. Baranowski, D. Czarnowski, A. Lisowska, P. Zabielski, J. Gorski, et al., Plasma sphingosine-1-phosphate concentration is reduced in patients with myocardial infarction, Med. Sci. Monit. 15 (9) (2009) CR490–3.
[46] M. Knapp, A. Lisowska, P. Zabielski, W. Musiał, M. Baranowski, Sustained decrease in plasma sphingosine-1-phosphate concentration and its accumulation in blood cells in acute myocardial infarction, Prostaglandins Other Lipid Mediat. 106 (2013) 53–61.
[47] M. Kurdi, C. Zgheib, G.W. Booz, Recent developments on the crosstalk between STAT3 and inflammation in heart function and disease, Front. Immunol. 9 (2018) 3029.
[48] N. Li, F. Zhang, Implication of sphingosin-1-phosphate in cardiovascular regulation, Front. Biosci. (Landmark Ed) 21 (2016) 1296–1313.
[49] V.P.M. van Empel, L.J. De Windt, Myocyte hypertrophy and apoptosis: a balancing act, Cardiovasc. Res. 63 (3) (2004) 487–499.

Appendix 2

The following pages contain list of primers and antibodies used in this thesis. They include:

1. List of rat gene primers, sequences and their manufacturer
2. List of mouse gene primers, sequences and their manufacturer
3. List of antibodies for immunohistochemistry analysis and their manufacturer

Appendix 2.1

List of rat gene primers, sequences and their manufacturer.

PRIMER	SEQUENCE	MANUFACTURER
TGFB1	Forward: 5'-CCA GCC GCG GGA CTC -3' Reverse: 5' -TTC CGT TTC ACC AGC TCC AT-3'	+Geneworks
TIMP1	Forward: 5'-GTA AAG ACC TAT AGT GCT GGC TG-3' Reverse: 5'-GAG CAT CTG ATC TGT CCA CAA-3'	*Sigma
SK1	Forward: 5'-CTT TAA ACT GAT GCT CAC CG-3' Reverse: 5'-TAC ATA GGG GTT TCT GGA TG-3'	Sigma
DEGS1	Forward:5'-ATC TTA GCG AAG TAT CCA GAG-3' Reverse:5'-CAG AGT CAT GGA ATG GTT AAG-3'	Sigma
S1PR1	Forward: 5'-AAA ACC AAG AAG TTC CAC C-3' Reverse: 5'-CCA CAA ACA TAC TTC CTT CC-3'	Sigma
S1PR2	Forward: 5'-CTC TTA TGG CAT CTT AGA AGA CAC C-3' Reverse: 5'-CAC AGA CAC ACA TAA ATA CCG-3'	Sigma
S1PR3	Forward: 5'-AAA ACG CTT AGA AGA CACC-3' Reverse: 5'-GTG TGT CTC TGA TGC TAA TC-3'	Sigma
COL 3A1	Forward: 5'-TTT CAA GAT CAA CAC TGA GG-3' Reverse: 5'-TAT TTC TCC GCT CTT GAG TTC-3'	Sigma
COL 1AI	Forward: 5'-TGG ATT CCA GTT CGA GAG TAT G-3' Reverse: 5'-AGT GAT AGG TGA TGT TCT GG-3'	Sigma
BMHC	Forward: 5'-TTG GCA CGG ACT GCG TCA TC-3' Reverse: 5'-GAG CCT CAA GAG TTT GCT GAA-3'	Sigma
ANP	Forward: 5'-ATC TGA TGG ATT TCA AGA ACC-3' Reverse: 5'-CTC TGA GAC GGG TTG ACT TC-3'	Sigma

BNP	Forward: 5'-ACA ATC CAC GAT GCA GAA GCT-3' Reverse: 5'-GGG CCT TGG TCC TTT GAG A-3'	Sigma
ASKA	Forward: 5'-TCG CGA CCT TAC TGA CTA CCT G Reverse: 5'-GCT TCT CTT TGA TGT CGC GC	Geneworks
MMP2	Forward: 5'-GGG TCC ATT CTG CCA GCA CTC-3' Reverse: 5'-CTC CAG AAC TTG TCT CCT GCA A-3'	Geneworks
GSK3B	Reverse:5'-TCC AGC ATT AGT ATC TGA GG-3' Forward:5'-CAC TCA AGA ACTGTC AAG TAA C-3'	Sigma
GATA4	Reverse:5'-CGG TTG ATA CCA TTC ATC TTG-3' Forward:5'-CCC CAA TCT CGA TAT GTT TG-3'	Sigma
18S	Forward: 5'-TCG AGG CCC TGT AAT TGG AA-3' Reverse:5'-CCC TCC AAT TGG ACC TCG TT-3'	Sigma

* Sigma, St. Louis, MO, USA; + Geneworks, Thebarton, SA, Australia

Appendix 2.2

List of mouse gene primers, sequences and their manufacturer.

Primer	Sequence	Manufacturer
TGFβ1	Forward: 5'-CCA GCC GCG GGA CTC-3' Reverse: 5'-TTC CGT TTC ACC AGC TCC AT-3'	*Sigma
CTGF	Forward: 5'-GCG GCG AGT CCT TCC AA-3' Reverse: 5'-CCA CGG CCC CAT CCA-3'	Sigma
TIMP1	Forward: 5'- GTA AAG ACC TAT AGT GCT GGC TG- 3' Reverse: 5'-GAG CAT CTG ATC TGT CCA CAA-3'	Sigma
TIMP2	Forward: 5'-GGT CAC AGA GAA GAG CAT CAA TG-3' Reverse: 5'- GTC CTC GAT GTC AAG AAA CTT C-3'	Sigma
Col 1a1	Forward: 5'-TGG ATT CCA GTT CGA GAG TAT G-3' Reverse: 5'-AGT GAT AGG TGA TGT TCT GG- 3'	Sigma
Coll 3a1	Forward: 5'-ACT CAA GAG TGG AGAATA CTG-3' Reverse: 5'-AAC ATG TTT CTT CTC TGC AC-3'	Sigma
MMP2	Forward: 5'-GGG TCC ATT CTG CCA GCA CTC- 3' Reverse: 5'-CTC CAG AAC TTG TCT CCT GCA A- 3'	Sigma
βMHC	Forward: 5'-TTG GCA CGG ACT GCG TCA TC- 3' Reverse: 5'- GAG CCT CAA GAG TTT GCT GAA- 3'	Sigma
ANP	Forward: 5'-ATC TGA TGG ATT TCA AGA ACC- 3' Reverse: 5'-CTC TGA GAC GGG TTG ACT TC- 3'	Sigma
BNP	Forward: 5'-ACA ATC CAC GAT GCA GAA GCT-3' Reverse: 5'-GGG CCT TGG TCC TTT GAG A- 3'	Sigma
S1PR1	Forward: 5'-CAT GAG GTG AAA TGT GAG AG-3' Reverse: 5'-AGT TGG TTG AAA TGG ATC AC-3'	Sigma
S1PR2	Forward: 5'-ATC CTG TCA TCT ATA CTG G G-3' Reverse: 5'-CAG AAA TGT CGG TGATGT AG-3'	Sigma
S1PR3	Forward: 5'-GAA CGA GAG CCT ATT TTC AAC- 3' Reverse: 5'-TCC TAG AGA CAG ATG GTT AC- 3'	Sigma
DEGS1	Forward:5'-ATC TTA GCG AAG TAT CCA GAG- 3' Reverse:5'-CAG AGT CAT GGA ATG GTT AAG- 3'	Sigma
SK1	Forward: 5'-CTT TAA ACT GAT GCT CAC CG- 3' Reverse: 5'-TAC ATA GGG GTT TCT GGA TG- 3'	Sigma
18s	Forward: 5'-TCG AGG CCC TGT AAT TGG AA- 3' Reverse:5' -CCC TCC AAT TGG ACC TCG TT- 3'	Sigma
GAPDH	Reverse: 5'-AGC CCA GGA TGC CCT TTA GT- 3' Forward: 5'-GAC ATG CCG CCT GGA GAA AC- 3'	Sigma

* Sigma, St. Louis, MO, USA; + Geneworks, Thebarton, SA, Australia

Appendix 2.3

List of antibodies for immunohistochemistry analysis and their manufacturer.

Antibody	Host	Dilution	Catalogue No.	Manufacturer
α-SMA	Rabbit monoclonal	1:2500	Ab124964	*Abcam
Coll 1	Rabbit Polyclonal	1:500	PAI-27396	! Invitrogen
Coll 3	Rabbit Polyclonal	1:200	PA5- 95595	Invitrogen
CD45	Rabbit Monoclonal	1:100	70257	#CST
CD68	Rabbit Polyclonal	1:1000	Ab125212	Abcam
pSMAD2	Rabbit Polyclonal	1:175	PA5-105000	Invitrogen
TGFβ1	Rabbit Polyclonal	1:200	Ab25121	Abcam

*Abcam, Cambridge, UK., ! Invitrogen, St.Louise, MO, USA. #Cell Signalling Technologies (CST), Danvers, MA, USA.

Appendix 3

The following pages contain individual lipidomics analysis data for chapter 5 in this thesis. They include:

1. List of individual lipids significantly altered in the plasma of I/R+Vehicle vs. sham and I/R+CIN038 vs. I/R+Vehicle
2. Individual lipids significantly altered in the liver of I/R+Vehicle vs. sham and I/R+CIN038 vs. I/R+vehicle.
3. Conditions for Tandem Mass Spectroscopy analysis

Appendix 3.1

List of individual lipids significantly altered in the plasma of I/R+Vehicle vs. sham and I/R+CIN038 vs. I/R+Vehicle. Significant alterations in individual lipids are highlighted in red font.

No.	Lipid Species	Mean Values		Percentage Difference I/R+Vehicle vs. Sham (%)	Direction of Change	p- Value (t-Test)	Mean Values	Percentage Difference CIN038 vs. Vehicle (%)	Direction of Change	p- Value (t-Test)
		Sham (± SEM)	I/R+vehicle (± SEM)				I/R+CIN038 (± SEM)			
1	CE(20:1)	627.71 ± 58.90	875.14 ± 51.90	39%	Increase	0.006	845.61 ± 60.47	3%	NS	0.715
2	CE(22:1)	237.08 ± 36.80	342.39 ± 30.53	44%	Increase	0.041	286.31 ± 54.59	16%	NS	0.382
3	DE(18:2)	2194.65 ± 193.48	1586.39 ± 95.14	28%	Decrease	0.008	1872.02 ± 163.33	18%	NS	0.148
4	DE(20:4)	3380.06 ± 278.79	2288.58 ± 234.16	32%	Decrease	0.008	2747.11 ± 402.77	20%	NS	0.338
5	DE(22:6)	1987.39 ± 254.91	1330.67 ± 177.46	33%	Decrease	0.045	1412.68 ± 143.06	6%	NS	0.723
6	FA(18:2)	23416.39 ± 1686.03	20399.00 ± 2050.55	13%	NS	0.289	27085.13 ± 2139.03	33%	Increase	0.037
7	LPC(18:1) [sn2]	21370.43 ± 1110.68	17811.19 ± 856.86	17%	Decrease	0.020	19437.80 ± 1243.79	9%	NS	0.296
8	LPC(18:1) [sn1]	51378.77 ± 2627.18	43637.20 ± 2358.87	15%	Decrease	0.044	47988.93 ± 2704.66	10%	NS	0.241
9	LPC(18:2) [sn2]	35486.98 ± 1272.79	30271.66 ± 1337.02	15%	Decrease	0.014	33718.25 ± 2224.49	11%	NS	0.201
10	LPC(22:5) [sn1] (n3)/LPC(22:5) [sn2] (n6)	587.69 ± 35.39	484.30 ± 18.95	18%	Decrease	0.015	551.85 ± 55.62	14%	NS	0.265
11	LPC(22:6) [sn1]	9350.41 ± 478.15	7830.58 ± 208.02	16%	Decrease	0.006	8812.68 ± 630.54	13%	NS	0.156
12	LPC(O-24:0)	11.74 ± 1.84	28.18 ± 2.18	140%	Increase	0.000	24.48 ± 1.79	13%	NS	0.206
13	LPC(O-24:1)	12.44 ± 1.82	16.93 ± 1.45	36%	NS	0.068	12.53 ± 0.99	26%	Decrease	0.022
14	PC(16:0_16:0)	12634.39 ± 553.19	10353.96 ± 687.48	18%	Decrease	0.024	11310.27 ± 818.83	9%	NS	0.383
15	PC(33:2)	1992.75 ± 148.74	1851.99 ± 69.99	7%	NS	0.373	1642.27 ± 58.87	11%	Decrease	0.034
16	PC(16:1_18:2)	10326.43 ± 904.34	10000.62 ± 633.67	3%	NS	0.765	8172.19 ± 556.40	18%	Decrease	0.044
17	PC(17:1_18:2)	788.50 ± 49.70	832.64 ± 25.30	6%	NS	0.413	687.31 ± 21.67	17%	Decrease	0.000
18	PC(P-16:0/16:0)	280.23 ± 16.25	301.26 ± 17.13	8%	NS	0.395	366.06 ± 12.37	22%	Increase	0.007
19	PC(P-18:0/20:4)	115.42 ± 5.24	148.65 ± 11.12	29%	Increase	0.024	161.59 ± 7.49	9%	NS	0.347
20	PC(P-20:0/20:4)	31.95 ± 1.66	48.26 ± 3.62	51%	Increase	0.002	48.36 ± 3.63	0.22%	NS	0.984
21	PE(P-16:0/18:1)	102.91 ± 8.55	72.33 ± 10.28	30%	Decrease	0.042	104.06 ± 18.11	44%	NS	0.145
22	PE(P-16:0/22:5) (n3)	231.55 ± 19.41	173.49 ± 15.36	25%	Decrease	0.030	236.19 ± 50.34	36%	NS	0.249
23	PI(18:0_20:3) (a)	62248.16 ± 4161.92	43309.02 ± 3677.10	30%	Decrease	0.004	45776.27 ± 4664.14	6%	NS	0.683
24	PI(18:0_22:6)	3663.48 ± 343.41	2597.30 ± 182.73	29%	Decrease	0.010	3057.90 ± 289.16	18%	NS	0.195
25	S1P(d18:1)	686.08 ± 55.43	519.33 ± 36.18	24%	Decrease	0.019	670.56 ± 73.59	29%	NS	0.082
26	SM(d18:2/16:0)	1944.04 ± 97.86	1580.53 ± 96.94	19%	Decrease	0.019	1658.06 ± 99.17	5%	NS	0.583
27	SM(34:3)	6.63 ± 0.61	4.08 ± 0.68	38%	Decrease	0.015	4.72 ± 0.54	16%	NS	0.475
28	SM(d18:1/17:0)/SM(d17:1/18:0)	152.97 ± 5.66	154.25 ± 6.98	1%	NS	0.893	189.62 ± 10.33	23%	Increase	0.011
29	SM(d18:2/17:0)	14.32 ± 0.69	12.07 ± 0.63	16%	Decrease	0.028	12.65 ± 1.45	5%	NS	0.717
30	SM(d18:2/18:0)	291.16 ± 15.43	239.76 ± 16.10	18%	Decrease	0.038	271.76 ± 17.27	13%	NS	0.192
31	SM(d18:2/18:1)	39.29 ± 1.95	29.19 ± 1.97	26%	Decrease	0.002	30.30 ± 1.31	4%	NS	0.646
32	SM(d18:2/20:0)	278.31 ± 17.06	217.53 ± 13.64	22%	Decrease	0.012	227.43 ± 14.52	5%	NS	0.625
33	SM(44:3)	18.32 ± 1.44	17.89 ± 1.14	2%	NS	0.815	22.25 ± 1.47	24%	Increase	0.031
34	TG(50:2) [NL-14:0]	1450.99 ± 184.83	2079.85 ± 204.08	43%	Increase	0.041	1813.01 ± 357.54	13%	NS	0.525
35	TG(56:6) [NL-20:4]	3522.31 ± 173.49	4300.26 ± 251.65	22%	Increase	0.028	4037.45 ± 526.33	6%	NS	0.658

Appendix 3.2

Individual lipids significantly altered in the liver of I/R+Vehicle vs. sham and I/R+CIN038 vs. I/R+vehicle.
Significant alterations in individual lipids are highlighted in red font.

No.	Lipid Species	Mean Values		Percentage Difference I/R+Vehicle vs. Sham (%)	Direction of Change	p- Value (t-Test)	Mean Values	Percentage Difference I/R+CIN038 vs. I/R+Vehicle (%)	Direction of Change	p- Value (t-Test)
		Sham (± SEM)	I/R+Vehicle (± SEM)				I/R+CIN038 (± SEM)			
1	CE(18:2)	27208.99 ± 5603.08	59761.75 ± 12044.99	119.64%	Increase	0.038	49176.68 ± 10185.71	17.71%	NS	0.511
2	CE(18:3)	1390.34 ± 173.53	2517.53 ± 448.61	81.07%	Increase	0.048	2137.45 ± 374.29	15.10%	NS	0.524
3	CE(22:1)	207.13 ± 30.51	132.84 ± 17.94	35.87%	Decrease	0.043	96.08 ± 18.08	27.67%	NS	0.166
4	CE(22:4)	147.90 ± 27.45	264.57 ± 28.99	78.88%	Increase	0.011	236.70 ± 44.92	10.54%	NS	0.609
5	Cer(d18:1/20:0)	267.86 ± 18.04	203.75 ± 21.05	23.93%	Decrease	0.039	210.28 ± 13.85	3.20%	NS	0.799
6	COH	93005.61 ± 3313.25	102051.19 ± 2455.43	9.73%	Increase	0.039	103798.68 ± 1884.28	1.71%	NS	0.579
7	DG(16:0_18:2)	25918.54 ± 3256.41	18419.64 ± 999.11	28.93%	Decrease	0.028	20169.40 ± 1770.82	9.50%	NS	0.401
8	DG(18:1_18:1)	146599.55 ± 29428.59	76251.47 ± 12306.26	47.99%	Decrease	0.030	81778.60 ± 12246.40	7.25%	NS	0.754
9	DG(18:1_18:2)	25173.21 ± 4262.33	14135.41 ± 1979.65	43.85%	Decrease	0.023	15018.48 ± 1907.45	6.25%	NS	0.752
10	DG(18:2_18:2)	2933.24 ± 561.55	1668.00 ± 276.46	43.13%	Decrease	0.047	1779.33 ± 217.48	6.67%	NS	0.755
11	DG(18:1_18:3)	1791.72 ± 455.47	692.67 ± 159.80	61.34%	Decrease	0.031	669.79 ± 145.79	3.30%	NS	0.917
12	DG(18:0_20:4)	45935.58 ± 2756.80	33215.81 ± 1591.84	27.69%	Decrease	0.001	32577.61 ± 1815.02	1.92%	NS	0.795
13	DG(18:2_20:4)	841.97 ± 107.31	508.16 ± 81.11	39.65%	Decrease	0.022	626.99 ± 65.15	23.39%	NS	0.268
14	DG(18:1_20:5)	365.42 ± 112.98	64.12 ± 26.34	82.45%	Decrease	0.011	95.29 ± 26.41	48.61%	NS	0.416
15	DG(18:1_22:5)	670.92 ± 159.68	138.57 ± 51.60	79.35%	Decrease	0.003	148.57 ± 51.38	7.22%	NS	0.892
16	DG(18:1_22:6)	8056.36 ± 1211.51	4800.45 ± 575.06	40.41%	Decrease	0.020	5421.82 ± 561.79	12.94%	NS	0.450
17	DG(18:2_22:6)	1806.52 ± 387.83	737.65 ± 141.92	59.17%	Decrease	0.012	965.22 ± 184.40	30.85%	NS	0.341
18	FA(18:1)	96844.09 ± 12679.38	60539.39 ± 8231.29	37.49%	Decrease	0.024	59300.24 ± 6019.54	2.05%	NS	0.905
19	FA(18:2)	33901.43 ± 4078.58	23739.60 ± 2019.33	29.97%	Decrease	0.030	23604.92 ± 1844.18	0.57%	NS	0.961
20	HexCer(d18:1/24:0)	351.23 ± 33.41	471.90 ± 28.00	34.36%	Increase	0.013	419.74 ± 30.01	11.05%	NS	0.220
21	LPC(24:0) [sn1]	16.13 ± 1.70	22.92 ± 1.02	42.09%	Increase	0.002	19.88 ± 1.37	13.26%	NS	0.093
22	LPC(26:0) [sn1]	37.21 ± 2.03	35.64 ± 0.98	4.21%	NS	0.469	39.34 ± 1.24	10.38%	Increase	0.031
23	LPC(O-18:0)	12.86 ± 1.76	19.81 ± 1.92	53.99%	Increase	0.019	16.14 ± 1.88	18.50%	NS	0.190
24	LPE(16:0) [sn1]	1394.24 ± 86.85	1161.86 ± 51.10	16.67%	Decrease	0.028	1039.71 ± 66.82	10.51%	NS	0.164
25	LPE(22:6) [sn2]	3311.17 ± 272.17	2640.77 ± 119.74	20.25%	Decrease	0.028	2328.06 ± 189.69	11.84%	NS	0.180
26	PC(28:0)	2.82 ± 0.96	7.11 ± 0.90	151.69%	Increase	0.006	6.74 ± 0.99	5.13%	NS	0.788
27	PC(31:0) (a)	45.09 ± 2.77	55.49 ± 3.33	23.07%	Increase	0.034	52.53 ± 3.28	5.33%	NS	0.535
28	PC(16:0_16:0)	12719.05 ± 419.74	13003.47 ± 229.97	2.24%	NS	0.539	11955.77 ± 340.40	8.06%	Decrease	0.020
29	PC(38:2)	2143.64 ± 89.91	2478.21 ± 76.99	15.61%	Increase	0.012	2264.55 ± 81.45	8.62%	NS	0.073
30	PC(O-16:0/16:0)	557.94 ± 62.42	855.30 ± 45.17	53.29%	Increase	0.001	741.21 ± 56.43	13.34%	NS	0.132
31	PC(O-32:1)	17.26 ± 1.53	24.90 ± 1.05	44.30%	Increase	0.001	24.08 ± 2.09	3.28%	NS	0.730
32	PC(O-32:2)	6.08 ± 1.12	10.91 ± 1.06	79.59%	Increase	0.007	9.42 ± 1.18	13.68%	NS	0.359
33	PC(O-34:1)	826.62 ± 53.99	1137.00 ± 39.84	37.55%	Increase	0.000	995.16 ± 45.59	12.47%	Decrease	0.031
34	PC(O-34:2)	203.36 ± 30.78	315.43 ± 17.71	55.11%	Increase	0.004	277.07 ± 25.05	12.16%	NS	0.227
35	PC(O-36:0)	10.56 ± 1.94	21.03 ± 1.43	99.14%	Increase	0.000	16.15 ± 1.44	23.21%	Decrease	0.027
36	PC(O-18:0/18:1)	36.91 ± 3.32	55.81 ± 2.29	51.20%	Increase	0.000	48.62 ± 3.01	12.88%	NS	0.074
37	PC(O-18:1/18:1)	65.14 ± 4.91	91.96 ± 4.64	41.17%	Increase	0.001	83.83 ± 4.59	8.84%	NS	0.229
38	PC(O-18:0/18:2)	55.43 ± 6.05	84.80 ± 4.74	52.99%	Increase	0.001	74.64 ± 5.89	11.98%	NS	0.196
39	PC(O-18:1/18:2)	160.18 ± 19.93	237.00 ± 11.44	47.96%	Increase	0.003	204.90 ± 18.41	13.55%	NS	0.156

40	PC(O-16:0/20:3)	113.53 ± 9.78	161.21 ± 9.16	41.99%	Increase	0.003	141.92 ± 12.30	11.97%	NS	0.225
41	PC(O-16:0/20:4)	464.30 ± 48.30	633.53 ± 32.72	36.45%	Increase	0.009	605.10 ± 53.49	4.49%	NS	0.656
42	PC(O-36:5)	59.97 ± 3.73	81.47 ± 6.56	35.84%	Increase	0.017	72.31 ± 7.68	11.24%	NS	0.376
43	PC(O-18:0/20:4)	107.58 ± 13.50	169.23 ± 11.34	57.30%	Increase	0.003	169.39 ± 15.73	0.09%	NS	0.994
44	PC(O-38:5)	605.63 ± 47.68	758.04 ± 32.85	25.17%	Increase	0.015	760.22 ± 68.51	0.29%	NS	0.977
45	PC(O-40:5)	16.37 ± 2.39	32.24 ± 2.55	96.97%	Increase	0.000	28.81 ± 3.36	10.64%	NS	0.427
46	PC(O-18:0/22:6)	98.93 ± 5.64	129.10 ± 6.32	30.49%	Increase	0.003	125.55 ± 7.17	2.75%	NS	0.714
47	PC(O-40:7) (a)	136.01 ± 7.77	170.31 ± 7.49	25.22%	Increase	0.006	156.91 ± 12.05	7.87%	NS	0.357
48	PC(P-16:0/16:0)	177.38 ± 13.02	276.90 ± 11.35	56.10%	Increase	0.000	319.82 ± 21.97	15.50%	NS	0.100
49	PC(P-16:0/16:1)	8.05 ± 2.07	14.96 ± 1.39	85.74%	Increase	0.011	19.04 ± 2.06	27.31%	NS	0.117
50	PC(P-16:0/18:1)	31.43 ± 5.40	59.69 ± 6.95	89.88%	Increase	0.007	62.20 ± 8.20	4.20%	NS	0.818
51	PC(P-16:0/18:2)	24.42 ± 9.91	81.54 ± 13.04	233.85%	Increase	0.004	78.29 ± 17.85	3.99%	NS	0.885
52	PC(P-16:0/18:3)	10.02 ± 0.66	14.97 ± 1.29	49.45%	Increase	0.006	13.79 ± 1.12	7.85%	NS	0.501
53	PC(P-35:2)(a)	19.51 ± 0.91	25.45 ± 1.77	30.42%	Increase	0.014	22.40 ± 1.88	11.99%	NS	0.252
54	PC(P-18:1/18:1)	12.93 ± 1.75	20.72 ± 1.83	60.31%	Increase	0.008	19.90 ± 1.88	3.94%	NS	0.759
55	PC(P-18:0/18:2)	9.06 ± 1.95	21.15 ± 2.03	133.38%	Increase	0.001	19.73 ± 2.80	6.73%	NS	0.685
56	PC(P-36:3)	28.12 ± 3.42	46.59 ± 4.09	65.66%	Increase	0.004	41.93 ± 5.16	10.01%	NS	0.488
57	PC(P-16:0/20:4)	221.46 ± 26.31	321.27 ± 21.42	45.07%	Increase	0.009	368.25 ± 30.93	14.62%	NS	0.228
58	PC(P-16:0/20:5)	12.01 ± 1.50	23.79 ± 2.69	98.11%	Increase	0.003	21.12 ± 3.42	11.21%	NS	0.548
59	PC(P-17:0/20:4) (a)	11.92 ± 1.35	18.00 ± 1.63	51.08%	Increase	0.013	18.74 ± 2.46	4.06%	NS	0.807
60	PC(P-17:0/20:4) (b)	9.26 ± 0.93	13.89 ± 0.93	49.99%	Increase	0.003	13.67 ± 1.27	1.56%	NS	0.891
61	PC(P-18:0/20:4)	39.80 ± 5.18	65.34 ± 5.18	64.20%	Increase	0.003	69.46 ± 6.19	6.31%	NS	0.616
62	PC(P-38:5) (a)	178.77 ± 16.82	243.19 ± 14.66	36.04%	Increase	0.011	241.54 ± 17.62	0.68%	NS	0.944
63	PC(P-16:0/22:6)	161.76 ± 11.49	195.56 ± 7.73	20.89%	Increase	0.023	205.94 ± 15.72	5.31%	NS	0.561
64	PC(P-20:0/20:4)	9.39 ± 1.48	17.32 ± 1.59	84.48%	Increase	0.003	17.34 ± 2.09	0.07%	NS	0.996
65	PC(P-18:0/22:5)	38.40 ± 3.33	53.58 ± 3.36	39.53%	Increase	0.006	47.85 ± 3.69	10.71%	NS	0.265
66	PC(P-18:0/22:6)	61.60 ± 5.10	75.35 ± 3.46	22.32%	Increase	0.035	78.42 ± 6.20	4.08%	NS	0.670
67	PC(P-18:1/22:6)	41.96 ± 3.93	52.94 ± 2.20	26.17%	Increase	0.021	49.35 ± 3.68	6.78%	NS	0.413
68	PE(P-16:0/18:1)	148.85 ± 21.22	154.42 ± 8.51	3.74%	NS	0.795	121.01 ± 11.13	21.63%	Decrease	0.028
69	PE(P-16:0/20:3)	131.84 ± 19.59	112.68 ± 6.81	14.54%	NS	0.328	79.17 ± 8.26	29.74%	Decrease	0.006
70	PE(P-16:0/22:4)	558.21 ± 31.18	715.36 ± 44.33	28.15%	Increase	0.014	640.98 ± 26.19	10.40%	NS	0.166
71	PE(P-18:0/20:4)	1447.93 ± 106.23	1820.13 ± 102.70	25.71%	Increase	0.024	1731.11 ± 104.47	4.89%	NS	0.551
72	PE(P-18:0/22:4)	77.08 ± 13.34	137.53 ± 11.07	78.43%	Increase	0.003	126.59 ± 7.90	7.95%	NS	0.432
73	PE(P-18:1/22:4)	171.30 ± 13.89	252.14 ± 12.63	47.19%	Increase	0.001	251.39 ± 10.94	0.30%	NS	0.964
74	PI(18:0_20:4)	328801.88 ± 17641.05	276743.96 ± 14234.67	15.83%	Decrease	0.034	284496.56 ± 11625.02	2.80%	NS	0.678
75	PI(18:0_22:5) (n3)	3764.14 ± 217.55	3160.25 ± 135.60	16.04%	Decrease	0.026	3381.57 ± 129.67	7.00%	NS	0.253
76	PS(38:5)	892.55 ± 44.82	1075.14 ± 63.03	20.46%	Increase	0.039	1199.86 ± 71.85	11.60%	NS	0.208
77	SM(d18:1/14:0)/SM(d16:1/16:0)	26.90 ± 8.74	76.93 ± 13.75	186.00%	Increase	0.011	71.62 ± 18.56	6.91%	NS	0.821
78	SM(d18:0/16:0)	352.53 ± 37.60	483.41 ± 35.94	37.13%	Increase	0.024	373.73 ± 37.09	22.69%	Decrease	0.048
79	SM(d18:2/16:0)	108.83 ± 17.59	182.81 ± 22.53	67.98%	Increase	0.024	162.13 ± 26.72	11.31%	NS	0.561
80	SM(d18:1/17:0)/SM(d17:1/18:0)	69.60 ± 10.32	109.08 ± 12.22	56.73%	Increase	0.029	114.97 ± 11.95	5.40%	NS	0.734

81	SM(d18:1/18:0)/SM(d16:1/20:0)	408.97 ± 24.97	516.74 ± 37.32	26.35%	Increase	0.037	544.33 ± 45.16	5.34%	NS	0.643
82	SM(d18:2/18:0)	46.62 ± 7.76	87.92 ± 13.81	88.60%	Increase	0.027	82.31 ± 16.87	6.38%	NS	0.800
83	SM(38:3) (b)	265.83 ± 19.58	250.34 ± 14.60	5.83%	NS	0.526	201.73 ± 15.96	19.42%	Decrease	0.037
84	SM(d19:1/24:1)	5.30 ± 1.69	13.16 ± 2.21	148.14%	Increase	0.016	12.73 ± 2.52	3.29%	NS	0.899
85	SM(44:2)	16.61 ± 1.03	22.21 ± 1.30	33.71%	Increase	0.005	20.21 ± 2.08	9.01%	NS	0.426
86	TG(48:0) [NL-16:0]	1950.24 ± 352.13	1000.87 ± 206.07	48.68%	Decrease	0.025	1455.02 ± 165.57	45.38%	NS	0.103
87	TG(48:1) [SIM]	3659.44 ± 839.49	1706.33 ± 388.04	53.37%	Decrease	0.038	2195.95 ± 690.45	28.69%	NS	0.544
88	TG(48:2) [NL-14:0]	2769.48 ± 623.18	1327.85 ± 317.32	52.05%	Decrease	0.044	1462.35 ± 314.83	10.13%	NS	0.767
89	TG(48:2) [NL-16:1]	14412.14 ± 3782.59	6232.22 ± 1539.01	56.76%	Decrease	0.046	6481.21 ± 1826.44	4.00%	NS	0.918
90	TG(48:2) [NL-18:2]	1331.67 ± 297.24	613.07 ± 124.48	53.96%	Decrease	0.029	692.66 ± 128.64	12.98%	NS	0.662
91	TG(48:2) [SIM]	10665.72 ± 2753.84	4615.09 ± 1046.43	56.73%	Decrease	0.040	5109.45 ± 1319.35	10.71%	NS	0.772
92	TG(48:3) [NL-14:0]	711.22 ± 212.56	259.97 ± 63.57	63.45%	Decrease	0.040	277.91 ± 54.69	6.90%	NS	0.833
93	TG(48:3) [NL-16:1]	4731.00 ± 1407.13	1803.06 ± 482.83	61.89%	Decrease	0.047	2060.43 ± 507.13	14.27%	NS	0.717
94	TG(48:3) [SIM]	4434.55 ± 1221.24	1678.39 ± 440.31	62.15%	Decrease	0.034	1807.82 ± 384.04	7.71%	NS	0.827
95	TG(50:1) [NL-16:0]	53766.43 ± 9389.50	27561.01 ± 4767.02	48.74%	Decrease	0.018	33942.99 ± 7925.13	23.16%	NS	0.499
96	TG(50:1) [NL-18:1]	25145.44 ± 4471.08	13752.11 ± 2305.12	45.31%	Decrease	0.029	15358.98 ± 2877.28	11.68%	NS	0.668
97	TG(50:1) [SIM]	13364.41 ± 2299.26	7131.31 ± 1228.01	46.64%	Decrease	0.022	8323.10 ± 1682.06	16.71%	NS	0.574
98	TG(50:2) [NL-16:1]	51825.99 ± 11801.29	24192.82 ± 5049.39	53.32%	Decrease	0.034	25860.52 ± 5928.19	6.89%	NS	0.833
99	TG(50:2) [NL-18:1]	51544.78 ± 10722.73	25509.79 ± 5462.56	50.51%	Decrease	0.035	27302.19 ± 5533.78	7.03%	NS	0.820
100	TG(50:2) [NL-18:2]	9082.51 ± 1650.20	4727.61 ± 705.58	47.95%	Decrease	0.019	5260.28 ± 831.95	11.27%	NS	0.631
101	TG(50:2) [SIM]	39687.43 ± 7872.29	18885.08 ± 3827.10	52.42%	Decrease	0.022	21580.89 ± 4362.33	14.27%	NS	0.648
102	TG(50:3) [NL-14:0]	3364.11 ± 740.88	1614.31 ± 364.90	52.01%	Decrease	0.038	1610.43 ± 250.90	0.24%	NS	0.993
103	TG(50:3) [NL-16:1]	56971.27 ± 14614.40	22464.52 ± 5421.09	60.57%	Decrease	0.028	25534.73 ± 5558.62	13.67%	NS	0.697
104	TG(50:3) [NL-18:2]	23055.20 ± 5141.27	9035.34 ± 1902.31	60.81%	Decrease	0.013	9992.21 ± 1845.43	10.59%	NS	0.722
105	TG(50:3) [NL-18:3]	720.01 ± 171.22	280.72 ± 49.28	61.01%	Decrease	0.015	323.77 ± 58.08	15.34%	NS	0.579
106	TG(50:3) [SIM]	43886.28 ± 10493.50	18112.73 ± 3972.38	58.73%	Decrease	0.024	20953.72 ± 3854.31	15.69%	NS	0.614
107	TG(50:4) [NL-14:0]	720.15 ± 224.31	246.82 ± 64.13	65.73%	Decrease	0.040	262.36 ± 42.06	6.30%	NS	0.842
108	TG(50:4) [NL-18:3]	2979.75 ± 966.41	776.85 ± 210.61	73.93%	Decrease	0.025	896.01 ± 181.80	15.34%	NS	0.674
109	TG(50:4) [NL-20:4]	89.61 ± 20.48	36.63 ± 9.06	59.12%	Decrease	0.022	41.20 ± 6.56	12.48%	NS	0.688
110	TG(50:4) [SIM]	14309.94 ± 4102.91	4956.65 ± 1221.58	65.36%	Decrease	0.029	5457.70 ± 1066.15	10.11%	NS	0.761
111	TG(51:0) [NL-16:0]	50.71 ± 12.90	18.72 ± 6.39	63.08%	Decrease	0.032	36.31 ± 5.76	93.94%	NS	0.056
112	TG(51:1) [NL-17:0]	523.64 ± 145.29	195.44 ± 34.08	62.68%	Decrease	0.027	267.26 ± 46.12	36.75%	NS	0.226
113	TG(51:1) [SIM]	775.44 ± 191.20	419.42 ± 74.55	45.91%	Decrease	0.078	447.82 ± 51.13	6.77%	NS	0.757
114	TG(51:2) [NL-15:0]	1182.61 ± 302.14	395.93 ± 79.41	66.52%	Decrease	0.013	480.77 ± 69.06	21.43%	NS	0.431
115	TG(51:2) [NL-17:0]	495.46 ± 125.81	184.29 ± 41.36	62.80%	Decrease	0.020	221.82 ± 31.07	20.36%	NS	0.478
116	TG(51:2) [NL-17:1]	3608.66 ± 782.84	1717.27 ± 382.62	52.41%	Decrease	0.034	1967.71 ± 372.90	14.58%	NS	0.645
117	TG(51:2) [SIM]	5714.10 ± 1192.66	3087.23 ± 493.58	45.97%	Decrease	0.043	3345.34 ± 408.38	8.36%	NS	0.692
118	TG(52:1) [NL-18:0]	7003.96 ± 1366.67	3174.23 ± 493.63	54.68%	Decrease	0.011	4115.99 ± 652.01	29.67%	NS	0.265
119	TG(52:1) [NL-18:1]	5531.55 ± 1163.29	2514.31 ± 368.42	54.55%	Decrease	0.015	3356.40 ± 668.70	33.49%	NS	0.285
120	TG(52:1) [SIM]	10735.09 ± 2070.33	4736.46 ± 735.76	55.88%	Decrease	0.009	6048.68 ± 905.40	27.70%	NS	0.275
121	TG(52:2) [NL-16:0]	159074.23 ± 32127.33	73915.72 ± 15571.55	53.53%	Decrease	0.022	79661.59 ± 13831.32	7.77%	NS	0.786
122	TG(52:2) [NL-18:2]	1730.50 ± 311.92	874.62 ± 104.43	49.46%	Decrease	0.012	976.60 ± 101.78	11.66%	NS	0.493

123	TG(52:2) [SIM]	112472.82 ± 21528.18	53917.64 ± 8975.32	52.06%	Decrease	0.015	59804.98 ± 9766.86	10.92%	NS	0.662
124	TG(52:3) [NL-16:1]	37748.79 ± 9260.59	19488.20 ± 3921.47	48.37%	Decrease	0.068	22556.76 ± 4271.31	15.75%	NS	0.603
125	TG(52:3) [NL-18:2]	99164.42 ± 20356.66	47008.10 ± 8588.70	52.60%	Decrease	0.022	48917.90 ± 7243.42	4.06%	NS	0.867
126	TG(52:3) [SIM]	90954.52 ± 16993.27	44400.14 ± 7518.47	51.18%	Decrease	0.016	49506.95 ± 7756.76	11.50%	NS	0.642
127	TG(52:4) [NL-16:1]	30991.20 ± 7336.86	12888.80 ± 3194.92	58.41%	Decrease	0.027	14275.11 ± 2861.89	10.76%	NS	0.750
128	TG(52:4) [NL-18:2]	58763.36 ± 13864.89	23708.53 ± 5037.34	59.65%	Decrease	0.020	24488.58 ± 4157.54	3.29%	NS	0.906
129	TG(52:4) [NL-18:3]	12963.32 ± 3477.77	4200.82 ± 954.20	67.59%	Decrease	0.016	4645.65 ± 858.22	10.59%	NS	0.733
130	TG(52:4) [SIM]	81688.15 ± 19075.28	34731.50 ± 7860.16	57.48%	Decrease	0.026	36979.00 ± 5939.42	6.47%	NS	0.822
131	TG(52:5) [NL-18:3]	7662.07 ± 2528.01	2031.15 ± 496.09	73.49%	Decrease	0.027	2359.89 ± 487.13	16.19%	NS	0.642
132	TG(52:5) [NL-20:4]	1965.70 ± 465.50	918.99 ± 150.33	53.25%	Decrease	0.032	909.27 ± 156.81	1.06%	NS	0.965
133	TG(52:5) [NL-20:5]	202.73 ± 70.34	50.27 ± 10.21	75.20%	Decrease	0.029	51.68 ± 9.13	2.80%	NS	0.919
134	TG(52:5) [SIM]	29290.33 ± 8340.78	9932.91 ± 2525.41	66.09%	Decrease	0.027	10107.87 ± 1861.32	1.76%	NS	0.956
135	TG(53:2) [NL-17:1]	161.13 ± 39.94	79.05 ± 14.10	50.94%	Decrease	0.051	77.38 ± 9.55	2.10%	NS	0.923
136	TG(53:2) [NL-18:1]	4111.86 ± 872.46	1869.77 ± 405.23	54.53%	Decrease	0.024	1932.17 ± 318.97	3.34%	NS	0.905
137	TG(53:2) [SIM]	4400.42 ± 899.23	2088.69 ± 421.94	52.53%	Decrease	0.024	2298.33 ± 327.00	10.04%	NS	0.699
138	TG(54:0) [NL-18:0]	161.90 ± 33.14	77.24 ± 16.34	52.29%	Decrease	0.025	80.23 ± 10.89	3.87%	NS	0.878
139	TG(54:1) [NL-18:1]	1750.89 ± 382.96	653.81 ± 100.43	62.66%	Decrease	0.007	707.43 ± 115.51	8.20%	NS	0.730
140	TG(54:1) [SIM]	6963.03 ± 1502.68	2709.18 ± 421.27	61.09%	Decrease	0.008	3065.42 ± 477.36	13.15%	NS	0.583
141	TG(54:2) [NL-18:0]	14039.41 ± 3037.12	7023.88 ± 1016.10	49.97%	Decrease	0.029	8689.84 ± 1226.24	23.72%	NS	0.309
142	TG(54:2) [NL-20:1]	23213.01 ± 4712.16	10453.58 ± 2361.83	54.97%	Decrease	0.020	11435.27 ± 2492.45	9.39%	NS	0.778
143	TG(54:2) [SIM]	38444.67 ± 7543.59	17899.73 ± 3328.41	53.44%	Decrease	0.016	20672.48 ± 3700.13	15.49%	NS	0.584
144	TG(54:3) [NL-18:2]	6511.97 ± 1098.96	3847.94 ± 610.03	40.91%	Decrease	0.040	4194.12 ± 640.72	9.00%	NS	0.700
145	TG(54:4) [NL-20:3]	7145.42 ± 1412.16	3324.12 ± 619.67	53.48%	Decrease	0.017	4078.65 ± 628.26	22.70%	NS	0.404
146	TG(54:5) [NL-18:3]	5789.32 ± 1380.52	2183.43 ± 492.22	62.29%	Decrease	0.016	2585.82 ± 497.78	18.43%	NS	0.573
147	TG(54:5) [NL-20:4]	10891.97 ± 2004.35	5575.76 ± 803.78	48.81%	Decrease	0.017	6125.14 ± 659.28	9.85%	NS	0.604
148	TG(54:5) [SIM]	37295.19 ± 7312.55	18462.35 ± 3455.24	50.50%	Decrease	0.024	19945.77 ± 3083.42	8.03%	NS	0.752
149	TG(54:6) [NL-18:3]	3407.74 ± 947.13	1237.25 ± 347.39	63.69%	Decrease	0.032	1230.62 ± 236.36	0.54%	NS	0.988
150	TG(54:6) [NL-20:4]	6275.27 ± 1210.36	2798.54 ± 411.02	55.40%	Decrease	0.009	3095.97 ± 375.26	10.63%	NS	0.600
151	TG(54:6) [NL-20:5]	4426.91 ± 1383.30	1323.60 ± 257.09	70.10%	Decrease	0.026	1384.67 ± 253.24	4.61%	NS	0.868
152	TG(54:6) [NL-22:6]	1877.72 ± 396.89	775.25 ± 132.75	58.71%	Decrease	0.011	1050.05 ± 214.79	35.45%	NS	0.291
153	TG(54:6) [SIM]	28244.14 ± 6610.68	11253.68 ± 2115.72	60.16%	Decrease	0.016	12361.52 ± 1782.70	9.84%	NS	0.694
154	TG(54:7) [NL-22:6]	5579.85 ± 1512.14	1877.07 ± 403.00	66.36%	Decrease	0.019	2382.18 ± 478.41	26.91%	NS	0.430
155	TG(54:7) [SIM]	14646.18 ± 4082.73	5024.23 ± 1029.47	65.70%	Decrease	0.022	5803.96 ± 962.82	15.52%	NS	0.587
156	TG(56:6) [NL-20:4]	3777.42 ± 588.30	1999.61 ± 270.40	47.06%	Decrease	0.010	2218.34 ± 211.76	10.94%	NS	0.532
157	TG(56:6) [NL-22:5]	5718.99 ± 1115.47	2279.01 ± 378.69	60.15%	Decrease	0.006	2700.80 ± 363.92	18.51%	NS	0.432
158	TG(56:6) [SIM]	17088.67 ± 3100.83	7777.61 ± 1206.22	54.49%	Decrease	0.008	9036.92 ± 1148.81	16.19%	NS	0.459
159	TG(56:7) [NL-20:4]	2167.88 ± 355.29	1109.77 ± 177.04	48.81%	Decrease	0.012	1283.63 ± 162.48	15.67%	NS	0.479
160	TG(56:7) [NL-20:5]	1414.61 ± 347.44	519.00 ± 112.07	63.31%	Decrease	0.016	624.54 ± 120.83	20.33%	NS	0.530
161	TG(56:7) [NL-22:5]	3290.76 ± 721.28	1277.41 ± 234.22	61.18%	Decrease	0.010	1448.35 ± 222.31	13.38%	NS	0.603
162	TG(56:7) [NL-22:6]	28623.65 ± 6418.99	11139.69 ± 2212.61	61.08%	Decrease	0.013	13522.00 ± 2479.50	21.39%	NS	0.483
163	TG(56:7) [SIM]	31257.26 ± 6320.18	13267.24 ± 2309.89	57.55%	Decrease	0.010	15033.74 ± 2155.96	13.31%	NS	0.583
164	TG(56:8) [NL-20:4]	660.26 ± 129.64	315.05 ± 49.98	52.28%	Decrease	0.016	359.94 ± 36.25	14.25%	NS	0.476
165	TG(56:8) [NL-20:5]	1001.60 ± 320.77	271.16 ± 64.16	72.93%	Decrease	0.024	346.85 ± 71.07	27.91%	NS	0.440

166	TG(56:8) [NL-22:6]	20208.71 ± 5239.83	7586.49 ± 1769.33	62.46%	Decrease	0.024	8405.04 ± 1568.61	10.79%	NS	0.733
167	TG(56:8) [SIM]	23987.96 ± 5946.37	9156.84 ± 1799.83	61.83%	Decrease	0.018	11087.94 ± 1917.61	21.09%	NS	0.472
168	TG(56:9) [NL-22:6]	2201.88 ± 635.31	829.47 ± 189.31	62.33%	Decrease	0.037	939.51 ± 173.12	13.27%	NS	0.673
169	TG(56:9) [SIM]	5496.77 ± 1432.17	2006.09 ± 412.03	63.50%	Decrease	0.020	2316.43 ± 378.09	15.47%	NS	0.586
170	TG(58:10) [NL-22:6]	1261.28 ± 316.82	464.12 ± 91.51	63.20%	Decrease	0.017	565.06 ± 107.43	21.75%	NS	0.484
171	TG(58:10) [SIM]	3051.72 ± 729.81	1202.02 ± 225.36	60.61%	Decrease	0.017	1484.90 ± 216.84	23.53%	NS	0.378
172	TG(58:8) [NL-22:6]	8136.27 ± 1783.74	3624.31 ± 675.37	55.45%	Decrease	0.021	4714.31 ± 1040.57	30.07%	NS	0.391
173	TG(58:8) [SIM]	8343.07 ± 1676.24	3911.60 ± 625.12	53.12%	Decrease	0.016	4687.44 ± 678.17	19.83%	NS	0.411
174	TG(58:9) [NL-22:6]	5514.06 ± 1276.11	2174.02 ± 499.01	60.57%	Decrease	0.018	2863.57 ± 572.26	31.72%	NS	0.376
175	TG(58:9) [SIM]	7603.07 ± 1595.14	3466.10 ± 625.33	54.41%	Decrease	0.019	4331.24 ± 756.54	24.96%	NS	0.390
176	TG(O-50:1) [NL-15:0]	28.28 ± 5.95	22.93 ± 2.56	18.93%	NS	0.387	33.01 ± 3.84	43.98%	Increase	0.042
177	TG(O-50:2) [SIM]	188.89 ± 43.18	143.01 ± 14.93	24.29%	NS	0.289	197.73 ± 16.55	38.26%	Increase	0.024
178	TG(O-52:1) [NL-16:0]	191.83 ± 27.34	180.14 ± 11.80	6.09%	NS	0.678	231.17 ± 18.35	28.33%	Increase	0.031
179	TG(O-52:2) [NL-16:0]	327.51 ± 40.93	377.20 ± 16.81	15.17%	NS	0.243	512.83 ± 44.95	35.96%	Increase	0.011
180	TG(O-52:2) [NL-17:1]	177.74 ± 23.85	181.02 ± 10.44	1.84%	NS	0.894	230.00 ± 16.43	27.06%	Increase	0.022
181	TG(O-52:2) [NL-18:1]	593.58 ± 83.85	615.72 ± 39.67	3.73%	NS	0.802	771.87 ± 50.80	25.36%	Increase	0.026
182	TG(O-54:2) [NL-17:1]	11.22 ± 2.70	12.97 ± 1.71	15.64%	NS	0.576	19.05 ± 2.13	46.91%	Increase	0.039
183	TG(O-54:3) [NL-17:1]	29.33 ± 5.74	33.68 ± 3.01	14.84%	NS	0.487	50.03 ± 4.95	48.54%	Increase	0.011
184	TG(O-54:3) [NL-18:1]	221.65 ± 30.87	215.84 ± 14.12	2.62%	NS	0.857	281.69 ± 17.04	30.51%	Increase	0.008
185	TG(O-54:4) [SIM]	353.80 ± 59.68	306.65 ± 24.65908	13.33%	NS	0.442	396.82 ± 28.36	29.41%	Increase	0.027
186	Ubiquinone	328.76 ± 30.99	240.55 ± 16.37398	26.83%	Decrease	0.017	249.35 ± 14.76	3.65%	NS	0.695

Appendix 3.3

Conditions for tandem mass spectrometry analysis of lipid species. [1]Mass spectrophometer1 resolution, [2]Mass spectrophometer2 resolution, [3]Retention time.

Compound Group	Compound Name	Precursor Ion	[1]MS1 Res	Product Ion	[2]MS2 Res	[3]Ret Time (min)	Collision Energy
AcylCarn	AcylCarnitine 10:0	316.3	Unit	85.1	Unit	0.829	30
AcylCarn	AcylCarnitine 12:0	344.3	Unit	85.1	Unit	1.183	30
AcylCarn	AcylCarnitine 12:1	342.3	Unit	85.1	Unit	0.979	30
AcylCarn	AcylCarnitine 13:0	358.3	Unit	85.1	Unit	1.355	30
AcylCarn	AcylCarnitine 14:0	372.3	Unit	85.1	Unit	1.752	30
AcylCarn	AcylCarnitine 14:0_OH	388.3	Unit	85.1	Unit	1.331	30
AcylCarn	AcylCarnitine 14:1	370.3	Unit	85.1	Unit	1.429	30
AcylCarn	AcylCarnitine 14:1_OH	386.3	Unit	85.1	Unit	1.093	30
AcylCarn	AcylCarnitine 14:2	368.3	Unit	85.1	Unit	1.128	30
AcylCarn	AcylCarnitine 15:0	386.3	Unit	85.1	Unit	2.027	30
AcylCarn	AcylCarnitine 16:0	400.4	Unit	85.1	Unit	2.42	30
AcylCarn	AcylCarnitine 16:0_OH	416.4	Unit	85.1	Unit	1.93	30
AcylCarn	AcylCarnitine 16:0d3	403.4	Unit	85.1	Unit	2.409	30
AcylCarn	AcylCarnitine 16:1	398.3	Unit	85.1	Unit	1.952	30
AcylCarn	AcylCarnitine 16:1_OH	414.3	Unit	85.1	Unit	1.566	30
AcylCarn	AcylCarnitine 17:0	414.4	Unit	85.1	Unit	2.706	30
AcylCarn	AcylCarnitine 18:0	428.4	Unit	85.1	Unit	3.078	30
AcylCarn	AcylCarnitine 18:0_OH	444.4	Unit	85.1	Unit	2.61	30
AcylCarn	AcylCarnitine 18:1	426.4	Unit	85.1	Unit	2.579	30
AcylCarn	AcylCarnitine 18:1_OH	442.4	Unit	85.1	Unit	2.132	30
AcylCarn	AcylCarnitine 18:2	424.3	Unit	85.1	Unit	2.133	30

-Table continued-							
AcylCarn	AcylCarnitine 18:3	422.3	Unit	85.1	Unit	1.76	30
AcylCarn	AcylCarnitine 20:3	450.3	Unit	85.1	Unit	2.514	30
AcylCarn	AcylCarnitine 20:3_OH	466.3	Unit	85.1	Unit	1.983	30
AcylCarn	AcylCarnitine 20:4	448.3	Unit	85.1	Unit	2.132	30
AcylCarn	AcylCarnitine 20:5	446.3	Unit	85.1	Unit	1.748	30
AcylCarn	AcylCarnitine 22:5	474.3	Unit	85.1	Unit	2.227	30
AcylCarn	AcylCarnitine 22:5_OH	490.3	Unit	85.1	Unit	1.885	30
AcylCarn	AcylCarnitine 22:6	472.3	Unit	85.1	Unit	2.046	30
AcylCarn	AcylCarnitine 24:0	512.3	Unit	85.1	Unit	4.859	30
AcylCarn	AcylCarnitine 24:0_OH	528.3	Unit	85.1	Unit	3.717	30
AcylCarn	AcylCarnitine 24:1	510.3	Unit	85.1	Unit	4.276	30
AcylCarn	AcylCarnitine 24:1_OH	526.3	Unit	85.1	Unit	3.096	30
AcylCarn	AcylCarnitine 26:0	540.3	Unit	85.1	Unit	5.708	30
AcylCarn	AcylCarnitine 26:1	538.3	Unit	85.1	Unit	4.858	30
CE	CE 14:0	614.6	Unit	369.3	Unit	11.372	10
CE	CE 15:0	628.6	Unit	369.3	Unit	11.528	10
CE	CE 16:0	642.6	Unit	369.3	Unit	11.643	10
CE	CE 16:1	640.6	Unit	369.3	Unit	11.382	10
CE	CE 16:2	638.6	Unit	369.3	Unit	11.227	10
CE	CE 17:0	656.6	Unit	369.3	Unit	11.759	10
CE	CE 17:1	654.6	Unit	369.3	Unit	11.527	10
CE	CE 18:0	670.7	Unit	369.3	Unit	11.907	10
CE	CE 18:0-d6 (IS)	676.7	Unit	375.3	Unit	11.897	10
CE	CE 18:1	668.6	Unit	369.3	Unit	11.653	10
CE	CE 18:2	666.6	Unit	369.3	Unit	11.433	10
oxLipid	CE 18:2_OH	682.6	Unit	369.3	Unit	10.73	10
CE	CE 18:3	664.6	Unit	369.3	Unit	11.237	10
CE	CE 20:0	698.7	Unit	369.3	Unit	12.111	10

- Table continued-							
CE	CE 20:1	696.7	Unit	369.3	Unit	11.906	10
CE	CE 20:2	694.7	Unit	369.3	Unit	11.683	10
CE	CE 20:3	692.6	Unit	369.3	Unit	11.484	10
CE	CE 20:4	690.6	Unit	369.3	Unit	11.329	10
oxLipid	CE 20:4_OH	706.6	Unit	369.3	Unit	10.708	10
CE	CE 20:5	688.6	Unit	369.3	Unit	11.135	10
CE	CE 22:0	726.7	Unit	369.3	Unit	12.302	10
CE	CE 22:1	724.7	Unit	369.3	Unit	12.099	10
CE	CE 22:4	718.7	Unit	369.3	Unit	11.515	10
CE	CE 22:5	716.6	Unit	369.3	Unit	11.37	10
CE	CE 22:6	714.6	Unit	369.3	Unit	11.216	10
oxLipid	CE 22:6_OH	730.6	Unit	369.3	Unit	10.536	10
CE	CE 24:0	754.7	Unit	369.3	Unit	12.49	10
CE	CE 24:1	752.7	Unit	369.3	Unit	12.289	10
CE	CE 24:4	746.7	Unit	369.3	Unit	11.746	10
CE	CE 24:5	744.7	Unit	369.3	Unit	11.536	10
CE	CE 24:6	742.7	Unit	369.3	Unit	11.37	10
Cer1P	Cer1P(d18:1/16:0)	618.424	Unit	264.3	Unit	5.295	29
Cer	Cer(d16:1/16:0)	510.6	Unit	236.3	Unit	6.501	25
Cer	Cer(d16:1/18:0)	538.6	Unit	236.3	Unit	7.652	25
Cer	Cer(d16:1/20:0)	566.6	Unit	236.3	Unit	8.922	25
Cer	Cer(d16:1/22:0)	594.6	Unit	236.3	Unit	9.994	25
Cer	Cer(d16:1/23:0)	608.6	Unit	236.3	Unit	10.109	25
Cer	Cer(d16:1/24:0)	622.6	Unit	236.3	Unit	10.202	25
Cer	Cer(d16:1/24:1)	620.6	Unit	236.3	Unit	10.003	25
Cer	Cer(d17:1/16:0)	524.6	Unit	250.3	Unit	7.043	25
Cer	Cer(d17:1/18:0)	552.6	Unit	250.3	Unit	8.243	25

-table continued-							
Cer	Cer(d17:1/20:0)	580.6	Unit	250.3	Unit	9.528	25
Cer	Cer(d17:1/22:0)	608.6	Unit	250.3	Unit	10.099	25
Cer	Cer(d17:1/23:0)	622.6	Unit	250.3	Unit	10.202	25
Cer	Cer(d17:1/24:0)	636.6	Unit	250.3	Unit	10.274	25
Cer	Cer(d17:1/24:1)	634.6	Unit	250.3	Unit	10.096	25
Cer	Cer(d18:1/14:0)	510.5	Unit	264.3	Unit	6.49	25
Cer	Cer(d18:1/16:0)	538.5	Unit	264.3	Unit	7.599	25
Cer	Cer(d18:1/18:0)	566.6	Unit	264.3	Unit	8.847	25
Cer	Cer(d18:1/19:0)	580.6	Unit	264.3	Unit	9.528	25
Cer	Cer(d18:1/20:0)	594.6	Unit	264.3	Unit	9.973	25
Cer	Cer(d18:1/21:0)	608.6	Unit	264.3	Unit	10.088	25
Cer	Cer(d18:1/22:0)	622.6	Unit	264.3	Unit	10.181	25
Cer	Cer(d18:1/23:0)	636.6	Unit	264.3	Unit	10.264	25
Cer	Cer(d18:1/24:0)	650.6	Unit	264.3	Unit	10.347	25
Cer	Cer(d18:1/24:1)	648.6	Unit	264.3	Unit	10.19	25
Cer	Cer(d18:1/26:0)	678.6	Unit	264.3	Unit	10.516	25
Cer	Cer(d18:1-d7/18:0) (IS)	573.6	Unit	271.4	Unit	8.805	25
Cer	Cer(d18:2/14:0)	508.5	Unit	262.3	Unit	5.718	25
Cer	Cer(d18:2/16:0)	536.5	Unit	262.3	Unit	6.709	25
Cer	Cer(d18:2/17:0)	550.5	Unit	262.3	Unit	7.138	25
Cer	Cer(d18:2/18:0)	564.6	Unit	262.3	Unit	7.872	25
Cer	Cer(d18:2/20:0)	592.6	Unit	262.3	Unit	9.154	25
Cer	Cer(d18:2/21:0)	606.6	Unit	262.3	Unit	9.825	25
Cer	Cer(d18:2/22:0)	620.6	Unit	262.3	Unit	10.035	25
Cer	Cer(d18:2/23:0)	634.6	Unit	262.3	Unit	10.138	25
Cer	Cer(d18:2/24:0)	648.6	Unit	262.3	Unit	10.221	25
Cer	Cer(d18:2/24:1)	646.6	Unit	262.3	Unit	10.043	25
Cer	Cer(d18:2/26:0)	676.6	Unit	262.3	Unit	10.388	25

-table continued-							
Cer	Cer(d19:1/16:0)	552.6	Unit	278.3	Unit	8	25
Cer	Cer(d19:1/18:0)	580.6	Unit	278.3	Unit	9.315	25
Cer	Cer(d19:1/20:0)	608.6	Unit	278.3	Unit	10.046	25
Cer	Cer(d19:1/22:0)	636.6	Unit	278.3	Unit	10.243	25
Cer	Cer(d19:1/23:0)	650.6	Unit	278.3	Unit	10.315	25
Cer	Cer(d19:1/24:0)	664.6	Unit	278.3	Unit	10.399	25
Cer	Cer(d19:1/24:1)	662.6	Unit	278.3	Unit	10.241	25
Cer	Cer(d19:1/26:0)	692.6	Unit	278.3	Unit	10.579	25
Cer	Cer(d20:1/22:0)	650.6	Unit	292.3	Unit	10.336	25
Cer	Cer(d20:1/23:0)	664.6	Unit	292.3	Unit	10.42	25
Cer	Cer(d20:1/24:0)	678.6	Unit	292.3	Unit	10.495	25
Cer	Cer(d20:1/24:1)	676.6	Unit	292.3	Unit	10.345	25
Cer	Cer(d20:1/26:0)	706.6	Unit	292.3	Unit	10.698	25
m18:0	Cer(m18:0/20:0)	580.6	Unit	268.4	Unit	10.216	35
m18:0	Cer(m18:0/22:0)	608.6	Unit	268.4	Unit	10.362	35
m18:0	Cer(m18:0/23:0)	622.6	Unit	268.4	Unit	10.445	35
m18:0	Cer(m18:0/24:0)	636.6	Unit	268.4	Unit	10.53	35
m18:0	Cer(m18:0/24:1)	634.6	Unit	268.4	Unit	10.359	35
m18:1	Cer(m18:1/18:0)	550.6	Unit	266.4	Unit	9.124	35
m18:1	Cer(m18:1/20:0)	578.6	Unit	266.4	Unit	10.027	35
m18:1	Cer(m18:1/22:0)	606.6	Unit	266.4	Unit	10.225	35
m18:1	Cer(m18:1/23:0)	620.6	Unit	266.4	Unit	10.308	35
m18:1	Cer(m18:1/24:0)	634.6	Unit	266.4	Unit	10.391	35
m18:1	Cer(m18:1/24:1)	632.6	Unit	266.4	Unit	10.233	35
Bile Acids	Cholic Acid	426.3	Unit	355.3	Unit	0.953	19
Bile Acids	Cholic Acid d4	430.3	Unit	359.3	Unit	0.941	19
COH	COH (161)	369.4	Unit	161.2	Unit	6.334	19
COH	COH-d7 (IS) (161)	376.4	Unit	161.2	Unit	6.209	19

-Table continued-							
DE	DE(16:0)	640.6	Unit	367.4	Unit	11.475	10
DE	DE(18:1)	666.6	Unit	367.4	Unit	11.423	10
DE	DE(18:1) ester d6 (IS)	672.6	Unit	373.4	Unit	11.423	10
DE	DE(18:2)	664.6	Unit	367.4	Unit	11.227	10
DE	DE(20:4)	688.6	Unit	367.4	Unit	11.114	10
DE	DE(20:5)	686.6	Unit	367.4	Unit	10.96	10
DE	DE(22:6)	712.6	Unit	367.4	Unit	11.052	10
Sterol - Other	dehydrodesmosterol 18:1	664.8	Unit	365.4	Unit	11.042	10
Sterol - Other	dehydrodesmosterol 18:2	662.8	Unit	365.4	Unit	11.104	10
Sterol - Other	dehydrodesmosterol 20:4	686.8	Unit	365.4	Unit	10.97	10
Bile Acids	Deoxycholic Acid	410.3	Unit	357.3	Unit	1.492	15
DG	DG 15:0 18:1 d7	605.5	Unit	299.5	Unit	9.485	25
DG	DG 30:0 -(14:0)	558.5	Unit	313.3	Unit	8.668	25
DG	DG 32:0 -(16:0)	586.5	Unit	313.2	Unit	9.974	25
DG	DG 32:1 -(16:1)	584.5	Unit	313.2	Unit	8.879	25
DG	DG 32:2 -(18:2)	582.5	Unit	285.2	Unit	8.02	25
DG	DG 34:1 -(18:1)	612.6	Unit	313.3	Unit	9.972	25
DG	DG 34:2 -(16:1)	610.5	Unit	339.2	Unit	9.101	25
DG	DG 34:2 -(18:2)	610.5	Unit	313.2	Unit	9.239	25
DG	DG 36:1 -(18:1)	640.6	Unit	341.3	Unit	10.117	25
DG	DG 36:2 -(18:1)	638.6	Unit	339.3	Unit	10.001	25
DG	DG 36:2 -(18:2)	638.6	Unit	341.3	Unit	10.033	25
DG	DG 36:3 -(18:2)	636.6	Unit	339.3	Unit	9.451	25
DG	DG 36:4 -(18:2)	634.5	Unit	337.2	Unit	8.528	25
DG	DG 36:4 -(18:3)	634.5	Unit	339.2	Unit	8.666	25
DG	DG 36:4 -(20:4)	634.5	Unit	313.2	Unit	9.026	25
DG	DG 38:4 -(20:3)	662.6	Unit	339.3	Unit	9.884	25
DG	DG 38:4 -(20:4)	662.6	Unit	341.3	Unit	10.01	25

-Table continued-							
DG	DG 38:5 -(20:4)	660.6	Unit	339.3	Unit	9.258	25
DG	DG 38:5 -(22:5)	660.6	Unit	313.3	Unit	9.205	25
DG	DG 38:6 -(20:4)	658.5	Unit	337.2	Unit	8.337	25
DG	DG 38:6 -(22:6)	658.5	Unit	313.2	Unit	8.824	25
DG	DG 38:6_NL 20:5	658.6	Unit	339.3	Unit	8.432	25
DG	DG 40:6_NL 22:5	686.6	Unit	339.3	Unit	9.609	25
DG	DG 40:6_NL 22:6	686.6	Unit	341.3	Unit	9.364	25
DG	DG 40:7_NL 22:6	684.6	Unit	339.3	Unit	8.961	25
DG	DG 40:8_NL 22:6	682.6	Unit	337.3	Unit	8.062	25
DG	DG(17:0_18:1) [NL-18:1]	626.5	Unit	327.5	Unit	10.066	25
DG	DG(17:1_18:1) [NL-18:1]	624.5	Unit	325.5	Unit	9.749	25
DG	DG(O-16:0_20:0) [NL-O16:0]	628.5	Unit	369.2	Unit	9.377	25
DG	DG(O-18:0/20:0) [NL-O18:0]	656.5	Unit	369.2	Unit	10.549	25
DG	DG(O-18:1/16:0) [NL-O18:1]	598.5	Unit	325.5	Unit	10.036	25
DG	DG(O-18:1/18:1) [NL-O18:1]	624.5	Unit	339.2	Unit	10.223	25
DG	DG(O-18:1/18:2) [NL-O18:1]	622.5	Unit	337.2	Unit	10.098	25
DG	DG(O-18:1/20:0) [NL-O18:1]	654.5	Unit	369.2	Unit	10.442	25
dhCer	dhCer 16:0	540.5	Unit	284.3	Unit	8.233	27
dhCer	dhCer 18:0	568.6	Unit	284.3	Unit	9.624	27
dhCer	dhCer 20:0	596.6	Unit	284.3	Unit	10.1	27
dhCer	dhCer 22:0	624.6	Unit	284.3	Unit	10.244	27
dhCer	dhCer 24:0	652.7	Unit	284.3	Unit	10.41	27
dhCer	dhCer 24:1	650.6	Unit	284.3	Unit	10.252	27
dhCer	dhCer(d18:0/13:0) d7	505.5	Unit	291.3	Unit	6.355	27
Sterol - Other	dimethyl-CE 18:1	696.6	Unit	397.3	Unit	11.832	10
Sterol - Other	dimethyl-CE 18:2	694.6	Unit	397.3	Unit	11.599	10
Sterol - Other	dimethyl-CE 20:4	718.6	Unit	397.3	Unit	11.505	10
Sterol - Other	dimethyl-CE 22:6	742.6	Unit	397.3	Unit	11.38	10

-Table continued-							
FFA	FA(14:0)-H	227.2	Unit	227.2	Unit	2.997	0
FFA	FA(15:0)-H	241.2	Unit	241.2	Unit	3.413	0
FFA	FA(16:0)-H	255.2	Unit	255.2	Unit	3.669	0
FFA	FA(16:1)-H	253.2	Unit	253.2	Unit	3.167	0
FFA	FA(16:2)-H	251.2	Unit	251.2	Unit	3.125	0
FFA	FA(17:0)-H	269.3	Unit	269.2	Unit	3.968	0
FFA	FA(17:1)-H	267.2	Unit	267.2	Unit	3.508	0
FFA	FA(18:0)-H	283.3	Unit	283.3	Unit	4.269	0
FFA	FA(18:1)-H	281.3	Unit	281.2	Unit	3.796	0
FFA	FA(18:1)-H d9	290.3	Unit	290.2	Unit	3.774	0
FFA	FA(18:2)-H	279.2	Unit	279.2	Unit	3.38	0
FFA	FA(18:3)-H	277.2	Unit	277.2	Unit	2.943	0
FFA	FA(20:2)-H	307.3	Unit	307.3	Unit	3.945	0
FFA	FA(20:3)-H	305.3	Unit	305.2	Unit	3.592	0
FFA	FA(20:4)-H	303.2	Unit	303.2	Unit	3.304	0
FFA	FA(20:4)-H d11	314.2	Unit	314.2	Unit	3.272	0
FFA	FA(20:5)-H	301.2	Unit	301.2	Unit	2.879	0
FFA	FA(22:4)-H	331.3	Unit	331.3	Unit	3.784	0
FFA	FA(22:5)-H	329.3	Unit	329.2	Unit	3.453	0
FFA	FA(22:6) d5	332.2	Unit	332.2	Unit	3.112	0
FFA	FA(22:6)-H	327.2	Unit	327.2	Unit	3.144	0
GD1	GD1(d18:1/24:0)	961.4897	Unit	264.3	Unit	10.794	63
GD1	GD1(d18:1/24:1)	960.4897	Unit	264.3	Unit	9.731	63
GM1	GM1(d18:1/16:0)	760.1	Unit	366.2	Unit	4.564	9
GM3	GM3(d18:1/16:0)	1153.7	Unit	264.3	Unit	4.701	61
GM3	GM3(d18:1/18:0)	1181.8	Unit	264.3	Unit	5.382	61
GM3	GM3(d18:1/20:0)	1209.8	Unit	264.3	Unit	6.189	61
GM3	GM3(d18:1/22:0)	1237.8	Unit	264.3	Unit	7.128	61

-Table continued-							
GM3	GM3(d18:1/24:0)	1265.8	Unit	264.3	Unit	8.212	61
GM3	GM3(d18:1/24:1)	1263.8	Unit	264.3	Unit	7.148	61
GM3	GM3(d18:2/24:1)	1261.8	Unit	262.3	Unit	6.439	61
MHC	Hex1Cer(d16:1/18:0)	700.6	Unit	236.3	Unit	6.427	35
MHC	Hex1Cer(d16:1/20:0)	728.6	Unit	236.3	Unit	7.492	35
MHC	Hex1Cer(d16:1/22:0)	756.7	Unit	236.3	Unit	8.716	35
MHC	Hex1Cer(d16:1/24:0)	784.7	Unit	236.3	Unit	9.915	35
MHC	Hex1Cer(d18:1/16:0)	700.6	Unit	264.3	Unit	6.354	35
MHC	Hex1Cer(d18:1/18:0)	728.6	Unit	264.3	Unit	7.418	35
MHC	Hex1Cer(d18:1/20:0)	756.6	Unit	264.3	Unit	8.632	35
MHC	Hex1Cer(d18:1/22:0)	784.7	Unit	264.3	Unit	9.873	35
MHC	Hex1Cer(d18:1/24:0)	812.7	Unit	264.3	Unit	10.124	35
MHC	Hex1Cer(d18:1/24:1)	810.7	Unit	264.3	Unit	9.883	35
MHC	Hex1Cer(d18:2/18:0)	726.6	Unit	262.3	Unit	6.654	35
MHC	Hex1Cer(d18:2/20:0)	754.6	Unit	262.3	Unit	7.689	35
MHC	Hex1Cer(d18:2/22:0)	782.7	Unit	262.3	Unit	8.937	35
MHC	Hex1Cer(d18:2/24:0)	810.7	Unit	262.3	Unit	9.978	35
DHC	Hex2Cer(d16:1/16:0)	834.6	Unit	236.3	Unit	5.056	49
DHC	Hex2Cer(d16:1/24:1)	944.7	Unit	236.3	Unit	8.022	49
DHC	Hex2Cer(d18:1/15:0) d7	855.6	Unit	271.3	Unit	5.406	49
DHC	Hex2Cer(d18:1/16:0)	862.6	Unit	264.3	Unit	5.846	49
DHC	Hex2Cer(d18:1/18:0)	890.7	Unit	264.3	Unit	7.516	49
DHC	Hex2Cer(d18:1/20:0)	918.7	Unit	264.3	Unit	7.895	49
DHC	Hex2Cer(d18:1/22:0)	946.7	Unit	264.3	Unit	9.136	49
DHC	Hex2Cer(d18:1/24:0)	974.8	Unit	264.3	Unit	10.006	49
DHC	Hex2Cer(d18:1/24:1)	972.7	Unit	264.3	Unit	9.124	49
DHC	Hex2Cer(d18:2/16:0)	860.6	Unit	262.3	Unit	5.204	49
DHC	Hex2Cer(d18:2/18:0)	888.7	Unit	262.3	Unit	6.054	49

-Table continued-							
DHC	Hex2Cer(d18:2/24:1)	970.7	Unit	262.3	Unit	8.212	49
THC	Hex3Cer(d18:1/16:0)	1024.7	Unit	264.3	Unit	5.519	61
THC	Hex3Cer(d18:1/17:0) (IS)	1038.7	Unit	264.3	Unit	5.949	61
THC	Hex3Cer(d18:1/18:0)	1052.7	Unit	264.3	Unit	6.408	61
THC	Hex3Cer(d18:1/20:0)	1080.7	Unit	264.3	Unit	7.421	61
THC	Hex3Cer(d18:1/22:0)	1108.8	Unit	264.3	Unit	8.626	61
THC	Hex3Cer(d18:1/24:0)	1136.8	Unit	264.3	Unit	9.816	61
THC	Hex3Cer(d18:1/24:1)	1134.8	Unit	264.3	Unit	8.604	61
MHC	HexCer(d18:1/15:0) d7	693.6	Unit	271.3	Unit	5.874	35
LPC	LPC 14:0	468.3	Unit	184.1	Unit	1.833	21
LPC	LPC 15:0	482.3	Unit	184.1	Unit	2.174	21
LPC	LPC 16:0	496.3	Unit	184.1	Unit	2.502	21
LPC	LPC 16:1	494.3	Unit	184.1	Unit	2.002	21
LPC	LPC 17:0	510.4	Unit	184.1	Unit	2.809	21
LPC	LPC 17:1	508.4	Unit	184.1	Unit	2.385	21
LPC	LPC 18:0	524.4	Unit	184.1	Unit	3.16	21
LPC	LPC 18:1	522.4	Unit	184.1	Unit	2.65	21
LPC	LPC 18:1 d7	529.4	Unit	184.1	Unit	2.639	21
LPC	LPC 18:2	520.3	Unit	184.1	Unit	2.204	21
oxLipid	LPC 18:2_OH	536.3	Unit	184.1	Unit	0.93	21
LPC	LPC 18:3	518.3	Unit	184.1	Unit	1.873	21
LPC(104)	LPC 18:3(104)	518.3	Unit	104.1	Unit	1.873	21
LPC	LPC 19:0	538.4	Unit	184.1	Unit	3.394	21
LPC	LPC 19:1	536.4	Unit	184.1	Unit	3.01	21
LPC	LPC 20:0	552.4	Unit	184.1	Unit	3.683	21
LPC	LPC 20:1	550.4	Unit	184.1	Unit	3.244	21
LPC	LPC 20:2	548.4	Unit	184.1	Unit	2.808	21
LPC	LPC 20:3	546.4	Unit	184.1	Unit	2.436	21

-Table continued-							
LPC(104)	LPC 20:3(104)	546.4	Unit	104.1	Unit	2.489	21
LPC	LPC 20:4	544.3	Unit	184.1	Unit	2.171	21
oxLipid	LPC 20:4_OH	560.3	Unit	184.1	Unit	1.466	21
LPC	LPC 20:5	542.3	Unit	184.1	Unit	1.798	21
LPC	LPC 22:0	580.4	Unit	184.1	Unit	4.22	21
LPC	LPC 22:1	578.4	Unit	184.1	Unit	3.725	21
LPC	LPC 22:4	572.4	Unit	184.1	Unit	2.669	21
LPC(104)	LPC 22:5(104)	570.4	Unit	104.1	Unit	2.351	21
LPC	LPC 22:5(a\b\c)	570.4	Unit	184.1	Unit	2.351	21
LPC	LPC 22:6	568.3	Unit	184.1	Unit	2.106	21
oxLipid	LPC 22:6_OH	584.3	Unit	184.1	Unit	1.615	21
LPC	LPC 24:0	608.5	Unit	184.1	Unit	4.911	21
LPC	LPC 26:0	636.5	Unit	184.1	Unit	5.749	21
LPCO	LPC(O-16:0)	482.4	Unit	104.1	Unit	2.853	23
LPCO	LPC(O-18:0)	510.4	Unit	104.1	Unit	3.481	23
LPCO	LPC(O-18:1)	508.4	Unit	104.1	Unit	2.98	23
LPCO	LPC(O-20:0)	538.4	Unit	104.1	Unit	3.984	23
LPCO	LPC(O-20:1)	536.4	Unit	104.1	Unit	3.533	23
LPCO	LPC(O-22:0)	566.5	Unit	104.1	Unit	4.62	23
LPCO	LPC(O-22:1)	564.4	Unit	104.1	Unit	4.026	23
LPCO	LPC(O-24:0)	594.5	Unit	104.1	Unit	5.423	23
LPCO	LPC(O-24:1)	592.5	Unit	104.1	Unit	4.63	23
LPCO	LPC(O-24:2)	590.5	Unit	104.1	Unit	4.155	23
LPCP	LPC(P-16:0)	480.3	Unit	104.1	Unit	2.832	25
LPCP	LPC(P-17:0) (a\b)	494.3	Unit	104.1	Unit	3.129	25
LPCP	LPC(P-18:0)	508.3	Unit	104.1	Unit	3.46	25
LPCP	LPC(P-18:1)	506.3	Unit	104.1	Unit	2.959	25
LPCP	LPC(P-20:0)	536.3	Unit	104.1	Unit	3.952	25

-Table continued-							
LPE	LPE 16:0	454.3	Unit	313.3	Unit	2.621	17
LPE	LPE 17:0	468.3	Unit	327.3	Unit	2.971	17
LPE	LPE 18:0	482.3	Unit	341.3	Unit	3.279	17
LPE	LPE 18:1	480.3	Unit	339.3	Unit	2.768	17
LPE	LPE 18:1 d7	487.3	Unit	346.3	Unit	2.747	17
LPE	LPE 18:2	478.3	Unit	337.3	Unit	2.322	17
LPE	LPE 20:4	502.3	Unit	361.3	Unit	2.279	17
LPE	LPE 22:6	526.3	Unit	385.3	Unit	2.214	17
LPEP	LPE(P-16:0)	438.3	Unit	266.4	Unit	2.971	19
LPEP	LPE(P-18:0)	466.3	Unit	294.4	Unit	3.568	19
LPEP	LPE(P-18:1)	464.3	Unit	292.4	Unit	3.088	19
LPEP	LPE(P-20:0)	494.3	Unit	322.4	Unit	4.093	19
LPI	LPI 13:0 (IS)	548.3	Unit	271.3	Unit	1.198	21
LPI	LPI 18:0	618.3	Unit	341.3	Unit	2.722	21
LPI	LPI 18:1	616.3	Unit	339.3	Unit	2.223	21
LPI	LPI 18:2	614.3	Unit	337.3	Unit	1.818	21
LPI	LPI 20:4	638.3	Unit	361.3	Unit	1.775	21
Sterol - Other	methyl-CE 18:0	684.6	Unit	383.3	Unit	11.982	10
Sterol - Other	methyl-CE 18:1	682.6	Unit	383.3	Unit	11.758	10
Sterol - Other	methyl-CE 18:2	680.6	Unit	383.3	Unit	11.526	10
Sterol - Other	methyl-CE 20:4	704.6	Unit	383.3	Unit	11.412	10
Sterol - Other	methyl-CE 22:6	728.6	Unit	383.3	Unit	11.308	10
mDE	methyldesmosterol (18:1)	680.6	Unit	381.4	Unit	11.526	10
mDE	methyldesmosterol (18:2)	678.6	Unit	381.4	Unit	11.36	10
MG	MG 18:1 d7	364.2	Unit	272.2	Unit	3.59	11
PA	PA(15:0_18:1) d7	685.6	Unit	570.6	Unit	6.073	13
PA	PA(34:1)	692.6	Unit	577.6	Unit	6.614	13

-Tabe continued-							
PA	PA(36:1)	720.6	Unit	605.6	Unit	7.629	13
PA	PA(36:2)	718.6	Unit	603.6	Unit	6.76	13
PA	PA(36:3)	716.6	Unit	601.6	Unit	6.04	13
PA	PA(36:4)	714.6	Unit	599.6	Unit	5.706	13
PA	PA(40:6)	766.6	Unit	651.6	Unit	6.235	13
PC	PC 28:0	678.5	Unit	184.1	Unit	5.071	25
PC	PC 30:0	706.5	Unit	184.1	Unit	5.863	25
PC	PC 31:0 (a\b)	720.6	Unit	184.1	Unit	6.269	25
PC	PC 31:1	718.5	Unit	184.1	Unit	5.621	25
PC	PC 32:0	734.6	Unit	184.1	Unit	6.832	25
PC	PC 32:1	732.6	Unit	184.1	Unit	6.05	25
PC	PC 32:2	730.5	Unit	184.1	Unit	5.431	25
PC	PC 33:0(a\b)	748.6	Unit	184.1	Unit	7.291	25
PC	PC 33:1	746.6	Unit	184.1	Unit	6.518	25
PC	PC 33:2	744.6	Unit	184.1	Unit	5.84	25
PC	PC 34:0	762.6	Unit	184.1	Unit	7.932	25
PC	PC 34:1	760.6	Unit	184.1	Unit	7.028	25
PC	PC 34:2	758.6	Unit	184.1	Unit	6.319	25
oxLipid	PC 34:2_OH	774.6	Unit	184.1	Unit	4.672	25
PC	PC 34:3(a\b\c)	756.6	Unit	184.1	Unit	5.725	25
PC	PC 34:4	754.5	Unit	184.1	Unit	5.378	25
PC	PC 34:5	752.5	Unit	184.1	Unit	4.909	25
PC	PC 35:1(a\b)	774.6	Unit	184.1	Unit	7.488	25
PC	PC 35:2(a\b)	772.6	Unit	184.1	Unit	6.745	25
PC	PC 35:3(a\b)	770.6	Unit	184.1	Unit	6.079	25
PC	PC 35:4	768.6	Unit	184.1	Unit	5.797	25
PC	PC 35:5	766.5	Unit	184.1	Unit	5.282	25

-Table continued-							
PC	PC 36:1	788.6	Unit	184.1	Unit	8.152	25
PC	PC 36:2(a\b)	786.6	Unit	184.1	Unit	7.246	25
PC	PC 36:3(a\b\c)	784.6	Unit	184.1	Unit	6.619	25
PC	PC 36:4(a\b)	782.6	Unit	184.1	Unit	6.006	25
oxLipid	PC 36:4(a\b)_OH	798.6	Unit	184.1	Unit	5.27	25
PC	PC 36:5(a\b)	780.6	Unit	184.1	Unit	5.598	25
PC	PC 36:6	778.5	Unit	184.1	Unit	5.122	25
PC	PC 37:4(a\b)	796.6	Unit	184.1	Unit	6.681	25
PC	PC 37:6	792.6	Unit	184.1	Unit	5.629	25
PC	PC 38:2	814.6	Unit	184.1	Unit	8.362	25
PC	PC 38:3	812.6	Unit	184.1	Unit	7.696	25
PC	PC 38:4(a\b\c)	810.6	Unit	184.1	Unit	6.973	25
PC	PC 38:5(a\b)	808.6	Unit	184.1	Unit	6.556	25
PC	PC 38:6(a\b)	806.6	Unit	184.1	Unit	5.953	25
oxLipid	PC 38:6(a\b)_OH	822.6	Unit	184.1	Unit	5.131	25
PC	PC 38:7(a\b\c)	804.6	Unit	184.1	Unit	5.386	25
PC	PC 39:5(a\b)	822.6	Unit	184.1	Unit	6.545	25
PC	PC 39:6(a\b)	820.6	Unit	184.1	Unit	6.482	25
PC	PC 40:4(a\b)	838.6	Unit	184.1	Unit	8.33	25
PC	PC 40:5(a\b)	836.6	Unit	184.1	Unit	7.622	25
PC	PC 40:6	834.6	Unit	184.1	Unit	7.077	25
PC	PC 40:7(a\b\c)	832.6	Unit	184.1	Unit	6.202	25
PC	PC 40:8	830.6	Unit	184.1	Unit	5.575	25
PC	PC 40:10	826.6	Unit	184.1	Unit	4.702	25
PC	PC 42:2	870.5	Unit	184.1	Unit	10.133	25
PC	PC 42:3	868.5	Unit	184.1	Unit	9.891	25
PC	PC 42:4	866.5	Unit	184.1	Unit	9.19	25
PC	PC 42:5 (a/b)	864.5	Unit	184.1	Unit	8.414	25

-Table continued-							
PC	PC 42:6 (a/b)	862.5	Unit	184.1	Unit	7.475	25
PC	PC 42:7	860.5	Unit	184.1	Unit	7.171	25
PC	PC 42:8	858.5	Unit	184.1	Unit	6.346	25
PC	PC 42:9	856.5	Unit	184.1	Unit	5.94	25
PC	PC 42:10	854.5	Unit	184.1	Unit	5.459	25
PC	PC 44:4	894.5	Unit	184.1	Unit	10.059	25
PC	PC 44:5	892.5	Unit	184.1	Unit	9.668	25
PC	PC 44:12	878.6	Unit	184.1	Unit	5.235	25
PC	PC(15:0_18:1) d7	753.6	Unit	184.1	Unit	6.486	25
PCO	PC(O-32:0)	720.6	Unit	184.1	Unit	7.556	25
PCO	PC(O-32:1)	718.5	Unit	184.1	Unit	7.011	25
PCO	PC(O-32:2)	716.6	Unit	184.1	Unit	6.207	25
PCO	PC(O-34:1)	746.6	Unit	184.1	Unit	7.733	25
PCO	PC(O-34:2)	744.6	Unit	184.1	Unit	6.967	25
PCO	PC(O-34:4)	740.6	Unit	184.1	Unit	5.903	25
PCO	PC(O-35:4)	754.5	Unit	184.1	Unit	6.486	25
PCO	PC(O-36:0)	776.6	Unit	184.1	Unit	9.915	25
PCO	PC(O-36:1)	774.6	Unit	184.1	Unit	8.959	25
PCO	PC(O-36:2)(a\b)	772.6	Unit	184.1	Unit	8.016	25
PCO	PC(O-36:3)(a\b)	770.6	Unit	184.1	Unit	7.237	25
PCO	PC(O-36:4)	768.6	Unit	184.1	Unit	6.892	25
PCO	PC(O-36:5)	766.5	Unit	184.1	Unit	6.277	25
PCO	PC(O-38:4)	796.6	Unit	184.1	Unit	8.024	25
PCO	PC(O-38:5)	794.6	Unit	184.1	Unit	7.025	25
PCO	PC(O-38:6)	792.6	Unit	184.1	Unit	6.681	25
PCO	PC(O-40:5)	822.6	Unit	184.1	Unit	8.108	25
PCO	PC(O-40:6)	820.6	Unit	184.1	Unit	7.78	25
PCO	PC(O-40:7)	818.6	Unit	184.1	Unit	6.941	25

-Table continued-							
PC	PC(O-42:4) (a/b)	852.5	Unit	184.1	Unit	9.976	25
PC	PC(O-42:5) (a/b/c)	850.5	Unit	184.1	Unit	9.564	25
PC	PC(O-42:6)	848.5	Unit	184.1	Unit	8.34	25
PC	PC(O-42:7)	846.5	Unit	184.1	Unit	8.012	25
PC	PC(O-42:8)	844.5	Unit	184.1	Unit	7.37	25
PC	PC(O-44:6)	876.5	Unit	184.1	Unit	9.669	25
PC	PC(O-44:7)	874.5	Unit	184.1	Unit	9.03	25
PC	PC(O-46:7) (a/b)	902.5	Unit	184.1	Unit	9.858	25
PC	PC(O-46:8)	900.5	Unit	184.1	Unit	9.274	25
PC(P)	PC(P-18:0/18:1) d9	781.6	Unit	184.1	Unit	8.746	25
PCP	PC(P-30:0)	690.4	Unit	184.1	Unit	6.386	25
PCP	PC(P-32:0)	718.5	Unit	184.1	Unit	7.388	25
PCP	PC(P-32:1)	716.6	Unit	184.1	Unit	6.572	25
PCP	PC(P-34:0)	746.6	Unit	184.1	Unit	8.611	25
PCP	PC(P-34:1)	744.6	Unit	184.1	Unit	7.617	25
PCP	PC(P-34:2)	742.5	Unit	184.1	Unit	6.831	25
PCP	PC(P-34:3)	740.6	Unit	184.1	Unit	6.195	25
PCP	PC(P-35:2)(a\b)	756.6	Unit	184.1	Unit	7.311	25
PCP	PC(P-35:4)(a\b)	752.6	Unit	184.1	Unit	6.341	25
PCP	PC(P-36:2)(a\b)	770.6	Unit	184.1	Unit	7.857	25
PCP	PC(P-36:3)	768.5	Unit	184.1	Unit	7.143	25
PCP	PC(P-36:4)	766.5	Unit	184.1	Unit	6.745	25
PCP	PC(P-36:5)	764.6	Unit	184.1	Unit	6.111	25
PCP	PC(P-37:4)(a\b)	780.5	Unit	184.1	Unit	7.215	25
PCP	PC(P-38:4)	794.6	Unit	184.1	Unit	7.845	25
PCP	PC(P-38:5)(a\b)	792.6	Unit	184.1	Unit	7.047	25
PCP	PC(P-38:6)	790.6	Unit	184.1	Unit	6.536	25
PCP	PC(P-40:4)	822.6	Unit	184.1	Unit	9.074	25

-Table continued-							
PCP	PC(P-40:5)(a\b)	820.6	Unit	184.1	Unit	7.938	25
PCP	PC(P-40:6)	818.6	Unit	184.1	Unit	7.602	25
PCP	PC(P-40:7)	816.6	Unit	184.1	Unit	6.67	25
PC	PC(P-42:5)	848.5	Unit	184.1	Unit	9.116	25
PC	PC(P-44:5)	876.5	Unit	184.1	Unit	10.007	25
PC	PC(P-46:7)	900.5	Unit	184.1	Unit	9.933	25
PC	PC(P-46:8)	898.5	Unit	184.1	Unit	9.125	25
PE	PE 32:0	692.5	Unit	551.5	Unit	7.179	19
PE	PE 32:1	690.5	Unit	549.5	Unit	6.365	19
PE	PE 34:1	718.5	Unit	577.5	Unit	7.388	19
PE	PE 34:2	716.5	Unit	575.5	Unit	6.635	19
PE	PE 34:3(a\b\c)	714.5	Unit	573.5	Unit	6.009	19
PE	PE 35:1(a\b)	732.6	Unit	591.5	Unit	7.849	19
PE	PE 35:2(a\b)	730.5	Unit	589.5	Unit	7.083	19
PE	PE 36:0	748.6	Unit	607.6	Unit	9.513	19
PE	PE 36:1	746.6	Unit	605.6	Unit	8.547	19
PE	PE 36:2(a\b)	744.6	Unit	603.5	Unit	7.628	19
PE	PE 36:3(a\b)	742.5	Unit	601.5	Unit	6.884	19
PE	PE 36:4	740.5	Unit	599.5	Unit	6.57	19
PE	PE 36:5(a\b)	738.5	Unit	597.5	Unit	5.872	19
PE	PE 37:4 (a\b)	754.6	Unit	613.5	Unit	7.008	19
PE	PE 38:3(a\b)	770.6	Unit	629.6	Unit	8.334	19
PE	PE 38:4	768.6	Unit	627.5	Unit	7.657	19
PE	PE 38:5(a\b)	766.5	Unit	625.5	Unit	6.882	19
PE	PE 38:6	764.5	Unit	623.5	Unit	6.361	19
PE	PE 39:6(a\b)	778.5	Unit	637.5	Unit	6.786	19
PE	PE 40:4	796.6	Unit	655.6	Unit	8.693	19
PE	PE 40:5(a\b)	794.6	Unit	653.6	Unit	7.972	19

-Table continued-							
PE	PE 40:6	792.6	Unit	651.5	Unit	7.424	19
PE	PE 40:7	790.5	Unit	649.5	Unit	6.64	19
PE	PE(15:0_18:1) d7	711.6	Unit	570.5	Unit	6.812	19
PE(O)	PE(O-34:1)	704.6	Unit	563.5	Unit	8.157	19
PE(O)	PE(O-34:2)	702.5	Unit	561.5	Unit	7.367	19
PE(O)	PE(O-36:3)(a\b)	728.6	Unit	587.5	Unit	7.66	19
PE(O)	PE(O-36:4)	726.5	Unit	585.5	Unit	7.293	19
PE(O)	PE(O-36:5)	724.5	Unit	583.5	Unit	6.623	19
PE(O)	PE(O-38:4)(a\b)	754.6	Unit	613.6	Unit	8.282	19
PE(O)	PE(O-38:5)(a\b)	752.6	Unit	611.5	Unit	7.553	19
PE(O)	PE(O-38:6)	750.6	Unit	609.5	Unit	7.061	19
PE(O)	PE(O-40:5)	780.6	Unit	639.6	Unit	8.556	19
PE(O)	PE(O-40:6)	778.5	Unit	637.5	Unit	8.217	19
PE(O)	PE(O-40:7)	776.6	Unit	635.5	Unit	7.194	19
PE(P)	PE(P-15:0/20:4)(a\b)	710.5	Unit	361.3	Unit	6.541	19
PE(P)	PE(P-15:0/22:6)(a\b)	734.5	Unit	385.3	Unit	6.31	19
PE(P)	PE(P-16:0/18:1)	702.5	Unit	339.3	Unit	8.051	19
PE(P)	PE(P-16:0/18:2)	700.5	Unit	337.3	Unit	7.242	19
PE(P)	PE(P-16:0/18:3)	698.5	Unit	335.3	Unit	6.531	19
PE(P)	PE(P-16:0/20:3)	726.5	Unit	363.3	Unit	7.661	19
PE(P)	PE(P-16:0/20:4)	724.5	Unit	361.3	Unit	7.126	19
PE(P)	PE(P-16:0/20:5)	722.5	Unit	359.3	Unit	6.467	19
PE(P)	PE(P-16:0/22:4)	752.6	Unit	389.3	Unit	7.943	19
PE(P)	PE(P-16:0/22:5)(a\b)	750.5	Unit	387.3	Unit	7.448	19
PE(P)	PE(P-16:0/22:6)	748.5	Unit	385.3	Unit	6.904	19
PE(P)	PE(P-17:0/20:4)(a\b)	738.6	Unit	361.3	Unit	7.607	19
PE(P)	PE(P-17:0/22:6)(a\b)	762.6	Unit	385.3	Unit	7.363	19
PE(P)	PE(P-18:0/18:1)	730.6	Unit	339.3	Unit	9.258	19

-Table continued-							
PE(P)	PE(P-18:0/18:1) d9	739.5	Unit	348.3	Unit	9.204	19
PE(P)	PE(P-18:0/18:2)	728.6	Unit	337.3	Unit	8.388	19
PE(P)	PE(P-18:0/18:3)	726.5	Unit	335.3	Unit	7.671	19
PE(P)	PE(P-18:0/20:3)	754.5	Unit	363.3	Unit	8.854	19
PE(P)	PE(P-18:0/20:4)	752.6	Unit	361.3	Unit	8.293	19
PE(P)	PE(P-18:0/20:5)	750.5	Unit	359.3	Unit	7.553	19
PE(P)	PE(P-18:0/22:4)	780.6	Unit	389.3	Unit	9.161	19
PE(P)	PE(P-18:0/22:5)(a\b)	778.5	Unit	387.3	Unit	8.63	19
PE(P)	PE(P-18:0/22:6)	776.6	Unit	385.3	Unit	8.036	19
PE(P)	PE(P-18:1/18:1)	728.6	Unit	339.3	Unit	8.346	19
PE(P)	PE(P-18:1/18:2)	726.5	Unit	337.3	Unit	7.503	19
PE(P)	PE(P-18:1/18:3)	724.5	Unit	335.3	Unit	6.728	19
PE(P)	PE(P-18:1/20:3)	752.5	Unit	363.3	Unit	7.975	19
PE(P)	PE(P-18:1/20:4)	750.5	Unit	361.3	Unit	7.417	19
PE(P)	PE(P-18:1/20:5)	748.5	Unit	359.3	Unit	6.747	19
PE(P)	PE(P-18:1/22:4)	778.5	Unit	389.3	Unit	8.153	19
PE(P)	PE(P-18:1/22:5)(a\b)	776.6	Unit	387.3	Unit	7.656	19
PE(P)	PE(P-18:1/22:6)(a\b)	774.5	Unit	385.3	Unit	7.184	19
PE(P)	PE(P-19:0/20:4)(a\b)	766.6	Unit	361.3	Unit	8.79	19
PE(P)	PE(P-20:0/18:1)	758.6	Unit	339.3	Unit	10.041	19
PE(P)	PE(P-20:0/18:2)	756.6	Unit	337.3	Unit	9.64	19
PE(P)	PE(P-20:0/20:4)	780.6	Unit	361.3	Unit	9.534	19
PE(P)	PE(P-20:0/22:6)	804.6	Unit	385.3	Unit	9.266	19
PE(P)	PE(P-20:1/20:4)	778.5	Unit	361.3	Unit	8.397	19
PE(P)	PE(P-20:1/22:6)	802.6	Unit	385.3	Unit	8.141	19
PG	PG 34:1	766.6	Unit	577.5	Unit	6.048	17
PG	PG 34:2	764.6	Unit	575.5	Unit	5.493	17
PG	PG 36:1	794.6	Unit	605.6	Unit	6.984	17

-Table continued-							
PG	PG 36:2	792.6	Unit	603.5	Unit	6.327	17
PG	PG(15:0_18:1) d7	759.6	Unit	570.6	Unit	5.63	17
PI	PI(15:0_18:1) d7	847.6	Unit	570.6	Unit	5.375	17
PI	PI 32:0	828.6	Unit	551.6	Unit	5.628	17
PI	PI 32:1	826.5	Unit	549.5	Unit	5.057	17
PI	PI 34:0	856.6	Unit	579.6	Unit	6.523	17
PI	PI 34:1	854.6	Unit	577.6	Unit	5.794	17
PI	PI 35:1	868.6	Unit	591.6	Unit	6.2	17
PI	PI 35:2	866.6	Unit	589.6	Unit	5.626	17
PI	PI 36:1	882.6	Unit	605.6	Unit	6.7	17
PI	PI 36:2	880.6	Unit	603.6	Unit	6.054	17
PI	PI 36:3(a\b\c)	878.6	Unit	601.6	Unit	5.468	17
PI	PI 36:4	876.6	Unit	599.6	Unit	5.204	17
PI	PI 37:4 (a\b)	890.6	Unit	613.6	Unit	5.583	17
PI	PI 37:6	886.6	Unit	609.6	Unit	5.478	17
PI	PI 38:2	908.6	Unit	631.6	Unit	6.919	17
PI	PI 38:3(a\b)	906.6	Unit	629.6	Unit	6.523	17
PI	PI 38:4	904.6	Unit	627.6	Unit	6.023	17
PI	PI 38:5(a\b)	902.6	Unit	625.6	Unit	5.383	17
PI	PI 38:6	900.6	Unit	623.6	Unit	5.076	17
PI	PI 39:6	914.6	Unit	637.6	Unit	5.393	17
PI	PI 40:4	932.6	Unit	655.6	Unit	6.887	17
PI	PI 40:5(a\b)	930.6	Unit	653.6	Unit	6.273	17
PI	PI 40:6	928.6	Unit	651.6	Unit	5.845	17
PIP	PIP1(38:4)	984.7	Unit	627.7	Unit	5.171	20
PS	PS 36:1	790.6	Unit	605.6	Unit	6.796	23
PS	PS 36:2	788.5	Unit	603.5	Unit	6.13	23
PS	PS 38:3	814.6	Unit	629.6	Unit	6.441	23

-Table continued-							
PS	PS 38:4	812.5	Unit	627.5	Unit	6.088	23
PS	PS 38:5	810.5	Unit	625.5	Unit	5.45	23
PS	PS 40:5	838.6	Unit	653.6	Unit	6.191	23
PS	PS 40:6	836.5	Unit	651.5	Unit	5.931	23
PS	PS(15:0_18:1) d7	755.5	Unit	570.5	Unit	5.441	23
S1P	S1P(d16:1)	352.2	Unit	236.3	Unit	1.409	12
S1P	S1P(d17:1)	366.2	Unit	250.3	Unit	1.699	12
S1P	S1P(d18:0)	382.2	Unit	284.3	Unit	2.219	12
S1P	S1P(d18:1)	380.2	Unit	264.3	Unit	2.038	12
S1P	S1P(d18:1) d7	387.2	Unit	271.3	Unit	2.027	12
S1P	S1P(d18:2)	378.2	Unit	262.3	Unit	1.558	12
SM	SM 31:1	661.5	Unit	184.1	Unit	4.673	29
SM	SM 32:0	677.6	Unit	184.1	Unit	5.316	29
SM	SM 32:1	675.5	Unit	184.1	Unit	5.028	29
SM	SM 32:2	673.5	Unit	184.1	Unit	4.489	29
SM	SM 33:1	689.6	Unit	184.1	Unit	5.401	29
SM	SM 34:0	705.6	Unit	184.1	Unit	6.187	29
SM	SM 34:1	703.6	Unit	184.1	Unit	5.822	29
SM	SM 34:2	701.6	Unit	184.1	Unit	5.177	29
SM	SM 34:3	699.5	Unit	184.1	Unit	4.705	29
SM	SM 35:1 (a\b)	717.6	Unit	184.1	Unit	6.217	29
SM	SM 35:2 (a\b)	715.6	Unit	184.1	Unit	5.737	29
SM	SM 36:1	731.6	Unit	184.1	Unit	6.811	29
SM	SM 36:2	729.6	Unit	184.1	Unit	6.039	29
SM	SM 36:3	727.6	Unit	184.1	Unit	5.452	29
SM	SM 37:1	745.6	Unit	184.1	Unit	7.386	29
SM	SM 37:2	743.5	Unit	184.1	Unit	6.528	29
SM	SM 38:1	759.6	Unit	184.1	Unit	7.995	29

-Table continued-							
SM	SM 38:2	757.6	Unit	184.1	Unit	7.06	29
SM	SM 38:3 (a\b)	755.6	Unit	184.1	Unit	6.288	29
SM	SM 39:1	773.7	Unit	184.1	Unit	8.61	29
SM	SM 40:0	789.7	Unit	184.1	Unit	9.639	29
SM	SM 40:1	787.7	Unit	184.1	Unit	9.15	29
SM	SM 40:2 (a\b)	785.7	Unit	184.1	Unit	8.121	29
SM	SM 40:3 (a\b\c)	783.6	Unit	184.1	Unit	7.236	29
SM	SM 40:4	781.5	Unit	184.1	Unit	6.276	29
SM	SM 41:0	803.7	Unit	184.1	Unit	9.988	29
SM	SM 41:1	801.7	Unit	184.1	Unit	9.671	29
SM	SM 41:2(a\b)	799.7	Unit	184.1	Unit	8.724	29
SM	SM 42:1	815.7	Unit	184.1	Unit	10.019	29
SM	SM 42:2 (a\b)	813.7	Unit	184.1	Unit	9.362	29
SM	SM 42:3	811.5	Unit	184.1	Unit	8.235	29
SM	SM 42:4	809.5	Unit	184.1	Unit	7.434	29
SM	SM 43:1	829.7	Unit	184.1	Unit	10.103	29
SM	SM 43:2 (a\b\c)	827.7	Unit	184.1	Unit	9.776	29
SM	SM 44:1	843.6	Unit	184.1	Unit	10.217	29
SM	SM 44:2	841.6	Unit	184.1	Unit	10.019	29
SM	SM 44:3 (a\b)	839.6	Unit	184.1	Unit	9.447	29
SM	SM(d18:1/15:0) d9	698.6	Unit	193.1	Unit	5.401	29
SPN	Sph(d16:1)	272.3	Unit	254.3	Unit	1.679	10
SPN	Sph(d17:1)	286.3	Unit	268.3	Unit	1.975	10
SPN	Sph(d18:1)	300.3	Unit	282.3	Unit	2.219	10
SPN	Sph(d18:2)	298.3	Unit	280.3	Unit	1.827	10
Sulfatides	Sulfatide (d18:1:/12:0) (ISTD)	724.8	Unit	264.3	Unit	3.907	56
Sulfatides	Sulfatide (d18:1:/16:0(OH)) [264]	796.8	Unit	264.3	Unit	4.789	56

-Table continued-							
Sulfatides	Sulfatide (d18:1:/16:0) [264]	780.8	Unit	264.3	Unit	4.94	56
Sulfatides	Sulfatide (d18:1:/24:0(OH)) [264]	908.8	Unit	264.3	Unit	8.361	56
Sulfatides	Sulfatide (d18:1:/24:0) [264]	892.8	Unit	264.3	Unit	8.627	56
Sulfatides	Sulfatide (d18:1:/24:1(OH)) [264]	906.8	Unit	264.3	Unit	7.254	56
Sulfatides	Sulfatide (d18:1:/24:1) [264]	890.8	Unit	264.3	Unit	7.516	56
TG	TG(48:0) [NL-16:0]	824.8	Unit	551.5	Unit	11.266	25
TG	TG(48:0) [NL-18:0]	824.8	Unit	523.5	Unit	11.266	25
TG SIM	TG(48:0) [SIM]	824.8	Unit	824.8	Unit	11.266	0
TG	TG(48:1) [NL-16:1]	822.8	Unit	551.5	Unit	11.102	25
TG	TG(48:1) [NL-18:1]	822.8	Unit	523.5	Unit	11.102	25
TG	TG(48:1) [NL-18:1] d7 ISTD	829.8	Unit	523.5	Unit	11.092	25
TG SIM	TG(48:1) [SIM]	822.8	Unit	822.8	Unit	11.102	0
TG	TG(48:2) [NL-14:0]	820.8	Unit	575.5	Unit	10.948	25
TG	TG(48:2) [NL-14:1]	820.8	Unit	577.5	Unit	10.938	25
TG	TG(48:2) [NL-16:1]	820.8	Unit	549.5	Unit	10.948	25
TG	TG(48:2) [NL-18:2]	820.8	Unit	523.5	Unit	10.958	25
TG SIM	TG(48:2) [SIM]	820.8	Unit	820.8	Unit	10.948	0
TG	TG(48:3) [NL-14:0]	818.8	Unit	573.5	Unit	10.813	25
TG	TG(48:3) [NL-16:1]	818.8	Unit	547.5	Unit	10.802	25
TG	TG(48:3) [NL-18:3]	818.8	Unit	523.5	Unit	10.844	25
TG SIM	TG(48:3) [SIM]	818.8	Unit	818.8	Unit	10.813	0
TG	TG(49:1) [NL-16:1]	836.8	Unit	565.5	Unit	11.194	25
TG	TG(49:1) [NL-17:1]	836.8	Unit	551.5	Unit	11.224	25
TG SIM	TG(49:1) [SIM]	836.8	Unit	836.8	Unit	11.204	0
TG	TG(50:0) [NL-18:0]	852.8	Unit	551.5	Unit	11.481	25
TG SIM	TG(50:0) [SIM]	852.8	Unit	852.8	Unit	11.481	0

-Table continued-							
TG	TG(50:1) [NL-14:0]	850.8	Unit	605.5	Unit	11.284	25
TG	TG(50:1) [NL-16:0]	850.8	Unit	577.5	Unit	11.293	25
TG	TG(50:1) [NL-18:1]	850.8	Unit	551.5	Unit	11.274	25
TG SIM	TG(50:1) [SIM]	850.8	Unit	850.8	Unit	11.284	0
TG	TG(50:2) [NL-14:0]	848.8	Unit	603.5	Unit	11.121	25
TG	TG(50:2) [NL-16:1]	848.8	Unit	577.5	Unit	11.121	25
TG	TG(50:2) [NL-18:1]	848.8	Unit	549.5	Unit	11.11	25
TG	TG(50:2) [NL-18:2]	848.8	Unit	551.5	Unit	11.131	25
TG SIM	TG(50:2) [SIM]	848.8	Unit	848.8	Unit	11.121	0
TG	TG(50:3) [NL-14:0]	846.8	Unit	601.5	Unit	10.967	25
TG	TG(50:3) [NL-14:1]	846.8	Unit	603.5	Unit	10.967	25
TG	TG(50:3) [NL-16:1]	846.8	Unit	575.5	Unit	10.967	25
TG	TG(50:3) [NL-18:2]	846.8	Unit	549.5	Unit	10.977	25
TG	TG(50:3) [NL-18:3]	846.8	Unit	551.5	Unit	11.018	25
TG SIM	TG(50:3) [SIM]	846.8	Unit	846.8	Unit	10.977	0
TG	TG(50:4) [NL-14:0]	844.8	Unit	599.5	Unit	10.843	25
TG	TG(50:4) [NL-18:3]	844.8	Unit	549.5	Unit	10.853	25
TG	TG(50:4) [NL-20:4]	844.8	Unit	523.5	Unit	10.915	25
TG SIM	TG(50:4) [SIM]	844.8	Unit	844.8	Unit	10.843	0
TG	TG(51:0) [NL-16:0]	866.7	Unit	593.4	Unit	11.563	25
TG SIM	TG(51:0) [SIM]	866.7	Unit	866.7	Unit	11.563	0
TG	TG(51:1) [NL-17:0]	864.8	Unit	577.5	Unit	11.376	25
TG SIM	TG(51:1) [SIM]	864.8	Unit	864.8	Unit	11.376	0
TG	TG(51:2) [NL-15:0]	862.8	Unit	603.5	Unit	11.212	25
TG	TG(51:2) [NL-17:0]	862.8	Unit	575.5	Unit	11.212	25
TG	TG(51:2) [NL-17:1]	862.8	Unit	577.5	Unit	11.222	25
TG SIM	TG(51:2) [SIM]	862.8	Unit	862.8	Unit	11.212	0
TG	TG(52:1) [NL-18:0]	878.8	Unit	577.5	Unit	11.499	25

-Table continued-							
TG	TG(52:1) [NL-18:1]	878.8	Unit	579.5	Unit	11.489	25
TG SIM	TG(52:1) [SIM]	878.8	Unit	878.8	Unit	11.489	0
TG	TG(52:2) [NL-16:0]	876.8	Unit	603.5	Unit	11.303	25
TG	TG(52:2) [NL-18:2]	876.8	Unit	579.5	Unit	11.324	25
TG SIM	TG(52:2) [SIM]	876.8	Unit	876.8	Unit	11.303	0
TG	TG(52:3) [NL-16:1]	874.8	Unit	603.5	Unit	11.14	25
TG	TG(52:3) [NL-18:2]	874.8	Unit	577.5	Unit	11.14	25
TG SIM	TG(52:3) [SIM]	874.8	Unit	874.8	Unit	11.154	0
TG	TG(52:4) [NL-16:1]	872.8	Unit	601.5	Unit	10.985	25
TG	TG(52:4) [NL-18:2]	872.8	Unit	575.5	Unit	11.006	25
TG	TG(52:4) [NL-18:3]	872.8	Unit	577.5	Unit	11.027	25
TG SIM	TG(52:4) [SIM]	872.8	Unit	872.8	Unit	11.01	0
TG	TG(52:5) [NL-18:3]	870.8	Unit	575.5	Unit	10.882	25
TG	TG(52:5) [NL-20:4]	870.8	Unit	549.5	Unit	10.924	25
TG	TG(52:5) [NL-20:5]	870.8	Unit	551.5	Unit	10.965	25
TG SIM	TG(52:5) [SIM]	870.8	Unit	870.8	Unit	10.872	0
TG	TG(53:2) [NL-17:1]	890.8	Unit	605.5	Unit	11.405	25
TG	TG(53:2) [NL-18:1]	890.8	Unit	591.5	Unit	11.384	25
TG SIM	TG(53:2) [SIM]	890.8	Unit	890.8	Unit	11.374	0
TG	TG(54:0) [NL-18:0]	908.8	Unit	607.5	Unit	11.908	25
TG SIM	TG(54:0) [SIM]	908.8	Unit	908.8	Unit	11.897	0
TG	TG(54:1) [NL-18:1]	906.8	Unit	607.5	Unit	11.707	25
TG SIM	TG(54:1) [SIM]	906.8	Unit	906.8	Unit	11.707	0
TG	TG(54:2) [NL-18:0]	904.8	Unit	603.5	Unit	11.507	25
TG	TG(54:2) [NL-20:1]	904.8	Unit	577.5	Unit	11.497	25
TG SIM	TG(54:2) [SIM]	904.8	Unit	904.8	Unit	11.507	0
TG	TG(54:3) [NL-18:1]	902.8	Unit	603.5	Unit	11.332	25
TG	TG(54:3) [NL-18:2]	902.8	Unit	605.5	Unit	11.342	25

-Table continued-							
TG SIM	TG(54:3) [SIM]	902.8	Unit	902.8	Unit	11.332	0
TG	TG(54:4) [NL-18:2]	900.8	Unit	603.5	Unit	11.168	25
TG	TG(54:4) [NL-20:3]	900.8	Unit	577.5	Unit	11.23	25
TG SIM	TG(54:4) [SIM]	900.8	Unit	900.8	Unit	11.175	0
TG	TG(54:5) [NL-18:3]	898.8	Unit	603.5	Unit	11.035	25
TG	TG(54:5) [NL-20:4]	898.8	Unit	577.5	Unit	11.097	25
TG SIM	TG(54:5) [SIM]	898.8	Unit	898.8	Unit	11.025	0
TG	TG(54:6) [NL-18:3]	896.8	Unit	601.5	Unit	10.901	25
TG	TG(54:6) [NL-20:4]	896.8	Unit	575.5	Unit	10.953	25
TG	TG(54:6) [NL-20:5]	896.8	Unit	577.5	Unit	10.974	25
TG	TG(54:6) [NL-22:6]	896.8	Unit	551.5	Unit	11.025	25
TG SIM	TG(54:6) [SIM]	896.8	Unit	896.8	Unit	10.901	0
TG	TG(54:7) [NL-20:5]	894.8	Unit	575.5	Unit	10.839	25
TG	TG(54:7) [NL-22:6]	894.8	Unit	549.5	Unit	10.871	25
TG SIM	TG(54:7) [SIM]	894.8	Unit	894.8	Unit	10.839	0
TG	TG(56:6) [NL-20:4]	924.8	Unit	603.5	Unit	11.115	25
TG	TG(56:6) [NL-22:5]	924.8	Unit	577.5	Unit	11.095	25
TG SIM	TG(56:6) [SIM]	924.8	Unit	924.8	Unit	11.105	0
TG	TG(56:7) [NL-20:4]	922.8	Unit	601.5	Unit	10.972	25
TG	TG(56:7) [NL-20:5]	922.8	Unit	603.5	Unit	10.982	25
TG	TG(56:7) [NL-22:5]	922.8	Unit	575.5	Unit	10.961	25
TG	TG(56:7) [NL-22:6]	922.8	Unit	577.5	Unit	11.044	25
TG SIM	TG(56:7) [SIM]	922.8	Unit	922.8	Unit	11.034	0
TG	TG(56:8) [NL-20:4]	920.8	Unit	599.5	Unit	10.848	25
TG	TG(56:8) [NL-20:5]	920.8	Unit	601.5	Unit	10.848	25
TG	TG(56:8) [NL-22:6]	920.8	Unit	575.5	Unit	10.9	25
TG SIM	TG(56:8) [SIM]	920.8	Unit	920.8	Unit	10.89	0
TG	TG(56:9) [NL-22:6]	918.8	Unit	573.5	Unit	10.765	25

-Table continued-							
TG SIM	TG(56:9) [SIM]	918.8	Unit	918.8	Unit	10.765	0
TG	TG(58:10) [NL-22:6]	944.9	Unit	599.5	Unit	10.784	25
TG SIM	TG(58:10) [SIM]	944.9	Unit	944.9	Unit	10.795	0
TG	TG(58:8) [NL-22:6]	948.8	Unit	603.5	Unit	11.053	25
TG SIM	TG(58:8) [SIM]	948.8	Unit	948.8	Unit	11.053	0
TG	TG(58:9) [NL-22:6]	946.9	Unit	601.5	Unit	10.909	25
TG SIM	TG(58:9) [SIM]	946.9	Unit	946.9	Unit	10.919	0
TG(O)	TG(O-50:1) [NL-15:0]	836.8	Unit	577.5	Unit	11.629	25
TG(O)	TG(O-50:1) [NL-16:0]	836.8	Unit	563.5	Unit	11.618	25
TG(O)	TG(O-50:1) [NL-17:1]	836.8	Unit	551.5	Unit	11.607	25
TG(O)	TG(O-50:1) [NL-18:1]	836.8	Unit	537.5	Unit	11.629	25
TG SIM	TG(O-50:1) [SIM]	836.8	Unit	836.8	Unit	11.618	0
TG(O)	TG(O-50:2) [NL-16:1]	834.8	Unit	563.5	Unit	11.41	25
TG(O)	TG(O-50:2) [NL-18:1]	834.8	Unit	535.5	Unit	11.43	25
TG(O)	TG(O-50:2) [NL-18:2]	834.8	Unit	537.5	Unit	11.472	25
TG SIM	TG(O-50:2) [SIM]	834.8	Unit	834.8	Unit	11.441	0
TG(O)	TG(O-50:3) [NL-18:2]	832.8	Unit	535.5	Unit	11.256	25
TG SIM	TG(O-50:3) [SIM]	832.8	Unit	832.8	Unit	11.245	0
TG(O)	TG(O-52:0) [NL-16:0]	866.8	Unit	593.5	Unit	12.029	25
TG SIM	TG(O-52:0) [SIM]	866.8	Unit	866.8	Unit	12.029	0
TG(O)	TG(O-52:1) [NL-16:0]	864.8	Unit	591.5	Unit	11.849	25
TG(O)	TG(O-52:1) [NL-18:1]	864.8	Unit	565.5	Unit	11.86	25
TG SIM	TG(O-52:1) [SIM]	864.8	Unit	864.8	Unit	11.86	0
TG(O)	TG(O-52:2) [NL-16:0]	862.8	Unit	589.5	Unit	11.638	25
TG(O)	TG(O-52:2) [NL-17:1]	862.8	Unit	577.5	Unit	11.638	25
TG(O)	TG(O-52:2) [NL-18:1]	862.8	Unit	563.5	Unit	11.628	25
TG SIM	TG(O-52:2) [SIM]	862.8	Unit	862.8	Unit	11.628	0
TG(O)	TG(O-54:2) [NL-17:1]	890.8	Unit	605.5	Unit	11.857	25

-Table continued-							
TG(O)	TG(O-54:2) [NL-18:1]	890.8	Unit	591.5	Unit	11.857	25
TG SIM	TG(O-54:2) [SIM]	890.8	Unit	890.8	Unit	11.867	0
TG(O)	TG(O-54:3) [NL-17:1]	888.8	Unit	603.5	Unit	11.646	25
TG(O)	TG(O-54:3) [NL-18:1]	888.8	Unit	589.5	Unit	11.646	25
TG SIM	TG(O-54:3) [SIM]	888.8	Unit	888.8	Unit	11.656	0
TG(O)	TG(O-54:4) [NL-17:1]	886.8	Unit	601.5	Unit	11.478	25
TG(O)	TG(O-54:4) [NL-18:2]	886.8	Unit	589.5	Unit	11.478	25
TG SIM	TG(O-54:4) [SIM]	886.8	Unit	886.8	Unit	11.489	0
Ubiquinone	Ubiquinone	880.7	Unit	197	Unit	10.819	17